



On the limits of cortical somatosensory plasticity and their functional consequences : a novel form of cross-border plasticity

Dolly-Anne Muret

► To cite this version:

Dolly-Anne Muret. On the limits of cortical somatosensory plasticity and their functional consequences : a novel form of cross-border plasticity. *Neurons and Cognition [q-bio.NC]*. Université Claude Bernard - Lyon I, 2015. English. NNT : 2015LYO10063 . tel-01186557

HAL Id: tel-01186557

<https://theses.hal.science/tel-01186557>

Submitted on 25 Aug 2015

HAL is a multi-disciplinary open access archive for the deposit and dissemination of scientific research documents, whether they are published or not. The documents may come from teaching and research institutions in France or abroad, or from public or private research centers.

L'archive ouverte pluridisciplinaire **HAL**, est destinée au dépôt et à la diffusion de documents scientifiques de niveau recherche, publiés ou non, émanant des établissements d'enseignement et de recherche français ou étrangers, des laboratoires publics ou privés.

THESE DE L'UNIVERSITE DE LYON

Délivrée par
L'UNIVERSITE CLAUDE BERNARD LYON 1

Ecole Doctorale Neurosciences et Cognition

DIPLOME DE DOCTORAT
(arrêté du 7 août 2006)

soutenue publiquement le 27 Avril 2015

par

Dolly-Anne MURET

**ON THE LIMITS OF CORTICAL SOMATOSENSORY PLASTICITY
AND THEIR FUNCTIONAL CONSEQUENCES:
A NOVEL FORM OF CROSS-BORDER PLASTICITY**

Directeur de thèse: **Dr. Alessandro Farnè, Ph.D.**
Co-encadrante: **Dr. Karen Reilly, Ph.D.**

JURY :	Pr. Arno Villringer, M.D., Ph.D., D.R.	Rapporteur
	Dr. Christian Xerri, Ph.D., D.R.	Rapporteur
	Dr. Luis Garcia-Larrea, M.D., Ph.D., D.R.	Examineur
	Pr. Gilles Rode, M.D, Ph.D.	Examineur
	Dr. Hubert R. Dinse, Ph.D.	Examineur
	Dr. Alessandro Farnè, Ph.D., D.R.	Examineur
	Dr. Karen T. Reilly, Ph.D.	Membre invité

Centre de Recherche en Neurosciences de Lyon, Equipe ImpAct (Integrative, Multisensory, Perception and Action Team), INSERM U1028, CNRS UMR5292, Lyon, France

UNIVERSITE CLAUDE BERNARD - LYON 1

Président de l'Université

M. François-Noël GILLY

Vice-président du Conseil d'Administration

M. le Professeur Hamda BEN HADID

Vice-président du Conseil des Etudes et de la Vie Universitaire

M. le Professeur Philippe LALLE

Vice-président du Conseil Scientifique

M. le Professeur Germain GILLET

Directeur Général des Services

M. Alain HELLEU

COMPOSANTES SANTE

Faculté de Médecine Lyon Est – Claude Bernard

Directeur : M. le Professeur J. ETIENNE

Faculté de Médecine et de Maïeutique Lyon Sud – Charles Mérieux

Directeur : Mme la Professeure C. BURILLON

Faculté d'Odontologie

Directeur : M. le Professeur D. BOURGEOIS

Institut des Sciences Pharmaceutiques et Biologiques

Directeur : Mme la Professeure C. VINCIGUERRA

Institut des Sciences et Techniques de la Réadaptation

Directeur : M. le Professeur Y. MATILLON

Département de formation et Centre de Recherche en Biologie Humaine

Directeur : Mme. la Professeure A-M. SCHOTT

COMPOSANTES ET DEPARTEMENTS DE SCIENCES ET TECHNOLOGIE

Faculté des Sciences et Technologies

Directeur : M. F. DE MARCHI

Département Biologie

Directeur : M. le Professeur F. FLEURY

Département Chimie Biochimie

Directeur : Mme Caroline FELIX

Département GEP

Directeur : M. Hassan HAMMOURI

Département Informatique

Directeur : M. le Professeur S. AKKOUCHE

Département Mathématiques

Directeur : M. le Professeur Georges TOMANOV

Département Mécanique

Directeur : M. le Professeur H. BEN HADID

Département Physique

Directeur : M. Jean-Claude PLENET

UFR Sciences et Techniques des Activités Physiques et Sportives

Directeur : M. Y. VANPOULLE

Observatoire des Sciences de l'Univers de Lyon

Directeur : M. B. GUIDERDONI

Polytech Lyon

Directeur : M. P. FOURNIER

Ecole Supérieure de Chimie Physique Electronique

Directeur : M. G. PIGNAULT

Institut Universitaire de Technologie de Lyon 1

Directeur : M. le Professeur C. VITON

Ecole Supérieure du Professorat et de l'Education

Directeur : M. le Professeur A. MOUGNIOTTE

Institut de Science Financière et d'Assurances

Directeur : M. N. LEBOISNE

“The greatest sense in our body is our touch sense. It is probably the chief sense in the processes of sleeping and waking; it gives us our knowledge of depth or thickness and form; we feel, we love and hate, are touchy and are touched, through the touch corpuscles of our skin.”

J. Lionel Tayler, *The Stages of Human Life*,

1921, p. 157

REMERCIEMENTS - ACKNOWLEDGEMENTS

This dissertation provides only a small foretaste of what these 4 years and a half have been: a journey fraught with adventures. Even if some of these adventures were far from being pleasant, each of them contributed to a long and, I hope fruitful, learning. Yeap, “learning” is definitely the take home message of this journey (and of this work ;-))! I learned so many things. Of course I learned a lot at the professional level, thanks to the so numerous opportunities that were offered to me, but also, and I would say more importantly, at the personal level. This is the reason why this journey is and will stay one of the most precious experiences I have been through. Consequently, I would like to thank each of the persons who significantly contributed to this amazing journey.

And my first thoughts are for you, Ale. Que dire Tout d’abord, merci d’avoir toléré mes nombreux mails truffés (et souvent dès l’objet) d’onomatopées : « Argh ... », « He he he », « Heuuu ... », « Mmmmh ... », « hum hum ... », « Oups ... » et j’en passe. Plus sérieusement, merci infiniment pour ton écoute, ton respect, et ta disponibilité malgré ton emploi du temps chargé, merci pour les discussions passionnantes (toujours trop courtes) que nous avons eu. Mais tu le sais, j’ai d’ors et déjà toute une liste de sujets à aborder lors des discussions qui nous attendent encore ;-). Merci d’être aussi passionné par ce que tu fais ... c’est un petit rien qui change tout et qui a rendu nos discussions si plaisantes! J’espère arriver à garder une passion aussi intacte. Je ne sais comment te remercier pour ton soutien à toute épreuve, pour les innombrables opportunités que tu m’as offertes et pour ta patience lors des quelques « crises » qui sont survenues tout au long de ces 4 ans et demi. Enfin (parce qu’il faut bien que j’arrête quelque part), un grand merci d’avoir permis que la franchise soit à la base de nos interactions ... même si j’en ai parfois peut-être trop usé, je t’en suis extrêmement reconnaissante car c’est une des valeurs que je chérie le plus.

Tout naturellement, mes pensées vont ensuite vers toi, Karen. Ca va faire maintenant plus de 5 ans que l’on travaille ensemble, et je n’ai pas vu le temps passer! Je ne pense pas te l’avoir jamais dis, mais je te suis extrêmement reconnaissante de m’avoir acceptée, en 200..9?, en tant que stagiaire de M2, de m’avoir initiée aux notions de plasticité corticale, et surtout, de m’avoir “ouvert” les portes de ce labo en me recommandant comme candidate auprès d’Alessandro. Je suis contente de t’avoir “suivie” jusqu’ici ;-). Mise à part ça, je tenais à te remercier pour ta constante réactivité et disponibilité durant ces années, pour les nombreuses fois où tu m’as proposé ton aide. Tu as toujours su te rendre disponible et je t’en remercie. Merci aussi d’avoir toujours été prête à corriger mon anglais ... si j’ai progressé, c’est sans nul doute à ton contact! Et ce n’était pas gagné d’avance ;-).

Merci à toi Fadila pour ton aide et tes conseils sur la dernière ligne droite, et d’une manière générale, merci à tous les chercheurs, qui font que ce laboratoire est extrêmement humain et collégial. C’est une chose précieuse dans ce milieu où la compétition tend à prendre de grandes proportions.

Merci aux secrétaires et ingénieurs ... avec une pensée spéciale pour Roméo que j’espère revoir très vite, mais aussi pour Christian, Olivier et Fred dont l’aide a été précieuse au début de

ce voyage pour développer mes setups/protocoles. Merci d'avoir été patients et toujours prêts à aider!

Mes pensées vont ensuite à mon autre "attache" à Lyon ... le "coin" MEG! Un grand merci à Jérémie Mattout pour avoir pris le temps de m'initier avec pédagogie aux bases de Matlab quand j'étais encore en Master, puis en première année de thèse. Je te serais à jamais redevable ... sans cela, je n'aurais pas pu accomplir la moitié de ce travail. Un immense merci à toi Sébastien, pour ton aide plus que précieuse même aux heures les plus tardives!! Merci pour ta patience, et d'avoir pris la peine de répondre à mes questions incessantes. Ca aura été une belle expérience ;-). Merci aussi à tous les membres du club MEG ... Françoise, Anne, Aline, Claude, ... merci pour les échanges et vos conseils avisés. Merci d'une manière générale à tous les membres de Dycog, pour m'avoir accueillie, que ce soit en Master ou pendant les quelques mois qu'a duré ma manip MEG ... petite pensée spéciale pour Gaëtan, Philippe, Margaux, Ludo, Yohana, et Manu!

The "formal" acknowledgements done, now I would like to thank my dear lab-mates with whom I shared so much these last four years. I do not know who to start with ... I simply love each one of you! Delphine, ma chère Dédé, ah la la, quel dommage que tu ne sois pas là, j'aurais adoré faire la choré de notre chère chanson ;). Merci pour nos pauses café du matin, pour les nombreuses « séances de thérapie » ... Selene, ou shorty pour les intimes (et ceux qui peuvent se permettre, he he he), que de péripéties tout au long de ces 4 ans! Je crois qu'on est rodées niveau montagnes russes ;). Olga, first of all, sorry for confusing your name with Inga's for so long when you arrived, you know, I'm not good at remembering names ... but I think I was slightly better at removing stitches ;). We had a lot of fun together, thanks a lot! I will never forget the canoe experience ;). To both of you, Selene and Olga, special thanks for taking care of me during the (most difficult) last months. I will call you mummy from now ;). Ouazna, ma chère Ouazna, ton arrivée dans le labo a changé bien des choses pour moi et tu le sais ;) ... et notre amitié qui s'est développée au fil du temps m'est précieuse. Petit coucou spécial à Mayes ;). Merci aussi à tous les nouveaux arrivants: Inga, Eric, Elisa. It was nice meeting you, and your coming to the lab was refreshing ☺. Petite pensée aussi aux "anciens" qui étaient présents dans les premières années de ma thèse, notamment Stéphane & Clément ... que dire de vous deux à part que vous nous manquez depuis votre départ ... petite pensée aussi pour Lucilla, Mumu, Laurence et bien d'autres, sans qui ce labo n'aurait pas été ce qu'il est.

Merci aussi à mes collègues « suisses » ... Marta, Polona et Alex : ah la la que de bon souvenir avec vous trois ... j'ai adoré nos petites sorties à Lausanne !! Merci à tous les autres du labo de l'EPFL pour leur accueil chaleureux : Elisa, Mariia, Roberto, Xavier, Jean-Paul, je suis heureuse de vous avoir rencontrés et d'avoir passé ce temps avec vous à Lausanne. Vous côtoyer m'a beaucoup appris et fait grandir. Enfin, Roberto ... cette étude IRMf aura été une sacrée aventure pour moi. Merci de m'en avoir donné l'opportunité.

Enfin, un grand merci à mes amis qui ont su être patients avec moi et tolérer mon côté associable des 6 derniers mois : Deborah, Sophie, Delphine, Christine & Jibé, et un peu plus loin en Belgique Yoyo et JC.

Et pour finir, je ne saurais comment remercier ma famille qui m'a entourée, encouragée et s'est adaptée à mon rythme de vie des dernières années : Dadou, Sweta, Eliath et man.

RÉSUMÉ EN FRANÇAIS

En plus de sa forte valence sociale et émotionnelle, le toucher joue un rôle prépondérant dans notre vie quotidienne, que ce soit pour pouvoir correctement saisir et manipuler des objets dans le but de réaliser une action, la plus primitive étant de se nourrir, ou pour simplement se mouvoir, la perception tactile émanant de nos pieds étant indispensable au maintien de notre position ainsi qu'à la bonne réalisation des mouvements des jambes. Au niveau cortical, les aires primaires dédiées à la perception tactile de l'ensemble de notre corps ont la particularité d'être organisées selon une cartographie détaillée, appelée *Homunculus*. Alors que la majorité de notre corps y est représenté avec la même continuité que celle de notre corps physique, cet *Homunculus* présente la particularité d'avoir la main et le visage représentés côte à côte alors que ces régions sont relativement distantes physiquement. Cette discontinuité que représente la frontière main-visage a été le sujet de nombreuses études, l'une des raisons ayant trait à la capacité fascinante qu'a notre cerveau à se réorganiser. En effet, de nombreuses études ont démontrées que suite à une perte permanente ou transitoire d'afférence sensorielle, survenant par exemple après une amputation ou une déafférentation, les cartes somatosensorielles primaires se réorganisent fortement, allant jusqu'à traverser cette frontière entre la main et le visage. Ce genre de plasticité liée à une perte d'afférence a été qualifiée de maladaptative du fait de son association à des symptômes douloureux chez ces patients. A l'inverse, alors que l'existence de réorganisations corticales induites par une augmentation d'afférence est connue depuis longtemps et a souvent été associée à des effets bénéfiques sur les performances tactiles et sensorimotrices, la qualifiant d'adaptative, la possibilité qu'une telle plasticité puisse avoir des effets au-delà de la frontière entre la main et le visage reste inexplorée. Mes travaux de thèse ont pour but d'apporter un début de réponse quant à cette question. Pour y parvenir, une première étude comportementale a permis de mettre en évidence qu'une stimulation cutanée répétée d'un doigt permettait non seulement d'améliorer la perception tactile localement, sur le doigt stimulé, mais avait aussi des répercussions sur la perception tactile du visage, en améliorant également l'acuité de la lèvre supérieure et de la joue. Cette première étude laissant penser qu'une augmentation d'afférence par stimulation répétée pourrait en effet traverser la frontière main-visage, deux études supplémentaires ont été réalisées en utilisant deux techniques d'imagerie cérébrales complémentaires, à savoir l'imagerie par résonnance magnétique à haute résolution (IRMf 7T), et la magnétoencéphalographie (MEG). La première d'entre elles (IRMf) révèle une augmentation de l'activation (signal BOLD en surplus de celui au repos) du doigt stimulé dans différentes sous-régions du cortex primaire somatosensoriel (l'aire de Brodmann 3b et 1),

associée à une augmentation de la désactivation (signal BOLD en défaut par rapport à celui au repos) évoquée en stimulant la lèvre. Ces deux sous-régions étant connues pour être impliquées dans le traitement des caractéristiques spatiales simples d'un stimulus tactile, les changements observés sont susceptibles d'être impliqués dans l'amélioration de l'acuité spatiale tactile observée ici aussi au niveau du doigt stimulé et des lèvres. De plus, cette étude est la première à rapporter que la désactivation observée suite à la stimulation de la lèvre est bilatérale (au sein des deux hémisphères), avec la particularité que la désactivation contralatérale à la lèvre stimulée a été trouvée plus dorsale que son homologue, la rendant par conséquent co-localisée avec les activations contralatérales évoquées par la stimulation des doigts de la main droite. Ce résultat suggère la présence d'un nouveau réseau "d'inhibition" entre les représentations de la main et du visage et requiert une investigation plus poussée. Pour finir, d'importants clusters ont été trouvés au niveau des sillons intrapariétaux et du cortex pariétal postérieur, ce qui suggère une intégration des effets de la stimulation répétée dans des régions corticales de plus haut niveau, impliquées notamment dans l'intégration multisensorielle, mais également dans des tâches de discrimination spatiales ou dans la représentation du "body schema". Quant à la seconde étude (MEG), les premiers résultats observés suggèrent une réorganisation de la distribution des représentations de la main et du visage, avec un éloignement respectif des représentations du doigt stimulé et de la lèvre, cohérent avec l'augmentation de l'activité "inhibitrice" observée pour la lèvre dans l'étude précédente. Les analyses dipolaires ont également mis en évidence une asymétrie entre les deux hémisphères quant à l'organisation somatotopique de la main et du visage. Ensemble, ces études révèlent donc qu'une plasticité adaptative induisant un bénéfice perceptif peut se propager sur de relativement grandes distances corticales, et notamment au-delà de la frontière entre la main et le visage jusque là impliquée essentiellement dans des processus maladaptatifs. De surcroît, nos résultats suggèrent l'implication de mécanismes plus complexes que prévu entre les représentations de la main et du visage, deux régions corporelles hautement sollicitées dans une palette d'activités que nous réalisons quotidiennement, allant des tâches les plus simple et primitives comme le fait de se nourrir, à des aspects beaucoup plus cognitifs et intégrés, comme notre communication non verbale. Une étude plus approfondie de ces différents niveaux d'interaction et de leurs répercussions au niveau perceptif se révèle indispensable. Pour finir, de part leurs aspects doublement positifs (augmentation d'afférence et gain perceptif), ces travaux ouvrent également une fenêtre sur un nouveau champ d'investigation pouvant avoir de réelles retombées sur les techniques mises en œuvre afin de promouvoir une réhabilitation de la perception du toucher, mais aussi des capacités motrices de patients cérébrolésés.

ABSTRACT

Touch plays a critical role in our daily life to grasp and manipulate objects, or simply walk. The primary somatosensory areas exhibit the striking feature of being somatotopically organized, giving rise to the so-called *Homunculus*. While most of our body surface is represented following an order similar to its physical continuity, the *Homunculus* displays a major discontinuity, the hand and the face being represented next to each other. The hand-face border has been widely used as a somatotopic hallmark to study one of the most fascinating features of our brain, its capacity for reorganization. Particularly, somatosensory plasticity was found to cross the hand-face border following deprivation of inputs. While it has long been known that increasing inputs also leads to cortical changes typically associated with perceptual benefits, whether such plasticity can cross the hand-face border remains unknown. My thesis work aimed to investigate this question. A first behavioural study revealed that increasing inputs to a finger improves not only the tactile acuity at this finger, but also at the face, suggesting a transfer of plastic changes across the hand-face border. To investigate this, two additional studies were performed using two complementary brain imaging techniques, namely high-field fMRI and MEG. In agreement with our hypotheses a reorganization of both hand and face representations was found. Altogether, this work reveals that adaptive plasticity leading to perceptual benefits can spread over large cortical distances, in particular across the hand-face border, and thus opens up a new window of investigation that may have a real impact in promoting rehabilitation.

RÉSUMÉ

Le toucher a un rôle critique dans notre vie quotidienne pour saisir, manipuler des objets, ou simplement marcher. Les aires primaires somatosensorielles présentent la particularité d'être organisées somatotopiquement, donnant lieu au dénommé *Homunculus*. Alors que la plupart de notre surface corporelle est représentée suivant un ordre similaire à sa continuité physique, l'*Homunculus* présente une discontinuité majeure, la main et le visage étant représentés côte à côte. La frontière main-visage a été souvent utilisée comme un repère pour étudier l'une des particularités les plus fascinantes de notre cerveau, sa capacité de réorganisation. En particulier, la plasticité somatosensorielle a été trouvée capable de traverser la frontière main-visage suite à une privation d'afférences. Alors qu'il est connu depuis longtemps que l'augmentation des afférences conduit également à des changements corticaux souvent associés à des bénéfices perceptifs, la possibilité qu'une telle plasticité puisse traverser la frontière main-visage reste inexplorée. Le travail de ma thèse a pour but d'examiner cette question. Une première étude comportementale a révélé que le fait d'augmenter les afférences d'un doigt améliore non seulement l'acuité tactile de ce doigt, mais aussi du visage, suggérant un transfert de changements plastiques au travers de la frontière main-visage. Afin d'examiner ceci, deux études supplémentaires ont été réalisées en utilisant deux techniques complémentaires d'imagerie cérébrales, à savoir l'IRMf et la MEG. En adéquation avec nos hypothèses, une réorganisation des représentations de la main et du visage a été trouvée. Dans l'ensemble, ce travail révèle qu'une plasticité adaptative menant à des bénéfices perceptifs peut se propager sur de larges distances corticales, en particulier au-delà de la frontière main-visage, et par conséquent ouvre une nouvelle fenêtre d'investigation pouvant avoir un réel impact dans la promotion de rééducation.

LIST OF ABBREVIATIONS

CNS	Central nervous system
VPL/M	Ventroposterior lateral/medial nucleus
SI/SII	Primary/secondary somatosensory cortex
MI	Primary motor cortex
BA3b, 3a, 1 and 2	Brodmann areas 3b, 3a, 1 and 2
PPC	Posterior parietal cortex
IPS/IPL	Intraparietal sulcus/lobule
SPL	Superior parietal lobule
SAI/II & FAI/II	Slowly/rapidly adapting afferents of type I or II
RF	Receptive field
EPSPs	Excitatory postsynaptic potentials
LTP/LTD	Long-term potentiation/depression
ICMS/ITMS	Intracortical/intrathalamic microstimulation
NMDA	N- <i>methyl</i> -D-aspartate
GABA	gamma-aminobutyric acid
STDP	Spike-timing-dependent plasticity
RSS	Repetitive somatosensory stimulation
2PDT	Two-point discrimination threshold
GOT	Grating orientation threshold
D1-5	Digits 1 to 5
fMRI	Functional magnetic resonance imaging
CBF	Cerebral blood flow
RFX	Random effects analysis
CoG	Centre of gravity
PBR/NBR	Positive/negative BOLD response
MEG/EEG	Magneto/electro-encephalography
SEP/SEF	Somatosensory evoked potential/field
ECD	Equivalent current dipole
GoF	Goodness of fit
ED	Euclidean distance

TABLE OF CONTENTS

INTRODUCTION.....	21
CHAPTER I: THE SOMATOSENSORY ASCENDING PATHWAY.....	23
I. THE SKIN: STRUCTURE AND MECHANORECEPTORS	23
II. SOMATOSENSORY SIGNAL CONDUCTION ALONG THE NEURAXIS	30
a. <i>The dorsal column-medial lemniscal pathway</i>	30
b. <i>The sensory trigeminal pathway</i>	33
III. TOPOGRAPHIC ORGANIZATION ALONG THE SOMATOSENSORY PATHWAY	35
a. <i>The spinal cord and brainstem</i>	35
b. <i>The somatosensory thalamus</i>	38
c. <i>The primary somatosensory cortex</i>	40
IV. ZOOM IN ON THE HAND AND FACE REGIONS	48
a. <i>The hand</i>	48
b. <i>The face</i>	55
V. THALAMOCORTICAL PROJECTIONS & HIGHER-ORDER CORTICAL AREAS	63
a. <i>Thalamocortical projections</i>	63
b. <i>Corticocortical projections arising from SI's subregions</i>	65
c. <i>Higher order somatosensory areas</i>	66
CHAPTER 2: SOMATOSENSORY PLASTICITY	73
I. CONCEPT/OVERVIEW	73
II. PLASTICITY FOLLOWING SENSORY DEPRIVATION	75
a. <i>Peripheral lesion or injury:</i>	75
b. <i>Central lesion or injury</i>	83
c. <i>Sensory deprivation without lesion</i>	87
d. <i>Mechanisms</i>	91
III. ACTIVITY-DEPENDENT PLASTICITY	100
a. <i>Restoration & modification of peripheral inputs in the context of rehabilitation</i> 100	
b. <i>Use-dependent plasticity: naturalistic cases</i>	103
c. <i>Training-dependent plasticity</i>	107
d. <i>Relevance of spatial/temporal dis/continuities</i>	112
IV. FUNCTIONAL CONSEQUENCES/RELEVANCE	115

CHAPTER 3: THE HEBBIAN PLASTICITY	125
I. CONCEPT.....	125
II. INDUCTION: FROM SYNAPSES TO THE SKIN	126
a. <i>Hebbian synaptic plasticity</i>	126
b. <i>Intracortical microstimulation</i>	127
c. <i>Temporally paired cutaneous stimulation</i>	128
III. REPETITIVE SOMATOSENSORY STIMULATION	129
a. <i>Description</i>	129
b. <i>RSS-induced perceptual and cortical changes</i>	131
c. <i>Non-mechanical RSS protocols</i>	134
SUMMARY & AIMS	135
EXPERIMENTAL CONTRIBUTIONS.....	137
STUDY 1: BEHAVIOURAL STUDY	139
STUDY 2: 7T FMRI STUDY.....	159
STUDY 3: MEG STUDY	233
GENERAL DISCUSSION.....	275
I. MAIN RESULTS	275
II. METHODOLOGICAL CONSIDERATIONS.....	277
III. TRAINING-DEPENDENT VS TRAINING-INDEPENDENT LEARNING	279
IV. UNDERLYING MECHANISMS:.....	281
a. <i>RSS-induced local plasticity</i>	281
b. <i>Specificity/generalization of the RSS-induced learning</i>	281
c. <i>Site of action of RSS</i>	286
V. THE HAND AND THE FACE: EVIDENCE FOR A SINGULAR “COUPLING”?	291
a. <i>Foetal development, cortical magnification & sensitivity</i>	291
b. <i>Language</i>	292
c. <i>Eating behaviour or the “bring-to-the-mouth neurons”</i>	293
CONCLUSION & FOLLOW-UP	295
REFERENCES.....	299

INTRODUCTION

In the evolution of the senses the sense of touch was undoubtedly the first to come into being. Touch is the parent of our eyes, ears, nose and mouth. It is the sense which differentiated into the others, a fact that seems to be recognized in the age-old adage that touch is “the mother of the senses”. Touch was one of the first senses to be studied directly in the brain of both human and non-human primates due to the easy access to the post-central gyrus, where the primary somatosensory cortex is located, during surgery and brain stimulation experiments. One of the famous discoveries resulting from such experiments consisted in the detailed description of the somatotopic organization of the primary somatosensory cortex, first reported by Penfield and Boldrey (1937, see Figure 1). Despite this early interest in the somatosensory system, this sense remains one of the least understood due to its complexity arising from the diversity of mechanoreceptors and afferents conveying tactile signals to the brain, which also makes the reproducibility and reliability of tactile stimulation difficult to achieve, and thus to compare between studies. However, touch, like vision, is primordial for several functions such as movement through its haptic component, especially necessary to perform fine grained movement such as precision grip, but also for higher functions, such as self perception and awareness. Among the whole body, the hand and the face have the particularity to share common features at different scales. Indeed, in addition to being the most magnified at the cortical level (in both the somatosensory and motor stripes), these body parts share high sensitivity and discrimination abilities, and are conjointly involved in basic and primitive functions such as feeding behaviour (reaching/grasping with hand and mouth) but also in higher cognitive functions such as the production and perception of communicative and emotional gestures.

The tactile information arising from the hand and from the face exhibits the particularity of being represented next to each other in the primary somatosensory cortex, whereas most of the information arising from the rest of our body surface is represented following an order similar to its physical continuity. This major discontinuity in the *Homunculus* has been widely used as a landmark to study one of the most fascinating features of our brain, its plasticity. In the 90ies, groundbreaking electrophysiological studies revealed that deprivation-induced somatosensory plasticity, up to then thought to be limited to few millimetres, could actually cross the hand-face border. Since then, numerous studies reported the presence of plastic changes in the cortical representations of the somatosensory cortex following reduction or increase of inputs, usually associated with perceptual changes. However, the functional relevance of cortical changes

regarding perception remains unclear. To better understand the relationship between cortical plastic changes and perceptual changes, my thesis work focused on investigating whether somatosensory changes, either behavioural and/or cortical, could transfer from the hand to the face.

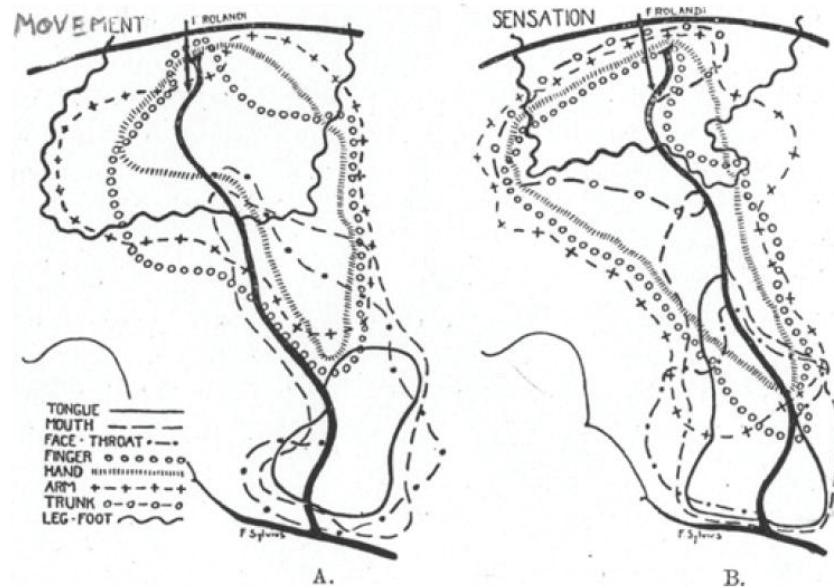


Figure 1 [from Penfield and Boldrey, 1937]. Schematic cartography of the movements and sensations reported by a human patient at the level of the tongue, mouth, face/throat, finger, hand, arm, trunk and leg/foot following electrical brain stimulation of the depicted regions within the primary motor (left) and somatosensory (right) cortices.

CHAPTER I: THE SOMATOSENSORY ASCENDING PATHWAY

Touch is the first sense that develops in utero, the foetus being capable of sensing the pressure caused by one hair touching his cheek starting from week 8 of the gestational period (Montagu, 1978), and the first response to electrical stimulation, the functional counterpart of the N20 in adults, being detected even prior to full-term age (Taylor et al., 1996; Pihko and Lauronen, 2004). This sense arises from the skin which is a highly complex organ, innervated by a wide array of specialized sensory neurones sensitive not only to pressure, but also to heat, cold, irritation, itch and pain (see Table 1 for a brief description of the different classes of sensory afferent nerves innervating the human skin).

I. The skin: structure and mechanoreceptors

The **skin** is the most widely distributed sensory organ, spanning in adults over an average area of 1.5-2.0m², which delimits our body and thus interfaces with the environment. Among the multiple functions of the skin (i.e. protection, temperature and evaporation regulation etc), this organ provides sensory information from our entire body. Mammalian skin is composed of three main layers: (i) the *epidermis*, an outer stratified squamous epithelium which provides waterproofing and serves as a barrier via keratinocytes, (ii) the *dermis*, which consists of a thicker, supporting layer of connective tissue and provides tensile strength and elasticity to the skin, which then sits on (iii) the *hypodermis*, which consists primarily of loose connective tissue and adipocytes and acts as an energy reserve. The thickness of the dermis, which is a densely innervated layer, varies from 0.5 mm over the eyelid to > 5.0 mm in glabrous skin. The two outer layers are tightly connected through the basement membrane and compose the *cutis* from which arise most of the somatic sensations through the numerous autonomic and sensory organs it contains.

The specialized **sensory receptors** in the cutaneous and subcutaneous tissues are dauntingly diverse. They include free nerve endings in the skin, nerve endings associated with specializations that act as amplifiers or filters, and sensory terminals associated with specialized transducing cells that influence the nerve ending by virtue of synapse-like contacts. Based on their functional features, this variety of receptors can be divided into three classes: mechanoreceptors, nociceptors, and thermoreceptors. Noci- and thermo-receptors are referred to as free nerve endings, whereas most other cutaneous receptors show some degree of

encapsulation, which helps determining the nature of the stimuli to which they respond. Despite their variety, all somatic sensory receptors work in fundamentally the same way: stimuli applied to the skin deform or otherwise change the nerve endings, which in turn affects the ionic permeability of the receptor cell membrane. Changes in permeability generate a depolarizing current in the nerve ending, thus producing a receptor (or generator) potential that triggers action potentials. This overall process, in which the energy of a stimulus is converted into an electrical signal in the sensory neuron, is called sensory transduction and is the critical first step in all sensory processing. Following this process, the action potentials are conveyed through the axons of sensory neurons, which constitute sensory fibres. The glabrous skin of the hand is innervated by 12 classes of afferent fibres (Table 1) comprising two broad classes of pain afferents (Greenspan, 1997), two types of thermoreceptive afferents (one selectively responsive to cooling and one to warming; Darian-Smith and Johnson, 1977), four types of proprioceptive afferents (Matthews, 1988), and four types of mechanoreceptive afferents responsive to mechanical deformation of the glabrous skin (described below).

Sensory afferent nerves			
Class	Modality	Axonal diameter (um)	Conduction velocity (m/s)
Myelinated			
A α	Proprioceptors from muscles and tendons	20	120
A β	Low-threshold mechanoreceptors	10	80
A δ	Cold, noxious, thermal	2.5	12
Unmyelinated			
C-pain	Noxious, heat, thermal	1	<1
C-tactile	Light stroking, gentle touch	1	<1
C-autonomic	Autonomic, sweat glands, vasculature	1	<1

Table 1 [from McGlone and Reilly, 2010]. Summary of the main characteristics of primary sensory afferents innervating the human skin.

Among the different modalities of information the skin encodes, the mechanical sensory signal (which is the one relevant to this work), is conveyed by large, myelinated fibres with conduction velocities in the A β range (80m/sec), which innervate cutaneous mechanoreceptors. Depending on the type of skin (hairy or glabrous), A β fibres are present at different densities and innervate slightly different structures. In hairy skin, A β fibres also innervate vascular structures and hair follicles that act as mechanical sensory receptors by detecting changes in hair position. In contrast, the glabrous skin is more abundantly and homogeneously innervated by A β fibres because of the high number of mechanoreceptors embedded within this type of skin (Figure 2, see Nolano et al., 2003; Provitera et al., 2007). Electrophysiological studies have identified four major types of mechanoreceptors in the glabrous skin of the **human hand** (see

Vallbo and Johansson, 1984; reviewed in Johnson, 2001), which are specialized for transducing complementary signals arising from skin mechanical stimulation such as vibration, indentation, pressure, cutaneous tension or more complex signals evoked by shapes/textures or moving stimuli. They comprise Meissner's corpuscles, Pacinian's corpuscles, Merkel cell-neurite complexes, and Ruffini's corpuscles (Figure 3). Based on **histology**, these mechanoreceptors are characterized by their location and structure. **Meissner's corpuscles**, which lie between the dermal papillae just beneath the epidermis, are elongated receptors formed by a capsule made of flattened supportive cells (Schwann cells) arranged as horizontal lamellae embedded in connective tissue. The centre of the capsule contains one or more afferent nerve fibres. They are the most common mechanoreceptors of glabrous skin, mainly expressed in hand palms and foot soles but also in lips, tongue, face, nipples and genitals. Their afferent fibres account for about 40% of the sensory innervation of the human hand. **Pacinian's corpuscles** are large (3-4mm in length) encapsulated endings located in the subcutaneous tissue (and more deeply in interosseous membranes and mesenteries of the gut). The Pacinian corpuscle has an onion-like capsule, made of concentric lamellae of fibrous connective tissue and fibroblasts lined by flat modified Schwann cells, in which the inner core of membrane lamellae is separated from an outer lamella by a fluid-filled space. One or more afferent axons lie at the centre of this structure. They make up 10–15% of the cutaneous receptors in the hand and the Pacinian's corpuscles located in interosseous membranes probably detect vibrations transmitted to the skeleton. **Merkel cell-neurite complexes** consist of a disc-shaped terminal composed of a specialized epithelial cell, the Merkel cell, in close apposition to an enlarged nerve terminal from a single myelinated A β fibre (reviewed in Halata et al., 2003). On the epidermal side Merkel cell exhibits finger-like processes extending between neighbouring keratinocytes. These complexes are found in the basal layer of the epidermis where they are precisely aligned with the papillae that lie beneath the dermal ridges. They account for about 25% of the mechanoreceptors of the hand and are particularly dense in the fingertips, lips, and external genitalia (Lacour et al., 1991). **Ruffini's corpuscles** are thin cigar-shaped encapsulated sensory endings constituted of small connective tissue cylinders. They are broadly distributed in the dermis as well as in ligaments and tendons. The long axis of the corpuscle is usually oriented parallel to the stretch lines in skin. They account for about 20% of the receptors in the human hand.

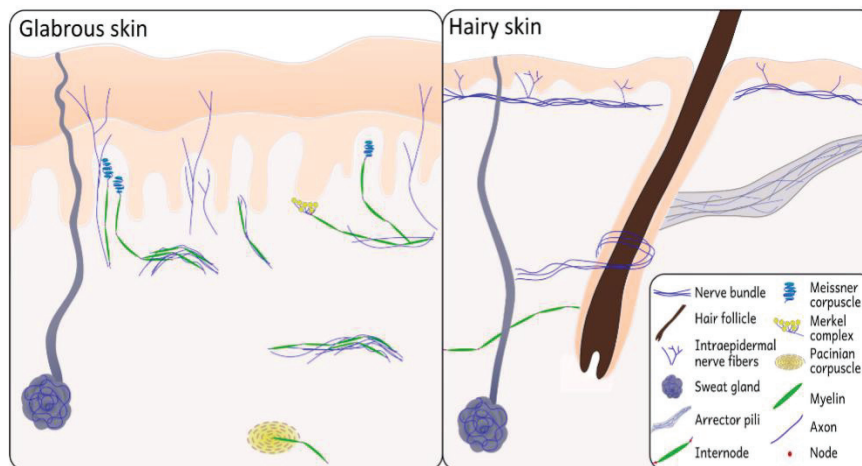


Figure 2 [from Myers et al., 2013]. Schematic representation of neural structures present in glabrous and hairy skin. Small sensory fibres branch off from dermal bundles to innervate the epidermis in both hairy and glabrous skin. In addition, autonomic innervation can be seen in sweat glands and arrector pili muscles (responsible for piloerection). The presence of large myelinated fibres in hairy skin is largely restricted to mechanoreceptive hair follicles; glabrous skin has a comparatively higher density of mechanoreceptive organs and afferent A β myelinated fibres.

Functionally, these receptors and their associated afferents are distinguished by three main features: the kind of stimuli to which they preferentially respond (vibration, moving or static stimuli ... etc), the dynamics of their responses (fast or slow adapting) and their receptive fields size (see Vallbo and Johansson, 1984). The second feature has been and is still the most commonly used to distinguish between mechano-sensory afferents. It refers to how these afferents behave in response to sustained skin stimulation: rapidly adapting fibres respond maximally, but briefly, to stimulation, their response decreasing quickly if the stimulus is maintained, while slowly adapting fibres keep firing as long as the stimulus is present, though at a diminished rate. Thus, these types of afferents provide complementary information about both the *dynamic* and *static* qualities of a stimulus. Among the four types of mechanoreceptors, two have been associated with rapidly adapting afferents (FAI and FAII) and two with slowly adapting afferents (SAI and SAII) (Knibestöl and Vallbo, 1970; Knibestol, 1973). **Rapidly adapting** cutaneous mechanoreceptors include Meissner's (FAI) and Pacinian's (FAII) corpuscles (Figure 3), which provide information primarily about the dynamics of mechanical stimuli.

1. The FAI system is particularly efficient at transducing information about the relatively low-frequency vibrations (~5 to ~40 Hz) that occur when textured objects are moved across the skin (low-frequency skin motion), and it provides the feedback signals required for grip control (Srinivasan et al., 1990). The centre of **Meissner's corpuscles** contains one or more afferent nerve fibres that generate rapidly adapting action potentials following minimal skin depression, which makes them especially sensitive to minute motion on the surface of the skin. They are protected from the confounding effects of large, low-frequency skin displacements by the fluid-filled corpuscle within which they reside.

2. The most important function served by the FAII system is the detection and transduction of high-frequency tissue deformation at the nanometre level. One or more rapidly adapting afferent axons lies at the centre of the multilayered, fluid-filled **Pacinian's corpuscle**, which again acts as a mechanical filter. In this case, its structure allows only transient disturbances at high frequencies (~40 to ~400 Hz) to activate the nerve endings, thus protecting against the confounding effects of high-amplitude, low-frequency stresses and strains that accompany manual tasks. Pacinian's corpuscles adapt more rapidly than Meissner's corpuscles and have a lower response threshold. These attributes suggest that Pacinian's corpuscles are involved in the discrimination of fine surface textures or other moving stimuli that produce high-frequency vibration of the skin.

Slowly adapting cutaneous mechanoreceptors include Merkel cell-neurite complexes (SAI) and Ruffini's corpuscles (SAII, see Figure 3).

1. The SAI system is considered to play a major role in the static discrimination of shapes, edges, and textures (see Johnson and Hsiao, 1992). **Merkel cell-neurite complexes** are especially sensitive to the spatial features of a stimulus due to their selective sensitivity to a particular component of tissue strain (strain energy density). This function is protected from the confounding effects of variations in contact pressure by the fact that strain energy density is relatively unaffected by changes in contact pressure. Whether the Merkel cell, the sensory neuron or both are sites of mechanotransduction is still a matter of debate. However, a recent study performed on mice showed that Merkel cells actively tune mechanosensory responses to facilitate high spatio-temporal acuity (Maksimovic et al., 2014). Keratinocytes may also play an important role in the normal functioning of the Merkel cell-neurite complex, the finger-like processes moving with skin deformation and epidermis cell movement. Selective stimulation of the SAI afferents in humans produces a sensation of light pressure.

2. The SAII system provides information used for the perception of limb conformation and for the perception of forces acting on the hand. **Ruffini's corpuscles** are supplied by one to three myelinated nerve fibres. Their orientation, parallel to the stretch lines in the skin, makes Ruffini's corpuscles particularly sensitive to the deep tissue strain produced by skin stretching, related to limb movements and/or position (i.e. proprioception). They are protected from the confounding effects of stimuli within their receptive fields by relative insensitivity to local skin deformation. They do not elicit any particular tactile sensation when stimulated electrically.

The second commonly used functional feature to distinguish between mechanoreceptors consists of the receptive field (RF) size associated with each type of afferent fibre (Johansson, 1978). Receptive field is a term originally coined by (Sherrington, 1906) to describe an area of the body surface where a stimulus could elicit a reflex. Hartline then extended the term to visual neurons (1938), and has been since extended to other sensory neurons. The somatosensory RF corresponds to the overall area of the skin that, when stimulated by indentation or hair deflection, elicits a reliable neural discharge in a given sensory neuron or fibre. The precise boundary of this area will depend to some extent on the intensity of the stimulus used, but with a given stimulus type I units (SAI and FAI afferents arising from Merkel cell-neurite complexes and Meissner's corpuscles) will be activated by a much smaller area of skin than type II units (SAII and FAII afferents arising from Ruffini's and Pacinian's corpuscles), meaning that they have smaller RFs (Figure 3, left panel). Consequently, the SAI and FAI fibre systems transmit neural images of events at the surface of the skin with relatively high spatial resolution, whereas the SAII and FAII systems convey information of a more global nature to the central nervous system. The resolution of the information transmitted from mechanoreceptors is also related to the fact that they are differently distributed across the skin. Indeed, they exhibit regional differences in innervation densities, the mechanoreceptors/afferents having small RFs (Merkel cell-neurite complexes and Meissner's corpuscles/SAI and FAI) showing a proximo-distal increasing gradient of innervation (i.e. greatest density in the fingertips), and those having larger RFs (Ruffini's and Pacinian's corpuscles/SAII and FAII) being more sparsely distributed with only small differences in density across the hand surface (Johansson and Vallbo, 1979; see Figure 3, right panel).

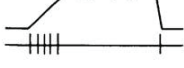
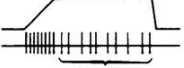


		ADAPTATION			
		Fast, no static response	Slow, static response present		
RECEPTIVE FIELDS	Small, sharp borders	 Edge sensitive FAI (43%) Meissner	 Irregular Edge sensitive SAI (25%) Merkel	INNERVATION DENSITY	
	Large, obscure borders	 FAII (13%) Pacini Golgi-Mazzoni	 Regular Sensitive to lateral skin stretch SAII (19%) Ruffini		

Figure 3 [from McGlone and Reilly, 2010; after Westling, 1986]. Characteristics of the four types of mechanoreceptors of the human hand. The central graphs schematically show the action potential discharges (lower traces) in response to ramp indentations of the skin (upper traces). The central panels also show the relative frequencies of occurrence of the four mechanoreceptor types, and the probable morphologic correlates. The black dots and shaded areas of the hand figures on the left panel represent typical receptive fields of type I (top) and type II (bottom) mechanoreceptors. The hand drawings on the right panel indicate the average densities of type I (top) and type II (bottom) mechanoreceptors.

While most of human research into skin sensory processing has focused on the glabrous surface of the hand (i.e. fingertips), a few studies also investigated the hairy skin. For instance, Essick and Edin (1995) described sensory fibres with similar properties in **human facial skin**, and more recently Nolano and colleagues (2013) found Meissner-like receptors, Merkel complexes and Ruffini-like receptors in the perioral hairy skin, as well as a gradient of innervation, with the density of myelinated fibres increasing from the supraorbital to the perioral skin, resembling the pattern found within the glabrous skin of the hand (Nolano et al., 2003). The similarities and differences in fingertip and face skin innervation will be detailed later (section Zoom in on the Hand and Face, page 48). In addition, the above “classification” has to be regarded only as an attempt to help understanding the complexity of mechanoreceptive $A\beta$ afferents. Indeed, the relationship between the cutaneous mechanoreceptors embedded in the skin and their presumed associated afferents (and so physiological responses to stimulation) is complex and remains to be clarified, each type of cutaneous receptor being always, even if differently, involved in the transduction of skin stimuli independently of its category (vibration, pressure etc). This is supported by histological evidence that a single afferent fibre can innervate

multiple receptors and single receptors can receive multiple (Paré et al., 2002), but also different class of afferent fibres (Reinisch and Tschachler, 2005).

In addition to $A\beta$ afferents, a growing body of evidence has revealed the presence of a population of mechanoreceptive unmyelinated C-fibres, found only in hairy skin, that respond preferentially (and vigorously) to low force, slowly moving mechanical stimuli traversing their RFs ($1-10 \text{ cm.s}^{-1}$, see Table 1; Vallbo et al., 1999). These nerve fibres have been classified as C-tactile afferents, and were first described by Johansson and colleagues (1988) using microneurography, and later by Nordin (1990). The functional role of C-tactile afferents is not fully understood, but their neurophysiological response properties, fibre class, and slow conduction velocities preclude them from playing a role in any form of rapid mechanical discriminative tasks, and point to a more limbic function, such as the emotional aspects of tactile perception (Essick et al., 1999). In agreement with this hypothesis, selective C-tactile stimulation has been found to activate the left anterior insular cortex (Olausson et al., 2002), an area involved in the processing of positive emotional feelings (Craig, 2009), and has recently been directly associated with pleasant tactile stimulation (Löken et al., 2009).

II. Somatosensory signal conduction along the neuraxis

Once the sensory transduction completed, cutaneous information is carried to the central nervous system (CNS) by several ascending pathways that run in parallel through the spinal cord, brainstem, and thalamus to reach the primary somatosensory cortex (SI) in the postcentral gyrus of the parietal lobe. SI projects in turn to the primary motor cortex (MI) in the precentral gyrus, to higher-order associative cortices in the parietal lobe, and back to the subcortical structures involved in mechanosensory information processing. Depending on the information carried, different ascending pathways are involved: discriminative touch and proprioceptive information arising from the body are carried through the dorsal column-medial lemniscal pathway and those arising from the face through the main sensory trigeminal pathway, while information about crude touch (i.e. non-discriminative), pain and temperature arising from the body is conducted through the spinothalamic (anterolateral) pathways, and those arising from the face through the spinal trigeminal pathway.

a. The dorsal column-medial lemniscal pathway

Mechanosensory information arising from the body is transmitted to the spinal cord by the previously mentioned $A\beta$ afferent sensory axons (see Figure 14 for detailed description of the hand innervation), whose neuronal cell bodies are located in the **dorsal root ganglia** associated

with each segmental spinal nerve. It is worth noting that each spinal nerve innervates a well-defined cutaneous territory, called a dermatome, thus leading to a “topographic” distribution of innervation along the spinal cord, each spinal segment being associated with a cutaneous territory (Figure 4).

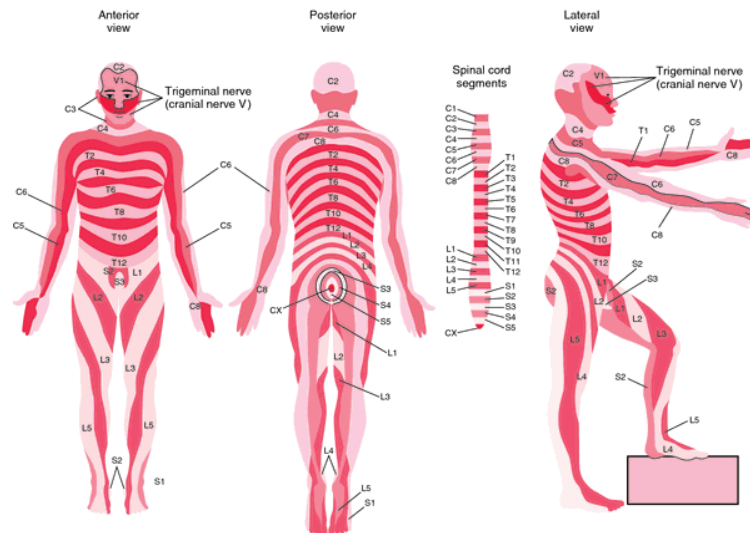


Figure 4 [from Thibodeau and Patton, 1999]. Segmental dermatome distribution of spinal nerves to the front, back, and side of the body. C, Cervical segments; T, thoracic segments; L, lumbar segments; S, sacral segments; CX, coccygeal segment.

Dorsal root ganglion cells are also known as first-order neurons because they initiate the three steps necessary to conduct sensory information to higher brain centres. The ganglion cells thus give rise on one side to long peripheral axons that end in the receptor specializations described above and, on the other side, to shorter central axons that reach the dorsal roots of each spinal cord segment (Figure 5). Immediately after entering the spinal cord, the major branch of the first-order axons ascends ipsilaterally through the dorsal columns of the cord, all the way to the lower medulla (i.e., lower part of the brainstem, consisting of the medulla, the pons and the midbrain), where it terminates by contacting second-order neurons in the **dorsal column nuclei**. Axons in the dorsal columns are separated into two tracts: the gracile tract in the medial subdivision, which conveys information from the lower half of the body (legs and trunk), and the cuneate tract in the lateral subdivision, which conveys information from the upper limbs and trunk. This organization is maintained as both tracts end up in two separate nuclei within the dorsal column nuclei, namely the **gracile** and **cuneate nuclei** (Figure 5). The fibres of the second-order neurons in the dorsal column nuclei form the internal arcuate tract which immediately crosses the midline (this crossing being called *decussation*) to form a tract on the contralateral side of the brainstem, named the **medial lemniscus**. This lemniscus then projects the **ventroposterior lateral** (VPL) nucleus of the thalamus, whose cells are the third-order

neurons of the dorsal column–medial lemniscal pathway (Figure 5). The fibres arising from the VPL then ascend in the posterior limb of the internal capsule and the corona radiata to terminate in the **primary somatosensory cortex (SI)** located in the postcentral gyrus.

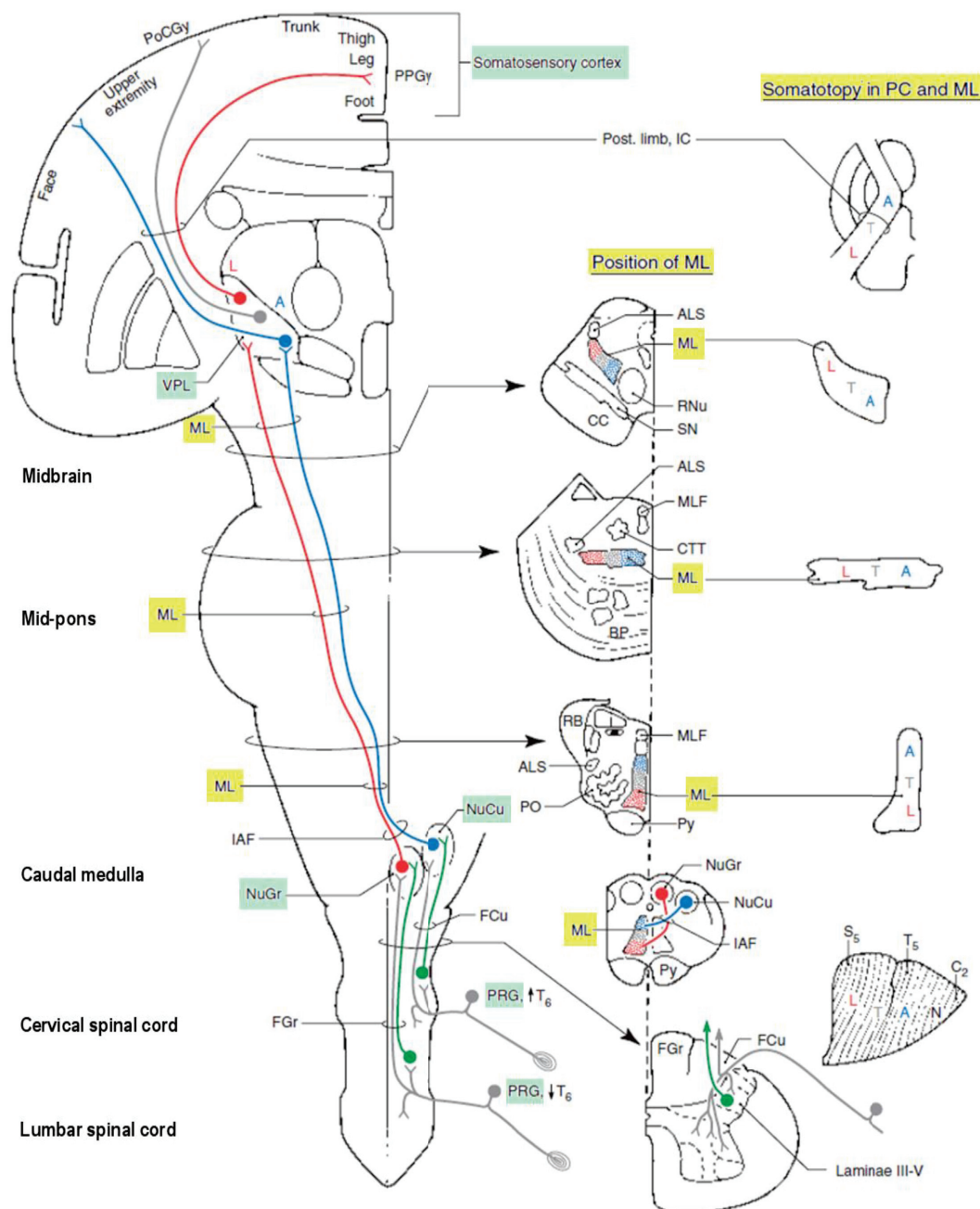


Figure 5 [modified from Haines, 2003]. *Left panel:* Schematic representation of the dorsal column–medial lemniscal pathway which carries mechanosensory information from the posterior third of the head and the rest of the body. The first-order neurons (bottom, in grey) located within the posterior (dorsal) root ganglia (PRG) synapse with the second-order neurons (centre, in red and blue) located respectively in the gracile (NuGr) and cuneate nuclei (NuCu). These neurons then project to the ventroposterior lateral (VPL) nucleus of the thalamus where they synapse with the third-order neurons (top, in red, grey and blue), which in turn project to the somatosensory cortex. *Central*

panel: transverse sections along the neuraxis showing the position of the medial lemniscus (ML, highlighted in yellow), with its somatotopic organization schematically represented in the *Right panel*: the colour-coded letters represent fibres conveying input from different body parts: A: upper extremities, L: lower extremities, N: neck, T: trunk).

b. The sensory trigeminal pathway

As mentioned earlier, the dorsal column–medial lemniscal pathway carries somatic information from the upper and lower body and from the posterior third of the head only. Mechanosensory information arising from the face is transmitted to the central nervous system via a different pathway, the **trigeminal somatosensory pathway** (Figure 6). The first-order neurons innervating the face (see Figure 18 for a detailed description of facial innervation) have their cell bodies located in the trigeminal ganglion. On one side these neurons give rise to the three main subdivisions of the **trigeminal nerve**, while on the other side they form the sensory roots of the trigeminal nerve. These $A\beta$ fibres enter the brainstem at the level of the pons to synapse with neurons in the **principal nucleus** (tripartite) of the trigeminal brainstem complex (Figure 6). This nucleus can be divided into dorsomedial and ventrolateral regions, the dorsomedial division receiving most of its primary afferent input from the oral cavity, and the ventrolateral division receiving input from all three branches of the trigeminal nerve. Then, as for the dorsal column–medial lemniscus, the projections of these second-order neurons located in the ventrolateral part of the principal nucleus decussate and ascend along the medial lemniscus via the **anterior** (or ventral) **trigemino-thalamic tract** (also called the trigeminal lemniscus) to reach the contralateral thalamus where they synapse with the third-order neurons located in the **ventroposterior medial (VPM) nucleus** (Figure 6). Neurons in the dorsomedial division of the principal sensory nucleus project to the ipsilateral VPM via the **posterior** (or dorsal) **trigeminothalamic tract**. Neurons located in the VPM nucleus (i.e., the third-order neurons) then project via the posterior limb of the internal capsule to the lateral part of the **primary somatosensory cortex (SI)** located in the postcentral gyrus.

Thus, mechanosensory pathways from the face and body join at the level of the mid-pons, this first single sensory map of the **entire body** being then projected onto the **ventroposterior complex of the thalamus**. However, it is worth noting that although the bulk of afferent input adheres either to the dorsal column–medial lemniscus or to the trigeminal pathway outlined above, a degree of mixing occurs, some axons responsible for cutaneous mechanoreception (the C-tactile afferents mentioned above) presumably running in the **spinothalamic pathway**, with the result that damage to the dorsal columns does not completely remove touch and pressure sensation. The spinothalamic tract will not be described here (for a brief review, see McGlone

and Reilly, 2010), but it ascends the entire length of the spinal cord and the entire brainstem, and is continuous with the medial lemniscus when it reaches the midbrain. The spinal trigeminal pathway synapses onto the spinal nucleus of the trigeminal complex mentioned above. Both tracts then enter the ventroposterior complex of the thalamus together, and thus must be taken into consideration.

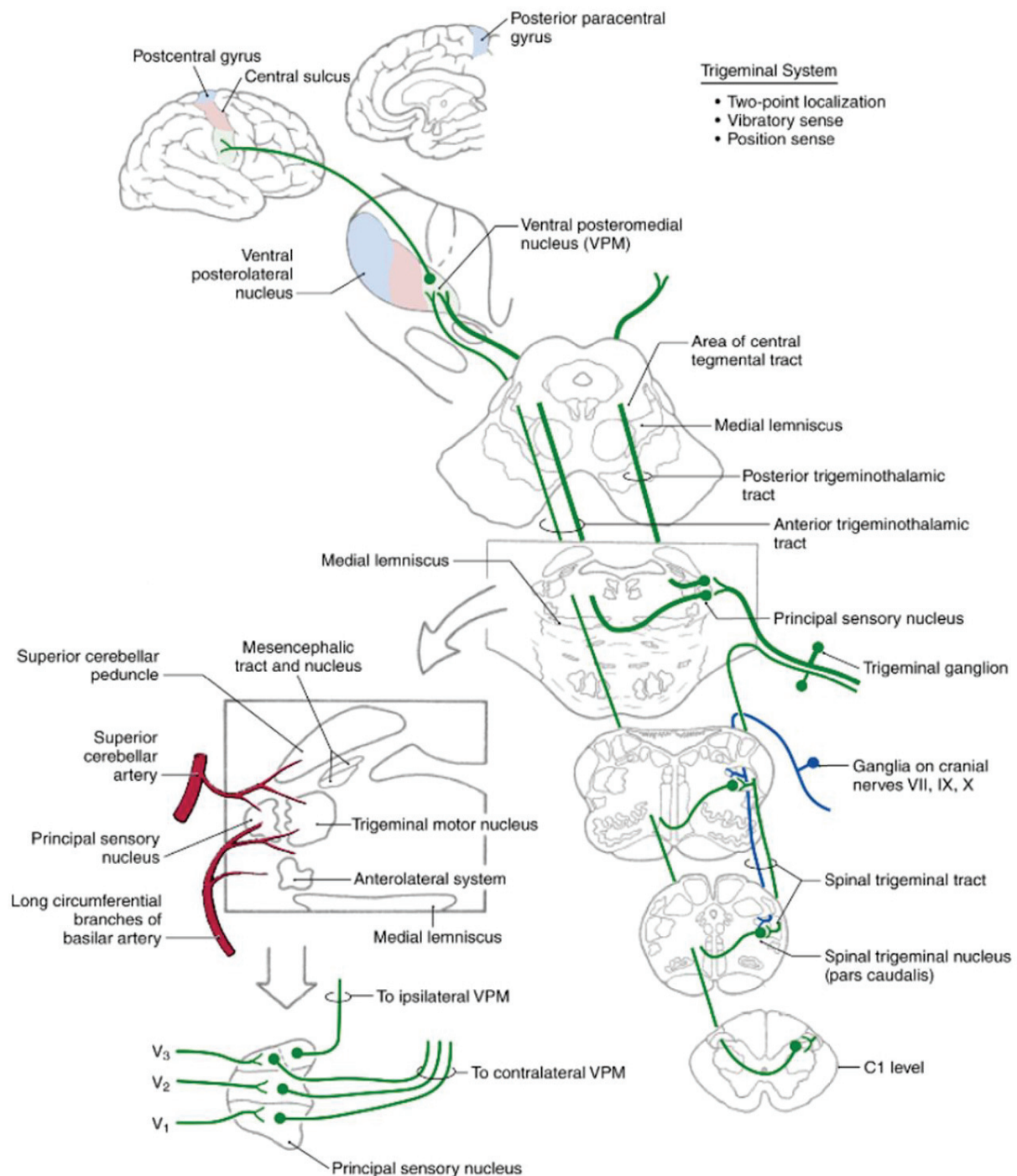


Figure 6 [from Haines, 2013]. Schematic representation of the trigeminal sensory pathway which carries mechanosensory information from the face. The first-order neurons located within the trigeminal ganglion synapse with the second-order neurons

located in the principal sensory nucleus at the pons level. These neurons then project to the ventroposterior medial (VPM) nucleus of the thalamus where they synapse with the third-order neurons, which in turn project to the somatosensory cortex. A zoom in on the pons is illustrated in the lower left part of the picture, with a second zoom showing the organization of the three trigeminal branches within the principal sensory nucleus. Note that some fibres arising from this nucleus do not cross the midline but instead project to the ipsilateral thalamus (VPM nucleus).

III. Topographic organization along the somatosensory pathway

a. The spinal cord and brainstem

One of the main features of the somatosensory system arise from its topographic organization, each part of the skin being represented in a well-defined order following, most of the time, the spatial continuity of the body. This organization, called somatotopy, is preserved along the neuraxis throughout the somatosensory pathways. While the somatotopy of cortical regions have been well described in humans (see paragraph c.), the organization of spinal and subcortical structures has been mainly investigated in animals. For instance, in addition to the rough mediolateral distribution of the gracile and cuneate tracts within the **spinal cord** (see Figure 5), a finer topographic organization of the **forelimb** has been reported in the **dorsal horn** of macaque (Florence et al., 1989) and squirrel monkeys (Florence et al., 1991), with the fingers being represented along the rostrocaudal axis, inputs from the dorsal hairy skin of the hand and the palm terminating lateral to the digits, and those from the forearm being split around the hand (see Figure 7). The authors noticed that this organization is quite similar to that observed in cats (Nyberg and Blomqvist, 1985; Brown et al., 1991) and rats (Molander and Grant, 1986), which suggests that this somatotopic organization is a common feature of the somatosensory system of mammals.

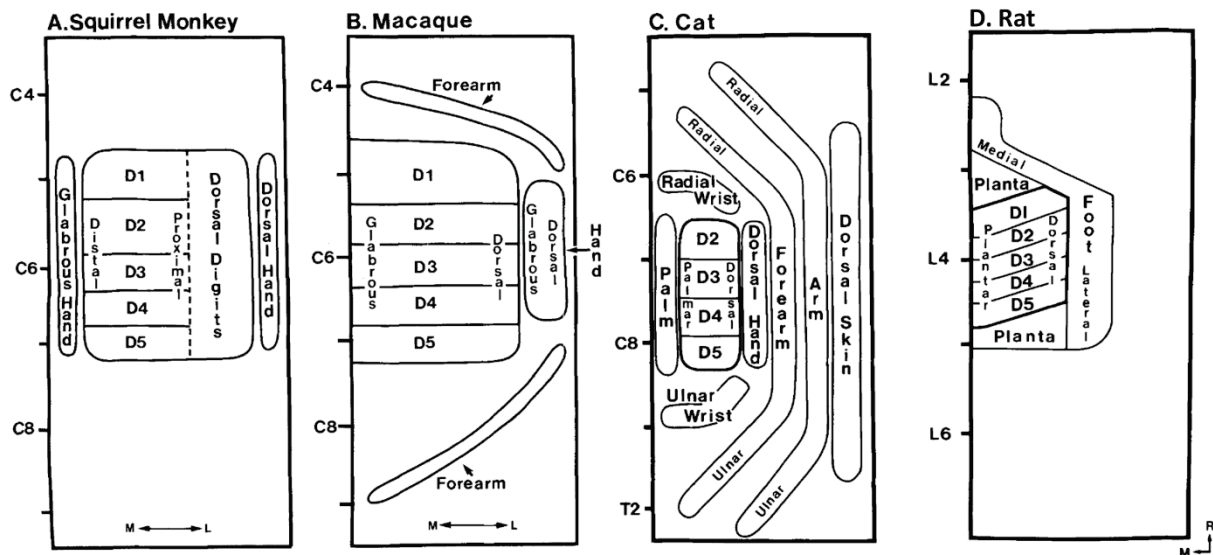


Figure 7 [modified from Florence et al., 1989, 1991]. Schematic representation of the somatotopic organization of afferent terminations in the dorsal horn of the spinal cord from the forelimb of (A) squirrel (A, from Florence et al., 1991) and macaque monkeys (B, from Florence et al., 1989), cats (C, based on results from Nyberg and Blomqvist, 1985), and rats (D, based on results from Molander and Grant, 1986). C4-T2 and L2-L6: cervical, thoracic and lumbar levels of the spinal cord; D1-D5: digits; M/L/R: medial/lateral/rostral directions.

This spatial organization is preserved along the dorsal columns before reaching the **dorsal column nuclei** in the lower **medulla** where an even more refined somatotopic organization has been found. Indeed, inputs from distal and proximal parts of the glabrous fingers are already well segregated at this level of the somatosensory pathway, with afferents from the proximal part terminating dorsal to those from the distal part. This organization was particularly observed in the ventral pars rotunda of macaque monkeys (Florence et al., 1989), the central zone of the **cuneate nucleus**, where the rest of the **hand** is organized so that inputs from digits D1-D5 terminate in a respective ventrolateral to dorsomedial sequence, the hairy skin of the digits, the palm, and the back of the hand being sequentially represented dorsal to the proximal glabrous digits (Figure 8). As the structure of the cuneate nucleus of humans closely resembles that of macaque monkeys, Florence et al. (1989) then extrapolated the topographic organization of forelimb afferents within the human cuneate nucleus, with the postulate of a similar pattern to that of macaque monkeys. But note that this extrapolation has to be considered carefully as some notable differences across species were later reported (Florence et al., 1991; Xu and Wall, 1999), the distal phalanges of the digits being for instance represented dorsally in the cuneate nucleus of squirrel monkeys and not ventrally as in macaques. The cuneate nucleus also contains maps of forelimb, trunk and face, which are located medial and lateral to the **hand map** with on

the lateral side the representations of the forelimb (usually radial surfaces), shoulder, chest, neck and side of the face region, and on the medial side the representations of forelimb (usually ulnar surfaces), shoulder, chest, trunk and proximal hindlimb (Xu and Wall, 1999). A similar topographic organization has been more recently confirmed within the **gracile nucleus** (containing afferents from the lower limbs and trunk) of several monkey species (Qi and Kaas, 2006), with the afferents from the tail, foot, distal leg and proximal leg being distributed along the mediolateral axis, and the toes 1-5 following a ventro-to-dorsal sequence.

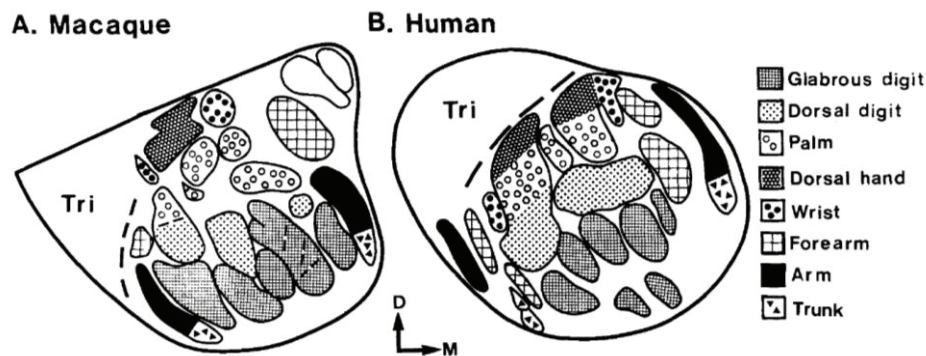


Figure 8 [from Florence et al., 1989]. Somatotopic organization of forelimb cutaneous regions into the pars rotunda of (A) macaque monkeys and (B) the proposed relation in humans based on histological observation of the substructures revealed by cytochrome oxidase (an enzyme related to metabolic activity) on human cuneate nuclei obtained post-mortem. Coronal views. Tri: triangularis nucleus. M/D: medial/dorsal directions.

Axons arising from both the cuneate and gracile nuclei then join to constitute the **medial lemniscus**, within which the somatotopic organization is maintained. But, as axons arising from the two nuclei cross each other in the process of the decussation, the orientation of the somatotopy changes from mediolateral to dorsoventral, with the upper extremities, the trunk and the lower extremities being sequentially more ventral (Figure 5). Then, the medial lemniscus gradually rotates laterally as it ascends through the brainstem, resulting in a somatotopy rotated by 90° at the level of the midbrain (see Figure 5), the upper extremities, trunk and lower extremities being then in a ventromedial to dorsolateral sequence. This is the configuration in which these fibres enter the **VPL nucleus** of the contralateral thalamus.

As for the **trigeminal pathway**, the three branches constituting the trigeminal nerve (see Figure 18) are somatotopically represented within the **principal sensory nucleus**, following an antero-posterior gradient with the ophthalmic branch (V₁) being the most anterior, followed by the maxillary branch (V₂) and the mandibular branch (V₃) being at the posterior part (see Figure 6). The afferent projections from the principal sensory nucleus also terminate somatotopically

within the **VPM nucleus** of the thalamus, so that the oral cavity is represented medially and the external facial structures are represented more laterally.

b. The somatosensory thalamus

As mentioned earlier, the ventroposterior complex of the thalamus is the first relay along the somatosensory pathway in which a large, **single and systematic representation of the whole body surface** is observed, with its medial (i.e., VPM) nucleus being devoted to the representation of the face and head, and its lateral (i.e., VPL) nucleus being devoted to the representation of the rest of the body. Both nuclei are separated by a prominent lamella of white matter, the arcuate lamella. Kaas et al. (1984) also reported fibre bands within the VPL nucleus of **squirrel monkeys**, subdividing the nucleus into four subnuclei containing respectively the representations of the hand, foot, tail and trunk/limbs (Figure 9). However, despite this parcellation of the ventroposterior complex, the representational continuity is provided by some cellular bridges. For instance, the representations of the distal limbs within the limbs/trunk subnucleus (labelled D on Figure 9) dorsally join those of the hand and foot located within their respective subnucleus (A & B). In a similar way, the face representation in VPM is separated from the hand subnucleus, but is continuous with the neck representation of the limbs/trunk subnucleus (D). The **hand** representation is dominated by large representations of the glabrous digits arranged mediolaterally from D1 to D5 and dorsoventrally from proximal to distal on each digit. Notably, fingertips are represented along a large band extending from the base of the nucleus to its rostral wall, fingertips being thus found both dorsorostrally and ventrally. Typically, the representation of digit 1 is less extensive than digit 2 and does not cover the entire medial wall of the subnucleus, which makes the index finger also adjacent to the **face** representation. This latter is mainly devoted to the hairy, glabrous and inner surfaces of the upper and lower lips, the representations of which are then joined laterally by the lateral and upper face (thus comprising the cheek), and dorsally by the lower chin and neck. Interestingly, the representations of the upper and lower lips join at the corner of the mouth along a mediolaterally oriented line, whose precise orientation appears to vary somewhat from case to case. Additionally, the cranium, ears, lateral face, trunk, limbs and gluteal regions are respectively represented in a mediolateral sequence within the **limbs/trunk** subnucleus, while the **foot** subnucleus exhibits a topographic organization similar to that of the hand, with the difference that the representation of the toes are rotated so that the rostral portion of each toe is medial to the caudal portion (see also Krubitzer and Kaas, 1987).

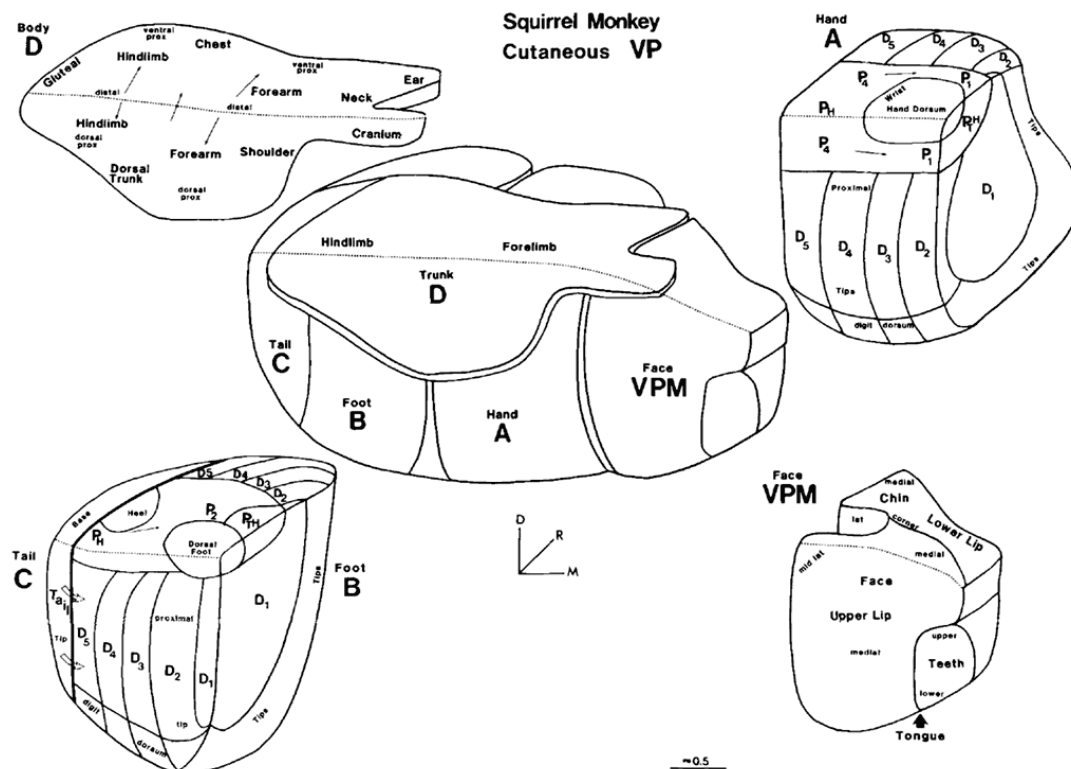


Figure 9 [from Kaas et al., 1984]. Summary of the somatotopic organization of the ventroposterior complex of the thalamus, divided into the VPM and VPL nuclei. VPL is further subdivided into four subnuclei respectively for the hand (A), the foot (B), the tail (C) and for the limbs/trunk (D). VPM represents the face. D/R/M: dorsal/rostral/medial directions.

Even if there are fewer and less detailed data from human recordings, some evidence from microelectrode mapping during stereotactic surgery of epileptic patients (Penfield and Jasper, 1954) or thalamotomy for treatment of involuntary motor disturbances (Ohye et al., 1990), suggests a somatotopic organization of the ventroposterior thalamus in **humans** comparable to that described in monkeys. These studies indicate that the face, upper limb and lower limb are represented in a medioventral to dorsolateral sequence, the tongue being more medial and the fingers, especially the thumb, being adjacent to the face (Figure 10).

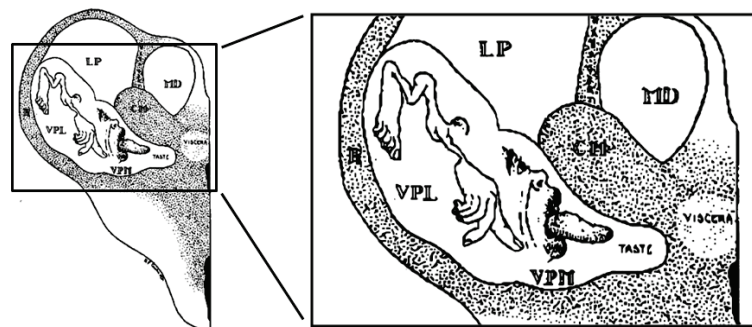


Figure 10 [modified from Penfield and Jasper, 1954]. Homunculus representation in the ventroposterior complex of the human thalamus. Coronal section.

c. The primary somatosensory cortex

The thalamocortical projections then convey the signal, whether from VPL or VPM, to somatosensory cortices by preserving the general somatotopic pattern (clusters of VP cells projecting to restricted cortical regions (Jones et al., 1982), which is responsible for the maps of the body that are an ubiquitous feature of early somatosensory cortical areas (Penfield and Rasmussen, 1950). Early electrophysiological mapping studies of the cortex identified two cortical areas responsive to peripheral tactile stimulation: the primary somatosensory cortex (SI) and the second somatosensory cortex (SII) (Woolsey and Fairman, 1946). But since then, electrophysiological and imaging studies have defined at least eight separate areas subserving somatosensation, arising from the subdivision of SI into four subregions (Brodmann's areas 3a, 3b, 1 and 2, see next paragraph), and the addition of the insular cortex (Schneider et al., 1993) and of two subdivisions of the posterior parietal cortex (Brodmann's areas 5 and 7b)(see). Here I will describe in details SI only, as our investigations, from behaviour to neuronal correlates, focused on this early somatosensory area.

The human primary somatosensory cortex is located in the parietal lobe along the posterior bank of the central sulcus (i.e., in the postcentral gyrus), and is divided into six distinct cytoarchitectonic layers (for a review see Mountcastle, 1997). Most of the thalamocortical projections arising from the ventroposterior complex of the thalamus terminate primarily in the 4th cortical layer and to a lesser extent, in layer 6 and lower layer 3 (Shanks and Powell, 1981) of the contralateral post-central gyrus. In addition to this vertical laminar distribution, SI is also subdivided into four subregions (namely, **Brodmann's areas (BAs) 3a, 3b, 1 and 2**, see Figure 23) that have been distinguished from each other based on their cytoarchitectonic structure (Brodmann, 1909; Vogt and Vogt, 1919). BA3b corresponds to the anterior bank of the postcentral gyrus, while BA3a lies in the fundus of the central sulcus. BA1 is located on the crown of the postcentral gyrus and reaches down into the postcentral sulcus, and finally, BA2 covers the posterior crown of the postcentral gyrus (Brodmann, 1909; Geyer et al., 1999). BA3b receives most of the projections arising from the ventroposterior thalamic complex, and is the site where the initial cortical processing of tactile discrimination takes place (see Figure 24 and next paragraph for further description of thalamocortical projections). This led to the suggestion that, for homogeny with other sensory fields, only area 3b should be referred to as “primary somatosensory cortex” (Merzenich et al., 1978). However, in this thesis the term primary somatosensory cortex (or SI) follows the nowadays classical terminology and thus refers to the entire postcentral gyrus (which includes BAs 3a, 3b, 1, and 2).

The first detailed cartography of the human primary somatosensory cortex was reported by Penfield and Boldrey in 1937, by the use of cortical stimulation in patients undergoing surgical procedures. Penfield started conducting these experiments in 1928, and in less than ten years he managed to carry out cortical stimulation studies in 163 fully conscious patients undergoing brain surgery for epilepsy. Data from 126 of these patients were good enough to be analyzed, allowing Penfield and Boldrey to publish their groundbreaking work in *Brain* in 1937. The authors rigorously reported any individual movement or sensation evoked by the stimulation of different points on the brain, ending up with 170 summarizing charts then condensed into the 16 illustrative charts that appear in Penfield and Boldrey's paper. In order to render the topography of their observations more legible, the authors then decided to add illustrations to their verbal descriptions and schematic charts, and thus asked a medical illustrator, Hortense Pauline Cantlie, to draw “a visual image and sequence of the cortical area”. This gave rise to the first *homunculus*, which was associated with both sensory and motor responses (Figure 11A). Thirteen years later, this first *homunculus* was revisited into a more precise representation of the cortical regions and their related body parts (Figure 11B). Notably, the sensory and motor responses were mapped separately onto a cross-section of the cerebral hemispheres with bars underlying the spatial sequence and relative extent of cortical areas controlling body part-related responses (either sensory or motor). On top of these sensory and motor topographic maps the representation of the body surface was resized according to the cortical magnification dedicated to each body part and superimposed for legibility. Sixty years later, this famous representation still serves as a reference, even if some additional revisions have since been made. These revisions concerned mainly the location of the genitals (Kell et al., 2005; Georgiadis et al., 2006), which constitute one of the two notable discontinuities within the SI homunculus, the other one (which we will discuss later on, see chapter Finger/face) involving the hand and face representations.

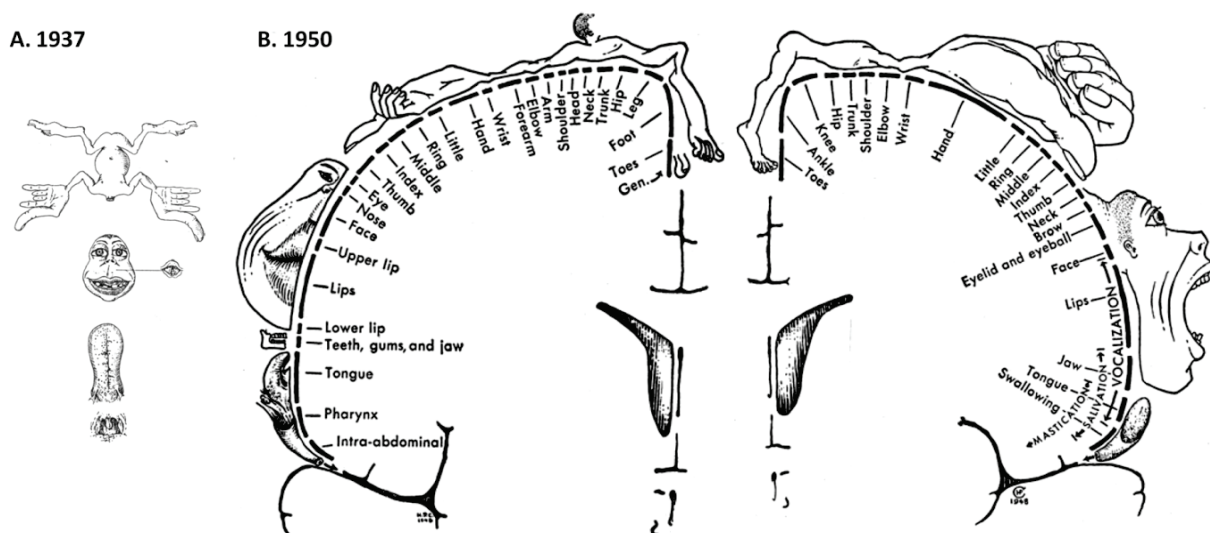


Figure 11 [adapted from Penfield and Boldrey, 1937 and Penfield and Rasmussen, 1950]. First (A) and revisited (B) versions of Penfield's *homunculus* illustrating the results obtained from the cortical stimulation of respectively 126 and 400 epileptic patients. (A) Each body part was drawn proportional to the size of the corresponding cortical area, thus illustrating the cortical magnification of the different body parts. (B) The revisited version represents more precisely the cortical areas and their relative surface, which when stimulated evoked either sensory (B, left panel) or motor (B, right panel) responses. The length of each bar drawn on the cortical surface provides an indication of the relative size of the cortical areas controlling the responses specific to its associated body part. Here again, the drawings superimposed at the periphery aim to illustrate the degree of cortical magnification associated with each body part.

Later on, some important experiments carried out in nonhuman primates (Powell and Mountcastle, 1959a, 1959b; Paul et al., 1972) provided the direct evidence that the cytoarchitectonic differences within SI previously described by Brodmann (1909), with the four distinct **BA**s **3a**, **3b**, **1** and **2**, must be regarded as distinct **functional entities**. Specifically, these authors demonstrated that neurons in BA3b and 1 respond primarily to contralateral low-threshold cutaneous stimulation as BA3b receives predominantly SA and FA cutaneous input, while BA1 receives FA cutaneous and deep input related to vibration sensation (i.e. Pacinian receptors). In contrast, neurons in BA3a respond mainly to stimulation of proprioceptors located in muscles spindles (Phillips et al., 1971) and those in BA2 process both tactile and proprioceptive stimuli (Iwamura and Tanaka, 1978) as they receive inputs principally from deep-laying receptors. Additional studies (Randolph and Semmes, 1974; Carlson, 1981) revealed that focal lesions of BA1 led to a specific deficit on texture discrimination tasks (hard/soft, roughness and line discrimination), while removal of BA2 induced a specific deficit on discrimination of object size, shape and curvature (square/diamond, convex/concave, size and curve discriminations, see also Yau et al., 2013). In contrast, following removal of BA3,

severe deficits were seen on all tactile tasks. The **interconnectivity** observed between these subregions is also quite informative regarding their functional properties. For instance, BA3b projects predominantly to BA1 via horizontal intracortical fibres, but also projects less densely to BA2 and BA3a (Vogt and Pandya, 1978; Burton and Fabri, 1995), and receives feedforward projections from BA3a, BA1 and BA2 (Burton and Fabri, 1995; Coq et al., 2004). BA1 primarily projects to BA2, but is also reciprocally connected with BA3a and BA3b (Jones et al., 1978; Pons and Kaas, 1986; Burton and Fabri, 1995). Finally, BA2 projects primarily to posterior areas (BA5 and BA7, see section V.c. of this chapter), but also exhibits connections with BA1, BA3a and BA3b (Vogt and Pandya, 1978; Pons and Kaas, 1986). Thus, a strong and sequential outflow of connections is observed from BA3b to BA1 and BA2 (Ruben et al., 2006), then from BA1 to BA2 and finally from BA2 to areas in the posterior parietal cortex, mainly BA5 and BA7. As a consequence, BA3b in non-human primates has small and relatively simple/homogeneous **RFs**, whereas RFs from BA1 were found to be larger and more complex (i.e., responding to multiple fingers; see Hyvarinen and Poranen, 1978; Iwamura et al., 1980, 1993; Sur, 1980). This complexification of RFs suggests a greater **convergence** of peripheral inputs in BA1 (see Iwamura, 1998; Ruben et al., 2006). Similarly, RFs for neurons in BA2 are typically larger than those in BA1 and RFs involving multiple digits and joints are common. Altogether, these studies led to the notion that BA3b is the site where the initial cortical processing of tactile discrimination takes place, while BA1 is more involved in texture discrimination (which requires the **integration** of different aspects of tactile inputs), and BA2 in size and shape recognition (i.e., even more integrated signal). In contrast, BA3a is mainly dedicated to proprioceptive signals processing (see Jones and Powell, 1969; Phillips et al., 1971).

Following these discoveries about the functional differences between these BAs, numerous electrophysiological studies performed on primates (e.g., Merzenich et al., 1978; Kaas et al., 1979; Nelson et al., 1980; Sur et al., 1982; Pons et al., 1985; Jain et al., 2001; Coq et al., 2004) revealed that the traditional SI somatotopy is actually divided into **four separate and complete representations of the body surface**, one within each of the BAs (see Figure 12 for a summary of the maps obtained in macaque monkeys). In agreement with Penfield's *homunculus*, the foot, leg, trunk, forelimbs, and face are represented in a medial to lateral arrangement within each of these subregions. Despite some differences (see Merzenich et al., 1978 and Sur et al., 1982 for details), the representations within BA3b and BA1 are roughly mirror-images of each other so that whatever skin surface is represented rostrally in BA3b is also represented caudally in BA1 (Sur et al., 1982; Jain et al., 2001). Some cutaneous responses were also found within BA2, with

again a somatotopic organization that is the mirror-image of that observed in BA1, and a possible fourth representation was found within BA3a (Merzenich et al., 1978; Kaas et al., 1979; Nelson et al., 1980; Coq et al., 2004). Moreover, the intrinsic interconnectivity observed between these subregions (at least BA3b, 1 and 2) appears to be also somatotopically organized (Pons and Kaas, 1986; Burton and Fabri, 1995).

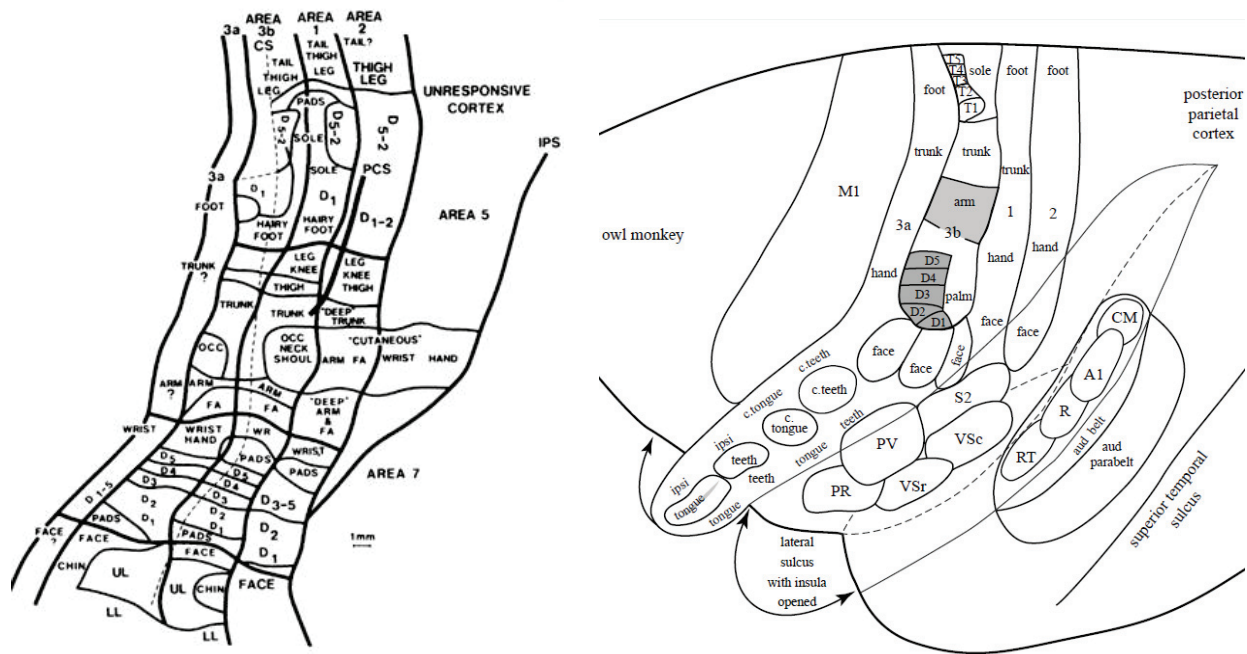


Figure 12 [left panel: from Mountcastle, 1997, after Kaas and Pons, 1988; right panel: from Kaas, 2005]. Somatotopic organization of the contralateral body surface in the four cytoarchitectural areas of the primary somatosensory cortex of macaque (left panel) and owl (right panel) monkeys. Left panel: CS: central sulcus, IPS: intraparietal sulcus, FA: forearm, LL: lower-lip, UL: upper-lip, D1-D5: digits of the contralateral hand. Right panel: c: contralateral, i: ipsilateral, PV: parietal ventral area, VSr & VSc: rostral and caudal ventral somatosensory areas, PR: parietal rostral area (see Coq et al., 2004).

Nowadays, the improvement in **brain imaging techniques** allows us to investigate the topographic organization of human somatosensory areas non-invasively. However, these techniques (mainly functional magnetic resonance imaging (fMRI) and magnetoencephalography (MEG), which have a relatively good spatial resolution) usually do not provide a spatial resolution sufficiently high enough to clearly distinguish between the four BAs. Thus, most imaging studies performed on **humans** usually refer globally to SI (i.e., postcentral gyrus). Beyond these technical considerations, it is surprising to note that the somatotopic organization of the **entire body surface** within SI, such as performed by Penfield, has rarely been investigated since then. To my knowledge, only one MEG study tried and managed to replicate Penfield's *homunculus* (Nakamura et al., 1998). The authors found a similar mediolateral

topographic organization of the body surface within the contralateral post-central gyrus, with the toes in the medial side of the hemisphere and the tongue in the most lateral region (Figure 13). But such mapping of about 40 regions is demanding and time consuming. This may explain why most of studies usually focus on specific (and few) body parts. Indeed, even if a few other MEG studies reported, with a less systematic approach, the somatotopic organization of some regions of distant body parts, such as the arm, leg and lip (Hoshiyama et al., 1997) or the dermatomes (i.e., cervical, thoracic, lumbar and sacral afferents; Itomi et al., 2000; Castillo and Papanicolaou, 2005), most studies usually focus solely on one body part at a time. For instance, the **hand** has been extensively investigated using either fMRI (e.g., Maldjian et al., 1999; Hlustík et al., 2001; McGlone et al., 2002; Sanchez-Panchuelo et al., 2010; Schweisfurth et al., 2011, 2014; Besle et al., 2013a, 2013b) or MEG recordings (e.g., Baumgartner et al., 1991; Forss et al., 1995; Tecchio et al., 1998; Mertens and Lütkenhöner, 2000; Druschky et al., 2002; Inoue et al., 2012; Jamali and Ross, 2013), likely due to its large cortical representation and its easy access to peripheral stimulation. Similarly, the **face**, also highly magnified at the cortical level, has been quite intensively investigated the last two decades using again either fMRI (Servos et al., 1999; Iannetti et al., 2003; Miyamoto et al., 2006; Blatow et al., 2007; Kopietz et al., 2009; Moulton et al., 2009; Lin et al., 2010) or MEG recordings (Yang et al., 1993; Mogilner et al., 1994; Hoshiyama et al., 1995, 1996; Nagamatsu et al., 2000; Disbrow et al., 2003a; Nguyen et al., 2004; Suzuki et al., 2004; Nevalainen et al., 2006; Sakamoto et al., 2008; Tamura et al., 2008). In contrast, the representations of the other body parts such as the arm (Servos et al., 1998), the legs (Shimojo et al., 1996; Del Gratta et al., 2000; Bao et al., 2012), the trunk and genitals (Kell et al., 2005; Rothmund et al., 2005) have been sparsely investigated. But except for the genitals, whose representation was reported to be between those of the toe and lower trunk (Kell et al., 2005), and for the face whose representation is still controversial (see next section IV.b.), most of these studies support the somatotopic arrangement of Penfield's *homunculus*.

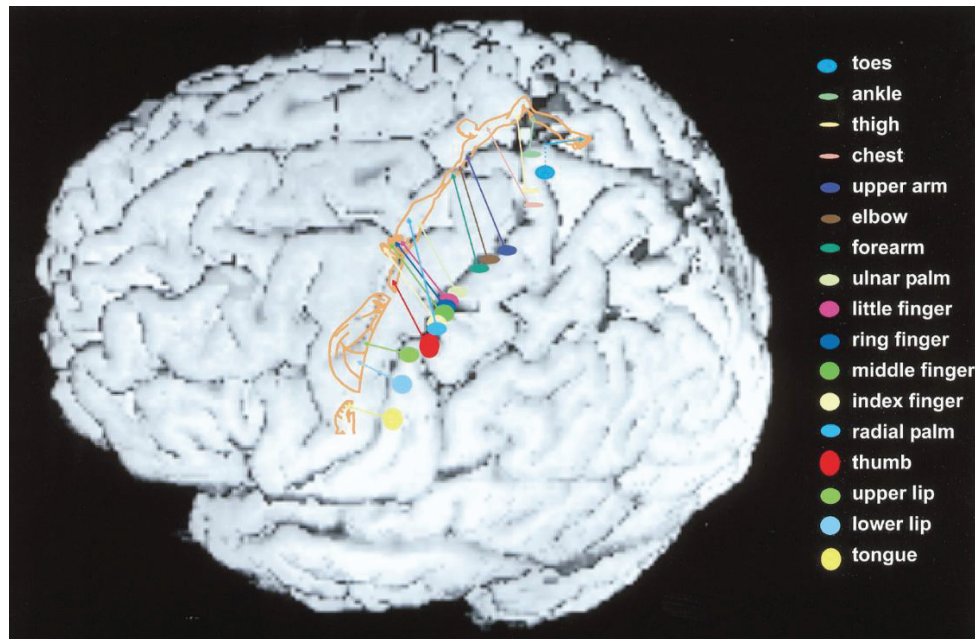


Figure 13 [from Nakamura et al., 1998]. Detailed somatotopy obtained by MEG and displayed on the MRI of one participant. Each receptive area, which was estimated to be located in the posterior bank of the central sulcus (BA3b), was projected onto the cortical surface. The size of each ellipse reflects the presumed size of the activated cortical area, but are displayed three times smaller than the predicted actual sizes. Note that the receptive area for the toes is in the medial side of the left hemisphere.

The development of **probabilistic cytoarchitectonic maps** based on an objective and systematic delineation and classification of the human cytoarchitectonic areas BA3a, 3b, 1 (Geyer et al., 1999, 2000) and 2 (Grefkes et al., 2001) over 10 post-mortem brains, and their recent integration in imaging analysis software (Eickhoff et al., 2005, 2007b), now allows parcellation of human SI and the assignment of imaging results (mostly from fMRI) to each of the four BAs. Using these probabilistic maps or the objective description of BAs described by Geyer, a somatotopic organization similar to the one reported by monkeys studies was consistently observed in human BA3b (Kurth et al., 2000; Blankenburg et al., 2003a; Overduin and Servos, 2004; van Westen et al., 2004; Nelson and Chen, 2008; Schweizer et al., 2008; Stringer et al., 2011; Martuzzi et al., 2014; Sánchez-Panchuelo et al., 2014), while BAs 1 and 2 were found to exhibit an overall higher somatotopic variability (Blankenburg et al., 2003a; Overduin and Servos, 2004; Nelson and Chen, 2008; Stringer et al., 2011; Martuzzi et al., 2014; Sánchez-Panchuelo et al., 2014). It is worth noting that in contrast to Kurth and colleagues (2000), two of these studies reported a somatotopy within BA2 (Martuzzi et al., 2014; Sánchez-Panchuelo et al., 2014), likely due to the higher spatial resolution of the fMRI recordings (7T instead of 1.5T). In addition, the possible discrepancies between these studies may arise from the huge variability in stimulation approaches, which range from strong electrical to air-puff

stimuli, passing by vibrotactile and brushing stimulation. Here again, it is worth emphasizing that most of these imaging studies investigated the somatotopy of the hand only. Eickhoff and colleagues (2008) are so far the only ones who mapped several regions distributed across the body surface (i.e., cheeks, arms and trunk) using cytoarchitectonic probabilistic maps. In addition to a *homunculus*-like somatotopy within SI, these authors reported robust bilateral activations to unilateral stimulation of the trunk and face within BAs 3b, 1 and 2, while the three BAs exhibited a more complex pattern of activation/deactivation for the hand (discussed later).

As briefly mentioned earlier, one striking feature of the somatotopic maps comes from the fact that the actual **proportions** of the body part surfaces are not preserved. Instead, while the fingertips and lips have the highest cortical magnification (e.g., Penfield and Boldrey, 1937; Kaas et al., 1979; Maldjian et al., 1999), the trunk and proximal limbs are disproportionately lowly represented given their actual physical size. Within the hand representation, the thumb and the index finger are also more represented than the other digits (Sutherling et al., 1992). This differential cortical magnification is the counterpart of the differential densities of receptors embedded in the skin across body parts, the fingertips and lips exhibiting the highest density of receptors. Together, this leads to the higher sensitivity observed at those body parts. But these differences in cortical magnification might also arise from different degrees in the functional relevance of body parts. Indeed, the **fingers** and the **lips** are particularly important for manipulation, feeding behaviour, facial expression and communication (language), which are preponderant functions for humans, but also non-human primates. Such distortions are also apparent in other species such as the rat, which has for instance, a huge part of its somatosensory cortex devoted to the whiskers, which are extensively used by the rat to explore its environment, safely move within it and localize anything relevant (another rat, food, ... etc).

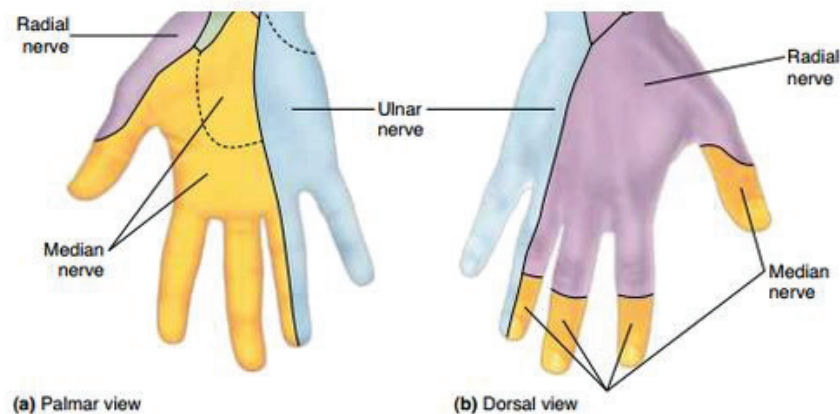
In addition to this well known location-based somatotopic organization, evidence for a sub-organization according to **afferent modalities** has been accumulating, suggesting that each submodality (i.e., FA and SA afferents) is separated into parallel processing channels from the skin to the cortex. In line with this, a modality-based organization was recently found within the dorsal column pathway (Niu et al., 2013). Similarly, a clusterisation of neurons according to their type of adaptation has been reported within the ventroposterior thalamus of squirrel monkeys (Dykes et al., 1981; Kaas et al., 1984), neurons related to slowly or rapidly adapting receptors being grouped within separate alternating aggregates. This modality-based somatotopic organization is then relayed to cortical areas 3b and 1, in which SA and RA neurons form alternating narrow bands (Paul et al., 1972; Sur et al., 1981; Schouenborg et al., 1986; Friedman et al., 2004; Pei et al., 2009). Approximately 20 to 55% (Paul et al., 1972; Sur et al.,

1981) of area 3b appears to be activated by SA inputs. While both RA and SA cell types are also found in area 1 (Paul et al., 1972; Nelson et al., 1980) the proportion of area 1 activated by SA inputs may be 5% or less (Paul et al., 1972), suggesting that few of the SA neurons in the ventroposterior thalamus project to area 1.

IV. Zoom in on the Hand and Face regions

a. The hand

The hand is one of the most complex movable parts of our body, comprising 27 bones with 14 phalanges for the fingers alone, and 20 intrinsic muscles. The hand is a special feature of primates and its particularity comes from the presence of opposable thumbs (i.e., having the ability to be brought into opposition to the other fingers), which renders possible the execution of the incredibly complex and refined movements involved in prehension and manipulation. The evolutionary relevance of the hand is likely to arise from the appearance of tool use and production in the paleolithic age, but in humans the hands also play an important function in body language. In addition, the fingers are some of the most densely innervated regions of the body, and thus one of the richest sources of tactile information. The hand's innervation is provided by three nerves: the median, ulnar and radial nerves (Figure 14). The **median nerve** originates from the lateral and medial cords of the brachial plexus (C5-T1) and is responsible for innervating the lateral (radial) three and a half digits on the palmar side. The dorsal branch innervates the distal phalanges of the index, middle and lateral half of the ring finger. The **ulnar nerve** innervates the ulnar third of the hand, both the palm and the back of the hand, as well as the pinkie and ulnar half of the ring finger. It originates from the medial cord of the brachial plexus (C8-T1). The **radial nerve** innervates the dorsum of the hand, from the thumb to the radial half of the ring finger, proximal to the distal interphalangeal joints. It originates from the posterior cord of the brachial plexus (C6-8). As mentioned earlier, these fibres, whose neuronal cell bodies are located in the dorsal root ganglia, then converge to the **gracile and cuneate nuclei** in the medulla before projecting to the VPL thalamic nucleus via the medial lemniscus (see section II.a. of this chapter).



modified from <http://epomedicine.com/medical-students/applied-anatomy-of-carpal-tunnel/>

Figure 14. Schematic distribution of the three nerves innervating the human hand.

As mentioned in the previous section, the functional organization of the hand representation within the four BAs constituting the “SI” area, has been extensively studied in non-human primates (e.g., Merzenich et al., 1978, 1987; Kaas et al., 1979; Iwamura et al., 1980; Nelson et al., 1980; Sur et al., 1982; Pons et al., 1985; Coq et al., 2004). The hand representation within SI is characterized by a dominant representation of the glabrous skin (Merzenich et al., 1978, 1987), with a particularly high magnification of the tips of the thumb and the index finger (Sutherling et al., 1992; Shoham and Grinvald, 2001). In addition to their sequential and topographic organization, a large **overlap** between finger representations has been repeatedly shown in electrophysiological (Iwamura et al., 1980) and optical imaging studies in monkeys (Chen et al., 2001; Shoham and Grinvald, 2001), which usually involved neighbouring fingers. As expected from the differential functional use of the fingers (i.e., the thumb and index fingers being highly solicited in grasping/prehension, manipulation of objects), the largest overlap was found between D3, D4 and D5 representations (see Figure 15).

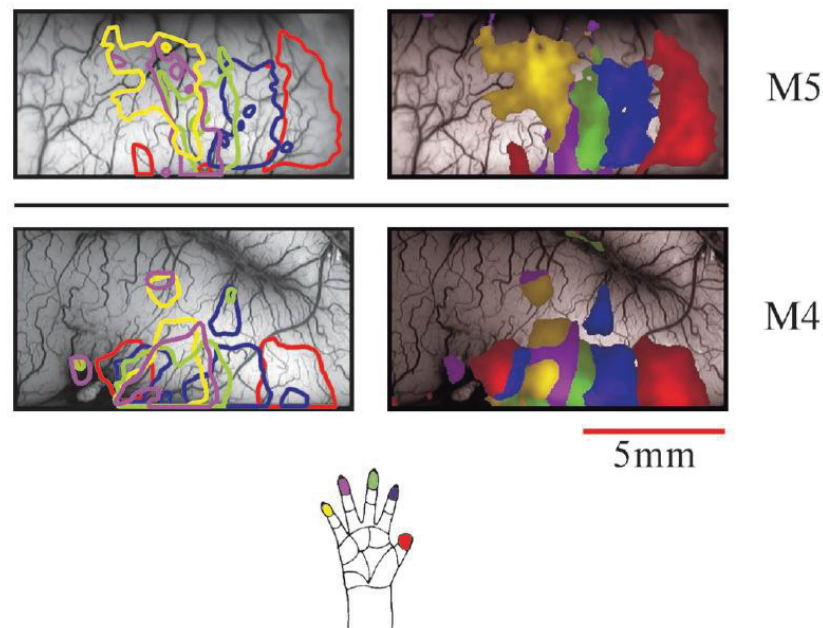


Figure 15 [from Shoham and Grinvald, 2001]. Somatotopic organization of the fingertips in two monkeys (left hemisphere maps for right-hand stimulation). The left maps show the contour lines (and thus overlap) of finger representations, while the right maps show which finger “wins” among others in cases of overlapping representations.

As in non-human primates, a consistent somatotopic arrangement of finger representations has been reported in humans within BA3b, BA1 and BA2 using fMRI (Kurth et al., 2000; Overduin and Servos, 2004; van Westen et al., 2004; Nelson and Chen, 2008; Schweizer et al., 2008; Martuzzi et al., 2014; Schweisfurth et al., 2014), with D1 located most lateral, anterior and inferior and D5 most medial, posterior and superior. In addition, while the fingers' activation peaks are usually well segregated, at least within BA3b and BA1 (Nelson and Chen, 2008; Stringer et al., 2011; Martuzzi et al., 2014), an overlap between finger representations, similar to that observed in electrophysiological studies, has been found in the human SI using fMRI (Maldjian et al., 1999; Krause et al., 2001; Besle et al., 2013b; Martuzzi et al., 2014) and optical imaging techniques (see Figure 16a; Canestra et al., 1998; Sato et al., 2005). Usually, the largest overlap is observed between neighbouring fingers, but some overlap also occurs between non-adjacent fingers (Kurth et al., 2000; Krause et al., 2001; Besle et al., 2013b; Martuzzi et al., 2014), and these overlaps have been reported within the three BAs (Krause et al., 2001; Besle et al., 2013b; Martuzzi et al., 2014). Note that, while the degree of overlap has been found to be correlated with stimulus intensity, it is not affected by correlation thresholds, which makes it consistent and argues against an unspecific 'spillover effect' (Krause et al., 2001).

But some differences are observable between the three BAs. First, the magnification and spread of finger representations along the gyrus seem to be different across BAs. Indeed, some studies reported a larger **Euclidean distance (ED)** between D1 and D5 peaks in BA3b than in BA1 (~16/17mm within BA3b according to Kurth et al., 2000; van Westen et al., 2004 vs ~14mm within BA1 according to Kurth et al., 2000), although another study reported that D1-D5 spanned over a similar distance within BA3b and BA1 (~15mm), but over a smaller one within BA2 (~8.6mm; Martuzzi et al., 2014). This discrepancy may come from some methodological differences, as the first study (Kurth et al., 2000) used electrocutaneous stimulation and computed the ED based on activation peaks, whereas the latter study used a brushing-like stimulation and computed ED based on the centre of mass of finger representations. Another study, in which fingertips were stimulated with air-puffs, also found that the relative distance between adjacent finger representations is in general 1.6 times larger in BA3b than in BA1 (Stringer et al., 2011), which was not the case in Martuzzi et al, 2014. I would like to emphasize here the huge variability observed in the literature, likely due, in addition to differences in analysis, to the use of different stimulation paradigms. Indeed, while electrocutaneous stimulation usually spreads along the entire finger and recruits most of the subcutaneous fibres, a mechanical stimulation is usually more focal (one or two phalanges) and is also more likely to recruit mechanoreceptors in a more specific manner. Ideally, the cortical representation should be carefully investigated and identified for each type of stimulation/receptor to facilitate comparisons across studies. Going back to the differential magnification of the fingers within the three mentioned BAs, an overall decrease of interdigit distances is, at least qualitatively, observed gradually from BA3b, to BA1 and BA2 in these studies. In addition, the relative magnification of the fingers is, as in monkeys, unbalanced, with the thumb exhibiting the largest representation among fingers and across BAs (Martuzzi et al., 2014). But here again some discrepancies (still attributable to stimulation and analyses differences) can be observed in the literature, some studies reporting instead the largest representation for the index finger (Maldjian et al., 1999). As a result of the differential degree of magnification, the degree of **overlap** between finger representations also varies from BA3b to BA2. Indeed, adjacent finger representations exhibit a gradual increase of overlap from BA3b to BA1/2 (Kurth et al., 2000; Krause et al., 2001; Besle et al., 2013b), with ~41% of overlap within BA3b, ~49% within BA1 and ~68% within BA2 (Kurth et al., 2000). But this increase in overlap is also observed between non-adjacent finger representations, with significantly larger overlap within BA1/2 (~25% within BA1, ~39% within BA2 => 23% in combined BA1/2) than within BA3b (~2% of overlap, see Kurth et al., 2000). In addition, while this degree of overlap was found to vary as a

function of stimulation intensity (Krause et al, 2001), its relative proportion is independent of the threshold used to compute the maps (Krause et al., 2001), and is not driven by extra-vascular contributions (Besle et al., 2013b), which goes against the idea that these overlaps are artefactual. Along this line, another type of analysis revealed that while a high specificity was observed within BA3b, the finger representations within BA1 and BA2 also strongly respond to adjacent fingers, with their response decreasing gradually with distance between fingers (Martuzzi et al., 2014). This gradual increase of overlap and thus decrease of specificity is coherent with the increase in RF complexity from BA3b to BA1 and B2 reported in electrophysiological studies in monkeys (see section III.c. of this chapter).

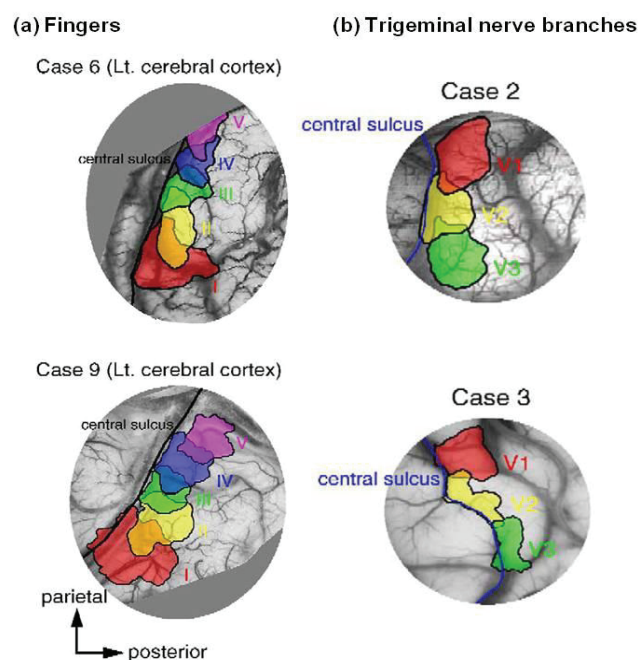


Figure 16 [from Sato et al., 2005]. Functional maps of fingers (a) and face (b) representations in the left somatosensory cortex (BA1) of four patients during surgical removal of tumors. The optical response areas evoked by transcutaneous electrical stimulation of each finger (D1, D2, D3, D4, D5) and trigeminal nerve branches (V1: supraorbital, V2: zygomaticofacial, V3: mental) are displayed on the vascular image of each patient's brain.

Going into a more refined mapping of the fingers/hand, several studies took advantage of the high spatial resolution of fMRI to investigate the cortical representation of the different **phalanges** and bases of each finger (Blankenburg et al., 2003a; Overduin and Servos, 2004; Schweisfurth et al., 2011, 2014; Sánchez-Panchuelo et al., 2012, 2014), as well as the palm (Blankenburg et al., 2003a), and looked at their relative distribution. These studies yielded somewhat different results. Some of them revealed a consistent somatotopic organization of the different phalanges along the anteroposterior axis, orthogonally oriented compared to the

“between-digit” maps (Blankenburg et al., 2003a; Sánchez-Panchuelo et al., 2012, 2014). From posterior to anterior, the representation of the finger is from base to tip within BA2 and BA3b, and reverses at the border with the neighbouring BA1 and BA3a, where it is represented from tip to base (see Figure 17). This result is in agreement with the electrophysiological literature showing a similar sequential organization in mirror-image of finger representations across BAs (e.g., Merzenich et al., 1978; Nelson et al., 1980). However, another group analyzed individual maps elicited by tactile stimulation of the three phalanges and the base of each finger of the right hand and found that among all the digits, only D5 exhibited a somatotopic organization of its phalanges within BA3b, with the base of D5 being consistently located medial to its fingertip, whereas no consistent pattern of organization was found for any of the other fingers (Schweissfurth et al., 2011, 2014). Another study mapped the three phalanges of D1, D2 and D4, but they performed only individual analyses without evaluating the existence of a consistent somatotopy across-subjects due to difficulties in map interpretation caused by limitations in cortical surface sampling (Overduin and Servos, 2004).

MEG also features a high spatial resolution, which allows the localization of dipole sources on the scale of millimetres. However, its intrinsic properties make MEG able to detect only fields oriented tangentially to the scalp (i.e., corresponding to a current oriented orthogonally to the scalp). Thus within the SI area, MEG is likely to detect mainly the activity arising from BA3b. As with fMRI, contradictory results have been reported regarding the distal-to-proximal distribution of the phalange representations. For instance, while no significant ordering was reported in two studies by Hashimoto et al. (1999a, 1999b), Hlushchuk et al. (2004) found, in agreement with electrophysiology studies and both Blankenburg et al, 2003 and Sanchez-Panchuelo et al, 2014, the proximal phalanx of D2 to be represented superior to its distal one. Yet, another study localized the third phalanx of D3 lateral to that of the first phalanx (Tanosaki and Hashimoto, 2004).

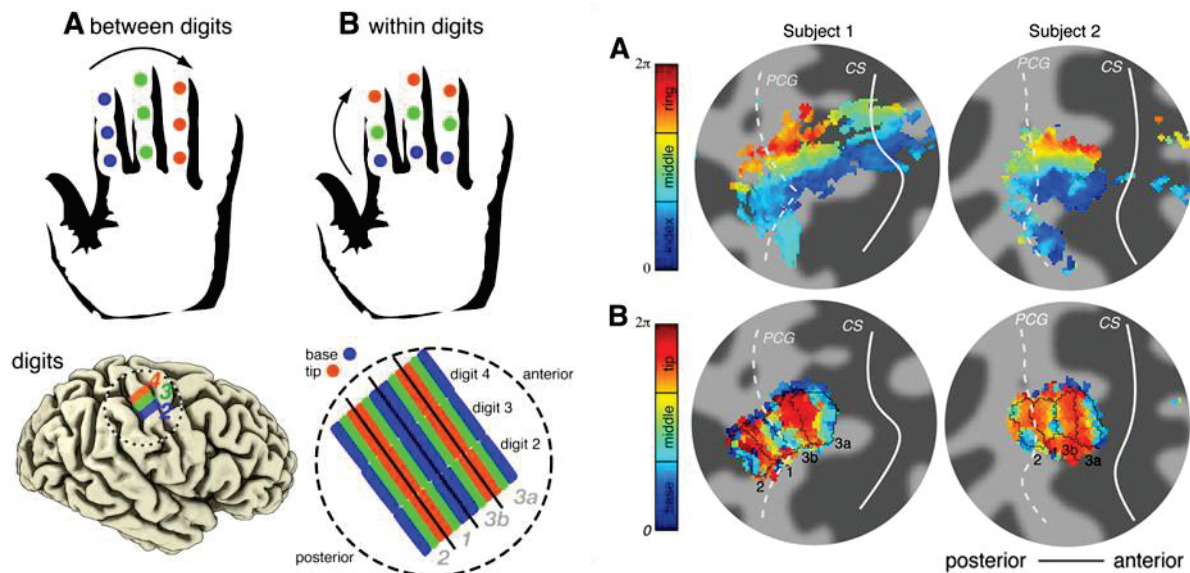


Figure 17 [from Sánchez-Panchuelo et al., 2014]. Left panel: schematic depiction of the between and within finger mapping, and their respective expected mapping within the SI region. Right panel: somatotopic maps obtained for two participants (A) between and (B) within fingers. Maps are displayed on a flattened cortical patch at the central cortical depth (dark grey: sulci, light grey: gyri). Black lines represent the delineation of the BAs based on the mirror reversal of the maps.

Here again several methodological differences could explain these discrepancies. The most striking difference is, again, the **stimulation modality** used to perform the mapping, but also the **surface** it encompasses, as well as its **frequency** (known to significantly change source localization, see Mogilner et al., 1994). While Blankenburg et al, 2003 delivered a large 7Hz non-painful electrical stimulation via electrodes covering approximately 15 mm² of D3 skin, Sanchez-Panchuelo et al, 2014 used a 30Hz vibrotactile stimulation of only ~1 mm² of skin, and Schweisfurth et al, 2011 & 2014 used a piezo-electric Braille display to stimulate at 32Hz, resulting in a fast varying pattern of stimulation across ~18 mm² of skin. Finally Overduin & Servos, 2004 used air-puff stimulation at a frequency of ~10Hz. This stimulation-related variability is similar for the MEG studies. Hashimoto et al, 1999a,b used a stimulation paradigm similar to Sanchez-Panchuelo et al, 2014 (vibrotactile, ~1 mm² of skin) but delivered at 200Hz instead of 30Hz on D2, and in his 2004 paper with Tanosaki used a relatively intense electrical stimulation delivered with ring electrodes at 4Hz on the interphalangeal parts of D3. Finally, Hlushchuk et al, 2004 used a ~2Hz pneumatically-driven mechanical stimulation covering ~8 mm² of skin. In addition to these differences in modality, surface and frequency of stimulation, the **intensity** used also varied largely, ranging from gentle indentation (Sanchez-Panchuelo et al, 2014: ~100 μm; Hashimoto et al, 1999a,b: ~200 μm) to high non-painful currents (Blankenburg et al, 2003: only 1 mA below pain threshold; Tanosaki & Hashimoto, 2004: 4 mA above the

highest sensory threshold among tested sites). Finally, it is worth noting that Sanchez-Panchuelo et al, 2014 stimulated the phalanges of the three digits they investigated, solely on the left hand and simultaneously, which might add some additional variability. Altogether, these discrepancies make it difficult to conclude about the pattern of organization of finger phalanges cortical representations. In addition, it should be reminded that the inter-digit differences of organization may possibly be due to their different functions within the hand (i.e., D1, D2, D3 being mostly involved in precision grip and D4, D5 supporting the others and allowing whole-hand prehension and power grip).

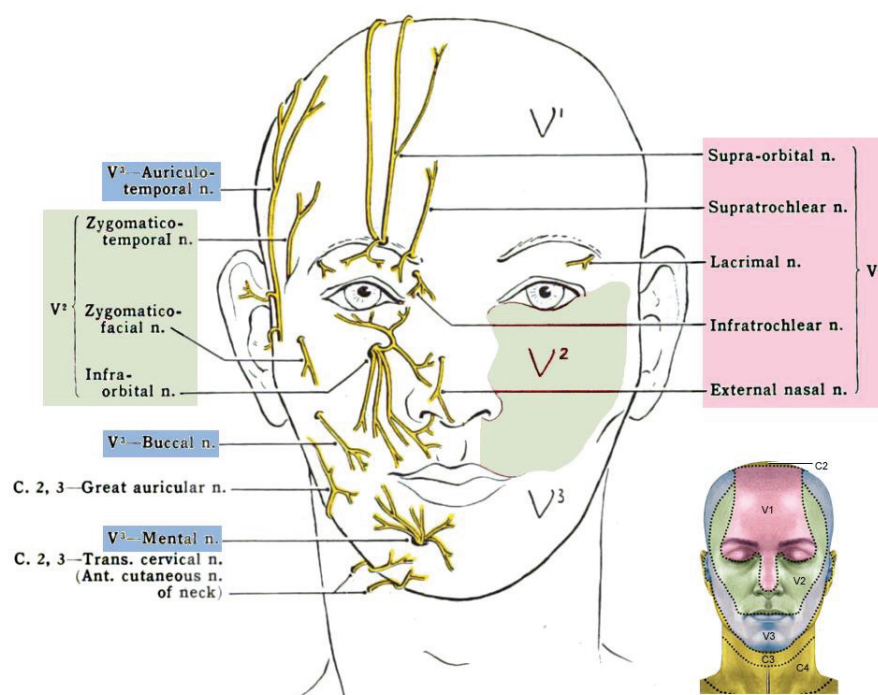
Overall, we can see from the literature that the hand's cortical representation is far from being simple and resolved, at least in humans. This complexity arises first from the huge variability in the stimulation paradigms employed, but also from the intrinsic limits of the imaging techniques used to investigate the human cortex non-invasively. Last, but not least, a non negligible variability may arise from the differences in function across fingers, which may also vary across individuals in regard to their respective experiences.

b. The face

Right after the hand, the face exhibits one of the most sensitive skin areas of our body. In addition, the face, especially in humans, is highly involved in the expression of emotions or most generally, of any communicative reactions in regards to the environment perceived through the five senses. The face comprises ~22 major muscles responsible for numerous functions, such as blinking, chewing (i.e., mastication), language production (i.e., speech) and as mentioned above, facial expressions. The lips themselves require approximately 10 muscles to achieve their full range of motion.

In classical anatomy textbooks, most sensory information from the face is reported to be carried by the Vth cranial nerve, but sensation from some parts of the mouth (such as the tongue), certain parts of the ear and of the meninges is carried by afferent fibres in cranial nerves VII (the facial nerve), IX (the glossopharyngeal nerve) and X (the vagus nerve). However, the cutaneous information arising from the face is carried by the Vth cranial nerve, which is subdivided into three major branches: the ophthalmic nerve (V₁), the maxillary nerve (V₂), and the mandibular nerve (V₃). The cutaneous areas innervated by the three branches have sharp borders with relatively little overlap (Figure 18). The three branches leave the skull through several foramina (i.e., holes in the skull: supraorbital, infraorbital, zygomaticofacial, incisive & mental foramina, superior orbital & inferior orbital fissures, foramen rotundum, ovale & spinosum). The **ophthalmic nerve (V₁)** carries sensory information from the scalp and

forehead, the upper eyelid, the conjunctiva and cornea of the eye, and the nose (except alae nasi). The **maxillary nerve (V₂)** innervates the lower eyelid, the cheek, the nostrils and the upper lip. The **mandibular nerve (V₃)** innervates the lower lip, the chin and jaw (except the angle of the jaw), and parts of the external ear. Thus, the lips are innervated by the infraorbital nerve, a branch of the maxillary nerve, and by the mental nerve, a branch of the mandibular nerve. This nerve arrangement provides a fully contralateral representation of the face to each hemisphere. Please note that each side of the upper-lip, and in particular the region in between the upper-lip and the nose, is innervated by the medial branch of the superior labial branch of the infraorbital nerve of this same side, and that these nerves have been reported to never meet its homologous branch from the other side of the face, nor to cross the midline to innervate part of the skin on the other side of the upper-lip region (see Hu et al., 2007). Thus each branch (left and right) exclusively innervates the upper-part of the lip from the midline to the left or right corner of the mouth. As mentioned previously, these fibres, whose neuronal cell bodies are located in the trigeminal ganglion, then converge in the **principal trigeminal nucleus** in the pons, before projecting to the VPM thalamic nucleus via the trigeminal lemniscus (see section II.b. of this chapter).



Modified from "Grant 1962 470" by Grant, John Charles Boileau - An atlas of anatomy, / by regions 1962.
Licensed under Public domain via Wikimedia Commons and <http://www.pennmedicine.org/encyclopedia>

Figure 18. Schematic representation of the three main branches of the trigeminal nerve innervating the face.

Even if it has received less attention than the hand, the face representation has been quite well described in non-human primates (e.g., Merzenich et al., 1978; Nelson et al., 1980; Sur et al., 1982; Lin et al., 1994; Jain et al., 2001; Toda and Taoka, 2002, 2004; Coq et al., 2004). Electrophysiological studies showed that despite some differences across monkey species, the representations of the upper and lower lips within BA3b and BA1 being sometimes reversed in owl monkeys (Merzenich et al., 1978) as compared to squirrel (Sur et al., 1982) and macaque monkeys (Nelson et al., 1980), the general location and organization of the face representation in the post-central gyrus is consistent. Within the postcentral gyrus, the face representation is located lateral to that of the hand, and clearly somatotopically organized within BA3a, BA3b and BA1 (Lin et al., 1994; Manger et al., 1995; Jain et al., 2001; Coq et al., 2004). In BA3b, the face is represented in a rostrocaudal sequence, three ovals adjacent to the hand representation corresponding respectively to the chin/lower-lip, upper-lip and neck/upper-face (Merzenich et al., 1978; Jain et al., 2001; Coq et al., 2004), whereas three or four more rostral ovals successively represent the contralateral teeth, tongue and the ipsilateral teeth and tongue (see Figure 19, Jain et al., 2001). Interestingly, the representation of the contralateral lower lip in BA3b has been repeatedly found to be split by the representation of the contralateral upper lip (e.g., Dreyer et al., 1975; Manger et al., 1995; Jain et al., 2001), making it a likely general feature of the trigeminal nerve representation in BA3b of primates. Then, as for the rest of the body, the face representation within BA1 mirrors that of BA3b and the neurons composing it exhibit larger RFs (Jain et al., 2001; Coq et al., 2004). Contrary to the hand, however, many of these RFs are located on both sides of the face, thus building bilateral representations of part of the face into one hemisphere (in particular, the lips). The face representation within BA2 has been less described, but a substantial number of neurons responding to lip stimulation were found to exhibit composite RFs covering both upper and lower lips (i.e., bilabial RFs), or more than one of five oral structures: lip, cheek mucosa, teeth/gingiva, tongue and palate (Toda and Taoka, 2002, 2004). In agreement with the BA3b to BA2 convergence, the relative incidence of neurons with composite RFs (especially for neurons activated by tongue and lip stimulation) is significantly higher in BA2 than in BA3b and BA1 (Toda and Taoka, 2004). Furthermore, the proportion of neurons having bilateral RFs increases gradually upon moving caudally from BA3b to BA2, suggesting a bilateral integration across SI subregions (Toda and Taoka, 2004). Similar to the thumb and index fingers within the hand representation, the lips exhibit the highest degree of cortical magnification within the face representation in BA3b, 1 & 2 (Dreyer et al., 1975; Merzenich et al., 1978; Nelson et al., 1980), likely due to its denser innervation (and thus sensitivity). Nearly all of the face SI neurons were found to respond to light tactile stimuli

and to exhibit a rapidly adapting response to tactile stimulation (82% of the neurons recorded by Lin et al., 1994). In addition, no significant difference in the ratio of slowly adapting to rapidly adapting neurons was found in BA3b and BA1 (Lin et al., 1994).

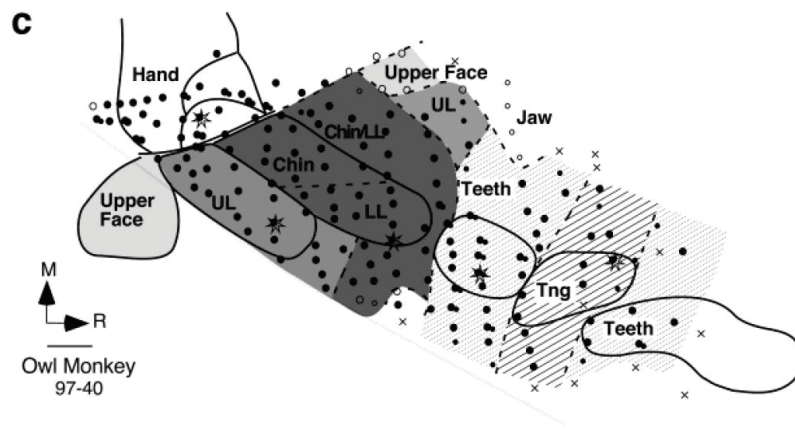


Figure 19 [from Jain et al., 2001]. Topography of the contralateral face and oral cavity representation in area 3b and the surrounding cortex in an owl monkey. Solid lines show the boundaries derived from the myeloarchitecture, dashed lines mark boundaries derived from the electrophysiological mapping data. The double hairline on the lateral side marks the location of the lateral sulcus. UL: upper-lip, LL: lower-lip, Tng: tongue, R/M: rostral/medial. Scale = 1mm.

As in non-human primates, while the somatotopic organization within the hand representation has been well described (see previous section), organization within the face representation in human S1 remains controversial. Indeed, while direct electrical stimulation of cortical fields (Penfield and Rasmussen, 1950) and more recent intraoperative optical imaging studies (Sato et al., 2002, 2005; Schwartz et al., 2004) have indicated a sequential representation of the forehead, cheek and chin in a superior-to-inferior order (i.e., an upright representation), imaging studies (fMRI and MEG) provide evidence for other possible organizations. A few studies reported an inverted (i.e., upside down) representation (Yang et al., 1993; Servos et al., 1999), whereas several other studies rather reported a huge overlap between face regions (Iannetti et al., 2003; Nguyen et al., 2004; Kopietz et al., 2009), suggesting no sharp somatotopic organization. For instance, the contralateral activation elicited by the stimulation of the forehead has been shown to overlap substantially and thus to not differ significantly from that of the lower lip (Iannetti et al., 2003) or of the cheek and chin (Kopietz et al., 2009). Similarly, an MEG study investigated six points on the face (two at the forehead, nose, cheek, chin and jaw), but did not find any difference in location among them (Nguyen et al., 2004). However, the authors highlighted the fact that the representations of these sites were located between the thumb and the lower lip representation (see Figure 20, Nguyen et al., 2004). The

representation of the neck, still debated, has been reported at the hand/face junction (Lin et al., 2010). Concerning the intraoral structures, the representation of the teeth has been found to be superior to that of the tongue and inferior to that of the lip in the rostral portion of the postcentral gyrus (corresponding to BA3b), which is consistent with the classical sensory homunculus of Penfield. However, this organization was less clear and the overlap between these representations significantly greater in the middle and caudal portions of the postcentral gyrus (likely BA1 and BA2) than that in the rostral portion (Miyamoto et al., 2006). Some other studies reported a gross somatotopic organization, with the lateral side of the upper lip being superior to the lower lip (at 0.6-1.1cm ED according to Mogilner et al., 1994; see also Hoshiyama et al., 1996; Disbrow et al., 2003a), and this latter one being more lateral than the cheek representation and more inferior, lateral and anterior than the index finger (Nevalainen et al., 2006). Quantitatively, the average ED between the P25m sources from the right index finger and from the face areas ranges from 1 to 1.5cm (right forehead 13.8 ± 8.3 mm (sd), right cheek 12.8 ± 4.6 mm, right lip 15 ± 4.6 mm and right chin 11.7 ± 4.2 mm, Nevalainen et al., 2006).

The face representational overlap previously observed was further confirmed by intraoperative optical imaging (Schwartz et al., 2004; Sato et al., 2005), however, the extent of overlap in the face region was quantitatively smaller than that in the finger region (see Figure 16, Sato et al., 2005). But according to the authors, this difference may come from the locations of the stimulation, which was applied to parts of the three trigeminal branches. Interestingly, the contralateral responses after lip stimulation were reported to be more ample than those of other face regions (Nevalainen et al., 2006), confirming the higher cortical magnification of the lips. In addition, the overall degree of cortical magnification of the human face was estimated to be similar to the one in monkeys (Schwartz et al., 2004).

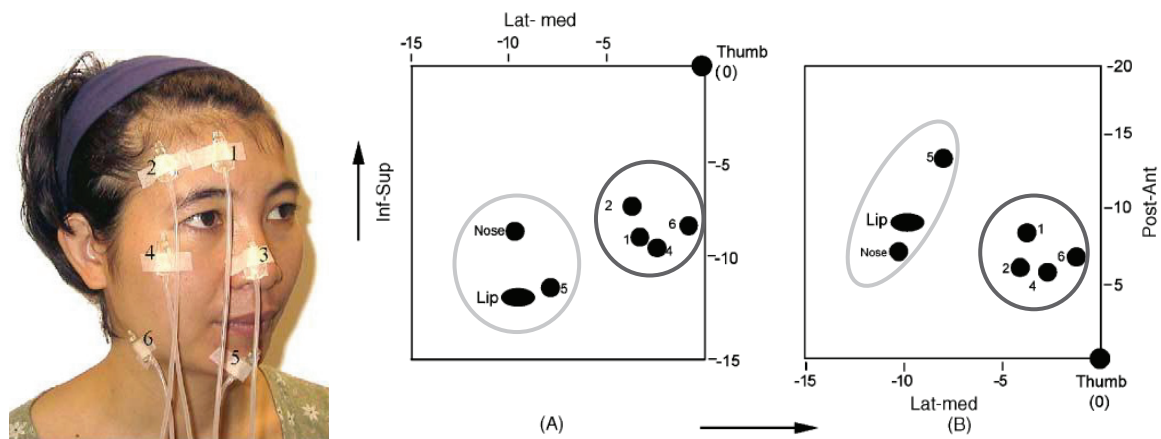


Figure 20 [modified from Nguyen et al., 2004]. Spatial relationship of the group ECD locations following stimulation of the right thumb, lower lip, and the six sites on the face illustrated on the picture (forehead 1 and 2, nose, cheek, chin and jaw). The location of each region is expressed relative to the thumb in the three dimensions (x : medio-lateral direction, y : anterior-posterior direction, z : superior-inferior direction).

More recently, a **segmental** organization of the face representation, similar to the one known for painful and heat stimuli (so called “onion-skin”, DaSilva et al., 2002), has been proposed for non-noxious tactile stimulation of the face (see Figure 21, Moulton et al., 2009). This organization consists of a rostro-caudal representation considered to be related to the vertical arrangement of the stimulation sites within the segmental “onion-skin” model, which is likely determined by segmental inputs from the trigeminal nucleus (Borsook et al., 2004). Due to its rather different distribution compared to that of the three trigeminal branches innervating the face (see Figure 18), the segmental model is a good candidate to explain the variability and the discrepancies of the results previously reported regarding face S1 representations in humans. Indeed, stimulation of areas innervated by a given trigeminal nerve division does not necessarily provide consistent results across studies, as these face areas may span over several segmental representations. Conversely, as a given segmental layer may span over face regions both distant and innervated by distinct trigeminal branches (e.g., the upper forehead innervated by V1 and the lateral lower jaw innervated by V3), distant sites on the face can be closely represented in the cortex (see Figure 21 left panel, Moulton et al., 2009). For example, looking back at the results obtained by Nguyen et al, 2004 (Figure 20), we can notice that the most peripheral/lateral sites of the face (highlighted in dark grey), correspond to the most external layers described by Moulton, and in agreement with the segmental organization (see sites 2, 4 and 3 from Figure 21), are closely grouped next to the thumb. In contrast, the lip, nose and chin tested in Nguyen’s study (highlighted in light grey), correspond to the central layer described by Moulton, and are similarly located more laterally and inferiorly. Finally, a previously mentioned intraoperative

optical imaging study reported a high overlap between peri-orbital and peri-buccal regions of the face (see Figure 21 right panel, Schwartz et al., 2004), which could correspond to the same layer of the segmental distribution, thus possibly explaining their overlap.

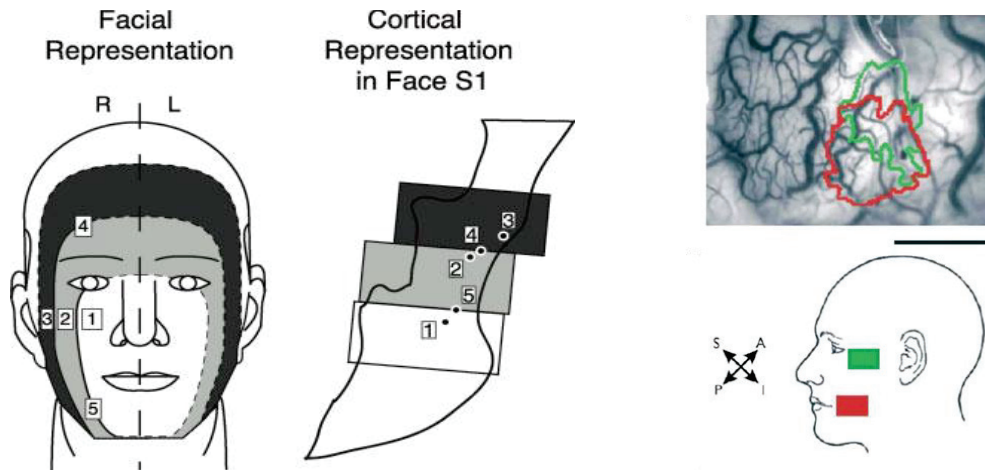


Figure 21. Left panel [from Moulton et al., 2009]: Schematic segmental representation of the face observed in SI. The black/white dots represent positive activation peaks identified for each stimulation site for the group. Dashed lines in the concentric ovals indicate putative extrapolated segmental boundaries. Right panel [from Schwartz et al., 2004]: Cortical representations obtained by intraoperative optical imaging of the peri-orbital (green) and peri-buccal (red) sites, whose stimulation location is illustrated on the schema. Activations are displayed on blood vessel map. Bar = 5mm.

Even if a more systematic mapping of the face regions has to be done to confirm this segmental organization, a few electrophysiological studies in monkeys have found a similar pattern of organization within SI subregions (BA3a, 3b, 1 & 2), with the midline of the face represented from top to bottom (i.e., from forehead to mental) along the mediolateral axis, and the more lateral parts of the face represented following concentric-like patterns along the anteroposterior axis (see Figure 22, Dreyer et al., 1975), more recently confirmed within BA3b (Manger et al., 1996).

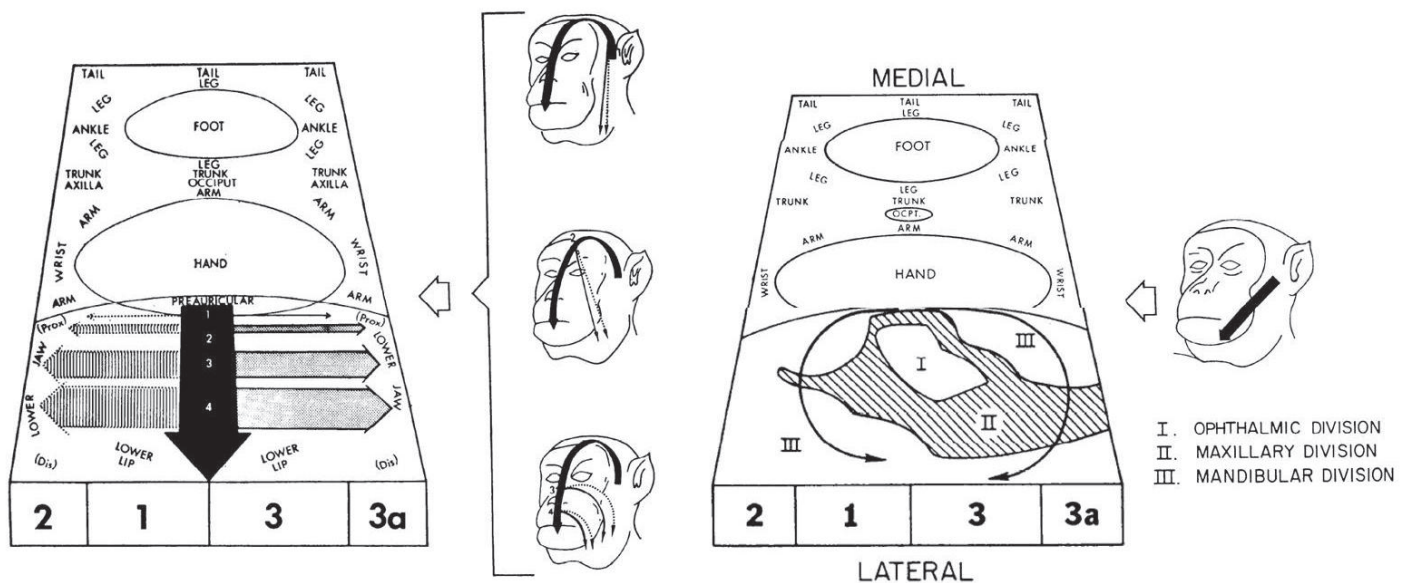


Figure 22 [modified from Dreyer et al., 1975]. Spatial distribution of the peripheral RFs of continuous sequences of cell columns in the face representation of SI region in macaque monkeys. The thick black arrow that crosses the cortical map from medial to lateral, describes a sequence of cell columns within BA1 and BA3b whose cutaneous RFs shift across body regions represented by the thick arrow drawn on the figurines. The thinner grey arrows, drawn orthogonal to the thick arrow on the schematic of the cortex, designate anteroposterior sequences (1-4) of cell columns whose RFs shift to describe paths (1-4) on the face.

Thus also for the face, and even more than for the hand, the literature does not provide a precise and detailed description of the intrinsic organization of the face representation at the cortical level. In particular, it has to be underlined that the differential representation of the face within the subregions of the human SI region (BA3b, BA1 and BA2) and the way tactile information arising from the face is processed across those regions has not yet been systematically investigated. One major limitation for mapping the face in humans via imaging techniques, comes from the issue of finding an appropriate and reliable stimulation paradigm, fully amagnetic to be compatible with both fMRI and MEG, capable of reaching the person's head in the fMRI tunnel, and delivering a stimulation sufficiently intense to be clearly perceived and to induce a clear brain response, but not too intense to avoid eliciting muscle contraction or blinks (mainly for MEG).

V. Thalamocortical projections & higher-order cortical areas

As briefly mentioned at the beginning of section III of this chapter, SI corresponds only to the “first” step of the cortical processing of cutaneous information. Other cortical areas, such as SII, the insular cortex, BAs 5 and 7b (see Figure 23 to localize BAs), are quickly involved in the process, and this starts as soon as the information is sent out from the thalamus.

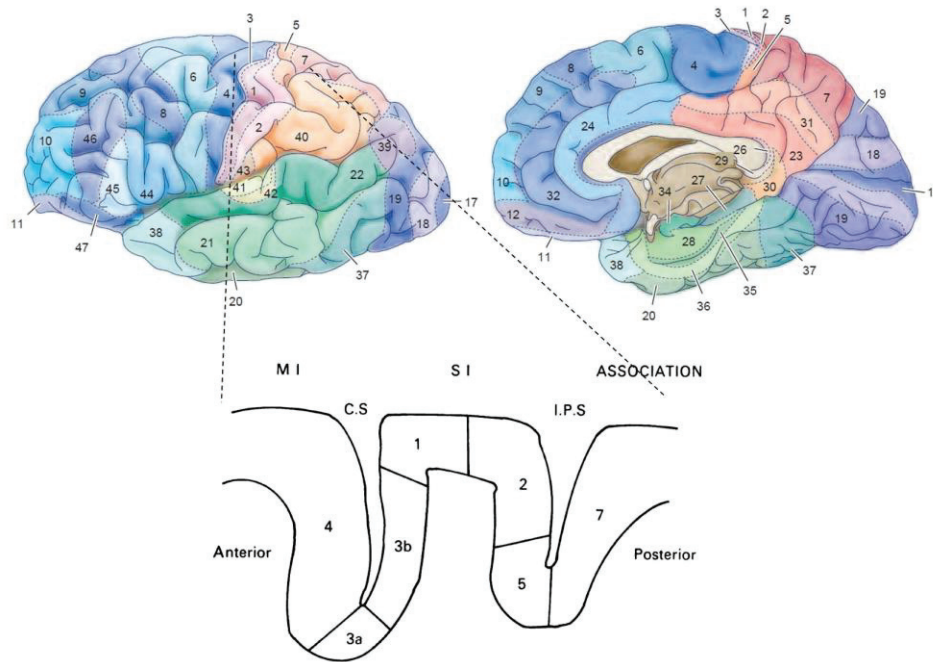


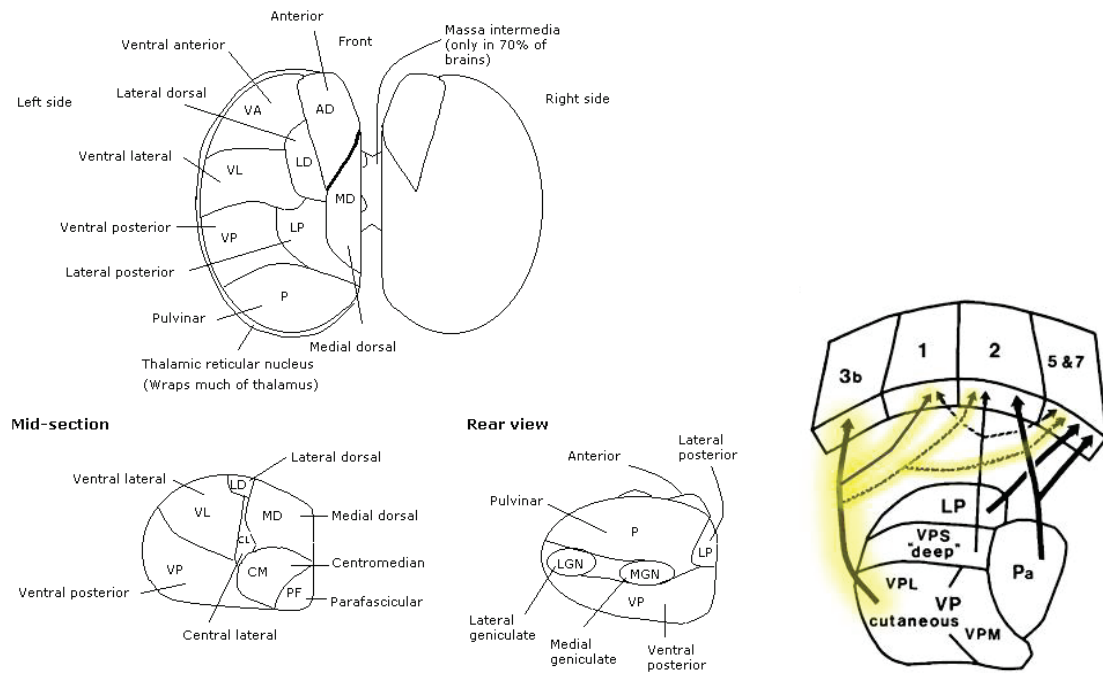
Figure 23 [modified from Purves et al., 2004 and Hyvarinen and Poranen, 1978]. **Upper panel:** cytoarchitectonic-based parcellation of the brain described by Brodmann in 1909. **Lower panel:** zoom of a section across the central sulcus at the level of the hand representation, highlighting the early somatosensory and motor cortical areas, with the precentral gyrus hosting the primary motor cortex (MI), the postcentral gyrus hosting SI region (comprising BA3a, BA3b, BA1 and BA2), and the posterior parietal cortex above the intraparietal sulcus (IPS), hosting BA5 and BA7 associative cortices.

a. Thalamocortical projections

The thalamus is often called the “gateway” of the cerebral cortex as it relays most of the sensory afferents (and motor efferents). However, the thalamus is not simply a relay structure, but rather plays an important integrative role prior to projecting to the overlying primary sensory cortices. The thalamus comprises 13 nuclei (see Figure 24, left panel). The lateral and medial nuclei of the **ventroposterior complex** of the thalamus (VPL and VPM) send somatotopically organized connections primarily to both BA3b and BA1 (see Figure 21, right panel; Whitsel et al., 1978; Lin et al., 1979; Nelson and Kaas, 1981), but also -to a lesser extent- to parts of BA2, BAs 5 & 7, and SII (Friedman and Murray, 1986; Krubitzer and Kaas, 1987). BA3a also

receives input from the ventroposterior complex, though its primary source of thalamic input appears to be from motor thalamic nuclei, such as the **ventral lateral** and **mediodorsal thalamic nuclei** (Huffman and Krubitzer, 2001). Several somatosensory cortical areas also receive inputs from other thalamic nuclei (see Figure 24; Pons and Kaas, 1985). For instance, the **ventroposterior superior nucleus** relays information from deep receptors mainly to BA2 (Kaas et al., 1984), BA3a (Jones and Friedman, 1982) and SII (Disbrow et al., 2002), but also sends sparse but somatotopically organized projections to BA3b (Cusick and Gould, 1990; Cerkevich et al., 2013), BA1 and BA5. The **anterior pulvinar**, which corresponds to the medial posterior nucleus in mammals other than primates, projects in a somatotopic manner to BA3b (Cusick and Gould, 1990; Cerkevich et al., 2013), BA2, BAs 5 & 7, as well as SII and the parietal ventral area (Krubitzer and Kaas, 1987, 1992). The **medial pulvinar** also projects to BA7b and the central lateral and the posterior nuclei to SII (Friedman and Murray, 1986). The **lateral posterior nucleus** projects to rostral BAs 5 and 7, and has reciprocal connections with SII (Krubitzer and Kaas, 1987), and the **ventroposterior inferior nucleus** projects mainly to SII (Friedman and Murray, 1986; Krubitzer and Kaas, 1992; Disbrow et al., 2002; Coq et al., 2004) and the parietal ventral area (Krubitzer and Kaas, 1992), but also to BA3b (Krubitzer and Kaas, 1987; Cusick and Gould, 1990; Cerkevich et al., 2013). Finally, the **ventroposterior oral nucleus**, which encodes information coming from deep receptors, relays muscle spindle signals to BA3a (Kaas et al., 1984). To conclude, the thalamocortical connections are quite complex, a single thalamic nucleus projecting to multiple cortical areas, but this network (and the processing of sensory information) is even more complicated by the fact that these connections are largely reciprocal, with cortical areas sending feedback projections to different thalamic nuclei (Guillery, 1995). It is also worth mentioning that while the main inputs to the ventroposterior complex of the thalamus arise from both the dorsal column and the trigeminal systems, this thalamic complex also receives substantial inputs relayed by the spinothalamic tract mentioned previously (e.g., Kenshalo et al., 1980).

Thalamus Dorsal View (top view).



from: <http://en.wikibooks.org/wiki/File:Constudthal.gif>

Figure 24. **Left panel:** Schema of the different nuclei forming the thalamus. **Right panel** [from Pons and Kaas, 1985]: Some of the multiple thalamocortical connections. Solid lines indicate major projections and dashed lines represent minor connections or connections that may not project to all parts of a given field. Collaterals of neurons from a single nucleus are not represented.

b. Corticocortical projections arising from SI's subregions

Apart from the interconnectivity already mentioned within SI (see section III.c. of this chapter), **BA3b** and **BA1** are also reciprocally connected with SII (Jones et al., 1978; Vogt and Pandya, 1978; Pons and Kaas, 1986; Burton et al., 1995), but **BA3b** projects less densely to SII (Vogt and Pandya, 1978). While there is no evidence that BA3b is connected with the primary motor cortex (M1) and BA5 (Jones et al., 1978; Vogt and Pandya, 1978), **BA1** is also reciprocally connected with M1, BAs 5 & 7 and the supplementary motor area (SMA) (Jones et al., 1978; Vogt and Pandya, 1978; Pons and Kaas, 1986; Burton and Fabri, 1995). In addition, **BA3b** and **BA1** also project to the retroinsular area and the granular insula (Burton et al., 1995). Finally, **BA2** primarily projects to BA5, but also exhibits reciprocal connections with M1, SII, the premotor cortex (BA6) and the SMA (Jones et al., 1978; Vogt and Pandya, 1978; Pons and Kaas, 1986). So to summarise, SI and SII are reciprocally connected in a topographically organized manner with each other and with M1 (Catani et al., 2012). Each of them sends further fibres in an organized manner to the SMA and the insula, but only SI projects to BAs 5 & 7 (Jones and Powell, 1969), mainly through BA2 and BA1, which both receive inputs from BA3b.

Outputs of SI can be summarized by the association of (i) a **ventral path** passing through SII to reach the caudal insula, areas of the temporal lobe and the premotor and prefrontal cortical areas, and (ii) a **dorsal path** passing by the superior parietal lobule (see Figure 25).

Figure 25 [modified from Squire et al., 2008, after Wall, 1988]. Schematic representation of the pathway conducting mechanosensory information from the ventroposterior complex of the thalamus to cortical areas.

The **secondary somatosensory cortex (SII)**, located along the superior bank of the lateral sulcus in the parietal operculum (BAs 40 & 43, see Figure 23), is the first relay of the somatosensory “ventral stream”. The first evidence for a human SII was based on another electrical stimulation study of Penfield (Penfield and Jasper, 1954). SII primarily receives convergent projections from SI, but as mentioned above, some third-order neurons from the thalamus also terminate directly in SII (Friedman and Murray, 1986; Krubitzer and Kaas, 1987, 1992; Disbrow et al., 2002). According to Robinson and Burton (1980), neurons in SII are rapidly adapting to hair or skin stimulation. Therefore, any projections to SII from the ventroposterior complex of the thalamus are likely to be from RA neurons. Functional imaging studies found SII to be bilaterally activated in response to nonpainful (Krubitzer et al., 1986; Disbrow et al., 2000; Del Gratta et al., 2002; Eickhoff et al., 2007a), and painful (Peyron et al., 1999; Ferretti et al., 2004; Baumgärtner et al., 2010; Lockwood et al., 2013) somatosensory

stimuli, especially when they are rare/deviant (Chen et al., 2008). But SII is also involved in higher-order processes of tactile stimuli, such as shape and texture discrimination (Health et al., 1984), attention (Mima et al., 1998; Backes et al., 2000; Chen et al., 2010; Goltz et al., 2013), learning (Pleger et al., 2003; Hodzic et al., 2004) and working memory of tactile surface texture (Harris et al., 2002; Kaas et al., 2013b). In monkeys, the SII region has been shown to be subdivided into three distinct areas (see Krubitzer et al., 1986, 1995; Cusick et al., 1989; Burton et al., 1995), referred to as area SII (not to be mistaken for the “SII region”), the parietal ventral area (PV) adjoining SI, and the ventral somatosensory area (VS), lying deeper in the lateral sulcus. An homologous subdivision of the human parietal operculum was later reported using functional imaging (Disbrow et al., 2000) and histological examinations (Eickhoff et al., 2006a, 2006c). The latter study led to the distinction of four distinct cytoarchitectonic areas (OP1-OP4) in the human parietal operculum (SII region). A topographical correspondence was reported between **OP4** and **PV**, **OP1** and **area SII**, **OP3** and **VS**, and the additional area **OP2** found in humans was attributed to the parietal-insular vestibular cortex in nonhuman primates. Similar to SI, and in agreement with electrophysiological studies in monkeys (Krubitzer et al., 1986, 1995; Burton et al., 1995), three distinct somatotopic body representations were found respectively within OP1, OP3 and OP4 (Eickhoff et al., 2007a), OP1 and OP4 being mirror-images of each other, sharing a common border at the representations of the face (superficial), hands (intermediate) and feet (deep in the fissure). In addition, many imaging studies revealed, even without considering the four subdivisions, an overall somatotopic organization within the parietal operculum (Maeda et al., 1999; Ruben et al., 2001; Ferretti et al., 2004; Nguyen et al., 2005; Malinen et al., 2006). Finally, physiological studies showed that compared to SI, SII neurons tend to have larger and more complex RFs (Krubitzer et al., 1986; Fitzgerald et al., 2006), which usually encompass over two or more fingers and responds to complex tactile stimuli, which supports the idea that SII is part of a serial processing scheme (see Pons et al., 1987, 1992; Iwamura, 1998) in addition to a parallel processing pathway (Knecht et al., 1996b; Rowe et al., 1996; Chung et al., 2014) going through the previously mentioned direct thalamocortical projections to the SII region. **PV (OP4)**, which is involved in sensorimotor integration, then projects densely and reciprocally to BA1, BA3b, BA7b, the parietal rostroventral area, frontal motor areas (such as the frontal eye field), the premotor cortex, posterior parietal areas (such as the IPS) and the medial auditory belt areas (Qi et al., 2002; Disbrow et al., 2003b), while area **SII (OP1)**, a purely somatosensory area, is densely interconnected with BA1 and BA3b, but also with PV, and BA7b within the same hemisphere (Burton et al., 1995; Disbrow et al., 2003b). Area SII (OP1) is additionally densely

interconnected, via massive transcallosal connections, to its homologue in the other hemisphere, which then projects intrahemispherically to BA7b and BA3b (Disbrow et al., 2003b, see Figure 26 for a summary). In contrast, PV has callosal connections limited to its homologue in New World monkeys (Disbrow et al., 2003b), plus to area SII in marmosets (Qi et al., 2002). In turn, the SII region projects to limbic structures, such as the amygdala and hippocampus (see Figure 25). This “ventral” path is believed to play an important role in tactile learning and memory.

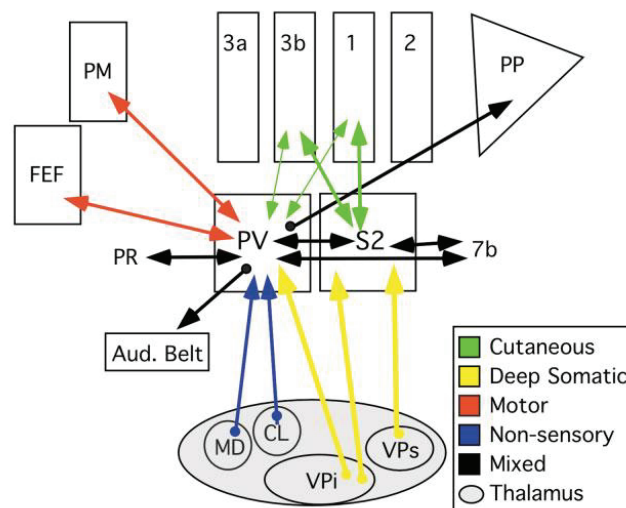


Figure 26 [from Disbrow et al., 2003b]. Summary of S2 and PV cortical connections (Disbrow et al., 2002, 2003b). FEF: frontal eye field, PM: premotor cortex, PP: posterior parietal cortex, MD & CL: non-sensory thalamic nuclei.

The other flow of information arising from SI goes through the “dorsal stream”, whose first relays are **BA 5 & 7**. BA5 and BA7 are part of the posterior parietal cortex (PPC), which is located posterior to SI and superior to the occipital lobe. These regions are associative sensory cortices that have been linked to a wide variety of high-level processing tasks, including multisensory (Huang et al., 2012; Sereno and Huang, 2014) and sensorimotor integration, and activation in association with language use. I will here provide a brief description of PPC to get an overview of its function within the somatosensory pathway.

BA5 is located immediately posterior to SI in the middle of the rostral bank of the intraparietal sulcus (IPS, see Figure 23). Like SII, BA5 receives direct projections from SI (Jones and Powell, 1969), primarily from BA2 (Vogt and Pandya, 1978) and dense thalamocortical projections from VPS, the anterior pulvinar and lateral posterior nuclei (Jones et al., 1978; Padberg et al., 2009), which respectively process inputs from muscles and joints and cutaneous inputs. Consequently, BA5 responds to stimulation of deep or cutaneous receptors on the contralateral hemibody. Unlike anterior parietal fields (BA3b, 1 & 2), which are proposed to be involved in more simple discrimination of object texture, shape and size (Randolph and

Semmes, 1974; Carlson, 1981; Murray and Mishkin, 1984), BA5 is involved in motor preparation (Burbaud et al., 1991; Snyder et al., 1997), in preshaping the hand before grasping an object (Debowy et al., 2001), and in generating body-centered coordinate systems for reaching (see Padberg et al., 2007 for review). In humans, BA5 has been reported to be involved in movement planning, and to be activated by forelimb movement execution and visualisation (Astafiev et al., 2003; Hanakawa et al., 2003; Diedrichsen et al., 2004). Similar to the “primary” areas (BA3b, 1 & 2), BA5 is somatotopically organized, but less precisely than BA2, with the proximal forelimb and trunk being represented medial to the distal forelimb and hand (Padberg et al., 2009; Huang et al., 2012). Strikingly, the forelimb and the hand are dominantly represented within this area (Padberg et al., 2009). In addition, BA5's touch responsive neurons exhibit RFs on average much larger and complex than those in BA1 and BA2 (Padberg et al., 2009), that can be contralateral, ipsilateral or bilateral and modulated by attentional states or experience (e.g., Iwamura et al., 1994; see Padberg et al., 2007 for review). The specialized cutaneous portion of BA5 then connects with BA7 and SII (Pons and Kaas, 1986). Parts of BA5 are also interconnected with M1 and more posterior parts of BA5 are connected with parts of the premotor cortex BA6 (Jones et al., 1978).

BA7 is located posterior to BA5 (see Figure 23) and superior to the occipital lobe, and is subdivided into several regions, with medially the precuneus, laterally the superior parietal lobule (SPL), at the base of which is the IPS, below which is the inferior parietal lobule (IPL), which in turn divides into BA39 (angular gyrus) and BA40 (supramarginal gyrus). Its lateral part, corresponding to **BA7b** (Vogt and Vogt, 1919), is more closely related to somatosensory and active motor functions (Vogt and Vogt, 1919; Leinonen et al., 1979; Robinson and Burton, 1980a, 1980b; Hyvärinen, 1981) than its medial part, namely **BA7a**, which has been linked to oculomotor functions (Vogt and Vogt, 1919; Mountcastle et al., 1975; Hyvärinen, 1981). BA5 and the SII area both send reciprocal and somatotopically organized connections to BA7b, but not to BA7a (Stanton et al., 1977; Neal et al., 1986; Pons and Kaas, 1986). BA7b also receives direct thalamocortical inputs from the anterior, medial and lateral pulvinar, the oral division of the pulvinar, the lateral posterior nucleus, the centrolateral and centromedial nuclei and the ventrolateral nucleus (Friedman and Murray, 1986; Padberg and Krubitzer, 2006), and inputs from BA1 (Pons and Kaas, 1986). Moreover, while no corticocortical fibres have been found between BA7a and BA7b (Neal et al., 1986), BA7a receives projections from extrastriate visual areas such as BAs 18 and 19 (Pandya and Kuypers, 1969; Stanton et al., 1977). Multiunit mapping of BA7 has revealed a somatotopic organization, with neurons responding to cutaneous stimulation of the face being located near the anterior tip of the IPS (close to SI face area), and

those related to the limbs more posteriorly (Hyvärinen, 1981). A large part of BA7 is related to hand sensorimotor performance (Sakata et al., 1973; Mountcastle et al., 1975), but a large part covering the most lateral part (in the BA7b region) is also related to face movements (Hyvärinen, 1981). Similar to BA5, BA7b generally exhibits large RFs, their size ranging from the tips of one or more digits to the entire body, and half of its RFs are bilateral (Robinson and Burton, 1980b). Concerning BA7 projections, while BA7a is reciprocally connected with the eye movement area of the frontal lobe (Pandya and Kuypers, 1969), BA7b has widespread connections with several frontal lobe premotor and motor areas (Pandya and Seltzer, 1982; Neal et al., 1987; Caminiti et al., 1996; Johnson et al., 1996). Overall, BA7 is preponderant to integrate visuo-tactile inputs to promote and guide arm, hand but also face and lip movements and coordination (e.g., in reaching to grasp an object).

PPC lesions that include BAs 5 & 7b were shown to induce deficits in arm and hand coordination in regards to the body posture and the shoulder-centered space (Rushworth et al., 1997a, 1997b), but to spare roughness discrimination abilities (Health et al., 1984). Conversely, electrical stimulation of these brain areas evokes complex movements such as arm and hand reaching, grasping or defensive movements, hand-to-mouth movements or face defensive and aggressive movements (Stepniewska et al., 2009b; see Figure 27). Altogether, BAs 5 & 7 seem to be preponderant for motor planning and spatial coordination of hand/arm movements in relation to proprioceptive and tactile information within body-part centred frames of reference, all these elements being necessary for an efficient interface between the hands and the object being explored (see Cohen and Andersen, 2002; Sereno and Huang, 2014; Vingerhoets, 2014).

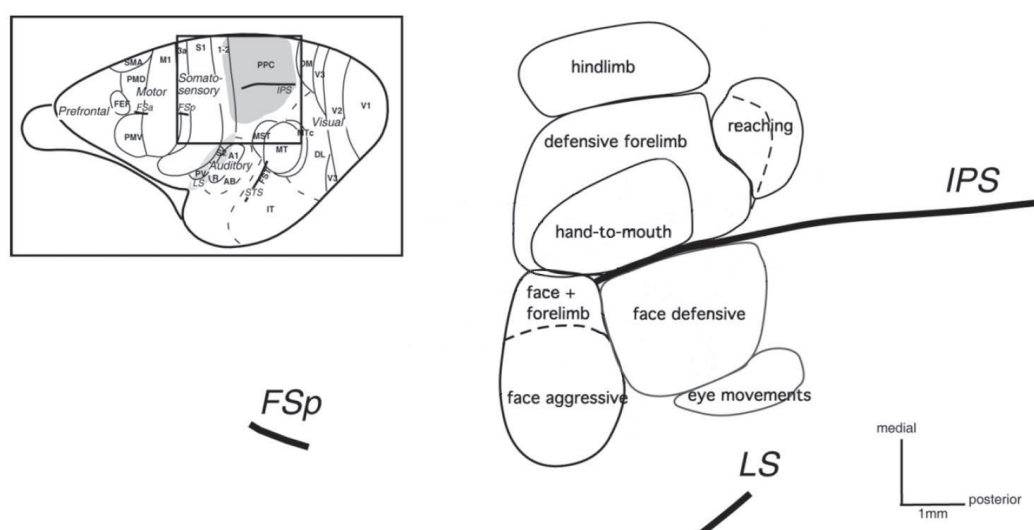


Figure 27 [modified from Stepniewska et al., 2009a]. Schematic representation of the different functional zones of PPC (outlined by solid lines) in galagos monkeys, defined by intracortical microstimulation (ICMS).

BAs 5 & 7 correspond to the “traditional” large divisions of PPC (Brodmann, 1909), but the latter has been further subdivided into various areas, identified by connection patterns, architecture and neuronal response properties in macaque monkeys. These areas include the anterior intraparietal area (AIP), the ventral intraparietal area (VIP), the medial intraparietal area (MIP), the lateral intraparietal area (LIP), and the posterior intraparietal area (PIP) (for review see Grefkes and Fink, 2005). **VIP** is located in the depth of IPS and receives projections from the visual area MT (Maunsell and van Essen, 1983), but also somatosensory inputs while projecting to frontal motor cortex (for review see Gentilucci et al., 1988; Graziano and Cooke, 2006; Avillac et al., 2007). Stimulation of VIP in macaques results in a sequence of movements that Cooke and colleagues (2003) described as defensive and avoidance movements (eye closure, facial grimacing, and hand movement to the face). **LIP** is connected to FEF and is involved in the control of eye movements (for review see Andersen and Buneo, 2002). **AIP** is considered to be involved in the visual guidance of grasping (see, e.g., Sakata et al., 1995; Fogassi et al., 2001), whereas a more posterior and medial region, the parietal reach region (PRR), occupied largely by the previously defined **MIP**, is thought to be involved in the spatial guidance of reaching (see, e.g., Batista et al., 1999).

In turn, PPC areas project to motor areas and multisensory associative cortex (see Figure 25). This “dorsal” path is believed to play an important role in prehension, grasping and manipulation of objects. Altogether, through the lateral sulcus (SII + Insula) and the posterior parietal areas (BAs 5 & 7), somatosensory information reaches (1) the **limbic** system (entorhinal cortex, amygdala and hippocampus), (2) the **motor** system (M1, SMA, BA6), and (3) the **multisensory** cortex in the superior temporal gyrus (see Figure 25).

An important feature of the nervous system is that at each synapse from the periphery to the brain, information from adjacent ascending fibres can be combined locally as each neuron receives projections from multiple neurons, thus leading to a **convergence** of the information (Iwamura, 1998). However, each neuron also projects to multiple neurons, causing an extensive **divergence** of ascending somatosensory projections. Thus, while gross somatotopy is preserved between the periphery and CNS, there is ample opportunity for each synaptic relay point to act as a station for the integration of information from spatially separate skin surfaces. This is reflected in the differences and the overall increase in complexity observed at the map and RF level along the somatosensory pathway. In addition to this periphery-to-central integration of the sensory information, a further **integration** occurs vertically through the six layers of the cortex. Indeed, experiments in rat and monkey somatosensory cortex indicate that the smallest RFs are found in layer 4, while supragranular and infragranular layers exhibit larger RFs (Simons, 1978;

Sur et al., 1985; Chapin, 1986; Armstrong-James and Fox, 1987). Together these data support the notion that at each level of cortical processing the neurons are sampling from a larger input space, receiving convergent information from the previous level, diverging out to the next level, and in the process, forming larger and more complexly integrated and combined RFs. In addition to this vertical flow of information, the substantial **horizontal interconnectivity** allows for integration of information from neighbouring regions and from specific, more distant cortical zones (Lorente de No, 1938). Horizontal connectivity may be of particular relevance in cortical map reorganization processes that will be detailed in the next chapter. Finally, while this bottom-up integration of the signal is preponderant and well-known, somatosensory information from cortical areas is also sent back to subcortical structures such as the thalamus, brainstem and spinal cord via massive **descending projections**. These pathways originate in sensory cortical fields and project to the thalamus, brainstem, and spinal cord. Although their physiological role is not well understood, it is generally assumed that descending projections modulate the ascending flow of sensory information at the level of the thalamus and brainstem.

To conclude, we can see from the literature (non-exhaustively) reviewed in this chapter that the somatosensory system is extremely complex, from the mechanoreceptors embedded in the skin to the higher order cortical areas and that its structure and function are still not fully understood, despite the numerous studies investigating it.

CHAPTER 2: SOMATOSENSORY PLASTICITY

I. Concept/Overview

For almost forty years, the previously described somatotopic organization of the cortex (i.e., *the homunculus*) was thought to be stable once the brain achieved its maturation at the adult stage. With regard to the RFs, they were -until recently- considered solely on the basis of their spatial feature, the classical definition of the RF of a somatosensory neuron being the overall area of the body surface eliciting significant variation in the neuron's firing rate when touched. However, when we explore objects with the hands, the multiple contacts between the skin and the object surface (which may be non-homogeneous) generate extraordinarily complex patterns of tactile inputs that, in addition, continuously change in time. In agreement with this observation, a temporal component has since been discovered to be a crucial feature of the RFs properties, making them intrinsically dynamic (see Nicolelis and Chapin, 1994; Nicolelis et al., 1997; Ghazanfar and Nicolelis, 1999; Brecht et al., 2003; Ramirez et al., 2014 for the somatosensory system). These spatiotemporal features of somatosensory neuron RFs are expressed by changes in their spatial selectivity as a function of time following stimulation (at the ms scale). For example, in the rat somatosensory thalamus, VPM neurons exhibit RFs that respond best to one whisker at the earliest post-stimulus time and then respond best to another whisker at a later time (Nicolelis and Chapin, 1994). Consequently, this spatiotemporal coupling is also reflected at the level of somatotopic maps, which also evolve with time. Thus, contrary to the initial view, the somatosensory system and its intrinsic somatotopic organization are far from being “static”, but rather process somatosensory information in a dynamic way. This relates to the concept of plasticity, an intrinsic property of the brain, which unveils its ability to adapt to our changing environment, but also determines and shapes our abilities to perceive and act in this same environment. Indeed, cortical connections and representations in the adult's brain are not static but rather dynamic and constantly changing in response to both peripheral manipulations and behaviourally important experience throughout life. Understanding the relationships between cortical maps reorganization and functional changes is a valuable and challenging step toward refining our knowledge of brain plasticity mechanisms which, in turn, could be exploited to implement, complement, or boost plasticity-induced perceptual, cognitive, or motor skill learning and rehabilitation.

As described in the previous chapter, most of the somatosensory relays and in particular the SI region are organized topographically, each body-part being represented following a well-

defined orderly arrangement. This peculiar organization makes the somatosensory cortices a particularly suitable model to study and quantify induced cortical plasticity by measuring changes in maps distribution/topography. Brain plasticity at this macroscopic level can be categorized either by **what** triggered the plastic changes (i.e., the event: reduction vs increase of inputs), by its functional **outcomes** (i.e. maladaptive vs adaptive) or by the **time-scale** over which the plastic changes occur (i.e. short vs long-term). The first categorization relies on the fact that sensory representations can be remodelled following peripheral or central changes in input sources or pattern. Numerous studies performed on animals or humans have indeed shown that plasticity can occur at great(er) or small(er) degree, following peripheral or central lesions, environmental manipulations, or an alteration in the incidence of sensory inputs. This reorganization is usually expressed in terms of shifted boundaries, location or volume changes of representational maps, as well as changes in the size and location of neuronal RFs. Moreover, the grain of spatial representation within sensory maps can be modified, as RFs are sharpened or expanded. The second way of categorizing brain plasticity focuses on the plasticity-induced functional outcomes, which in a dichotomic approach, can be seen as adaptive or maladaptive. To a first approximation, we can distinguish “positive” (or adaptive) cortical plasticity induced, for example, by a perceptual or motor training that leads to some benefits (e.g., enhanced performance), from “negative” (or maladaptive) plasticity, resulting in functional impairments as a consequence, for example, of nerve injury, amputation or brain damage. In reality though, things appear to be more complicated, making this classification attempt not fully viable due to its subjectivity (i.e. what can be considered “positive” or “negative”?) and to the fact that it does not capture the different aspects of the outcomes evoked at all possible levels (e.g. cross-modal plasticity or side effects). Finally, the last proposed factor of classification of brain plasticity relies on its temporal feature, which is one of the most important to keep in mind throughout the reading of my work. Indeed, by definition brain plasticity refers to dynamic processes of change/reorganization, which develop and evolve with time. However, most of the studies investigating this phenomenon are limited in time and thus zoom in on the involved processes during a limited time window. As a result, brain plasticity can refer to different processes (or at least different degrees of evolution of these processes) depending on whether it is short-term or long-term plasticity. On top of these attempts of classification, brain plasticity can be assessed either at the structural or at the functional level.

Given its involvement in most neuronal processes (e.g. during developmental maturation processes, memory, learning, recovery etc), gaining a better understanding of cortical plasticity is still a huge challenge for neuroscientists, from a purely fundamental point of view, as well as

with the ultimate purpose of improving clinical rehabilitation strategies. Indeed, being capable of promoting or strengthening CNS functions that are lost or weakened by guiding/enhancing cerebral plasticity would be a huge achievement for brain plasticity research. In this work, the functional aspects will be favoured, with a particular emphasis first on the different forms of plastic changes with regard to the events triggering them, and second on the functional outcomes and relevance of these plastic changes, while the temporal feature of plastic change will be emphasized when needed. Moreover, despite the fact that plastic changes can occur at each relay along the somatosensory pathway, I intentionally focused on plastic changes occurring at the cortical level as this level is the one under investigation in this work.

II. Plasticity following sensory deprivation

a. Peripheral lesion or injury:

Interrupting signal transduction along sensory pathways was one of the first experimental manipulations used to probe brain plasticity in animals. The early demonstrations of adult somatosensory plasticity were reported after peripheral nerve damage or amputation in the somatosensory cortex of several animal species, but mainly in **monkeys**.

Deafferentation resulting from **amputation of one or a few digits** (from upper or lower limb) has been shown to induce plastic changes within SI. Immediately after amputation, many neurons in the deprived cortical area of flying-foxes (Calford and Tweedale, 1988) and rats (Byrne and Calford, 1991) were not silent, but rather became responsive to stimulation of directly adjoining skin territories within a few minutes after denervation. Interestingly, these enlarged RFs shrank back to their initial size and position in the week following amputation (Calford and Tweedale, 1988). Because of their short time-scale, these plastic changes have been interpreted as originating from removal of inhibition and the subsequent shrinkage as the re-establishment of the inhibitory balance in the affected cortex and its inputs. However, similarly restricted amputation in monkeys revealed more gradual reorganization within SI (Rasmusson, 1982). The deprived digit's cortical representation (digit 5) was initially totally **unresponsive**, for as long as 2 weeks, before showing RFs extending over large regions of the hand within 8 weeks (Figure 28, A), tending to shrink back to more restricted regions mostly on the neighbouring finger (digit 4) and palm 16 weeks post-amputation (Figure 28, B). Despite these possible species-dependent time course discrepancies, these studies in flying-foxes, rats or monkeys revealed that restricted amputation leads to rather rapid **changes in SI RF properties**. A similar emergence of new tactile RFs following digit amputation was also reported in the

ventroposterior lateral (VPL) thalamus of rats (Shin et al., 1995) and monkeys (Rasmusson, 1996), but most changes have been investigated at the cortical level. The subcortical contribution to cortical reorganization is discussed later (page 91).

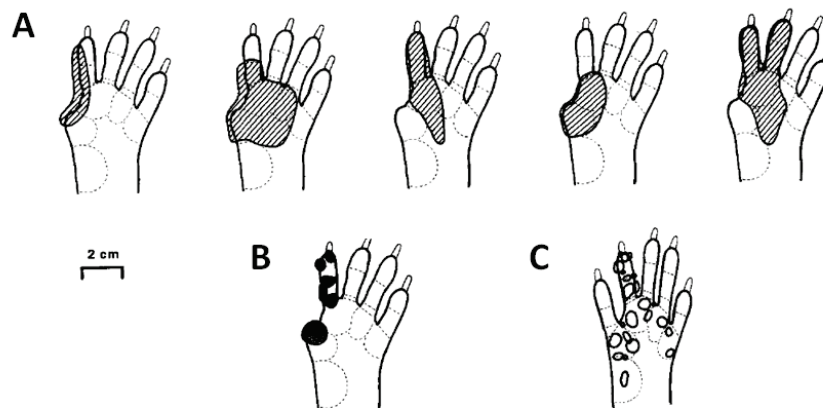


Figure 28 [modified from Rasmusson, 1982]. **A)** Examples of “large” RFs obtained from the fifth digit area of 8- to 16-week post-amputation animals. **B)** Representative “small” RFs obtained from the fifth digit region of the 16-week post-amputation animals. **C)** Representative RFs obtained in intact animals from the fourth digit and the palm areas.

In parallel with these RF translocations, a significant reorganization has been found within cortical maps 2-9 months after multiple-digit amputation (Merzenich et al., 1984), but also median nerve transection (Merzenich et al., 1983a, 1983b). A detailed investigation of **cortical changes** over time revealed a similar time course of evolution in monkeys that had undergone a more extensive deafferentation induced by median nerve transection, thus depriving the cortex of inputs from the glabrous surface of digits D1-D3 (Merzenich et al., 1983b). Immediately after transection, a large portion of areas 3b and 1 was unresponsive, but came to be excited by inputs from peripherally neighbouring skin surfaces over the course of a few weeks (Figure 29).

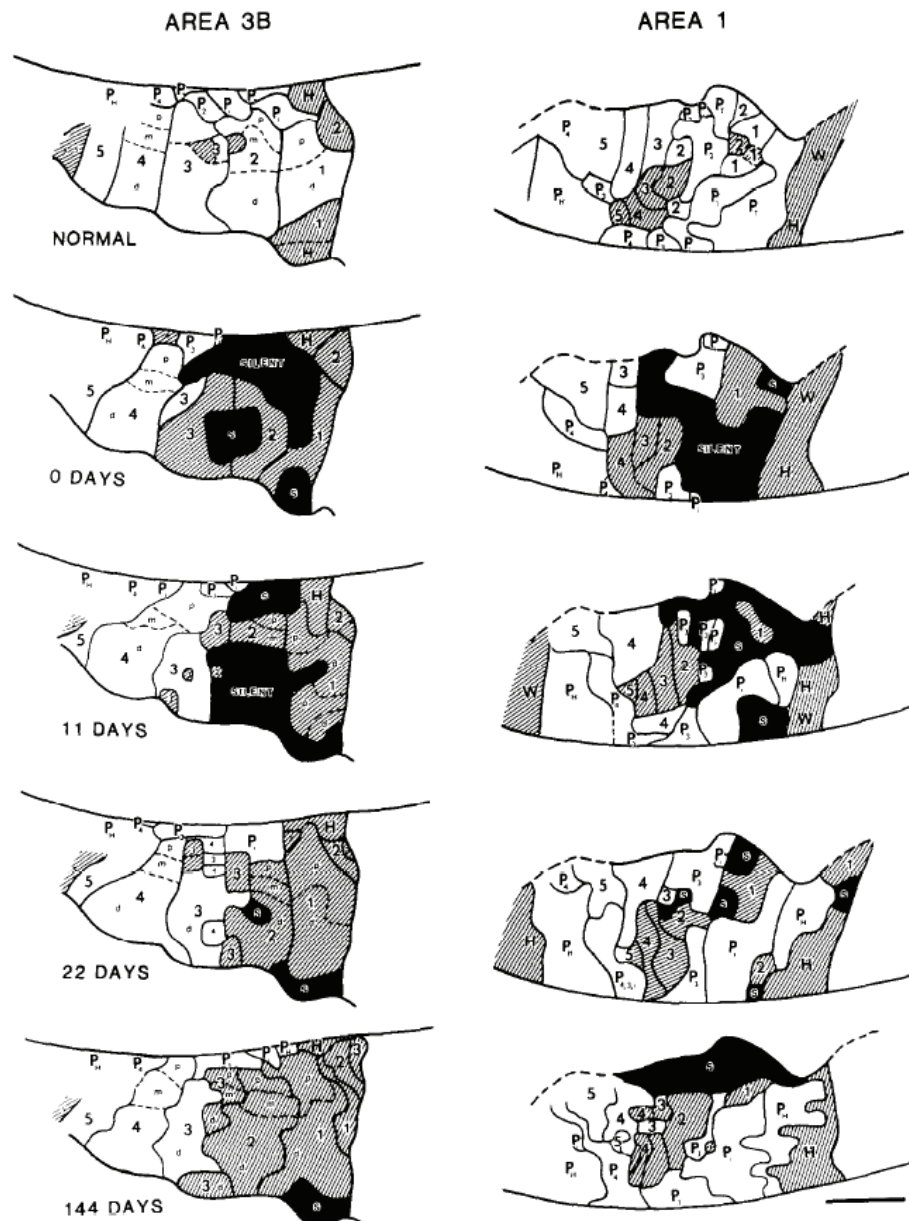


Figure 29 [from Merzenich et al., 1983b]. Progression of the reorganization of the cortical map in response to median nerve transection. Somatotopic representation of the hand in areas 3b (left) and 1 (right) derived from a single squirrel monkey before (top), immediately after, and 11, 22 and 144 days after transection of the median nerve. Numbers 1–5 represent the digits; the letters p, m, and d represent the proximal, middle, and distal portion of each finger. *Hatched areas* represent the dorsal surface of the hand, and *black* represents silent areas (not driven by cutaneous stimulation).

But in all cases, topographic plasticity remained relatively **local**, as most of the changes involved the representation of the intact, immediately adjacent digit or palm regions, without affecting the representation of more distant digits, such as digit 5 (D5). This reorganization consisted of an expansion of neighbouring cortical representations into the deprived cortex, resulting in new cortical maps which initially possessed a crude somatotopy that over time

transformed into a highly topographic representation. Some authors initially estimated that the major topographic changes were limited to a cortical zone extending 500-700 μm on either side of the initial boundaries of the amputated digits (Merzenich et al., 1984). In addition to this apparent “**spatial limit**” of reorganization, significant residual cortically silent regions have been found up to 2-8 months after multiple-digit amputation (Merzenich et al., 1984). This indicates that the deprived cortex failed to completely regain responsiveness even several months after the lesion, and suggests the existence of some additional limitations in the amount of possible reorganization at the cortical level. Interestingly, and in contrast with the findings of this multiple-digit amputation experiment (Merzenich et al., 1984), another monkey study found no evidence of unresponsive cortex 2-5 months following transection of both median and ulnar nerves, which deprives a larger cortical region of inputs from the glabrous surface of the entire hand (Garraghty and Kaas, 1991). Despite the larger amount of deprivation, the corresponding (deprived) cortical territories were in all cases responsive to the dorsal surface of the hand and/or digits innervated by the intact radial nerve.

The incongruity of these results compared to those reported in cases of more restricted “digit-amputation” (Rasmusson, 1982; Merzenich et al., 1983a, 1983b, 1984) led the authors to investigate whether the pattern of peripheral deafferentation could explain these discrepancies in the **limits** of cortical reorganization (Garraghty et al., 1994). To this aim, they induced in monkeys a deafferentation mimicking multiple-digit amputation by transecting either radial and ulnar nerves (D4-D5 amputation-like) or radial and median nerves (D1-D3 amputation-like). With such deafferentation patterns, and in agreement with Merzenich and colleagues' studies, the authors found that a large zone of the deprived area was still unresponsive 3-11 months post-lesion. In light of the opposite results obtained following ulnar and median nerves transection (Garraghty and Kaas, 1991), the authors thus concluded that incomplete reorganization occurs (at least in monkeys) only if the deafferentation involves both glabrous and hairy skin surfaces. Based on this interpretation, Garraghty and colleagues developed a model proposing the concept of “dominant” and “latent” inputs reaching the cortex. According to this model, “inputs from each of the three cutaneous nerves of the hand have a “dominant” cortical territory where neurons are activated in the intact animal, and an additional “latent” cortical territory where activation is possible after removal of competitively advantaged inputs” (see Garraghty et al., 1994). Supported by the evidence that new RFs located exclusively on the dorsal surface of the hand have been found in monkeys following median nerve transection (Merzenich et al., 1983a, 1983b), the authors suggested the existence of a preferential (and immediate) access of “latent” inputs from the radial nerve (but not the ulnar nerve) to the deprived “median nerve cortex”,

supposedly via an “unmasking” of existing horizontal connections or thalamocortical inputs that were previously suppressed by inhibitory circuitry. In line with the literature at this time, this study raised the idea that the reorganization that can occur in somatosensory cortex following peripheral sensory loss is **constrained** by the precise pattern of somatosensory deprivation, meaning that there is a **limitation** to the set of new RFs that cortical neurons can acquire. Moreover, this model also highlighted the idea of **competition** between inputs reaching the cortex, usually represented between adjacent cortical areas.

Remarkably, reorganization over a much greater scale was reported by Pons and colleagues in the early nineties, with the first demonstration of a massive cortical reorganization in **monkey SI** spanning over 1-2 cm across the hand-face border (Pons et al., 1991), while the previously reported reorganization following digit amputation (Merzenich et al., 1984) or median nerve transection (Merzenich et al., 1983a, 1983b) did not exceed a few millimetres. In this study, Pons and colleagues investigated the reorganizational changes within areas 3b and 1 of monkeys that had undergone somatosensory **deafferentation** of an entire forelimb (and upper trunk) more than **12 years** earlier (via dorsal root transection at C2-T4 level, i.e. dorsal rhizotomy). Typically, each side of the hand-face border region in macaque somatosensory cortex is composed of the representation of the chin and lower jaw on the face side, and of the representation of the thumb on the hand side (see Figure 12 and Figure 19). Electrophysiological recordings revealed that the **entire deprived arm area** (10 mm in extent) had developed novel responses to stimulation of neighbouring skin regions, including a relatively small portion of the **face (from the chin to the lower jaw)**. These results suggest that the cortical representation of the face had “taken over” or “invaded” the deprived cortical region initially representing the arm. Interestingly, the topographical organization was maintained within the reorganized/new face map in a highly systematic manner. As mentioned earlier, different types of deprivations can lead to different extents of reorganization. Just as deprivation induced by nerve transection or digit amputation differs in apparently significant ways (see Garraghty et al, 1994), there are also potentially significant differences between deprivations induced by rhizotomy and those induced by transection of peripheral processes. For example, many, if not most, dorsal root ganglion cells (and their central processes) survive section of their peripheral processes (see Wall et al., 1988), while with dorsal rhizotomy, the central processes of the cells lying in the rhizotomized ganglia degenerate, leaving vacated synaptic sites in central structures. This argument was considered to be a good explanation for the astonishing large-scale reorganization reported by Pons and colleagues (1991). However, similar large-scale plastic changes crossing the hand-face border have been subsequently reported within monkey areas 3b and 1 following

long-lasting (1-13 years) **hand or forelimb amputation** (Florence and Kaas, 1995; Florence et al., 1998, 2000). Thus the degeneration of dorsal root ganglion cells cannot fully account for this cross-border plasticity. Rather, as this amount of reorganization goes beyond the estimated limits of thalamocortical divergence (i.e., the maximal range of projection of a single thalamocortical axon, see Merzenich et al., 1983a; Jones, 2000), it has been proposed that sprouting at subcortical and/or cortical levels may account for the cortical magnification of plasticity (see Mechanisms section, page 91). In line with the previously mentioned nerve injury studies, these results suggest that the extent of cortical reorganization (and reactivation) depends on the **pattern** of deprivation (and pre-existing innervation) rather than on the actual extent of deprivation (at the skin and cortical level).

Similar to median nerve deprivation, compiling evidence comes from **trigeminal nerves lesion** studies, especially in rodents, which typically exhibit a well-ordered cortical organization of clearly distinguishable areas called barrels, each barrel processing the tactile information from a single whisker (see Petersen, 2007; Feldmeyer et al., 2013 as reviews). Consequently, lesions in the rat trigeminal system have become an important model for the study of CNS organization and pattern generation (see Brecht et al., 2003; Wilent and Contreras, 2005; Erzurumlu et al., 2006; Pouchelon et al., 2012; Ramirez et al., 2014 and Wu et al., 2011 as a review) and its neuroplastic effects have been studied extensively (see Fox, 1992; Phoka et al., 2012 and Feldman and Brecht, 2005; Frostig, 2006; Margolis et al., 2014 for reviews). It is well demonstrated, for example, that if all the whiskers but one are removed - by follicle destruction, plucking or trimming, which can be considered as an “amputation” - the cortical representation of the spared whisker typically expands (thus overlapping with the adjacent ones) and becomes more responsive (Fox, 1992, reviewed in Feldman and Brecht, 2005). Similarly, infraorbital nerve crush¹ immediately results in a large cortical area unresponsive to vibrissal deflection, but instead responsive to stimulation of the forepaw **digits** (Kis et al., 1999), suggesting an expansion of the digit representation into the barrel cortex. This expansion was still observed 3 weeks after injury and the cortical maps fully returned to their initial state 60 days after injury. Together with the monkey literature on amputation, these results show that plasticity **across the cortical hand-face border** is bidirectional, the face representation invading that of the hand following its amputation/deafferentation, but the opposite being also possible, with the hand representation invading that of the deprived face.

¹ Nerve crush is a commonly used procedure in which a nerve is squeezed, thus blocking transiently the signal conduction, but without sectioning the nerve fibres, which allows for recovery and regeneration.

In humans, a similar large-scale remodelling occurs in somatosensory areas following sensory deprivation, the one occurring across the hand-face border being particularly well documented. Indeed, marked intrusion of the face representation into the former hand area has been repeatedly found in the contralateral postcentral gyrus of upper-limb amputees using EEG/MEG (Elbert et al., 1994; Yang et al., 1994; Elbert et al., 1997; Flor et al., 1995, 1998; Knecht et al., 1996a; Birbaumer et al., 1997; Montoya et al., 1998; Grüsser et al., 2001a, 2001b; Karl et al., 2001) and fMRI (Borsook et al., 1998). Moreover, the amount of cortical plasticity found in humans (13-35mm in Yang et al., 1994; 13mm in Elbert et al., 1997; 17mm in Knecht et al., 1996a), inferred from the amount of shift of the face representation into the deprived area, was found to be similar to that observed in monkeys (1-2cm, Pons et al., 1991). The face regions invading the deafferented arm/hand cortical area comprised alternatively the chin, lower jaw and cheek (Yang et al., 1994), the chin (Elbert et al., 1994; Flor et al., 1995), the lip/corner of the mouth (Flor et al., 1995, 1998; Birbaumer et al., 1997; Elbert et al., 1997; Montoya et al., 1998; Grüsser et al., 2001a, 2001b). However, no systematic mapping of the face was performed in these studies on amputees, which would provide a clearer idea of which face regions are involved in such plastic changes and to which extent these changes occur. In addition, some plasticity of the trunk representation, the other neighbour of the hand/arm representation, has also been observed, in the form of an extension of its representation into the hand/arm representation (Kew et al., 1997). The variability in the amount and in the topography of cortical plasticity, on top of methodological differences across studies, is likely to arise from other confounding variables such as the age at which the amputation occurred, the amount of time since the amputation, the level of the amputation and thus the size of the residual limb, the cause of the amputation (traumatic or for therapeutic reasons), and the presence of phantom sensations and pain. Indeed, traumatic amputees experiencing phantom pain exhibit a higher amount of plastic changes (22.2mm in Flor et al., 1998; 20.25mm in Birbaumer et al., 1997; Grüsser et al., 2001a), than pain-free amputees (2.7mm in Flor et al., 1998; 3.36mm in Flor et al., 1995; Birbaumer et al., 1997; Grüsser et al., 2001a). The amount of reorganization observed has also been closely related to the degree of telescoping sensation and painful referred sensations (Grüsser et al., 2001a) (see Functional consequences section, page 115).

Altogether, these studies in monkeys and humans reveal that a decrease in sensory input following hand/arm **amputation or deafferentation** results in an “invasion” of the deprived cortical representation primarily by the neighbouring cortical areas such as the face and the trunk, whose innervation has remained intact. However, it is worth noting that in most of these studies reporting a massive cortical reorganization, a massive loss of **motor outputs** co-occurs with the loss of somatosensory inputs. Indeed, nerve injury and amputation of a limb involves the complete and sudden truncation of all the afferent and efferent fibres that were innervating this limb, triggering an extensive reorganization in the somatosensory cortex, but also in the motor cortex (Ojemann and Silbergeld, 1995; Pascual-Leone et al., 1996). In both cases the cortical regions surrounding the representation (including the face) of the deafferented/missing limb expand into the deprived cortex. Given the close interaction/strong interconnectivity between SI and M1 (Porter, 1997; Rocco and Brumberg, 2007; Catani et al., 2012), the concurrently induced motor plasticity is likely to contribute extensively to the large-scale cortical plasticity reported within SI, but also to the associated subcortical changes (see Mechanisms section, page 91). In addition, and more importantly, cortical neuroplastic changes are not restricted to the cortex contralateral to the deafferentation/amputation, but also affect the **ipsilateral hemisphere** (i.e., “intact hemisphere”), taking the form of expressed as an expansion of the intact hand’s representation (Calford and Tweedale, 1990; Elbert et al., 1997; Werhahn et al., 2002). This remodelling is likely to arise from an inter-hemispheric disinhibition (Werhahn et al., 2002; Simoes et al., 2012), but also from use-dependent plasticity induced by a compensatory over-use of the intact limb (Elbert et al., 1997). Over-use of the remaining limb is also the most likely explanation for the increased representation of the intact hand recently reported within the deprived cortex of the ipsilateral hemisphere (i.e., contralateral to the amputation; Frey et al., 2008; Bogdanov et al., 2012; Makin et al., 2013a). The fact that major plastic changes also occur within the ipsilateral hemisphere has to be carefully kept in mind when (re)reading the human studies referring to large-scale plastic changes. Indeed, many of these studies (Elbert et al., 1994; Flor et al., 1995, 1998; Birbaumer et al., 1997; Grüsser et al., 2001a; Karl et al., 2001) quantified the cortical changes by comparing both hemispheres, because they assumed the ipsilateral one to be “intact” and unchanged. This could have led to misleading results.

b. Central lesion or injury

One way of avoiding confusion in assessing plasticity comes from cases of partial or complete transection of the dorsal columns, which prevents specifically the somatosensory inflow from the spinal cord. Unilateral transection of the dorsal columns at the C3/C4 level disrupts afferents from the entire hand (and lower body), while leaving intact some inputs from the arm, as well as those from the face. Consequently, such a lesion performed in monkeys extensively deprives portions of the forelimb, trunk, and hindlimb cortical representations in area 3b (Jain et al., 1997). A large number of studies described massive reorganization following such deafferentations (reviewed in Kaas et al., 2008; Xerri, 2012; Nardone et al., 2013; Qi et al., 2014). In particular, large-scale cortical changes across the hand-face border similar to those reported by Pons and colleagues (1991) were observed within BA3b of these monkeys 6 to 22 months and up to more than one year after the lesion using microelectrode recordings (Jain et al., 1997, 2000, 2008; Tandon et al., 2009), and more than two years after lesion using fMRI (Dutta et al., 2013). Here again, the reorganization was expressed as an “invasion” of the deprived hand territory by the neighbouring cortical areas (namely the representations of the face and arm), but dominantly by the face representation (see Figure 30 A-C). Interestingly, in case of partial section preserving the afferents from digits 4 & 5 and the adjoining palm, these afferents not only continued to activate neurons within their normal cortical target territories, but after 5 or more weeks their area of activation greatly expanded, invading the deafferented cortical areas initially dedicated to the other regions of the hand (see Figure 30 D&E, Jain et al., 1997). Neurons in the reorganized parts of cortex exhibited large RFs and those responding to stimulation of the face had RFs located either on the face alone, mostly on the chin, or on both the hand and the face (Jain et al., 2008).

In rats, similar transection of the spinal cord, but at the midthoracic level, revealed that the deafferented hindlimb regions in SI became responsive to electrical stimulation of the unaffected forepaw as early as three days after the lesion (Endo et al., 2007). However, such reorganization was not observed when the forepaw (and any other body part) was mechanically stimulated (Jain et al., 1995). Indeed, these authors failed to detect any responses in the hindlimb cortical representation deafferented as a consequence of unilateral section of the dorsal funiculus at thoracic levels. Thus, in contrast to Endo’s study, Jain’s results suggest that forelimb inputs do not substitute for missing hindlimb inputs in SI in rats. The discrepancy between these studies may arise from the stimulation paradigms used to elicit post-lesion responses, the electrocutaneous stimulation used in Endo’s study being likely to activate the spinothalamic pathway in addition to the dorsal column pathways (Chang and Shyu, 2001). Interestingly, a

more recent study using mechanical somatosensory stimulation reported in addition to a large unresponsive cortical area, an expansion of the lower lip representation into the deprived forepaw representation within SI (Martinez et al., 2010), which is in line with the monkey results.

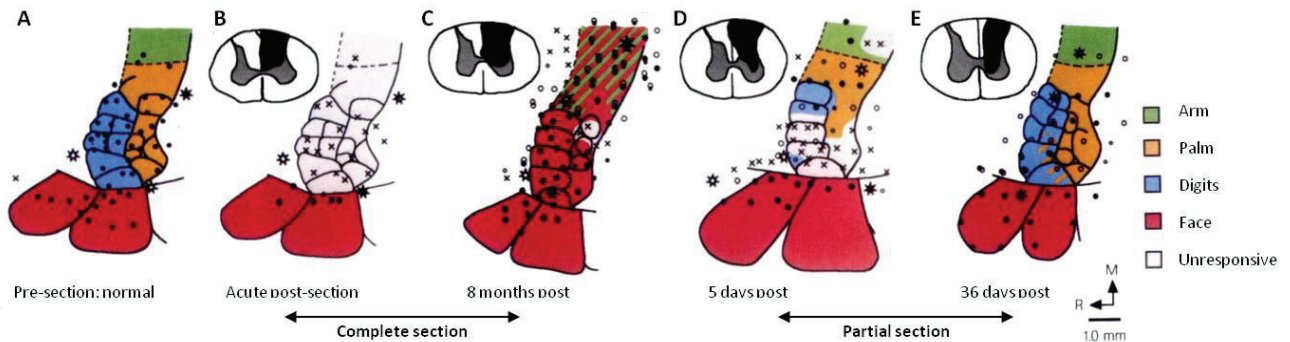


Figure 30 [modified from Jain et al., 1997]. Effects of unilateral dorsal column section at the C3/C4 level on the hand, face and arm representations in the contralateral area 3b. **A.** Normal map of an adult owl monkey in area 3b before, and **B.**, immediately after a complete contralateral dorsal column section. No responses are evoked in the hand region after section. **C.** Eight months after **complete** section, hand, arm cortex respond to stimulation of chin. **D&E.** From five to thirty-six days after a **partial** section, the initially unresponsive deafferented portions of the hand representation are progressively invaded by the cortical territory of the preserved dorsal column inputs from digits 4 and 5 and adjoining palm.

Unfortunately, in humans such focal lesions of the dorsal columns are rare, and obviously impossible to induce experimentally. Thus most of the human cases arise from spinal cord injuries, which can lead to lesion of several other tracts such as the spinothalamic or the motor descending fibres, making these cases quite similar to amputation cases. Together with the fact that motor impairments are the most incapacitating for the patients, most of the studies investigated the induced plasticity at the motor level (see Nardone et al., 2013 for a review). As an example, similarly to the previously reported study of midthoracic spinal cord transection (Endo et al., 2007), an expansion of the motor cortical hand area toward that of the leg was found in both hemiplegic and paraplegic patients using PET imaging (Bruehlmeier et al., 1998). Similarly, patients with complete thoracic spinal cord injury revealed a shift of the activation maxima evoked during elbow movement (Lotze et al., 1999). Other studies, however, investigated the consequences of spinal cord injury on the somatosensory system. For example, the study of a patient suffering from a complete spinal cord injury at the T6-level and who was experiencing referred sensations on the ipsilateral chest when the left or right forearm were stimulated, revealed the activation of both the forearm and the chest cortical representations

when the forearm regions inducing the referred sensation were stimulated (Moore et al., 2000). This was not the case for other parts of the forearms which did not induce referred sensations. Interestingly, these activation foci were separated by more than 1.6cm of nonresponsive cortex, suggesting that cortical plasticity can be expressed between nonadjacent representations. Plastic changes were also observed within SI following complete thoracic spinal cord injury, with the representation of the little finger shifting ~13mm medially toward the deprived lower body representation (Henderson et al., 2011). In addition, the amount of cortical reorganization was positively correlated with the gray matter volume in the deprived cortical area, and negatively correlated with the fractional anisotropy in the little finger representation.

Altogether, and despite some differences across species and the variability in the induced lesion, one can appreciate that similar to the amputation and nerve injury cases, the deafferentation induced by hemi-sectioning the spinal cord is followed by a massive somatosensory and motor cortical reorganization, the deafferented area being progressively invaded by its cortical neighbours. In particular, a lesion limited to the dorsal columns in monkeys, revealed exactly the same pattern of large-scale plasticity across the hand-face border, the face representation invading the deprived cortical area as soon as 6 months after deafferentation. However, results of such experiments can be difficult to interpret because, unlike nerve injury experiments, it is more difficult to consistently achieve the complete section of the dorsal columns without damaging pathways in the adjacent lateral and ventral tracts and the spinal gray matter. Conversely, it is also difficult to determine the extent and source of any remaining fibres, particularly if there are only a few.

Another way of evaluating the patterns of cortical reorganization is to ablate a part of the cortex dedicated to a body part to observe how the remaining cortex reacts (see Xerri, 2012 for review of plasticity following stroke). For instance, weeks to months after removing all cortex responsive to light touch on the glabrous surface of D3 in owl monkeys, some recording sites in cortex next to the lesion that were formerly responsive to other parts of the hand become responsive to D3 (Jenkins and Merzenich, 1987). Thus, there was recovery of some of the cortical inputs previously removed by the lesion. Yet, the amount of cortex activated by inputs from D3 remained relatively small, and larger lesions including the cortex devoted to digits 2-to-5 were not followed by the recovery of representations of these digits. Thus, there was a redistribution of the damaged representations that has been demonstrated both in the vicinity of the injury, and in remote regions. Indeed, following stroke involving the representations in cortical area 3b of specific skin surfaces in monkeys, a post-lesional re-emergence of the representation of the fingertips, engaged in a behavioural task, was observed in novel locations

within area 3b. In monkeys who had reacquired sensorimotor skill after retraining, an enlargement of the representation of the fingers in cortical area 1 was reported, as well as a striking emergence of a new representation of the cutaneous fingertips in area 3a, predominantly within zones that were previously excited only by proprioceptive inputs (Xerri et al., 1998). These findings support the existence of an experience-dependent post-lesional plasticity.

Altogether, there is evidence that somatosensory deafferentation, induced either via amputation, nerve injury or central lesions, induces massive cortical reorganization that is capable of “crossing” the hand-face border. The possible mechanisms underlying such a large-scale plasticity will be discussed later (see Mechanisms section page 91), but at this stage, one has to consider the fact that this massive reorganization has been reported following extensive lesions, which, as repeatedly mentioned along this section, brings some confounds as it removes other components such as **motor efferents** in the case of amputation, nerve or spinal cord injuries, but also proprioceptive and sometimes nociceptive afferents, and so on. Moreover, and more importantly, a **lesion** by definition consists of the section or destruction of fibres, which is likely to give rise to the death of their cell bodies and thus in turn leads to a massive atrophy and neuronal loss along the somatosensory pathway. Note that depending on the manner and the level at which the lesion is performed, the amount of neuronal loss is likely to vary, and thus may account for some of the variability observed across deafferentation types. Consequently, the plasticity observed following such deafferentations likely involves both specific and general compensatory phenomena and the intrinsic plastic property of the healthy brain. In addition, all the previously cited studies reporting large-scale plasticity across the hand-face border (except Jain et al., 1997; Kis et al., 1999) referred to long-lasting deafferentations, which had occurred at least 6 months before the related plasticity was investigated. Thus, in addition to its lesional aspects, such “**long-term**” plasticity is likely to involve and to be mediated by multiple mechanisms that may develop over time both sequentially and in parallel. Indeed, while several electrophysiological studies investigated the time course of **local** plastic changes (see the beginning of the section Peripheral lesion or injury; Rasmusson, 1982; Merzenich et al., 1983b), few studies reporting **large-scale** reorganization investigated the time course of these changes. Those who did confirmed the idea that different processes might be involved over time. For instance, while an expansion of the face representation into the deafferented hand region was reported within BA3b 6 months (Jain et al., 1997) or 22 to 23 months (Jain et al., 2008) after complete or partial unilateral dorsal column lesion in monkeys, this same region was found

unresponsive immediately after the lesion (Jain et al., 1997, 2008), thus revealing no reorganization at this early/acute stage. In contrast, a progressive reactivation of the deafferented hand region by the spared hand/palm afferents (already described above, see Figure 30) was observed 5 to 36 days after the lesion. That is, in-between the unresponsive state and the face “invasion” phase described at 6 months even after partial section of the dorsal columns (similar to the complete section case shown on the figure; Jain et al., 1997). Together with the studies on local (small-range) plastic changes, these studies underline the critical importance of time when considering plasticity, which intrinsically consists of ongoing processes. We should thus be careful when interpreting the results of experiments which usually take a single snapshot of this process at a given time point.

Having these caveats in mind, one could wonder what kind of plasticity occurs in an intact brain following deprivation of somatosensory inputs, especially on a short time scale.

c. Sensory deprivation without lesion

The closest non-lesional cases of sensory “deprivation” are the cases of **congenital malformation or aplasia**. In contrast to traumatic amputees, little or no cortical reorganization was found in congenital aplasics (6.9mm in Flor et al., 1998; Montoya et al., 1998). But the imaging resolution and the sample size used in these studies might not have been high enough to unveil the related cortical changes. In contrast, electrophysiological and tracer recordings in a monkey with congenital malformation of the left foot (missing toes 1, 3 and 5) revealed an abnormal arrangement of the foot representation throughout the lemniscal pathway (from spinal cord to area 3b) with an expanded representation of the plantar region, but also an abnormal representation of the intact foot in the ipsilateral spinal cord and area 3b (Liao et al., 2014). Note that this latter evidence of an ipsilateral reorganization is consistent with the previously raised point regarding the “intact” hemisphere. While the plasticity observed in these congenital cases is obviously non-lesional, it results from even longer time-scale changes that have taken place since the earliest developmental stages. This leaves the matter of short-term effects of sensory-deprivation unsolved.

A more viable way of answering such a question is to investigate the short-term reorganization occurring after local anaesthesia of a body part. For instance, **restricted anaesthesia** of a single toe in rats, leads to an expansion of the remaining toes RFs within 5min of deafferentation, the deprived cortical area becoming responsive to stimulation of neighbouring regions (Byrne and Calford, 1991; Calford and Tweedale, 1991). While these initial changes were quite similar to those found following digit amputation, as soon as the

anaesthesia wore off (~10-30min after anaesthesia onset), RFs shrank but never returned back to precisely the same boundaries as before anaesthesia. In addition, despite this shrinking, most of the RFs remained larger than originally (Byrne and Calford, 1991; Calford and Tweedale, 1991), suggesting some consequences at a longer time-scale. Similar results were obtained following local anaesthesia of the hindlimb (Panetsos et al., 1995), and anaesthesia of the perioral region of rats, with an immediate reorganization of the deprived barrel cortex which developed new (i.e., “unmasked”, see Mechanisms section page 91) tactile responses (Faggin et al., 1997; Katz et al., 1999).

Another way of “simulating” deafferentation effects without damaging the neural structures is via **environmental impoverishment**. Indeed, rats exposed for 80-115 days to an environment that reduces the otherwise typical tactile inflow, the topographic cortical organization is profoundly disrupted, with the forepaw representation in SI being interspersed with islets driven by proprioceptive inputs (see Figure 31; Xerri et al., 1996). In addition, the RFs recorded in the remaining cutaneous zones were drastically enlarged. Both cortical map shrinkage and RF enlargement were also observed in rats subjected to 7 days of forelimb **immobilization** (see Figure 31; Xerri et al., 1996) or to hindlimb unloading² for 2 weeks (Langlet et al., 1999; Dupont et al., 2001), which also dramatically decreases the rate of cutaneous stimulation. On a much longer time-scale, **age-related plasticity** can be considered as an even more naturalistic model of sensory deprivation. Indeed, when compared to young animal, similar RF enlargements and disruption/fragmentation of the somatotopic organization of cortical maps were reported in aged rats (Spengler et al., 1995; Coq and Xerri, 2000). The representational degradation was found to be partially offset or accentuated by housing in enriched or impoverished environments respectively (Coq and Xerri, 2001). In humans, an expansion of the hand representation (as assessed by an increased distance between D2 and D5 dipoles) close to 40%, was found in elderly as compared to younger participants (Kalisch et al., 2009).

² Hindlimb unloading consists in an experimental model of hindlimb sensory deprivation, which was commonly used in earth to mimic the effects of microgravity. This technic is characterized by the absence of weight-bearing and by a reduced motor activity, which also reduces considerably the activation of the cutaneous receptors located on the foot sole.

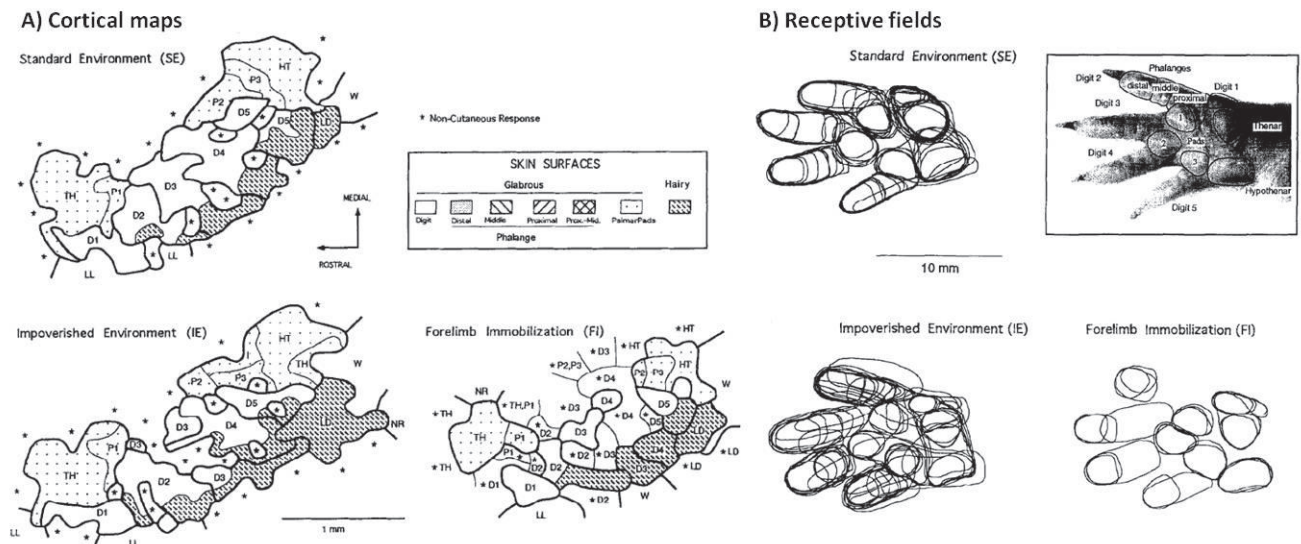


Figure 31 [modified from Xerri et al., 1996]. Effects of rats housing in an impoverished environment and of 7 days of forelimb immobilization on **A)** the hand representation within SI, and on **B)** SI receptive fields size and distribution. D1-D5: digits 1-5, TH: thenar pad, P1-P3: pads 1-3, I: insular zone, HT: hypothenar pad, LL: lower lip, W: wrist, LD: large dorsum.

In humans, the early studies investigating the effect of local anaesthesia on SI used ischemic nerve block (e.g., Rossini et al., 1994; Werhahn et al., 2002), which results in an acute and reversible deprivation of somatosensory and motor inputs, but also in ischemic pain. Other authors using drug anaesthetics reported also on burning pain during these procedures (Buchner et al., 1995). However, (phantom) pain is known to be closely related to cortical plasticity within SI (e.g., Flor et al., 1995; Wrigley et al., 2009; Gustin et al., 2012), making it difficult to distinguish the effects of somatosensory deprivation from the effects of pain produced by ischemic nerve block, or from some interaction of these factors. Rossini and colleagues (1994) overcame this issue by applying an anaesthetic cream on the ischemic fingers (i.e., four out of the five fingers, the remaining finger being either D1, D3 or D5). This procedure completed, the authors observed significant changes of the equivalent current dipoles (ECDs) of the remaining (unanaesthetized) finger after a relatively brief period of sensory deprivation (~20min). This plasticity was expressed by a shift of the dipole source of this finger towards the deprived area (corresponding to the four other fingers). Interestingly, while D1 and D5 respectively shifted towards the representations of the other (anaesthetized) fingers, D3 (i.e., middle finger) did not exhibit a shift of its ECD when the four other fingers (D1, D2, D4 & D5) were anaesthetized (Figure 32), which is remarkably consistent with the symmetry of the deprivation (two fingers deprived on each side of the tested finger). Considering that the ECD reconstruction corresponds more or less to the centre of gravity (CoG) of the representation, one can assume that while D3's

ECD did not shift, its representation could have enlarged, but symmetrically. This hypothesis was further suggested by the authors regarding the tendency of D3's ECD to deepen. Finally, and in agreement with the previously cited animal studies, the changes reported in this study took progressively place during the anaesthesia phase, but were persisting even immediately after sensation regain.

More recent human studies favoured the use of pharmacological anaesthesia (by injection or cutaneous application) to avoid pain induction. A similar expansion and shift of the neighbouring cortical areas towards the deprived region were found following 80min of forearm anaesthesia, with the hand representation expanding into that of the forearm (Björkman et al., 2009). Interestingly, within a similar time-scale (1h), anaesthesia of the radial and medial three-quarters of the hand resulted in a shift of both the lower lip and D5 cortical representations towards each other (see Figure 32; Weiss et al., 2004). Their intact cortical representations being on each side to the deprived area, these shifts strongly support an “invasion”, likely mediated by an expansion of the lip and the unaffected finger representations into the partially deprived hand region. In addition, an increased amplitude of the N20/P20, P27 and N30 components of the somatosensory evoked potentials by stimulation of the median nerve were observed during anaesthesia of the ipsilateral ulnar nerve (Tinazzi et al., 1997). These components being known to be generated respectively in BA3b (N20/P20 and N30) and BA1 (P27), these results thereby suggest a strong modulation of SI activity in response to the deafferentation of a neighbouring region.

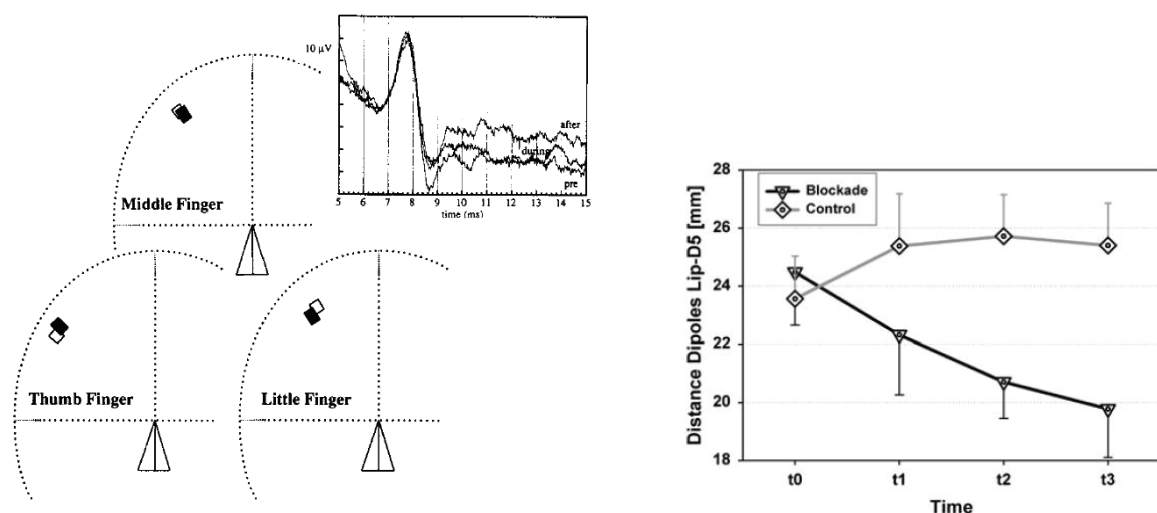


Figure 32 [from Rossini et al., 1994 & Weiss et al., 2004]. **Left panel:** Antero-posterior view of the localizations of the ECDs of the responses induced by stimulation of the test finger (either D1, D3 or D5) in the control phase (empty symbols) and when the four other fingers (non-stimulated) were anaesthetized (filled symbols) (note that the induced ischemic pain was relieved by application of an anaesthetic cream). **Right panel:**

Effects of local anaesthesia of the radial and median three-quarters of the hand on the cortical representations of the lower-lip region and D5 (assessed by distance between their respective ECDs).

Altogether, we can see that anaesthesia, even if transient, spatially local and preserving the integrity of the somatosensory pathway, may induce significant cortical reorganization within SI, and in particular appears to replicate similar large-scale cortical reorganization as those described following amputation, nerve or dorsal columns injuries, with the “invasion” of the face representation into that of the hand. Thus, cortical plasticity across the hand-face border can be induced following a pure deprivation of somatosensory inputs and on a remarkably short-term scale.

d. Mechanisms

A critical issue is to understand **how** large-scale/cross-border cortical changes are mediated in the adult brain. The first obvious point to take into consideration is that the topographic reorganizations observed after **long-term** deafferentation (i.e., amputation, nerve injury and spinal cord injury) are not limited to the cortex, but rather occur at each relay of the somatosensory pathway. Indeed, similar to that found at the cortical level, an invasion of the deafferented area by the neighbouring regions was observed in the ventroposterior nucleus of the **thalamus** following peripheral nerve injury (e.g., Churchill et al., 2001), unilateral dorsal column lesion (e.g., Graziano and Jones, 2009), or amputation (e.g., Rasmusson, 1996; Chowdhury et al., 2004). But none of these studies investigated whether large-scale plasticity occurred across the hand-face border. The only evidence of such plastic changes at the thalamic level was reported following long-lasting (ranging from 18 months to 12 years) deafferentation by **lesion**, such as dorsal root section (Jones and Pons, 1998), unilateral dorsal columns lesion (Jain et al., 2008), and amputation (Florence et al., 2000). Similar to that found in BA3b, this plasticity was expressed by an expansion of the face representation into the deprived forelimb region of the ventroposterior nucleus of the thalamus. In humans, the use of microelectrode recordings revealed that the thalamic representation of amputees' stump was increased (Lenz et al., 1998), invading that of the amputated limb (Davis et al., 1998). In addition, the thalamic firing pattern was also increased (Lenz et al., 1998). It seems, therefore, that the thalamus exposed to input-deprivation reacts with the same long-term topographic plastic phenomena as the cortex. At the **brainstem** level, expansion of the intact neighbouring representation was also found to occur after cutting of the median and ulnar nerves to the hand (Churchill et al., 2001), transection of the dorsal roots caudal to L3 (Dostrovsky et al., 1976), long-lasting (> 1 year)

amputation (Florence and Kaas, 1995; Jain et al., 2000), or dorsal columns lesion (Jain et al., 2000). The latter two studies specifically reported a similar expansion of the brainstem face representation into that of the deprived hand area.

Conversely, reorganization of the adult brain following hand deafferentation also takes place in **higher somatosensory areas** such as SII and PV (Tandon et al., 2009). Interestingly, while in BA3b the invasion concerned only the chin representation, at ~30% of the recording sites in areas SII and PV the expanded face representation did not include chin inputs, but included instead other parts of the face such as the upper-lip, the cheek or the whole hemiface, which is consistent with the integrative property of these higher order areas. Similar differences in the details of reorganization were reported between the ventro-posterior thalamic nucleus and BA3b (Florence et al., 2000; Jain et al., 2008). Moreover, Tandon's study also suggests that the spinothalamic pathway, which remained intact, is unlikely to play a role in the observed large-scale reorganization as its integrity did not prevent the large-scale expansion of the face representation in SII and PV. Consequently, since there are two major inputs to area SII and PV in primates, namely area 3b and direct thalamic inputs from the VPI nucleus (which receives dense inputs from the spinothalamic tracts), the authors concluded that the reorganization observed in areas SII and PV is likely to arise from and reflect changes in area 3b, which is the only source of altered inputs to SII and PV.

Altogether, these findings show that the extensive reorganization following long-term lesion-related deafferentation occurs at multiple levels along the neuraxis. This suggests that the large-scale cortical reorganization is likely to reflect that observed in the ventroposterior thalamic nucleus that may, in turn reflect that which occurs in the cuneate nucleus of the brainstem. It has been proposed that such processes could be mediated by **sprouting** of new connections targeting the dorsal horn of the spinal cord and the brainstem, as observed in adult macaque monkeys after forelimb or hindlimb amputation (Florence and Kaas, 1995; Wu and Kaas, 2002). In a similar way, neonatal forelimb removal (Lane et al., 1995) or dorsal root avulsion (Sengelaub et al., 1997) in rats resulted respectively in invasion of the cuneate nucleus by sciatic nerve primary afferents or by gracile projections. Interestingly, sprouting and growth of intact face afferents was also reported from the trigeminal **brainstem** complex into the cuneate nucleus (Jain et al., 2000). Similar connections from the trigeminal to the cuneate nuclei have also been reported following injection of tracers in the trigeminal ganglion (Marfurt and Rajchert, 1991). Although the spread of axon terminals in the **cuneate nucleus** is limited, it undoubtedly activates a number of cuneate neurons, which relay to the contralateral **ventroposterior thalamic nucleus** where an even larger area of the deprived nucleus may be

activated (Davis et al., 1998; Jones and Pons, 1998). Then, a relay from the ventroposterior nucleus to area 3b probably further amplifies the process, so that an even more extensive reorganization may occur in the cortex, likely with the help of other mechanisms, including unmasking of previously existing connections at different processing levels (further described below). In addition, sprouting has also been reported in the somatosensory **cortex** (Florence et al., 1998), with expanded lateral connections in BA3b and BA1 following long-lasting amputation and constraint forelimb. Thus the somatosensory cortical reorganization may benefit from both local and bottom-up convergence/divergence processes along the somatosensory pathway, relatively small modifications at the periphery ending up magnified at the cortical level by the divergence of neuron projections (see Figure 33 and Kaas et al., 1999; Jones, 2000 for reviews). In agreement with this hypothesis, a slow but progressive withdrawal of lemniscal and thalamocortical axons has been reported following cuneate tract section at the cervical level in monkeys (Graziano and Jones, 2009), while dendritic arbors reorganization resulting in a medial shift of the hand-face cortical border has been observed in rats following forepaw deafferentation (Hickmott and Steen, 2005). Conversely, similar considerations have been offered for the alterations at subcortical levels, which receive the strong top-down regulatory influence of efferent connections from the sensory cortex to the thalamic and brainstem/spinal relays (Ergenzinger et al., 1998; Kaas, 1999).

In humans, an abnormal pattern of intrinsic connectivity has been reported within the deafferented SI hand/arm area of amputees (Kew et al., 1997). In addition, the reorganization within SI induced by complete thoracic spinal cord injury was found to be negatively correlated with local changes in fractional anisotropy (as SI reorganization increased, the extent of “aligned structures” decreased) (Henderson et al., 2011), which could reflect intracortical changes in fibre density, axonal diameter or myelination. These results support the idea that SI reorganization results from sprouting of new lateral connections.

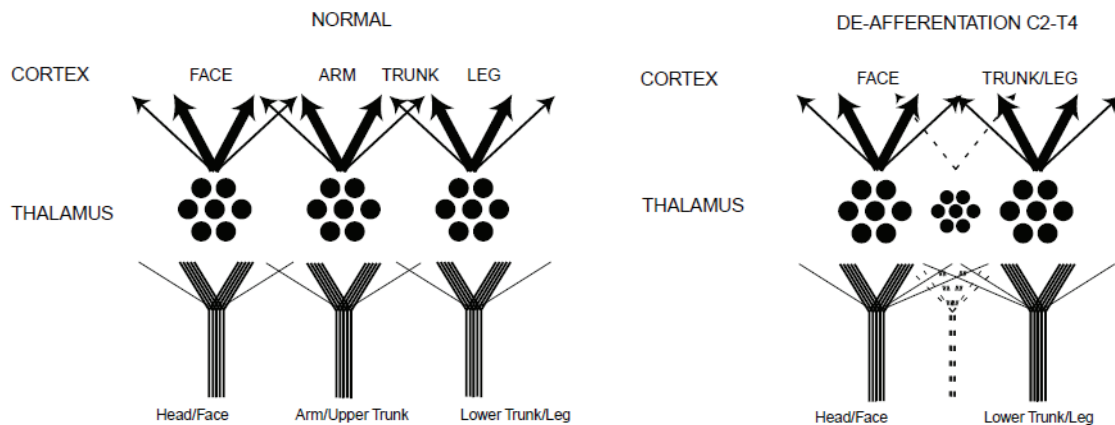


Figure 33 [from Jones, 2000]. Schematic representation of the sequential divergence in the projections along the somatosensory pathway from the dorsal column and trigeminal nuclei to the ventroposterior thalamic nucleus before reaching the somatosensory cortex in a normal monkey (left panel) or in a monkey who underwent a dorsal root section at the C2-T4 level. This deafferentation leads to atrophy and reorganization within the thalamus, which is then magnified at the cortical level, giving rise to the face and trunk invasion into the deafferented cortex.

Note that the most rapid changes mentioned above involved reorganization of the dendritic arborization (Hickmott and Steen, 2005), which took place progressively from 7 to 28 days after deprivation. While such changes can be considered to occur on a short-term time scale compared to sprouting and axonal withdrawal processes, they resulted in a mean shift of the hand-face border reaching 250µm at the final stage. Thus, even if occurring over a period of weeks, these processes cannot account for the large-scale reorganization that has been observed within shorter time-scales. Indeed, numerous studies have shown that reorganization (i.e., “invasion”) between neighbouring areas can occur within hours or even minutes after sensory interruption in animals, and has been observed within each relay of the somatosensory pathway. For instance, local **cortical** reorganization occurs within a few minutes following restricted (single-digit) amputation (Rasmusson and Turnbull, 1983; Calford and Tweedale, 1988, 1991; Byrne and Calford, 1991), or nerve injury (Merzenich et al., 1983b). Similar changes within the **thalamus** have been reported following anaesthesia (Nicoletis et al., 1993; Shin et al., 1995) or single-digit amputation (Shin et al., 1995). In contrast, no change in response magnitude was found in rats following whisker deprivation (see Fox et al., 2002 for review). Finally, short-term plasticity at the **brainstem** level was found after anaesthesia (Pettit and Schwark, 1993), or dorsal root transection (Dostrovsky et al., 1976). In addition, a few electrophysiological studies simultaneously recorded within several relays along the neuraxis. Local **anaesthesia** (via lidocaine injections) of the maxillary gum, the whisker pad or in different regions of the upper lip of rats revealed an immediate and simultaneous sensory reorganization at all levels of the

neuraxis, with an expansion of the remaining RFs and the deprived region becoming responsive to neighbouring whiskers (Faggin et al., 1997). Moreover, no significant differences between the overall spatial extent of reorganization and the percentage of neurons exhibiting unmasked responses in the cortex and thalamus were found, suggesting that reorganization evenly occurred along the whole system. Similar changes within the VPM thalamic nucleus and SI have been reported following capsaicin injections in the lip of rats (Katz et al., 1999), which strongly stimulated nociceptive fibres before silencing them. Here again, RF change rates were comparable in SI and VPM (57-49%). Altogether, one can see that within minutes, the whole somatosensory pathway is capable of reorganization following transient or lesion-induced inputs deprivation. But note that all the short-term topographic changes observed in these studies were limited to the neighbouring unaffected parts of the same limb that was undergoing the sensory deprivation. Reorganization at a larger-scale, for instance across the hand-face border, was not investigated.

Another study investigating the changes along the neuraxis reported that trigeminal nerve crush in rats induced few or no short-term changes with the brainstem (Pr5) and thalamus (VPM). Shortly after nerve crush (starting from a few minutes), the large unresponsive cortical vibrissal representation responded to stimulation of the forepaw digits but, surprisingly, to no other parts of the face (see Figure 34; Kis et al., 1999). This expansion was still present 3 weeks after injury (~10 days after nerve regeneration onset) and cortical maps fully returned to their initial state by 60 days after crushing. These results show that, while a few plastic changes take place in the brainstem and thalamus following transient peripheral deafferentation, an **immediate** (and most) significant reorganization was observed at the cortical level (i.e., SI) across the hand-face border, with an expanded representation of the digits that, though transient, was stable for at least 3 weeks. Thus, while the role played by plasticity taking place in subcortical structures remains somewhat controversial, the cortical reorganization occurring within minutes after sensory loss has been clearly demonstrated. Note that despite the fact that such plastic changes could be considered as short-term as those reported by Hickmott and Steen (2005) (from 7 to 28 days), the amount of reorganization observed across the hand-face border here is at the *mm* scale rather than the *μm* scale.

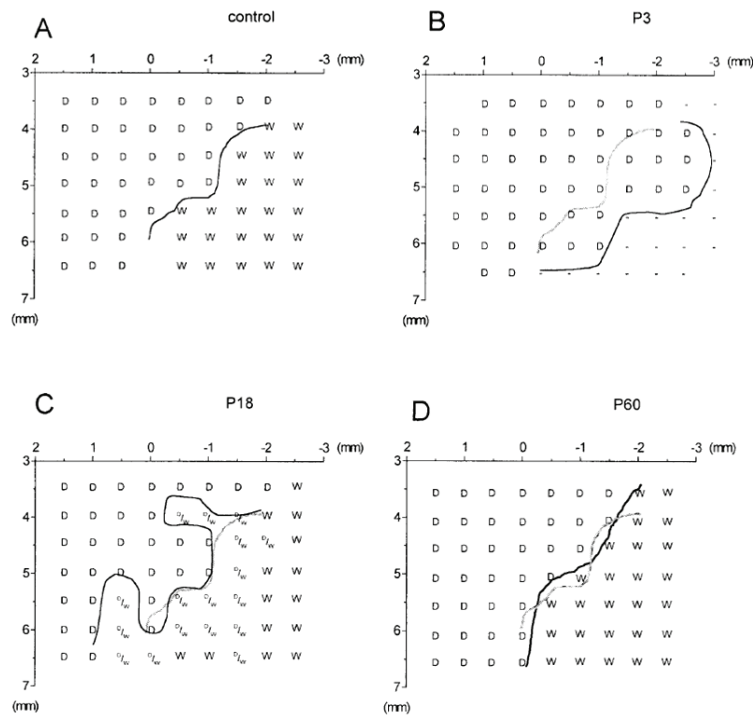


Figure 34 [from Kis et al., 1999]. Reorganization in SI digit and whisker representations induced by crushing and subsequent regeneration of the contralateral infraorbital nerve. (A) Representation of the posterolateral border between digit and whisker representations at baseline. (B) Contralateral trigeminal nerve crush resulted in a large unresponsive area to whisker stimulation invaded by responses evoked by digit stimulation 3 days after nerve crush, resulting in a shift of the hand-face border into the deprived area. (C) The expanded digit representation and the return of whisker responses (at 7-10 days after crush) resulted in an overlapping zone exhibiting responses to both digital and vibrissal stimulation. (D) 60 days after crushing, the hand-face border almost regained its original location.

In **humans**, short-term plastic changes have been found at the cortical level following **anaesthesia** of part of, or the whole upper-limb (Rossini et al., 1994; Tinazzi et al., 1997; Weiss et al., 2004; Björkman et al., 2009; Petoe et al., 2013). But here again, few studies investigated large-scale reorganization across body-parts. Björkman and colleagues reported an expansion of the hand representation into that of the anaesthetized forearm around 80 minutes after deprivation (the face representation was not investigated in this study). Weiss and colleagues (2004) reported that the cortical representation of the lower-lip invaded the deprived D1/D2/D3 cortical region within one hour of pharmacological blockade (Weiss et al., 2004). Interestingly, while long-term disruption of median nerve transmission due to carpal tunnel syndrome (symptoms > 11 months) was associated with increased somatosensory evoked potentials (SEPs) at the spinal, brainstem and cortical levels (Tinazzi et al., 1998), no change at the spinal and subcortical levels were found following transient (non-lesional) anaesthesia of the ulnar

nerve (Tinazzi et al., 1997). Instead, markedly increased SEPs were reported at the cortical level, with in particular, a more pronounced reorganization within BA3b as compared to BA1 (Tinazzi et al., 1997). This latter result is in agreement with electrophysiological results showing more marked RF reorganization within area 3b than in area 1 (Merzenich et al., 1983a, 1983b). Knowing that the carpal tunnel syndrome in the former study was associated with median nerve lesions at the distal territories, the two studies suggest that different processes might subserve the reorganization induced respectively by long-term lesional somatosensory disruptions (such as nerve & spinal cord injuries, amputation) and short-term reversible interventions (such as anaesthesia). Together with the electrophysiological results previously mentioned, the likely contribution of subcortical structures to the cortical reorganization has to be further demonstrated and clarified, especially following transient non-lesional deprivations. But apart from this consideration, these studies all agree on the fact that somatosensory deprivation induces a rapid cortical reorganization, which can occur over a large-scale.

Given that these short-term plastic changes occur too quickly to be subserved by collateral sprouting, or any other changes in neuronal morphology, one potential explanation is the **unmasking** of previously existing, but silent connections (Merzenich et al., 1984; Nicolelis et al., 1993; Rossini et al., 1994; Faggin et al., 1997; Tinazzi et al., 1997; Katz et al., 1999). The most likely mechanism for unmasking is a **disinhibition** of these previously silent connections (Jacobs and Donoghue, 1991; Tremere et al., 2001a, 2001b; Weiss et al., 2004; Lu et al., 2014). Indeed, the discreteness of cortical representations is actively maintained, at least in part, by **lateral intracortical inhibition** (e.g. Tremere et al., 2001b) emanating from a cortical zone receiving coherent input from regions of the body surface and exerting its influence on adjacent regions. Somatosensory deprivation may thus lead to changes in the **balance of excitatory and inhibitory** postsynaptic potentials with the neighbouring areas. Such changes have been found mainly for the GABAergic system (e.g., Jones, 1993; Tremere et al., 2001a, 2001b; Jasmin et al., 2003), GABA antagonists leading to a decrease of inhibition. Due to this disinhibition, the relatively widespread and previously silent thalamocortical projections (e.g., Rausell et al., 1998; Barbay et al., 1999) and cortico-cortical connections (Smits et al., 1991; Zarzecki et al., 1993) may become functional. This disinhibition would account for the rapid rate at which cortical reorganization can take place after a decrease in sensory inputs, by rendering the deafferented neurons hypersensitive to and thus activated by weak inputs coming from adjacent representations, which would otherwise be inhibited. This disinhibition is further supported by the numerous reports of an enhanced spontaneous activity (i.e., hyperexcitability) following deafferentation (e.g., Rasmusson et al., 1992; Taub et al., 1995; Knecht et al., 1996). The

disinhibition further implies an extended network of connectivity across somatosensory cortical representations to structurally support such a process. This “unmasking” of latent connections could later on be supplemented or even replaced by changes in synaptic efficacy, and/or by growth processes, such as sprouting.

Altogether, the plastic changes observed following different ways of inducing deafferentation (i.e., amputation, nerve and spinal cord injuries and anaesthesia), highlight that the induced reorganization evolves with time, and may thus depend on **different mechanisms having different time courses**, with short time-scale processes (minutes to hours), possibly relying on the unmasking of pre-existing -but silent- thalamocortical and cortico-cortical connections, and longer time-scale processes (weeks to months), possibly based upon the sprouting of thalamocortical and cortico-cortical projections. To these mechanisms, homeostatic processes can be added, aimed at regaining a balanced brain activity (Vitureira et al., 2012; Lu et al., 2014).

However, I would like to emphasize that despite the fundamental differences between somatosensory deprivation cases involving or not a lesion (already mentioned at the end of the II.a. and II.b. sections), both cases are usually considered to be similar and are jointly mentioned when referring to brain plasticity due to somatosensory deprivation. The processes subserving the induced plasticity are, however, likely different. Thus, a direct comparison of these two deprivation classes should be systematically investigated within the same species and obviously at equal, but multiple, time-scales. For instance, to my knowledge the effects of long-term anaesthesia at all levels of the neuraxis have not yet been investigated. In addition, while cortical reorganization could result from subcortical plastic changes, the converse also holds, with the effects observed at the subcortical level following anaesthesia possibly resulting from changes in corticothalamic connections (top-down regulation processes). Indeed, simultaneous recordings from the rat forepaw areas of both SI and VPL nucleus 20 minutes after anaesthesia onset (by injection of lidocaine), revealed a massive decrease of the thalamocortical connectivity and a small decrease of the corticothalamic (corticofugal) connectivity (Jung and Shin, 2002). Conversely, a non negligible number of corticothalamic connections were potentiated following anaesthesia onset (see Figure 35).

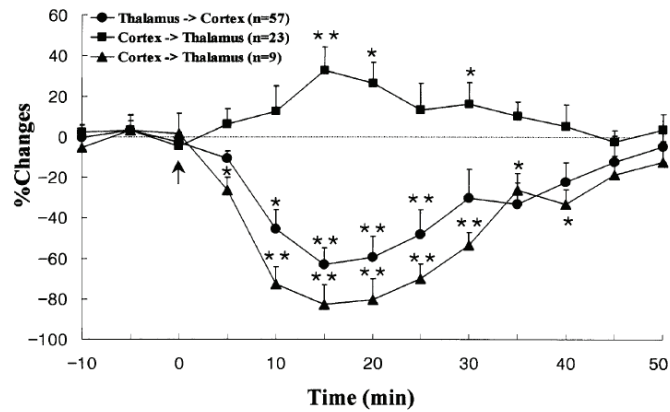


Figure 35 [from Jung and Shin, 2002]. Averaged temporal changes of synaptic strengths between SI and the VPL thalamic nucleus during forepaw anaesthesia in rats. The arrow indicates the onset of anaesthesia (i.e., the subcutaneous injection of lidocaine). * $P < 0.05$, ** $P < 0.01$, compared to the values in absence of anaesthesia.

In addition, the repeatedly observed invasion of the deprived territory by neighbouring representations following deafferentation has led to the concept of an ongoing process of **competition** between sensory surfaces for dynamic allocation of representational space (see Buonomano and Merzenich, 1998). Since then, competition-based plasticity has gained a large consensus among neuroscientists. Following deafferentation, however, the first consequence of the loss of somatosensory inputs is that a given cortical representation is rendered “empty” (i.e., deprived), thus allowing for potential competitive “invasions”. But what would happen in the absence of sensory deprivation? Which kind of plasticity could we observe across somatosensory representations following enhancement of somatosensory inputs? Could we still observe large-scale plastic changes with behaviourally relevant perceptual consequences? Would competition processes still be involved? To address these questions, a recent and quickly expanding field of research has started investigating the potential involvement of cortical plasticity as one of the processes subserving perceptual learning and recovery of function, both relying on an activity-dependent (also called experience-dependent) modulation of somatosensory inputs.

III. Activity-dependent plasticity

a. Restoration & modification of peripheral inputs in the context of rehabilitation

Complementarily to the deafferentation cases reported in the previous section, the most intuitive cases to study in regard of activity-dependent plasticity are patients who have undergone surgical restoration of peripheral inputs, either by allograft (transplantation) or nerve regeneration/redirection, as these cases allow us to assess whether deprivation-induced plasticity is reversible.

In monkeys, **nerve regeneration** following suture of a previously cut nerve is known to result in reactivation of much of its original cortical territory (for reviews, see Merzenich and Jenkins, 1993; Navarro, 2009). However, the somatotopic re-organization remains highly abnormal (Florence et al., 1994), many neurons having multiple RFs such that neurons at the same cortical site respond to stimulation of nonadjacent skin areas, and conversely, many parts of the skin innervated by the regenerated nerve being represented in non-contiguous chunks of cortex. In contrast, if a nerve is crushed instead of cut and allowed to regenerate, the axons regenerate into their original fascicles, and a complete restoration of cortical maps is observed. For instance following complete median nerve crush the digits' somatotopic organization within area 3b was fully restored 142 days after injury (Wall et al., 1983). Similarly, restoring inputs by means of nerve redirection induces an expansion of the SI representation of the re-innervated regions in rats (Marasco and Kuiken, 2010).

In humans, percutaneous microneurography performed 7 to 23 months following complete transection with subsequent **suture or graft** of the median or ulnar nerves revealed significant changes in RFs of SAI and FAI afferents, with multiple RFs innervated by a single afferent and unusually small or large RFs (Mackel et al., 1985). At the cortical level, similar median nerve transection and repair revealed that more than 1 year postoperatively the BOLD signal within SI evoked by stimulation of the hand covered a smaller area located more superiorly than the area activated in controls (Taylor et al., 2009). This decreased activity was co-localized with grey matter reductions, which were negatively correlated with measures of sensory recovery (mechanical and vibration detection). While these results from nerve repair cases clearly show the occurrence of cortical plastic changes in these patients, they do not clearly address the differential contribution of deprivation and repair-induced plastic changes. In contrast, **allograft** of a limb following amputation was found to at least partially reverse the deprivation-induced

plasticity. For instance, Giraux and colleagues (2001) showed that after bilateral hand graft, hand representations which were originally shifted towards that of the face due to deprivation, expanded toward their normal location 6 months after transplantation. A similar “recapture” of the pre-amputation SI hand territory was more recently found to occur as early as 4 months post-transplantation (Frey et al., 2008). Similarly, toe-to-finger **transplantation** was found to result in successful “substitution” of cortical representations in the long-term (average of 5 years post-transplantation), the transplanted toe being located in the expected location of the previously missing finger representation (Chen et al., 2006). In addition, the transplanted toe (now finger) exhibited an expanded representation compared to the other (normal) fingers. Interestingly, a quite recent study investigated the time course of cortical changes following similar transplantation, but over a shorter time-scale (Hadoush et al., 2012). Somatosensory evoked field (SEF) recordings revealed responses evoked by stimulation of the transplanted toe (now D2) as soon as 4 weeks after surgery, and its representation was found very close to that of the intact D5 of the same hand (ED = 3.7mm). But over time (weeks 12 and 24), this distance increased (to 5.9mm and 7.4mm respectively) as did the dipole strength (from 9nAm at week 4 to 17.3 nAm at week 12 and to 18.6nAm at week 24), whereas latencies decreased (from 76.5ms at week 4 to 69.7ms at week 12 and to 67ms at week 24). While these studies, both in animals and in humans, show that deprivation-induced plasticity can be partially reversed by restoring the missing inputs, the process of restoration and the end result could not be controlled which means that the amount of input restored is thus difficult to quantify and thereby difficult to link to the cortical reorganization induced by this restoration.

To overcome this issue, active increase of somatosensory inputs can be triggered in monkeys to evaluate and quantify the subsequent restoration of cortical organization (for a review, see Xerri, 2012). For instance, monkeys **trained** to perform a small-object retrieval sensorimotor task after having undergone cortical microlesion of the glabrous finger representation within area 3b, had a re-emergence of the representation of the fingertips engaged in the task, but in novel locations in areas 3b and 3a (Xerri et al., 1998). Following median nerve cut and repair, **sensory enrichment** was also found to increase the proportion of small and well localized RFs compared to monkeys raised in non-enriched environments (see Figure 36; Florence et al., 2001). Interestingly, these RF changes were consistently observed within area 3b, but not within the ventroposterior thalamic nucleus, suggesting that enhanced sensory inputs primarily affect cortical maps.

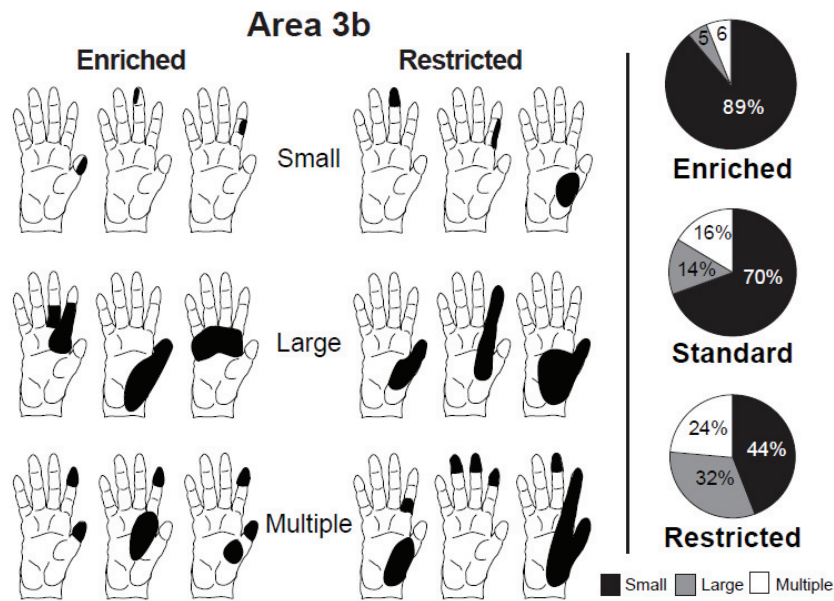


Figure 36 [from Florence et al., 2001]. **Left:** Examples of small, large and multiple RF classes in area 3b found in the monkeys that had sensory enrichment of the median nerve cut hand and in the sensory restricted monkeys. **Right:** Relative proportions of the three classes of RFs (small, large and multiple) in monkeys reared with sensory enriched, restricted or standard environments.

Together, these findings clearly demonstrate that deprivation-induced plastic changes at the cortical level can be mostly reversed by restoring somatosensory inputs. This is also true for plasticity occurring across the hand-face border. However, while such restoration-induced plasticity can be considered as activity-dependent plasticity, the restored inputs are highly perturbed due to the reafferentation process involved in the transplants, which inevitably leads to afferent changes and re-innervation errors. Accounting for these confounding aspects, a few interesting studies have investigated the plastic changes following therapeutic limb elongations performed in dwarfs. Such intervention, performed at the lower-limb level, results in an enlargement and in a progressive ventral shift of the foot representation in SI, but also in signal changes in the superior and inferior parietal regions (SPL and IPL) up to 6 months after intervention (Di Russo et al., 2006). This evidence highlights the fact that plastic changes also occur in the case of limb modification, likely due to the subsequent modification of the limb's use to adapt to its new length.

b. Use-dependent plasticity: naturalistic cases

Similarly, extensive training leading to an expertise in a given domain is also accompanied by use-dependent plastic changes. One type of expertise that has been studied is the one acquired by **musicians** throughout practice. For instance, the cortical representation of the digits of the left hand of string players, which are strongly solicited for rapid and precise individual movements on the strings, were found to be larger than that of their right hand (less solicited), or than the left fingers of non-musicians (Elbert et al., 1995). Interestingly, the amount of cortical reorganization in the representation of the fingering digits was correlated with the age at which the person had begun to play, but not with the amount of practice. This confirms the involvement of the plastic capacity of the CNS at early stages of life in such learning, as half of the studied musicians started to practice before the age of 10. A subsequent study further revealed that in string players, D2 and D1 were located more anteriorly and the D2-D5 distance was greater than in controls (Hashimoto et al., 2004). In the somatosensory modality, **blind people** learning Braille develop a highly sophisticated perceptual skill when they become proficient Braille readers. Using SEP recordings and transcranial magnetic stimulation (TMS), a larger sensorimotor cortical representation was found for the right index reading finger as compared with the left non-reading finger or with the right finger of non-Braille readers (Pascual-Leone and Torres, 1993). In contrast, representations of parts of the hand that were not solicited in Braille reading were smaller than in non-readers hands. Interestingly, in blind people who use more than one finger to read Braille, in addition to a substantial enlargement of the reading finger representations a disordered topographical arrangement of the finger representations has also been observed within SI (Sterr et al., 1998a, 1998b). In contrast, neither the disordered representations, nor comparable mislocalizations were observed in one-finger Braille readers or in sighted controls. These few examples clearly demonstrate that cortical representation changes not only follow sensory deprivation and can be reversed by restoring sensory inputs, but they show that intense use and practicing in a healthy context also results in plastic changes that seem to be the “inverse” of those observed after deprivation. But note that these expertise-related plastic changes follow either long-term training/practice, usually initiated during childhood when the brain exhibits higher plastic capacities, or are associated with long-term cross-modal plasticity (i.e., from vision to touch). So these cases might reflect rather extreme positions on the continuum of the plastic changes occurring in adult brain. Furthermore, “over-use” can also result in **pathological cases**. For instance, individuals who perform high precision hand movements such as musicians, engineers, architects and writers may become affected by focal hand dystonia, which has been shown to be associated with reorganization of

the dystonic (Braun et al., 2003) and non-dystonic (Meunier et al., 2001) hand representations in SI, but also with altered sensorimotor integration across fingers (Tamburin et al., 2002).

In animals, a similar naturalistic induction of use-dependent somatosensory plasticity can be achieved through **sensory enrichment**. Following the early evidence that environmental manipulations affect the areal organization of the cortex (e.g. Diamond et al, 1976), numerous electrophysiological studies, mainly performed in rats, highlighted the influence and relevance of naturalistic sensory solicitation. For instance, a pioneer study investigated the effects of natural nursing behaviour in rats on the cortical representation of the ventrum surface (Xerri et al., 1994; Rosselet et al., 2006). Compared to virgin or postpartum age-matched rats, lactating rats exhibited an enlarged representation of the ventral trunk skin, especially of the nipple-bearing skin (almost twofold), which was associated with a concomitant decrease in RF size. Interestingly, these cortical changes did not alter the topographical organization of SI, which remained well ordered. In monkeys, these authors described a similar expansion of the representation of the fingertips that were highly solicited in a difficult small-object retrieval task, with a closely corresponding reduction in RF size (Xerri et al., 1996). Similarly, rats housed for 80 to 115 days in an enriched environment exhibited a substantial enlargement of the cutaneous forepaw representation which was associated with smaller glabrous RFs and with fewer representational discontinuities (see Figure 37; Xerri et al., 1996; Coq and Xerri, 1998; see also Polley et al., 2004). Interestingly, this higher cortical magnification was predominant for the protuberant glabrous skin, more likely to be stimulated (i.e., digit tips and palmar pads), whereas the hairy skin representation remained unchanged (Coq and Xerri, 1998). Finally, neurons were more sensitive to light tactile stimulation in rats exposed to an enriched environment than in rats exposed to a standard environment. Altogether, these results demonstrate the importance of sensory experience, even at the adult stage, in modifying cortical representations, and corroborate the view that cortical representations are maintained in a permanent state of use-dependent fluctuation (see next section).

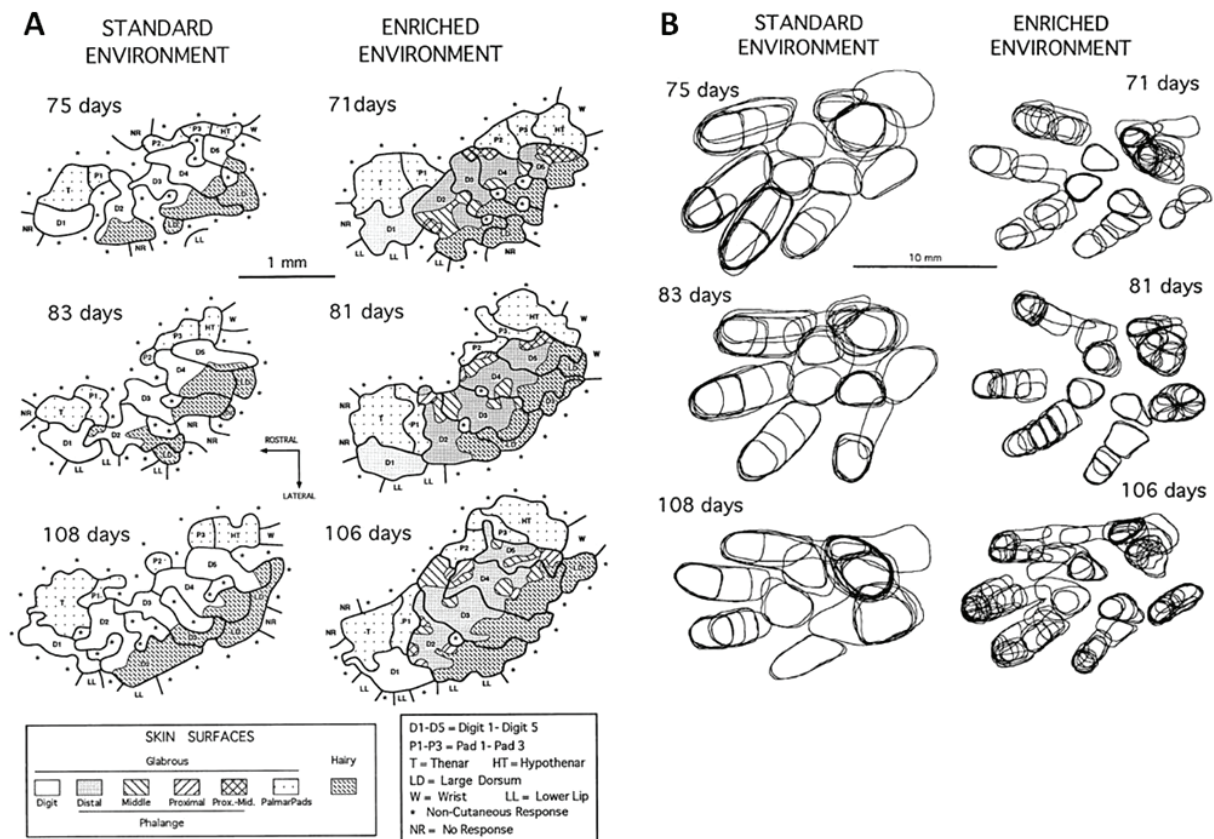


Figure 37 [from Coq and Xerri, 1998]. Influence of housing in either a standard or enriched environment (after different durations of housing) on **A**) electrophysiological maps of the skin surfaces of the forepaw within SI, and on **B**) the size and spatial distribution of glabrous skin RFs in the same rats. Multiple RFs are not shown.

As mentioned earlier (see the section Sensory deprivation without lesion page 87), the inverse situation of **immobilizing** a limb for one or more weeks, which also dramatically constraints and decreases the occurrence of somatosensory stimulation, results in both SI cortical map shrinkage and RF enlargement (Xerri et al, 1996; Dupont et al, 2001; Langlet et al, 1999). Similar results have been obtained in humans, but most reports refer to the plastic changes induced within the motor cortex. For instance, a decreased cortical area devoted to the unused anterior tibialis muscle was observed following ankle immobilization (Liepert et al., 1995), the amount of reorganization being correlated with the duration of immobilization and quickly reversed by voluntary muscle contraction. This latter fact led the authors to interpret the origin of these cortical changes as being functional rather than morphological. Similarly, subcutaneous injections of Botulinum toxin to treat hemifacial spasms (i.e., involuntary phasic or tonic contractions of facial muscles), induced an expansion of the contralateral motor “representation” of the hand ipsilateral to facial muscle contractions towards the face representation, as measured by TMS two weeks after treatment (Liepert et al., 1999). Recently,

however, similar injections (but for aesthetic purposes) were further associated with a reduction of event-related potentials (ERPs) induced by tactile stimulation of both thumbs, but at longer latencies (Haenzi et al., 2014). Thus, despite an obvious major contribution of reorganization of motor efferent signals, the somatosensory components are also affected by such interventions. But whether these changes arise from the direct “deprivation” of somatosensory inputs due to immobilization, or whether they arise from a “second-order” plasticity resulting from the motor reorganization remains unknown.

Altogether, the results mentioned in this section provide evidence that cortical representations are strongly modulated by “naturalistic” variations of either the environment or the use of a limb. But to my knowledge, in contrast with the deprivation-related plasticity cases, no systematic investigation of the spatial limits of such activity- or use-dependent plasticity has been attempted. However, note that both environmental- and use-related plastic changes involve a strong contribution of the limb motor component, either transplanted, immobilized or stimulated by its displacement in an enriched environment. Thus, even in these cases the pure contribution of increased somatosensory inputs is difficult to isolate. Despite this, these results provide a clear demonstration of the strong influence of both activity-dependent sensory inputs and motor outputs in driving cortical plastic changes.

c. Training-dependent plasticity

Along the same lines, but focusing more specifically on the somatosensory modality, changes in the somatotopic organization of cortical maps have been repeatedly observed following tactile training, which is easy to implement in laboratory conditions. For instance, reorganization of the hand representation was reported in monkeys who were trained over 10 days to maintain contact with a rotating disk, thus producing an extensive cutaneous stimulation of a restricted part of the skin on the distal phalanges of one or two digits (Jenkins et al., 1990). Similar to sensory enrichment cases, the observed reorganization was expressed in terms of an expansion of the cortical representations of these stimulated digits, associated with reduced cutaneous RF size. In addition, the borders between the representations of individual digits and digit segments shifted in parallel. Interestingly, a significant lateral translocation of the borders between the representations of the hand and the face was recorded in all cases, suggesting again a close interaction between these representations. Finally, the rostral border of BA3b was also shifted towards BA3a, which is normally activated by deep (proprioceptive) receptors, suggesting a potentiation of cutaneous over deep receptor activation (Jenkins et al., 1990). This latter hypothesis was then confirmed in animals trained to detect tactile frequency differences on a single digit segment over a period of 20 weeks (Recanzone et al., 1992c), in which an emergence of a large cutaneous representation of the trained cutaneous region was observed within BA3a, replacing the normal representation of deep receptors in this field. Two other studies from this series further investigated the cortical changes observed in these monkeys. Electrophysiological mapping of their hand representations within BA3b confirmed the previous report of Jenkins by revealing a 1.5- to 3-fold increase in the cortical representation of the stimulated skin location (Recanzone et al., 1992d). This enlargement was also accompanied by an increased topographic complexity, but also by larger and more overlapping RFs within the trained region (Recanzone et al., 1992d). This enlargement of RFs, which strikingly contrasts with the shrinkage repeatedly reported so far, is likely to arise from the fact that in this study, somatosensory stimuli were invariantly delivered to the same skin location (see the end of the section “Temporally paired cutaneous stimulation” for further discussion of this point, page 128). Additionally, the temporal response characteristics of neurons from BA3b revealed a sharpening of their response that could be accounted for by a large subpopulation of neurons that had highly coherent responses, suggesting an increased neuronal coherence (Recanzone et al., 1992e). Thus, in contrast to BA3a neurons, frequency discrimination training led to an alteration of spatial and temporal response properties of BA3b neurons, which was found to be correlated with changes in frequency discrimination performance (Recanzone et al., 1992e).

Together, these results confirm the preponderant role of BA3b in processing tactile information relevant for acuity performance and further demonstrate its involvement in tactile learning processes through training. In addition, these reports clearly highlight that solely increasing somatosensory input through **training**, even if at a restricted skin region, results in a consistent enlargement of the representation of the stimulated regions within BA3b, which can lead to alterations of the hand-face border.

In humans, a few studies investigated the cortical correlates of somatosensory training, but with less clear results than those of animal studies. For instance, humans trained over a 22 days period in a tactile frequency discrimination task similar to that used by Recanzone and colleagues did not show any changes of the cortical representation of the trained finger (left-D4) as assessed by MEG recordings, despite a steep and long-lasting behavioural improvement (Imai et al., 2003). In the spatial domain, another study reported changes in effective connectivity within both subcortical (bilateral insula, bilateral putamen, bilateral thalamus, and cerebellum) and pre-SMA areas rather than somatosensory cortical regions in participants who underwent a tactile microspatial discrimination training at the right-D2 fingertip over 14 sessions lasting ~1h each (Sathian et al., 2013). This spatial stimulation pattern consisted of three aligned dots, with the middle one being slightly off-set either towards the left or the right, yielding an arrow-like pattern whose direction had to be discriminated. Thus, in contrast to the previously cited monkey studies, the representational changes in humans induced by tactile training seem to be more difficult to capture, likely due to the poor spatial resolution of brain imaging techniques compared with invasive electrophysiological recordings. But despite this challenge, a larger number of studies investigating the cortical correlates of tactile learning is indeed required. Apart from these two studies in which a restricted cutaneous area was involved in the training phase, numerous studies in the late 90's - early 2000's combined training (either temporal or spatial) with what I will call “**pairing**” of different cutaneous regions, predominantly the fingers. This enthusiasm for pairing procedures arose from earlier studies demonstrating the crucial role of temporally correlated inputs in inducing macroscopic representational reorganization (more detailed in the next section, page 112) both in monkeys (e.g., Clark et al., 1988) and in humans (e.g., Mogilner et al., 1993), these studies having themselves inherited from classical electrophysiological studies investigating pairing-induced LTP processes at the synaptic level (i.e., Hebbian plasticity or spike-timing dependent plasticity, more detailed in next chapter, page 125).

One of the first studies in which somatosensory training was combined with finger pairing was performed by Wang and colleagues (1995) in adult owl monkeys. These authors had the ingenious idea of “reversing” the natural pattern of tactile stimulation within the hand by delivering a synchronous tactile stimulation across distal phalanges of several fingers (D2, D3 & D4), while another synchronous stimulation was delivered to the middle or proximal segments of the same digits, but both bars being jittered, thus inducing an abnormal asynchronous stimulation of within-finger segments. In addition to these cross-finger pairing and within-finger unpairing, monkeys were trained to temporally discriminate and recognize stimulation patterns over 4-6 weeks. Using electrophysiological recordings the authors found that the synchronous stimulation of the three fingers resulted in a “fusion” of their cortical representations in BA3b, whereas the finger segments to which stimuli were applied asynchronously had representations that were segregated more than usual (Wang et al., 1995). In addition, RFs corresponding to these cortical regions were found to enlarge to span over the multiple stimulated digit segments. Note that as in the study by Recanzone and colleagues (1992a, 1992b, 1992c, 1992d) described above, this many-fold RF enlargement is likely arising from invariant stimulated skin locations (discussed in section “Temporally paired cutaneous stimulation”, page 128). Interestingly, in addition to SI, these authors also investigated the VPL thalamic nucleus, and reported no changes at its level, supporting the idea that the induced representational changes are cortical in origin. A similar protocol applied in humans over a 3-4 weeks period revealed, in addition to a behavioural improvement, a significant training-related decrease in the magnitude of the current dipole strength corresponding to the source of the contralateral activity evoked by stimulation of the trained hand (Spengler et al., 1997). This decreased dipole strength was interpreted by the authors as either a decrease of the neuronal population contributing to the signal or a decrease in the temporal and spatial coherence in the evoked activity. Remaining in the tactile temporal domain, participants trained to detect changes in tactile frequency applied either to D2+D3+D4 or only to D2+D4 of the right hand, had modulated steady-state evoked responses for D3, which varied across the three days of training (Liu et al., 2000). While the results were difficult to interpret due to changes in strength of cortical activation across sessions, this study further illustrates how SI representational maps can be dynamically modulated by use/activity-dependent processes. Considering the fact that both sensory enrichment and training at a restricted single cutaneous region seem to induce an enlargement of the stimulated region's representation, an additional process is likely to be concurrently involved in the three previously mentioned studies (Wang et al., 1995; Spengler et al., 1997; Liu et al., 2000), the synchronous stimulation (or pairing) of non-adjacent cutaneous regions tending to move the stimulated

representations towards each other, eventually fusing them into a “new” representation with digit-overlapping fields. Interestingly, a more recent electrophysiological study in monkeys trained to detect temporal differences in tap pairs delivered to two adjacent digits (D1-D2 or D2-D3), revealed that absolute synchrony is not necessary to induce “fusion-like” cortical changes as demonstrated by Wang and colleagues (1995). Indeed, after 4 weeks of training, similar cortical reorganization of fingers representations were observed with stimulus onset asynchronies ranging from 100 to 200ms (Blake et al., 2005). Note that, as in Recanzone and Wang's studies, RFs at sites responsive to the taps enlarged more than twofold (discussed in section “Temporally paired cutaneous stimulation”, page 128). In humans, an additional study further underlined the importance of inputs temporal characteristics, but also the role of attention in representational changes. Participants performed the same (micro)spatial discrimination task as in Sathian and colleagues (2013) (i.e., three dots arrow-like pattern), but in contrast to that study, training was simultaneously applied to left-D1 and left-D5 over a period of 4 weeks (~20h). Interestingly, while EEG recordings during training (in which participants had to identify the direction of the “arrow”) revealed an increased distance (in ED and theta polar angle) between D1 and D5 cortical representations, both moving further apart from each other, passive stimulation of these fingers (with a two-point probe) during EEG recordings performed before and after training revealed a shift of their representations in the opposite direction, the dipoles of both fingers being closer to each other after training (see Figure 38; Braun et al., 2000). While the latter result is consistent with the “fusion” expected due to the synchronous stimulation of the fingers (Wang et al., 1995), the increased distance observed during training is likely to be accounted for by the attentional weight required during the discrimination task due to the need to isolate the stimuli (thus likely the pools of neurons activated by D1 and D5 stimuli in SI) in order to discriminate them. Later studies confirmed this hypothesis by showing similar increased segregation between finger representations as soon as the attentional task started, thus excluding the involvement of training in such changes (Braun et al., 2002; Iguchi et al., 2002). Overall, these different reports clearly demonstrate the relevance and crucial role of both the spatial and temporal parameters of somatosensory inputs in shaping representational maps of the body, and that this modelling is highly dynamic, with representations being constantly modulated depending on the context, task, and attentional demands.

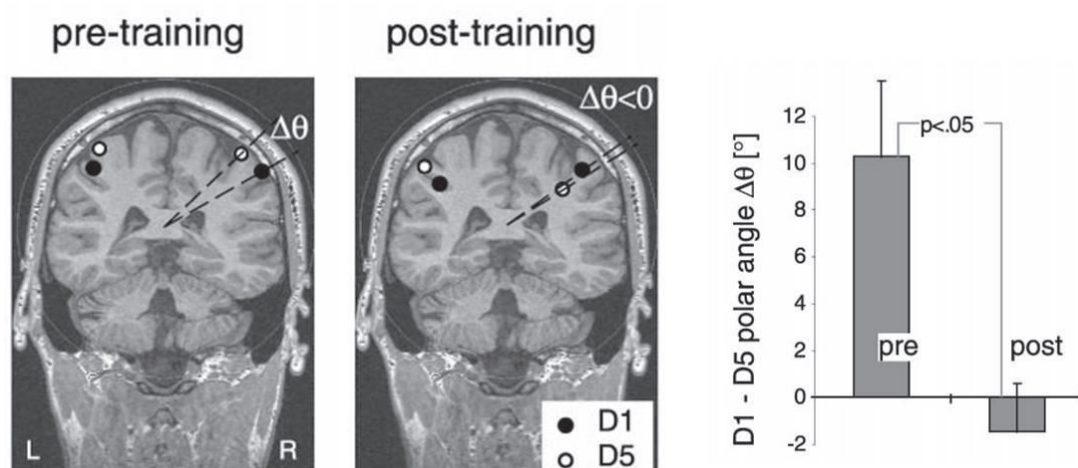


Figure 38 [from Braun et al., 2000]. Neuroelectric source imaging data obtained during passive tactile stimulation sessions Pre and Post training. **Left panel:** Coronal section through the postcentral gyrus of an experimental participant showing the decrease in theta polar angle between the cortical representations of the first and fifth digit after training. **Right panel:** Mean theta polar angle between the D1 and D5 dipoles obtained at the group level for the pre- and post-training sessions.

Thus, apart from complex naturalistic environments, simple protocols such as repetitive stimulation of a restricted cutaneous region through training on temporal or spatial tactile discrimination tasks induce representational changes that are somewhat opposite to those observed following permanent or transient somatosensory deprivation, the representation of the stimulated region expanding. While these changes seem to be more difficult to capture in humans (likely due to the relatively poor spatial resolution of brain imaging techniques), cortical reorganization was more easily observed in case of extensive training involving temporal pairing (i.e., simultaneous stimulation) across fingers, but also under conditions requiring attention. Note that, as mentioned above, different processes might be involved in these latter cases due to the combination of both local and pairing stimulations. In addition, some confounding reorganization could also arise from the involvement of attentional task-related processes, which are also likely to differ according to the type of task (i.e., spatial or temporal). Indeed, attentional modulation is known to affect somatosensory organization (Noppeney et al., 1999; Braun et al., 2002; Iguchi et al., 2002; Goltz et al., 2013). But the major point raised by these reports is that activity-dependent plastic changes are strongly affected by the degree of local synchrony of concurrent sensory inputs delivered to the cortex. Given this crucial influence of inputs temporal pattern, an obvious consideration is that the spatial distribution, and in particular, continuity between cutaneous regions is one of the founding principles which drives temporal correlation of sensory events.

d. Relevance of spatial/temporal dis/continuities

Accordingly, the earliest studies which originally investigated the relevance of the temporal correlation of inputs in driving cortical changes, without the confound of training-induced cortical reorganization, altered the temporal pattern of inputs by directly altering the spatial cutaneous continuity, either by inducing **syndactyly** or by **translocating** skin islands. Given that in primates, and especially humans, different fingers usually receives non-simultaneous somatosensory inputs, partly due to their high dexterity and motor independence, a surgical intervention fusing the skin of adjacent fingers would inevitably alter inputs coincidence and thus produce abnormal input correlation patterns across digits. In monkeys, recordings made from area 3b months after surgically-induced syndactyly revealed that instead of being restricted to a single digit, a number of RFs extended across the line of the syndactyly onto the surgically joined skin of both fused digits (Clark et al., 1988; Allard et al., 1991). Interestingly, the authors showed that this could not be the result of a mechanical spread of the stimulus or of sprouting of peripheral nerves across digits, since RFs remained on two digits when recordings were made immediately after the digits were separated. In addition, this intervention resulted in the disappearance of the normally present discontinuity between the representations of these digits, suggesting their “fusion” or the apparition of a new representation dedicated to both digits (Clark et al., 1988; Allard et al., 1991), likely reflecting also the induced changes in hand use. Similar results were obtained at the synaptic level, with an increased incidence of excitatory postsynaptic potentials (EPSPs) evoked from adjacent fingers within the fused finger representations in SI (Zarzecki et al., 1993). Taken together, these results clearly support the hypothesis that the somatotopic representation of the body-surface in the adult cortex is influenced by the temporal correlation of afferent inputs, which primarily results from the spatial continuity across skin regions. Horizontal corticocortical connections represent one of the most likely substrates for mediating these activity-dependent plastic changes (Smits et al., 1991; Zarzecki et al., 1993). In humans, disorganized finger representations were also observed in patients with congenital syndactyly, their representations being unusually small and overlapping (Mogilner et al., 1993). Conversely, surgical separation of the fused fingers of these patients induced a segregation of their cortical representations within weeks of surgery, by 3 to 9 mm. Interestingly, a more recent study investigated the temporal dynamics of such cortical changes by non-surgically (glove-based) **webbing** index-to-little fingers of healthy participants for 5h (thus inducing an artificial, reversible syndactyly). This ingenious intervention revealed an initial decrease in the distance between the representations of D2 and D5 after only 30 min of webbing (B1 in Figure 39), followed by a subsequent increase that lasted for about 2h (B2-B4 in

Figure 39), before returning to baseline values after about 4h of finger webbing (B5 in Figure 39; Stavrinou et al., 2007). These observations further confirm that the mechanisms underlying cortical reorganization are extremely rapid in their expression.

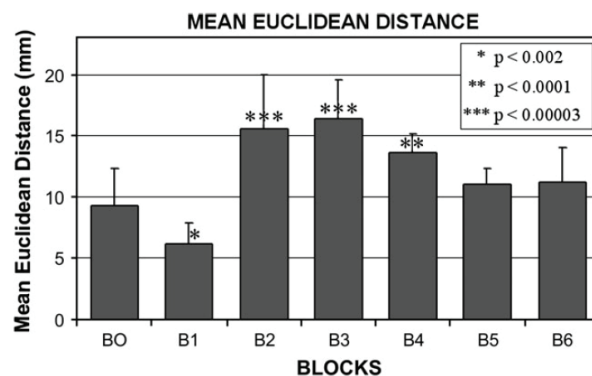


Figure 39 [from Stavrinou et al., 2007]. Mean Euclidean distance between D2 and D4 dipoles before (B0), during (every hour: B1-B5) and after (B6) finger webbing in humans, as measured by MEG. Statistical significance with respect to B0 is indicated.

Another way of disrupting the cutaneous continuity and thus of altering the temporal pattern of somatosensory inputs is to translocate pieces of skin. In monkeys, **transplantation** of skin and its neurovascular supply from one finger to an adjacent finger appeared to result in an integration of the transplanted skin representation with that of surrounding skin to form the cortical representation of the digits (Clark et al., 1986). More recently, Rosselet and colleagues (2008) investigated the effects of rotating by 180° a vascularised and innervated pedicle flap of the ventrum skin bearing nipples in rats on the somatotopic map organization. Two weeks after parturition and nursing, electrophysiological mapping of the ventrum skin revealed that compared with non-nursing rats, nursing rats had a reincorporation of the rotated skin flap representation into an updated topographical organization of the cortical map, as well as a higher incidence of neurons with split RFs resulting from the surgical separation of formerly adjoining skin surfaces. This suggests that the nursing-induced cutaneous stimulation of this region helped integrating the newly induced continuity of formerly separated skin surfaces. In line with this, RFs that included newly adjacent skin surfaces on both sides of the scar line emerged in nursing rats. Interestingly, subsequent local anaesthesia of the skin flap induced a RF translocation within 2-3 min that reversed the nursing-induced RF changes, such that single RFs located on the skin flap shifted back towards their original locations assessed before parturition (Rosselet et al., 2008). The influence of the temporal pattern of somatosensory inputs has also been shown in humans, a study revealing a reduction of D1-D3 cortical distance when stimulation during the mapping procedure was delivered to digits 1, 3 and 5 in this fixed sequence, as compared to

randomly (Braun et al., 2000b). But it should be emphasized that the interstimulus intervals (ISIs) used in this study were fixed at 250ms, which first, is likely to induce adaptation due to stimulation repetition, and second, is highly similar to the study of Blake and colleagues (2005), who found a fusion of cortical representations after stimulating two adjacent digits with ISIs of 200ms. A last remark concerns the matter of what should be considered synchronous or asynchronous inputs. Obviously, purely coincident inputs correspond literally to what one refers to when speaking about synchrony. But, should we consider the procedure of stimulation employed in Braun et al, 2000b and Blake et al, 2005 as asynchronous? Or is the fact of delivering a constant temporal pattern of stimuli (i.e., with fixed jittered stimuli) the relevant feature captured by neuronal activity before leading to the observed representational changes? Conversely, what can be considered an asynchronous stimulation? Purely randomized stimuli, free of any repeated pattern?

Despite these last remarks, these studies performed either in rats, monkeys or humans, clearly demonstrate the relevance of the body-surface **spatial continuity** in determining and shaping the **temporal pattern** of afferent activity, which in turn also shapes the CNS organization and in particular the cortical representational maps. Different mechanisms are thought to subserve this activity-dependent plasticity, such as Hebbian-like spike-timing dependent plasticity (STDP) involving changes in the excitatory-inhibitory balance through long-term potentiation (LTP) and long-term depression (LTD) processes. These mechanisms will be further discussed in the next chapter (Chapter 3: The Hebbian plasticity, page 125).

To conclude, we have seen throughout this chapter that cortical map reorganization within the somatosensory system, and in particular cortical reorganization occurring across the hand-face border, has been primarily demonstrated after **permanently or transiently depriving** the cortex of its normal inputs either by **lesioning** afferents somewhere along the somatosensory pathway, or by **local anaesthesia** of a cutaneous region. Then, we saw that these plastic changes can be reversed by **restoring inputs** either through nerve or limb graft in humans, or through training/sensory enrichment in animals. We also saw that under non-pathological conditions (i.e., healthy subjects), **increasing sensorimotor inputs/outputs** either by undergoing an extensive practice leading to a sensorimotor expertise or by evolving in an enriched environment, also induces remarkable representational changes at the cortical level. Similarly, **increasing more specifically somatosensory inputs** through training on a tactile task or by delivering tactile stimuli with a specific temporal pattern also results in drastic changes in the topographic organization of somatosensory cortical areas. However, to my knowledge, the limits of such plastic changes have not been systematically investigated, in particular regarding their

possible spread across the hand-face border. In addition, the issue of understanding the functional relevance of these cortical changes remains unsolved despite numerous attempts. A short review of this literature will be described in the following section.

IV. Functional consequences/relevance

One of the most intriguing and yet unsolved challenges consists in understanding the functional relevance of cortical plasticity. It is indeed important to establish whether the observed changes in maps topography are associated with changes in cognitive or perceptual performance. In addition, better understanding the functional consequences of such plastic changes would help to develop new rehabilitative therapies targeting the induction of adaptive plasticity to promote recovery. But so far, the links between cortical and behavioural changes are far from being solved, numerous discrepant results having been reported, even at the level of early somatosensory areas such as SI.

The cortical reorganization following transient or permanent suppression of somatosensory inputs is thought to offer no benefit and has rather been associated with negative outcomes, such as **pain** (Flor et al., 1995; Birbaumer et al., 1997; Karl et al., 2001), and has led to the idea of “maladaptive” plasticity. In particular, large-scale SI reorganization observed across the hand-face border in amputees/deafferented patients has been positively correlated with the intensity of phantom limb pain (PLP) (Flor et al., 1995; Montoya et al., 1998; Karl et al., 2001). In favour of such an association, a larger amount of cortical reorganization, as measured by face invasion, was observed in traumatic amputees with PLP than in pain-free (congenital or traumatic) amputees (Birbaumer et al., 1997; Flor et al., 1998; Montoya et al., 1998; Grüsser et al., 2001a). Conversely, transient release of PLP induced by local anaesthesia of the stump (Birbaumer et al., 1997) or by 4 weeks of mirror training (Foell et al., 2013) was associated with a reversal of the cortical reorganization within SI, the lip representation shifting back to its original location. In line with these studies, another interesting case report showed that local anaesthesia of the left face in the context of dental treatments temporarily released the pain of a patient experiencing severe neuropathic pain in his left upper-limb following brachial plexus avulsion (Hozumi et al., 2011). This pain alleviation was further associated with the disappearance of the illusory finger sensations evoked by face stimulation (i.e., referred sensations), and these effects lasted 2h, the time for the anaesthesia to resorb. Since this patient reported the same referred sensation as that reported in the literature showing hand/face border changes mainly following amputation (see “Plasticity following sensory deprivation” section page 75), the authors speculated that local anaesthesia of the mouth shrank the mouth/face representation and subsequently expanded the

somatotopic representation of the hand/upper limb within the sensorimotor cortices (see Figure 40), resulting in amelioration of the neuropathic pain in the upper limb and in the disappearance of the referred sensations from the face to the phantom. Interestingly, a short but promising report revealed that 2 weeks of asynchronous tactile stimulation of the stump and ipsilesional lip in six upper-limb amputees, aiming to induce a segregation of their cortical representation based on Wang and colleagues' work (1995), resulted in an increase of the lip dipole moment that was significantly correlated with **PLP reduction** (Huse et al., 2001). While this increased lip dipole moment suggests an enlargement of its cortical representation, as no shift of this dipole was reported, this result could support an increased invasion of the face towards the deprived hand region, as well as away from it. But beyond the matter of invasion accentuation or reversal, this result could simply reflect a strengthening or potentiation of the cortical representation surrounding the deprived region, thus rather reinforcing and accelerating the plastic processes already in progress, whose aim is to re-allocate the deprived cortical area to remaining body parts to make cortical maps conform to the new body configuration. Note that an improved **tactile perception** as measured by absolute and two-point discrimination tasks, was also reported at the stimulated sites (stump and lip) compared with the contralateral sides. Thus, while the previous reports associate pain with enlarged representation of the lip (and pain release to its shrinkage), this latter report suggests the opposite by associating the expansion of the lip representation with pain release and increased tactile perception.

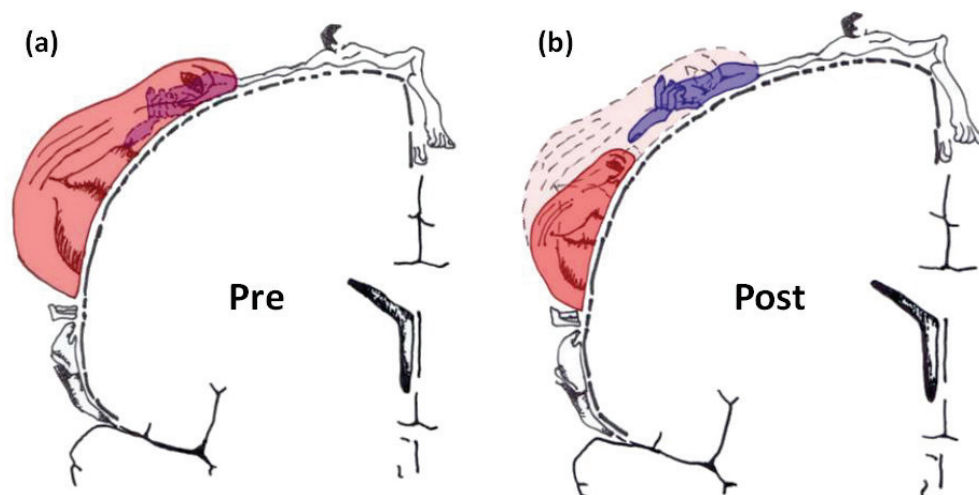


Figure 40 [from Hozumi et al., 2011]. Schematic representation of the somatotopic reorganization occurring in the sensorimotor cortices following deafferentation by a brachial plexus avulsion injury (a) and its hypothetical normalization by application of local anaesthesia to the mouth (b).

When considering **non-painful sensations**, reports converge towards a much more complicated pattern of relationships between cortical plasticity and perceptual changes. Indeed, while it has been proposed (Ramachandran et al., 1992b; Ramachandran, 1993; Jain, 2002) that the plasticity-induced overlap between face and hand regions within somatosensory cortices may provide an anatomical and neurophysiological substrate for referred phantom sensations that are experienced by patients with limb amputation (Ramachandran, 1993; Ramachandran and Hirstein, 1998; Hozumi et al., 2011), and nerve or spinal cord injury (Moore et al., 2000; Pourrier et al., 2010), the large-scale SI reorganization observed in amputees was not found to be correlated with non-painful phantom sensations (Flor et al., 1995). However, the repeated observations of referred sensations to the phantom fingers when stimulating the face in amputees (see Figure 41; e.g., Ramachandran et al., 1992a, 1992b; Halligan et al., 1993; Borsook et al., 1998) is strikingly congruent with the cortical plastic changes also repeatedly observed across the hand-face border. In addition to pain, the reorganization observed in amputees was also found to be correlated with the number of sites from which painful stimuli evoked referred sensations (Knecht et al., 1996a, 1998), and with **telescoping sensations** (Katz, 1992; Grüsser et al., 2001a), but not with tactile thresholds (either thermal, electric or spatial) assessed at the stump (Grüsser et al., 2001a). Thus, while a clear (and almost linear) link has been observed between SI reorganization and pain, the link with other perceptual changes remains largely unclear. However, it's worth noting that in all these studies, non-painful mechanical stimulation was used during brain imaging procedures, yielding to the expectation of repercussions primarily on non-nociceptive functions. In line with this, the presumed consistent and reliable relationship between pain and plasticity has been recently questioned by a study suggesting that PLP is rather related to a preserved hand representation, and to a reduced sensorimotor connectivity (Makin et al., 2013b). Thus, both painful and some non-painful sensations seem to be related to cortical changes, but through a complex association. In addition, it is likely that the measure used to quantify the reorganization in most of the previous studies was not precise enough to catch this relationship. Indeed, in amputees the plasticity was usually quantified by the relative ED between the intact face and the mirrored projection of the intact hand representation into the deprived hemisphere, which supposes first an initial "pseudo-perfect" symmetry between hand representations (quite hazardous at the individual level), and second the absence of reorganization of the intact hand representation, which has actually been disconfirmed several times (see Elbert et al., 1997; Frey et al., 2008; Björkman et al., 2012; Makin et al., 2013a; Moore et al., 2013). In agreement with these remarks, different results were obtained with other approaches. For instance, fMRI recordings performed when inducing

referred sensations revealed different clusters of activation within SI corresponding to the regions from which, but also to which **referred sensations** were evoked (Moore et al., 2000), even if these body parts did not exist anymore (Björkman et al., 2012). Similarly, the use of a higher fMRI resolution (3T) revealed a quite substantial cortical reorganization within SI and M1 in pain-free lower-limb amputees experiencing phantom sensations (Simoes et al., 2012). Finally, artificially-induced referred sensations in healthy participants using the rubber hand illusion, were found to be positively correlated with an increased distance between the fingers (D1 and D5) involved in the illusion (Schaefer et al., 2006). Thus, taken together these studies stress the need for a more refined evaluation and quantification of plastic changes, by combining methodological approaches but also by simultaneously observing the plastic changes from different but complementary perspectives.

Some perceptual changes, such as referred sensations, may also arise from plastic changes in higher integrative cortical areas, such as SII. Indeed, the sites from which referred sensations were mainly reported in upper-limb amputees are a large part of the ipsilateral face that includes the chin, upper lip, and cheek (Cronholm, 1951; Ramachandran et al., 1992a, 1992b). These face regions correspond to those from which inputs have been found to invade the hand representation within SI but also SII and PV in monkeys (i.e., OP1 and OP4 in humans) (Tandon et al., 2009). Moreover, the one-to-one relationship between the stimulated face sites and the phantom hand areas to which sensations were elicited (see Figure 41, Ramachandran et al., 1992b; Halligan et al., 1993; Yang et al., 1994; Knecht et al., 1996a; Borsook et al., 1998), strongly suggests the involvement of a somatotopically organized cortical area. Finally, these referred sensation maps appear to be modality-specific - at least in the acute phase (Borsook et al., 1998), and to evolve with time (Halligan et al., 1994; Knecht et al., 1998) in the same way cortical maps do. The involvement of higher order cortical areas is consistent with the fact that restoration of visuo-motor inputs/outputs alleviates PLP (see Flor and Diers, 2009 as a review for rehabilitative sensorimotor training). However, referred sensations were also reported following microstimulation of the deafferented thalamic region, which supports the contribution of subcortical reorganization (Davis et al., 1998). As a corollary, these results also indicate that, as for the issue of understanding which site along the neuraxis is responsible for the observed large-scale cortical reorganization, the origin of the associated perceptual changes remains unclear and is more likely to arise from the contribution of the different relays along the somatosensory pathway rather than from one specific site.

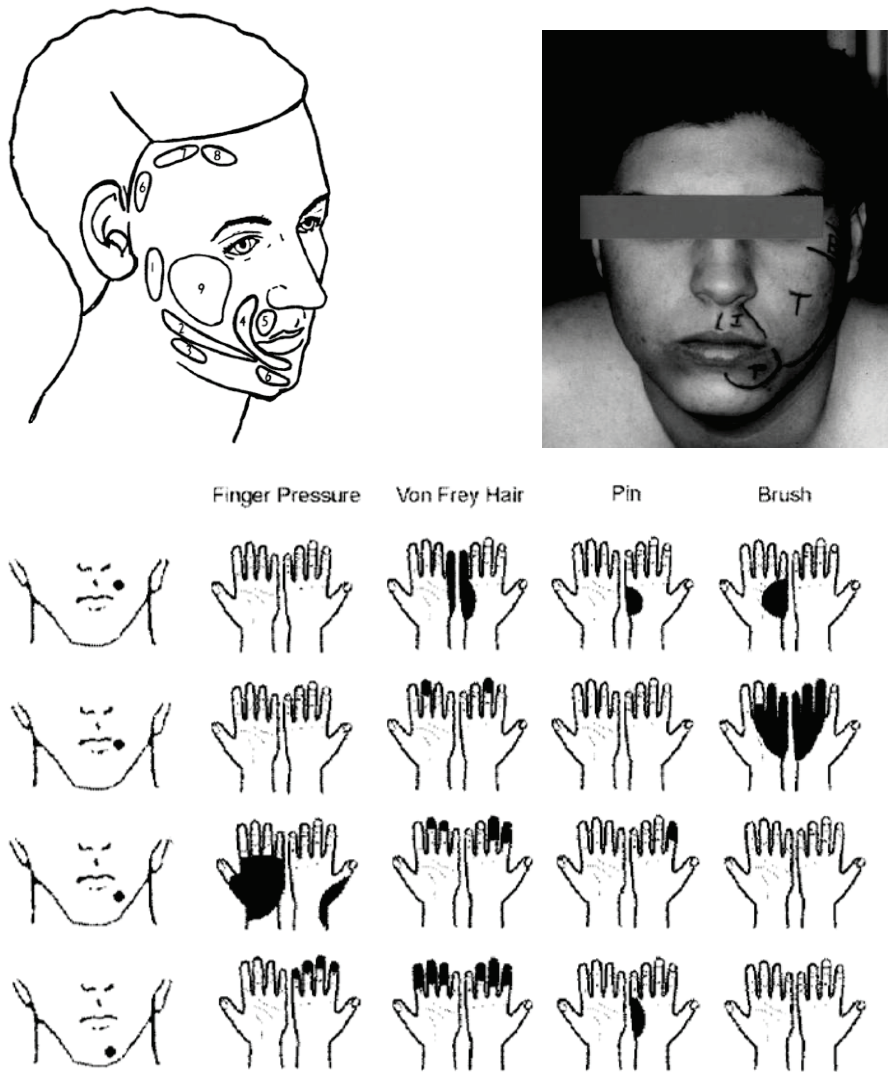


Figure 41. Example of cases reporting referred sensations across the hand-face border. **Top left** [from Halligan et al., 1993]: The regions on the right side of the face of patient DM which elicited precisely localized referred sensations in the phantom hand: 1 = elbow; 2 = lower arm; 3 = wrist; 4 = palm; 5 = generalized area of the fingers (with occasional specific reference to the middle and ring fingers); 6 = little finger; 7 = finger tips; 8 = base of fingers; 9 = no referred sensations. **Top right** [from Ramachandran and Hirstein, 1998]: Regions on the left side of patient VQ's face which elicited precisely localized referred sensations in the phantom digits 4 weeks after amputation. The region labelled 'T' always evoked sensations in the phantom thumb, 'P' from the pinkie, 'I' from the index finger, and 'B' from the ball of the thumb. **Bottom** [from Borsook et al., 1998]: Somatotopic representation of referred phantom sensations in the hand following stimulation of the face with different stimuli 24 h after amputation. The sites used were on the same side as the amputation. No phantom sensations were elicited by stimulation of sites on the opposite side of the face. Phantom activation of the arm was seen in more lateral stimulation sites (3 cm lateral to the corner of the mouth).

Apart from this consideration, while pain is obviously a negative outcome, referred sensations and more generally phantom sensations, even if not painful, do not provide any

benefit but rather some confusion regarding which body part has been touched. Thus, the cortical reorganization giving rise to these sensations, but also in some cases to PLP, is usually considered as “maladaptive”. In contrast, similar deprivation-induced plasticity has also been associated with **positive (and functionally relevant) outcomes**. For instance, increased **tactile spatial acuity** was observed at the homologous hand (Werhahn et al., 2002; Björkman et al., 2004b), but also at the lips (see Figure 42; Weiss et al., 2004) following hand anaesthesia via ischemic or pharmacological nerve blockade respectively. In addition, while the acuity changes observed at the homologous hand were not observed following foot ischemic nerve blockade (Werhahn et al., 2002), partial hand anaesthesia was also associated with increased **mislocalization** of touch in the intact ulnar portion of the hand, from D4 to its neighbour D3 whose nerve supply was blocked (Weiss et al., 2004). Together these results underline a spatial selectivity of both cortical and behavioural changes, consistent with the neighbouring cortical representation of the hand and face and with the strong transcallosal reciprocal connections between homotopic regions within SI (for review see Iwamura et al., 2001). As these gains in tactile spatial acuity were identified shortly after the onset of deafferentation, and no change in nerve transduction or subcortical structures was found (Werhahn et al., 2002), these behavioural changes seemingly arose from mechanisms subserved by existing connections within SI. One possible mechanism is disinhibition between adjacent cortical representation through removal of existing lateral inhibition via anaesthesia, which could account for both the cortical enlargement resulting in the hand-face “invasion” and the improved acuity at the lips.

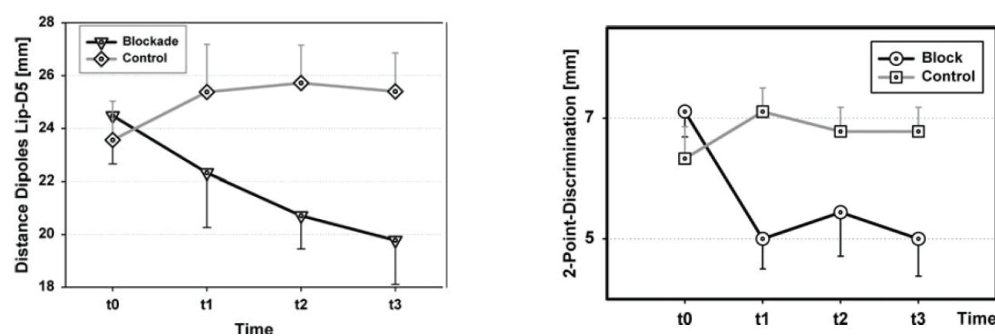


Figure 42 [from Weiss et al., 2004]. Effects of local anaesthesia of the radial and median three-quarters of the hand on: **Left panel:** the distance between Lip and D5 cortical representations (assessed by ECDs), and **Right panel:** the lip spatial acuity following hand anaesthesia (assessed by two-point discrimination thresholds).

Similar to Weiss and colleagues, Gandevia and Phegan (1999) reported enhanced perceived size of the lips following thumb anaesthesia either by nerve block or cooling, while that of the adjacent finger (D2) was not altered. In line with the hypothesis mentioned earlier, increased spatial acuity was also reported at the hand level following anaesthesia of the above forearm

(Björkman et al., 2004a, 2009; Petoe et al., 2013), and was associated with an expansion of the hand representation within SI (Björkman et al., 2009), and with increased intracortical inhibition (Petoe et al., 2013). But changes on the homologous hand were not systematically observed (Björkman et al., 2004a, 2009). Altogether, these results demonstrate that a similar event triggering reorganization, in this case sensory deprivation, can be associated with both negative and positive outcomes. However, note that since the origin of these cortical and functional changes is by definition negative, both outcomes have been interpreted mainly in terms of competition, with the absence of a given input releasing the lateral inhibition between adjacent cortical regions, and resulting in both cortical and functional changes. But competitive processes might by itself be regarded as negative, as the “winner” always wins to the detriment of another.

Conversely, an increase in sensory inputs (i.e., the opposite of deprivation) produces an expansion in the corresponding cortical representation zone, similar to that observed for intact cortical areas adjacent to a deprived region. But in the case of use-dependent or afferent-increase cortical reorganization, this expansion has almost always been associated with the development of skills and with outcomes that are **advantageous** to the individual. For instance, an expanded hand representation was reported in string players (Elbert et al., 1995), supposedly subserving the enhanced **manual dexterity** of these musicians. A greater absolute and spatial **tactile acuity** was also recently reported in pain-free musicians as compared to non-musicians or to musicians with chronic pain (Zamorano et al., 2015). Similarly, long-term training in Braille reading was associated with enlarged cortical representations of the reading fingers (Pascual-Leone and Torres, 1993; Sterr et al., 1998a, 1998b), which was linked with the fact that blind Braille readers were found to outperform sighted people in terms of tactile acuity (Van Boven et al., 2000; Goldreich and Kanics, 2003; Wan et al., 2010; Norman and Bartholomew, 2011; Wong et al., 2011). However, as mentioned earlier, these initially adaptive plastic changes can result in **disadvantageous** consequences due to over-use, such as, in the case of musicians, focal hand **dystonia** due to the fusion of finger cortical representations (Elbert et al., 1998). Similarly in blind Braille readers, representations of the reading fingers were found to be topographically disordered (Pascual-Leone and Torres, 1993; Sterr et al., 1998a, 1998b), and an enhanced frequency of **mislocalization** of tactile stimuli was further found between reading fingers in multiple-digit blind readers (Sterr et al., 1998b, 2003). Thus, the functional benefits acquired by extensive practice seem to have some “side-effects”, resulting in either pathological cases such as dystonia, or in deficits in other tasks (i.e., tactile localization in blind Braille readers). Together with the deprivation-related literature, this evidence suggests that use-dependent

cortical reorganization can also lead to negative outcomes, and thus can be sometimes as “maladaptive” as the deprivation-induced reorganization.

Other reports of cortical representational expansion arise from rehabilitation cases. For instance, the restoration of the hand cortical representation found by Giraux and colleagues (2001) in an amputee who underwent bilateral hand graft, was found to be associated with **tactile extinction** at the functional level (Farnè et al., 2002). The authors showed that simultaneous stimulation of the ipsilateral face extinguished hand tactile perception soon after the graft, in accordance with the face representation invading that of the deprived hand, and 6 months after, but no longer at 11 months post-operatively. The authors interpreted this ipsilateral face-hand extinction as a perceptual counterpart of the remapping that occurs after allograft and further stressed that such results highlight the inherently competitive nature of sensory representations. Similar “tactile extinction” was observed in an earlier report describing the case of an amputee whose referred sensations could be suppressed by simultaneously touching her intact hand and the face evoking referred sensations (Ramachandran and Hirstein, 1998). Interestingly, this extinction was not observed when the face was simultaneously touched with other body-parts (i.e., contralateral shoulder, chest or thigh), suggesting here again a somatotopy-based spatial selectivity but this time through topographically organized transcallosal connections, known to be mostly inhibitory. Another interesting case report concerns a patient who underwent a toe-to-index transplantation (Hadoush et al., 2012). MEG recordings in this patient revealed a progressive recovery of the index finger representation over time (weeks 12 and 24), as measured by an increased D2-D5 ED, together with an increased strength and a decreased latency of D2’s dipole, and these cortical changes were paralleled by recovery of **hand sensitivity**. Altogether, these three case reports tend to underline the **adaptive** aspects of plastic changes in rehabilitation, increased cortical representation being associated with sensory recovery, but also with tactile extinction in early recovery stages.

Focussing on the somatosensory level, while an improved **temporal discrimination** associated with an enlarged finger representation was found in monkeys (Recanzone et al., 1992a), the relationship between cortical changes and behavioural performance is less clear in humans. Indeed, humans trained 3-4 weeks in a temporal discrimination task exhibited enhanced performance with complete transfer of learning to the contralateral hand, and these changes were associated with a unilateral decrease in the hand dipole strength (Spengler et al., 1997). This dipole strength decrease was discussed by the authors as reflecting either a decrease of the neuronal population contributing to the signal (i.e., representational shrinkage) or a decrease in the temporal and spatial coherence in the evoked activity. But while the authors concluded that

the attenuation of SEFs and the complete learning transfer indicate learning in associative cortical areas rather than plasticity in early sensory areas, I would consider an alternative simple interpretation, which arises directly from the task used in their protocol. Indeed, participants were instructed to localize a certain pattern of tactile stimulation (i.e., two consecutive stimulations) either at the distal or at the proximal segments of D2-D4 (i.e., same protocol as Wang et al., 1995). The task requiring a clear distinction between two locations, shrinkage of their representations and RFs would thus help to perform the task. And such functional shrinkage could be driven by task-related attentional modulation (Braun et al., 2002). In addition, another report of improved performance in participants who trained for 30 days in a frequency discrimination task, did not observe any cortical changes as assessed by MEG (Imai et al., 2003). Finally, a study comparing the cortical correlates observed during and after spatial tactile training revealed changes in opposite directions (Braun et al., 2000a). Indeed, while during training the distance between the cortical representations of the fingers involved in the task increased, this same distance decreased after training, when fingers were passively stimulated. And this latter decrease was correlated with an increased frequency of **mislocalizations** attributed to more distant fingers (Braun et al., 2000a; Schweizer et al., 2001). The authors concluded that the discrimination training tended to isolate pools of neurons activated by D1 or D5 stimuli in SI (likely thanks to attentional processes), whereas the passive stimulation tended to enlarge/move the territories toward each other, possibly resulting in an overlap increasing the probability of tactile mislocalizations. Altogether, while the functional consequences of tactile training have been quite abundantly described in humans, their links to the changes in cortical representational maps remain unclear. In addition, while animal studies clearly suggest that tactile training and improved performance are related to enlarged cortical representations (Jenkins et al., 1990; Recanzone et al., 1992a, 1992c, 1992d, 1992e), these changes were not observed in humans following similar protocols.

Although it is outside the scope of the thesis, it should be recalled that age-dependent changes also bring to cortical enlargement, but associated with opposite perceptual effects. Indeed, a similar expansion of the hand cortical representation was reported in elderly (60-85 years old), but was associated with strong **decline in tactile spatial acuity** (Kalistch et al., 2009). Similar results were observed with electrophysiological recordings in rats, enlarged SI representations being correlated with sensorimotor deficits (Spengler et al., 1995). So in this case, the enlargement of cortical representation was associated with negative outcomes and not with enhanced acuity as in Recanzone's paper (1992a).

Altogether, in this section I reviewed findings showing that a given representational change such as a cortical expansion has been associated with: (i) phantom sensations following amputation and spinal cord injury, and (ii) sometimes pain release (PLP); (iii) increased tactile acuity following anaesthesia or expertise (i.e., musician/Braille readers); (iv) enhanced sensorimotor skills with expertise such as in musicians, Braille readers or any learner; (v) sensorimotor recovery following graft or transplantation; but also (vi) different kinds of pain such as phantom limb pain, back pain or neuropathic pain; (vii) increased mislocalization of tactile stimuli following anaesthesia, over-use or tactile training; (viii) some pathologies such as dystonia; and (ix) somatosensory deficits in elderly. Thus seemingly identical ‘phenomenological’ expressions of cortical plasticity within SI can be either associated with “positive” (adaptive) or “negative” (maladaptive) outcomes, exhibiting sometimes entirely opposite effects on a given task. Thus, whilst there is an intuitive advantage in developing a larger cortical representation as a result of skill acquisition, this overview of some of its other functional outcomes clearly underlines that the significance of cortical reorganization remains largely unclear, and even questions the presence of a functional significance of cortical plasticity. It could be that cortical reorganization *per se* is neither positive nor negative for individuals, the valence of its effects being likely to depend on multiple factors, such as the nature of the event triggering the reorganization, the context in which this event occurs, the level at which the somatosensory pathway is affected and the environmental or task-related demands placed upon the individual. Thus, if one wants to achieve a better understanding of the complex relationships linking cortical and behavioural changes, all these potentially confusing factors must be minimized or at least controlled, as much as possible. The work done in this thesis is an attempt to contribute to this huge challenge faced by the scientific community, and in particular here the somatosensory community. To avoid the confounding aspects of lesional and motor contributions mentioned throughout the section “Plasticity following sensory deprivation” (page 75), we chose the model of activity-dependent plastic changes induced in a healthy population and the use of a pure somatosensory protocol designed to precisely control for input pattern.

CHAPTER 3: THE HEBBIAN PLASTICITY

I. Concept

As briefly mentioned in the section “Relevance of spatial/temporal dis/continuities” of the previous chapter, one of the most likely mechanisms underlying activity-dependent plastic changes is based on Hebb’s postulate. Indeed, numerous investigations suggested the crucial relevance of input temporal pattern for shaping and modulating the brain functional circuitry (see Buonomano and Merzenich, 1998 for a review).

The idea of brain plasticity started to receive wide acceptance in the 1940s when the theory of neural plasticity got some popularity thanks to Donald Hebb, who was claiming that “cells that fire together, wire together”. Hebb introduced a concept in which an increase in synaptic efficacy arises from episodes of high temporal correlation between pre- and post-synaptic activity (Hebb, 1949). Such a plastic mechanism is now known as “Hebbian learning” or “Hebbian plasticity”. Later, Jacques Paillard supported the theory of brain plasticity by stating that “The term plasticity is only appropriate in terms of the ability of a system to achieve novel functions, either by transforming its internal connectivity or by changing the elements of which it is made” (see Will et al., 2008 for an English translation and commentaries). New enthusiasm for Hebb’s theory was then provided by the fundamental description of long-term potentiation (LTP) and depression (LTD) mechanisms (Bliss and Lomo, 1973; Wigström and Gustafsson, 1986) and is now commonly advocated to explain some types of associative learning in which simultaneous activation of cells leads to pronounced increases in synaptic strength. In addition to LTP and LTD mechanisms, the crucial role of the relative timing between pre- and post-synaptic activity led to the concept of spike-timing-dependent plasticity (STDP). STDP was revealed by the demonstration that LTP is induced when pre-synaptic activity preceded post-synaptic activity by tens of milliseconds, whereas LTD is induced when spiking occurs in the reverse order (post-synaptic before pre-synaptic) (e.g., Markram et al., 1997; Feldman, 2000; see Dan and Poo, 2004, 2006 for reviews). Although the preponderance of STDP processes in driving activity-dependent plasticity has been recognized, their implementation was mostly done in vitro and in vivo in animals, before being adapted to humans.

In this chapter, I will briefly describe the different protocols that have been used to induce Hebbian plasticity by emphasizing how this plasticity, which was first described in vitro at the synaptic level, was also reported following stimulation of parts of the cortex, and then peripheral sensors. Consequently, I will first describe the principles of Hebbian synaptic plasticity, before

zooming out to the plastic changes observed following **intracortical microstimulation** (ICMS). Then, I will describe how these protocols were adapted to **non-invasive protocols** that could be applied in animals but also in humans, for which plastic changes are mainly investigated at the level of the entire brain, leading to the observation of representational plasticity. Finally, I will describe in more detail the perceptual and cortical consequences observed following the protocol of repetitive somatosensory stimulation, which was used as a mean of inducing transient plastic changes in the present work.

II. Induction: from synapses to the skin

a. Hebbian synaptic plasticity

As mentioned above, the Hebbian learning rule was first described and then investigated at the synaptic level. This gave rise to the Hebbian synaptic plasticity, which was first reported in hippocampal neurons (e.g. Kelso et al., 1986). When presynaptic input from CA3 axons was paired with postsynaptic depolarization, the amplitude of the EPSPs was enhanced in a long-lasting way and referred to as LTP. This form of associative plasticity is of particular interest because it is an instantiation of Hebb's postulate according to which simultaneous pre- and post-synaptic activity results in the strengthening of the synaptic connection. A particular subtype of the glutamate receptor, the N-methyl-D-aspartate (NMDA) receptor (see Fan et al., 2014 for a review), mediates this process by permitting the influx of Ca^{2+} , which in turn increases post-synaptic excitation and is a critical early step in the induction of LTP, when a postsynaptic depolarization arrives in presence of glutamate (see Bliss and Collingridge, 1993; Nicoll and Malenka, 1995). LTP is also found at the cortical level, and, even if more complex, is highly similar to that observed in the hippocampus and can be induced in both cortical slices and in vivo. One of the first demonstrations of Hebbian synaptic plasticity in the cortex was with intracellular recordings from cat motor cortex in vivo (Baranyi and Fehér, 1981), by pairing synaptic input from the ventrolateral nucleus of the thalamus with stimulation of a second pathway or intracellular depolarization. Three main protocols have been used to induce LTP at the cortical level: (a) tetanus, often a 100-Hz, 1-s stimulus applied to the afferent pathway; (b) theta-burst stimulation, in which 10 brief bursts at 5 bursts/s are applied, with each burst consisting of 4 pulses at 100 Hz, again delivered to the afferent pathway; and (c) through pairing, in which intracellular depolarization of the postsynaptic cell is paired with low-frequency afferent stimulation. These protocols are likely to differ significantly in their physiological relevance but the general hypothesis is that manipulations that decrease inhibition or increase the NMDA current result in more robust LTP.

b. Intracortical microstimulation

One level of investigation above, *in vivo* ICMS has been successfully used to induce short-term and reversible plastic changes in various cortical regions, including motor (e.g., Gu and Fortier, 1996), somatosensory (Recanzone et al., 1992b; Dinse et al., 1993, 1997; Spengler and Dinse, 1994; Benali et al., 2008), auditory (e.g., Sakai and Suga, 2001) and visual (e.g., Godde et al., 2002) cortices. Typically, ICMS consists in repetitive electrical pulse trains that are delivered intracortically via a microelectrode, and which activate a cortical volume of tens or hundreds of microns depending on the intensity used. This stimulation results in nearly simultaneous activation of all local pre- and post-synaptic elements as well as the modulatory inputs projecting to that same cortical locus. Therefore, this stimulation generates the type of temporally coincident responses necessary to induce Hebbian plastic changes. The short time scale and reversibility of ICMS-induced changes support the idea that ICMS modulates synaptic efficiency in neuronal networks.

Applied over the primary somatosensory cortex of monkeys or rats, ICMS has been shown to induce transient changes in the somatotopic map in area 3b. For instance, significant extension of the cortical representation of a restricted skin region was reported up to several hundred microns away from the conditioning microstimulation site (Recanzone et al., 1992b; Spengler and Dinse, 1994). Interestingly, these representational changes were reversible 6 to 8 hours after termination of ICMS (Spengler and Dinse, 1994), and were accompanied by changes in RFs location and size following different patterns. Indeed, while some RFs shifted toward or away from the microstimulation site, others shifted and expanded to include the RF of the microstimulation site (Recanzone et al., 1992b). Interestingly, ICMS of SI in rats and of BA3b in monkeys, revealed an increased correlation in the activity not only of neuron pairs separated by about 250 μ m, but also of pairs separated by 300-800 μ m or more, revealing an emergence of long-range functional coupling (Dinse et al., 1993). Furthermore, this increased coupling was positively correlated with a several-fold increase of RFs overlap, changes in RF size and response latency. These effects were initially detected 15min after ICMS.

Altogether, these results demonstrate that ICMS, which is considered to induce Hebbian-like plastic changes, results in substantial changes in cortical representations, and notably in an expansion of the stimulated representation. However, ICMS, as well as the “classical” protocols used to induce LTP, can be regarded as artificial and non-physiological experimental procedures, compared to natural cutaneous stimulations.

c. Temporally paired cutaneous stimulation

Under more ecological circumstances, similar Hebbian plastic changes occur when tactile inputs are temporally paired. Indeed, given the somatotopic organization of the body surface at the cortical level, two neighbouring cutaneous points that are stimulated in close temporal proximity are more likely to elicit synchronous firing of neighbouring neurons. In terms of the excitatory intracortical connections in cortical networks, Hebbian learning should drive neurons engaged by behaviourally important stimuli to respond to them in a more temporally coherent manner. This kind of synchronous stimulation, or pairing protocol, has been extensively used in rodents, by trimming or plucking a subset of whiskers. Neural responses to deprived whiskers rapidly decrease and cause the weakening and shrinking of the representation of deprived whiskers within the map. In contrast, the responses to spared whiskers increase slowly, and lead to the strengthening and expanding of the representation of spared whiskers within the map (Fox, 1992; Diamond et al., 1993; Sellien and Ebner, 2007). The dynamic relocation of cortical processing space from deprived inputs toward spared inputs will optimize sensory processing (see Feldman and Brecht, 2005 for a review).

The induction of cortical reorganization following temporally paired cutaneous stimulations was also described in monkeys (Recanzone et al., 1992c; Wang et al., 1995) and in humans (Spengler et al., 1997; Liu et al., 2000) via training, and was initially tested by syndactyly and webbing experiments (described in section Relevance of spatial/temporal dis/continuities, page 112). Interestingly, a study performed in both rats and humans using a pairing paradigm of natural tactile stimulation revealed an expansion of the cortical representation of the stimulated hindpaw in SI of rats associated with enlarged RFs, while a similar procedure resulted in an enhanced tactile acuity at the stimulated fingers (Godde et al., 1996). This study was the first suggesting the relevance of adapting somatosensory pairing protocols to humans, and provided the evidence that such stimulation may have functional outcomes.

However, it is worth noting that the enlargement of RFs size observed in rats may appear contradictory to the improved discrimination observed in humans. Indeed, given that tactile acuity resolution is considered to be determined by the spacing between RF centres (Goodwin and Wheat, 2004), a decrease in RFs size is usually expected to obtain an improved discrimination. But, note that an enlarged cortical representation was also observed, suggesting an increase in the number of neurons activated by the stimulation and thus processing the tactile information. In addition, discrepancies in the direction of RF size changes has been frequently observed. Among the possible explanations, the pattern and location of somatosensory

stimulation is thought to affect RFs size. Indeed, while studies in which stimuli were applied with a significant trial-by-trial variability in location (e.g. Xerri et al., 1994) or in which stimuli moved across the skin (e.g. Jenkins et al., 1990) repeatedly reported RFs size shrinkage following training/stimulation exposure, studies in which stimuli were applied at an invariant skin location (e.g. Recanzone et al., 1992a, 1992c, 1992d, 1992e; Wang et al., 1995) reported in contrast enlarged RFs for the trained region (see section previous chapter). This was interpreted as a consequence of the fact that by Hebbian plasticity, any input into the cortex driven from the invariantly stimulated skin location would be integrated into a necessarily larger receptive field. In contrast, when stimuli move across the hand (as in Jenkins et al., 1990) or are delivered to inconstant skin locations (as in Xerri et al., 1994), each small sector of skin is an effective source of competitive input for the Hebbian network, and receptive fields therefore shrink in size as the zones of representation of the engaged skin surface grow in size. Note also that RFs and cortical map changes induced by naturalistic sensory enrichment were found to follow different time courses (Rosselet et al., 2006), the RF size reduction occurring earlier than map expansion. Thus, the onset at which both are recorded must be taken into consideration.

Aside from this parenthetical remark about RFs, we can see that similarly to ICMS, temporally paired cutaneous stimulation results in substantial reorganization of the cortical representation of the stimulated site. In addition, applied in humans, such protocol appears to alter tactile acuity. The paradigm introduced by Godde and colleagues, now commonly referred as repetitive somatosensory stimulation, was then extensively used to investigate the link between cortical plastic changes and perceptual changes in humans. This literature will be described in the following section.

III. Repetitive somatosensory stimulation

a. Description

As underlined in the previous sections of this chapter, the preponderance of the temporal coincidence to induce plastic changes has been widely demonstrated. Spike-timing-dependent plasticity together with LTP and LTD of synaptic transmission are the most likely processes driving activity-dependent plasticity. However, the induction of such processes is typically performed invasively in animals, either in slice preparations or intracortically in vivo, which makes its implementation in humans difficult, if not impossible. The paradigm introduced by Godde and colleagues (1996), or repetitive somatosensory stimulation (RSS), corresponds to an adaptation of the classical Hebbian protocols into an ecological stimulation that can be

implemented in humans, and which allow for a complete control of the timing and spatiotemporal allocation of the stimulation in order to systematically study brain plasticity and its functional relevance (see Beste and Dinse, 2013; Parianen Lesemann et al., 2015 for recent reviews). Consistent with the Hebbian postulate, RSS consists in a passive simultaneous stimulation of cutaneous receptive fields for a few hours. Since Godde and colleagues (1996), a substantial number of studies confirmed that RSS induces cortical changes associated with changes in tactile perceptual abilities comparable to those occurring after application of active perceptual learning paradigms (described in detail below). However, in contrast to classical training-dependent procedures, RSS presents the characteristic of being completely passive and devoid of attentional or cognitive control processes (i.e., training-independent, Beste and Dinse, 2013).

Several lines of evidence strongly suggest that RSS relies on Hebbian synaptic plasticity and reflects LTP-like plasticity in SI. First, RSS effects (both cortical and behavioural) were found to be N-methyl-D-aspartate (NMDA) receptor-dependent (Dinse et al., 2003), this receptor being known to be crucial for LTP induction. Similarly, RSS behavioural effects were also found to be dependent on cholinergic mechanisms which are known to participate in NMDA receptor-dependent neuroplasticity (Bliem et al., 2008). In addition, an Hebbian-like “co-activation” of several RFs has been proven to be crucial for the induction of plastic/behavioural changes (Pleger et al., 2003; Ragert et al., 2008). In line with this, opposite perceptual changes have been reported following *in vitro*-like protocols of high- and low-frequency RSS, discrimination being improved following high-frequency stimulation, whereas low-frequency stimulation resulted in an impaired acuity (Ragert et al., 2008). These results indicate that brief stimulation protocols resembling those used in cellular LTP and LTD studies can induce meaningful and persistent alterations in tactile discrimination in humans. This evidence further supports the Hebbian action of RSS. Finally, the short time-scale over which RSS cortical and behavioural effects occur (up to 8 hours; Godde et al., 2000) further supports the fact that RSS relies on Hebbian-like transient changes in synaptic efficiency.

Most studies using this protocol applied RSS on the tip of the right index finger (right-D2) (Godde et al., 1996, 2000, 2003; Pleger et al., 2001, 2003; Dinse et al., 2003, 2006; Hodzic et al., 2004; Ragert et al., 2008; Gibson et al., 2009; Schlieper and Dinse, 2012; Freyer et al., 2012, 2013; Höffken et al., 2012), while few other studies applied RSS on two- or more adjacent fingers (Pilz et al., 2004; Kalisch et al., 2007, 2008; Smith et al., 2009; Kowalewski et al., 2012), or on the whole hand with a specific glove (e.g., Golaszewski et al., 2012). I will describe in the following sections the behavioural and cortical plastic changes obtained following RSS,

with a particular emphasis on single-finger stimulation as this procedure was the one used in the present work.

b. RSS-induced perceptual and cortical changes

First, the consequences of RSS-induced plasticity on tactile perception was assessed using tactile **spatial discrimination** tasks, mainly the two-point discrimination task (2PDT) and the grating orientation task (GOT). Following two (Godde et al., 2000) to three hours (Pleger et al., 2001, 2003; Dinse et al., 2003, 2006; Godde et al., 2003; Hodzic et al., 2004) of RSS at the right-D2 fingertip, a substantial improvement in spatial acuity has been observed at the stimulated fingertip, the effect size ranging between 13 and 28.8% (Parianen Lesemann et al., 2015). Conversely, the acuity at the homologous finger was repeatedly found to remain stable after RSS at right-D2 (Godde et al., 2000, 2003; Pleger et al., 2001, 2003; Dinse et al., 2003, 2006). However, apart from the homologous finger, few reports investigated the selectivity of RSS-induced perceptual changes. Among these studies, one reported that the spatial acuity at the adjacent major finger (right-D3) remained stable (Godde et al., 2000), while another study only reported that the dipole source of the adjacent thumb (right-D1) was not affected by RSS at right-D2 (Pleger et al., 2001). Moreover, it is worth noting that in the former study the acuity at right-D3 was tested on a small sample of participants (i.e., 7), and that a high variability was observable (see Figure 43).

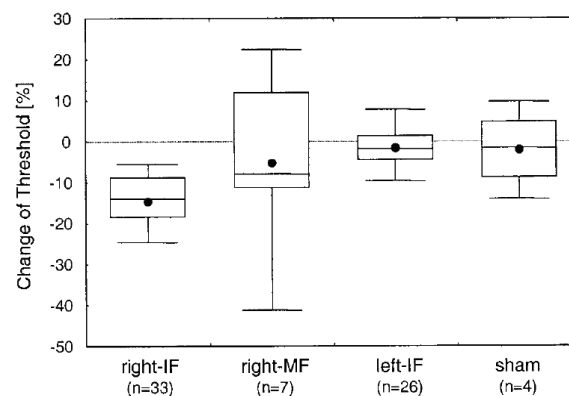


Figure 43 [from Godde et al., 2000]. Relative changes (Post-Pre in %) of discrimination thresholds were measured at the tip of right-IF (i.e., right-D2), right-MF (i.e., right-D3), and left-IF (i.e., left-D2) after RSS was applied to right-D2. In addition, the result of a sham stimulation applied to right-D2 is shown.

These results led the authors to interpret RSS discrimination changes as highly specific to the stimulated finger. In contrast to two or three hours, 30min of RSS was found not enough to yield significant changes in tactile discrimination (Godde et al., 2000). Regarding the time course of recovery, the improved tactile acuity was found still present 2 to 4h after RSS, but returned to baseline within 8h after RSS (Godde et al., 2000). Finally, the same authors reported that RSS at right-D2 cumulated over 3 consecutive days (2h/day) delayed the recovery time up to 72h. Interestingly, in contrast to tactile spatial discrimination, an impaired **frequency discrimination** was reported at the stimulated fingertip following RSS (Hodzic et al., 2004), suggesting a trade-off between spatial and temporal discrimination abilities. But to date, this has been the only one report showing that RSS acts on temporal aspects of tactile perception. Altogether, these studies reveal that RSS applied at a fingertip substantially improves its tactile spatial discrimination.

RSS has been demonstrated to reliably induce a transient **cortical plasticity** of the stimulated finger's representation in rats (Godde et al., 1996) but also in humans (Pleger et al., 2001, 2003; Dinse et al., 2003; Godde et al., 2003; Hodzic et al., 2004). Depending of the imaging technique employed, this plasticity has been described in terms of an enlargement of the finger's representation within SI (Figure 44; Pleger et al., 2003; Hodzic et al., 2004), and/or by a shift of its centre of gravity (CoG) or dipole source toward the thumb representation (Pleger et al., 2001; Dinse et al., 2003; Godde et al., 2003; Hodzic et al., 2004). Similar changes were also observed within the secondary somatosensory cortex (Figure 44; Pleger et al., 2003; Hodzic et al., 2004). Conversely, no significant cortical changes were observed for the homologous finger (left-D2; Pleger et al., 2001, 2003; Dinse et al., 2003; Godde et al., 2003; Hodzic et al., 2004) and, although on a relatively small sample of participants (n=5), for the adjacent thumb (right-D1; Pleger et al., 2001). Additionally, an increase in cortical excitability was reported after RSS, as measured by dipole strength (Pleger et al., 2001), BOLD signal intensity (Pleger et al., 2003), or paired-pulse SEP recordings (Höffken et al., 2007). Given that an increased excitability is considered as a typical signature of effective LTP induction, this increased excitability together with the expansion of the representation of the stimulated finger suggest that RSS lead to the recruitment of latent connections and/or to fast modulations of synaptic efficiency. Interestingly, the amount of shift (Pleger et al., 2001; Dinse et al., 2003; Hodzic et al., 2004), enlargement (Pleger et al., 2003) and cortical excitability (Höffken et al., 2007) of the finger representation was found to be correlated with its spatial discrimination performance. Thus, the improved discrimination is likely to arise from a recruitment of processing resources (see Gilbert et al., 2001 for more general discussion).

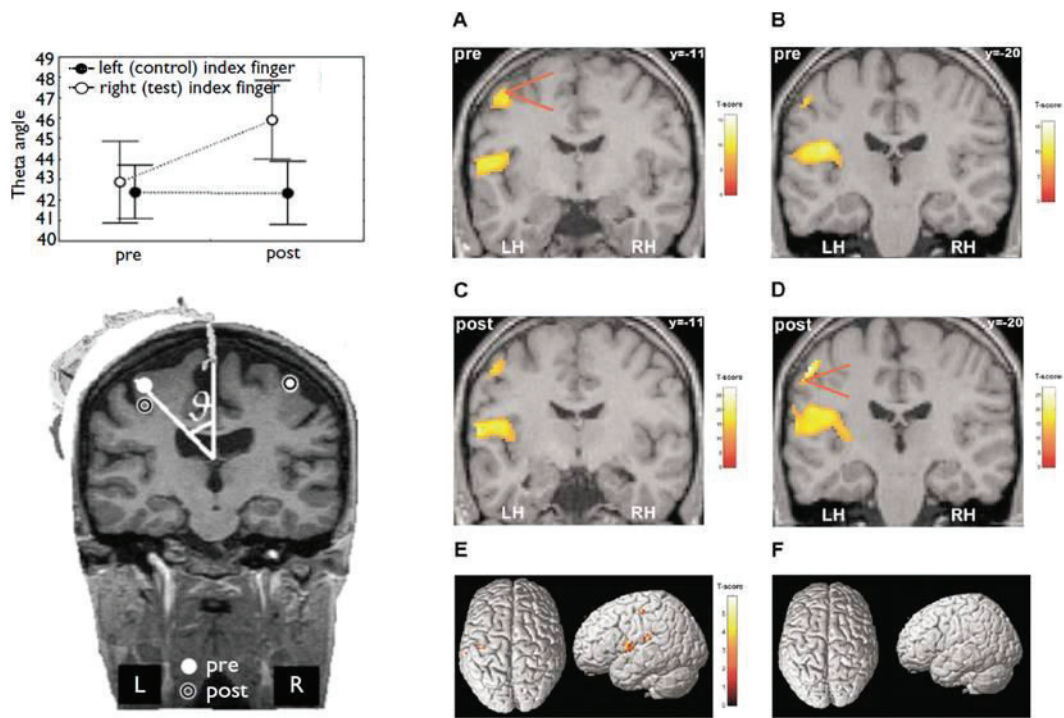


Figure 44. **Left** [from Godde et al., 2003]: Mean theta angles of the dipoles corresponding to the contralateral representations of each index finger (stimulated and control) before and after RSS. A representative example of dipole locations is illustrated below, with the dipoles corresponding to the contralateral representations of each finger before (filled circles) and after (open circles) RSS. **Right** [from Pleger et al., 2003]: (A-D): Fixed-effects analysis showing BOLD signals detected pre (A and B) and post (C and D) RSS in the contralateral SI and in the contralateral and ipsilateral SII (LH/RH: left/right hemisphere). S1 parameters: Pre-RSS [cluster level = 255 vox; T-score = 10.12; MNI template coordinates (mm) = -46, -11, 50 (x,y,z)]; Post-RSS [cluster level = 1091 vox; T-score = 20.23; -56, -21, 50 (x,y,z)]. (E) RFX analyses (paired t-test pre vs post) revealed significant changes of right-D2 activated patterns localized in the contralateral SI and SII [threshold: $p = 0.001$ uncorrected; S1 parameters: 22 v; T-score = 5.92; -44, -18, 54 (x,y,z)]. (F) No changes of BOLD activity were found contralateral to the control left-D2.

As previously mentioned, few studies applied RSS on **multiple fingers**. In such cases, the stimulation was delivered either synchronously or asynchronously to the different fingers (Pilz et al., 2004; Kalisch et al., 2007). After 3h of RSS applied synchronously to D2 and D3 or to D3 and D4, mislocalization between these fingers increased by approximately 37.5%, and was associated with a “merge” of the cortical representations of these fingers in the contralateral SI (Pilz et al., 2004). In contrast, asynchronous stimulation led to a decreased number of mislocalizations (i.e., improved localization) by approximately 22%, which was accompanied by a “segregation” of the cortical representation of the stimulated finger (Pilz et al., 2004). When applied on all the fingers of the right hand, synchronous RSS led to an improved spatial

discrimination associated with an increased rate of mislocalization to more distant fingers, whereas after asynchronous RSS no significant perceptual change was observed (Kalisch et al., 2007). Interestingly, in contrast to spatial acuity, tactile sensitivity as assessed by absolute thresholds was unaffected by RSS (Kalisch et al., 2007). Altogether, these studies suggest that when several fingers are submitted to RSS, synchrony is necessary to drive spatial discrimination improvement locally on each finger, whereas asynchrony seems to involve a slightly different mechanism. It is worth noting here that when applied to several fingers, RSS might act at two different scales: a first that I will consider as “local”, arising from the synchronous stimulation of several RFs at each fingertip, and a second arising from the synchronous or asynchronous across fingers. But this hypothesis needs further investigation.

c. Non-mechanical RSS protocols

In addition, while the stimulation of the RSS protocol was originally mechanical (Godde et al., 1996, 2000, 2003; Pleger et al., 2001, 2003; Dinse et al., 2003; Höffken et al., 2007; Kalisch et al., 2007; Ragert et al., 2008; Freyer et al., 2012, 2013), many studies used different variants of RSS, and in particular **electrical** stimulation (Smith et al., 2009; Kalisch et al., 2010; Freyer et al., 2012, 2013; Kowalewski et al., 2012; Schlieper and Dinse, 2012; Ladda et al., 2014). In contrast to mechanical stimulation which is basically transmitted via Meissner or Merkel mechanoreceptors, electrical stimulation activates much more afferents: Ia large muscle afferents, group Ib afferents from Golgi, SAI and FAII tactile afferents (Campbell, 1999; Kimura, 2013). This wide recruitment of afferents led electrical stimulation to be favoured in the context of rehabilitation. For instance, electrical RSS of the fingers of stroke patients suffering from sensory loss (Smith et al., 2009), or of elderly people affected by age-related somatosensory decline (Kalisch et al., 2010), resulted in an improved sensory discrimination but also in an enhanced sensorimotor performance.

To conclude, we saw in this chapter that altering the temporal pattern of somatosensory inputs is an efficient way to drive activity-dependent plastic changes via Hebbian plasticity, while avoiding the confounding aspects of lesional, motor and attentional contributions. Adapted from classical pairing protocols, RSS has been proven to be efficient in inducing a transient somatosensory plasticity in healthy population. Interestingly, this plasticity has been associated with substantial changes, an notably improvements, in tactile perception.

SUMMARY & AIMS

As described in the introduction of this work, we know from the literature that the tactile information arising from the hand and the face are cortically neighbours, and that in case of sensory loss cortical plastic changes can occur across the hand-face border, but are associated with different functional consequences (either adaptive or maladaptive). On the other hand, restoring and more generally increasing somatosensory inputs also leads to cortical changes that are more systematically associated with adaptive outcomes. Among the different alternatives available to increase somatosensory inputs, RSS relies on the well-known Hebbian plasticity processes and yields training-independent learning by passively increasing somatosensory inputs. Applied at the right index fingertip RSS results in a substantial, though transient, reorganization of the stimulated finger representation within SI, which is typically associated with a local improvement in tactile spatial discrimination. However, the eventuality that RSS (or any other activity-dependent protocol) may have remote effects to other body-parts, for instance its cortical neighbour the face, has not been investigated so far. To address this question, while also providing new elements aiming to better understand the perceptual relevance of cortical plastic changes, we conducted three studies which will be described in the following section.

Briefly, a first behavioural study (**study 1**) was conducted in healthy participants to investigate whether three hours of RSS applied at the index fingertip could alter tactile discrimination at the face, and whether such transfer follows a pattern “competition-like”. Then, two imaging studies were conducted to investigate the cortical correlates of RSS-induced changes within SI. Ultra-high field (7T) functional magnetic resonance imaging (fMRI, **study 2**) and magnetoencephalography (MEG, **study 3**) were respectively used due to their complementarity.

EXPERIMENTAL CONTRIBUTIONS

STUDY 1: BEHAVIOURAL STUDY

Prior investigations of the topographical limits of the RSS-induced perceptual and cortical changes only examined the hand, namely the fingers adjacent to the stimulated index finger (Godde et al., 2000; Pleger et al., 2001) and the homologous finger on the opposite hand (e.g., Godde et al., 2000, 2003; Pleger et al., 2001, 2003), with the conclusion that RSS-induced changes were largely local, both behaviourally and neurally. On the other hand, numerous studies reported large-scale plastic changes across the hand-face border following somatosensory deprivation (Pons et al., 1991; Elbert et al., 1994; Jain et al., 1997, 2008; Weiss et al., 2004), which were associated with perceptual changes (Ramachandran et al., 1992b; Halligan et al., 1993; Farnè et al., 2002; Weiss et al., 2004). Little is known, however, about whether such cross-border changes can be induced by *increasing* afferent input under non-pathological conditions, for instance through RSS-like learning processes.

Thus, in a first behavioural experiment, we investigated whether the RSS-induced improvement of tactile acuity observed at the stimulated fingertip, could cross the hand-face border and affect the face tactile acuity. To this aim, we assessed two-point discrimination thresholds at both upper-lips and cheeks in addition to both index fingers, respectively before and after RSS of the right index finger. To control for any contribution of training or of duration of the experiment, a control group in which participants underwent the exact same procedure, but with the RSS being off, was additionally tested.

The **two-point discrimination threshold (2PDT)** was first introduced by Weber in 1834 (Weber, 1996) as a measure of tactile spatial acuity, a measure that has subsequently become an important, albeit highly controversial, measure of human hand function. This threshold is defined as the shortest distance between two contact points that could be perceived as distinct, as opposed to just one. Due to its easy implementation, the 2PD task has been widely used to assess cutaneous innervation and central somatosensory function (Dellon and Kallman, 1983; Van Boven and Johnson, 1994; Lundborg and Rosén, 2004; Parianen Lesemann et al., 2015). It has been assumed that two points are distinguishable from one only when the two points are sufficiently separated to evoke spatially distinct foci of neural activity (Vallbo and Johansson, 1978). Accordingly, the 2PDT has been assumed by many to reflect the size and spacing of cutaneous RFs, particularly the innervation density of SAI afferents, which convey fine spatial information (Johansson and Vallbo, 1979; Johnson, 2001).

However, the validity of 2PD task as a measure of spatial acuity has been questioned (Johnson and Phillips, 1981; Craig and Johnson, 2000; Lundborg and Rosén, 2004; Tong et al., 2013). This controversy arises from the fact that 2PDT has sometimes been reported to fall under the receptor spacing (i.e., near 0 mm; Johnson and Phillips, 1981), suggesting that participants may exploit a **non-spatial cue** to perform the 2PD task (Craig and Johnson, 2000). Indeed, two closely spaced points elicit fewer action potentials in the underlying SAI afferents than does a single point of equal indentation (Vega-Bermudez and Johnson, 1999). Consequently, the overall response magnitude could provide a non-spatial cue (i.e., intensity cue) helping to perform the 2PD task. This means that participants would be able to infer whether a stimulus consisted of two closely spaced points or one without actually perceiving two distinct points pressing against the skin. This makes 2PDT extremely dependent on the **criterion** that participants adopt for responding that they perceive two points. Finally, another issue arises from the lack of **standardization** of reliable technique of 2PD assessment.

The most prominent alternative to the classical 2PDT discussed in the literature is the grating orientation threshold (GOT), in which a grating consisting of equidistant grooves and ridges (with varying width) is presented in one of two orientations, which has to be discriminated by the participant (Van Boven and Johnson, 1994; Craig and Johnson, 2000). However, potential confounds in the GOT task are unknown contributions of visual cortical processing (Sathian and Zangaladze, 2002) and anisotropy of the task performance (Vega-Bermudez and Johnson, 2004; Gibson and Craig, 2005). But, despite these different critics and the differences in the type of stimulation, 2PDT and GOT are roughly equivalent (Dinse et al., 2006; Bruns et al., 2014).

Considering the controversy of GOT and the fact that 2PDT is probably the most used (and known) method to evaluate tactile spatial acuity, we adopted several precautions regarding our method of assessing 2PDT. First, home-made devices were used to deliver a reliable stimulation with a constant application force. These devices also prevented participants to move the tested area. Then, the instructions for the task were carefully delivered to the participants, to ensure the use of a single criterion: to respond that they feel two points **ONLY** when clearly feeling two distinct points, and not a larger point, bar or anything else. These simple precautions made our 2PDT assessment reliable, as repeatedly confirmed in the literature (Godde et al., 2000, 2003; Pleger et al., 2001, 2003; Dinse et al., 2003, 2006). This method was kept similar across the three studies reported here.

Touch improvement at the hand transfers to the face

Dollyane Muret^{1,2,*}, Hubert R. Dinse³,
Silvia Macchione^{1,2},
Christian Urquizar^{1,2},
Alessandro Farnè^{1,2,4},
and Karen T. Reilly^{1,2,4}

The hand–face border is one of the most prominent features of the primate somatosensory cortex. A reduction of somatosensory input, following amputation or anesthesia, induces perceptual changes across this border that are explained by plastic competitive mechanisms [1–4]. Whether cross-border plasticity can be induced by learning processes relying on increased somatosensory input has been unclear. Here we report that training-independent learning [5] improves tactile perception, not only at the stimulated index finger, but also at the unstimulated face. These findings demonstrate that learning-induced tactile improvement can cross the hand–face border, suggesting that facilitation-based plasticity may operate in the healthy human brain.

Perceptual improvement can be induced by protracted training but also by brief training-independent learning through repetitive somatosensory stimulation (RSS) [5–7]. Applied to the index finger, RSS reliably improves tactile acuity at this finger [6,7], presumably via functional reorganization within somatosensory cortices [6]. Prior investigations concluded that RSS-induced changes were local, as no changes were found either at the adjacent or homologous fingers [7]. To investigate the possible spread of learning-induced changes across the hand–face border we applied RSS to the right index fingertip of healthy participants and tested tactile acuity at the unstimulated face. In experiment 1, two-point discrimination thresholds were assessed using force-controlled devices at the right (stimulated) and left (control) index fingertips (right/left-D2) and above the right and left upper-lip (right/left-Lip) in two groups of 15 participants before and after a three-hour period during which the

RSS device was either ON (RSS_{Exp1}) or OFF (Control_{Exp1}) (Figure S1).

To ensure our RSS protocol replicated the well-established finger-specific improvement of tactile acuity, fingertip thresholds were submitted to a rmANOVA. The triple interaction ($F_{(1,28)} = 5.90$, $P = 0.022$) revealed a significant decrease in right-D2 threshold after RSS in the RSS_{Exp1} group (Bonferroni-corrected: $P_{Bonf} = 0.002$), but no changes at left-D2 in this group or at either finger in the Control_{Exp1} group (P -values > 0.9) (Figure 1A). This acuity gain ($-15.26\% \pm 3.85$) is consistent with previous work (-15.6% on average; Supplemental Results in the Supplemental Information).

A double interaction from the same analysis on the lip data ($F_{(1,28)} = 7.37$, $P = 0.011$) revealed significantly lowered thresholds only in the RSS_{Exp1} group ($P_{Bonf} = 0.002$; $P > 0.9$ in Control_{Exp1} group) (Figure 1A). This indicates a transfer of the RSS-induced behavioural effect across the hand–face border,

likely arising from a spread of plastic changes from the right-D2 somatosensory representation [6] into the face region through horizontal intracortical connections. Although limited in number, these cross-border connections undergo Hebbian-based plastic changes [8] and are the most likely substrate for the interactions observed between the hand and face [2,3].

Notably, tactile improvement was side-specific at the fingers, but not at the lips, making transcallosal transfer unlikely. Instead, given the bilateral representation of the lips within the primary somatosensory cortex [9], the bilateral improvement observed at the lips may arise from transfer of right-D2's representational changes [6] to the neighbouring lips region within the left somatosensory cortices. To test this model of side-specificity, in experiment 2 (Supplemental Information) we measured two-point discrimination thresholds not only at the fingers and lips, but also at the cheeks (represented more

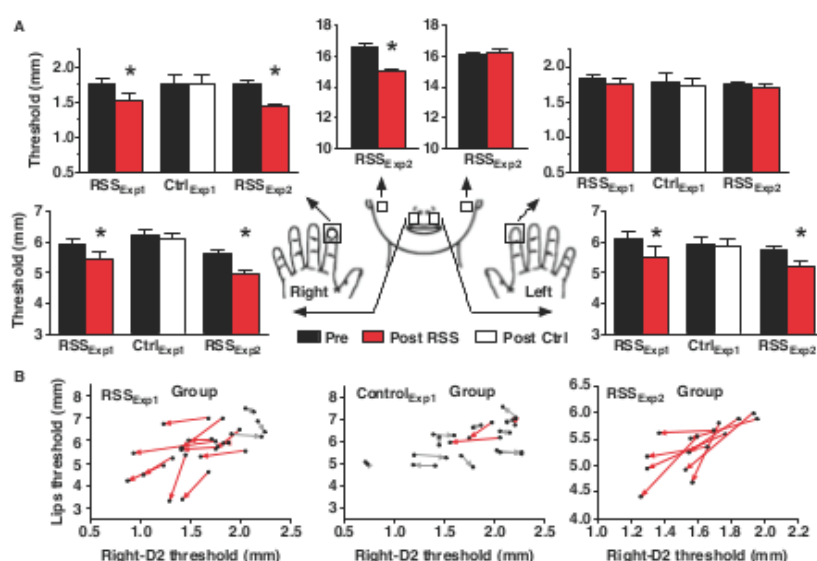


Figure 1. Improvement of touch acuity transfers from the finger to the face. (A) Mean two-point discrimination threshold pre (black) and post the procedure applied to the right-D2 (RSS: red; Control: white), assessed at right/left-D2, right/left-Lip and right/left-Cheek (mean \pm SEM; see also Figures S1 & S2). Repeated measures ANOVAs on data from the fingers, lips, and cheeks followed by Bonferroni-corrected post-hoc tests revealed significant threshold decreases ($*P_{Bonf} < 0.05$) at right-D2, both sides of the upper-lip, and right-Cheek in the RSS groups only (Supplemental Results). (B) Vectors showing the consistent relationship between threshold changes at the lips and right-D2 for each participant in the RSS_{Exp1} (left panel), Control_{Exp1} (central panel) and RSS_{Exp2} (right panel) groups. The starting and ending points of vectors respectively represent pre- and post-session thresholds. Red vectors indicate parallel threshold decreases at both right-D2 and lips, whereas grey vectors illustrate other combinations of threshold changes (see also Figure S1).



contralaterally [9]), before and after RSS (RSS_{Exp2} group). In addition to replicating the significant threshold decreases at both upper-lips ($F_{(1,7)} = 18.25$, $P = 0.004$) and at the right- ($F_{(1,7)} = 36.56$, $P_{\text{Bonf}} < 0.001$) but not left-D2 ($P > 0.9$; Figure 1A), a side-specific effect was also found for the cheek ($F_{(1,7)} = 21.32$, $P < 0.001$), with a significant improvement at the right-Cheek only ($P_{\text{Bonf}} = 0.005$; Figure 1A), thus supporting our model.

D-prime analyses confirmed sensitivity gains for right-D2, right-Cheek and both upper-lips (RSS_{Exp1}: all P_{Bonf} -values ≤ 0.027 , RSS_{Exp2}: all P_{Bonf} -values ≤ 0.045), with no slackening of participants' response criterion in either experiment (Supplemental Table S1). Furthermore, the stable pattern observed in the equally-sized Control_{Exp1} group, whose baseline thresholds were similar to those of the RSS_{Exp1} group (P -values ≥ 0.8), rules out unspecific contributions of training or attention.

Threshold decreases at the left- and right-Lip were correlated with each other ($r = 0.57$, $P = 0.026$), but not with right-D2 threshold decrease (P -values ≥ 0.4 ; Supplemental Results). However, 12/15 RSS_{Exp1} participants and all RSS_{Exp2} participants had decreased thresholds at both the right-D2 and lips, whereas this was true for only 3/15 Control_{Exp1} participants (Figure 1B). Interestingly, all RSS_{Exp2} participants also exhibited acuity gains at both the right-D2 and right-Cheek, which tended to correlate ($r = 0.70$, $P = 0.051$). Averaging across experiments, the mean threshold at the lips and right-Cheek decreased respectively by 10.8% (± 2.8) and 9.8% (± 3.6), which represent 62.4% and 56.6% of the improvement observed at right-D2 (Figure S1C).

The distribution of threshold changes combined with the high proportion of transfer strengthens the hypothesis of a large and robust spread of plastic changes across the hand-face border. Consistent with the intra-hemispheric shift of right-D2's representation following RSS [6], the correlation between gains at both upper-lips and the side-specificity at other body parts support the intra-hemispheric hypothesis. Since there is currently

no evidence that RSS effects transfer to other fingers [7], our findings further imply that training-independent perceptual improvement transfers across the hand-face border, without necessarily transferring within the hand. This may be surprising given the position of the thumb's representation (between that of the index and face [10]), but is consistent with results showing that the thumb's cortical representation is unchanged after RSS of the right-D2 [6]. This might be due to differences in remote and local circuit properties [8], with long-range facilitatory connections allowing hand-face transfer and shorter-range lateral inhibition preventing inter-finger transfer.

The cross-border perceptual improvements reported here provide evidence that passively increasing input to a body part can positively affect touch perception at cortically close, but physically distant body-parts, and thus reveal a novel perceptual learning phenomenon whereby improvement transfers across the hand-face border. To date, the theoretical framework within which hand-face border crossings have been interpreted has been one of 'competition' [1-4], whereby the face cortical area invades the deprived territory after permanent or transient removal of hand afferent inputs [3,4]. Although the present findings might rely on the same connections, the functional context (increased input) and subsequent consequences (acuity gain at non-contiguous body parts) indicate the need to extend the framework of cross-border plasticity beyond 'competition', which might apply to specific conditions of dramatically reduced afferent inputs, to generate new models of cortical plasticity that also account for 'facilitation' based forms of cross-border plasticity.

Supplemental Information

Supplemental Information includes supplemental results, experimental procedures, two figures and one table, and can be found with this article online at <http://dx.doi.org/10.1016/j.cub.2014.07.021>.

Acknowledgments

This work was supported by ANR-11-LABX-0042, FRM, McDonnell Foundation and SFB874 grant by the German Research

Foundation. We thank F. Volland for the setup and reviewers for their helpful comments.

References

1. Ramachandran, V.S., Stewart, M., and Rogers-Ramachandran, D.C. (1992). Perceptual correlates of massive cortical reorganization. *Neuroreport* 3, 583-586.
2. Farnè, A., Roy, A.C., Giraux, P., Dubernard, J.M., and Sirigu, A. (2002). Face or hand, not both: perceptual correlates of reafferentation in a former amputee. *Curr. Biol.* 12, 1342-1346.
3. Weiss, T., Miltner, W.H.R., Liepert, J., Meissner, W., and Taub, E. (2004). Rapid functional plasticity in the primary somatomotor cortex and perceptual changes after nerve block. *Eur. J. Neurosci.* 20, 3413-3423.
4. Jain, N., Qi, H.-X., Collins, C.E., and Kaas, J.H. (2008). Large-scale reorganization in the somatosensory cortex and thalamus after sensory loss in macaque monkeys. *J. Neurosci.* 28, 11042-11060.
5. Beste, C., and Dinse, H.R. (2013). Learning without training. *Curr. Biol.* 23, R489-R499.
6. Pleger, B., Dinse, H.R., Ragert, P., Schwenkreis, P., Malin, J.P., and Tegenthoff, M. (2001). Shifts in cortical representations predict human discrimination improvement. *Proc. Natl. Acad. Sci. USA* 98, 12255-12260.
7. Godde, B., Stauffenberg, B., Spengler, F., and Dinse, H.R. (2000). Tactile coactivation-induced changes in spatial discrimination performance. *J. Neurosci.* 20, 1597-1604.
8. Paullus, J.R., and Hickmott, P.W. (2011). Diverse excitatory and inhibitory synaptic plasticity outcomes in complex horizontal circuits near a functional border of adult neocortex. *Brain Res.* 1416, 10-25.
9. Nevalainen, P., Ramstad, R., Isotalo, E., Haapanen, M.-L., and Lauronen, L. (2006). Trigeminal somatosensory evoked magnetic fields to tactile stimulation. *Clin. Neurophysiol.* 117, 2007-2015.
10. Nakamura, A., Yamada, T., Goto, A., Kato, T., Ito, K., Abe, Y., Kachi, T., and Kakigi, R. (1998). Somatosensory homunculus as drawn by MEG. *Neuroimage* 7, 377-386.

¹INSERM U1028, CNRS UMR5292, Lyon Neuroscience Research Center, ImpAct Team, Lyon, France. ²University Claude Bernard Lyon I, Lyon, France.

³Neural Plasticity Laboratory, Institute for Neuroinformatics, Ruhr-University, Clinic of Neurology, BG University Hospital Bergmannsheil, Bochum, Germany.

⁴These authors contributed equally to the work.

*E-mail: dollyane.muret@inserm.fr

The editors of Current Biology welcome correspondence on any article in the journal, but reserve the right to reduce the length of any letter to be published. All Correspondence containing data or scientific argument will be refereed. Queries about articles for consideration in this format should be sent by e-mail to cbiol@current-biology.com

Supplemental Information:
Touch improvement at the hand transfers to the face

Dollyane Muret, Hubert R. Dinse, Silvia Macchione, Christian Urquizar,

Alessandro Farnè, Karen T. Reilly

Supplemental Results:

Multiple-Baseline stability of two-point discrimination thresholds

Experiment 1: Right-D2 and lip thresholds obtained at Pre-sessions S1 and S2 were analyzed for baseline stability. No significant main effects or interactions were found for either right-D2 or right-Lip thresholds (two repeated measures ANOVAs, all P values > 0.05). Only a significant main effect of Session was observed for left-Lip thresholds (repeated measures ANOVA, $F_{(1,28)} = 7.86$, $P = 0.012$), with S2 thresholds being higher than S1 thresholds. No significant interaction with the factor Group was found for this lip ($F_{(1,28)} = 0.37$, $P = 0.55$). As there was no effect of Session in the direction of task learning (i.e., no threshold reduction) for any of the four tested sites, performance at S1 and S2 was averaged to compute a Pre-session threshold measure.

Experiment 2: Right-D2, lip, and cheek thresholds obtained at Pre-sessions S1 and S2 were analyzed for baseline stability. No significant main effects or interactions were found for any of the six tested body-parts (six repeated measures ANOVAs, all P values > 0.05).

Analyses comparing Pre (S2 or average of S1 and S2 when available)/Post (Exp1: $n = 30$, Exp2: $n = 8$)

Thresholds

Experiment 1: A three-way repeated measures ANOVA with Session (Pre/Post), Digit (left-D2/right-D2) and Group (RSS/Control) as factors showed a significant main effect of Session ($F_{(1,28)} = 6.49$, $P = 0.016$) and a Session x Digit x Group interaction ($F_{(1,28)} = 5.90$, $P = 0.022$). This interaction revealed a significant threshold decrease at right-D2 in the RSS_{Exp1} group only ($P = 0.0006$; $P_{Bonf} = 0.002$; all P values > 0.9 for the Control_{Exp1} group, Figure 1A & S2).

A three-way repeated measures ANOVA with Session (Pre/Post), Lip (left-Lip/right-Lip) and Group (RSS/Control) as factors showed a significant main effect of Session ($F_{(1,28)} = 15.34$, $P = 0.0005$) and a Session x Group interaction ($F_{(1,28)} = 7.37$, $P = 0.011$). This interaction revealed a significant threshold decrease at the lips in the RSS_{Exp1} group only ($P = 0.0004$; $P_{Bonf} = 0.002$; all P values > 0.9 for the Control_{Exp1} group, Figure 1A & S2).

Experiment 2: A two-way repeated measures ANOVA with Session (Pre/Post) and Digit (left-D2/right-D2) as factors showed a significant main effect of Session ($F_{(1,7)} = 55.05$, $P = 0.0001$), a significant main effect of Digit ($F_{(1,7)} = 10.68$, $P = 0.014$) and a significant Session x Digit

interaction ($F_{(1,7)} = 36.56$, $P = 0.0005$). This interaction revealed a significant threshold decrease at right-D2 only ($P = 0.0001$; $P_{Bonf} = 0.0002$, Figure 1A & S2).

A two-way repeated measures ANOVA with Session (Pre/Post) and Lip (left-Lip/right-Lip) as factors showed a significant main effect of Session ($F_{(1,7)} = 18.25$, $P = 0.0037$) with a significant threshold decrease at both sides of the upper-lip after RSS (Figure 1A & S2).

A two-way repeated measures ANOVA with the factors Session (Pre/Post) and Cheek (left-Cheek/right-Cheek) showed a significant main effect of Session ($F_{(1,7)} = 54.10$, $P = 0.0001$) and a significant Session x Cheek interaction ($F_{(1,7)} = 21.32$, $P = 0.0024$). This interaction revealed a significant threshold decrease at the right-Cheek only ($P = 0.0027$; $P_{Bonf} = 0.0054$, Figure 1A & S2).

Threshold changes

To better quantify the RSS-induced changes in 2PDT, the difference in threshold between the Pre- and Post-sessions was expressed as a percentage of the Pre-session threshold.

Both local (i.e., right-D2) and remote (i.e., left and right upper-lip and right-Cheek) changes in tactile perception were present in the majority of participants (Figure S1C). While in the Control_{Exp1} group (white bars) and at the left-Cheek in the RSS_{Exp2} group threshold changes were approximately equally distributed around zero, most of the participants in both the RSS_{Exp1} and RSS_{Exp2} groups (dark and light red bars) had reduced thresholds after RSS, suggesting a consistent effect of RSS.

Threshold changes in spatial discrimination previously reported in the RSS literature, assessed with either 2-Point Discrimination (2PD) test or Grating Orientation Test (GOT):

[S1] -18.25% (n = 35; 2PD)	[S5] -20% (n = 12; 2PD)
[S2] -15.50% (n = 21; 2PD)	[S6] -12.60% (n = 16; 2PD)
[S3] -12.60% (n = 16; 2PD)	[S7] -16% (n = 11; GOT)
[S4] -19% (n = 14; 2PD)	[S8] -14.20% (n = 78; 2PD)

Weighted mean (by sample size) = -15.55%; Weighted SD = 2.30%

Mean = -16.02%; SD = 2.84%

Correlations

Experiment 1: Correlations were calculated on the data from the RSS_{Exp1} group between the change in two-point discrimination performance at the right-D2 fingertip and at both sides of the upper-lip. No significant correlations were found between threshold changes at the right-D2 and either side of the upper-lip (right-D2/left-Lip, $r = 0.23$, $P = 0.41$; right-D2/right-Lip, $r = 0.06$, $P = 0.83$), but threshold changes at both sides of the upper-lip were correlated ($r = 0.57$, $P = 0.026$). In the $Control_{Exp1}$ group no significant correlation was found between threshold changes at both sides of the upper-lip ($r = -0.0372$, $P = 0.895$).

Experiment 2: No significant correlations were found between threshold changes at the right-D2 and either side of the upper-lip (right-D2/left-Lip, $r = -0.02$, $P = 0.96$; right-D2/right-Lip, $r = -0.42$, $P = 0.30$), but threshold changes at the right-D2 tended to correlate with threshold changes at the right-Cheek ($r = 0.70$, $P = 0.051$).

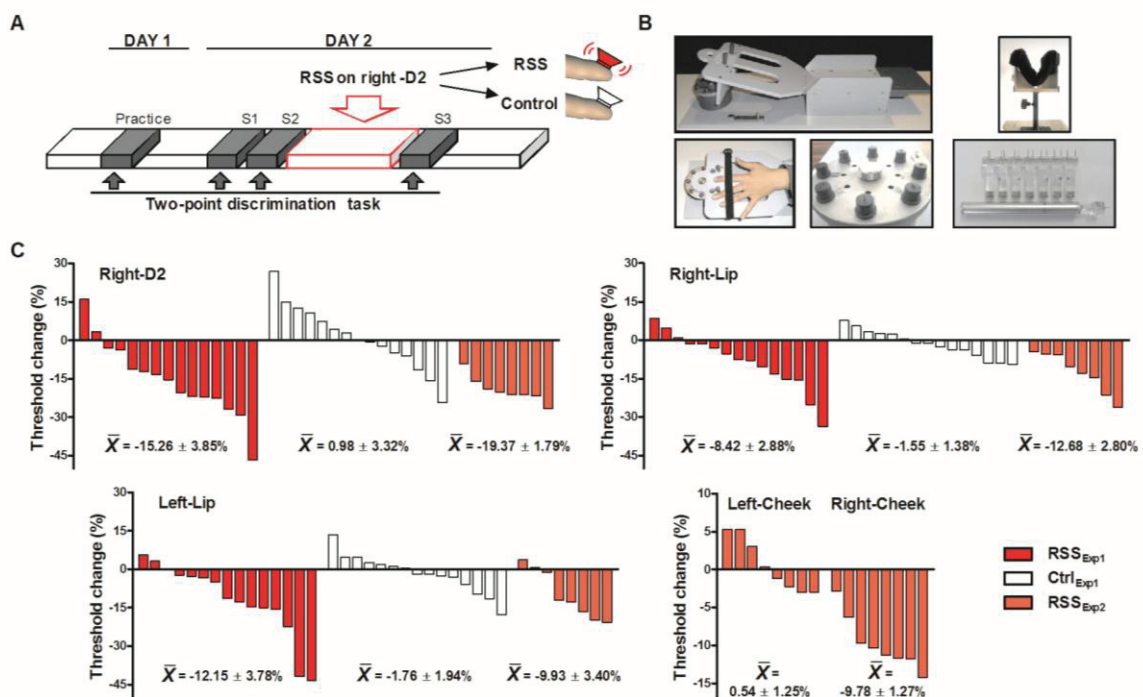


Figure S1, related to Experimental Procedures and Figure 1. Experimental design, testing devices and individual threshold changes following the procedure (RSS on or off) at the body-parts showing significant changes.

(A) Experimental design: 2PDT were assessed at right/left-D2, right/left-Lip and right/left-Cheek in a practice session and three experimental sessions (S1-S3) on two consecutive days. Participants were blindfolded and instructed to promptly answer whether they were touched by one or two tips. The RSS device was attached to the right-D2 for three hours between S2 and S3

with the stimulator switched on for the RSS_{Exp1} and RSS_{Exp2} groups and off for the $Control_{Exp1}$ group. When available, the average of S1 and S2 2PDTs was used to calculate the baseline (Pre-session) (otherwise threshold at S2 was used for the Pre-session threshold). Pre-session was then compared with 2PDT values measured in S3 (Post-session). **(B)** Spring mounted devices used to deliver nearly constant-force stimulation for 2PDT assessment on right/left-D2 (left), and on right/left-Lip and right/left-Cheek (right). **(C)** Rank ordered distributions of individual participant threshold changes in 2PDT (% of Pre-session) shown for the RSS_{Exp1} (dark-red bars), $Control_{Exp1}$ (white bars) and RSS_{Exp2} (light-red bars) groups for sites that showed significant changes at the group level in the RSS groups: the right-D2, the right and left upper-lips, and the right-Cheek. The bottom right panel also shows the same data for the non-affected left-Cheek in the RSS_{Exp2} (light-red bars). Each bar corresponds to a single participant. Values are rank ordered so a given participant is not represented in the same position across graphs. The average threshold changes at the group level are indicated below each distribution (\bar{X} referring to mean \pm SEM).

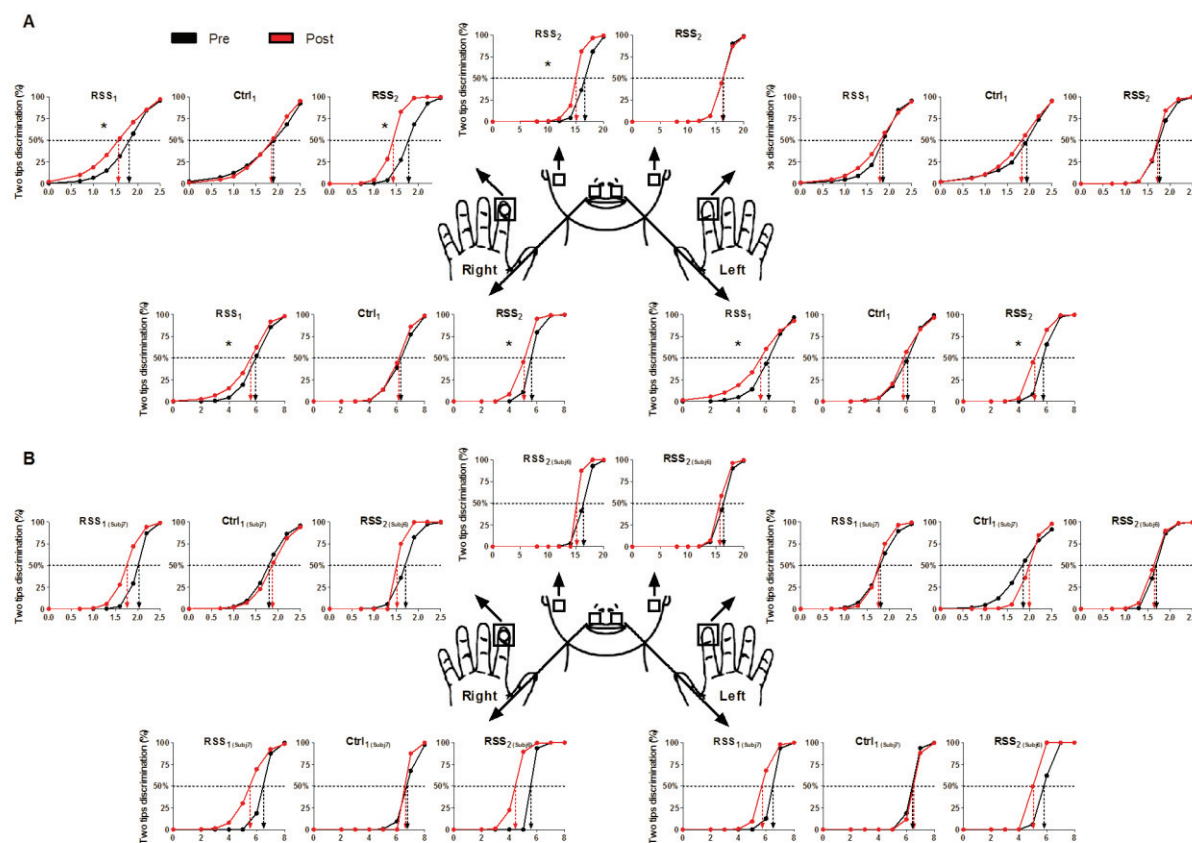


Figure S2, related to Figure 1. Mean and single subject psychometric curves, before and after the procedure (RSS on or off) at each tested body-part for each group.

(A) Psychometric curves averaged over all individual regression curves for each tested distance, Pre (black) and Post (red) the procedure applied to the right-D2. Asterisks highlight the cases

where a significant threshold decrease was obtained (repeated measures ANOVAs on data from the fingers, lips, and cheeks followed by Bonferroni-corrected post-hoc tests, $*P_{Bonf} < 0.05$, see Figure 1A). **(B)** Single subject psychometric curves from individuals representative of each group, Pre (black) and Post (red) the procedure applied to the right-D2. Arrows indicate thresholds at 50% correct detection.

Analyses comparing S2/Post (Exp1: $n = 30$):

Thresholds

A three way repeated measures ANOVA with factors Session (S2/Post), Digit (left-D2/right-D2) and Group (RSS/Control) showed a significant main effect of Session ($F_{(1,28)} = 5.47$, $P = 0.027$) and a Session x Digit x Group interaction ($F_{(1,28)} = 4.92$, $P = 0.035$). This interaction revealed a significant threshold decrease at right-D2 in the RSS_{Exp1} group only ($P = 0.006$; $P_{Bonf} = 0.026$; all P values > 0.9 for the Control_{Exp1} group).

A three way repeated measures ANOVAs with factors Session (S2/Post), Lip (left-Lip/right-Lip) and Group (RSS/Control) showed a significant main effect of Session ($F_{(1,28)} = 24.57$, $P = 0.00003$) and a Session x Group interaction ($F_{(1,28)} = 11.19$, $P = 0.002$). This interaction revealed a significant threshold decrease at both lips in the RSS_{Exp1} group only ($P = 0.00002$; $P_{Bonf} = 0.00006$; all P values > 0.9 for the Control_{Exp1} group).

Threshold changes

RSS_{Exp1} group:

Right-D2: $-13.67 \pm 3.92\%$ (mean \pm SEM).

Right-Lip: $-10.86 \pm 2.98\%$.

Left-D2: $-4.34 \pm 2.90\%$.

Left-Lip: $-13.76 \pm 3.53\%$.

Control_{Exp1} group:

Right-D2: $2.73 \pm 3.36\%$.

Right-Lip: $-1.46 \pm 1.60\%$.

Left-D2: $-0.62 \pm 6.41\%$.

Left-Lip: $-2.57 \pm 2.00\%$.

Correlations

As for when they were calculated with respect to the average of S1 and S2, threshold changes observed in the RSS_{Exp1} group showed no significant correlations between changes at the right-D2 and at either side of the upper-lip (right-D2/left-Lip, $r = 0.29$, $P = 0.30$; right-D2/right-Lip, r

= 0.02, $P = 0.93$). Again similar to the calculation based upon the S1-S2 average, threshold changes at both sides of the upper-lip were correlated ($r = 0.59$, $P = 0.02$).

In the Control_{Exp1} group, no significant correlation was found either between right-D2 and either side of the upper-Lip, nor between both sides of the upper-Lip (all P values > 0.08).

Analyses comparing Pre (average of S1 and S2) /Post for the lip data (RSS_{Exp1}: $n = 11$):

A two-way repeated measures ANOVA with Session (Pre/Post) and Lip (left-Lip/right-Lip) as factors, showed a significant main effect of Lip ($F_{(1,10)} = 7.71$, $P = 0.02$), the thresholds at the right-Lip being smaller than at the left-Lip, and a significant main effect of Session ($F_{(1,28)} = 7.72$, $P = 0.02$) reflecting a threshold decrease at both sides of the upper-lip after RSS.

			Pre-session	Post-session	Paired t-test		
			Mean \pm SD	Mean \pm SD	t	P	P_{Bonf}
Experiment 1 (Pre: S1 & S2 average or S2 only)	<i>d-prime</i>	Right-D2	0.93 \pm 0.35	1.22 \pm 0.55	-3.23	0.0060*	0.024*
		Left-D2	0.87 \pm 0.35	0.96 \pm 0.44	-1.34	0.20	
		Right-Lip	0.81 \pm 0.31	1.00 \pm 0.35	-3.18	0.0067*	0.027*
		Left-Lip	0.71 \pm 0.39	0.97 \pm 0.59	-3.59	0.0029*	0.012*
	<i>ln(Beta)</i>	Right-D2	0.57 \pm 0.09	0.52 \pm 0.15	1.37	0.19	
		Left-D2	0.57 \pm 0.09	0.55 \pm 0.12	0.54	0.60	
		Right-Lip	0.55 \pm 0.11	0.59 \pm 0.07	-1.57	0.14	
		Left-Lip	0.49 \pm 0.19	0.48 \pm 0.25	0.12	0.90	
Experiment 2 (Pre: S1 & S2 average)	<i>d-prime</i>	Right-D2	0.89 \pm 0.24	1.37 \pm 0.15	-8.14	0.00008*	0.0005*
		Left-D2	0.96 \pm 0.13	1.00 \pm 0.15	-1.05	0.33	
		Right-Lip	0.93 \pm 0.08	1.15 \pm 0.18	-4.30	0.0035*	0.021*
		Left-Lip	0.87 \pm 0.09	1.11 \pm 0.17	-3.71	0.0075*	0.045*
		Right-Cheek	0.66 \pm 0.15	1.01 \pm 0.09	-7.97	0.0001*	0.0006*
		Left-Cheek	0.75 \pm 0.06	0.73 \pm 0.14	0.36	0.73	
	<i>ln(Beta)</i>	Right-D2	0.58 \pm 0.12	0.63 \pm 0.03	-0.88	0.41	
		Left-D2	0.63 \pm 0.03	0.64 \pm 0.05	-1.19	0.27	
		Right-Lip	0.63 \pm 0.01	0.65 \pm 0.02	-1.56	0.16	
		Left-Lip	0.61 \pm 0.02	0.65 \pm 0.02	-3.76	0.0071*	0.042*
		Right-Cheek	0.52 \pm 0.08	0.65 \pm 0.01	-5.06	0.0015*	0.009*
		Left-Cheek	0.57 \pm 0.02	0.57 \pm 0.06	0.52	0.62	
Experiment 1 (Pre: S2)	<i>d-prime</i>	Right-D2	0.97 \pm 0.39	1.22 \pm 0.55	-2.64	0.0193*	0.077
		Left-D2	0.87 \pm 0.35	0.96 \pm 0.44	-1.34	0.20	
		Right-Lip	0.76 \pm 0.30	1.00 \pm 0.35	-3.98	0.0014*	0.005*
		Left-Lip	0.67 \pm 0.43	0.97 \pm 0.59	-4.64	0.0004*	0.001*
	<i>ln(Beta)</i>	Right-D2	0.57 \pm 0.10	0.52 \pm 0.15	1.57	0.14	
		Left-D2	0.57 \pm 0.09	0.55 \pm 0.12	0.54	0.60	
		Right-Lip	0.54 \pm 0.12	0.59 \pm 0.07	-1.81	0.09	
		Left-Lip	0.46 \pm 0.25	0.48 \pm 0.25	-0.56	0.58	

Table S1, related to Results in Main Text. Signal Detection Theory values.

Mean *d-prime* and *ln(Beta)* values at the Pre- (either the average of S1 and S2 or S2 only) and Post-session for each tested area for both the RSS_{Exp1} and RSS_{Exp2} groups. Paired t-test results are presented in the last column, $*P_{Bonf} < 0.05$. Participants from the second experiment were

more conservative (favouring 1 rather than 2 responses) after the RSS stimulation for the left-Lip and the right-Cheek, which could have yielded higher thresholds. Instead, the observed threshold decreased (confirmed by the significant increase in *d-prime* values). Therefore, in both experiments we observed improved discrimination, with no slackening of response criterion. The comparison of the S2 and Post sessions revealed significant *d-prime* increases at right-D2 (which did not survive the Bonferroni correction), right-Lip and left-Lip without criterion changes, as for when the comparison was made between the Post-session and the average of S1 and S2.

†Average of S1 and S2 for all 30 subjects for the right-D2 and right-Lip and for 20 subjects for the left-Lip. S2 only for 10 subjects for the left-Lip and for all 30 subjects for the left-D2.

Supplemental Experimental Procedures:

Participants

Thirty-two healthy volunteers participated in the first experiment. Participants were randomly assigned to one of two groups: RSS_{Exp1} or Control_{Exp1}. Two participants (one from each group) were excluded from the final analyses because their percent threshold change between S2 and S3 was more than 2.5 SDs above the average threshold change in their group. Groups were similar in terms of average age and number of males/females (RSS_{Exp1}: $n = 15$, mean age = $20.53 \pm \text{SD } 2.26$ years, 8 females. Control_{Exp1}: $n = 15$, mean age = $23.42 \pm \text{SD } 3.10$ years, 8 females). Eight healthy volunteers participated in the second experiment (RSS_{Exp2}: mean age = $23.25 \pm \text{SD } 1.67$ years, 7 females).

All participants were right-handed according to the Edinburgh Handedness Inventory [S9] (RSS_{Exp1}: mean score = $75.34 \pm \text{SD } 20.65\%$; Control_{Exp1}: mean score = $77.86 \pm \text{SD } 15.78\%$; RSS_{Exp2}: mean score = $73.75 \pm \text{SD } 24.46\%$), and they all gave written informed consent before participating. The protocol was approved by the ethics committee of Lyon, and was performed in accordance with the Declaration of Helsinki.

Experimental Design

During the Practice session (Day1), detailed instructions were given, informed consent was obtained, and two-point discrimination thresholds (2PDT) were measured. This session allowed participants to become familiar with the task, but the data were not included in any analyses

(Figure S1A). This Practice session and sessions S1 and S2 ensured that discrimination performance before RSS was stable and allowed us to separate RSS-induced changes from potential changes related to familiarization with the task.

Based upon previous studies reporting no threshold change at left-D2 [S2-S6, S8], and because we did not expect to see a threshold change on the left-Lip, the initial design of the first experiment tested 2PDT at the left-D2 and left-Lip in S2 and S3 only. However, when a preliminary analysis on the data from 4 participants from the RSS_{Exp1} group revealed changes in left-Lip threshold between S2 and S3 (i.e., after RSS), we modified our protocol to include assessments of left-Lip threshold in all four sessions. Data from the new design were obtained for 20 out of the 30 participants who participated in Experiment 1.

In the second experiment, thresholds of the six tested areas (left/right-D2, left/right-Lip and left/right-Cheek) were assessed in all four sessions (Practice, S1, S2 and S3) in all participants.

Within a session, each area was tested in a separate block, and for a given participant the order of blocks was maintained across sessions. Block order was randomized across participants.

Repetitive Somatosensory Stimulation (RSS) Protocol

We used an RSS protocol that is known to induce plastic changes in the somatosensory cortex [S2-S7, S10-S12]. This method is effective and relatively simple to implement. It relies on the Hebbian postulate as it simultaneously co-activates several cutaneous receptive fields, thus producing temporally correlated inputs necessary to give rise to Hebbian plasticity [S13, S14].

In the three groups (RSS_{Exp1}, Control_{Exp1} and RSS_{Exp2}) a small 8 mm diameter solenoid controlled by an MP3 player was taped to the volar surface of the right-D2 fingertip for three hours. In both the RSS_{Exp1} and RSS_{Exp2} groups this solenoid delivered brief (10ms) supra-threshold tactile stimuli with inter-stimulus intervals ranging from 100 to 3000 ms and following a Poisson distribution (average stimulation frequency of 1Hz). In the Control_{Exp1} group the stimulation was turned off. All participants could freely move during the real and control stimulation period (3 hours) and were instructed to continue with their daily activities without paying attention to the device, but to avoid intensive use of their fingers (i.e. they were not allowed to either write or type on a keyboard).

Two-point discrimination task

In Experiment 1 tactile two-point discrimination thresholds (2PDT) were assessed at four locations using a two-alternative forced-choice task: the tips of both index fingers [distance from fingertip: 5.40 ± 1.82 mm; distance from finger edge: 5.59 ± 0.69 mm (mean \pm SD)], and both sides of the upper-lip region [distance from mid-lip: 20.00 ± 4.52 mm (mean \pm SD); midway between the upper-lip and the base of the nose]. In Experiment 2, 2PDT were assessed at six locations using the same paradigm: the tips of both index fingers [distance from fingertip: 6.25 ± 2.12 mm; distance from finger edge: 5.13 ± 1.64 mm (mean \pm SD)], both sides of the upper-lip region [distance from mid-lip: 10.00 ± 0.00 mm (mean \pm SD); midway between upper-lip and nose], and both cheeks [distance from the corner of the mouth: 5.13 ± 0.58 cm; midway between the ear and the corner of the mouth at $46.09 \pm 5.25\%$ of the distance ear-mouth: 11.13 ± 0.44 cm (mean \pm SD)]. The tested lip areas are innervated by two independent nerves: each side of the upper-lip is innervated by the medial branch of the superior labial branch of the infraorbital nerve and these nerves never cross the midline [S15]. Thus, measurements at both sides of the upper-lip could not influence each other at the peripheral level. For each participant the location of each tested area was kept constant across sessions.

2PDT were assessed using eight probes, one with a single tip and seven with two tips separated by various distances. Shaft length was 1.9 mm for the finger probes and 8 mm for the lip and cheek probes. Shaft and tip diameters were identical for all probes (shaft: 0.7 mm; tip: approximately 200 μ m). The distances tested were predetermined and remained constant for all participants but differed between fingertips (0.7, 1.0, 1.3, 1.6, 1.9, 2.2, 2.5 mm), lips (2, 3, 4, 5, 6, 7, 8 mm) and cheeks (8, 10, 12, 14, 16, 18, 20 mm) because of basic sensitivity differences between these regions. For every site, each probe was tested 8 times in a pseudo-randomized order (no more than two consecutive repetitions of the same probe), resulting in 64 trials (approximately 10 minutes). Tips were always presented parallel to the longitudinal axis of the fingers and face. To avoid the problem of variations in application pressure when using handheld tips [S16, S17], we used two specially-designed spring-mounted apparatuses that controlled application force across trials.

The left images in panel B of Figure S1 show the apparatus used to assess 2PDT at the index fingertips. The eight probes were mounted on a rotatable disc which permitted rapid and unpredictable switching between distances. The participant's arm rested on the device with the index finger positioned over a small hole and the index, middle, and ring fingers strapped down to prevent them moving. Participants were instructed to relax the hand and the forearm, and to

remain still. The probes were brought into contact with the participant's finger by the experimenter pulling the device down towards the rotatable disc with an application force of between 150 and 200 mN [S11]. The fingertip remained in contact with the probes for approximately 1 second and participants were required to promptly give their oral response ("one" or "two"). The experimenter then lifted up the participant's hand, rotated the disc to present the next probe and continued until all probes had been presented eight times. Care was taken to prevent participants from moving their finger or pressing it down on the probes.

The apparatus used to test 2PDT on the skin above the upper-lip and on the cheeks is shown in the right images in panel B of Figure S1. The probes were mounted on individual plexiglass sticks with ferromagnetic bases (4.5 cm long). Probes were applied by inserting them into the end of a metal tube (length: 12.5 cm; diameter: 1.5 cm) which contained a spring that was calibrated to obtain an almost constant application force (between 190 and 290 mN). When applied to the skin, the plexiglass stick moved approximately 1 cm into the tube and a magnet prevented it from rotating or tilting. The participant's head was stabilized using a chin/head rest and their hands rested on the table. They were instructed to keep their face and hands relaxed and still. Stimulation was manually delivered by the experimenter perpendicularly to the skin surface to ensure that both tips (for the seven two-tip probes) touched the skin's surface at the same time. After each trial the experimenter changed the plexiglass base and presented the next probe until all probes had been presented eight times.

At the beginning of each finger, lip or cheek testing block the single probe and the two-tip probe with the largest tip separation (2.5 mm for the fingertip; 8 mm for the lips; 20 mm for the cheeks) were presented three times to the participant while the experimenter said "one" or "two". Once participants declared that they clearly felt the difference between these two probes the testing began and lasted approximately 10 minutes for each body-part.

Analyses

For each participant and for each area the mean of the verbal responses ('one' or 'two') was plotted as a function of distance between the probes and the psychometric function was fitted with a binary logistic regression [S8]. **Threshold** was determined from the fitted data and was defined as the distance at which participants responded "two" 50% of the time.

S1 and S2 thresholds were statistically analyzed for stability using repeated measures ANOVAs with, in Experiment 1, the two factors Group (Control/RSS) and Session (S1/S2) and in Experiment 2, the factor Session (S1/S2). Separate ANOVAs were performed for the right-D2,

right-Lip, and left-Lip data (left-D2 data were not collected at S1) of Experiment 1 and for data from each of the six tested body-parts (fingers, lips, cheeks) of Experiment 2.

Pre (average of S1 and S2 or S2 alone) and Post (S3) thresholds were statistically analyzed using (for Experiment 1) two three-way repeated measures ANOVAs (one for the lips one for the fingers) with factors Group (Control/RSS), Side (Left/Right), and Session (Pre/Post) or (for Experiment 2) three two-way repeated measures ANOVAs (one for each pair of body-parts) with factors Side (Left/Right) and Session (Pre/Post).

Threshold changes between Pre- and Post-sessions were determined for each subject as a percentage of the Pre-session threshold (average of S1 and S2, or S2 alone):

$$\frac{\text{Threshold Post} - \text{Threshold Pre}}{\text{Threshold Pre}} * 100.$$
 For each tested area the average threshold change was calculated.

Three correlations were performed within the RSS_{Exp1} group to compare threshold changes at the left and right upper-lip and between each side of the upper-lip and the right-D2. Six correlations were performed within the RSS_{Exp2} group to compare threshold changes at the left and right upper-lip, at the left and right-cheek and between each side of the upper-lip or cheek and the right-D2 (4 correlations).

To test for changes in discrimination sensitivity and response criterion (Signal Detection Theory), we calculated the false alarm and hit rates and using the MATLAB Palamedes toolbox for one-alternative forced choice (PAL_SDT_1AFC_PHFtoDP, MATLAB v.r2010a) we derived the discriminative index (*d-prime value*) and the criterion shift index (*ln(Beta) value*) [S18]. Statistical analysis was performed using paired t-tests corrected for multiple comparisons (Bonferroni), comparing sessions (Pre vs. Post) within both the RSS_{Exp1} (four t-tests) and the RSS_{Exp2} (six t-tests) groups.

All statistical analyses were conducted using Statistica[®] (v.9.0, StatSoft). Data were checked for normality using Kolmogorov-Smirnov tests. Bonferroni post-hoc analyses were performed and corrected for multiple comparisons (Bonferroni). All data are expressed as mean \pm standard error of the mean (SEM).

Supplemental References:

- S1. Godde, B., Spengler, F., and Dinse, H. R. (1996). Associative pairing of tactile stimulation induces somatosensory cortical reorganization in rats and humans. *Neuroreport* 8, 281–5.
- S2. Godde, B., Stauffenberg, B., Spengler, F., and Dinse, H. R. (2000). Tactile coactivation-induced changes in spatial discrimination performance. *J. Neurosci.* 20, 1597–604.
- S3. Pleger, B., Dinse, H. R., Ragert, P., Schwenkreis, P., Malin, J. P., and Tegenthoff, M. (2001). Shifts in cortical representations predict human discrimination improvement. *Proc. Natl. Acad. Sci. U.S.A.* 98, 12255–60.
- S4. Pleger, B., Foerster, A.-F., Ragert, P., Dinse, H. R., Schwenkreis, P., Malin, J.-P., Nicolas, V., and Tegenthoff, M. (2003). Functional imaging of perceptual learning in human primary and secondary somatosensory cortex. *Neuron* 40, 643–53.
- S5. Godde, B., Ehrhardt, J., and Braun, C. (2003). Behavioral significance of input-dependent plasticity of human somatosensory cortex. *Neuroreport* 14, 543–6.
- S6. Dinse, H. R., Ragert, P., Pleger, B., Schwenkreis, P., and Tegenthoff, M. (2003). Pharmacological modulation of perceptual learning and associated cortical reorganization. *Science* 301, 91–4.
- S7. Hodzic, A., Veit, R., Karim, A. A., Erb, M., and Godde, B. (2004). Improvement and decline in tactile discrimination behavior after cortical plasticity induced by passive tactile coactivation. *J. Neurosci.* 24, 442–6.
- S8. Dinse, H. R., Kleibel, N., Kalisch, T., Ragert, P., Wilimzig, C., and Tegenthoff, M. (2006). Tactile coactivation resets age-related decline of human tactile discrimination. *Ann. Neurol.* 60, 88–94.
- S9. Oldfield, R. C. (1971). The assessment and analysis of handedness: the Edinburgh inventory. *Neuropsychologia* 9, 97–113.
- S10. Pilz, K., Veit, R., Braun, C., and Godde, B. (2004). Effects of co-activation on cortical organization and discrimination performance. *Neuroreport* 15, 2669.
- S11. Kalisch, T., Tegenthoff, M., and Dinse, H. R. (2007). Differential effects of synchronous and asynchronous multifinger coactivation on human tactile performance. *BMC Neurosci.* 8, 58.
- S12. Gibson, G. O., Makinson, C. D., and Sathian, K. (2009). Tactile co-activation improves detection of afferent spatial modulation. *Exp. Brain Res.* 194, 409–17.
- S13. Clark, S. A., Allard, T., Jenkins, W. M., and Merzenich, M. M. (1988). Receptive fields in the body-surface map in adult cortex defined by temporally correlated inputs. *Nature* 332, 444–5.
- S14. Wang, X., Merzenich, M. M., Sameshima, K., and Jenkins, W. M. (1995). Remodelling of hand representation in adult cortex determined by timing of tactile stimulation. *Nature* 378, 71–5.
- S15. Hu, K.-S., Kwak, J., Koh, K.-S., Abe, S., Fontaine, C., and Kim, H.-J. (2007). Topographic distribution area of the infraorbital nerve. *Surg. Radiol. Anat.* 29, 383–88.
- S16. Johnson, K. O., and Phillips, J. R. (1981). Tactile spatial resolution. I. Two-point discrimination, gap detection, grating resolution, and letter recognition. *J. Neurophysiol.* 46, 1177–92.
- S17. Craig, J. C., and Johnson, K. O. (2000). The two-point threshold: not a measure of tactile spatial resolution. *Curr. Dir. Psychol. Sci.* 9, 29–32.
- S18. Ragert, P., Kalisch, T., Bliem, B., Franzkowiak, S., and Dinse, H. R. (2008). Differential effects of tactile high- and low-frequency stimulation on tactile discrimination in human subjects. *BMC Neurosci.* 9, 9.

TRANSITION TO IMAGING STUDIES

Instead of an impaired tactile acuity, (as one may have expected from the tactile improvement at the fingertip, based on the literature showing competitive processes between neighbouring cortical areas), we report that *increasing* input at the right index finger of healthy participants through RSS improved tactile perception not only at the stimulated fingertip, but also at the unstimulated lips and cheek. These findings demonstrate that perceptual improvement induced by finger stimulation crosses the face-hand border in a novel 'competition-free' manner, and suggest that competition is not the only mechanism behind cross-border plasticity, but that facilitation-based plasticity can be harnessed to produce large-scale changes in the healthy human brain.

Together with the fact that an expansion and a shift of the cortical representation of the RSS-stimulated finger (i.e., right-D2) has been extensively reported in SI (Pleger et al., 2001, 2003; Godde et al., 2003; Hodzic et al., 2004), the behavioural results of this first study bring to the prediction that: (i) the lips representation may also be affected and enlarged after RSS of right-D2, (ii) such an enlargement would possibly lead to a shift of their centre of gravity or dipole sources, and (iii) these shifts might be toward the RSS-stimulated finger.

In order to investigate the cortical correlates of these behavioural changes, two imaging studies were then performed with the same RSS protocol and behavioural task to allow a direct comparison between perceptual and cortical changes. Among the neuroimaging techniques available, fMRI and MEG exhibit the highest spatial resolution achievable non-invasively in healthy participants, which makes them the most suitable to investigate the subtle changes we are expecting.

STUDY 2: 7T FMRI STUDY

Among functional neuroimaging techniques, fMRI is indubitably the most extensively used since the discovery of its potential for studying brain function in the early 1990s. This technique relies on the detection of changes in cerebral blood flow (CBF) that exceed changes in tissue oxygen consumption, which is tightly linked to neuronal activity. This phenomenon is called neurovascular coupling. Although this link was discovered quite early by Charles Roy and Charles Sherrington in 1890 (Roy and Sherrington, 1980), one century passed before the first description of fMRI and its blood oxygenation level dependent (BOLD) signal by Seiji Ogawa in the 1990. Based on earlier works by Thulborn and colleagues (Thulborn et al., 1982) and by Pauling's and Coryell's who discovered the paramagnetic nature of deoxyhemoglobin, making it a good indicator to measure blood flow to the brain (Pauling and Coryell, 1936), Ogawa and colleagues measured blood flow changes in rodents using a strong magnetic field (7.0 Tesla) MRI. To show these blood flow changes were related to functional brain activity, they manipulated the blood oxygen level (later called BOLD signal) by changing the proportion of oxygen breathed by the animals, and scanned them while monitoring brain activity with EEG (Ogawa et al., 1990). Since then, fMRI has come to dominate the brain imaging field due to its low invasiveness, high spatial resolution, and relatively wide availability and easy use.

As fMRI relies on the detection of changes in blood oxygenation, it provides only an indirect measure of brain activity. The basic principle of the underlying neurovascular coupling relies on that fact that in case of neuronal activity, blood flow to the brain increases to bring to the neurons the amount of glucose and oxygen (in the form of oxygenated hemoglobin) they need. Usually the brought-in oxygen is more than the oxygen consumed in burning glucose, and this causes a net decrease in deoxyhemoglobin in that brain area (see Figure 45). This changes the magnetic property of the blood, making it interfere less with the magnetization and its eventual decay induced by the MRI process.

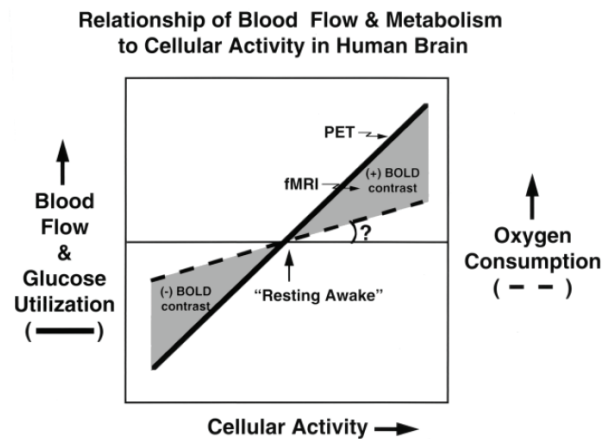


Figure 45 [from Raichle, 1998]. Summary of the basic principle on which BOLD signal relies, i.e., the relationship between blood flow, glucose utilization and oxygen consumption, and the cellular activity of the brain during changes in functional activity. The changes occurring in o blood flow and glucose utilization exceed changes in oxygen consumption.

Beyond this theoretical principle, the exact relationship between BOLD signal and the underlying neural activity is still not fully understood (for reviews on neurovascular coupling, see Shibasaki, 2008; Vanzetta and Grinvald, 2008; Kim and Ogawa, 2012). However, electrophysiological studies in animals support the idea that positive BOLD response (PBR; i.e., above baseline levels) reflects an increase in neural activity (Logothetis et al., 2001; Arthurs and Boniface, 2003; Devor et al., 2005; Goloshevsky et al., 2008; Huttunen et al., 2008; Bentley et al., 2014). Conversely, negative BOLD response (NBR; i.e., below baseline levels) has been recently increasingly investigated, and while its neurophysiological significance raised considerable debate, accumulating evidence suggests that NBR is tightly coupled with local decreases in neuronal activity below spontaneous activity (see Figure 46; Shmuel et al., 2006; Boorman et al., 2010; Kennerley et al., 2012; Schäfer et al., 2012; Bentley et al., 2014; Mullinger et al., 2014).

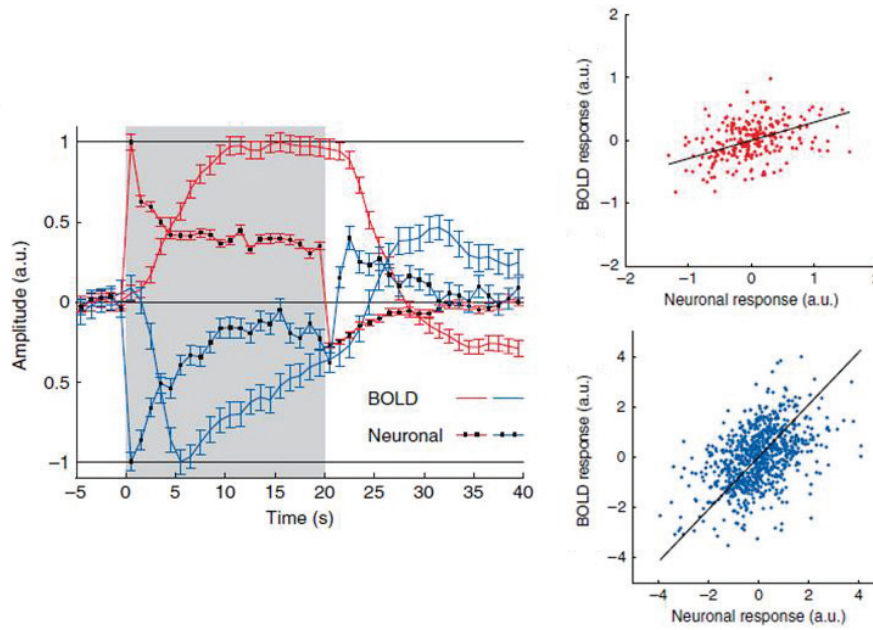


Figure 46 [from Shmuel et al., 2006]. **Left:** Dynamics of BOLD signal and neuronal activity. red: PBR and increases neuronal activity; blue: NBR and decreases in neuronal activity. **Right:** Scatter plots of the trial-by-trial amplitude of the PBR (red) and NBR (blue) as a function of respectively the increase and decrease in neuronal activity.

In this first imaging experiment, we choose to exploit the high spatial resolution of ultra-high field fMRI (7T) to investigate the cortical changes induced by RSS, with regard to the behavioural changes observed at both the finger and face level. Both PBR and NBR were considered.

Cortical correlates of perceptual changes transferring from the finger to the lips in human SI revealed by 7T fMRI

Dollyane Muret^{1,2}, Roberto Martuzzi³, Hubert R. Dinse^{4,5}, Karen T. Reilly^{1,2}, Alessandro Farnè^{1,2*}, Olaf Blanke^{3,6*}

¹ Lyon Neuroscience Research Centre (CRNL), Integrative, Multisensory, Perception, Action and Cognition (ImpAct) Team, INSERM U1028, CNRS UMR5292, 69000 Lyon, France;

² University Claude Bernard Lyon 1, 69000 Lyon, France;

³ Laboratory of Cognitive Neuroscience & Centre for Neuroprosthetics, Ecole Polytechnique Fédérale de Lausanne (EPFL), Lausanne, Switzerland;

⁴ Neural Plasticity Laboratory, Institute for Neuroinformatics, Ruhr-University;

⁵ Clinic of Neurology, BG University Hospital Bergmannsheil, Bochum, Germany;

⁶ Department of Neurology, University Hospital, Geneva, Switzerland.

* These authors contributed equally to the study

Corresponding author: Dollyane Muret, Neuroscience Research Centre, 16 avenue du Doyen Lépine, 69100 Bron, France. E-mail: dollyane.muret@inserm.fr.

Acknowledgements: This work was supported by the McDonnell foundation, ANR DFG and Labex cortex. We thank F. Hadj-Bouziane and Angelika Lingnau for their precious advices regarding the fMRI analysis.

Abstract

Better understanding the functional relevance of cortical plasticity is still a major challenge. Within the primary somatosensory cortex (SI), large-scale plastic changes have been reported across the hand-face border following deafferentation and correlated with phantom sensations and pain. While similar representational changes, but associated with perceptual benefits, have been observed locally following learning, the possible extent across the hand-face border has not yet been investigated. To address this question, we used a repetitive somatosensory stimulation, known to induce an expansion of the cortical representation of stimulated finger, associated with an improved tactile acuity at this finger, which was recently found to transfer to the face. Using ultra-high field magnetic resonance imaging (7T fMRI) to precisely map the cortical representations of each finger and lip within SI sub-regions, we report an enlarged activation of the stimulated finger within BA3b and BA1, but also a decreased volume of activation for the adjacent finger after RSS ($p=.049$). Interestingly, we also report the presence of contralateral deactivations evoked by lips stimulation which were co-localized with the contralateral activation elicited by finger stimulation. This lip deactivation within the contralateral BA3b was found to expand after RSS. Altogether, these results not only report the major contribution of BA3b and BA1 sub-regions to the RSS-induced effects, but also suggest the presence of a new interaction between the hand-face mediated by activation/deactivation processes.

Introduction

One of the most intriguing and yet unsolved challenges faced by the neuroscientific community is to understand the functional significance of cortical plasticity. Within the primary somatosensory cortex (SI), large-scale reorganizations after permanent or transient reduction of afferent input (Pons et al., 1991; Weiss et al., 2004) have been extensively investigated during the last 25 years due to its striking feature of crossing the hand-face “boundary”. The mechanisms subserving such large-scale plastic changes are assumed to act on competitive processes, intrinsically present between neighbouring areas, for instance by releasing intracortical inhibition (Tremere et al., 2001b), unmasking corticocortical connections (Smits et al., 1991) or a combination of both. This cortical plasticity, which typically displays an expansion of the face representation into that of the deprived hand area, was found to correlate with phantom sensations and pain (Flor et al., 1995; Davis et al., 1998; but see Makin et al., 2013), and thus considered as maladaptive.

Quite surprisingly, despite the fact that similar expansion of cortical representations (mostly of the fingertips) has been repeatedly observed following an increase in somatosensory input (Recanzone et al., 1992d; Wang et al., 1995; Pleger et al., 2003; Hodzic et al., 2004), their possible extent across the hand-face border has never been investigated. Such a gap into our knowledge about large-scale plasticity due to augmented somatosensory stimulation is even more astonishing when considering that, in contrast to deprivation cases, these input-increase or activity-dependent plastic changes were invariably associated with enhanced tactile acuity (Recanzone et al., 1992a; Godde et al., 2000; Pleger et al., 2003; Hodzic et al., 2004; Zamorano et al., 2015) or augmented sensorimotor skills in experts such as musicians (Elbert et al., 1995) or Braille readers (Pascual-Leone and Torres, 1993; Sterr et al., 1998b). Trying to fill this gap, here we tested the limits and functional repercussions of such beneficial (or adaptive) somatosensory plasticity.

To this aim, we built upon a recent study (Muret et al., 2014) in which we showed that repetitive somatosensory stimulation (RSS) of the right index finger (right-D2), known to improve tactile acuity locally at this fingertip (Godde et al., 2000; Pleger et al., 2003), actually improves tactile acuity also remotely, at the level of the upper-lip (bilaterally) and cheek (ipsilaterally). Since the local behavioural effects of RSS have consistently been associated with plastic reorganization within SI (see Parianen Lesemann et al., 2015 for a review), as expressed by an enlargement of the cortical representation of the stimulated finger (Pleger et al., 2003;

Hodzic et al., 2004), we hypothesised that larger scale reorganization may accompany the remote effects induced by RSS at the lips, thus crossing the hand-face border.

Ultra-high field functional magnetic imaging (7T fMRI) has recently proven its reliability in providing detailed somatosensory maps of individual finger representations within SI (Sánchez-Panchuelo et al., 2012; Besle et al., 2013b), and even within different sub-regions of SI, as recently shown by Martuzzi and colleagues (Martuzzi et al., 2014). Taking advantage of the ultra-high spatial resolution of this technique, we examined in depth the RSS-induced cortical plasticity, with a special focus on the differential contribution of the three Brodmann areas (BA) involved in tactile information processing within SI, namely areas 3b, 1 and 2 (BA3b, BA1 and BA2). In addition, to assess the spatial limits of this form of adaptive plasticity, we investigated whether RSS-induced cortical plasticity can cross the hand-face border under non-pathological conditions.

Materials and Methods

Participants. Fourteen healthy volunteers (mean age = $23.21 \pm \text{SD } 3.60$ years, 7 females) participated in the study. One participant was excluded from further analyses due to excessive head motion (more than 2mm) during fMRI scanning. All participants were right-handed according to the Edinburgh Handedness Inventory (Oldfield, 1971; mean score = $70.95 \pm \text{SD } 25.54\%$), and gave written informed consent before participating. All procedures were approved by the Ethics Committee of the Faculty of Biology and Medicine of the University of Lausanne, and the study was conducted in accordance with the Declaration of Helsinki.

Experimental time course. The experiment took place over two consecutive days. During the first day, participants were familiarized with the experimental procedure and a first measure of tactile spatial acuity was assessed. On the second day, another measure of tactile acuity was acquired before a first session of fMRI recordings, then repetitive somatosensory stimulation (RSS) was applied to the right index finger for three hours. Afterward the RSS, a new set of fMRI and tactile spatial acuity measures were acquired, with the order of these two measures counterbalanced across participants (see Figure 1 for a schematic representation of the experimental time course).

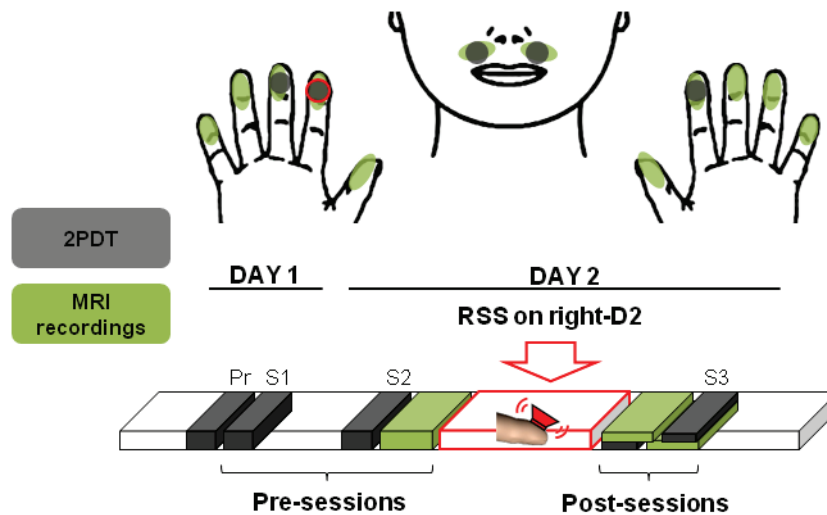


Figure 1. Experimental time course. Two-point discrimination thresholds (2PDT) were assessed at right/left-D2, right-D3 and right/left-Lip in a practice session and three experimental sessions (S1-S3) distributed over two consecutive days. On the second day, the RSS device was attached to the right-D2 for three hours between S2 and S3. In order to assess cortical plasticity, the cortical representations of both sides of the upper-lips and each finger on both hands were mapped during two fMRI sessions acquired before and after the RSS procedure. After RSS, the order between the fMRI and tactile acuity sessions was counterbalanced across participants.

Repetitive Somatosensory Stimulation (RSS) Protocol. The RSS protocol consist in the simultaneous co-activation of several cutaneous receptive fields in a limited portion of a fingertip, thus producing temporally correlated inputs necessary to drive Hebbian plasticity (Clark et al., 1988; Wang et al., 1995). A small 8 mm diameter solenoid controlled by an MP3 player was taped to the volar surface of the right-D2 fingertip. For three hours this solenoid delivered supra-threshold tactile stimuli with inter-stimulus intervals ranging from 100 to 3000 ms and following a Poisson distribution (average stimulation frequency of 1Hz). Participants could freely move during the stimulation period and were instructed to continue with their daily activities without paying attention to the device, but to avoid intensive use of their fingers (i.e., they were not allowed to either write or type on a keyboard).

Tactile spatial acuity assessment. To assess tactile spatial acuity, two-point discrimination thresholds (2PDT) were measured using a two-alternative forced-choice task at both index fingertips (left-D2 & right-D2), the right middle fingertip (right-D3), and both sides of the upper-lip region, three times before (Practice, S1 and S2) and once after (S3) 3 hours of RSS applied to the right-D2. During the Practice session (Day1), detailed instructions were given and informed consent was obtained before the 2PDT assessment. This session allowed participants to become familiar with the task, but data were not analyzed. Sessions S1 and S2 allowed to test

whether discrimination performance before RSS was stable and allowed us to separate RSS-induced changes from potential changes related to familiarization with the task. Based upon previous studies reporting that learning due to practice/familiarization transfers to the homologous finger (Sathian and Zangaladze, 1997, 1998; Harris et al., 2001; Harrar et al., 2014), together with other studies showing no threshold change at left-D2 following RSS on right-D2 (Godde et al., 2000, 2003; Pleger et al., 2001, 2003; Dinse et al., 2003, 2006), 2PDT at left-D2 was assessed in S2 and S3 only. Within a session each area was tested in a separate block, and for a given participant the order of blocks was maintained across sessions, but block order was randomized across participants. For each participant the location of each tested area was kept constant across sessions [distance from fingertip: 5.69 ± 2.29 mm and distance from finger edge: 6.00 ± 0.91 mm (mean \pm SD); distance from mid-lip: 18.38 ± 2.66 mm (mean \pm SD), midway between the upper-lip and the base of the nose].

2PDTs were assessed using a set of eight probes, one with a single tip and seven with two tips separated by various distances. Shaft length was 1.9 mm for the finger probes and 8 mm for the lip and cheek probes. Shaft and tip diameters were identical for all probes (shaft: 0.7 mm; tip: approximately 200 μ m). The distances tested were predetermined and remained constant for all participants but differed between index fingertips (0.7, 1.0, 1.3, 1.6, 1.9, 2.2, 2.5 mm), middle fingertip (1.0, 1.4, 1.8, 2.2, 2.6, 3.2, 4 mm) and lips (2, 3, 4, 5, 6, 7, 8 mm) because of absolute sensitivity differences between these regions. At the beginning of each testing block, the single probe and the two-tip probe with the largest tip separation (2.5 mm for index fingertips; 4 mm for the middle fingertip; 8 mm for the lips) were presented three times to the participant while the experimenter said "one" or "two". Once participants declared that they clearly felt the difference between these two probes the testing was started and lasted 10 to 15 minutes for each body-site. For every site, each probe was tested 8 times in a pseudo-randomized order (no more than two consecutive repetitions of the same probe), resulting in 64 trials. Tips were always presented parallel to the longitudinal axis of the fingers and face.

To avoid the problem of variations in application pressure when using handheld tips (Johnson and Phillips, 1981; Craig and Johnson, 2000), we used two specially-designed spring-mounted apparatuses that controlled application force across trials (for details, see Muret et al., 2014 supplemental data). Briefly, for fingertips, the eight probes were mounted on a rotatable disc which permitted rapid and unpredictable switching between distances while the participant's arm rested on the device with the tested fingertip positioned over a small hole. Participants were blindfolded and instructed to relax the hand and forearm and to remain still. The probes were brought into contact with the participant's finger by the experimenter pulling

the device down towards the rotatable disc with an application force of between 150 and 200 mN (Kalisch et al., 2007). The fingertip remained in contact with the probes for approximately 1 second and participants were required to promptly give their oral response (“one” or “two”). The experimenter then lifted up the participant's hand, rotated the disc to present the next probe and continued until all probes had been presented eight times. Care was taken to prevent participants from moving their finger. Similarly, for the lips, probes were mounted on individual plexiglass sticks with ferromagnetic bases (4.5 cm long) and were used to deliver the stimulation by inserting them into the end of a metal tube (length: 12.5 cm; diameter: 1.5 cm) which contained a spring that was calibrated to obtain an almost constant application force (between 190 and 290 mN). When applied to the skin, the plexiglass stick moved approximately 1 cm into the tube and a magnet prevented it from rotating or tilting. The participants' head was stabilized by a chin-head rest and their hands rested on the table. They were instructed to keep their face and hands relaxed and still. Stimulation was manually delivered by the experimenter perpendicularly to the skin surface to ensure that both tips (for the seven two-tip probes) touched the skin's surface at the same time. After each trial the experimenter changed the plexiglass base and presented the next probe until all probes had been presented eight times.

Procedure for fMRI data acquisition. During fMRI sessions, participants lay supine in the scanner with both arms comfortably stretched along the side of their body in the magnet bore. Just before being slowly moved into the scanner, a custom-made MRI-compatible device was fixed on the 32-channel coil to deliver tactile stimulation to each of the upper-lips with a constant application force and location (Figure 2). This device consisted of 2 brushes attached to a plastic joint which allowed pendular displacement along the medio-lateral axis of each brush independently. The position of each brush was adjustable with respect to the distance from the coil, which allowed the position of the brushes to be adapted to each participant's face configuration and head size.

Two casts were used to maintain the forearm, the wrist and the two first phalanges of each finger aligned in the same position, and to maintain each finger well-separated from each other, thus preventing inadvertent stimulation of multiple-fingers. Additionally, to maintain tactile stimulation parameters stable across Pre/Post RSS sessions, these casts allowed access only to the distal phalange of each finger and prevented any change of the hand posture over the course of the acquisition.

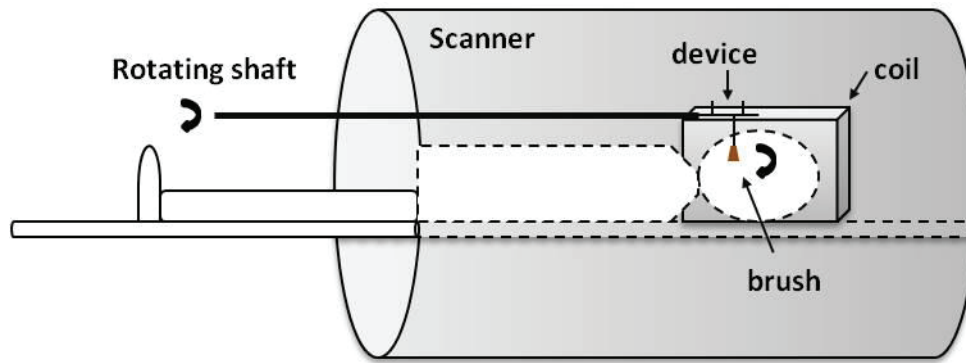


Figure 2. MRI-compatible apparatus used to stroke the lips. The experimenter stayed at the entrance to the bore and sequentially stimulated the fingertips and the upper-lip using either a tooth brush or the shaft whose rotation induced a pendular displacement of the brush that was attached to the coil.

Two functional runs were acquired per session, with one run per hemibody. The order in which each side was tested was kept constant across sessions but counter-balanced across participants. The experimenter was positioned at the entrance to the bore where she could easily reach and stroke the distal phalange of each digit with a tooth brush and could control the shafts attached to the lip stimulator attached to the coil. Stimulation was delivered on the distal phalange of each finger along the longitudinal axis, and on one side of the upper-lip along the medio-lateral axis of the face. Each body-site was repeatedly stroked independently for 24 s, followed by 12 s of rest, in the following order: D1 (thumb), D3 (middle), D5 (little), D2 (index), D4 (ring) and Lip. This sequence was repeated four times per run, resulting in a scan time of 12 min per run. To minimize the variability of the stroking procedure all stimulations were performed by the same experimenter (DM) who kept a similar pace and pressure on the fingers across subjects. Each stroke lasted 400–700 ms and digits were stroked at a frequency of ~ 1 Hz, leading to approximately 25 strokes per stimulation block.

MRI data acquisition. Images were acquired on a short-bore 7T scanner (Siemens Medical, Germany) with a 32-channel coil Tx/Rx RF-coil (Nova Medical, USA). Functional images were acquired using sinusoidal readout EPI sequence (Speck et al, 2008) and comprised 34 axial slices (in-plane resolution 1.3mm^2 ; slice thickness 1.3mm ; no gap) placed over the postcentral gyrus (approximately orthogonal to the central sulcus, see Figure 3) in order to cover the primary somatosensory cortex ($\text{TR} = 2.4\text{s}$, $\text{TE} = 27\text{ms}$, matrix size 160×160 , $\text{FOV} = 210\text{mm}$, GRAPPA = 2). Two functional runs (one for each hemibody) were acquired before and after the RSS procedure, comprising 371 volumes each. To aid coregistration, two whole-brain EPI volumes with 91 slices (1.3mm^3 resolution) were also acquired before and after the procedure. To aid in the delineation of the Brodmann areas, a 1mm^3 resolution anatomical volume was

acquired at the beginning of the first session (Pre) using the MP2RAGE sequence (TR = 5.5s, TE = 2.82ms, TI1 = 0.75s, TI2 = 2.35s, TRmpage = 5.5s, see Marques et al, 2010).

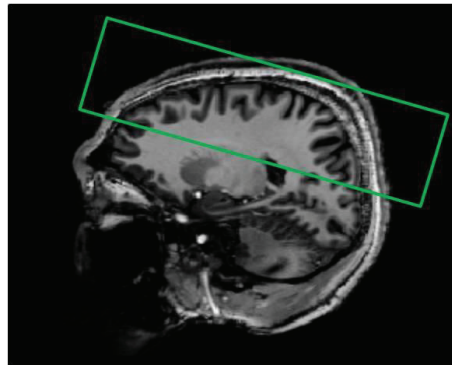


Figure 3. Position of the 34 axial slices acquired during functional recordings shown on the structural MRI of an individual participant.

Behavioural data analysis. For each participant and for each body-site the mean of the verbal responses ('one' or 'two') was plotted as a function of distance between the probes and the psychometric function was fitted with a binary logistic regression (Dinse et al., 2006). Threshold values were determined from the fitted data and were defined as the distance at which participants responded "two" 50% of the time. S1 and S2 thresholds for each body-site (except left-D2 as data were not collected at S1) were separately analyzed for stability using repeated measures ANOVA (rmANOVA) with the factor Session (S1, S2). Pre (average of S1 and S2) and Post (S3) thresholds were analyzed using separate two-way rmANOVAs with factors Side (Left/Right) and Session (Pre/Post) respectively for the index fingertips and upper-lips datasets and using a one-way rmANOVA with factor Session (Pre/Post) for the right-D3 dataset. Furthermore, threshold changes between Pre- and Post-sessions were determined for each subject as a percentage of the Pre-session threshold (average of S1 and S2): $\frac{Threshold_{Post} - Threshold_{Pre}}{Threshold_{Pre}} * 100$. Mean threshold changes were calculated for each of the five tested areas and were then submitted to a one-way rmANOVA to assess differences in threshold change across body-sites. Three linear correlations (Pearson) were performed to compare threshold changes at the left and right upper-lip and between each side of the upper-lip and the right-D2. To assess whether threshold changes were related to changes in discrimination sensitivity and/or in response criterion (Signal Detection Theory), false alarm and hit rates were systematically calculated and used to compute the discriminative index (*d-prime value*) and the criterion shift index (*ln(Beta) value*) using the Palamedes toolbox for one-alternative forced choice (PAL_SDT_1AFC_PHFtoDP, MATLAB R2010a). These indices were then statistically analyzed using five paired t-tests comparing sessions (Pre vs. Post). All statistical analyses were

conducted using Statistica[®] (v.10, StatSoft). Data were checked for normality using Kolmogorov-Smirnov tests. Post-hoc analyses were performed using Bonferroni tests (mentioned in the text as p_{Bonf}). All group data are expressed as mean \pm standard error of the mean (SEM).

Imaging data analysis. Statistical analyses were conducted using SPM8[®] (v.5236, Wellcome Trust Centre for Neuroimaging, London, UK). Functional volumes were temporally realigned to the second slice acquired, spatially realigned to the average of both volumes using 6th degree B-spline interpolation, and the whole brain EPI was coregistered to this mean EPI functional volume. The MP2RAGE volume was then coregistered to the whole brain EPI image using rigid body transformations and 6th degree B-spline interpolation.

Functional analyses were conducted both in the MNI (Montreal Neurological Institute) space for standard group analyses, and in the native space as proposed in Martuzzi et al. (2014), in order to better take into account the inter-individual variability regarding both structural and functional aspects of the data. In line with this, and with the idea of preserving the initial resolution as much as possible, the realigned functional volumes were smoothed with a 4mm (full-width half-maximum) isotropic Gaussian kernel (FWHM) for the MNI space analysis, but with a 2mm FWHM isotropic Gaussian kernel for the native space analysis. In both cases statistical analyses were then performed using the General Linear Model (GLM), which included two regressors per region (the canonical hemodynamic response function: HRF and its time derivative), the motion parameters as nuisance regressors, and also included a high-pass filter set to 432s to filter low-frequency drifts. Using this model the response evoked by the stimulation of each area was estimated independently from the others by means of t -contrasts over the HRF regressors of each individual area. Both positive (activity > rest) and negative (activity < rest) contrasts were computed. In addition, Post-Pre contrasts were computed to later assess their possible co-variation with perceptual changes.

For the MNI space analysis contrasts from the Post-session were coregistered together with the mean EPI functional volume of the Post-session, to the mean EPI functional volume of the Pre-session, and resliced using 6th degree B-spline interpolation. The MP2RAGE volume was then segmented and used to compute a template of the group normalized to the standard MNI template using DARTEL algorithms. The resulting normalization parameters were then applied to the previously computed t -contrasts with no additional smoothing (voxel size, 1mm³). These normalized contrasts were inserted into a random-effect model to compute both one-sample (activity > or < rest) and paired t -tests (Post > Pre or Post < Pre), the former contrasts being then

used to visually inspect data and to compute the centres of gravity (CoG) of the resulting clusters, whereas the latter contrasts allowed evaluation of the RSS-induced changes. To assess the relationship between individual RSS-induced changes in BOLD signal and perceptual changes in discrimination thresholds, Pearson correlations were performed by entering the individual (normalized) Post-Pre contrasts in a second level analysis, where 2PDT threshold changes were inserted as covariates. Given our strong a priori predictions, the resulting activation maps were examined within SI only using a composite of the BA3b, BA3a, BA2 and BA1 maximum probabilistic maps available in the Anatomy Toolbox (Eickhoff et al., 2005, 2006b, 2007b) as region of interest (ROI), and thresholded at $p < 0.001$ uncorrected (due to the use of ROI), with a minimum cluster size of 10 voxels.

For the native space analysis, the t -contrasts resulting from the GLM (smoothed at 2mm) were used to compute positive and negative maps of each area (10 fingers and both lips) from each session (Pre and Post), by selecting the voxels that survived a threshold of $p < 0.05$ (FDR corrected). To assess whether the FDR-corrected thresholds used to compute the maps were similar across areas and sessions, they were submitted to a three-way rmANOVA (Session*Side*Area). The only significant difference observed was higher thresholds for D4 than for D1 and D2 (both p_{LSD} values < 0.035), higher thresholds for D5 than for the other fingers (all p_{LSD} values < 0.05), and lower thresholds for the Lip than for the other areas (all p_{LSD} values < 0.002). No main effects or interactions between the factors Session or Side were observed, suggesting that thresholds were comparable for both hemi-bodies before and after the RSS procedure. This was further confirmed by separate two-way rmANOVAs (Session*Side) applied on the FDR-corrected thresholds of each area, which revealed no main effect or interaction with the factor Session. Each individual map (positive or negative) and contrast from the Post-session was then coregistered together with the mean EPI functional volume of the Post-session, to the mean EPI functional volume of the Pre-session, and resliced using nearest neighbour and 6th degree B-spline interpolations respectively, the former one being used to avoid any spillover effect due to interpolation. Anatomical masks were manually delineated for each participant based on his/her own structural MRI, which was previously skull-stripped and coregistered to the whole brain EPI before being both resliced to the mean EPI functional volume using 6th degree B-spline interpolation. Delineation of BA3b, BA1 and BA2 was performed using the guidelines provided by cytoarchitectonic studies (Geyer et al., 1999, 2000; Grefkes et al., 2001), with BA3b being defined as the posterior bank of the central sulcus, BA1 as the crown of the postcentral gyrus, and BA2 as the posterior bank of the postcentral gyrus. These masks, corresponding to our regions of interests (ROIs), were then applied on the

individual functional maps (positive or negative) to constrain the analyses to BA3b, BA1 and BA2 anatomically defined at the individual level. Within each BA and body-site representation the volume of activation was assessed by quantifying the number of voxels surviving the threshold ($p_{\text{corr}} < 0.05$), and the volume of overlap between representations was also quantified. To account for the fact that different levels of activation could arise between Pre and Post sessions (e.g., from fatigue), but also between the two hemi-bodies (recorded in two separate runs), we normalized activation volumes to the total volume of activation obtained for all body-sites in a hemibody for each session, (i.e., sum of the volumes of activation obtained in both hemispheres for the 6 areas of one side in a given session). This was done for each BA. The CoG of each representation was also computed by weighting the coordinates of each voxel by its *beta* value (i.e., BOLD signal intensity) and the Euclidean distance (ED) between CoGs of different body-sites was calculated as following:

$$ED = \sqrt{(x_a - x_b)^2 + (y_a - y_b)^2 + (z_a - z_b)^2}$$

where x , y and z refer to the 3D Cartesian coordinates of the two body-sites a and b . Volumes and ED differences across body-sites, BAs, and sessions were assessed using rmANOVAs (detailed in the Results section), followed by LSD Fisher post-hoc tests ($p_{\text{LSD}} < 0.05$).

Results

The thresholds obtained at right-D2, right-D3 and the lips in the pre-sessions S1 and S2 were analyzed to ascertain multiple baseline stability. No significant differences were found for any of the body-sites (four rmANOVAs, all p values > 0.08). A two-way rmANOVA on two-point discrimination thresholds of index fingertips, showed a significant interaction Side x Session ($F_{(1,12)} = 13.35$, $p = 0.003$). Bonferroni post-hoc tests revealed that thresholds at right-D2 significantly decreased following the RSS procedure ($p_{\text{Bonf}} = 0.014$), whereas thresholds obtained at left-D2 remained stable ($p_{\text{Bonf}} > 0.90$, Figure 4). The post-RSS threshold of right-D2 was also significantly smaller than that of its homologue post-RSS ($p_{\text{Bonf}} = 0.028$). A similar analysis performed on thresholds of both sides of the upper-lips revealed a significant main effect of Session ($F_{(1,12)} = 22.75$, $p < 0.0005$), the thresholds from both upper-lips being significantly smaller after RSS of right-D2 (Figure 4). Altogether, these results confirm our previous findings (Muret et al., 2014) that three hours of RSS applied to the right-D2 significantly improves spatial discrimination not only locally, (i.e., at the stimulated fingertip), but also remotely (i.e., at both sides of the upper-lip), without affecting the homologous index fingertip (left-D2). In addition, the results from the present study further revealed that the

thresholds of the right-D3 also remained stable (see Figure 4) after the same amount of RSS applied to the right-D2 (from 2.39 ± 0.31 mm pre-RSS to 2.37 ± 0.36 mm post-RSS, $p > 0.8$).

D-prime analyses confirmed sensitivity gains exclusively for right-D2 and both upper-lips (right-D2: $t_{(12)} = -2.48$, $p = 0.029$, right-Lip: $t_{(12)} = -4.57$, $p < 0.0007$, left-Lip: $t_{(12)} = -3.75$, $p = 0.003$), with no slackening of participants' response criterion in either experiment (Figure 5).

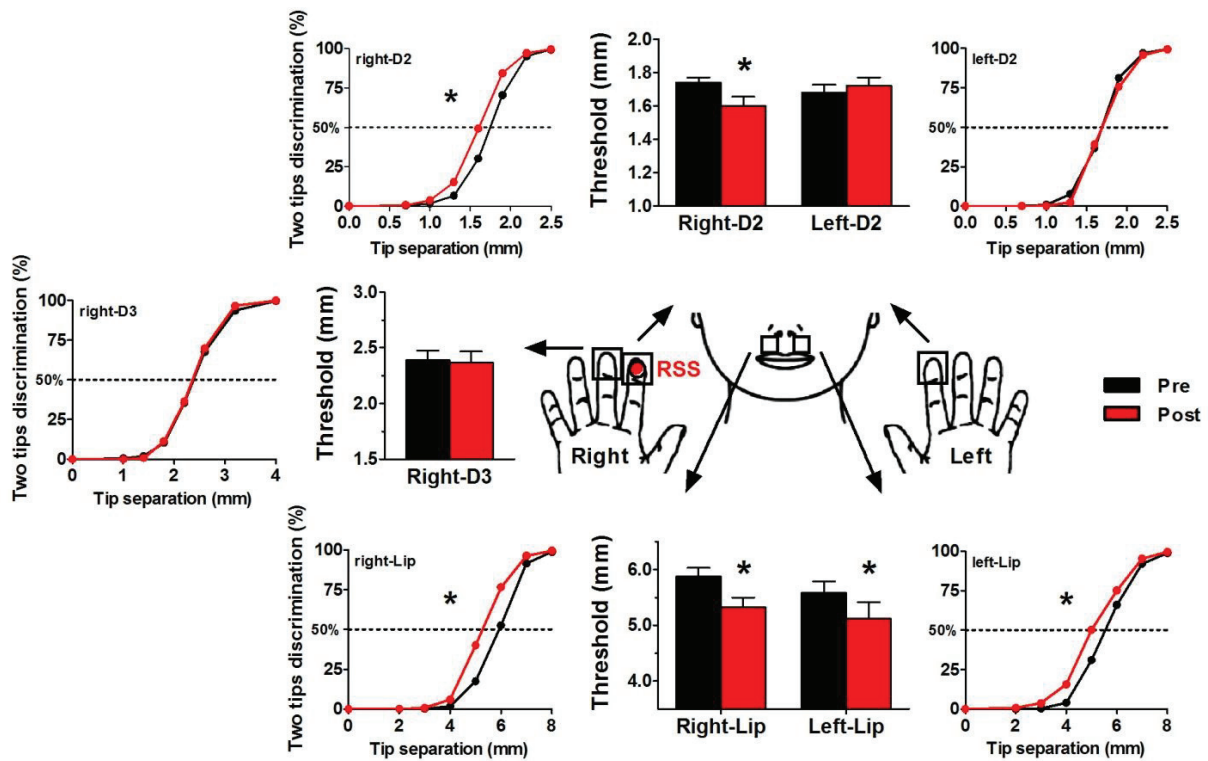


Figure 4. Mean psychometric curves and thresholds (mm), before and after the RSS procedure at each tested body-site. Psychometric curves averaged over all individual regression curves for each tested distance, Pre (black) and Post (red) RSS applied to the right-D2. The mean thresholds obtained Pre and Post RSS are represented for each area on the bar plots, with the same colour code. Asterisks highlight the cases where a significant threshold decrease was obtained from the thresholds analyses (three rmANOVAs on data from the index fingers, major finger and lips followed by Bonferroni post-hoc tests, * $p_{Bonf} < 0.05$).

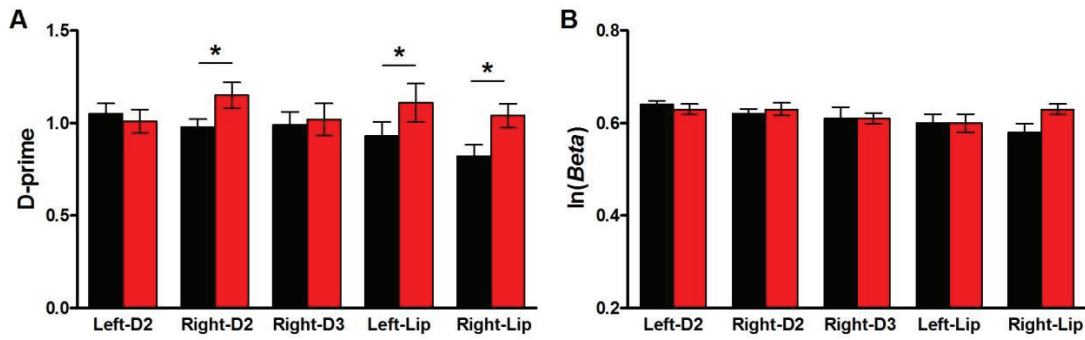


Figure 5. Signal detection theory values across sessions. (A) Mean *d-prime* and (B) mean $\ln(\text{Beta})$ values obtained for each area, Pre (black) and Post (red) RSS of right-D2.

* $p < 0.05$

To compare the RSS-induced changes obtained across body-sites, the difference in threshold between the Pre- and Post-sessions was expressed as a percentage of the Pre-session threshold, and these values were submitted to a one-way rmANOVA. This analysis revealed different threshold changes across body-sites ($F_{(4,48)} = 5.35$, $p = 0.001$), with the changes observed at right-D2 ($p_{\text{Bonf}} = 0.032$), right-Lip ($p_{\text{Bonf}} = 0.008$) and left-Lip ($p_{\text{Bonf}} = 0.011$) being significantly different from left-D2 threshold changes (Figure 6, upper panel). Similar to the first report of such RSS-induced transfer of tactile acuity improvement from the finger to the lips (Muret et al., 2014) the majority of participants exhibited decreased thresholds at both the right-D2 and lips (i.e., 84.6% here with 11 participants out of 13, and 80% in Muret et al., 2014 with 12 participants out of 15), while threshold changes were approximately equally distributed around zero (i.e., no change) at the other areas (i.e., left-D2 and right-D3, see Figure 6, left and right columns). In addition, the mean threshold at the right- and left-Lip decreased respectively by 9.33% (± 1.90) and 8.90% (± 2.43), which represents 121% and 116% of the improvement observed at right-D2 ($-7.66 \pm 3.07\%$).

In contrast to the straightforward pattern observed between threshold changes at right-D2 and the lips (Figure 6, right column, middle plot), the pattern observed between right-D2 and either left-D2 or right-D3 reveals that among the participants for whom the RSS protocol turned out to be effective locally (i.e., exhibiting right-D2 threshold decrease after RSS), half of them had a similar threshold decrease at the homologous or adjacent finger (Figure 6, right column, upper and lower plots, red arrows), while the other half instead had increased thresholds at these finger following RSS (blue arrows). Interestingly, no threshold increase was observed at the lips following RSS (Figure 6, right column, middle plot).

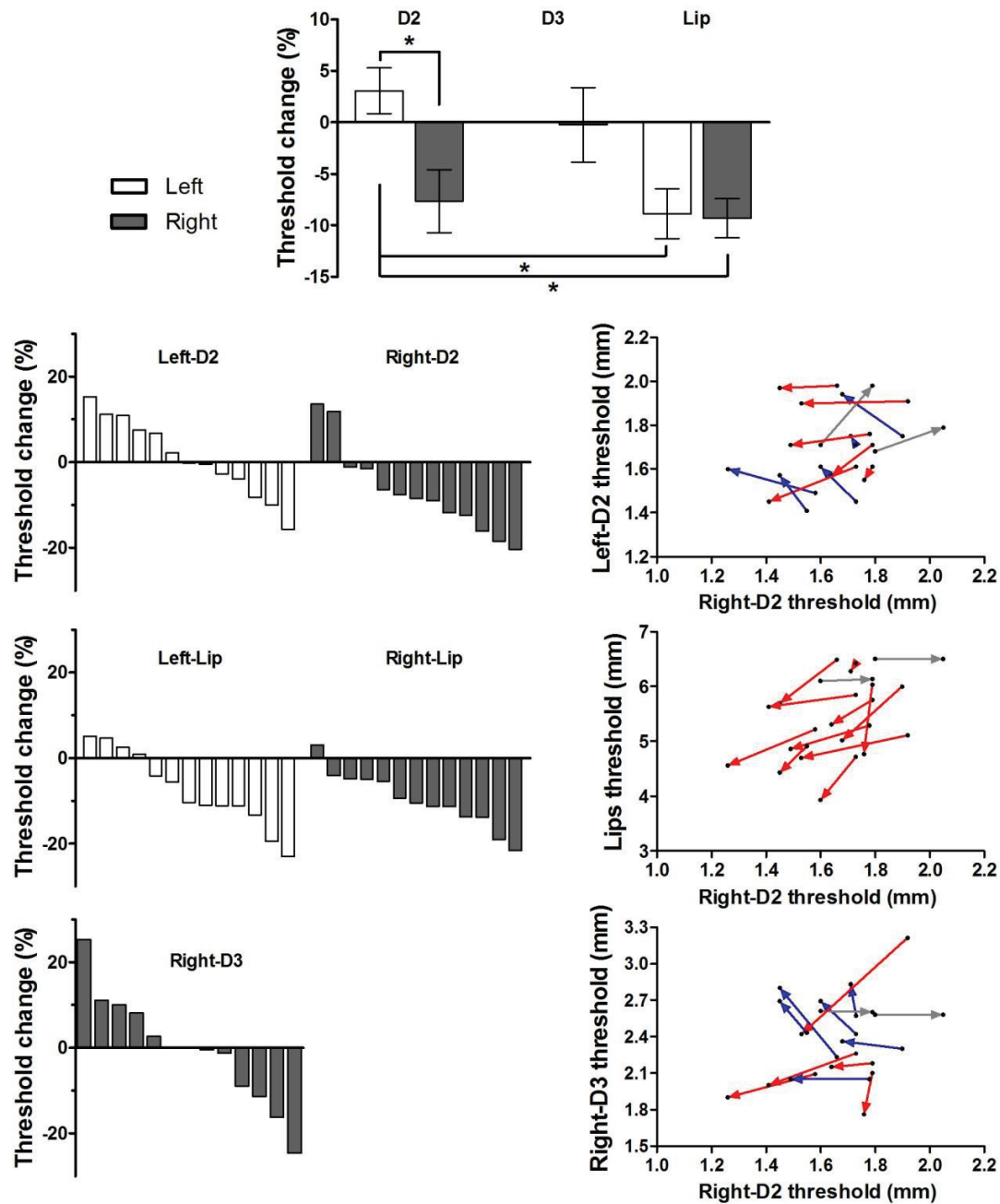


Figure 6. Group and individual threshold changes. **Upper panel:** Average threshold changes at the group level for each tested area (mean \pm SEM). * $p_{Bonf} < 0.05$. **Left column:** Rank ordered distributions of individual participant threshold changes in 2PDT (% of Pre-session) shown for each tested area. Each bar corresponds to a single participant. Values are rank ordered so a given participant is not represented in the same position across graphs. **Right column:** Vectors showing the relationship between threshold changes at right-D2 and: left-D2 (top), the lips (middle), and right-D3 (bottom), for each participant. The starting and ending points of vectors respectively represent pre- and post-session thresholds. Red vectors indicate parallel threshold decreases at both right-D2 and the other body-site (i.e., lips, left-D2 or right-D3), whereas blue vectors illustrate a decreased threshold at right-D2 and an increased at the

other area. Grey vectors illustrate the two participants having an increased threshold at right-D2 after RSS.

Random-effect (RFX) analyses - Region of Interest (SI)

RFX analyses were first computed using one-sample t-tests to get a first qualitative overview of the data at our group level. As expected, large positive BOLD responses (PBR, activity > rest) were found in the postcentral gyrus, before and after RSS. These responses were predominantly contralateral for the fingers, with the notable exception of the thumb, which also exhibited a small but significant ipsilateral cluster. In contrast, touch evoked responses were bilateral for the lips (see Figure S1 for whole-EPI and S2 for ROI maps). Similarly to Pleger and colleagues (2003), an enlargement of the cluster size and an enhancement of the BOLD signal amplitude were observed for right-D2 PBR following RSS (Figure 7; Pre: cluster-level = 1574 voxels (vox); T-score = 7.70; MNI template coordinates (mm): [-50 -20 52] [x y z]. Post: 5969 vox; T-score = 13.03; [-55 -21 45]). In addition, an ipsilateral cluster emerged at the Post-session (see Figure 7, bottom right panel; 138 vox; T-score = 5.23; [53 -19 37]). In contrast, no changes were observed for the homologous left-D2 PBR after RSS (Figure 8; Pre: 1403 vox; T-score = 7.72; [51 -21 56]. Post: 1179 vox; T-score = 7.70; [51 -21 56]).

The CoG of each activation cluster was computed for each body-site and session. The Euclidean Distance (ED) between Pre and Post CoGs was calculated and considered as a measure of the CoG shift. In apparent contrast to Pleger et al. (2003), most of the body-sites exhibited a shift of their CoG, ranging from 0.68 to 8.67mm (Table 1), but with no specific shift of right-D2 CoG.

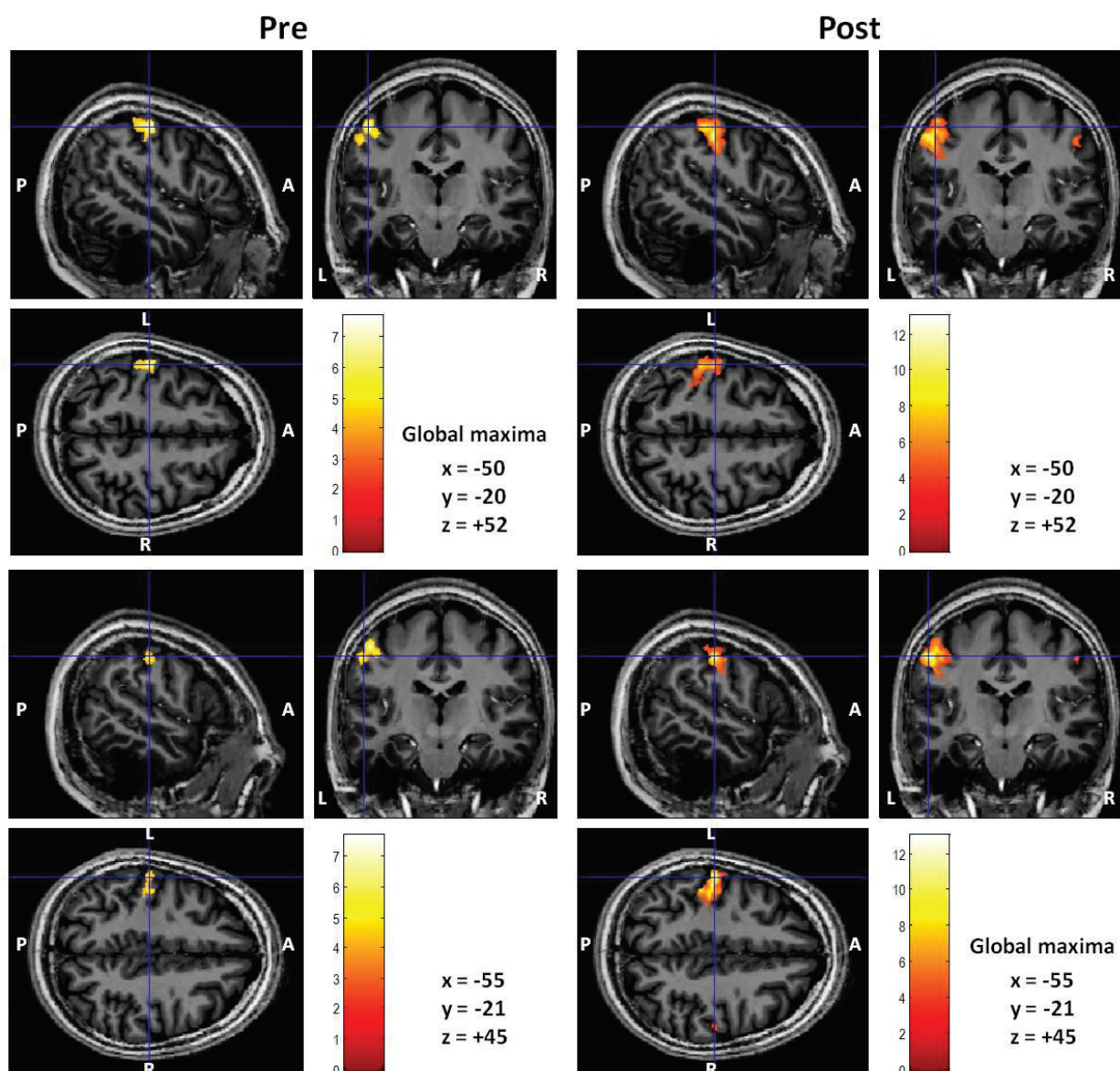


Figure 7. Group positive BOLD response (PBR) obtained from random-effects analysis using one-sample t-tests (stimulation > rest, $p_{uncorr} < 0.001$, minimum cluster size = 10vox) following stimulation of right-D2 respectively Pre (left) and Post (right) RSS. PBR maps are displayed on the MP2RAGE volume of an individual participant (normalized into MNI), whose three anatomical planes are shown (sagittal, coronal and axial). Two different positions (x , y , z in MNI coordinates) are shown between the upper and lower row, corresponding to the location of the respective peaks of activation. Note the enlarged area and the increased intensity of PBR post-RSS. A: anterior, P: posterior, L: left, R: right.

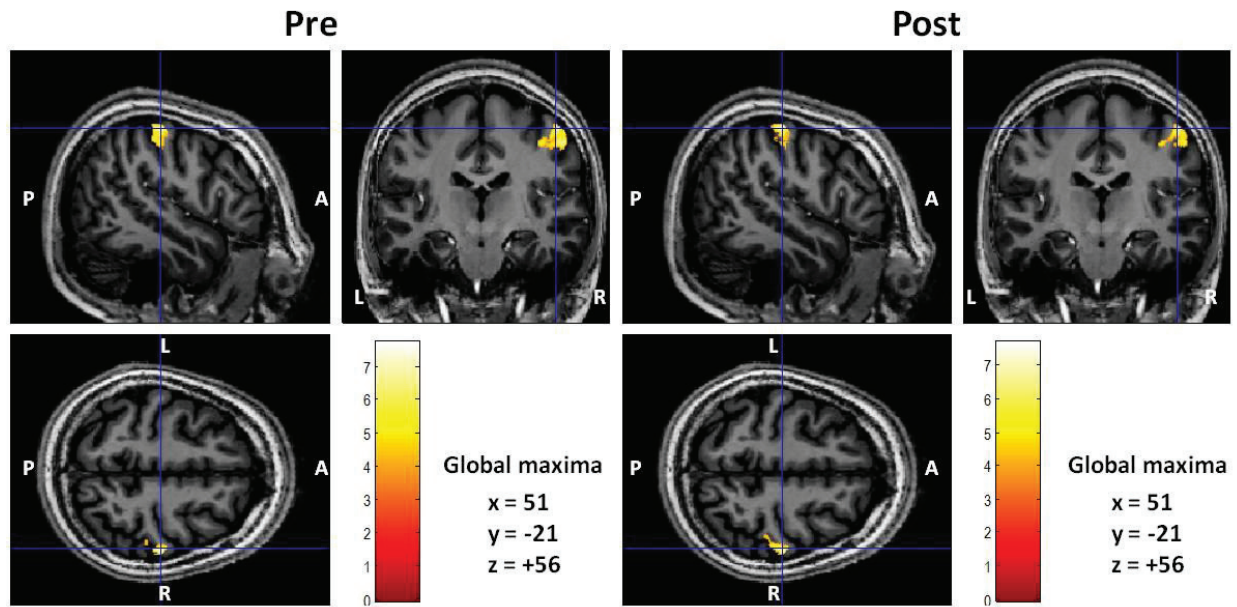


Figure 8. Group positive BOLD response (PBR) obtained from random-effects analysis using one-sample t-tests (stimulation > rest, $p_{uncorr} < 0.001$, minimum cluster size = 10vox) following stimulation of left-D2 respectively Pre (left) and Post (right) RSS. The respective peaks of activation are exactly at the same position (x , y , z in MNI coordinates). A: anterior, P: posterior, L: left, R: right.

	Pre (mm)			Post (mm)			Shift (mm)
	x	y	z	x	y	z	Post-Pre
Left-D1	51.93	-18.52	47.44	54.30	-14.99	48.48	2.64
Left-D2	49.39	-20.79	51.49	48.89	-20.67	53.18	1.78
Left-D3	47.13	-24.01	55.83	47.02	-23.12	58.84	3.15
Left-D4	44.99	-24.01	62.11	44.99	-24.68	62.22	0.68
Left-D5	42.53	-25.60	66.93	45.02	-26.35	64.99	3.25
Left-Lipc	54.12	-14.59	37.96	60.13	-13.46	37.94	6.11
Left-Lipi	-59.12	-19.01	38.00	-59.30	-18.68	37.41	0.70
Right-D1	-45.68	-26.57	49.46	-49.91	-24.23	47.56	5.19
Right-D2	-50.19	-22.61	49.93	-47.35	-24.87	48.87	3.78
Right-D3	-45.90	-26.58	54.16	-47.31	-26.67	53.95	1.42
Right-D4	-43.82	-30.12	60.86	-45.45	-28.14	54.14	4.39
Right-D5	-43.46	-31.98	60.86	-42.40	-31.90	58.52	2.57
Right-Lipc	-55.46	-16.36	37.02	-54.04	-16.04	38.76	2.57
Right-Lipi	57.13	-13.73	38.52	51.45	-11.43	44.65	8.67

Table 1. Cartesian coordinates (x, y, z, MNI space) and amount of CoG shift for each cluster of PBR (RFX one-sample t-test, stimulation > rest, $p_{uncorr} < 0.001$, minimum cluster size = 10vox) obtained for each body-site across sessions.

In contrast to PBR, negative contrasts (activity < rest) revealed activity into a more distributed network resembling the default mode network (Figure S1; Raichle et al., 2001; Greicius et al., 2003; Brookes et al., 2011; Passow et al., 2015), which is known to be task-dependent down-regulated (Fox et al., 2005). Within our ROI, these negative BOLD responses (NBR) were most of the time observed within the ipsilateral hemisphere for the fingertips, but within both hemispheres for the lips (Figure S3). Notably, the NBRs elicited by finger stimulation appeared to be highly overlapped and located more anterior relative to the post-central gyrus than that elicited by lip stimulation. Similar to the findings of Amedi's group on the negative bold somatotopy of the motor homunculus (Zeharia et al., 2012), the NBR of the lips were not located in the mirror PBR maps, but more dorsally (Figure 9, two first brain displays). Using the PBR evoked by all body-sites as masks, the contralateral NBR evoked by lip stimulation was co-localized only with the contralateral PBR evoked by the stimulation of all

fingers from the same side (Figure 9). Note that while the PBR evoked by lip stimulation was predominantly assigned to BA3b and BA1, the NBR was primarily assigned to BA2 (Figure 9). NBR being too widespread, changes in their volumes, BOLD signal amplitude or CoG location were difficult to assess qualitatively.

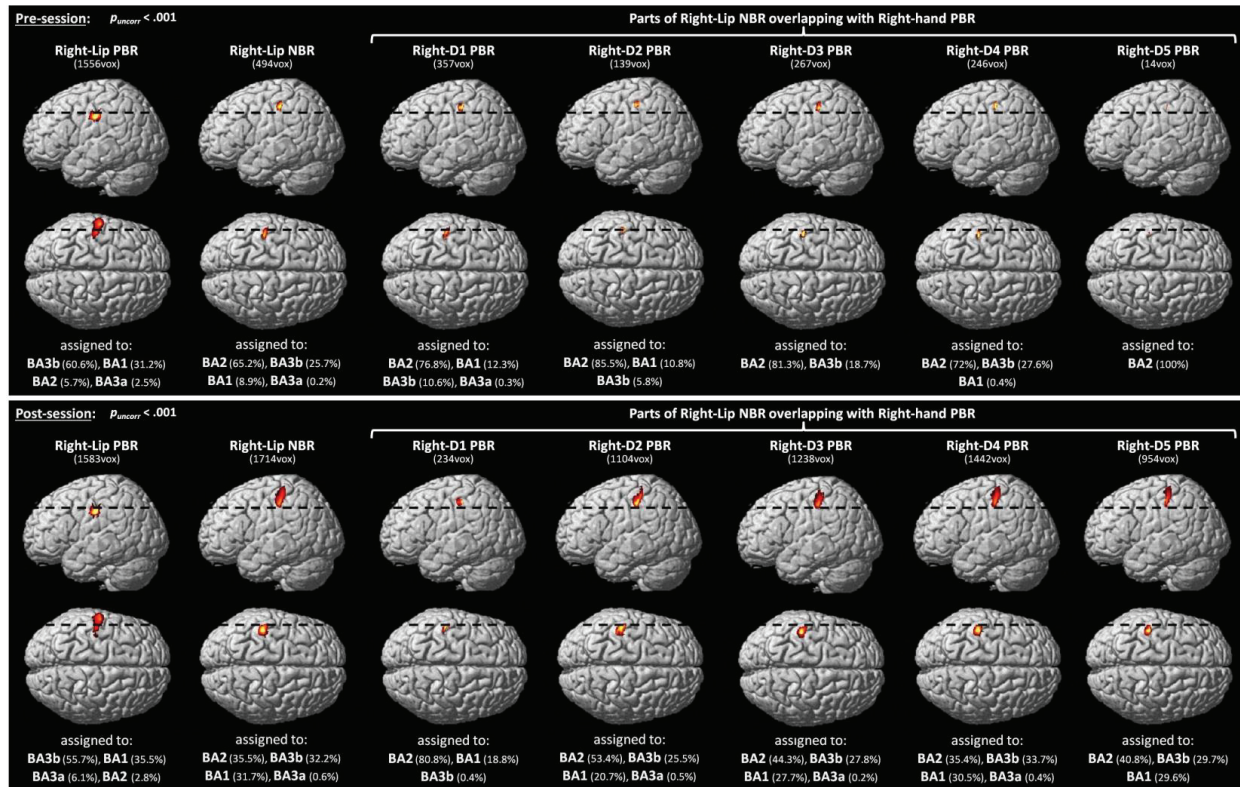


Figure 9. Localization of the group negative BOLD response (NBR) obtained from random-effects analysis using one-sample t-tests ($p_{uncorr} < 0.001$, minimum cluster size = 10vox) following stimulation of right-Lip respectively Pre (upper panel) and Post (lower panel) RSS. Sagittal and radial views are shown for each cluster. The two first brain displays show respectively the PBR and the NBR evoked by right-Lip stimulation within the contralateral hemisphere. Note that the NBR is much more dorsal than the PBR. The dashed lines highlight the clear separation between both. The five other brain displays show the portion of the NBR being co-localized with the contralateral PBR evoked by each finger of the right hand (used as masks). Note that while this co-localization is more striking at the Post-session (lower panel), it is already present at the Pre-session (upper panel). The assignment of each cluster performed using the Anatomy toolbox is indicated below each cluster. Similar results were observed for the left-Lip.

To assess the RSS-induced volume enlargement of right-D2 PBR were analyzed using RFX paired t-tests ($p_{uncorr} < 0.001$, minimum cluster size = 10vox). Post-Pre contrasts (Post-Pre > rest = Post > Pre) revealed for right-D2 four different clusters, which suggests a significant increase of right-D2 BOLD response following RSS. Two of these clusters were located within the left (contralateral) hemisphere (cluster1: 14 vox; T-score = 4.27; [-48 -15 40]; cluster2: 12

vox; T-score = 4.30; [-46 -17 35]), and the two others were within the right (ipsilateral) hemisphere (cluster3: 17 vox; T-score = 4.60; [49 -16 44]; cluster4: 11 vox; T-score = 4.73; [41 -18 35]). With the use of cytoarchitectonic probabilistic maps, the contralateral clusters were respectively assigned to BA3b with a probability of 100% for cluster1, and with a probability of 91.7% for cluster2, the remaining 8.3% assigning it to BA3a (Figure 10). Regarding the ipsilateral clusters, they were respectively assigned with a 100% probability to BA3b (cluster3) and to BA3a (cluster4) (Figure 10). Interestingly, using the group PBR maps resulting from the one-sample t-tests ($p_{\text{uncorr}} < 0.001$) as masks, parts of the contralateral clusters were co-localized with the right-D2 PBR within BA3b obtained at the Post-session (9 voxels from cluster1, and 3 voxels from cluster2), but other parts were additionally co-localized with the right-Lip PBR within BA3b obtained at the Post-session (9 voxels from cluster1 and 11 voxels from cluster2). In addition, parts of the ipsilateral cluster4 (7 voxels) were co-localized with the right-D1 ipsilateral NBR obtained within BA3a at the Post-session.

In contrast, no changes of BOLD activity were found for the homologous finger left-D2 or for any other regions, except two ipsilateral clusters respectively for left and right-D5 (left-D5: 49 vox; T-score = 6.16; [-52 -36 52]. right-D5: 20 vox; T-score = 5.13; [50 -39 58]). While the latter cluster was assigned at 100% to right BA1, the cluster obtained for left-D5 was assigned at 67.3% to left BA1 and at 32.7% to left BA2. The inverse paired t-test contrasts (Pre-Post > rest == Post < Pre) were also computed. Among all the body-sites, only one significant cluster (14 vox; T-score = 4.94; [30 -42 72]) was found for right-D1 within the right hemisphere, thus ipsilaterally to the stimulation. Using probabilistic maps, this cluster was assigned at 92.9% to right BA1, and at 7.1% to right BA3b.

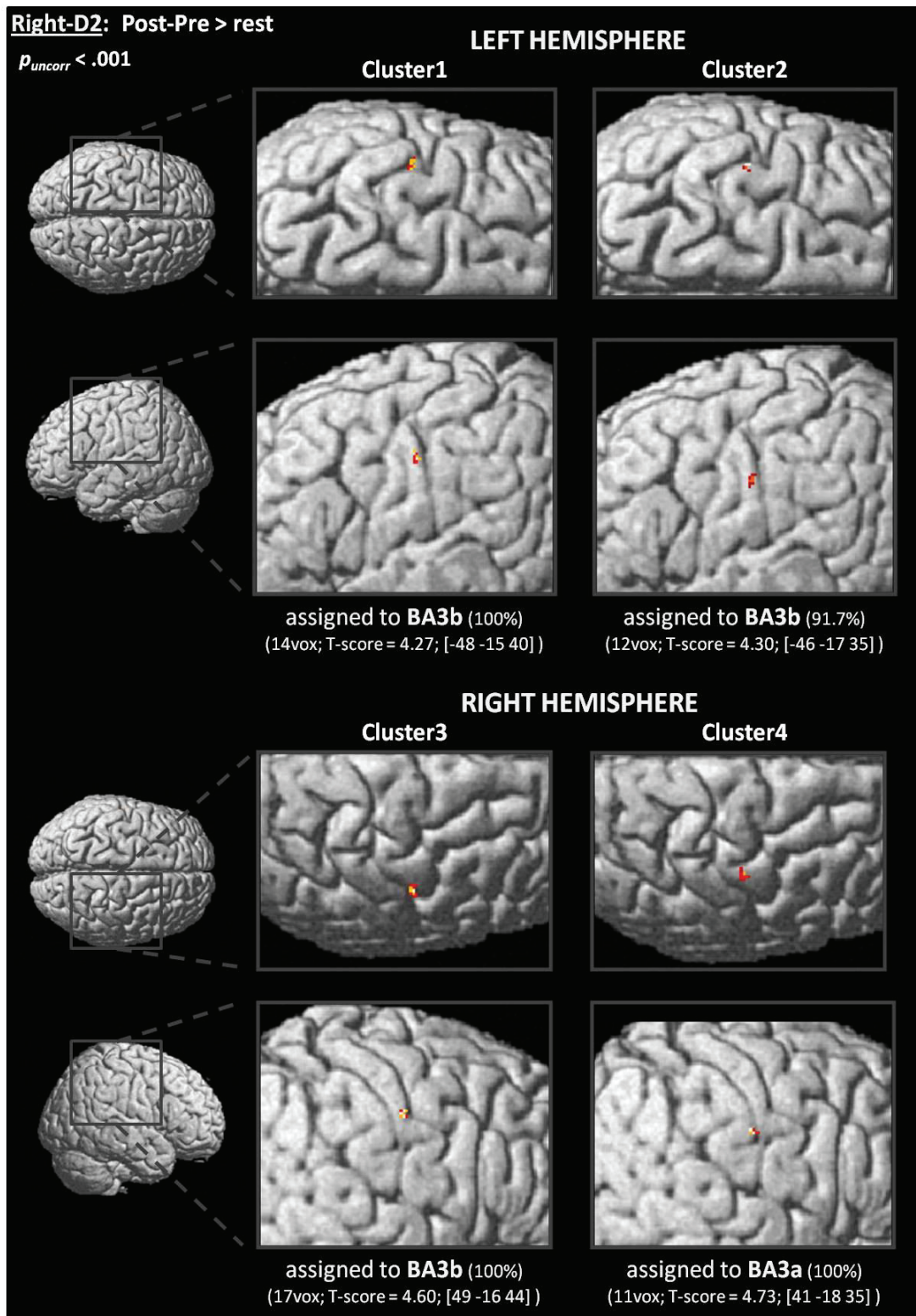


Figure 10. Differential group BOLD response between Pre and Post sessions following right-D2 stimulation, obtained from random-effects analysis using paired t-tests (Post-Pre > rest, $p_{uncorr} < 0.001$, minimum cluster size = 10vox). Among the four clusters revealed by the analysis, two were located within the left hemisphere (upper panel), while the other two were located within the right hemisphere (lower panel). The assignment of each cluster was performed using the Anatomy toolbox, and is indicated below each cluster. [x, y, z in MNI coordinates].

To assess whether the PBR changes observed for right-D2 are related to the 2PDT changes previously reported, linear correlations (Pearson) were performed using the individual Post-Pre contrasts with the individual 2PDT threshold changes inserted as covariates. While no significant correlation was found with right-D2 threshold changes, a significant negative correlation was found within SI between the RSS-induced changes in the PBR volumes evoked by right-D2 stimulation and the 2PDT changes found at the left-Lip ($p_{uncorr} < 0.001$, minimum cluster size = 10vox). Three clusters exhibited this correlation, one located within the left hemisphere (cluster1: 106 vox; T-score = 6.85; [-39 -36 41]) was assigned to BA2 at 100% (Figure 11, left), while the two other clusters located in the right hemisphere (cluster2: 204 vox; T-score = 5.90; [42 -37 56]; cluster3: 14 vox; T-score = 4.61; [53 -31 56]) were fully assigned to BA2 and BA1 respectively (Figure 11, right).

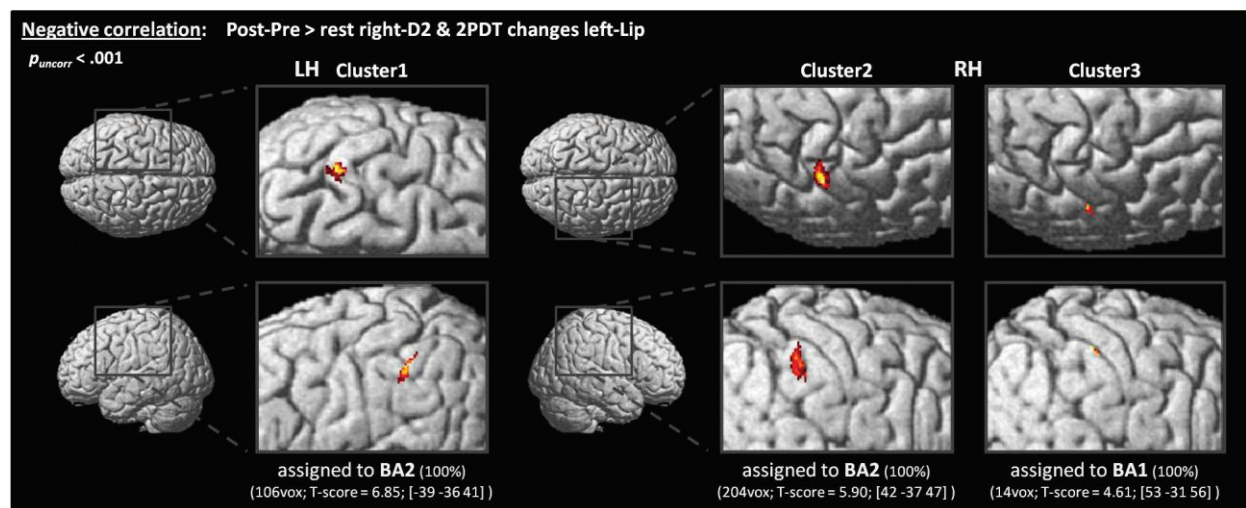


Figure 11. Correlation analysis to assess the relationship between the RSS-induced BOLD signal changes found for right-D2 and the two-point discrimination threshold changes obtained at the individual level. Results revealed a significant negative correlation between BOLD changes at right-D2 and the perceptual changes at left-Lip only ($p_{uncorr} < 0.001$, minimum cluster size = 10vox). Among the three clusters revealed by the analysis, one was located within the left hemisphere (left panel), while the other two were located within the right hemisphere (right panel). The assignment of each cluster was performed using the Anatomy toolbox, and is indicated below each cluster. [x, y, z in MNI coordinates].

Native space analyses - Positive contrasts

To investigate more subtle somatotopic changes across body-sites, analyses were also performed in the native space as suggested by Martuzzi et al. (2014). All the data hereafter are thus displayed relative to the original coordinates of acquisition and have not been reoriented relative to the bicommissural (i.e., AC-PC) plane. Differently from Martuzzi et al. (2014), here

maps were determined using FDR-corrected thresholds, and thus allowed for areal overlaps. As expected, all participants exhibited PBR (positive t-contrasts: activity > rest) within the postcentral gyrus. While responses were predominantly contralateral for the fingers, bilateral PBR were consistently observed following stimulation of either side of the upper-lip (Figure 12). Some PBR were also observed ipsilateral to the stimulated fingers, but inconsistently across participants. An overview of the maps obtained at the individual level is shown in Figure 13, with two representative slices (axial and sagittal) per participant. Despite some overlaps, a clear somatotopic organization was systematically observed along the anterior bank of the postcentral gyrus (corresponding to BA3b), with the fingers being represented in a dorso-medial to ventro-lateral sequence from D5 to D1, and the lips being located ventro-laterally (Figure 13). In contrast, the crown and the posterior bank of the postcentral gyrus exhibited much more overlaps between representations, yielding to a less distinguishable somatotopic organization. This result is in agreement with previous imaging studies demonstrating a larger areal overlap between finger representation in BA1/2 than in BA3b (Krause et al., 2001; Besle et al., 2013b).

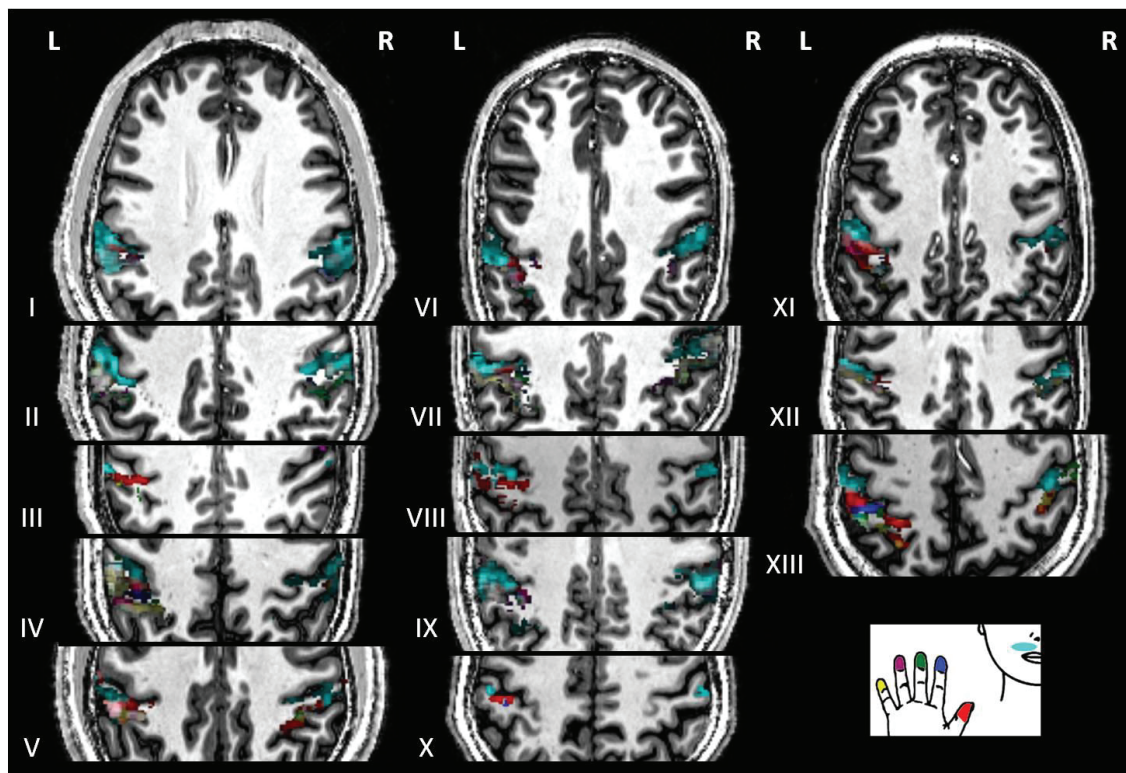


Figure 12. Bilateral SI PBR evoked by right-Lip stimulation obtained at the Pre-session in the native individual space. One representative axial slice is shown for each of the participants (I to XIII). Body-sites are colour-coded (see inset in the right lower corner), and overlaps result in mixed colours (white when all the areas are superimposed). Note that the ipsilateral PBR to lip stimulation varied with the amount of global activation (e.g., smaller but present in participants III and X, showing the smallest overall activity).

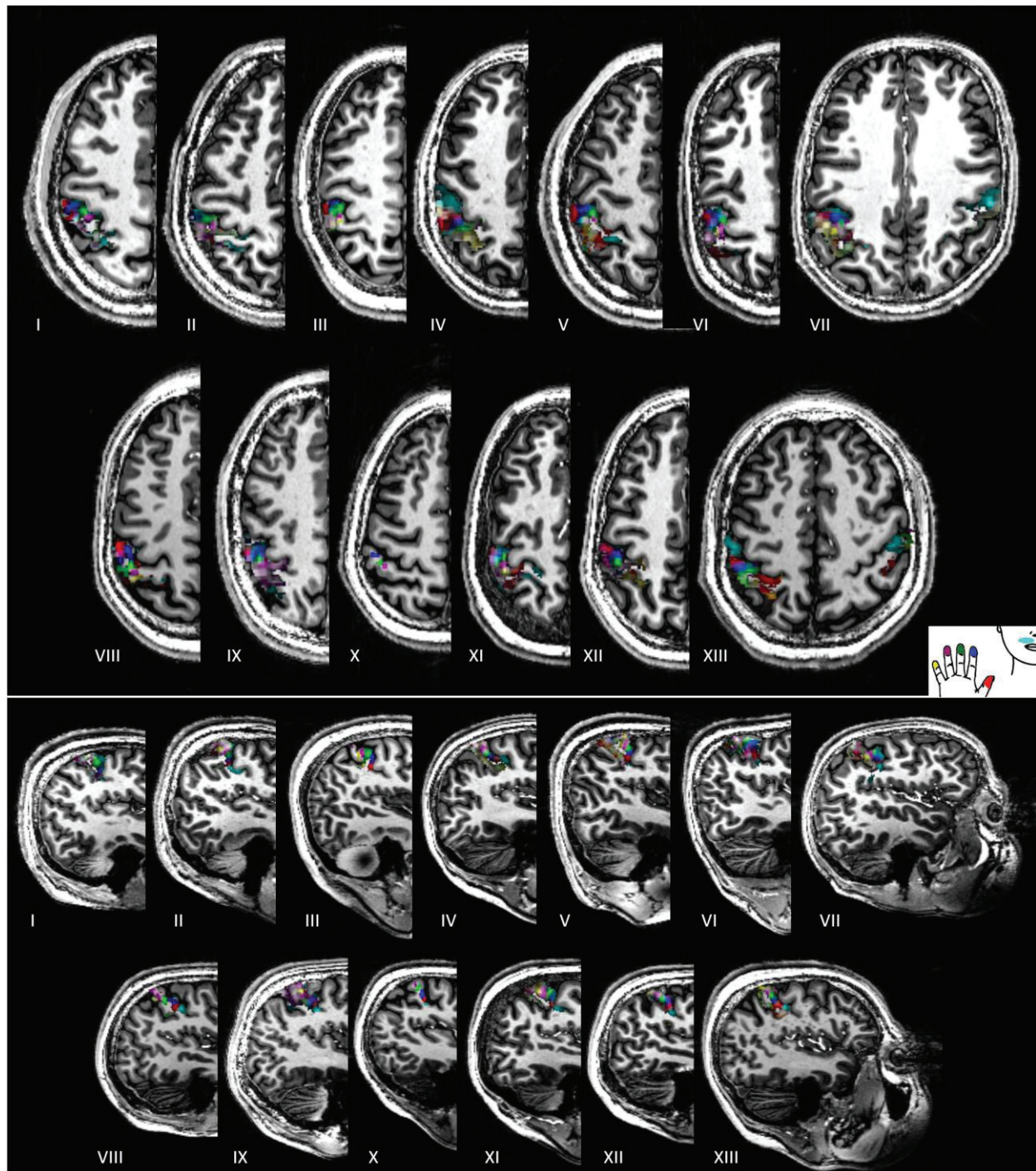


Figure 13. Native space individual somatotopic organization of PBR obtained following stimulation of the right hemibody within the contralateral SI during the Pre-session. One representative axial (top) and sagittal (bottom) slices are shown for each participant (I to XIII). Body-sites are colour-coded (see inset), and overlaps result in mixed colours (white when all the areas are superimposed).

These results on the overall distribution of PBR to fingers stimulation are consistent with previous reports (Kurth et al., 2000; Krause et al., 2001; Stringer et al., 2011; Besle et al., 2013b; van der Zwaag et al., 2013; Martuzzi et al., 2014). To assess whether the enhancement of right-D2 PBR observed at the group level (Figure 10) was also observable in data from the

native space, the volumes of body-sites PBR were extracted from the previous maps and further analyzed.

First, looking at the total volume of the three sub-regions (i.e., BA3b, BA1 and BA2), a two-way rmANOVA (BAs*Session) revealed a significantly smaller volume of PBR for BA3b than for BA1 and BA2 (Figure 14; $F_{(2,24)} = 10.01$, $p < 0.001$, post-hoc tests: BA3b < BA1, $p_{LSD} < 0.001$; BA3b < BA2, $p_{LSD} = 0.008$). This result is in apparent contrast to the report of Martuzzi et al. (2014), in which BA2 was found smaller than BA3b and BA1. This discrepancy is likely to arise from a major difference in how maps were computed here, whereby overlaps were allowed. As the focus of the present study was not to assess the absolute volume differences across sub-regions or even body-sites, but rather to investigate the relative volume changes across sessions, the total volume of each sub-region (BAs) was further analyzed separately.

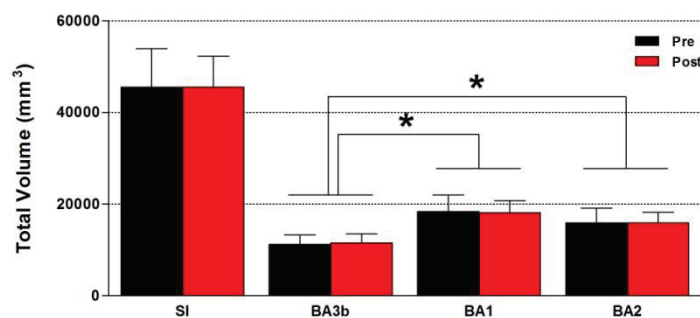


Figure 14. Total volume (mm³) of PBR within SI and the sub-regions BA3b, BA1 and BA2 of both hemispheres, before (black) and after (red) the RSS procedure. * $p < 0.05$.

When considering sub-regions volumes across body sides, hemispheres and sessions, two participants who lacked suprathreshold ipsilateral PBR (expected for the lips) in at least one session and within at least two of the three BAs (participant VIII within BA3b & BA2; participant X within BA3b, BA1 and BA2) were removed from further analysis. Another argument in favour of this rejection was that these same participants also lacked contralateral PBR for at least one body-site within at least two of the three BAs (participant VIII within BA3b & BA2; participant X within BA1 & BA2). This resulted in 11 participants exhibiting responses for all the body-sites (within the contralateral hemisphere for all regions and within the ipsilateral hemisphere for the lips) within BA3b and BA1. Within BA2, two further participants were lacking PBR, one (participant III) for left-D4 and left-D5 within their contralateral right hemisphere (RH) at the Pre-session solely, and the other one (participant XII) for left-Lip within its ipsilateral left hemisphere (LH) at the Post-session. To keep our sample size as big as possible, these two participants were removed only from BA2 analysis, which was thus based on a sample of 9 participants.

PBR volumes within each sub-region were analyzed across sessions with body side and hemisphere as factors (i.e., three-way rmANOVA Session*Side*Hemisphere). First, the analysis performed on **SI** as a whole ($n = 11$; Figure 15, top left), revealed a significant difference between hemispheres ($F_{(1,10)} = 6.02, p = 0.034$), with a larger PBR volume within the left ($25\,712.67 \pm 3\,606.45 \text{ mm}^3$, mean \pm sem) than the right hemisphere ($22\,544.91 \pm 3\,707.26 \text{ mm}^3$). In addition, a significant interaction between the body side and hemisphere ($F_{(1,10)} = 61.75, p < 0.001$) revealed, as expected, larger PBR volumes within the contralateral hemisphere compared to the ipsilateral one (Left: $RH > LH$; Right: $LH > RH$; LH: $Right > Left$; RH: $Left > Right$, all p_{LSD} values < 0.001). No significant effect or interaction with the factor Session was observed at this level ($p > 0.3$).

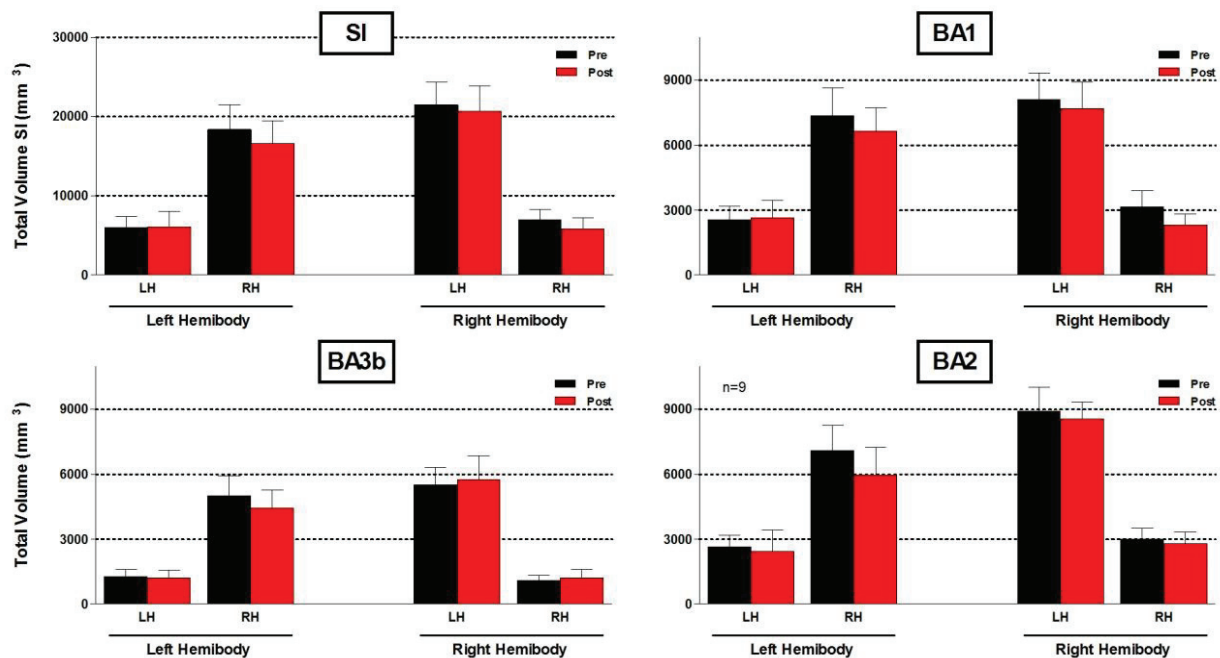


Figure 15. Total PBR volumes (mm^3) evoked by the stimulation of each hemibody, within SI and the three sub-regions (BA3b, BA1 and BA2) of each hemisphere (LH: left hemisphere, RH: right hemisphere), before (black) and after (red) the RSS procedure. Statistical results are detailed in the text. Note that SI, BA3b and BA1 volumes include the average of 11 participants, whereas those of BA2 include 9 participants.

Similar results were found within **BA3b** ($n = 11$; Figure 15, bottom left), with larger volumes within LH than within RH ($F_{(1,10)} = 5.41, p = 0.042$), and larger PBR volumes within the contralateral hemisphere than within the ipsilateral one ($F_{(1,10)} = 47.59, p < 0.001$; Post-hoc tests: Left: $RH > LH, p_{LSD} = 0.002$; Right: $LH > RH, p_{LSD} < 0.001$; LH: $Right > Left, p_{LSD} < 0.001$; RH: $Left > Right, p_{LSD} = 0.001$). Within **BA1** ($n = 11$; Figure 15, top right) and **BA2** ($n = 9$; Figure 15, bottom right), the difference between hemispheres was no longer observed, but

larger volumes were still observed within the contralateral hemisphere compared to the ipsilateral one (BA1: $F_{(1,10)} = 54.21$, $p < 0.001$; Post-hoc tests: all p_{LSD} values < 0.001 - BA2: $F_{(1,8)} = 72.92$, $p < 0.001$; Post-hoc tests: all p_{LSD} values < 0.001). In addition, **BA2** volumes contralateral to the right hemibody (i.e., within LH) were significantly larger than that contralateral to the left hemibody (i.e., within RH) ($p_{\text{LSD}} = 0.026$). Altogether, these results suggest a similar pattern between hemispheres and body sides for the three BAs, with larger PBR volumes within the hemisphere contralateral to the stimulation than the ipsilateral one being consistent across BAs.

As for SI, no significant changes were observed across sessions, suggesting no effect of RSS over the global PBR volumes within either sub-region. More importantly, this finding allows excluding any variation in response volumes potentially due to fatigue or other unspecific factors between sessions. Because the two hemi-bodies were stimulated by the same experimenter in two different runs with either her right or left hand, we refrain from interpreting the larger volumes observed in the left hemisphere as compared to the right one. Instead, we expressed the volumes obtained for each body-site as a percentage of the total volume obtained for a given sub-region (BAs) after stimulating this hemibody, within the two hemispheres. These volumes used to normalize body-site volumes (i.e., sum of the volumes of activation within both hemispheres obtained for either hemibody) were statistically stable and similar across sessions and hemibody sides (one two-way rmANOVAs Session*Side per BA).

From the resulting (normalized) volumes, those corresponding to the contralateral PBR for the fingers and to the bilateral responses for the lips were selected (i.e., the only regions for which all the 11 participants exhibited PBR). Separate analyses of the three BAs (three-way rmANOVA Session*Hemisphere*Area) revealed volume differences between body-sites, regardless of the hemisphere, or session (BA3b: $F_{(6,60)} = 7.936$, $p < 0.001$; BA1: $F_{(6,60)} = 17.15$, $p < 0.001$; BA2: $F_{(6,48)} = 5.321$, $p < 0.001$).

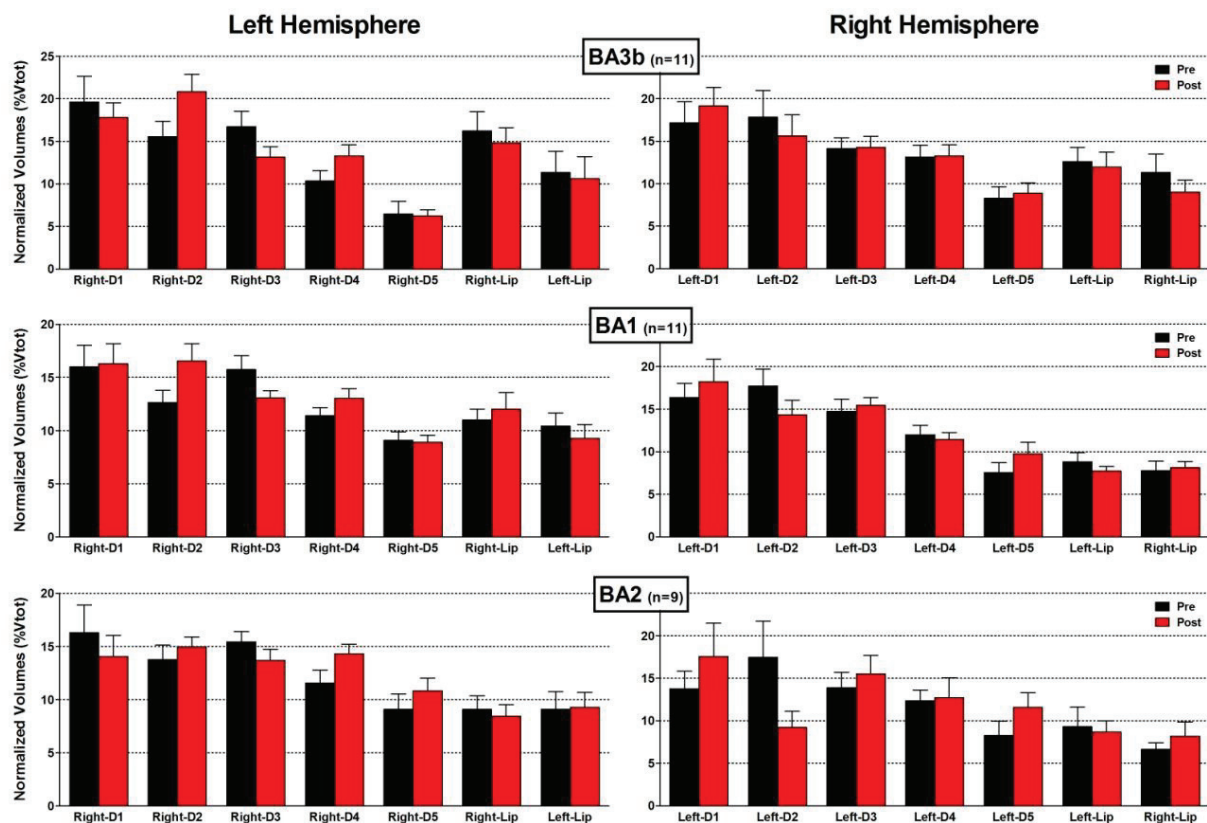


Figure 16. Normalized volumes (% volume total of the sub-region) of PBR evoked by the stimulation of each body-site from each body side, within each of the three sub-regions BA3b, BA1 and BA2 in each hemisphere, before (black) and after (red) the RSS procedure. Note that within each hemisphere, the volumes of the ipsilateral lip are showed in addition to the contralateral body-sites. Significant volume differences were obtained only between body-sites, not interfering with the hemisphere or the session. Statistical results are detailed in the text.

Within **BA3b** (Figure 16, top), PBR from D5 were significantly smaller than those from all other areas, but the ipsilateral lip (i.e., left-Lip within LH and right-Lip within RH; all p_{LSD} values < 0.011), while PBR from D1 were significantly larger than those observed for D3, D4 and D5 and the lips (all p_{LSD} values < 0.048). Finally, PBR from D4 were smaller than those observed for D2 ($p_{LSD} = 0.012$), and PBR of the ipsilateral lip were also significantly smaller than those from D2 and D3 (both p_{LSD} values < 0.041). Within **BA1** (Figure 16, middle), the volume differences between body-sites was less pronounced, with PBR from D1, D2 and D3 being larger than those from D4, D5 and the lips (all p_{LSD} values < 0.015), and with the PBR from D5 and the ipsilateral lip being significantly smaller than that from D4 (both p_{LSD} values < 0.008). Finally, few differences were observed within **BA2** (Figure 16, bottom), with D1, D2 and D3 showing larger PBR than those observed from D5 and the lips (all p_{LSD} values < 0.032), the latter having smaller PBR than those from D4 (both p_{LSD} values < 0.035).

Thus, while D1 & D2 seem to display the largest representation across BAs, D5 and the ipsilateral lip exhibit the smallest representations within BA3b, and are followed by the contralateral lip, whose representation seems to decrease from BA3b to BA2. These results are in agreement with previous reports showing a higher degree of cortical magnification for D1 and D2 in both monkeys (Sutherling et al., 1992; Shoham and Grinvald, 2001) and humans (Maldjian et al., 1999; Martuzzi et al., 2014). Apart from these differences in volumes across body-sites, no differences were observed across hemispheres or sessions (see Figure 16). This suggests that the effects induced by RSS, if any, might be masked by the huge differences across body-sites.

To overcome this issue and directly compare the PBR volumes obtained for homologous body-sites across sessions, the normalized volumes were then analyzed separately. Within **BA3b** ($n = 11$; Figure 17, top), a two-way rmANOVA showed a significant interaction for D2 fingertips ($F_{(1,10)} = 5.08, p = 0.048$), revealing a significant increase of right-D2 PBR after RSS ($p_{\text{LSD}} = 0.047$). A significant main effect of Session was found for D3 ($F_{(1,10)} = 4.99, p = 0.049$), but displaying a decrease of D3 PBR after RSS, though visual inspection of the data (Figure 17, top) suggests the effect may be predominantly driven by right-D3. Finally, a significant difference between sides was found for D5 ($F_{(1,10)} = 7.80, p = 0.019$), the PBR of left-D5 (thus within RH) being larger than its homologue within LH. Within **BA1** ($n = 11$; Figure 17, middle), a similar interaction as in BA3b was found for D2 PBR ($F_{(1,10)} = 11.76, p = 0.006$), revealing here again a significant enlargement of right-D2 BOLD response after RSS ($p_{\text{LSD}} = 0.027$), but also a significant decrease of left-D2 PBR after RSS ($p_{\text{LSD}} = 0.047$). However, a significant difference between the Pre-sessions of both fingers was also observed ($p_{\text{LSD}} = 0.007$), which could partly explain the interaction. Finally, a significant difference between sides was found for the contralateral lip ($F_{(1,10)} = 5.15, p = 0.047$), the PBR of the right-Lip being larger than that of the left-Lip. Lastly, no significant changes were observed within **BA2**, likely due to a too small sample ($n = 9$). However, despite the small sample, the variability observed (Figure 17, bottom) seems reasonable, and allows to distinguish a tendency for a decrease of left-D2 PBR, as found within BA1.

Altogether, these results suggest that RSS induced an increase of right-D2 PBR, primarily within BA3b, but extending significantly to BA1. This enlargement of right-D2 representation was accompanied by a significant decrease of (mainly the right) D3 PBR within BA3b, and by a tendency for left-D2 PBR to shrink within BA1. Somewhat surprisingly, no changes across sessions were observed for the upper-lips.

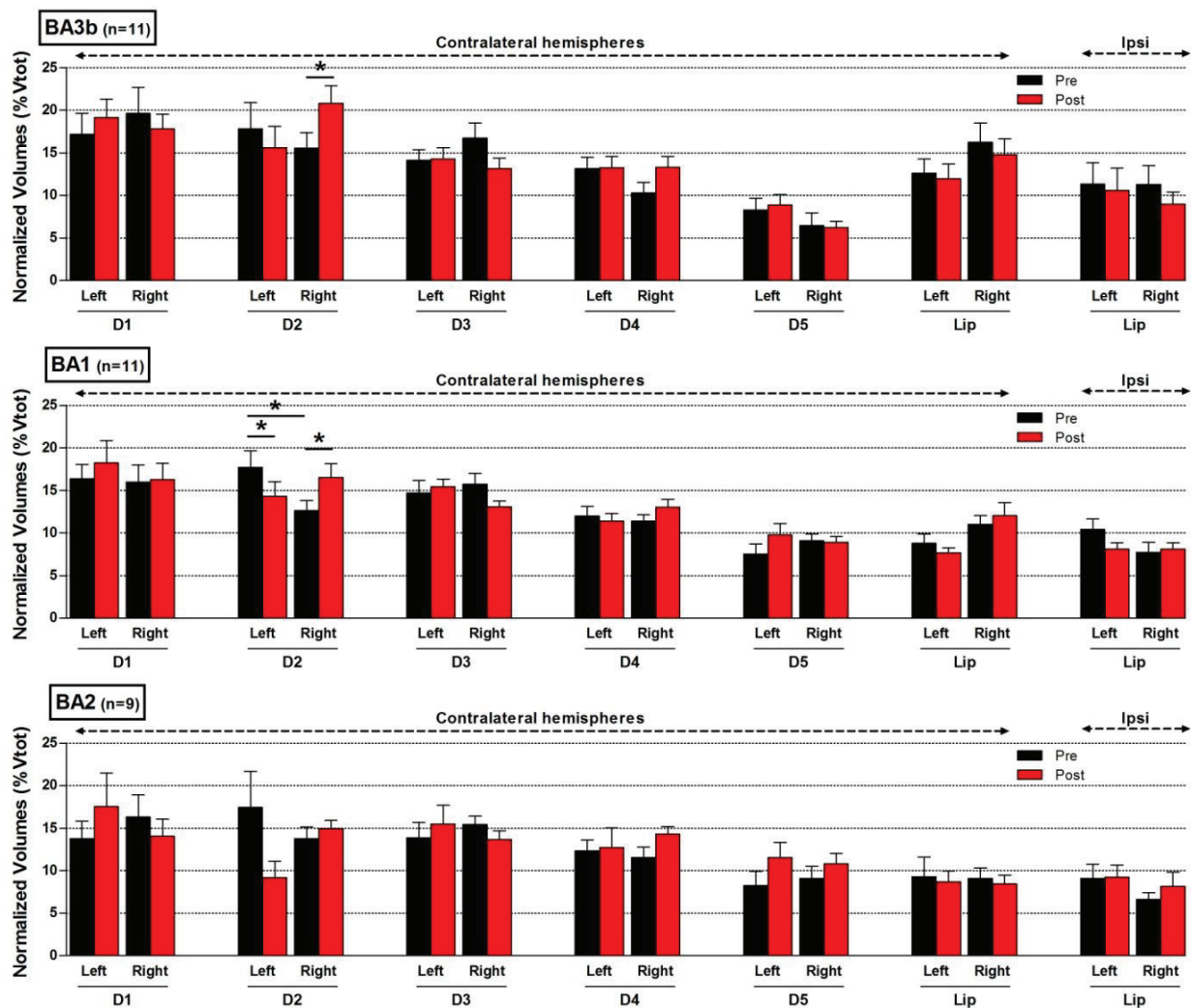


Figure 17. Same normalized PBR volumes (%Vtot) as in Figure 15, but grouped by body-sites within each of the three sub-regions BA3b, BA1 and BA2, to directly compared homologous body-sites (i.e., the two sides of the body) and their changes in volume across sessions (Pre-RSS: black, Post-RSS: red). Note that for the six first body-sites (i.e., the five fingers and the lip), the volumes of PBR obtained within their respective contralateral hemispheres are compared, while for the last body-site (i.e., the second lip), the volumes of PBR compared are those located within their respective ipsilateral hemispheres. A two-way rmANOVA (Session*Side) was applied on each body-site. * $p < 0.05$.

To assess the possible link between the significant volume changes observed at these body-sites and sub-regions, they were submitted to Pearson's correlations. While no significant correlation was found between right-D2 and right-D3 volume changes within BA3b ($p = 0.101$), nor between right-D2 volume changes within BA3b and left-D2 volume changes within BA1 ($p = 0.218$), a significant positive correlation was observed between volume changes of right-D2 PBR within BA3b and those within BA1 (Figure 18; $r = 0.8273$, $p = 0.002$). Notably, the equation linking these two variables exhibited a slope whose coefficient was below 1, suggesting that a higher amount (almost twice more) of volume changes were occurring within BA3b to get the same amount of changes within BA1.

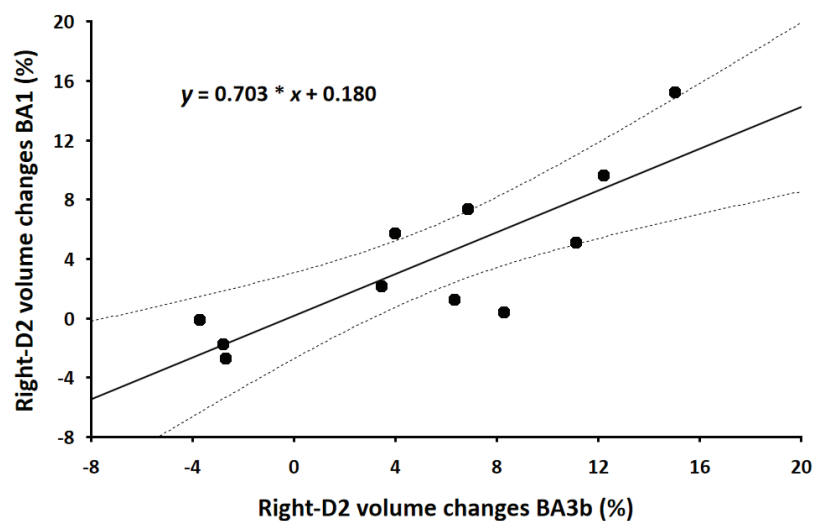


Figure 18. Relationship between right-D2 PBR volume changes within BA3b and BA1 (%Post-Pre). The linear (Pearson) correlation is significant ($p < 0.05$).

To investigate whether these enlargements of right-D2 representation altered its degree of overlap with the other areas, we computed both the proportion of D2 PBR overlapping with the PBR from other body-sites, and the proportion of the other body-sites PBR being overlapped with D2 PBR (i.e., we expressed the volumes of overlaps as a proportion of either D2's volume or of the volumes of the other body-sites). Within **BA3b**, the proportion of D2 PBR overlapping with those from the other body-sites was significantly higher with its direct neighbours (i.e., D1 and D3), than with the non-adjacent body-sites ($F_{(4,40)} = 20.19$, $p < 10^{-6}$, all p_{LSD} values < 0.005), with respectively 39.08% (± 4.69) and 45.03% (± 5.28) of D2 overlapping with D1 and D3, instead of 27.45% (± 6.37), 15.4% (± 3.61) and 18.44% (± 2.89) with D4, D5 and Lip. Conversely, these same volumes of overlap corresponded to 40.40% (± 6.39), 49.72% (± 5.05), 33.04% (± 6.80), 29.73% (± 6.81), and 19.77% (± 3.28) of the representations of these other body-sites (i.e., in the same order: D1, D3, D4, D5 and Lip). Within **BA1**, the proportion of D2 overlapping with the other body-sites was higher than in BA3b, and a significant gradient of

overlap was observed from D3, to D1, D4, D5 and Lip ($F_{(4,40)} = 58.45$, $p < 10^{-6}$, all p_{LSD} values < 0.005), with respectively 67.71% (± 4.55), 57.70% (± 5.31), 48.23% (± 6.37), 37.04% (± 5.97) and 21.24% (± 3.31) of overlap. Conversely, these same volumes of overlap corresponded to 67.36% (± 4.89), 59.96% (± 6.55), 58.13% (± 6.47), 56.42% (± 7.26), and 34.97% (± 5.97) of the representations of these other body-sites (i.e., in the same order: D3, D1, D4, D5 and Lip). These values reveal a gradient of overlap consistent with the literature for the adjacent fingers (see Kurth et al., 2000). For the with non-adjacent body-sites, the proportion of relative overlaps were slightly higher, but these values were calculated in a slightly different way. However, no significant changes in the proportion of overlap were observed across sessions.

Despite the fact that similar behavioural results were found when analyzing data from the 11 participants used for BA3b and BA1 analyses, (i.e., significant threshold decreases for right-D2 ($F_{(1,10)} = 13.70$, $p = 0.004$, post-hoc: $p_{Bonf} = 0.049$) and both sides of the upper-lips ($F_{(1,10)} = 21.78$, $p < 0.001$), whereas thresholds remained stable at left-D2 and right-D3 (both p values > 0.4)), no significant correlation between behavioural and PBR volume changes was found for any of the affected body-sites, likely due to our too small sample size.

Native space analyses - Negative contrasts

All participants also showed NBR (activity $<$ rest) within the postcentral gyrus. Interestingly, these ‘negative maps’ were observed within both hemispheres. However, although larger volumes were observed within the ipsilateral hemispheres (see Figure 22), contralateral NBR were more consistent across individuals, making their statistical analysis possible. First, to compare qualitatively the distribution of these negative maps with that of the positive maps analyzed previously (see Figure 12 and Figure 13), we observed these maps at the same brain slices. When considering the brain regions where the upper-lip PBR were found bilaterally (Figure 12, cyan), few NBR were observed at the individual level (Figure 19, cyan). In contrast, when considering the regions where hand PBR were observed (Figure 13, cyan), 11 out of the 13 participants exhibited large NBR evoked by upper-lip stimulation (Figure 20, cyan), and these responses were predominantly contralateral. Concerning the fingertips, some NBR were observable at this level, sometimes more ipsilaterally, sometimes more contralaterally depending on participants (Figure 20). Larger NBR evoked by finger stimulation were found slightly more dorsally. These observations suggest that NBR were located globally higher in the brain than PBR, and notably, the NBR evoked by lip stimulation were observed at the same brain levels as the fingers PBR. Note that the ipsilateral activity evoked by stimulating the different body-sites was generally much more overlapping than the one evoked within the

contralateral hemisphere (especially for the fingers). Apart from the clear distinction between the NBRs evoked by lip and finger stimulation, no consistent somatotopic organization was observed. While the finding of ipsilateral NBR following hand stimulation has increasingly been documented in recent years (Hlushchuk and Hari, 2006; Kastrup et al., 2008; Klingner et al., 2010, 2011; Schäfer et al., 2012; Malinen et al., 2014; Mullinger et al., 2014), to the best of our knowledge this is the first report of contralateral NBR following hand and face stimulation.

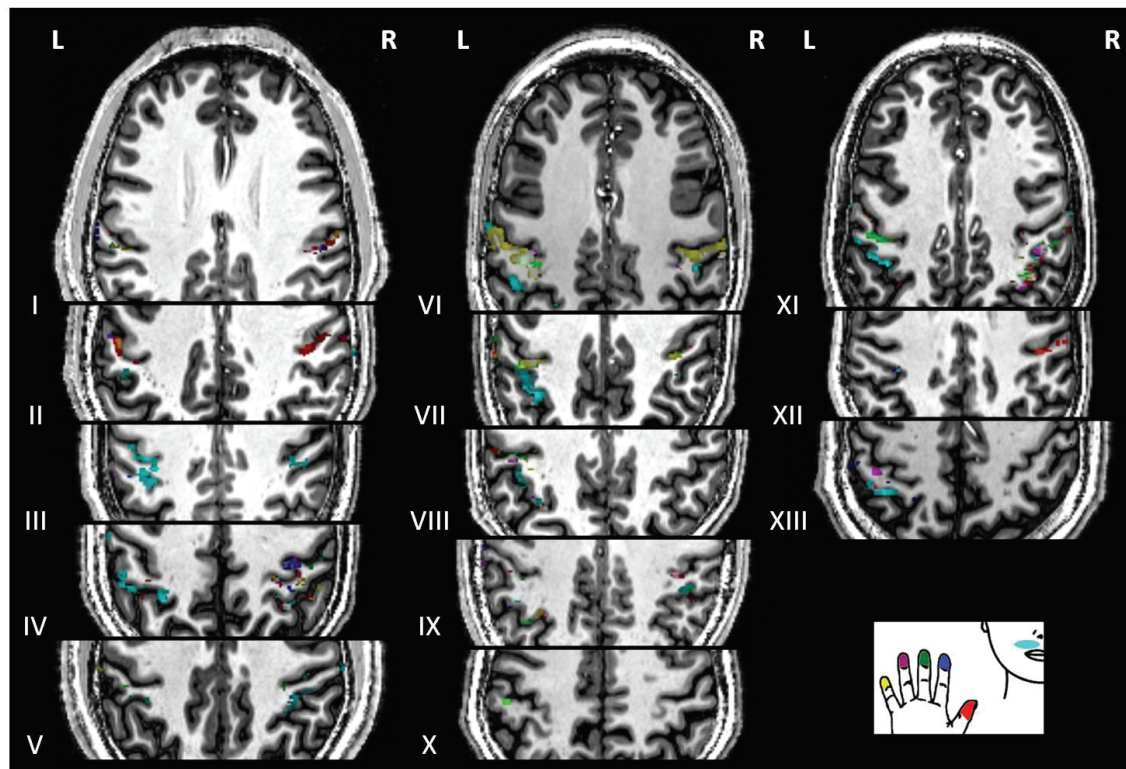


Figure 19. NBR maps obtained at the Pre-session following right hemibody stimulation in the native space of individuals, at the same axial slices as in Figure 11 for each of the participants (I to XIII). Body-sites are colour-coded (see schema), and overlaps result in mixed colours (white when all the areas are superimposed). Note that compared to Figure 19, few lip NBR is observed at these lip PBR levels (see Figure 11).

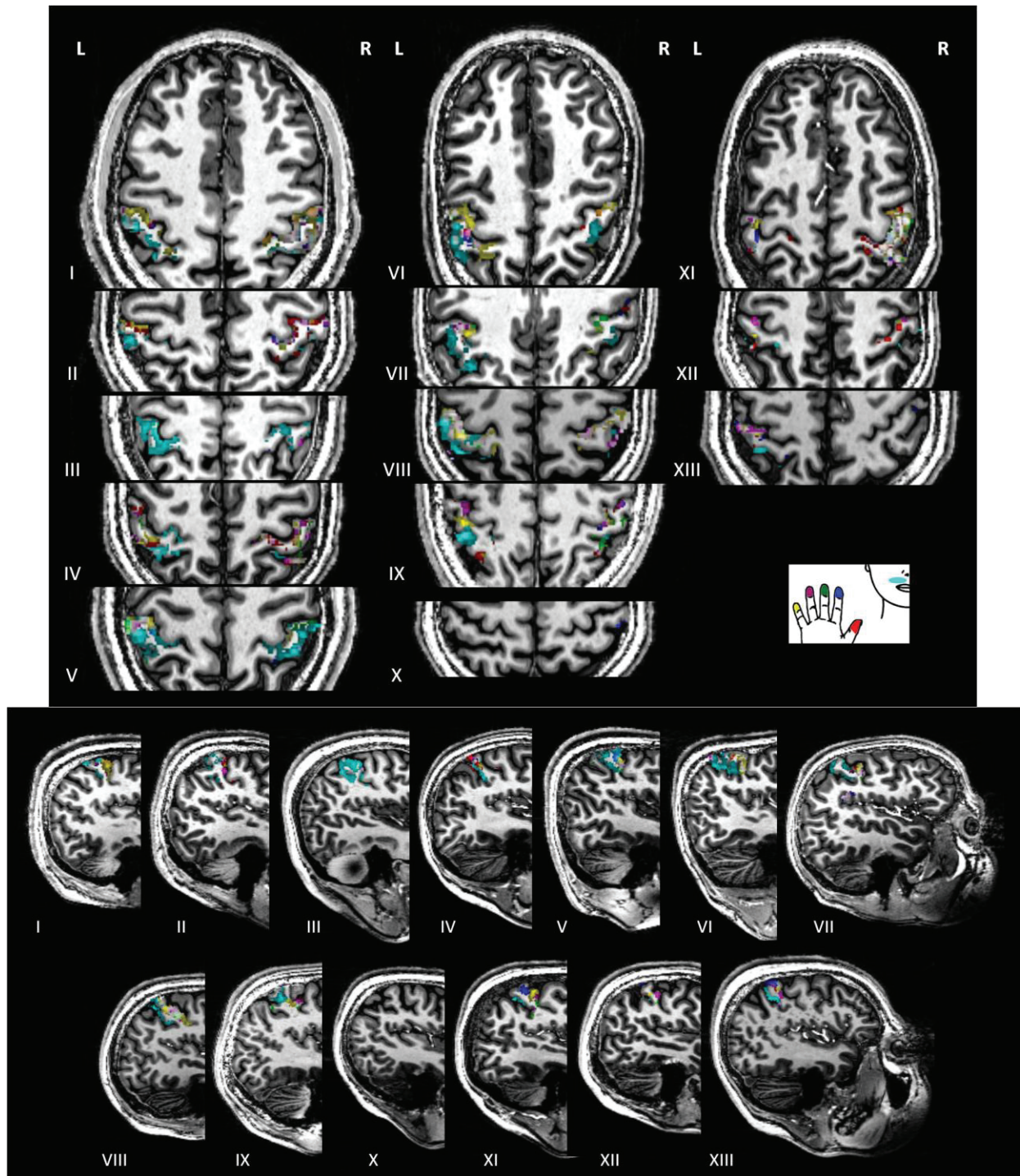


Figure 20. Native space individual NBR maps obtained at the Pre-session following right hemibody stimulation. The same axial (top) and sagittal (bottom) slices as in Figure 12 are shown for each of the participants (I to XIII). Body-sites are colour-coded (see schema), and overlaps result in mixed colours (white when all the areas are superimposed).

Similar to positive contrasts, the total volumes of NBR among the three sub-regions were quantified based on data from the 13 participants, and a two-way rmANOVA (BAs*Session) revealed significantly larger volumes within BA3b than within BA1 and BA2 (Figure 21; $F_{(2,24)} = 8.52$, $p = 0.002$, post-hoc tests: BA3b > BA1, $p_{LSD} = 0.001$; BA3b > BA2, $p_{LSD} = 0.002$). Note that the overall amount of negative BOLD is approximately twice as smaller than that of the positive BOLD at SI level. Here again, no difference across sessions was observed.

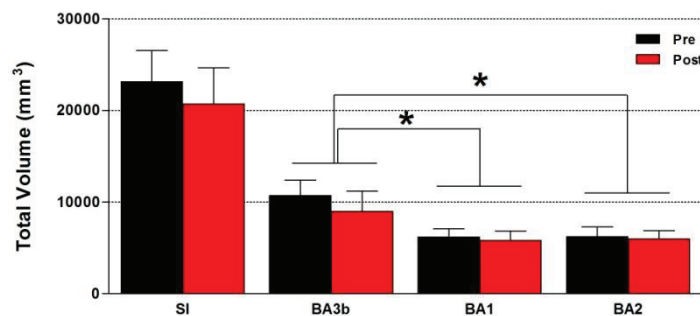


Figure 21. Total volumes (mm³) of all NBR maps within SI and the three sub-regions BA3b, BA1 and BA2, before (black) and after (red) the RSS procedure. * $p < 0.05$.

The four participants who were lacking PBR within several sub-regions (i.e., participant VIII and X excluded for BA3b and BA1 analysis and participants III and XII excluded for BA2 analysis), also lacked NBR for several body-sites in all sub-regions. They were thus excluded from further analysis as for the positive BOLD analysis, resulting in a sample of 9 participants.

Looking at the distribution of negative BOLD across body sides and hemispheres (rmANOVA Session*Side*Hemisphere), first within **SI**, a larger volume of NBR was found following stimulation of the left body side compared to the right side ($F_{(1,8)} = 7.03$, $p = 0.030$). This larger NBR was further found to be specific to the ipsilateral hemisphere ($F_{(1,8)} = 14.22$, $p = 0.005$), the volume of negative BOLD evoked within the left hemisphere following stimulation of the left hemibody being significantly larger than all other side or hemisphere (Figure 22, top left; all $p_{LSD} < 0.028$). Similar results were found within **BA3b** (Figure 22, bottom left), where the NBR evoked by stimulation of the left hemibody was larger than that of the right side ($F_{(1,8)} = 7.98$, $p = 0.022$), this effect being driven by the ipsilateral hemisphere ($F_{(1,8)} = 14.56$, $p = 0.005$; all $p_{LSD} < 0.024$). While similar results were found within **BA1** (Figure 22, top right; $F_{(1,8)} = 5.09$, $p = 0.054$) and **BA2** (Figure 22, bottom right; $F_{(1,8)} = 10.11$, $p = 0.013$), post-hoc tests revealed significantly larger volumes within the hemisphere ipsilateral to the stimulation of the left hemibody compared to its contralateral hemisphere (BA1: $p_{LSD} = 0.014$; BA2: $p_{LSD} = 0.009$) and to the hemisphere contralateral to the right hemibody solely (BA1: $p_{LSD} = 0.011$; BA2: $p_{LSD} = 0.012$).

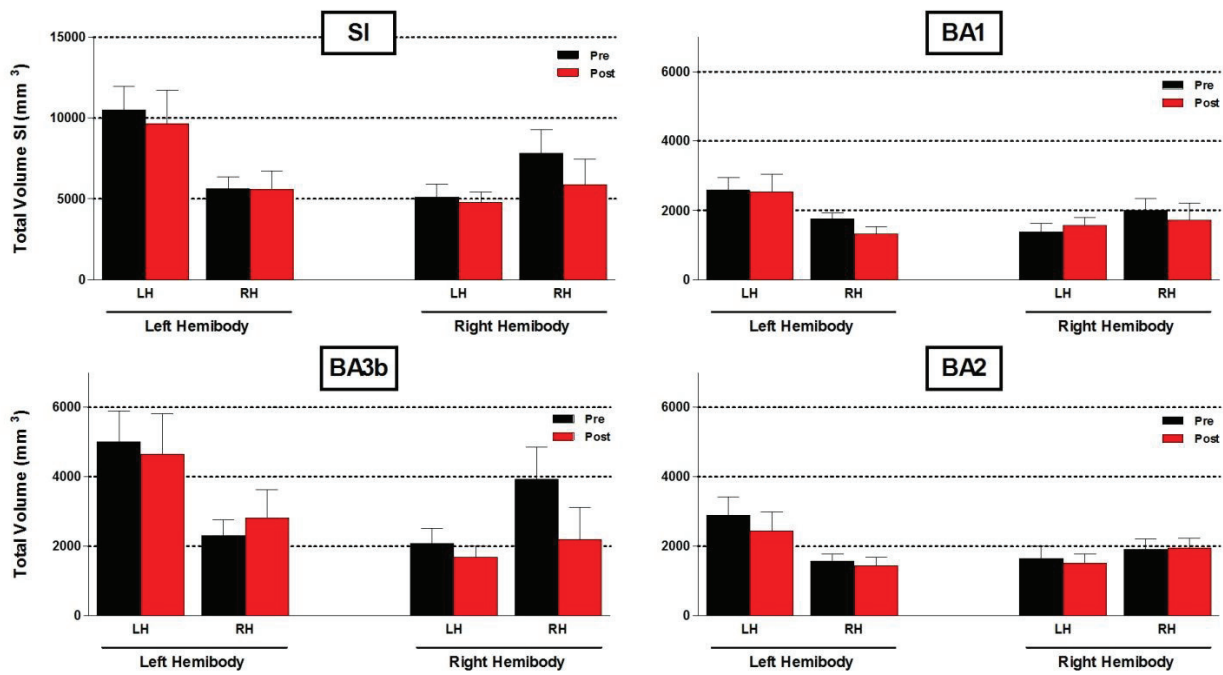


Figure 22. Total volumes (mm³) of NBR evoked by the stimulation of each hemibody, within SI and the three sub-regions BA3b, BA1 and BA2 of each hemisphere (LH: left hemisphere, RH: right hemisphere), before (black) and after (red) the RSS procedure. Statistical results are detailed in the text. Note that these volumes arise from the average of 9 participants.

Similar to the positive contrasts, volumes were then normalized to the total volume obtained within each sub-regions for each hemibody and session. No difference between sessions was observed for these volumes, but here again, the volumes elicited after stimulation of the left hemibody were larger than those elicited by the right hemibody within BA3b solely ($F_{(1,8)} = 7.98, p = 0.022$), with only a tendency for BA1 ($F_{(1,8)} = 5.09, p = 0.054$).

Surprisingly, despite the larger amount of negative BOLD within the ipsilateral hemispheres at the group level ($n = 9$), NBR were more reliably and systematically observed within the contralateral hemisphere. Thus, the volumes obtained from the contralateral hemisphere were analyzed together with the ipsilateral volumes obtained for the lips.

BA3b and BA1 were the sub-regions for which negative BOLD signal was consistently observed across body-sites and participants. Indeed, NBR were detected for the 9 participants after stimulation of all body-sites, except ipsilateral lips within BA3b and D2 fingertip within BA1. NBR were more disparate within BA2, thus precluding statistical analysis. Within **BA3b** (Figure 23, top), when comparing the body-sites for which the 9 participants exhibited activity (i.e., not for the ipsilateral lip), significant differences were found between their volumes ($F_{(5,40)} = 3.33, p = 0.013$), with a significantly larger volume of negative BOLD evoked by stimulating

the lip within their respective contralateral hemisphere than those elicited by stimulating D1, D2, D3, D4 (all p_{LSD} values < 0.046). In addition, D5 volume was found significantly larger than that of D2 ($p_{LSD} = 0.027$), and a significant interaction between sessions and body-sites was found ($F_{(5,40)} = 2.63$, $p = 0.038$), with a volume of NBR evoked within the contralateral BA3b region by lip stimulation significantly enhanced after RSS ($p_{LSD} < 0.001$). Despite a clear tendency for this effect to be driven by the right-Lip (see Figure 23, top left), the interaction with the hemisphere was not significant, suggesting an increased volume for both lips within their respective contralateral hemisphere. Within **BA1** (Figure 23, middle), submitting data from the body-sites for which negative BOLD was elicited in each of the 9 participants to a three-way rmANOVA (i.e., all body-sites except D2), revealed a similar pattern of volume differences across body-sites as within BA3b ($F_{(5,40)} = 9.26$, $p < 0.001$), with a significantly larger volume of NBR evoked by stimulating the lips within their respective contralateral hemisphere than those elicited by stimulating all other body-sites (i.e., D1, D3, D4, D4 and ipsilateral lip; all p_{LSD} values < 0.002). In addition, the ipsilateral lip exhibited a significantly larger volume of NBR than D3 ($p_{LSD} = 0.021$). Finally, a significant interaction between sessions and hemispheres ($F_{(5,40)} = 7.11$, $p = 0.028$) revealed an enhanced volume of negative BOLD after RSS for the right hemibody ($p_{LSD} = 0.015$), the latter being also significantly larger than that evoked by stimulating the left hemibody after RSS ($p_{LSD} = 0.047$). As previously mentioned, **BA2** sub-region was not statistically analyzed due to the lack of data for too many body-sites (see Figure 23, bottom).

In summary, these results reveal not only the presence of contralateral negative BOLD activity following finger stimulation, but also, and for the first time, an even larger contralateral volume of negative BOLD signal following lip stimulation. This larger contralateral deactivation following lip stimulation was statistically confirmed within BA3b and BA1. A tendency for a gradual increase of this contralateral deactivation from BA3b to BA2 is detectable by visual inspection (Figure 23) despite the lack of data from one participant within BA2. In addition to the differences across body-sites, a significant increase of the contralateral NBR following RSS was already observable within BA3b.

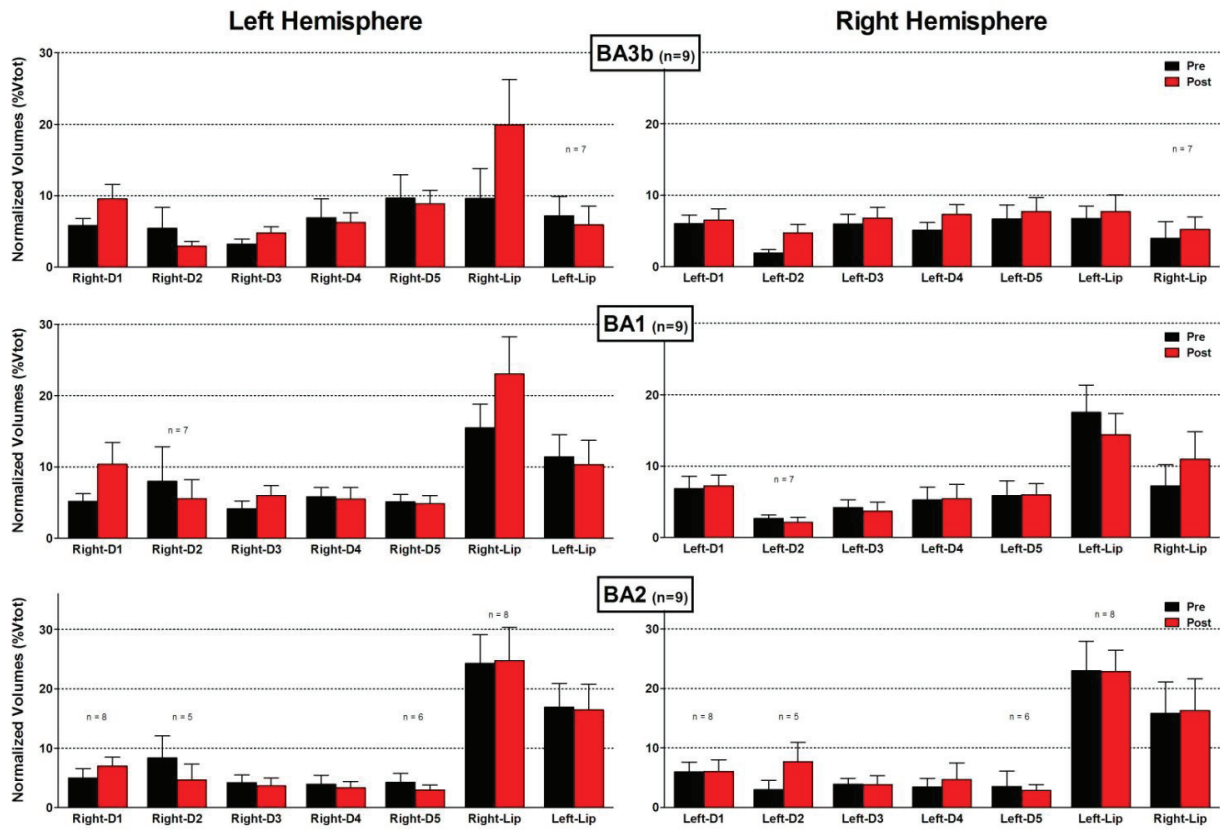


Figure 23. Normalized volumes (% volume total of the sub-region) of NBR evoked by the stimulation of each body-site from each body side, within each of the three sub-regions BA3b, BA1 and BA2 in each hemisphere, before (black) and after (red) the RSS procedure. Note that within each hemisphere, the volumes of the ipsilateral lip are showed in addition to the contralateral body-sites. Significant volume differences were obtained only between body-sites, not interfering with the hemisphere or the session. Statistical results are detailed in the text.

As done for the positive contrast, normalized contralateral volumes were further analyzed separately for each body-site (two-way rmANOVAs). Within **BA3b** ($n = 9$; Figure 24, top), apart from a significantly larger volume for left-D3 than for right-D3 ($F_{(1,8)} = 6.61, p = 0.033$), the contralateral NBR evoked by lips stimulation increased significantly after RSS ($F_{(1,8)} = 7.74, p = 0.024$), with no difference across hemispheres, in line with the previous analysis. In addition, a tendency for NBR from D1 to increase after RSS was observed ($F_{(1,8)} = 5.09, p = 0.054$). This trend turned significant within **BA1** ($n = 9$; Figure 24, middle), revealing larger NBR following RSS for D1 ($F_{(1,8)} = 6.84, p = 0.031$) regardless of hemisphere, though seemingly predominant for right-D1 (Figure 24, middle). Finally, the contralateral negative BOLD elicited by right-Lip stimulation was found significantly larger than that evoked by left-Lip stimulation ($F_{(1,10)} = 5.15, p = 0.047$).

Altogether, these results suggest that RSS resulted in an increase of the NBR elicited by lips stimulation within their respective contralateral BA3b sub-region, a similar RSS-induced increase being observed following D1 stimulation within BA1. Moreover, despite the lack of side differences, these changes were preferentially driven by the right side of the body.

No significant correlation (Pearson) was found between these negative BOLD volume changes observed across BAs (all p values > 0.05).

To investigate whether the RSS-induced increase of the lips NBR altered its degree of overlap with the NBR from other body-sites, we computed both the proportion of Lip NBR (the contralateral response) overlapping with the NBR from other body-sites, and the proportion of the other body-site NBR being overlapped with Lip NBR. Within **BA3b**, the proportion of Lip NBR overlapping with those from the other body-sites was significantly different across body-sites ($F_{(4,32)} = 4.97$, $p = 0.003$). For instance, a higher overlap was found with D1 than with D3, D4 and D5 (all p_{LSD} values < 0.009), with respectively 15.40% (± 3.38) of Lip overlapping with D1 instead of 5.03% (± 1.39), 6.27% (± 1.95) and 8.21% (± 1.97) with D3, D4 and D5. In addition, the Lip NBR was significantly more overlapping with D2 NBR ($10.53\% \pm 2.86$) than with D3 ($p_{LSD} = 0.042$). Conversely, these same volumes of overlap corresponded to 22.80% (± 5.82), 23.92% (± 6.80), 10.08% (± 3.04), 10.36% (± 3.25), and 12.32% (± 4.06) of the NBR of these other body-sites (i.e., in the same order: D1, D2, D3, D4 and D5). These latter proportions were significantly higher for D1 and D2 than for the other fingers ($F_{(4,32)} = 10.36$, $p < 10^{-4}$, all p_{LSD} values < 0.001). However, no significant changes in the proportion of overlap were observed across sessions.

Similar to PBRs, no correlation was found between 2PDT changes and NBR volume changes for any of the affected body-sites (Lips in BA3b and D1 in BA1; all p values > 0.05).

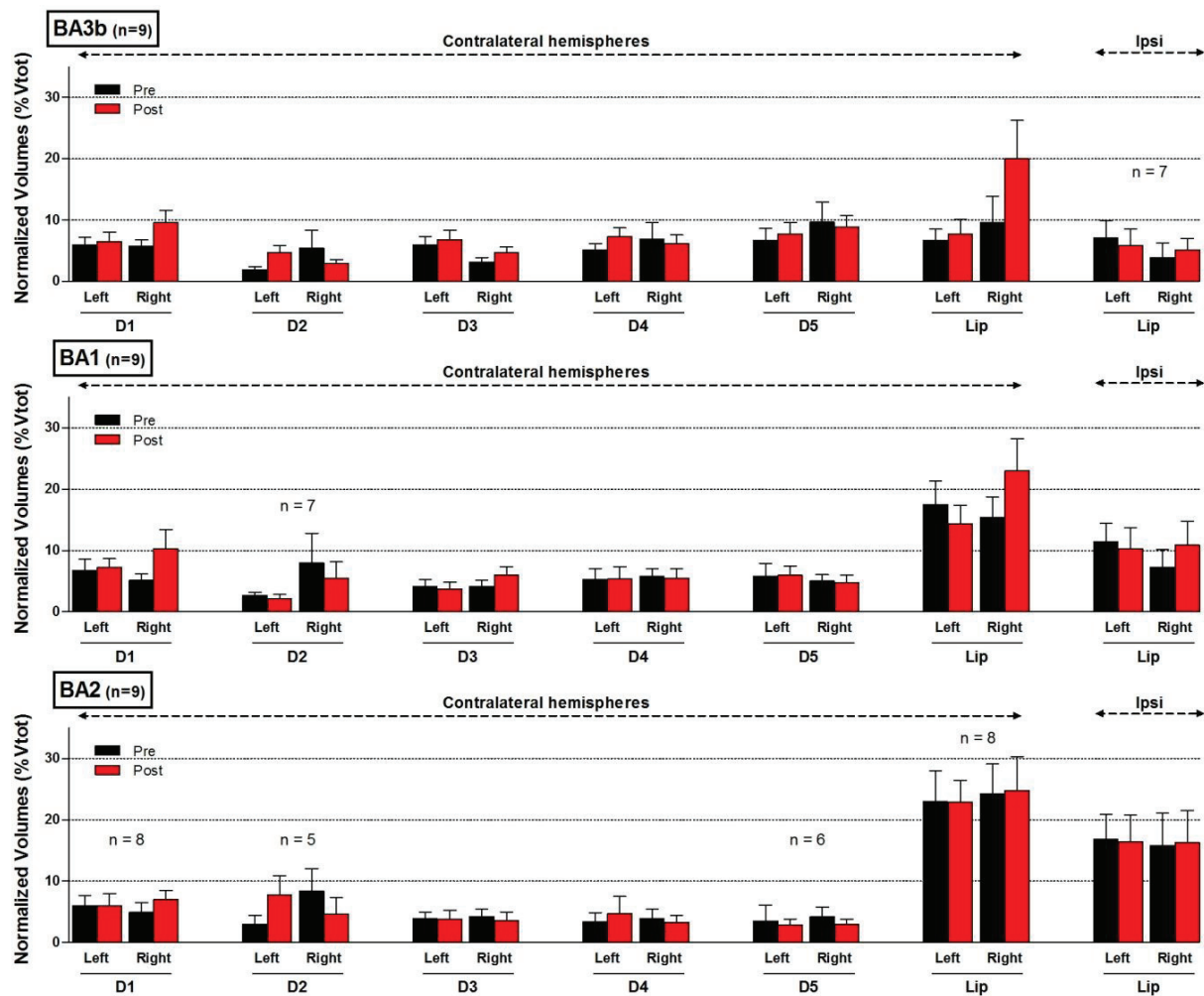


Figure 24. Same normalized NBR volumes (%Vtot) as in Figure 23, but grouped by body-sites within each of the three sub-regions BA3b, BA1 and BA2, to directly compared homologous body-sites (i.e., the two sides of the body) and their changes in volume across sessions (Pre-RSS: black, Post-RSS: red). Note that for the six first body-sites (i.e., the five fingers and the lip), the volumes of NBR obtained within their respective contralateral hemispheres are compared, while for the last body-site (i.e., the second lip), the volumes of NBR compared are those located within their respective ipsilateral hemispheres. A two-way rmANOVA (Session*Side) was applied on each body-site. * $p < 0.05$.

Finally, no correlation was found between the RSS-induced increased PBR within BA3b for right-D2 and the increased NBR found within BA3b for the lips, as well as between the changes of volumes of PBR for right- and left-D2 within BA1 and the increased NBR evoked by D1 stimulation within BA1.

Random-effect (RFX) analysis - “whole-EPI”

In addition to these RFX and native space ROI analyses, a whole-EPI RFX paired t-test analysis of right-D2 ($p_{uncorr} < 0.001$, minimum cluster size = 100 voxels) revealed four clusters of enhanced PBR following RSS (Figure 25). The first cluster (756 vox; T-score = 6.53; [-12 - 27 70]) was assigned to left BA4a with a probability of 42.5%, and the second (725 vox; T-score = 6.49; [57 -51 45]) to the right intraparietal lobule (IPL) and right intraparietal sulcus (IPS). More specifically, 35.9% of this cluster was assigned to PFm, 27% to PGa, 19.4% to hIP1 and 1.4% to hIP2. Finally, 73% of the third cluster (141 vox; T-score = 6.22; [42 -18 38]) was assigned to right BA4p, 12.1% to BA3b and 7.8% to BA3a, and the last cluster (139 vox; T-score = 5.96; [-41 -16 43]) to left BA4p (71.2%), BA3b (18%), BA4a (6.5%) and BA3a (0.7%).

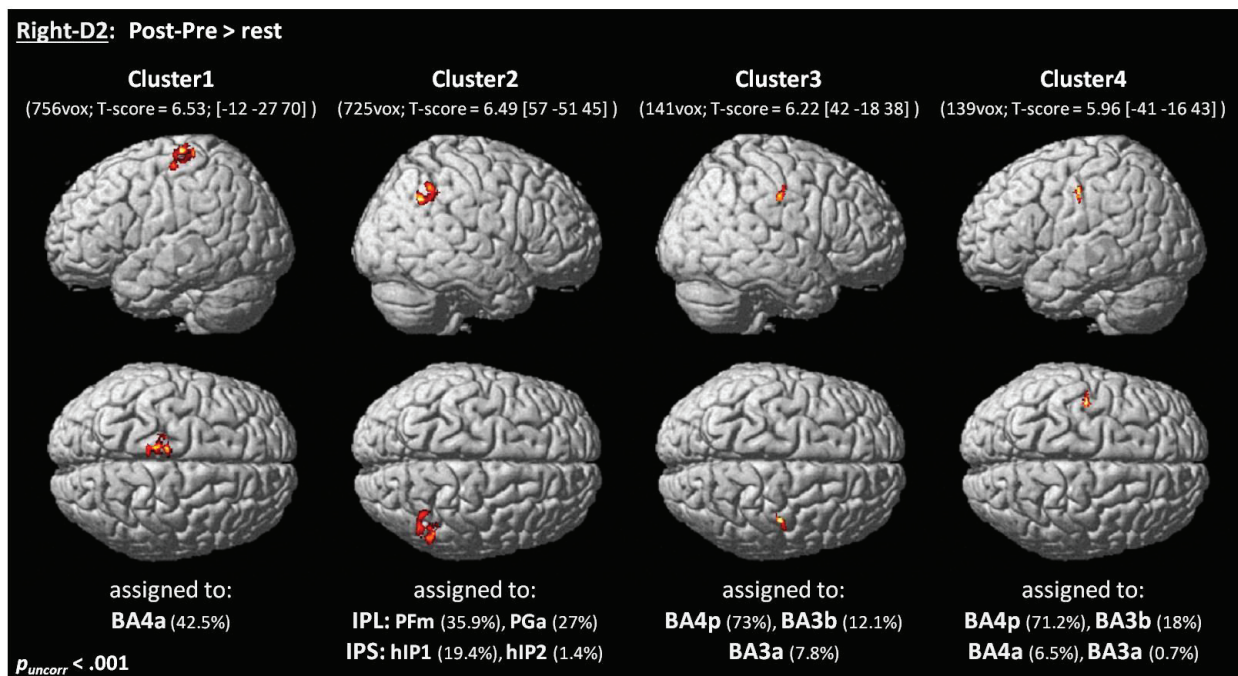


Figure 25. Differential group BOLD response between Pre and Post sessions following right-D2 stimulation, obtained from random-effects analysis using paired t-tests (Post-Pre > rest, $p_{uncorr} < 0.001$, minimum cluster size = 100vox) for right-D2. Among the four clusters revealed by the analysis, two were located within the left hemisphere (cluster 1 and 4), while the other two were located within the right hemisphere (cluster 2 & 3). The assignment of each cluster was performed using the Anatomy toolbox, and is indicated below each cluster. [x, y, z] in MNI coordinates.

Unexpectedly, when entering 2PDT as covariates, the whole-EPI RFX paired t-test analysis of right-D2 revealed several clusters of correlation. Notably, 2PDT changes at right-D2 were negatively correlated with BOLD signal changes (Post-Pre) within the SPL (BA5 and BA7), IPS and IPL. Similarly, 2PDT at left-Lip were negatively correlated with BOLD signal changes (Post-Pre) at right-D2 within SPL (BA7), IPS, BA2 and IPL (see Figure 26 for more details).

The more these cortical regions were activated, the more 2PDT decreased (i.e., improved discrimination). Conversely, a positive correlation was found between BOLD signal changes (Post-Pre) at right-D2 and right-D3 2PDT changes. This cluster was partly assigned to MI (BA4a and BA4p).

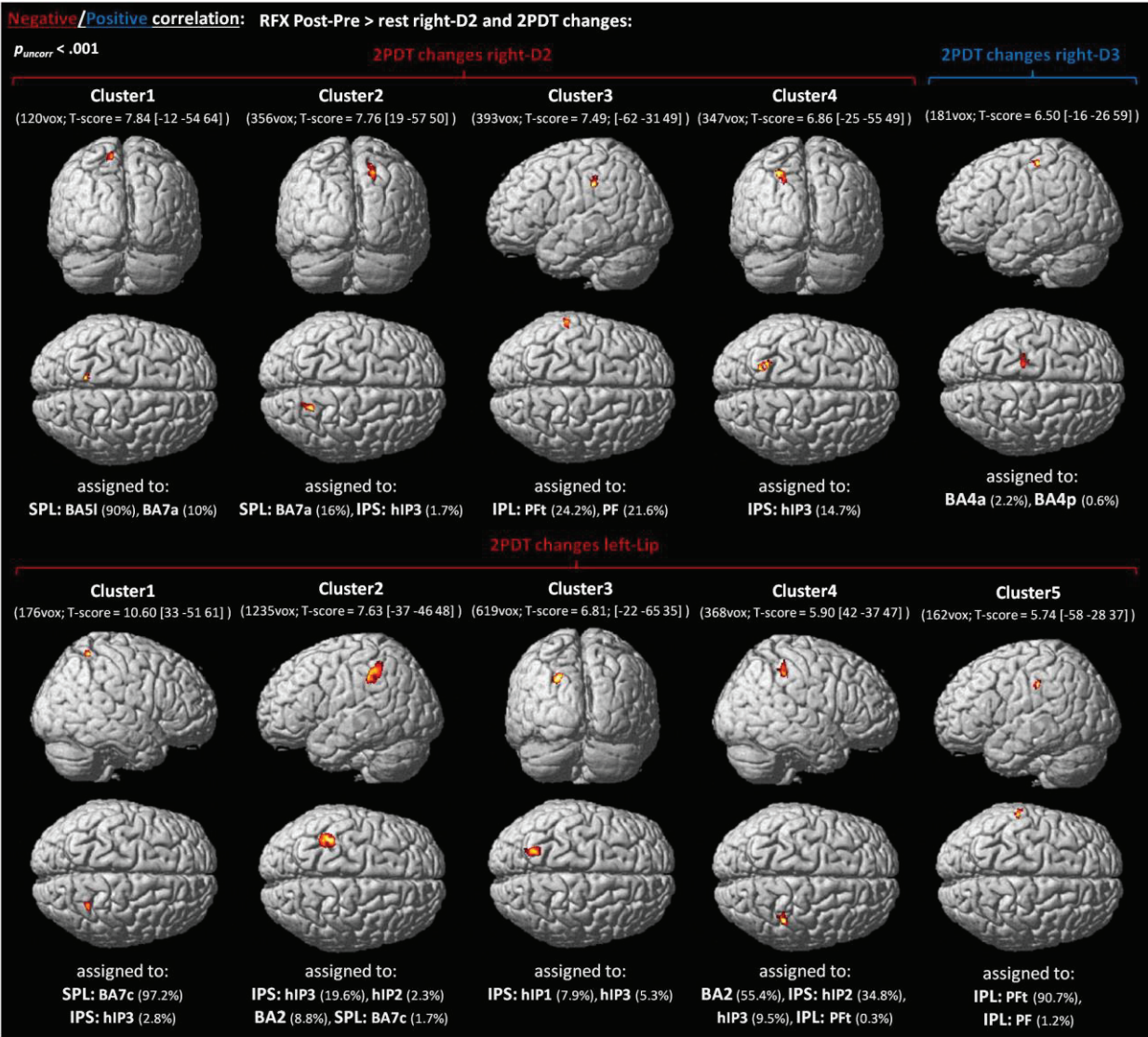


Figure 26. Correlation analysis to assess the relationship between the RSS-induced BOLD signal changes found for right-D2 and the two-point discrimination threshold changes obtained at the individual level. Results revealed a significant negative correlation between BOLD changes at right-D2 and the perceptual changes at right-D2 and left-Lip ($p_{uncorr} < 0.001$, minimum cluster size = 100vox). The assignment of each cluster was performed using the Anatomy toolbox, and is indicated below each cluster. [x, y, z in MNI coordinates].

Discussion

The purpose of this study was to take advantage of ultra-high field fMRI to identify first, the involvement of SI subregions BA3b, 1 and 2 in the somatosensory plastic changes that are obtained through training-independent learning, such as RSS; Second to investigate whether the recently reported remote changes induced by finger-RSS on the unstimulated region of the upper-lips reflect not only a behavioural, but also functional plastic changes that cross the hand-face border within SI sub-regions.

In agreement with our previous study (Muret et al., 2014), we found that three hours of RSS of right-D2 fingertip improved the spatial acuity not only at this finger, but also at both sides of the upper-lip. Additionally, this study provides the evidence that spatial acuity on right-D3 also remained unchanged. In parallel with these behavioural effects, several RSS-induced BOLD changes were observed at the cortical level. **First**, using standard group analysis (RFX) we found that the right-D2 response expanded following RSS within both hemispheres. Similar enhanced BOLD responses were also observed for both little fingers within their ipsilateral hemispheres. Finally, a decreased BOLD response was observed after RSS for right-D1 within the ipsilateral hemisphere. **Second**, a native space analysis similar to that proposed by Martuzzi and colleagues (2014) also revealed an enlarged contralateral PBR for right-D2 after RSS. In addition, decreased contralateral PBRs were found for right-D3 and for left-D2. Conversely, enhanced contralateral NBRs after RSS were found for the lips and the thumbs. Finally, exploration of the whole-EPI following RFX Post-Pre contrasts revealed large clusters located within the anterior part of the left primary motor cortex (BA4a) and the right intraparietal lobule and sulcus (IPL/IPS) for the stimulated finger (right-D2), and BOLD changes within these regions covaried with the perceptual threshold changes.

Behavioural results

The changes in tactile spatial discrimination observed here support and confirm our previous findings that RSS at right-D2 improves not only its tactile acuity, but also that of the upper-lips (Muret et al., 2014). Compared with the first report of this finding, the overall amount of threshold decrease for the three affected body-sites was smaller (right-D2: -7.66 ± 3.07 % instead of -15.26 ± 3.85 %; Lips: -9.11 ± 1.76 % instead of -10.29 ± 2.96 %). In addition to replicating these effects, the lack of threshold changes at the adjacent finger (i.e., right-D3) confirms a previous report by Godde and colleagues in a smaller sample of participants (Godde et al., 2000), and further defines a limit in the “spread” of the RSS-induced perceptual changes within the hand region. In addition, the different patterns of threshold changes at the different

body-sites suggest that a decreased threshold at right-D2 is more likely to be associated with an increased threshold at the adjacent finger than at the homologous finger. Together, these results are consistent with the presence of intracortical inhibitory connections between adjacent representations (Négyessy et al., 2013), and thus reinforce the hypothesis that short-range lateral inhibition (Simões et al., 2001) might be one of the mechanisms limiting the spread of RSS-induced effects between fingers. This is further supported by the previous report that the cortical representation of the adjacent thumb remains unchanged after RSS of right-D2 (Pleger et al., 2001). Conversely, the consistent decrease in lip thresholds suggests that different mechanisms underlie lip threshold changes after RSS of the right-D2.

Positive and Negative BOLD significance

BOLD (i.e., blood oxygenation level-dependent) signal is the most commonly used measure among the different possibilities provided by fMRI techniques. This signal is directly linked to the level of deoxyhemoglobin content in the cerebral blood, which is indirectly related to neural activity. The principle is quite simple: increased neural activity supposedly yields to a local increase in cerebral blood flow (CBF) greater than the increase in oxygen consumption by the neurons in activity, resulting in a decrease in deoxyhemoglobin content. As deoxyhemoglobin is paramagnetic by nature, its decrease translates into an increased magnetic resonance signal relative to the pre-stimulus baseline period (i.e., PBR). While the exact relationship between BOLD signal and the underlying neural activity is still not fully understood (for reviews on neurovascular coupling, see Shibasaki, 2008; Vanzetta and Grinvald, 2008; Kim and Ogawa, 2012), electrophysiological studies in animals support the idea that PBR reflects an increase in neural activity. For instance, PBR amplitude has been shown to correlate with increases in intracortical local field potential (LFP) (Logothetis et al., 2001; Devor et al., 2005; Bentley et al., 2014), but also with increases in the amplitude of somatosensory evoked potentials (SEPs) (Goloshevsky et al., 2008; Huttunen et al., 2008). A similar coupling between SI BOLD changes and SEP amplitudes has been found in humans (Arthurs and Boniface, 2003), and more recently, BOLD changes were associated with changes in the spectral profile of neuronal activity among several spectral bands (Rosa et al., 2010).

In contrast to PBR, NBR consists in a decrease in BOLD signal below pre-stimulus baseline levels. While this aspect of BOLD signal has long been disregarded, NBR has been increasingly investigated over the last 10 years, and has raised considerable debate regarding the underpinning mechanisms and its neurophysiological significance (see Kim and Ogawa, 2012). However, accumulating evidence from recent electrophysiological studies suggests that NBR is

tightly coupled with local decreases in neuronal activity below spontaneous activity (Shmuel et al., 2006), and with comparable decreases in LFP and multi-unit activity (Shmuel et al., 2006; Boorman et al., 2010; Kennerley et al., 2012; Bentley et al., 2014). While deep cortical layers were found to be involved (De Celis Alonso et al., 2008; Boorman et al., 2010), NBR is also likely to reflect activity in astrocytes (e.g., Sloan et al., 2010). In humans, the NBR evoked either by tactile or visual stimuli was found to be associated with decreases in CBF and oxygen consumption in primary sensory cortices (Shmuel et al., 2002; Wade and Rowland, 2010; Schäfer et al., 2012; Mullinger et al., 2014), and its average amplitude has been shown to increase with increasing stimulus duration and intensity (Shmuel et al., 2002; Klingner et al., 2010), analogous to the behaviour of the PBR. NBR within SI/MI has also been found to be negatively correlated with both the mu (8-13Hz) power and SEP amplitude (Mullinger et al., 2014). Altogether, these studies suggest that NBR may reflect inhibitory processes. Further support for this view comes from increasing evidence that NBR is associated with an increase in perceptual detection thresholds, suggesting that NBR reflects a functionally relevant measure of neuronal deactivation (Bressler et al., 2007; Kastrup et al., 2008; Klingner et al., 2010; Schäfer et al., 2012).

Positive BOLD distribution

Regardless of the analysis (RFX or native space), our mapping procedure revealed a consistent PBR in the post-central gyrus contralaterally to the stroked finger, and in both hemispheres following lip stroking. While the former is now well accepted, the **bilateral representation of the lips** remains somewhat controversial as some imaging studies report no ipsilateral activity following face stimulation (Stippich et al., 1999; Suzuki et al., 2004; Kopietz et al., 2009). However, in agreement with several imaging studies of face regions (Nagamatsu et al., 2000; Disbrow et al., 2003a; Nevalainen et al., 2006; Blatow et al., 2007; Eickhoff et al., 2008; Lin et al., 2010; Nash et al., 2010), including the lips (Nagamatsu et al., 2000; Disbrow et al., 2003a; Nevalainen et al., 2006; Blatow et al., 2007; Nash et al., 2010) our results bring strong evidence in support of a bilateral representation of the upper-lip region within SI. The lack of an ipsilateral representation in some of the previous studies might have arisen from insufficient strength in tactile stimulation leading to low levels of activation (Stippich et al., 1999; Kopietz et al., 2009), or from low signal to noise ratio particularly crucial for dipole source reconstruction in electrophysiological imaging (Suzuki et al., 2004). It is worth noticing that each side of the upper-lip is innervated by the medial branch of the superior labial branch of the infraorbital nerve, which never crosses the midline (Hu et al., 2007). In addition, the tested

sites at the upper-lips were located away from the midline (average at 18.38 ± 2.66 mm) for the behavioural testing, and the stroking never crossed the midline during the fMRI mapping. This positioning ensures that the bilateral PBR that we report here in SI emerges from unilateral peripheral innervation of the upper-lip. We also observed some ipsilateral PBR following finger stimulation, but this was inconsistent across participants. While this has been a subject of controversy, the existence of an **ipsilateral representation of the hand** within SI is now relatively well accepted, since both electrophysiological studies in animals (Iwamura et al., 1994; Zarei and Stephenson, 1996) and imaging studies in humans provide evidence in this direction (Schnitzler et al., 1995; Hansson and Brismar, 1999; Nihashi et al., 2005; Sutherland and Tang, 2006; Blatow et al., 2007).

The **ipsilateral representations** observed for both fingers and lips have two possible origins, either subcortical or cortical. First, it has been proposed that uncrossed fibres directly projecting to the ipsilateral SI or projections to both hemispheres may arise from the thalamus (Hoshiyama et al., 1996). However, the former appears to be unlikely as unilateral stimulation of the lip has been shown to elicit a strict contralateral activation within the ventroposterior thalamus, but bilateral activations in SI (Nash et al., 2010). Similarly, while neurons with bilateral RFs in the hindlimb region were found SI in awake macaque monkeys (Taoka et al., 2000), microstimulation of the stump representation in the thalamus of amputees induced referred sensation limited to the same hemi-body (Davis et al., 1998). While the available evidence does not support a thalamic origin, the ipsilateral responses could be caused by spread through transcallosal connections. Such callosal connections have been shown to vary in density among SI sub-regions, with few between BA3b, more between BA1 and relatively dense callosal connections between BA2 (Killackey et al., 1983; Manzoni et al., 1984; Iwamura, 2000; Iwamura et al., 2001). Additionally, these connections were found to be much denser for the representations of the face and trunk than for the glabrous hand (Killackey et al., 1983), which is consistent with the stronger ipsilateral activation found for the lip than for the fingers reported here and in previous studies (Blatow et al., 2007; Eickhoff et al., 2008; Nash et al., 2010).

In line with the literature (Penfield and Rasmussen, 1950; Nakamura et al., 1998), a **somatotopic organization** of the PBRs was observed, the finger representations from D5 to D1 being sequentially more ventral and anterior, with the lip representations located more ventrally and anterior than D1. This somatotopic organization was more distinguishable within BA3b than BA1 and BA2, as confirmed by the increase in PBR **overlap** observed from BA3b to BA1. Primarily found for the fingers, with larger areal overlap between finger representation in BA1/2 than in BA3b (Krause et al., 2001; Besle et al., 2013b; Martuzzi et al., 2014), similar results

were observed for the face with larger overlaps between the representations of the lower lip, teeth and tongue in the portions of the post-central gyrus corresponding to BA1 and BA2 (Miyamoto et al., 2006). Notably, here we additionally report a substantial overlap between D2 and the Lip representations, which also increases from BA3b to BA1 (19.77% of the PBR from the lip overlapping with that from D2 in BA3b, which turned to 34.97% in BA1). Finally, the larger PBRs observed for D1 and D2 in the native space analysis suggest a higher magnification of D1 and D2 across BAs, and a lower magnification of D5 and the ipsilateral Lip. These results are in agreement with the literature showing a higher degree of cortical magnification of D1 and D2 in monkeys (Sutherling et al., 1992; Shoham and Grinvald, 2001) and in humans (Maldjian et al., 1999; Martuzzi et al., 2014).

Negative BOLD distribution

In contrast to PBR, negative contrasts revealed activity in a more distributed network resembling the default mode network (Raichle et al., 2001; Greicius et al., 2003; Brookes et al., 2011; Passow et al., 2015), which is known to be down-regulated in a task-dependent manner (Fox et al., 2005). A similar widespread network has already been reported following electrical median nerve stimulation (Taylor and Davis, 2009; Klingner et al., 2011), and is likely to reflect a deactivation of the cortical regions not involved in tactile processing.

Within SI, RFX analyses revealed a consistent **ipsilateral NBR** following **finger** stimulation. This ipsilateral deactivation has already been reported in the literature (Hlushchuk and Hari, 2006; Arthurs et al., 2007; Eickhoff et al., 2008; Kastrup et al., 2008; Schäfer et al., 2012; Mullinger et al., 2014), but most of the time following strong electrical median nerve stimulation near motor (Kastrup et al., 2008; Schäfer et al., 2012; Mullinger et al., 2014) or pain (Arthurs et al., 2007) thresholds. Here, we show that an ecological brushing stimulation of individual fingers also results in ipsilateral NBRs. In previous reports this ipsilateral NBR has mainly been observed within BA3b and BA1 sub-regions (Hlushchuk and Hari, 2006; Eickhoff et al., 2008), where microelectrode recordings in monkeys revealed a predominant inhibition (Lipton et al., 2006). In agreement with these findings, here we found that the ipsilateral NBRs evoked by fingers brushing were located on the anterior wall of the post-central gyrus, and that larger volumes of NBR were found in BA3b than BA1 and BA2. Given that in contrast to BA3b and BA1, BA2 appears to contain a bilateral hand representation in monkeys (Iwamura et al., 1994) or a bilateral PBR in humans (Nihashi et al., 2005; Eickhoff et al., 2008), but also dense homologous callosal connections (Killackey et al., 1983), the ipsilateral NBR observed within BA3b and BA1 has been hypothesized to arise from a “serial” process, the contralateral PBR

sequentially travelling from BA3b to BA1 and BA2 through inter-areal intracortical connections, then transferring to the other hemisphere through BA2 transcallosal connections, this ipsilateral PBR within BA2 being then likely responsible for the NBR in BA3b and BA1 via inter-areal intracortical backward connections (Hlushchuk and Hari, 2006). This hypothetical model of indirect interhemispheric inhibition still remains the most probable, but requires further investigation.

A major novel finding of the current study is that it provides the first evidence for NBRs across body-sites at the somatosensory level, allowing the assessment of their relative distribution and possible somatotopic organization. At both group and individual levels, **ipsilateral NBRs** elicited by **finger** stimulation were highly overlapping, suggesting no clear somatotopic organization. Interestingly, while these ipsilateral NBRs were consistently observed at the group level (RFX), their presence was less systematic across individuals and body-sites, not all participants showing NBR for each body-site in all sessions. The presence of RFX ipsilateral NBRs despite some inconsistencies across individuals is likely to arise from the fact that these NBRs were large, highly overlapping and at relatively similar locations across participants. This suggests that the NBRs evoked ipsilaterally following fingers stroking may reflect a somatosensory deactivation processing that does not target any particular homotopic regions. In contrast, **contralateral NBRs** were consistently observed across participants and body-sites at the individual level, but not at the group level (RFX). This apparent discrepancy most likely arises from the fact that these contralateral NBRs were substantially smaller than the ipsilateral ones and not consistently distributed and localized, making it difficult to capture them at the group level. To the best of our knowledge, such a somatosensory contralateral NBR was previously reported only once, following imperceptible (subliminal) electrical finger stimulation (Blankenburg et al., 2003b). These authors interpreted this NBR as reflecting an increased activity of local inhibitory interneurons. While this contralateral NBR could be thought to arise from vascular stealing due to the presence of juxtaposed PBR (see Harel et al., 2002; Kannurpatti and Biswal, 2004), recent studies in rodents suggest that such NBR might rather reflect surround inhibition (De Celis Alonso et al., 2008; Boorman et al., 2010; Kennerley et al., 2012), a process that has been extensively studied in the barrel cortex (e.g., Derdikman et al., 2003). To conclude on the NBR from the fingers, presuming that this negative BOLD reflects an inhibition-like deactivation, the ipsilateral NBRs are likely to reflect a “global” somatosensory inhibition of the homologous hand, not necessarily somatotopically organized, while the contralateral NBR is more likely to reflect lateral-inhibition processes.

Another major novel finding of our study is that lip stimulation evoked large NBRs, within both hemispheres. In addition, these NBRs were located more dorsal than the lip PBR and co-localized with the PBR of the fingers/hand. In contrast to the hand, the NBR elicited by stimulation of the **face**, and notably the lips, has never been investigated. The only study in which both PBR and NBR elicited by cheek stimulation were assessed within SI reported a strong bilateral PBR only (Eickhoff et al., 2008). However, it is worth noting that the authors only investigated the ipsilateral hemisphere using ROIs defined based on the positive contrasts. In agreement with their results, we observed only a few NBRs at the same localizations as PBRs evoked by lip stimulation.

Thus, here we provide the first evidence that the somatosensory cortex might actually be composed of two homunculi: the first one is the traditional homunculus based on activations, while the second and new one would be a ‘negative’ version of the traditional homunculus, which would be detectable only by analyzing NBRs. In addition, the new somatosensory homunculus seems to be spatially inverted, as finger and lip regions appeared swapped. This negative homunculus may arise from a direct (i.e., via thalamocortical projections) or indirect increase in inhibitory interneuron activity, since electrophysiological studies demonstrated that NBR is related to decreases in neural activity in deep cortical layers (De Celis Alonso et al., 2008; Boorman et al., 2010), which are known to contain such interneurons (Gibson et al., 1999; Swadlow, 2003). The precise nature and origin of such a negative homunculus remains to be investigated, however. Interestingly, a similar negative based homunculus, which is also swapped in term of somatotopy, has been recently reported for the primary motor cortex by Zeharia and colleagues (Zeharia et al., 2012). Most interestingly in relation to the neurofunctional mechanisms behind the behavioural transfer of plasticity from the finger to the lips, here we found that, while the PBR evoked by lip stimulation was predominantly assigned to BA3b and BA1, the NBR was primarily assigned to BA2, where neuronal excitation (Iwamura et al., 1994) and PBR (Nihashi et al., 2005) were found bilaterally following hand stimulation. This co-localization of lip NBR and fingers PBR may thus represent a novel substrate for interactions between these two regions, without requiring the involvement of long-range intracortical connections, which have been found to be rare, at least within BA3b (Manger et al., 1996; Fang et al., 2002).

RSS-induced changes in SI

While this study provides novel evidence of differential patterns of NBR within SI, its primary purpose was to assess how the RSS procedure may modulate somatotopic patterns both locally at the stimulated finger and remotely at the unstimulated lips. As expected, the RFX paired t-tests revealed an enlargement of the contralateral PBR associated with right-D2 stroking (the finger that underwent RSS). This result is in keeping with those reported by Pleger and colleagues (2003). However, in contrast to Pleger and colleagues who reported a lateral shift of right-D2 by 11.9 mm, we found a non-selective shift for each tested body-site, with right-D2 shifting only by 3.78 mm. It is important to note, however, that Pleger and colleagues calculated the shift based on a fixed-effect analysis, which does not take into consideration the inter-individual variability, meaning that this large shift could be driven by only a few participants. Inspection of their individual data suggests an average shift of only 6.80 ± 9.1 mm (\pm sd), including one participant who had a 30mm shift (the others all shifting less than 13mm). Notwithstanding this methodological consideration from previous fMRI data, a lateral shift of the RSS-stimulated finger has been previously reported with other, electrophysiological imaging techniques (Pleger et al., 2001; Dinse et al., 2003; Godde et al., 2003). Thus, considering the significant enlargement of right-D2 PBR, the smaller shift reported here suggests a more symmetrical enlargement than in previous studies. In addition, the current study is the first that allows for comparison among the effects induced by RSS on the representation of the stimulated finger with those of other unstimulated sites on the same hemi-body. In this respect, we observed non-selective shifts of the PBR of other body-sites, which may underline the dynamic property of cortical maps. Indeed, to our knowledge, no study systematically investigated the test-retest reliability of the absolute localization of PBR CoGs. The only study reporting test-retest data for finger PBRs (Martuzzi et al., 2014) revealed similar absolute and non-selective shifts in the retest session (1.7 ± 1.2 mm for D1, 3.2 ± 3.1 mm for D2, 2.3 ± 1.3 mm for D3, 2.2 ± 1.5 mm for D4, and 2.2 ± 2.5 mm for D5). Given the temporal dynamics of receptive fields (see Nicolelis et al., 1997; Ramirez et al., 2014) and of transient plastic changes in SI (Stavrinou et al., 2007), cortical maps could exhibit similar properties, making them to be constantly and dynamically fluctuating. This could explain the non-selective shifts reported here. Also at odds with Pleger and colleagues' findings, we did not find a linear correlation between right-D2 acuity improvement and cortical enlargement. Again, methodological differences should be underlined, as to avoid removing possible effects from the control homologous finger, here we did not use side-corrected difference maps to perform the correlation, and found only a negative correlation between right-D2 cortical changes (located within bilateral BA2 sub-region and right

BA1) and left-Lip threshold changes. Yet, at the behavioural level we observed a tendency towards a positive correlation between right-D2 and left-Lip threshold changes ($r = 0.52$, $p = 0.066$). All in all, the present results substantiate the enlargement of right-D2 following RSS. The purpose was then to use the ultra-high resolution of 7T fMRI to investigate in more detail the contribution of SI sub-regions to this enlargement and to RSS-induced behavioural effects.

RSS-induced changes within BA3b

BA3b is considered to be the true primary somatosensory cortex as it receives the bulk of thalamocortical projections. Within BA3b, a significant enlargement of **right-D2** contralateral PBR was observed with both RFX and native space analyses. Given that it has been suggested that BOLD changes reflect the input and intracortical processing of a given area rather than its spiking output (Logothetis et al., 2001), this increased PBR elicited by stimulation of the finger that underwent RSS could either arise from an increased thalamocortical input, from an increased intracortical processing, or both. Given that RSS drives Hebbian-like plastic changes, this enlarged PBR is likely to reflect recruitment of cortical processing resources and/or an enhanced synaptic efficacy through potentiation (see Beste and Dinse, 2013 for a review). In line with this resource recruitment hypothesis, a decrease in **D3's** PBR that was mostly driven by right-D3 was found after RSS in the native space analysis. This suggests that part of the resources recruited to enhance the processing of tactile information on the right-D2 after RSS might have been drawn from the adjacent right-D3 finger. Interestingly, although the cortical changes for these two areas were not correlated, the cortical changes observed for right-D2 and right-D3 are consistent with the behavioural data, which show improved tactile acuity for right-D2 but not for right-D3.

In addition, an ipsilateral cluster emerged at the group level (RFX) after RSS when right-D2 was stroked. Given that hand stimulation evokes NBR in the ipsilateral BA3b (Hlushchuk and Hari, 2006; Eickhoff et al., 2008) associated with local inhibition (Lipton et al., 2006), this ipsilateral cluster resulting from the Post-Pre contrast is likely to reflect a decrease in NBR (i.e., less negative after RSS). This type of relationship between positive and negative BOLD responses has recently been demonstrated by inducing somatosensory adaptation in humans (Klingner et al., 2014). These authors found that a high frequency unilateral electrical stimulation of the median nerve not only decreased the contralateral PBR (indicative of adaptation), but also increased the ipsilateral NBR. Together, these results suggest the presence of widespread changes in the excitatory/inhibitory balance between hemispheres.

Interestingly, the RFX analysis revealed that the cortical regions recruited in favour of right-D2 after RSS were partly co-localized with the right-Lip PBR within the contralateral BA3b at the Post-session. While this has to be confirmed with a more refined analysis in the native space, based on the relationship found by Klingner with adaptation, it could be hypothesized that due to this co-localization, the increased right-D2 PBR may have occurred to the detriment of the right-Lip PBR which might then have resulted in an increased NBR within the lip's ipsilateral hemisphere. What we found, however, was an increased NBR for both **lips** and within their contralateral hemispheres. While this bilateral effect is likely to arise from the bilateral representation of the lips, based on the hypothesis presented above it is surprising that we did not find a similar effect for the ipsilateral lip representation. These results suggest that the interhemispheric balance in the processing of tactile information may be different for the face. Indeed, the “hemispheric rivalry” observed for the hands (with the ipsilateral NBR in BA3b and BA1) is likely to be related to the need to dissociate tactile information arising from the two hands when manipulating objects (usually done bimanually). Instead, the use we make of lips does not require such dissociation. This idea is consistent with the fact that in contrast to the hand, the lips' ipsilateral activity was found to be positive within all SI sub-regions (Eickhoff et al., 2008). In addition, while the exact nature and interaction between SI sub-regions regarding the processing of tactile information arising from the hands is still unclear despite many investigations, that arising from the face is completely obscure. Our results represent a starting point for such an investigation. Interestingly, despite the absence of a correlation (likely due to the small sample size, $n=9$), the increased lip NBR following RSS of right-D2 was bilateral, as was the acuity improvement. This hypothetical link between NBR and tactile acuity is further supported by the recent evidence that the NBR elicited by hand stimulation is associated with an increased detection threshold on the opposite hand (Kastrup et al., 2008; Klingner et al., 2014).

Overall, we can see that as early as within BA3b, RSS-induced cortical changes are observed for the body-sites exhibiting tactile threshold changes. But these cortical changes affect both activation and deactivation processes, which suggests that RSS modulates a complex excitatory/inhibitory balance across body-sites, SI sub-regions, and hemispheres.

RSS-induced changes within BA1

Within BA1 the native space analysis revealed an increase in PBR for **right-D2**, similar to that observed in BA3b. Given the strong interconnectivity between SI sub-regions (Vogt and Pandya, 1978; Burton and Fabri, 1995), this effect could arise from a transfer of the RSS-

induced effects from BA3b to BA1. But another possibility would be a direct effect of RSS on BA1 via the thalamocortical projections reaching BA1 (Whitsel et al., 1978; Lin et al., 1979; Nelson and Kaas, 1981). However, the positive linear correlation found between the changes observed within BA3b and BA1 supports a transfer from BA3b to BA1. The slope of this correlation further suggests that larger changes should occur within BA3b to get substantial changes within BA1. Interestingly, this increased PBR for right-D2 was associated with a significant decrease of the PBR evoked by stroking **left-D2**. This result suggests a transfer of the RSS-induced effects to the other hemisphere (i.e., BA1), which is consistent with the electrophysiological literature reporting more transcallosal connections between homologous BA1 regions than between BA3b (Killackey et al., 1983; Manzoni et al., 1984; Iwamura, 2000; Iwamura et al., 2001). The decrease in left-D2 PBR is also consistent with the increased activity emerging within the ipsilateral BA3b (discussed above), and with the absence of threshold changes at this fingertip. Together, these results are likely to reflect a homeostatic process that counterbalances the RSS-induced increased response observed for right-D2, perhaps via indirect interhemispheric inhibition. But the exact nature and interactions between homologous representations within a given hemisphere remains to be clarified. Note that while a difference between PBR volumes was also observed at baseline for left-D2 and right-D2, the same trend was found within BA3b and BA2, suggesting general inter-hemispheric difference. In addition to these PBR changes, the contralateral NBR elicited by **thumb** stroking increased following RSS of right-D2. D1 being adjacent to the finger that underwent RSS, this increased NBR within the contralateral hemisphere is likely to reflect an increased lateral inhibition (discussed in the Negative BOLD distribution paragraph). But if this were the case then it should have also been observed for right-D3, but there was only a tendency that did not reach significance. This is likely due to the fact that the higher cortical magnification of the thumb and index fingers means that their volumes represent a higher proportion of the total evoked activity, which makes it easier to catch any changes.

In addition to these changes observed at the native space, RFX paired t-tests also revealed an enhanced activity for both little fingers and a decreased activity (either decreased PBR or increased NBR) for right-D1, all within their respective ipsilateral hemispheres. These unexpected changes might reflect a “by-product” of the increased lateral inhibition suggested above and of the increased ipsilateral activity observed for right-D2, though this possibility awaits for further investigations. Here again, while this effect is likely to, an interpretation is difficult and would be highly speculative.

To conclude, our results suggest that the RSS-induced effects reach BA1, likely through BA3b, and reveal that in both BA1 and BA3b the pattern of changes for right-D2 is similar. Our results also suggest the presence of some inhibition in BA1, both intra (right-D1) and interhemispheric (mainly left-D2).

RSS-induced changes within BA2

While data from BA2 were not consistent enough to perform the native space analysis, RFX analyses revealed no significant changes within this sub-region. However, this does not preclude BA2 from being involved in the RSS-induced effects. Instead, the significant negative correlation found between the RSS-induced changes for right-D2 BOLD signal and the perceptual changes observed at left-Lip rather suggest the opposite. Two of the clusters were localized within each BA2 sub-region, while the last one was assigned to right BA1. Altogether, it is difficult to conclude about BA2's role in RSS.

RSS-induced changes within BA3a

In addition to the three sub-regions described above, an increase in activity was also observed within BA3a after RSS. This was observed for right-D2 within both hemispheres (with 8.3% of cluster2 and 100% of cluster4). While this result seems at first surprising, an emergence of cutaneous responses in the hand representation of BA3a have been previously reported in monkeys following training in tasks increasing tactile inputs (Recanzone et al., 1992c) or sensorimotor skills (Xerri et al., 1998). While BA3a neurons are usually classified as “deep” in origin because they respond specifically to inputs arising from muscle and joint spindles (Powell and Mountcastle, 1959a), electrophysiological recordings have revealed sub-threshold responses of BA3a neurons from cutaneous mechanoreceptors (Zarzecki and Wiggin, 1982; Zarzecki et al., 1983; Kang et al., 1985), and cutaneous RFs are occasionally defined within BA3a (see Tanji and Wise, 1981). Thus, RSS appears to also affect these neurons. This effect might be linked to the previously reported RSS-induced haptic improvement (Kalisch et al., 2008, 2010; Kowalewski et al., 2012). Indeed, the enhanced tactile acuity, associated with an enhanced kinaesthesia, is likely to improve the integration of both object conformation hold by the fingers and the finger/hand position, and movement to maintain fine grasping while performing arm movements to end up with release of the object in a specific place (i.e., pegboard task).

RSS-induced changes within BA4a and PPC

While the previous analyses highlighted the contributions of SI sub-regions in the RSS-induced cortical changes, some interesting hints about the implication of other cortical areas arise from the whole-EPI analysis. Indeed, to the best of our knowledge, this is the first evidence of RSS-induced changes within BA4a and the posterior parietal cortex (PPC), including the intraparietal sulcus (IPS) and the superior parietal lobule (SPL).

Even if primarily associated with the motor cortex, BA4a has been shown to be involved in the processing of either purely somatosensory information, in case of complex tactile stimulation such as moving pins (Terumitsu et al., 2009), or in haptic discrimination tasks (Geyer et al., 1996; Eickhoff et al., 2005) involving somatosensory, proprioceptive and motor processing. Regarding PPC, this region has been found to be activated in cases of **complex moving stimuli** generating a texture sensation such as rubbing a sponge (Fabri et al., 1999, 2001), which is quite similar to the brushing used here for the fMRI mapping. The involvement of SPL and IPS in tactile motion direction discrimination was also reported (Nakashita et al., 2008). But occasionally, activation of PPC either ipsilateral (Del Gratta et al., 2000; Nihashi et al., 2005) or contralateral (Forss et al., 1995; Mauguière et al., 1997) was found following electrical stimulation. Previous studies have also implicated the superior parietal cortex in tactile (and visual) spatial attention specifically when **attention** was focused close to the hands, in peripersonal space (see Macaluso and Maravita, 2010 for a review), and in **working memory** representations of actively explored tactile textures (Kaas et al., 2013b). Additionally, IPS and SPL were found to be involved in macrospatial discrimination tasks such as the grating orientation task, but also in microspatial spacing discrimination tasks resembling the 2PDT (Sathian et al., 1997; Stoesz et al., 2003; Zhang et al., 2005). Still along these same lines, shape, length and texture perception and discrimination were found to activate the anterior part of IPS and SPL (Roland et al., 1998; Bodegård et al., 2001; Stoeckel et al., 2004). PPC was also involved in two-point discrimination (Akatsuka et al., 2008). Thus the enhanced activity that we report within BA4a and PPC following RSS of right-D2 appears to reveal changes in higher order cortical areas, which may reflect or actually contribute to improved spatial discrimination abilities following RSS. This seems to be confirmed by the negative correlations found between the enhanced activity in bilateral PPC and both right-D2 and left-Lip acuity changes. In line with this, the right posterior IPS was also found to be involved in **tactile spatial discrimination learning**, within which the level of activity significantly predicted individual acuity thresholds (Stilla et al., 2007).

Interestingly, although tactile stimuli were applied to the right hand of right-handed people, the enhanced activity in PPC was found mainly in the right hemisphere. This may reflect right cerebral hemisphere dominance. Similar right lateralization has been reported for tactile shape perception (Sadato et al., 2000), somatosensory stimulation of different kinds (Coghill et al., 2001; Hagen et al., 2002).

Conclusion

To conclude we found that three hours of RSS of right-D2 fingertip improved the spatial acuity not only at this finger, but also at both sides of the upper-lip, while the acuity of left-D2 and right-D3 remained unchanged. In parallel with these behavioural effects, an expansion of right-D2 response was found following RSS within the contralateral BA3b and BA1. In addition, decreased contralateral PBRs were found for right-D3 and for left-D2 respectively within the contralateral BA3b and BA1. Unexpectedly, we also report an enhanced contralateral NBRs for the lips within BA3b, and for the thumbs within BA1. Interestingly, while no linear correlation was found between PBR and NBR changes, the PBR changes observed within BA3b and BA1 for right-D2 were positively correlated. Finally, exploration of the whole-EPI following RFX Post-Pre contrasts revealed large clusters located within the anterior part of the left primary motor cortex (BA4a) and the right intraparietal lobule and sulcus (IPL/IPS) for the stimulated finger (right-D2), and BOLD changes within these regions covaried with the perceptual threshold changes. Thus, in addition to replicating the well-established enlargement of right-D2 representation, this study reports a differential contribution of SI sub-regions to RSS-induced effects, and the possible involvement of higher-order cortical regions. Furthermore, this study provides evidence for the existence of NBR evoked by lip stroking, which in contrast to PBR, are co-localized with the hand PBR. This latter result asks for a revision of the concepts of cortical “representations” and of their “borders”, the presence of intermingled positive and negative responses making them more complex. Finally, this lip-related NBR was modulated by RSS of the finger, suggesting the existence of remote cortical effects of RSS, and further, that plastic changes observed across the hand-face border in the literature could be related to modulations in NBR.

Supplementary Data

Whole-EPI - Positive and Negative RFX one-sample t-tests at baseline:

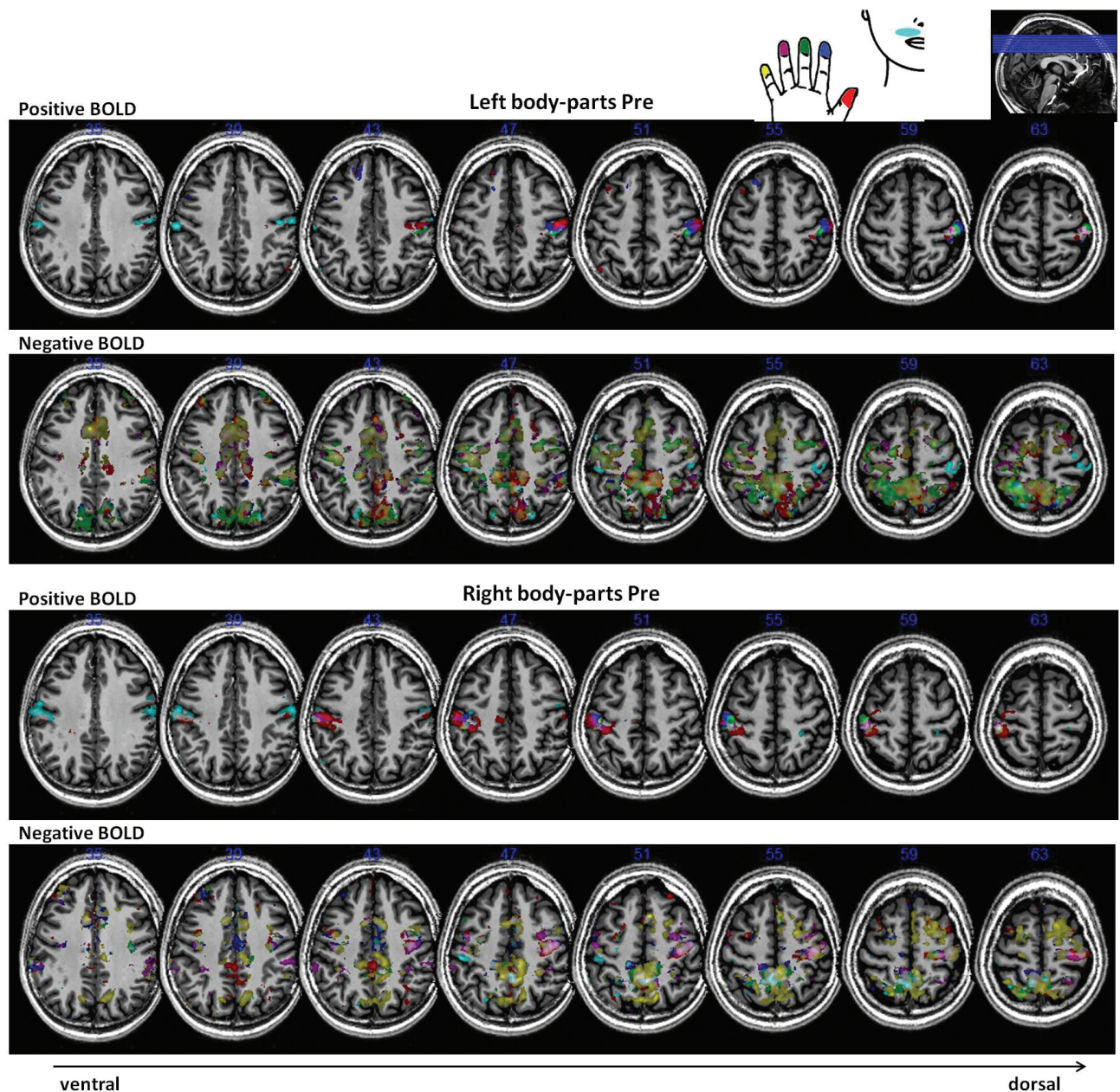


Figure S1. Example of whole-EPI group activations (positive BOLD) and deactivations (negative BOLD) obtained from random-effects analysis using one-sample t-tests (stimulation > rest or stimulation < rest, $p_{uncorr} < 0.001$) following stimulation of left (top) and right (bottom) body-sites at baseline. The same eight axial slices are shown across sides and sessions, along the ventro-dorsal axis. Each body-site is color-coded (see upper schema: red: D1, blue: D2, green: D3, violet: D4, yellow: D5, cyan: Lip). Overlaps result in mixed colors (white when all the areas are superimposed).

ROI - Positive RFX one-sample t-tests (activity > rest):

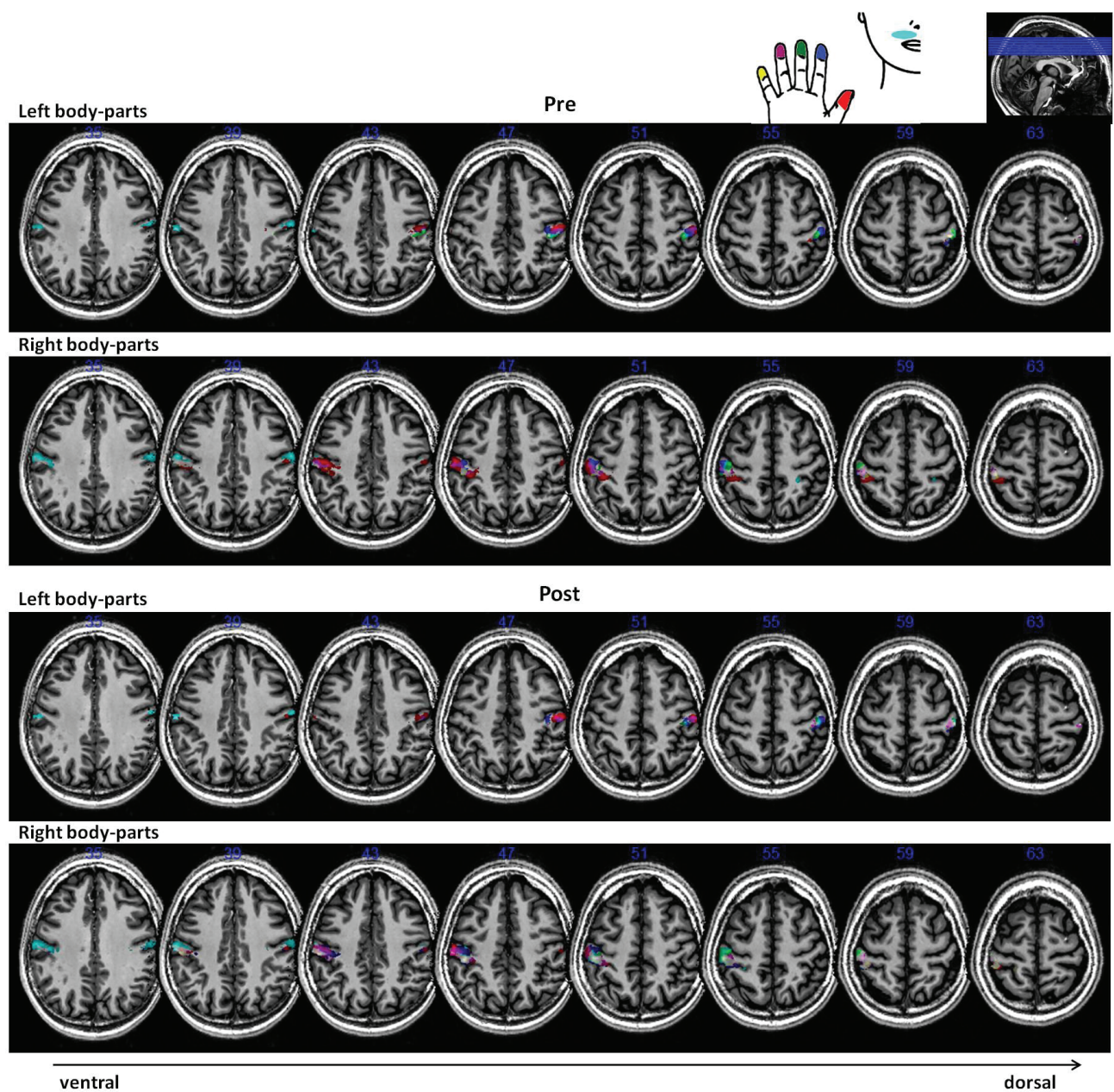


Figure S2. Group activations within SI obtained from random-effects analysis using one-sample t-tests (stimulation > rest, $p_{uncorr} < 0.001$) following stimulation of right and left body-sites respectively Pre (top) and Post (bottom) RSS. The same eight axial slices are shown across sides and sessions, along the ventro-dorsal axis. Each body-site is color-coded (see upper schema: red: D1, blue: D2, green: D3, violet: D4, yellow: D5, cyan: Lip). Overlaps result in mixed colors (white when all the areas are superimposed).

ROI - Negative RFX one-sample t-tests (activity < rest):

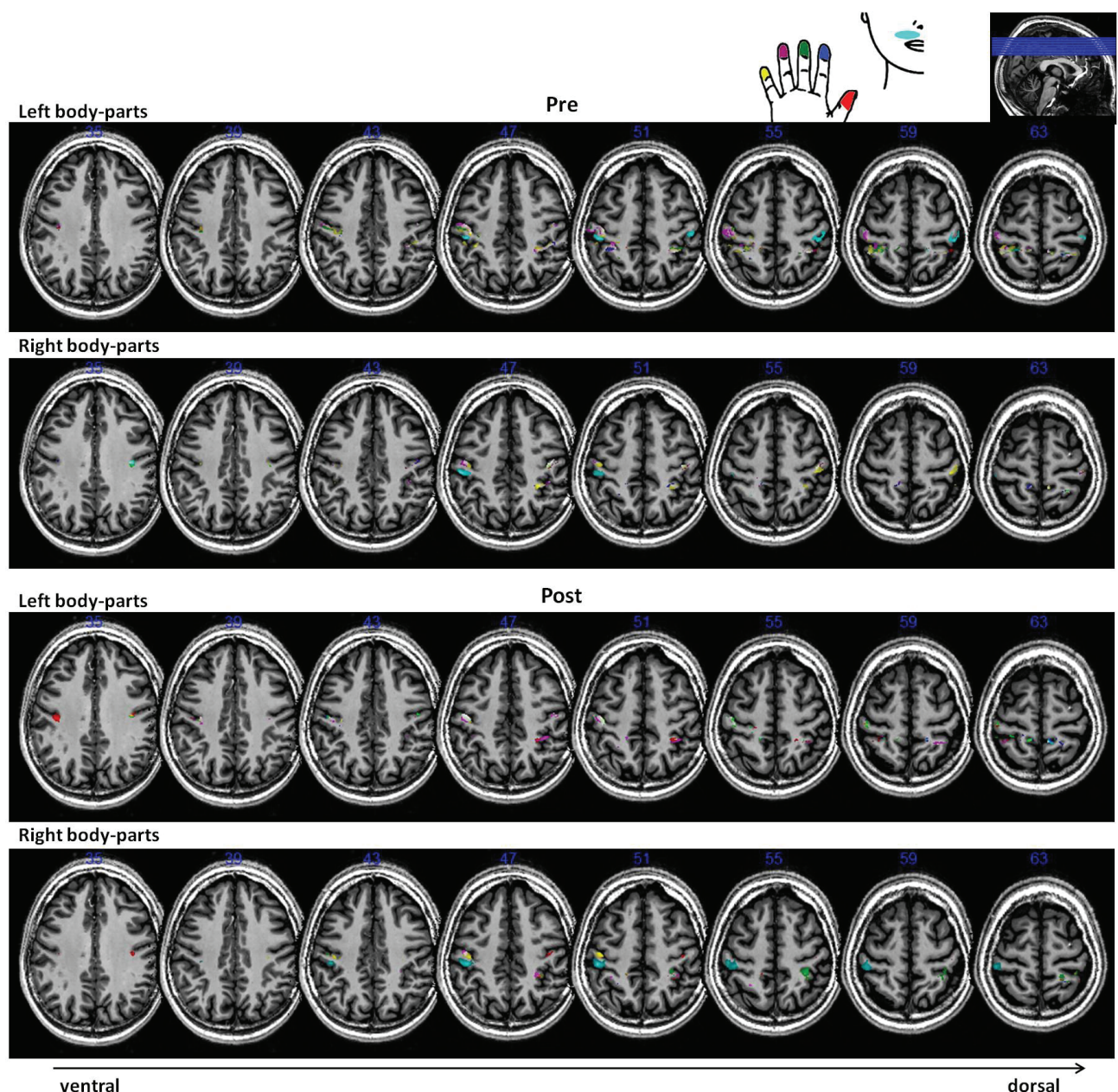


Figure S3. Group deactivations within SI obtained from random-effects analysis using one-sample t-tests (stimulation < rest, $p_{uncorr} < 0.001$) following stimulation of right and left body-sites respectively Pre (top) and Post (bottom) RSS. The same eight axial slices as for the activation maps are shown across sides and sessions, along the ventro-dorsal axis. Note that the lips deactivations are located much more dorsally than are their activations. Each body-site is color-coded (see upper schema: red: D1, blue: D2, green: D3, violet: D4, yellow: D5, cyan: Lip). Overlaps result in mixed colors (white when all the areas are superimposed).

References

- Akatsuka K, Noguchi Y, Harada T, Sadato N, Kakigi R (2008) Neural codes for somatosensory two-point discrimination in inferior parietal lobule: An fMRI study. *Neuroimage* 40:852–858.
- Arthurs O. J, Boniface S. J (2003) What aspect of the fMRI BOLD signal best reflects the underlying electrophysiology in human somatosensory cortex? *Clin Neurophysiol* 114:1203–1209.
- Arthurs OJ, Donovan T, Spiegelhalter DJ, Pickard JD, Boniface SJ (2007) Intracortically distributed neurovascular coupling relationships within and between human somatosensory cortices. *Cereb Cortex* 17:661–668.
- Bentley WJ, Li JM, Snyder AZ, Raichle ME, Snyder LH (2014) Oxygen level and LFP in task-positive and task-negative areas : bridging BOLD fMRI and electrophysiology. *Cereb Cortex*:1–12.
- Besle J, Sánchez-Panchuelo R-M, Bowtell R, Francis S, Schluppeck D (2013) Event-related fMRI at 7T reveals overlapping cortical representations for adjacent fingertips in S1 of individual subjects. *Hum Brain Mapp* 35:2027–2043.
- Beste C, Dinse HR (2013) Learning without training. *Curr Biol* 23:R489–R499.
- Blankenburg F, Taskin B, Ruben J, Moosmann M, Ritter P, Curio G, Villringer A (2003) Imperceptible stimuli and sensory processing impediment. *Science* (80-) 299:1864.
- Blatow M, Nennig E, Durst A, Sartor K, Stippich C (2007) fMRI reflects functional connectivity of human somatosensory cortex. *Neuroimage* 37:927–936.
- Bodegård A, Geyer S, Grefkes C, Zilles K, Roland PE (2001) Hierarchical processing of tactile shape in the human brain. *Neuron* 31:317–328.
- Boorman L, Kennerley AJ, Johnston D, Jones M, Zheng Y, Redgrave P, Berwick J (2010) Negative blood oxygen level dependence in the rat: a model for investigating the role of suppression in neurovascular coupling. *J Neurosci* 30:4285–4294.
- Bressler D, Spotswood N, Whitney D (2007) Negative BOLD fMRI response in the visual cortex carries precise stimulus-specific information. *PLoS One* 2.
- Brookes M, Woolrich M, Luckhoo H, Price D, Hale, Stephenson M, Barnes G, Smith S, Morris P (2011) Investigating the electrophysiological basis of resting state networks using magnetoencephalography. *PNAS* 108:16783–16788.
- Burton H, Fabri M (1995) Ipsilateral intracortical connections of physiologically defined cutaneous representations in areas 3b and 1 of macaque monkeys: projections in the vicinity of the central sulcus. *J Comp Neurol* 355:508–538.
- Clark SA, Allard T, Jenkins WM, Merzenich MM (1988) Receptive fields in the body-surface map in adult cortex defined by temporally correlated inputs. *Nature* 332:444–445.
- Coghill RC, Gilron I, Iadarola MJ (2001) Hemispheric lateralization of somatosensory processing. *J Neurophysiol* 85:2602–2612.
- Craig JC, Johnson KO (2000) The Two-Point Threshold : Not a Measure of Tactile Spatial Resolution. *Am Psychol Soc* 9:29–32.
- Davis KD, Kiss ZHT, Luo L, Tasker RR, Lozano AM, Dostrovsky JO (1998) Phantom sensations generated by thalamic microstimulation. *Nature* 391:385–387.

- De Celis Alonso B, Lowe AS, Dear JP, Lee KC, Williams SCR, Finnerty GT (2008) Sensory inputs from whisking movements modify cortical whisker maps visualized with functional magnetic resonance imaging. *Cereb Cortex* 18:1314–1325.
- Del Gratta C, Penna S Della, Tartaro A, Ferretti A, Torquati K, Bonomo L, Romani GL, Rossini PM (2000) Topographic organization of the human primary and secondary somatosensory areas. *Neuroreport* 11:2035–2043.
- Derdikman D, Hildesheim R, Ahissar E, Arieli A, Grinvald A (2003) Imaging spatiotemporal dynamics of surround inhibition in the barrels somatosensory cortex. *J Neurosci* 23:3100–3105.
- Devor A, Ulbert I, Dunn AK, Narayanan SN, Jones SR, Andermann ML, Boas D a, Dale AM (2005) Coupling of the cortical hemodynamic response to cortical and thalamic neuronal activity. *PNAS* 102:3822–3827.
- Dinse HR, Kleibel N, Kalisch T, Ragert P, Wilimzig C, Tegenthoff M (2006) Tactile coactivation resets age-related decline of human tactile discrimination. *Ann Neurol* 60:88–94.
- Dinse HR, Ragert P, Pleger B, Schwenkreis P, Tegenthoff M (2003) Pharmacological modulation of perceptual learning and associated cortical reorganization. *Science* 301:91–94.
- Disbrow E a, Hinkley LBN, Roberts TPL (2003) Ipsilateral representation of oral structures in human anterior parietal somatosensory cortex and integration of inputs across the midline. *J Comp Neurol* 467:487–495.
- Eickhoff SB, Grefkes C, Fink GR, Zilles K (2008) Functional lateralization of face, hand, and trunk representation in anatomically defined human somatosensory areas. *Cereb cortex* 18:2820–2830.
- Eickhoff SB, Heim S, Zilles K, Amunts K (2006) Testing anatomically specified hypotheses in functional imaging using cytoarchitectonic maps. *Neuroimage* 32:570–582.
- Eickhoff SB, Paus T, Caspers S, Grosbras M-H, Evans AC, Zilles K, Amunts K (2007) Assignment of functional activations to probabilistic cytoarchitectonic areas revisited. *Neuroimage* 36:511–521.
- Eickhoff SB, Stephan KE, Mohlberg H, Grefkes C, Fink GR, Amunts K, Zilles K (2005) A new SPM toolbox for combining probabilistic cytoarchitectonic maps and functional imaging data. *Neuroimage* 25:1325–1335.
- Elbert T, Pantev C, Wienbruch C, Rockstroh B, Taub E (1995) Increased cortical representation of the fingers of the left hand in string players. *Science* (80-) 270:305–307.
- Fabri M, Polonara G, Del Pesce M, Quattrini a, Salvolini U, Manzoni T (2001) Posterior corpus callosum and interhemispheric transfer of somatosensory information: an fMRI and neuropsychological study of a partially callosotomized patient. *J Cogn Neurosci* 13:1071–1079.
- Fabri M, Polonara G, Quattrini A, Salvolini U, Del Pesce M, Manzoni T (1999) Role of the corpus callosum in the somatosensory activation of the ipsilateral cerebral cortex: An fMRI study of callosotomized patients. *Eur J Neurosci* 11:3983–3994.
- Fang P, Jain N, Kaas JH (2002) Few intrinsic connections cross the hand-face border of area 3b of new world monkeys. *J Comp Neurol* 454:310–319.
- Flor H, Elbert T, Knecht S, Wienbruch C, Pantev C, Birbaumer N, Larbig W, Taub E (1995) Phantom-limb pain as a perceptual correlate of cortical reorganization following arm amputation. *Nature* 375:482–484.
- Forss N, Jousmäki V, Hari R (1995) Interaction between afferent input from fingers in human somatosensory cortex. *Brain Res* 685:68–76.

- Fox MD, Snyder AZ, Vincent JL, Corbetta M, Van Essen DC, Raichle ME (2005) The human brain is intrinsically organized into dynamic, anticorrelated functional networks. *PNAS* 102:9673–9678.
- Geyer S, Ledberg A, Schleicher A, Kinomura S, Schormann T, Bürgel U, Klingberg T, Larsson J, Zilles K, Roland PE (1996) Two different areas within the primary motor cortex of man. *Nature* 382:805–807.
- Geyer S, Schleicher A, Zilles K (1999) Areas 3a, 3b, and 1 of human primary somatosensory cortex. Microstructural organization and interindividual variability. *Neuroimage* 10:63–83.
- Geyer S, Schormann T, Mohlberg H, Zilles K (2000) Areas 3a, 3b, and 1 of human primary somatosensory cortex. Spatial normalization to standard anatomical space. *Neuroimage* 11:684–696.
- Gibson JR, Beierlein M, Connors BW (1999) Two networks of electrically coupled inhibitory neurons in neocortex. *Nature* 402:75–79.
- Godde B, Ehrhardt J, Braun C (2003) Behavioral significance of input-dependent plasticity of human somatosensory cortex. *Neuroreport* 14:543–546.
- Godde B, Stauffenberg B, Spengler F, Dinse HR (2000) Tactile coactivation-induced changes in spatial discrimination performance. *J Neurosci* 20:1597–1604.
- Goloshevsky AG, Silva AC, Dodd SJ, Koretsky AP (2008) BOLD fMRI and somatosensory evoked potentials are well correlated over a broad range of frequency content of somatosensory stimulation of the rat forepaw. *Brain Res* 1195:67–76.
- Grefkes C, Geyer S, Schormann T, Roland P, Zilles K (2001) Human somatosensory area 2: observer-independent cytoarchitectonic mapping, interindividual variability, and population map. *Neuroimage* 14:617–631.
- Greicius MD, Krasnow B, Reiss AL, Menon V (2003) Functional connectivity in the resting brain: a network analysis of the default mode hypothesis. *PNAS* 100:253–258.
- Hagen MC, Zald DH, Thornton T a, Pardo J V (2002) Somatosensory processing in the human inferior prefrontal cortex. *J Neurophysiol* 88:1400–1406.
- Hansson T, Brismar T (1999) Tactile stimulation of the hand causes bilateral cortical activation: a functional magnetic resonance study in humans. *Neurosci Lett* 271:29–32.
- Harel N, Lee S-P, Nagaoka T, Kim D-S, Kim S-G (2002) Origin of negative blood oxygenation level-dependent fMRI signals. *J Cereb blood flow Metab* 22:908–917.
- Harrar V, Spence C, Makin TR (2014) Topographic generalization of tactile perceptual learning. *J Exp Psychol Hum Percept Perform* 40:15–23.
- Harris JA, Harris IM, Diamond ME (2001) The topography of tactile learning in humans. *J Neurosci* 21:1056–1061.
- Hlushchuk Y, Hari R (2006) Transient suppression of ipsilateral primary somatosensory cortex during tactile finger stimulation. *J Neurosci* 26:5819–5824.
- Hodzic A, Veit R, Karim AA, Erb M, Godde B (2004) Improvement and decline in tactile discrimination behavior after cortical plasticity induced by passive tactile coactivation. *J Neurosci* 24:442–446.
- Hoshiyama M, Ryusuke K, Koyama S, Kitamura Y, Shimojo M, Watanabe S, Kakigi R (1996) Somatosensory evoked magnetic fields following stimulation of the lip in humans. *Electroencephalogr Clin Neurophysiol* 100:96–104.

- Hu K-S, Kwak J, Koh K-S, Abe S, Fontaine C, Kim H-J (2007) Topographic distribution area of the infraorbital nerve. *Surg Radiol Anat* 29:383–388.
- Huttunen JK, Gröhn O, Penttonen M (2008) Coupling between simultaneously recorded BOLD response and neuronal activity in the rat somatosensory cortex. *Neuroimage* 39:775–785.
- Iwamura Y (2000) Bilateral receptive field neurons and callosal connections in the somatosensory cortex. *Philos Trans R Soc Lond B Biol Sci* 355:267–273.
- Iwamura Y, Iriki A, Tanaka M (1994) Bilateral hand representation in the postcentral somatosensory cortex. *Nature* 369:554–556.
- Iwamura Y, Taoka M, Iriki A (2001) Bilateral activity and callosal connections in the somatosensory cortex. *Neurosci* 7:419–429.
- Johnson KO, Phillips JR (1981) Tactile spatial resolution. I. Two-point discrimination, gap detection, grating resolution, and letter recognition. *J Neurophysiol* 46:1177–1192.
- Kaas AL, van Mier H, Visser M, Goebel R (2013) The neural substrate for working memory of tactile surface texture. *Hum Brain Mapp* 34:1148–1162.
- Kalisch T, Tegenthoff M, Dinse HR (2007) Differential effects of synchronous and asynchronous multifinger coactivation on human tactile performance. *BMC Neurosci* 8:58.
- Kalisch T, Tegenthoff M, Dinse HR (2008) Improvement of sensorimotor functions in old age by passive sensory stimulation. *Clin Interv Aging* 3:673–690.
- Kalisch T, Tegenthoff M, Dinse HR (2010) Repetitive electric stimulation elicits enduring improvement of sensorimotor performance in seniors. *Neural Plast* 2010:690531.
- Kang R, Herman D, MacGillis M, Zarzecki P (1985) Convergence of sensory inputs in somatosensory cortex: interactions from separate afferent sources. *Exp brain Res* 57:271–278.
- Kannurpatti SS, Biswal BB (2004) Negative functional response to sensory stimulation and its origins. *J Cereb blood flow Metab* 24:703–712.
- Kastrup A, Baudewig J, Schnaudigel S, Huonker R, Becker L, Sohns JM, Dechent P, Klingner C, Witte OW (2008) Behavioral correlates of negative BOLD signal changes in the primary somatosensory cortex. *Neuroimage* 41:1364–1371.
- Kennerley AJ, Mayhew JE, Boorman L, Zheng Y, Berwick J (2012) Is optical imaging spectroscopy a viable measurement technique for the investigation of the negative BOLD phenomenon? A concurrent optical imaging spectroscopy and fMRI study at high field (7 T). *Neuroimage* 61:10–20.
- Killackey HP, Gould HJ, Cusick CG, Pons TP, Kaas JH (1983) The relation of corpus callosum connections to architectonic fields and body surface maps in sensorimotor cortex of new and old world monkeys. *J Comp Neurol* 219:384–419.
- Kim S-G, Ogawa S (2012) Biophysical and physiological origins of blood oxygenation level-dependent fMRI signals. *J Cereb Blood Flow Metab* 32:1188–1206.
- Klingner CM, Hasler C, Brodoehl S, Witte OW (2010) Dependence of the negative BOLD response on somatosensory stimulus intensity. *Neuroimage* 53:189–195.
- Klingner CM, Hasler C, Brodoehl S, Witte OW (2014) Excitatory and inhibitory mechanisms underlying somatosensory habituation. *Hum Brain Mapp* 35:152–160.

- Klingner CM, Huonker R, Flemming S, Hasler C, Brodoehl S, Preul C, Burmeister H, Kastrup A, Witte OW (2011) Functional deactivations: multiple ipsilateral brain areas engaged in the processing of somatosensory information. *Hum Brain Mapp* 32:127–140.
- Kopietz R, Sakar V, Albrecht J, Kleemann AM, Schöpf V, Yousry I, Linn J, Fesl G, Wiesmann M (2009) Activation of primary and secondary somatosensory regions following tactile stimulation of the face. *Clin Neuroradiol* 19:135–144.
- Kowalewski R, Kattenstroth J, Kalisch T, Dinse HR (2012) Improved acuity and dexterity but unchanged touch and pain thresholds following repetitive sensory stimulation of the fingers. *Neural Plast* 2012.
- Krause T, Kurth R, Ruben J, Schwiemann J, Villringer K, Deuchert M, Moosmann M, Brandt S, Wolf K-J, Curio G, Villringer A (2001) Representational overlap of adjacent fingers in multiple areas of human primary somatosensory cortex depends on electrical stimulus intensity: an fMRI study. *Brain Res* 899:36–46.
- Kurth R, Villringer K, Curio G, Wolf K-J, Krause T, Repenthin J, Schwiemann J, Deuchert M, Villringer A (2000) fMRI shows multiple somatotopic digit representations in human primary somatosensory cortex. *Neuroreport* 11:1487–1491.
- Lin C-CK, Sun Y, Huang C-I, Yu C-Y, Ju M-S (2010) Cortical activation by tactile stimulation to face and anterior neck areas: an fMRI study with three analytic methods. *Hum Brain Mapp* 31:1876–1885.
- Lin CS, Merzenich MM, Sur M, Kaas JH (1979) Connections of areas 3b and 1 of the parietal somatosensory strip with the ventroposterior nucleus in the owl monkey (*Aotus trivirgatus*). *J Comp Neurol* 185:355–372.
- Lipton ML, Fu K-MG, Branch C a, Schroeder CE (2006) Ipsilateral hand input to area 3b revealed by converging hemodynamic and electrophysiological analyses in macaque monkeys. *J Neurosci* 26:180–185.
- Logothetis NK, Pauls J, Augath M, Trinath T, Oeltermann A (2001) Neurophysiological investigation of the basis of the fMRI signal. *Nature* 412:150–157.
- Macaluso E, Maravita A (2010) The representation of space near the body through touch and vision. *Neuropsychologia* 48:782–795.
- Makin TR, Scholz J, Filippini N, Henderson Slater D, Tracey I, Johansen-Berg H (2013) Phantom pain is associated with preserved structure and function in the former hand area. *Nat Commun* 4:1–8.
- Maldjian JA, Gottschalk A, Patel RS, Detre JA, Alsop DC (1999) The sensory somatotopic map of the human hand demonstrated at 4 Tesla. *Neuroimage* 10:55–62.
- Malinen S, Renvall V, Hari R (2014) Functional parcellation of the human primary somatosensory cortex to natural touch. *Eur J Neurosci* 39:738–743.
- Manger PR, Woods TM, Jones EG (1996) Representation of face and intra-oral structures in area 3b of macaque monkey somatosensory cortex. *J Comp Neurol* 371:513–521.
- Manzoni T, Barbaresi P, Conti F (1984) Callosal mechanism for the interhemispheric transfer of hand somatosensory information in the monkey. *Behav Brain Res* 11:155–170.
- Martuzzi R, van der Zwaag W, Farthouat J, Gruetter R, Blanke O (2014) Human finger somatotopy in areas 3b, 1, and 2: A 7T fMRI study using a natural stimulus. *Hum Brain Mapp* 35:213–226.
- Mauguière F, Merlet I, Forss N, Vanni S, Jousmäki V, Adeleine P, Hari R (1997) Activation of a distributed somatosensory cortical network in the human brain. A dipole modelling study of

- magnetic fields evoked by median nerve stimulation. Part I: Location and activation timing of SEF sources. *Electroencephalogr Clin Neurophysiol* 104:281–289.
- Miyamoto JJ, Honda M, Saito DN, Okada T, Ono T, Ohyama K, Sadato N (2006) The representation of the human oral area in the somatosensory cortex: a functional MRI study. *Cereb cortex* 16:669–675.
- Mullinger KJ, Mayhew SD, Bagshaw a P, Bowtell R, Francis ST (2014) Evidence that the negative BOLD response is neuronal in origin: a simultaneous EEG-BOLD-CBF study in humans. *Neuroimage* 94:263–274.
- Muret D, Dinse HR, Macchione S, Urquizar C, Farnè A, Reilly KT (2014) Touch improvement at the hand transfers to the face. *Curr Biol* 24:R736–R737.
- Nagamatsu K, Nakasato N, Hatanaka K, Kanno A, Iwasaki M, Yoshimoto T, Nakasato CAN (2000) Neuromagnetic localization of N15, the initial cortical response to lip stimulus. *Neuroreport* 12:1–5.
- Nakamura A, Yamada T, Goto A, Kato T, Ito K, Abe Y, Kachi T, Kakigi R (1998) Somatosensory homunculus as drawn by MEG. *Neuroimage* 7:377–386.
- Nakashita S, Saito DN, Kochiyama T, Honda M, Tanabe HC, Sadato N (2008) Tactile-visual integration in the posterior parietal cortex: a functional magnetic resonance imaging study. *Brain Res Bull* 75:513–525.
- Nash PG, MacEfield VG, Klineberg IJ, Gustin SM, Murray GM, Henderson L a. (2010) Bilateral activation of the trigeminothalamic tract by acute orofacial cutaneous and muscle pain in humans. *Pain* 151:384–393.
- Négyessy L, Pálfi E, Ashaber M, Palmer C, Jákl B, Friedman RM, Chen LM, Roe AW (2013) Intrinsic horizontal connections process global tactile features in the primary somatosensory cortex: neuroanatomical evidence. *J Comp Neurol* 521:2798–2817.
- Nelson RJ, Kaas JH (1981) Connections of the ventroposterior nucleus of the thalamus with the body surface representations in cortical areas 3b and 1 of the cynomolgus macaque , (Maca ca fascicularis). *J Comp Neurol* 199:29–64.
- Nevalainen P, Ramstad R, Isotalo E, Haapanen M-L, Lauronen L (2006) Trigeminal somatosensory evoked magnetic fields to tactile stimulation. *Clin Neurophysiol* 117:2007–2015.
- Nicolelis M a. ., Ghazanfar A a, Faggin BM, Votaw S, Oliveira LM. (1997) Reconstructing the engram: simultaneous, multisite, many single neuron recordings. *Neuron* 18:529–537.
- Nihashi T, Naganawa S, Sato C, Kawai H, Nakamura T, Fukatsu H, Ishigaki T, Aoki I (2005) Contralateral and ipsilateral responses in primary somatosensory cortex following electrical median nerve stimulation--an fMRI study. *Clin Neurophysiol* 116:842–848.
- Oldfield RC (1971) The assessment and analysis of handedness: the Edinburgh inventory. *Neuropsychologia* 9:97–113.
- Parianen Lesemann FH, Reuter E-M, Godde B (2015) Tactile stimulation interventions: Influence of stimulation parameters on sensorimotor behavior and neurophysiological correlates in healthy and clinical samples. *Neurosci Biobehav Rev* 51:126–137.
- Pascual-Leone A, Torres F (1993) Plasticity of the sensorimotor cortex representation of the reading finger in Braille readers. *Brain* 116:39–52.
- Passow S, Specht K, Adamsen TC, Biermann M, Brekke N, Craven AR, Ersland L, Grüner R, Kleven-Madsen N, Kvernenes O-H, Schwarzl Müller T, Olesen RA, Hugdahl K (2015) Default-mode network functional connectivity is closely related to metabolic activity. *Hum Brain Mapp*.

- Penfield W, Rasmussen T (1950) The cerebral cortex of man: a clinical study of localization of function. New York Macmillan Compagny.
- Pleger B, Dinse HR, Ragert P, Schwenkreis P, Malin JP, Tegenthoff M (2001) Shifts in cortical representations predict human discrimination improvement. *Proc Natl Acad Sci USA* 98:12255–12260.
- Pleger B, Foerster A-F, Ragert P, Dinse HR, Schwenkreis P, Malin J-P, Nicolas V, Tegenthoff M (2003) Functional imaging of perceptual learning in human primary and secondary somatosensory cortex. *Neuron* 40:643–653.
- Pons TP, Garraghty PE, Ommaya AK, Kaas JH, Taub E, Mishkin M (1991) Massive cortical reorganization after sensory deafferentation in adult macaques. *Science* 252:1857–1860.
- Powell TPS, Mountcastle VB (1959) Some aspects of the functional organization of the cortex of the postcentral gyrus of the monkey: a correlation of findings obtained in a single unit analysis with cytoarchitecture. *Bull Johns Hopkins Hosp* 105:133–162.
- Raichle ME, MacLeod a M, Snyder a Z, Powers WJ, Gusnard D a, Shulman GL (2001) A default mode of brain function. *PNAS* 98:676–682.
- Ramirez A, Pnevmatikakis E a, Merel J, Paninski L, Miller KD, Bruno RM (2014) Spatiotemporal receptive fields of barrel cortex revealed by reverse correlation of synaptic input. *Nat Neurosci* 17:866–875.
- Recanzone GH, Jenkins WM, Hradek GT, Merzenich MM (1992a) Progressive improvement in discriminative abilities in adult owl monkeys performing a tactile frequency discrimination task. *J Neurophysiol* 67:1015–1030.
- Recanzone GH, Merzenich MM, Jenkins WM (1992b) Frequency discrimination training engaging a restricted skin surface results in an emergence of a cutaneous response zone in cortical area 3a. *J Neurophysiol* 67:1057–1070.
- Recanzone GH, Merzenich MM, Jenkins WM, Grajski K a, Dinse HR (1992c) Topographic reorganization of the hand representation in cortical area 3b owl monkeys trained in a frequency-discrimination task. *J Neurophysiol* 67:1031–1056.
- Roland PE, O’Sullivan B, Kawashima R (1998) Shape and roughness activate different somatosensory areas in the human brain. *PNAS* 95:3295–3300.
- Rosa MJ, Kilner J, Blankenburg F, Josephs O, Penny W (2010) Estimating the transfer function from neuronal activity to BOLD using simultaneous EEG-fMRI. *Neuroimage* 49:1496–1509.
- Sadato N, Ibañez V, Deiber MP, Hallett M (2000) Gender difference in premotor activity during active tactile discrimination. *Neuroimage* 11:532–540.
- Sánchez-Panchuelo R-M, Besle J, Beckett A, Bowtell R, Schluppeck D, Francis S, Sanchez-panchuelo RM (2012) Within-digit functional parcellation of Brodmann areas of the human primary somatosensory cortex using functional magnetic resonance imaging at 7 tesla. *J Neurosci* 32:15815–15822.
- Sathian K, Zangaladze A (1997) Tactile learning is task specific but transfers between fingers. *Percept Psychophys* 59:119–128.
- Sathian K, Zangaladze A (1998) Perceptual learning in tactile hyperacuity: complete intermanual transfer but limited retention. *Exp Brain Res* 118:131–134.

- Sathian K, Zangaladze C a a, Hoffman JM, Grafton ST (1997) Feeling with the mind ' s eye. *Neuroreport* 8:3877–3881.
- Schäfer K, Blankenburg F, Kupers R, Grüner JM, Law I, Lauritzen M, Larsson HBW (2012) Negative BOLD signal changes in ipsilateral primary somatosensory cortex are associated with perfusion decreases and behavioral evidence for functional inhibition. *Neuroimage* 59:3119–3127.
- Schnitzler A, Salmelin R, Salenius S, Jousm V, Hari R (1995) Tactile information from the human hand reaches the ipsilateral primary somatosensory cortex. *Neurosci Lett* 200:25–28.
- Shibasaki H (2008) Human brain mapping: Hemodynamic response and electrophysiology. *Clin Neurophysiol* 119:731–743.
- Shmuel A, Augath M, Oeltermann A, Logothetis NK (2006) Negative functional MRI response correlates with decreases in neuronal activity in monkey visual area V1. *Nat Neurosci* 9:569–577.
- Shmuel A, Yacoub E, Pfeuffer J, Van de Moortele PF, Adriany G, Hu X, Ugurbil K (2002) Sustained negative BOLD, blood flow and oxygen consumption response and its coupling to the positive response in the human brain. *Neuron* 36:1195–1210.
- Shoham D, Grinvald A (2001) The cortical representation of the hand in macaque and human area S-I: high resolution optical imaging. *J Neurosci* 21:6820–6835.
- Simões C, Mertens M, Forss N, Jousmäki V, Lange J, Lütkenhöner B, Hari R (2001) Functional overlap of finger representations in human SI and SII cortices. *J Neurophysiol* 86:1661–1665.
- Sloan HL, Austin VC, Blamire a. M, Schnupp JWH, Lowe a. S, Allers K a., Matthews PM, Sibson NR (2010) Regional differences in neurovascular coupling in rat brain as determined by fMRI and electrophysiology. *Neuroimage* 53:399–411.
- Smits E, Gordon DC, Witte S, Rasmusson DD, Zarzecki P (1991) Synaptic potentials evoked by convergent somatosensory and corticocortical inputs in raccoon somatosensory cortex : substrates for plasticity. *J Neurophysiol* 66:688–695.
- Stavrinou ML, Penna S Della, Pizzella V, Torquati K, Cianflone F, Franciotti R, Bezerianos A, Romani GL, Rossini PM (2007) Temporal dynamics of plastic changes in human primary somatosensory cortex after finger webbing. *Cereb Cortex* 17:2134–2142.
- Sterr A, Müller MM, Elbert T, Rockstroh B, Pantev C, Taub E (1998) Perceptual correlates of changes in cortical representation of fingers in blind multifinger Braille readers. *J Neurosci* 18:4417–4423.
- Stilla R, Deshpande G, LaConte S, Hu X, Sathian K (2007) Posteromedial parietal cortical activity and inputs predict tactile spatial acuity. *J Neurosci* 27:11091–11102.
- Stippich C, Hofmann R, Kapfer D, Hempel E, Heiland S, Jansen O, Sartor K (1999) Somatotopic mapping of the human primary somatosensory cortex by fully automated tactile stimulation using functional magnetic resonance imaging. *Neurosci Lett* 277:25–28.
- Stoeckel MC, Pollok B, Schnitzler A, Witte OW, Seitz RJ (2004) Use-dependent cortical plasticity in thalidomide-induced upper extremity dysplasia: Evidence from somaesthesia and neuroimaging. *Exp Brain Res* 156:333–341.
- Stoesz MR, Zhang M, Weisser VD, Prather SC, Mao H, Sathian K (2003) Neural networks active during tactile form perception: common and differential activity during macrospatial and microspatial tasks. *Int J Psychophysiol* 50:41–49.
- Stringer EA, Chen LM, Friedman RM, Gatenby C, Gore JC (2011) Differentiation of somatosensory cortices by high-resolution fMRI at 7 T. *Neuroimage* 54:1012–1020.

- Sutherland MT, Tang AC (2006) Reliable detection of bilateral activation in human primary somatosensory cortex by unilateral median nerve stimulation. *Neuroimage* 33:1042–1054.
- Sutherling WW, Levesque MF, Baumgartner C (1992) Cortical sensory representation of the human hand: size of finger regions and nonoverlapping digit somatotopy. *Neurology* 42:1020–1028.
- Suzuki T, Shibukawa Y, Kumai T, Shintani M (2004) Face area representation of primary somatosensory cortex in humans identified by whole-head magnetoencephalography. *Jpn J Physiol* 54:161–169.
- Swadlow H a (2003) Fast-spike interneurons and feedforward inhibition in awake sensory neocortex. *Cereb Cortex* 13:25–32.
- Tanji J, Wise SP (1981) Submodality distribution in sensorimotor cortex of the unanesthetized monkey. *J Neurophysiol* 45:467–481.
- Taoka M, Toda T, Iriki a., Tanaka M, Iwamura Y (2000) Bilateral receptive field neurons in the hindlimb region of the postcentral somatosensory cortex in awake macaque monkeys. *Exp Brain Res* 134:139–146.
- Taylor KS, Davis KD (2009) Stability of tactile- and pain-related fMRI brain activations: An examination of threshold-dependent and threshold-independent methods. *Hum Brain Mapp* 30:1947–1962.
- Terumitsu M, Ikeda K, Kwee IL, Nakada T (2009) Participation of primary motor cortex area 4a in complex sensory processing: 3.0-T fMRI study. *Neuroreport* 20:679–683.
- Tremere L, Hicks TP, Rasmusson DD (2001) Role of inhibition in cortical reorganization of the adult raccoon revealed by microiontophoretic blockade of GABA A receptors. *J Neurophysiol* 86:94–103.
- Van der Zwaag W, Kusters R, Magill A, Gruetter R, Martuzzi R, Blanke O, Marques JP (2013) Digit somatotopy in the human cerebellum: a 7T fMRI study. *Neuroimage* 67:354–362.
- Vanzetta I, Grinvald A (2008) Coupling between neuronal activity and microcirculation: implications for functional brain imaging. *HFSP J* 2:79–98.
- Vogt B a, Pandya DN (1978) Cortico-cortical connections of somatic sensory cortex (areas 3, 1 and 2) in the rhesus monkey. *J Comp Neurol* 177:179–191.
- Wade AR, Rowland J (2010) Early suppressive mechanisms and the negative blood oxygenation level-dependent response in human visual cortex. *J Neurosci* 30:5008–5019.
- Wang X, Merzenich MM, Sameshima K, Jenkins WM (1995) Remodelling of hand representation in adult cortex determined by timing of tactile stimulation. *Nature* 378:71–75.
- Weiss T, Miltner WHR, Liepert J, Meissner W, Taub E (2004) Rapid functional plasticity in the primary somatomotor cortex and perceptual changes after nerve block. *Eur J Neurosci* 20:3413–3423.
- Whitsel BL, Rustioni A, Dreyer D a, Loe PR, Allen EE, Metz CB (1978) Thalamic projections to SI in macaque monkey. *J Comp Neurol* 178:385–410.
- Xerri C, Merzenich MM, Peterson BE, Jenkins W (1998) Plasticity of primary somatosensory cortex paralleling sensorimotor skill recovery from stroke in adult monkeys. *J Neurophysiol* 79:2119–2148.
- Zamorano AM, Riquelme I, Kleber B, Altenmüller E, Hatem SM, Montoya P (2015) Pain sensitivity and tactile spatial acuity are altered in healthy musicians as in chronic pain patients. *Front Hum Neurosci* 8:1–9.

- Zarei M, Stephenson JD (1996) Ipsilateral and bilateral receptive fields in rat primary somatosensory cortex. *Neuroreport* 7:647–651.
- Zarzecki P, Blum PS, Bakker DA, Herman D (1983) Convergence of sensoru inputs upon projection neurons of somatosensory cortex: vestibular, neck, head, and forelimb inputs. *Exp brain Res* 50:408–414.
- Zarzecki P, Wiggan DM (1982) Convergence of sensory inputs upon projection neurons of somatosensory cortex. *Exp brain Res* 48:28–42.
- Zeharia N, Hertz U, Flash T, Amedi A (2012) Negative blood oxygenation level dependent homunculus and somatotopic information in primary motor cortex and supplementary motor area. *PNAS* 109:18565–18570.
- Zhang M, Mariola E, Stilla R, Stoesz M, Mao H, Hu X, Sathian K (2005) Tactile discrimination of grating orientation: fMRI activation patterns. *Hum Brain Mapp* 25:370–377.

STUDY 3: MEG STUDY

MEG is another functional neuroimaging technique whose use has been considerably rising since the late 1990s. The increasing interest for this technique arises from several features of MEG. First, unlike fMRI, MEG provides a direct measure of brain activity as it measures the magnetic fields generated by the currents arising from neuronal activity. In addition, MEG also has a higher temporal resolution, events with time scales on the order of milliseconds being resolved. Even if slightly below than that of fMRI, the spatial resolution of MEG is still excellent, sources can be localized with millimetre precision. This makes MEG highly complementary to fMRI, which has a higher spatial resolution but a pretty low temporal resolution.

Despite the fact that MEG was described earlier than fMRI, the first measure having been done by the physicist David Cohen in 1968 (Cohen, 1968), MEG has long been less popular than fMRI, likely due to the higher complexity of the signals and of the algorithms required to analyze it. David Cohen later used the first superconducting sensor (or SQUID, superconducting quantum interference devices) to improve MEG signal measurement (Cohen, 1972). This was cumbersome, and, in the 80s, MEG manufacturers began to arrange multiple sensors into arrays to cover a larger area of the head. Present-day MEG arrays are set in helmet-shaped dewar that typically contain 300 sensors, covering most of the head. In this way, MEGs of a subject or patient can now be accumulated rapidly and efficiently.

Magnetic fields are generated by current flows, which in the brain originate primarily from intracellular currents flowing from the dendrites to the soma. Since current dipoles must have similar orientations to generate magnetic fields that reinforce each other, it is often the layer of pyramidal cells, which are situated perpendicular to the cortical surface, which gives rise to measurable magnetic fields. To generate a signal that is detectable, approximately 50,000 active neurons are needed (Okada, 1983). Despite the fact that magnetic fields pass unaffected through brain tissue and the skull, making it possible to be recorded outside of the head, these fields are extremely small. To account for this, MEG signals are typically recorded by superconducting sensors within a shielded room to eliminate the magnetic interference found in a typical urban environment. Given that magnetic fields are orthogonally oriented relatively to the current flow (Maxwell's equations), only the activity of neurons that are orientated tangentially to the scalp surface project measurable portions of their magnetic fields outside of the head, thus measurable with MEG sensors (see Figure 47). This limitation of MEG makes it sensitive mainly to neurons

(as said above, primarily pyramidal cells) typically located in the sulci, which in most of the case is not problematic when investigating primary sensory cortices.

In many instances, the net currents from which magnetic fields originates can be thought as current dipoles having a given position, orientation and magnitude (also called dipole strength), but no spatial extent. Using complex algorithms, these dipoles can be reconstructed using equivalent current dipole (ECD) models. A high goodness of fit of the field produced by the modelled ECD to the real measurement provides a reasonable justification for the application of the model. The accuracy of the localization of ECD is usually in the range of few millimetres.

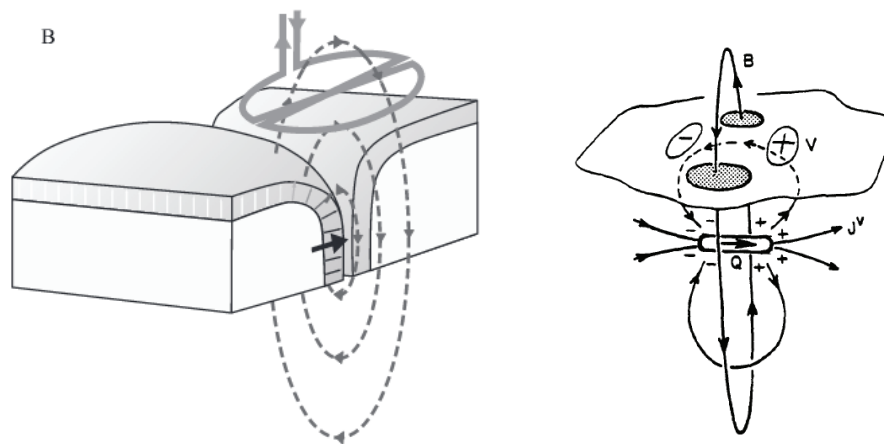


Figure 47. **Left** [from Korvenoja, 2007]: Illustration of an MEG sensor (planar gradiometer) above the cortex measuring the gradient of magnetic fields (dotted lines with arrows indicating their flow) generated by the current source (black arrow) oriented tangentially to the scalp. **Right** [from Williamson and Kaufman, 1990]: Representation of a current dipole \mathbf{Q} associated with intracellular current and the magnetic field \mathbf{B} that it produces. The extracellular charge density is represented by + and - signs, and \mathbf{J}^v indicates the accompanying extracellular current density.

Neuromagnetic correlates of an adaptive plasticity across the hand-face border in human somatosensory cortices

Dollyane Muret^{1,2*}, Sébastien Daligault³, Hubert R. Dinse^{4,5}, Claude Delpuech³, Jérémie Mattout⁶, Karen T. Reilly^{1,2}, Alessandro Farnè^{1,2}.

¹ INSERM U1028, CNRS UMR5292, Lyon Neuroscience Research Centre, Integrative, Multisensory, Perception, Action and Cognition (ImpAct) Team, Lyon, France;

² University Claude Bernard Lyon I, Lyon, France;

³ CERMEP, MEG Department, Bron, France;

⁴ Neural Plasticity Laboratory, Institute for Neuroinformatics, Ruhr-University;

⁵ Clinic of Neurology, BG University Hospital Bergmannsheil, Bochum, Germany;

⁶ INSERM U1028, CNRS UMR5292, Lyon Neuroscience Research Centre, Brain Dynamics and Cognition (Dycog) Team, Lyon, France.

* E-mail: dollyane.muret@inserm.fr

Abstract

It is well established that permanent or transient reduction of somatosensory inputs (following deafferentation or anaesthesia) induces plastic changes across the hand-face border. Whether such cross-border changes can be induced by increasing rather than decreasing afferent inputs remains poorly understood. We recently found that a repetitive somatosensory stimulation (RSS) at a fingertip, which is known to induce a local training-independent learning paralleled by local plastic changes within the primary somatosensory cortex (see Beste & Dinse, 2013), induces plastic changes and a similar perceptual learning across the hand-face border, altering the face representation (Muret et al., in preparation) and perception (Muret et al., 2014). Here we used magnetoencephalography to provide a complementary view over the mechanisms underlying RSS-induced cortical reorganization across the hand-face border, by investigating its electrophysiological correlates. We report significant changes in dipole location after RSS, both for the stimulated finger and for the lips. These results confirm the presence of plastic changes crossing the hand-face border following an increase of inputs.

Introduction

Most of our knowledge about large-scale somatosensory plasticity comes from cases of permanent or transient reduction of inputs. In particular, massive cortical reorganization has been repeatedly observed across the face-hand border, with the representation of the face expanding and shifting towards that of the deprived hand (Pons et al., 1991; Jain et al., 1997; Weiss et al., 2004; Tandon et al., 2009; Dutta et al., 2013). Whether such cross-border changes can be induced by increasing rather than decreasing afferent inputs remains poorly understood despite its potential impact in promoting adaptive plasticity remotely. We recently found that repetitive somatosensory stimulation (RSS) of a single fingertip, which has long been known to induce both a local plasticity within the primary somatosensory cortex (SI) and a local improvement in tactile acuity (for reviews see Beste and Dinse, 2013; Parianen Lesemann et al., 2015), also alters remotely the face representation (Muret et al., in preparation) and improves its tactile acuity (Muret et al., 2014). These observations suggest a transfer of plastic changes across the hand-face border. Indeed, following RSS of the right index finger (right-D2) we observed reorganization of the face representation within BA3b, which took the form of an increase of the negative BOLD response (NBR) evoked by lip stimulation (Muret et al., in preparation). Strikingly, this NBR was co-localized with the more “traditional” positive BOLD response evoked by index finger stimulation in the contralateral hemisphere. Given that the neurovascular coupling underlying such BOLD signal changes is still under investigation and debated (Hoffmeyer et al., 2007; Huttunen et al., 2008; Moore and Cao, 2008; Rosa et al., 2010; Devonshire et al., 2012), and that magnetoencephalography (MEG) allows for a direct measure of neuronal activity with a sufficiently high spatial resolution to distinguish between lip and finger somatosensory sources (Nakamura et al., 1998), we used MEG to further investigate the neurophysiological substrates of these plastic changes, in order to provide a complementary perspective over the mechanisms underlying RSS-induced cortical changes. The benefits of comparing electrophysiological and functional magnetic resonance imaging signals have already been proven (Thees et al., 2003; Tuunanen et al., 2003; Stoeckel et al., 2007).

Given that the local plasticity induced in the finger representation was previously found to be expressed by a shift of the right-D2 equivalent current dipole (ECD) toward that of the thumb (Pleger et al., 2001; Godde et al., 2003), we investigated whether RSS-induced cortical changes across the hand-face border were accompanied by changes in the configuration of neuromagnetic dipole sources.

Experimental Procedures

Participants. Twenty-five healthy volunteers (mean age = $22.24 \pm \text{SD } 2.71$ years, 13 females) were tested and four participants were removed from the analyses due to poor signal to noise ratio and to artefacts. All participants were right-handed according to the Edinburgh Handedness Inventory (Oldfield, 1971; mean score = $82.93 \pm \text{SD } 18.37\%$), and they all gave written informed consent before participating. The protocol was approved by the ethics committee of Lyon, and was performed in accordance with the Declaration of Helsinki.

Experimental time course. Figure 1 shows the time-course of the experiment which took place over two consecutive days. On the first day, participants underwent a practice session to familiarize themselves with the tactile task, followed by a first assessment of their tactile spatial acuity. The next day, another measure of tactile acuity was acquired before a first session of MEG recordings, immediately followed by 3 hours of repetitive somatosensory stimulation (RSS) of the right index finger. Immediately after the RSS a second set of MEG recordings and tactile acuity assessments were performed, the order between these two last sessions being counterbalanced across participants (see Figure 1). The structural MRI of each participant was acquired in the days following the experiment, usually the next day.

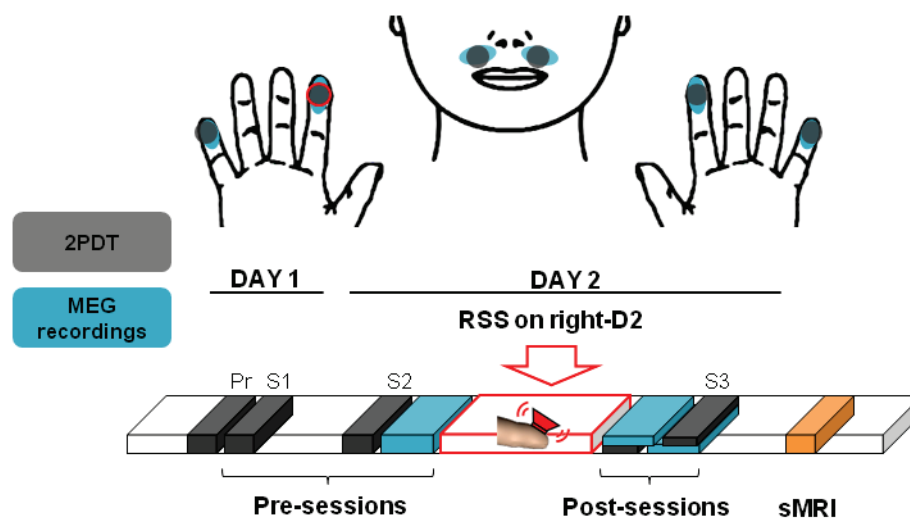


Figure 1. Experimental time course. Two-point discrimination thresholds (2PDT) were assessed at right/left-D2, right/left-D5 and right/left-Lip in a practice session and three experimental sessions (S1-S3) distributed over two consecutive days. On the second day the RSS device was attached to the right-D2 for three hours between S2 and S3. Additionally, mapping of the cortical representations of the four tested fingers and both sides of the upper-lips was performed during two MEG sessions acquired just before and after the RSS procedure. After RSS, the order between the MEG and tactile acuity sessions was counterbalanced across participants.

Repetitive Somatosensory Stimulation (RSS) Protocol. We used an RSS protocol that is known to induce plastic changes in the somatosensory cortex (Godde et al., 2000, 2003; Pleger et al., 2001, 2003; Dinse et al., 2003; Hodzic et al., 2004; Pilz et al., 2004; Kalisch et al., 2007; Gibson et al., 2009). This method is effective, relatively simple to implement, and relies on Hebbian-like plasticity processes as it simultaneously co-activates several cutaneous receptive fields, thus producing temporally correlated inputs necessary to drive plasticity (Clark et al., 1988; Wang et al., 1995). A small 8 mm diameter solenoid controlled by an MP3 player was taped to the volar surface of the right-D2 fingertip for three hours. This solenoid delivered brief (10ms) supra-threshold tactile stimuli with inter-stimulus intervals ranging from 100 to 3000 ms and following a Poisson distribution (average stimulation frequency of 1Hz). Participants could freely move during the stimulation period and were instructed to continue with their daily activities without paying attention to the device, but to avoid intensive use of their fingers (i.e., they were not allowed to either write or type on a keyboard).

Tactile spatial acuity assessment. To assess tactile spatial acuity, two-point discrimination thresholds (2PDT) were measured using a two-alternative forced-choice task and force-controlled devices, at both index fingertips (left-D2 & right-D2), both little fingertips (left-D5 & right-D5), and both sides of the upper-lip region, three times before (Practice, S1 and S2) and once after (S3) 3 hours of RSS applied to the right-D2. During the Practice session (Day1), detailed instructions were given and informed consent was obtained before 2PDT assessment. This session allowed participants to become familiar with the task, but the data were not included in any analyses. This Practice session and sessions S1 and S2 ensured that discrimination performance before RSS was stable and allowed us to separate RSS-induced changes from potential changes related to familiarization with the task. Based upon previous studies reporting no threshold change at left-D2 following RSS on right-D2 (Godde et al., 2000, 2003; Pleger et al., 2001, 2003; Dinse et al., 2003, 2006), and on other studies showing that learning due to practice/familiarization transfers to the homologous finger (Harris et al., 2001; Harrar et al., 2014), 2PDT at left-D2 were assessed in S2 and S3 only. Within a session, each area was tested in a separate block, and for a given participant the order of blocks was maintained across sessions while block order was randomized across participants. For each participant the location of each tested area was kept constant across sessions [distance from fingertip: 5.17 ± 1.74 mm and distance from finger edge: 5.19 ± 1.13 mm (mean \pm SD); distance from mid-lip: 14.88 ± 0.82 mm (mean \pm SD), midway between the upper-lip and the base of the nose]. To ensure as precisely as possible that assessments were performed on a constant location throughout sessions, the location of 2PDT assessment was marked on the first day before

starting the first session (and renewed if necessary the second day), using a 10 mm circular stamp soaked in an invisible ink visible with a UV lamp (see Figure 2, A). These marks were also used to position the pneumatically-driven stimulators used during the MEG mapping procedure on the same locations (see “Magnetoencephalography data acquisition” section). It is important to note that the tested lip areas are innervated by two independent nerves as each side of the upper-lip is innervated by the medial branch of the superior labial branch of the infraorbital nerve and these nerves never cross the midline (Hu et al., 2007). Thus, measurements at both sides of the upper-lip could not influence each other at the peripheral level. For each participant the location of each tested area was kept constant across sessions.

2PDT were assessed using eight probes, one with a single tip and seven with two tips separated by various distances. Shaft length was 1.9 mm for the finger probes and 8 mm for the lip and cheek probes. Shaft and tip diameters were identical for all probes (shaft: 0.7 mm; tip: approximately 200 μ m). The distances tested were predetermined and remained constant for all participants but differed between index fingertips (0.7, 1.0, 1.3, 1.6, 1.9, 2.2, 2.5 mm), little fingertips (1.0, 1.4, 1.8, 2.2, 2.6, 3.2, 4 mm) and lips (2, 3, 4, 5, 6, 7, 8 mm) because of basic sensitivity differences between these regions. At the beginning of each finger or lip testing block the single probe and the two-tip probe with the largest tip separation (2.5 mm for index fingertips; 4 mm for little fingertips; 8 mm for the lips) were presented three times to the participant while the experimenter said "one" or "two". Once participants declared that they clearly felt the difference between these two probes the testing began and lasted 10 to 15 minutes for each body-site. For every site, each probe was tested 8 times in a pseudo-randomized order (no more than two consecutive repetitions of the same probe), resulting in 64 trials. Tips were always presented parallel to the longitudinal axis of the fingers and face.

To avoid the problem of variations in application pressure when using handheld tips (Johnson and Phillips, 1981; Craig and Johnson, 2000), we used two specially-designed spring-mounted apparatuses that controlled application force across trials (see Muret et al., 2014 supplemental data for details). Briefly, for fingertip assessments, the eight probes were mounted on a rotatable disc which permitted rapid and unpredictable switching between distances. The participant's arm rested on the device with the tested fingertip positioned over a small hole while the other fingers were strapped down to prevent any motion. Participants were blindfolded and instructed to relax the hand and the forearm, and to remain still. The probes were brought into contact with the participant's finger by the experimenter pulling the device down towards the rotatable disc with an application force of between 150 and 200 mN (Kalisch et al., 2007). The fingertip remained in contact with the probes for approximately 1 second and participants

were required to promptly give their oral response (“one” or “two”). The experimenter then lifted up the participant's hand, rotated the disc to present the next probe and continued until all probes had been presented eight times. Care was taken to prevent participants from moving their finger or pressing it down on the probes. Similarly for the lips assessments, probes were mounted on individual plexiglass sticks with ferromagnetic bases (4.5 cm long) and were used to deliver the stimulation by inserting them into the end of a metal tube (length: 12.5 cm; diameter: 1.5 cm) which contained a spring that was calibrated to obtain an almost constant application force (between 190 and 290 mN). When applied to the skin, the plexiglass stick moved approximately 1 cm into the tube and a magnet prevented it from rotating or tilting. The participant's head was stabilized using a chin/head rest and their hands rested on the table. They were instructed to keep their face and hands relaxed and still. Stimulation was manually delivered by the experimenter perpendicularly to the skin surface to ensure that both tips (for the seven two-tip probes) touched the skin's surface at the same time. After each trial the experimenter changed the plexiglass base and presented the next probe until all probes had been presented eight times.

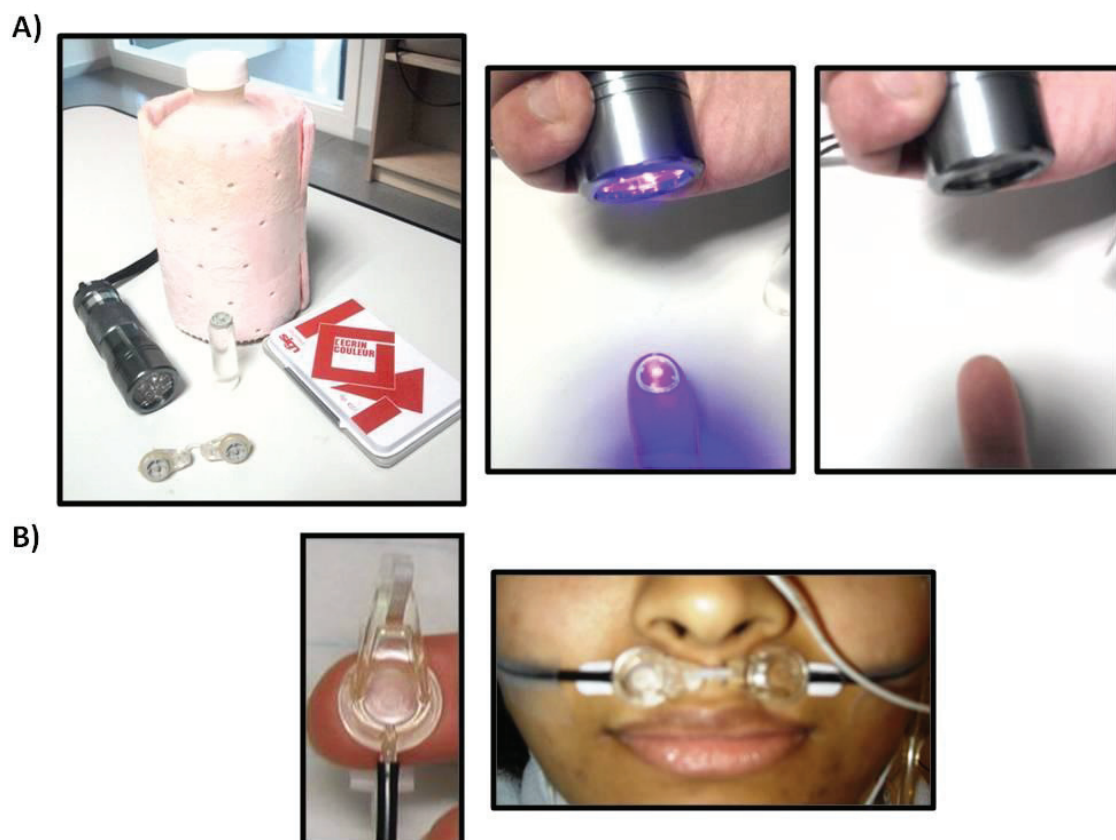


Figure 2. Devices and procedure used to deliver a reliable stimulation during MEG recordings at a constant location throughout sessions, but also to systematically assess tactile acuity within the same cutaneous area. **A)** Pictures showing the circular stamp and the UV-visible ink used to precisely mark the tested locations. **B)** Pictures

illustrating the pneumatically-driven stimulator (8mm diameter) fixed either to a fingertip or to the lips with the membrane contacting the skin and the tubes conducting the compressed-air coming from outside of the shielded room.

Magnetoencephalography data acquisition. Recordings were carried out using a 275-channel whole-head MEG system (CTF-275 by VSM Medtech Inc.) with continuous sampling rate of 600Hz, a 150Hz low-pass filter, and third-order spatial gradient noise cancellation. During the two MEG sessions, participants lay supine in a magnetically-shielded recording room with the head comfortably maintained by cushions to limit involuntary movements. Oblique electro-oculogrammes (EOG) were acquired with bipolar electrodes. The exact position of the head with respect to the sensors was determined by measuring magnetic signals produced by currents in three indicator coils fixed to the nasion and the preauricular points (fiducial points). Their location was continuously recorded and checked at the beginning of each block to ensure that head movements did not exceed 5mm. In order to maintain the exact same position across sessions the coils and EOG electrodes remained on the participant's head between the two MEG sessions.

The stimulation system was pneumatically driven and electronically controlled from the command board outside of the shielded room. This system had eight individually controlled channels, each consisting of a pneumatic valve connected by a plastic tube to a membrane (8mm of diameter). Prior to starting the experiment, the temporal onset and time course of the stimulation was carefully measured for each of the eight channels using a force sensor positioned next to the membrane. The average of 100 stimulations revealed a constant delay of 30ms in each of the tubes (see Figure 3), which was taken into consideration for further analyses. The six channels/tubes with the closest delays were selected for our six stimulators. For each participant, the membranes used to deliver the mechanical stimulation were carefully checked and replaced if damaged, and then fixed at each of the tested body-sites (D2, D5 and upper-lip bilaterally) using double adhesive tape combined with regular adhesive tape. At the beginning of each MEG session care was taken to position each stimulator exactly at the same location as 2PDT assessments thanks to the UV-visible marks made beforehand (see Figure 2, B). This ensured a precise correspondence between the location of behavioural and MEG acquisitions throughout sessions. Tactile stimuli were delivered at constant supra-threshold intensity (0.8 bars) using 30ms square-wave pulses interleaved by a delay ranging from 400 to 600ms by 10ms steps. Before each session participants were asked whether the tactile stimulation was clearly perceived at all body-sites, with a comparable subjective intensity across the six body-sites, and if necessary the fixation of the membranes was adjusted.

Each MEG session was subdivided into four blocks during which each body-site was stimulated 125 times, resulting in 500 stimulations per area per session. The stimulated regions and intervals between stimulations were pseudo-randomized, allowing no more than one consecutive repetition at the same location or with the same ISI, and ensuring that the number of repetitions (location or ISI) was equally distributed across body-sites and blocks. To mask the noise made by the stimulators participants listened to 60 dB white noise presented binaurally through air-conducting tubes with foam ear tips. Participants were instructed to remain as still as possible, to fixate a cross drawn at the centre of a board positioned 50cm away from their eyes (to avoid eye saccades), and to avoid blinking during the stimulation period. Every 30 stimulations the white noise was interrupted for 3s, notifying a rest period during which participants were instructed/allowed to freely close the eyes and blink. Few minutes of rest were additionally taken in between each block.

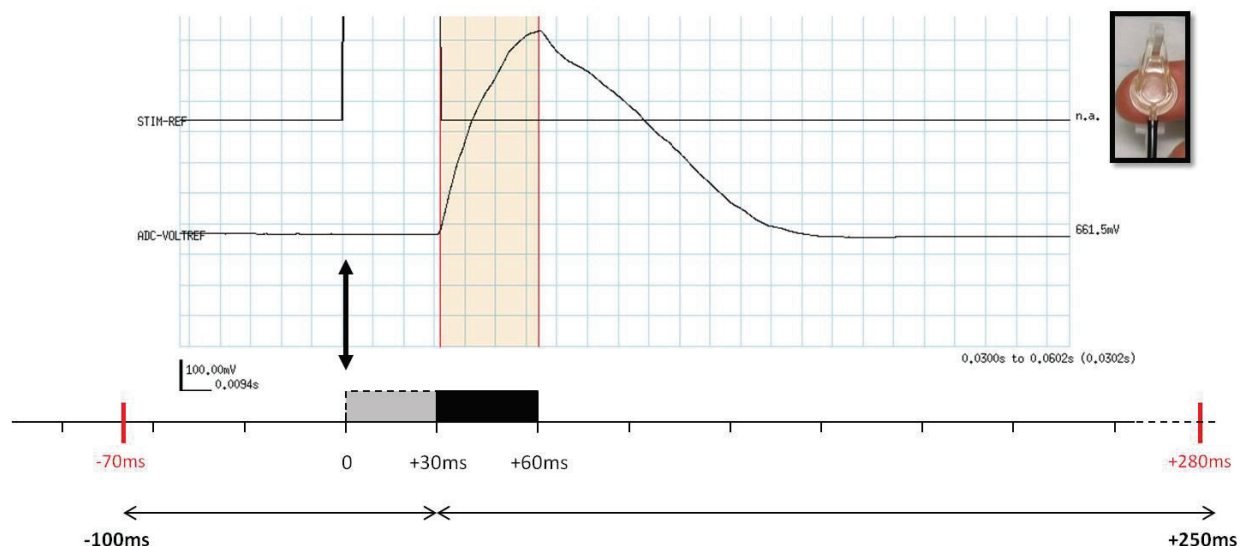


Figure 3. Mean onset and time course of the pneumatically-driven tactile stimulation used during MEG recordings as measured by a force captor positioned next to the membrane. The time course below the graph shows the onset of the stimulus trigger (0), the onset of the stimulus corrected for the delay (+30ms), and the peak of the stimulus force profile (+60ms) as well as the time window used for further analyses: [-70 +280]ms uncorrected to obtain a final analysis window [-100 +250]ms where 0 represents the onset of the tactile stimulation.

Behavioural data analysis. For each participant and for each area the mean of the verbal responses ('one' or 'two') was plotted as a function of distance between the probes and the psychometric function was fitted with a binary logistic regression (Dinse et al., 2006). Threshold was determined from the fitted data and defined as the distance at which participants responded "two" 50% of the time. S1 and S2 thresholds were statistically analysed for stability using

repeated measures ANOVAs (rmANOVAs) with the factor Session (S1/S2). Separate rmANOVAs were performed for the right-D2, right-D5, right-Lip, and left-Lip data (left-D2 and left-D5 data were not collected at S1). To assess whether the S2 session of left-D2 and left-D5 were different from the S2 session of right-D2 and right-D5, two paired t-tests were performed. Pre (average of S1 and S2) and Post (S3) thresholds were analysed using three two-way rmANOVAs (one for each pair of body-sites) with factors Side (Left/Right) and Session (Pre/Post). Threshold changes between Pre- and Post-sessions were determined for each subject as a percentage of the Pre-session threshold (average of S1 and S2): $\frac{Threshold\ Post - Threshold\ Pre}{Threshold\ Pre} * 100$. Mean threshold changes were calculated for each of the six tested areas and were then submitted to a one-way rmANOVA to assess differences in threshold change across regions. Three linear correlations (Pearson) were performed to compare threshold changes at the left and right upper-lip and between each side of the upper-lip and the right-D2. To assess whether threshold changes were related to changes in discrimination sensitivity and/or in response criterion (Signal Detection Theory), false alarm and hit rates were systematically calculated and used to compute the discriminative index (*d-prime value*) and the criterion shift index (*ln(Beta) value*) using the Palamedes toolbox for one-alternative forced choice (PAL_SDT_1AFC_PHFtoDP, MATLAB v.r2010a). These indices were then statistically analyzed using five paired t-tests comparing sessions (Pre vs. Post), corrected for multiple comparisons (Bonferroni). All statistical analyses were conducted using Statistica® (v.10, StatSoft). Data were checked for normality using Kolmogorov-Smirnov tests. Post-hoc analyses were performed using Bonferroni tests (mentioned in the text as p_{corr}). All group data are expressed as mean \pm standard error of the mean (SEM).

Magnetoencephalography data analysis. Neuromagnetic analyses were conducted using CTF softwares (VSM Medtech Inc.). The first step in the offline processing involved visual inspection of all datasets for muscle artefacts rejection. Datasets were then low-pass filtered to 100Hz before being segmented into epochs of 350ms including a period of 250ms post-stimulus (corrected) and a pre-stimulus baseline of 100ms. Trials coinciding with eye movements (i.e., blink, saccades etc) were automatically rejected on the basis of EOG recordings, all trials with EOG activity exceeding 20 μ V being rejected. Subsequently, all trials were visually inspected to check and if necessary adjust trials rejection. Using the remaining trials, the mean head position was calculated and trials in which head motion exceeded the average by 3mm were rejected. Then the mean head position was re-calculated separately for each condition and used to correct for head motion. These pre-processing steps resulted in an average of 404 (\pm 15.72) (out of 500)

artefact-free trials per condition. For each of the six conditions (Area, Side and Session) artefact-free trials were averaged using the 100ms pre-stimulus for baseline correction. The averaged somatosensory evoked magnetic fields (SEFs) were then visually explored with DataEditor CTF software and a trigger was placed over the peak of the first prominent component.

To allow for an anatomical correspondence to participants' brain, MEG data were coregistered to each participant's structural MRI using the position of the coils as landmarks. A multi-spherical headmodel was computed based on individuals' brain shape and used for dipole source reconstruction. Please note that it has been suggested that realistically shaped head models offer a significant advantage over spherical head models only when dipole sources are located at depths greater than 10-20mm below the brain surface (i.e. subcortical structures) (see Yvert et al., 1996), which is not the case of the present study. The three fiducial points defined a head-based Cartesian coordinate system with the origin at the midpoint between the left and right preauricular points. The y -axis ran along the medio-lateral (M/L) direction from the right to the left preauricular points, x -axis (orthogonal to y -axis) along the antero-posterior (A/P) direction, forward through the nasion, and z -axis along the dorso-ventral (D/V) direction, upwards orthogonal to the xy plane (see Figure 6).

For source identification, dipole source analysis using equivalent current dipoles (ECDs) was used to model local cerebral activations using a multi-spherical head model. For fingertip data, a single ECD was fitted as most of the activity was expected to be in the contralateral hemisphere. In contrast, two ECDs were fitted for the lips due to multiple MEG (Hoshiyama et al., 1996; Disbrow et al., 2003a; Nevalainen et al., 2006) and fMRI (Iannetti et al., 2003; Blatow et al., 2007; Eickhoff et al., 2008; Lin et al., 2010) reports showing a bilateral response following lip stimulation. Data from all MEG channels over a time interval of 7ms around the peak were used to solve the inverse problem. Given that lip's sources were expected to be bilateral and symmetrical, a minimal sphere was systematically used to exclude the centre of the headmodel from the source space in order to minimize the convergence of bilateral dipoles. The radius of this minimal sphere was set to 35% (i.e., 2.57 ± 0.02 cm) of each participant's headmodel radius. An extra dipole (excluded from further analyses) was added if the dipole model did not explain 90% of the variance of the magnetic field (Wühle et al., 2010, 2011). In total, 19 additional dipoles (for 9 participants) were required for the fingertips (most of the time due to small ipsilateral activity), while only 6 were needed for the lips (for 2 participants). These procedures resulted in ECDs explaining more than 95% of the variance (95.45 ± 0.47 %) for the fingertips, and more than 97% of the variance for the lips (97.25 ± 0.28 %). To ensure that the

goodness-of-fit (GoF) did not vary across sessions the error of fit percentages were submitted to a three-way rmANOVA with the factors Session (Pre/Post), Area (D2, D5 and Lip) and Side (Left/Right). While this analysis revealed a significant difference of GoF between Areas ($F_{(2,40)} = 16.37, p < 10^{-5}$), with significantly smaller error of fit for the lips than for the fingers (Fisher post-hoc tests, both p_{LSD} values $< 5 \cdot 10^{-4}$), no effect or interaction with the factor Session was found (see Figure 4). An additional analysis with separate two-way rmANOVA (Session*Side) for each of the three body-sites confirmed that for a given body-site the GoF remained stable across sessions (all p values > 0.05).

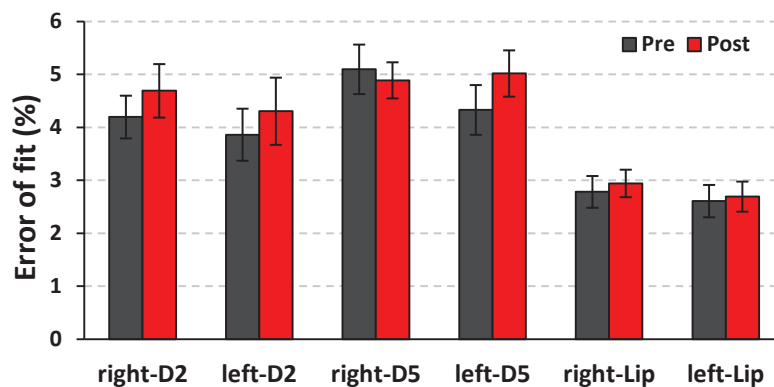


Figure 4. Mean error of fit expressing the percentage of the variance of the magnetic field not explained by the dipole model used to reconstruct the source of each of the tested body-sites.

For each participant ECDs were superimposed onto their MRI images to identify source locations with respect to anatomical structures. Examination of the resulting images revealed erroneous localization of the ipsilateral activity evoked by lip stimulation, confirmed by large volumes of confidence: $209.20 \pm 170.18 \text{ mm}^3$ (14 participants with volumes larger than 5 mm^3). Consequently, ipsilateral dipoles were excluded from further analyses. In contrast, the volumes of confidence were in the order of $2.65 \pm 0.96 \text{ mm}^3$ for the contralateral lip dipoles and $2.60 \pm 1.37 \text{ mm}^3$ for the contralateral fingertip dipoles. These small volumes of confidence provide the information that the error in dipole localization was less than 1mm in radius ($0.78 \pm 0.08 \text{ mm}$). To ensure that this incertitude in localization did not vary across sessions, the mean radius of the volumes of confidence were submitted to a three-way rmANOVA with the factors Session (Pre/Post), Area (D2, D5 and Lip) and Side (Left/Right). This analysis revealed no significant differences across Areas or Sessions (see Figure 5). Running separate two-way rmANOVAs (Session*Side) on each of the three body-sites did not reveal any further differences.

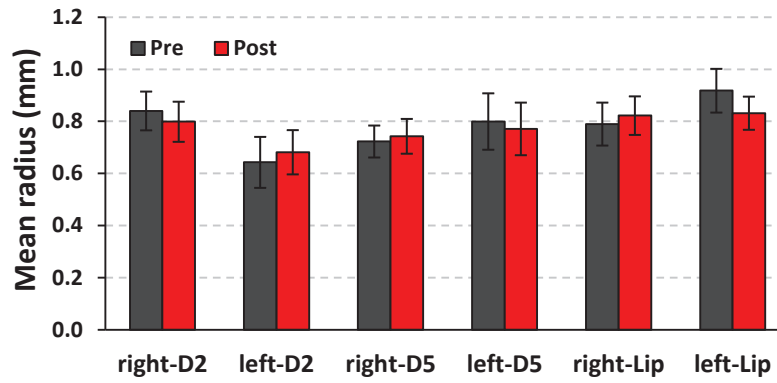


Figure 5. Mean radius (mm) of the volumes of confidence, providing the incertitude in dipole location obtained for each of the tested body-sites.

Dipole positions, originally expressed in the Cartesian coordinate system, were also defined by their polar coordinates, computed following the standard formula described in Figure 6. The eccentricity (or radius, r) is defined as the distance from the centre of the Polar coordinate system (here the centre of the headmodel), theta angle (θ) is positive on both sides, from 0° to 180° , upward to downward, while phi angle (φ) is positive on the right side, from 0° to 180° , upward to downward, and negative on the left side (due to the use of the "four quadrant inverse tangent" function). The Euclidean Distance (ED) between dipoles was calculated from their dipole location in the Cartesian system as following:

$$ED = \sqrt{(x_a - x_b)^2 + (y_a - y_b)^2 + (z_a - z_b)^2}$$

x , y and z referring to the 3D Cartesian coordinates of the two body-sites a and b .

Statistical analyses of peak latencies, dipoles coordinates and strength were performed using repeated measures analysis of variance (rmANOVA) and post-hoc Fisher's tests (mentioned in the text as p_{LSD}).

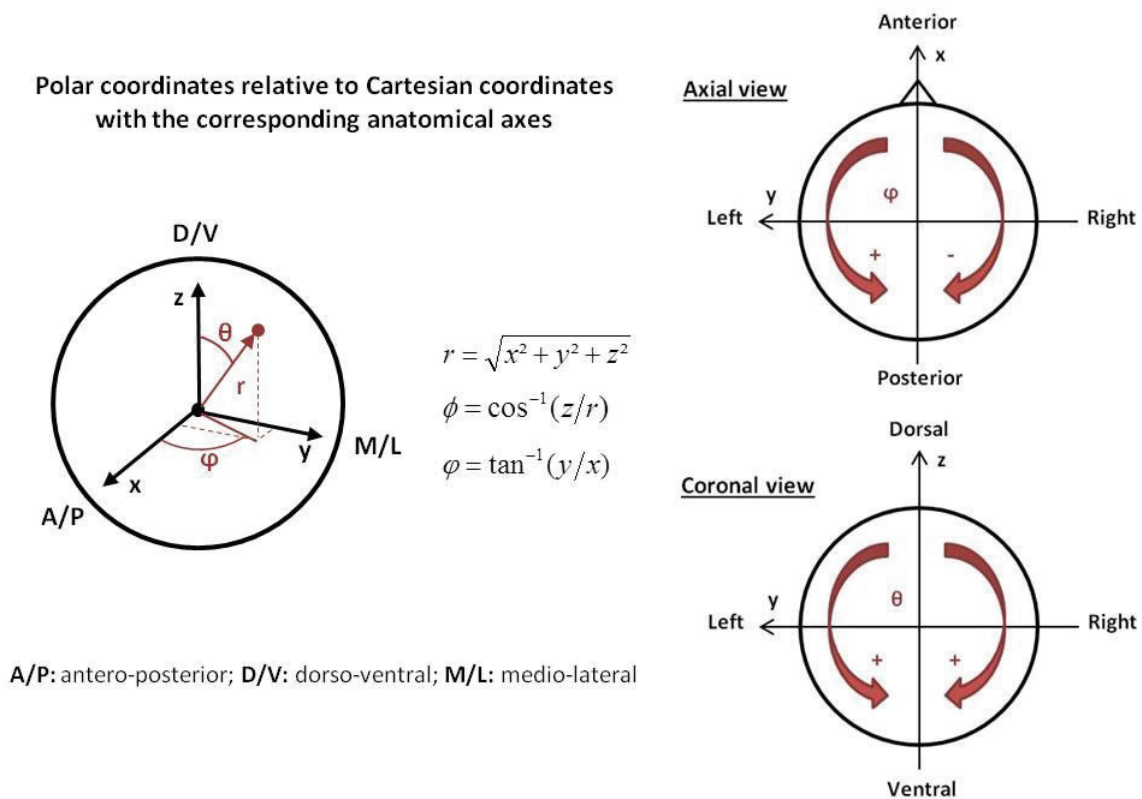


Figure 6. Cartesian and polar coordinate systems. **Left panel:** Schematic representation of the Cartesian coordinate system centred to the headmodel origin of each participant, from which polar coordinates were computed according to the equations. The spatial correspondence of each polar coordinate is illustrated in red among the Cartesian coordinates (black), as well as the three main anatomical axes (antero-posterior, dorso-ventral and medio-lateral). **Right panel:** the sign and directional changes of both ϕ and θ polar angles are illustrated on axial and coronal view respectively. Note that the "four quadrant inverse tangent" was used to facilitate ϕ angle analysis.

Results

Behavioural data

Analysis of the thresholds obtained at baseline for right-D2, right-D5 and the lips revealed no significant differences between S1 and S2 for any of these body-sites (four rmANOVAs, all p values > 0.12). As thresholds at left-D2 and left-D5 were assessed solely at S2, two paired t -tests confirmed that their thresholds were not statistically different from those obtained for their homologue at S2 (both p values > 0.7). A two-way rmANOVA (Session*Side) on the thresholds from both index fingertips revealed a significant interaction ($F_{(1,20)} = 4.82, p = 0.040$), indicating a significant decrease of right-D2 thresholds following RSS ($p_{Bonf} = 0.002$) while left-D2 thresholds remained stable ($p_{Bonf} > 0.90$; Figure 7). The post-RSS threshold obtained at right-D2 was also significantly lower than that obtained at left-D2 pre and post-RSS (both p_{Bonf} values $<$

0.018). A similar analysis performed on thresholds from both sides of the upper-lip revealed a significant main effect of Session only ($F_{(1,20)} = 11.47, p < 0.003$), with thresholds from both upper-lips being significantly lower after RSS of right-D2 (Figure 7). Together, these results confirm our previous findings (Muret et al., 2014 and results from the fMRI study) that three hours of RSS applied to the right-D2 significantly improves spatial discrimination not only at the stimulated fingertip but also at both sides of the upper-lip, without affecting the left-D2. In the present study, thresholds were additionally assessed at both little fingertips and their analysis revealed that they were stable across sessions. These latter results further demonstrate the limit in the “spread” of the RSS-induced perceptual changes across fingers of the same hand, something that was already reported for the adjacent middle finger following RSS on right-D2 (Godde et al, 2000; Muret et al, 2014).

D-prime analyses confirmed sensitivity gains for right-D2 and right-Lip (right-D2: $t_{(20)} = -2.63, p = 0.016$, right-Lip: $t_{(20)} = -2.42, p = 0.025$), with no slackening of participants’ response criterion for any region (Figure 8).

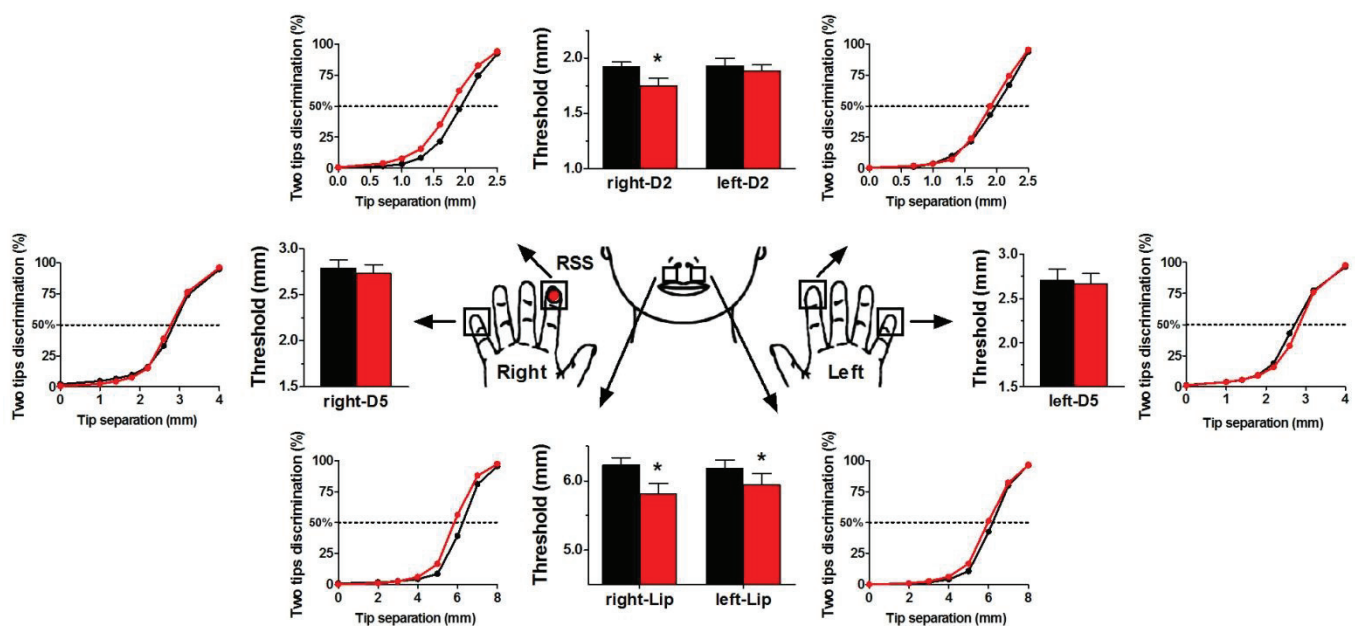


Figure 7. Mean psychometric curves and thresholds (mm) before and after the RSS procedure at each tested body-site. Psychometric curves averaged over all individual regression curves, Pre (black) and Post (red) RSS applied to the right-D2. The mean thresholds obtained Pre and Post RSS are represented for each area on the bar plots with the same colour code. Asterisks highlight the cases where a significant threshold decrease was obtained from the threshold analyses (three rmANOVAs on data from the index fingers, little fingers and lips followed by Bonferroni post-hoc tests, * $p_{Bonf} < 0.05$).

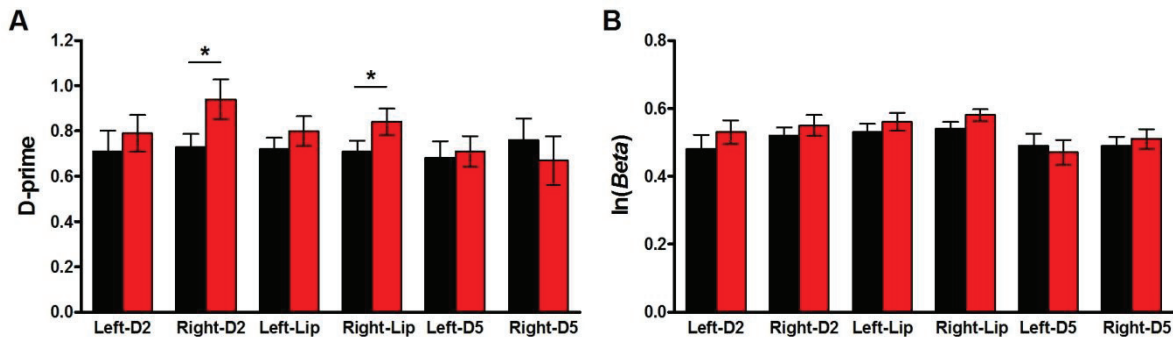


Figure 8. Signal detection theory values across sessions. **(A)** Mean d' -prime and **(B)** mean $\ln(Beta)$ values obtained for each area, Pre (black) and Post (red) RSS of right-D2.

Comparison of the amount of threshold change at each body-site did not reveal any further patterns of interest. In contrast to the first report of this transfer (Muret et al., 2014), no significant correlation was found between threshold changes obtained at each side of the upper-lip. In comparison with the previous study, however, in this study more participants did not exhibit a threshold decrease at right-D2 (5/21 instead of 2/15), resulting in a lower proportion of participants (57% (12/21) compared with 80% (12/15)) who had decreased thresholds at both the right-D2 and lips. In addition, the mean threshold decreases at right-D2 and the right- and left-Lip were lower than those observed in Muret et al., 2014 (i.e., respectively $-8.91 \pm 3.35\%$, $-6.73 \pm 2.04\%$ and $-3.80 \pm 2.18\%$, instead of $-15.26 \pm 3.85\%$, $-8.42 \pm 2.88\%$ and $-12.15 \pm 3.78\%$).

Despite observing a smaller threshold decrease after RSS in this study than in our previous study (Muret et al., 2014), the pattern of changes at right-D2 and the lips was similar for the two studies when only participants exhibiting threshold decrease at right-D2 were selected (Figure 9, upper left).

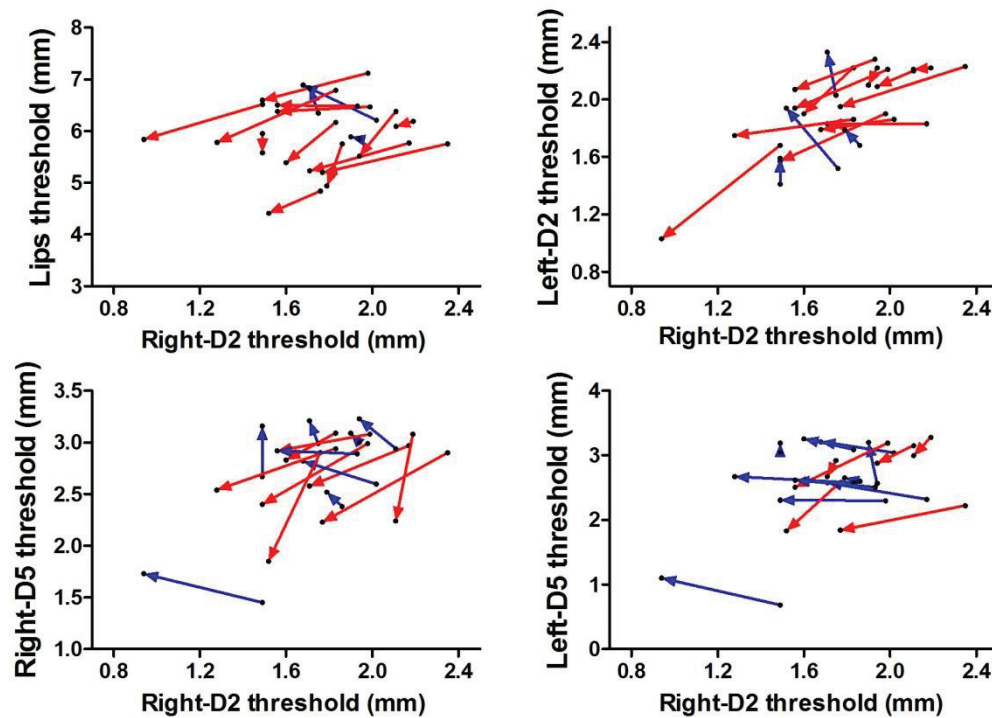


Figure 9. Vectors showing the relationship between threshold changes at right-D2 and the lips (upper left), left-D2 (upper right), right-D5 (bottom left), and left-D5 (bottom right) for each of the participants for who RSS worked (i.e., exhibiting a threshold decrease for right-D2). The starting and ending points of vectors respectively represent pre- and post-session thresholds. Red vectors indicate parallel threshold decreases at both right-D2 and the other body-site (i.e., lips, left-D2, right-D5 or left-D5), whereas blue vectors illustrate a decreased threshold at right-D2 and an increase at the other area.

Neuromagnetic data

Significant somatosensory evoked fields (SEFs) were identified for all participants with a first prominent peak observed on average at 60.1 ms (± 8.5 , SD) following fingertip stimulation and at 47.4 ms (± 6.9 , SD) following upper-lip stimulation (see Figure 10 for a representative example). These latencies are in agreement with the literature reporting a first component from 55ms to 75ms following finger/hand stimulation (e.g., Braun et al., 2000; Mertens et al., 2000; Hlushchuk et al., 2004; Zhu et al., 2007; Onishi et al., 2010; Wühle et al., 2011), and around 40ms following lips/face stimulation (Mogilner et al., 1994; Disbrow et al., 2003a; Nguyen et al., 2004; Nevalainen et al., 2006).

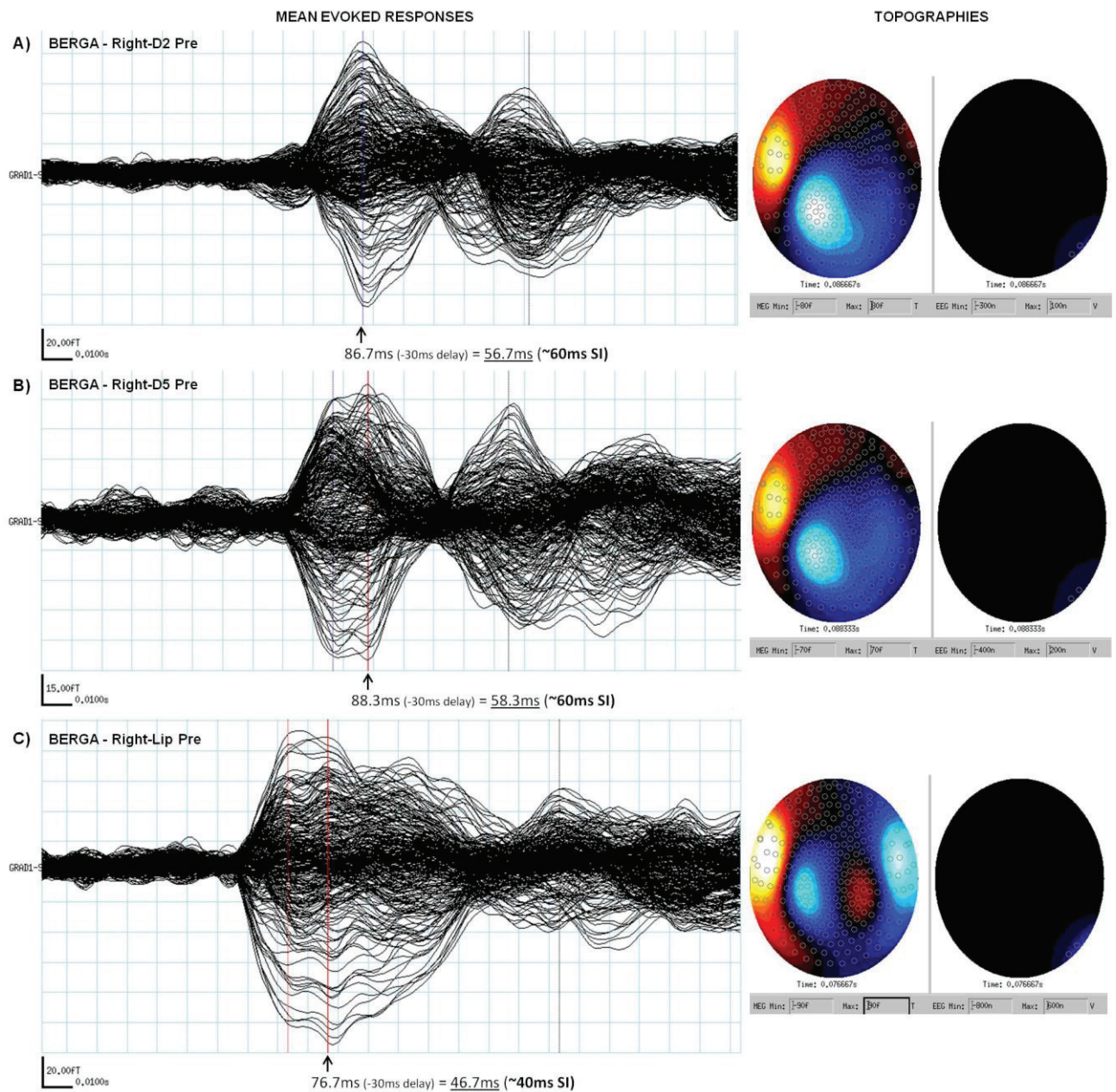


Figure 10. Illustration of the mean evoked responses and of their topographies projected at the captor level from a single participant. The left panels show the somatosensory evoked fields (SEFs) computed by averaging artefact-free trials obtained following stimulation of A) right-D2, B) right-D5, and C) right-Lip at the Pre-session. The vertical lines represent the triggers used to select the peak of each component and the arrows below these lines indicate their raw and delay-corrected latencies. The right panels show the topography of the fields corresponding to the peak highlighted by the arrow in left panels projected at the sensor/scalp level.

To assess whether these peak latencies varied across sessions or body-sites, values were submitted to a three-way rmANOVA (Session*Area*Side; Figure 11). This analysis revealed a significant decrease in peak latencies after RSS ($F_{(1,20)} = 6.14$, $p = 0.022$), but also significant differences between body-sites ($F_{(2,40)} = 66.71$, $p < 10^{-6}$), with as expected, shorter peak latencies for the lips than for the fingertips (both p_{LSD} values $< 10^{-6}$). Given this difference between lips and fingertips separate two-way rmANOVAs (Session*Side) were then applied to their datasets. Analysis of fingertip peak latencies revealed significantly shorter latencies for the left fingers than for the right ($F_{(1,20)} = 4.43$, $p = 0.048$), and the significant decrease of peak latencies after RSS was still observed ($F_{(1,20)} = 6.46$, $p = 0.019$). In contrast, no significant differences were observed for the lips.

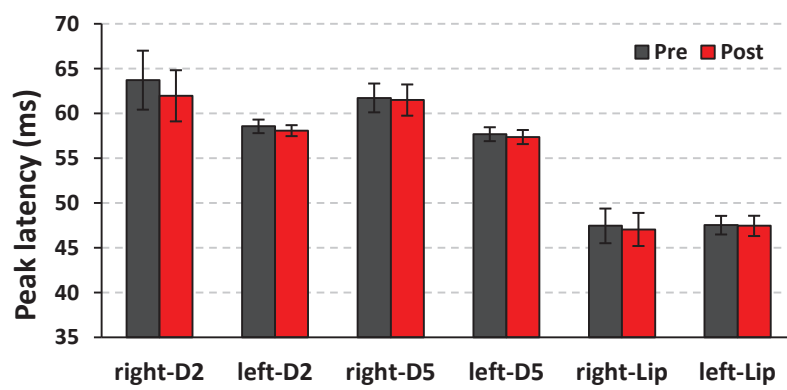


Figure 11. Mean peak latencies (ms) of the first prominent component obtained Pre (black) and Post (red) RSS following stimulation of each of the tested body-sites: right- and left-D2, right- and left-D5, right- and left-Lip.

The topography of the magnetic fields observed at the sensor level for these components revealed that the one evoked by finger stimulation arose predominantly from the contralateral hemisphere (Figure 10, A & B), but that the component evoked by lip stimulation arose from both hemispheres, as an inverted pattern was observed (Figure 10, C). Because of the nature of the stimulation employed for the mapping procedure (i.e., mechanical), and given the orientation of SI subregions and the fact that MEG sensors predominantly record the activity arising tangentially from the scalp, these responses are likely to arise from activity within BA3b. Reconstruction of the sources of these components using ECDs confirmed this hypothesis, as dipoles were located at the proximity of the post-central gyrus (see Figure 12 for a representative example). A somatotopic organization was observable at the individual level (Figure 12), but also across individuals (Figure 13), with D5, D2 and the Lip being sequentially more ventral and anterior. This organization is consistent with Penfield's homunculus (Penfield and Boldrey, 1937), but also with more recent somatotopic mapping using MEG (Nakamura et al., 1998).

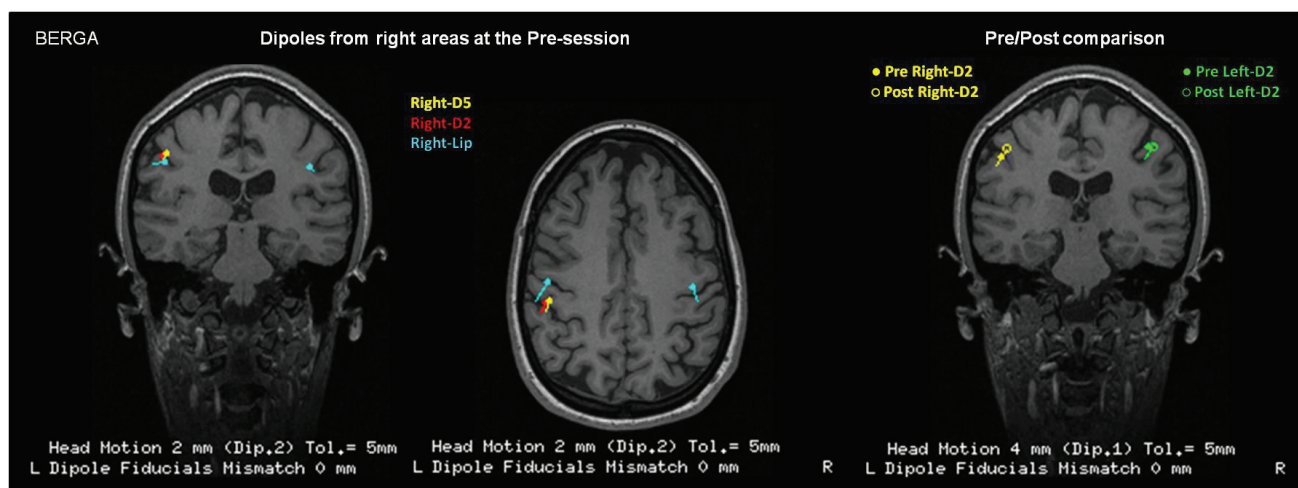
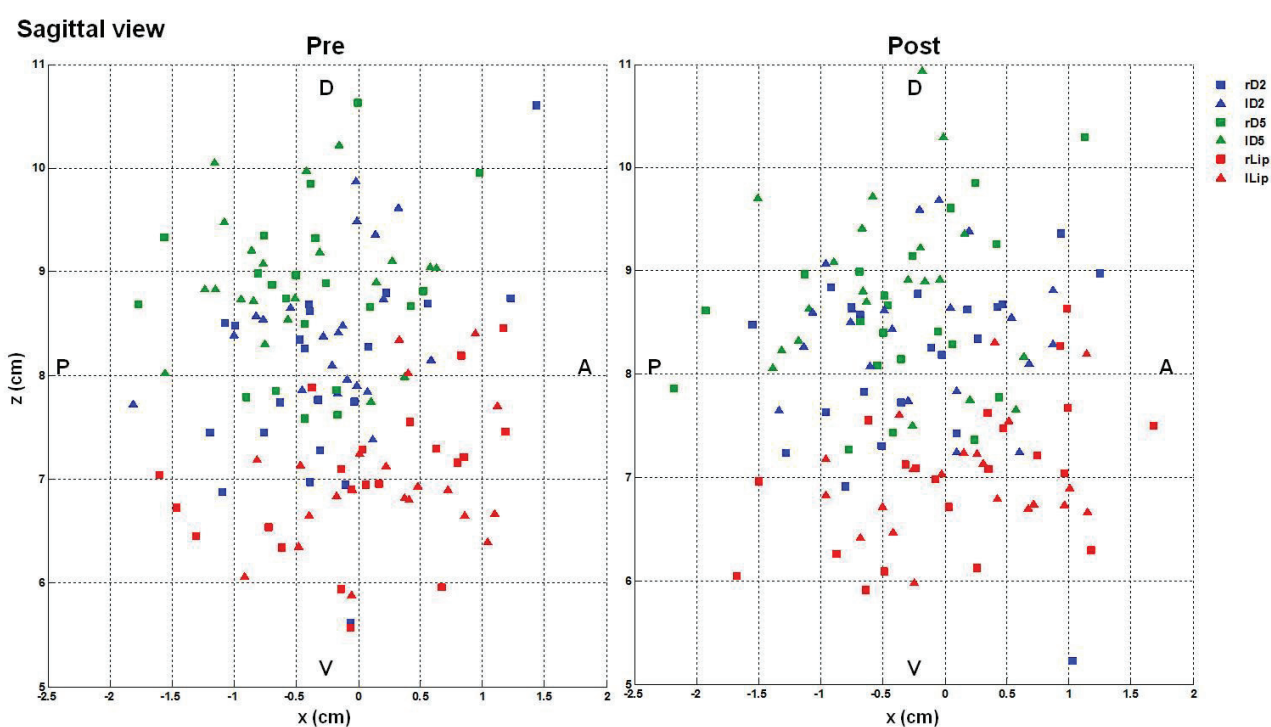


Figure 12. Illustration of dipole localizations from a single participant overlaid on his structural MRI. **Left panel:** coronal and axial view of the ECDs from right body-sites (right-D5: yellow; right-D2: red; right-Lip: cyan) obtained at the Pre-session. Note the bilateral dipole obtained for the right-Lip and the somatotopic organization with D5-D2-Lip being sequentially more ventral and anterior. Note also that due to large volumes of confidence, the ipsilateral lip dipole was excluded from further analyses. **Right panel:** comparison of the dipole location Pre (filled circle) and Post (empty circle) RSS, obtained for right-D2 (yellow) and left-D2 (green). Note the upward shift of the right-D2 ECD at the Post-session.



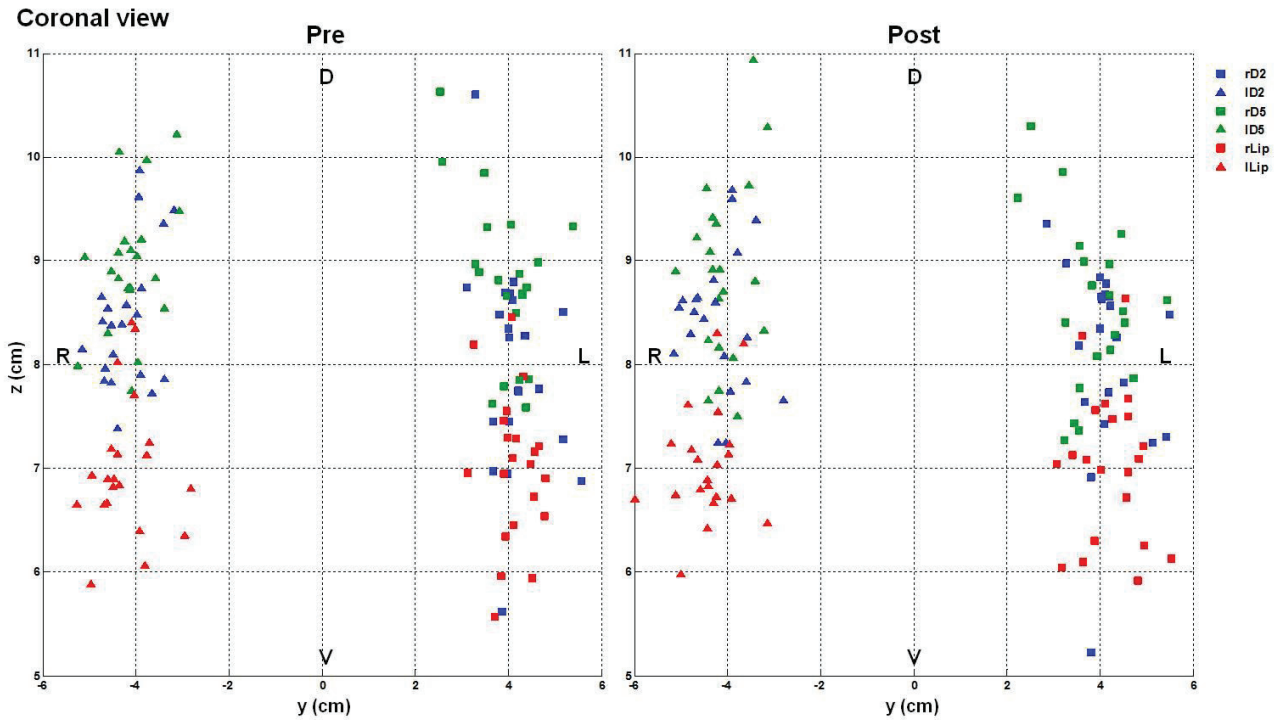


Figure 13. Sagittal (top) and coronal (bottom) view of the contralateral ECDs of all individuals obtained Pre (left) and Post (right) RSS for all tested body-sites: D2 (blue), D5 (green) and Lips (red). The body side is differentiated by marker shapes: right (square), left (triangle). The centre of the referential corresponds to the centre of the headmodel of each participant, which had a similar size (radius: 7.33 ± 0.05 cm). Note here again the overall somatotopic organization with D5-D2-Lip being sequentially more ventral and anterior.

Since our goal was to detect possible RSS-induced changes in dipole localization, the next step was to quantify Pre-Post differences among individuals. These analyses were performed within both the Cartesian and the Polar coordinate systems, and gave rise to multiple differences between body-sites related to their somatotopic organization that we will describe first. Note that only the significant RSS-induced changes are indicated by asterisks on the graphics.

Somatotopic organization:

Body-sites differences in dipole localization were first assessed by analyzing the **Polar coordinates** (Figure 16). Significant differences in the eccentricity (i.e., radius) of the ECDs of the different body-sites were observed (three-way rmANOVA; $F_{(2,40)} = 29.08$, $p < 10^{-6}$), with a gradual increase in radius from the lip, to D2, to D5 (all p_{LSD} values < 0.032). The same gradual increase from the lip, to D2, to D5 was also found for the phi angle (three-way rmANOVA; $F_{(2,40)} = 16.81$, $p < 10^{-5}$), while as expected, the inverse pattern was observed for the theta angle (three-way rmANOVA; $F_{(2,40)} = 127.39$, $p < 10^{-6}$, all p_{LSD} values $< 10^{-5}$). Together, these results demonstrate a clear somatotopic organization, with D5, D2 and the Lip being sequentially more

ventral (as revealed by theta angles) and anterior (as revealed by phi angles). This result is consistent with the somatotopic organization described in the literature (Penfield and Boldrey, 1937; Nakamura et al., 1998) and qualitatively observed in Figure 13. In addition, the eccentricity (i.e., radius) was significantly smaller for the ECDs of the right body-sites than for that of the left ($F_{(1,20)} = 23.94, p < 10^{-4}$). Running separate two-way rmANOVAs (Session*Side) on each body-site confirmed this difference was present at all three body-sites (D2: $F_{(1,20)} = 16.50, p < 0.001$; D5: $F_{(1,20)} = 14.42, p = 0.001$; Lip: $F_{(1,20)} = 10.43, p = 0.004$).

Differences in the distance between body-site ECDs were also assessed by computing their relative **Euclidean Distances (EDs)** (Figure 16). At baseline, the ED between D2 and D5 ECDs was on average 10.61 mm (± 1.50 , SEM). These values are in agreement with those previously reported in the MEG literature (Elbert et al., 1995; Nakamura et al., 1998; Tecchio et al., 1998; Stavrinou et al., 2007; Inoue et al., 2013). Similar to the Polar analysis, significant differences were found between these relative EDs (three-way rmANOVA; $F_{(2,40)} = 46.76, p < 10^{-6}$), with the D2-D5 distance being smaller than the distance between the lip and D2, itself smaller than the Lip-D5 distance (all $p_{LSD} < 5 \cdot 10^{-5}$). In addition, an interaction between relative distances and sides was found ($F_{(2,40)} = 6.65, p = 0.003$), with the ED between D2 and D5 being larger on the right side than on the left ($p_{LSD} = 0.018$), while both sides were similar for the Lip-D5 and Lip-D2 EDs (both p_{LSD} values > 0.05). This latter result suggests a larger representation of the right hand compared to the left one, perhaps due to handedness. Separate two-way rmANOVAs (Session*Side) on each body-site further revealed that the Lip-D2 ED was significantly smaller on the right side than on the left ($F_{(1,20)} = 5.87, p = 0.025$). This was not the case for Lip-D5 EDs. Similar rmANOVAs performed separately on each **Cartesian coordinate** (x , y and z) revealed that the gradual increase in the relative distance from D2-D5, to Lip-D2 and Lip-D5 was predominantly driven by differences along the z axis (see Supplemental Results). This was also true for the side difference observed for the Lip-D2 distance.

The relative distances between body-site ECDs were also evaluated by calculating their differential **Polar coordinates** (Figure 17). As for the relative EDs, a gradually increasing Δ theta angle was found from D2-D5, to Lip-D2, with the largest Δ theta angle being reported for Lip-D5 ECDs (three-way rmANOVA; $F_{(2,40)} = 38.56, p < 10^{-6}$; all p_{LSD} values $< 5 \cdot 10^{-4}$). This suggests that ED differences are essentially present along the dorso-ventral direction, and thus confirms the similar gradual increase observed along the z axis. Some differences were also observed at the level of both eccentricity and phi angles, with a significantly smaller Δ radius between D2-D5 ECDs than between the Lips and the fingertips (three-way rmANOVA; $F_{(2,40)} = 8.88, p < 0.001$; all p_{LSD} values < 0.021), and a larger Δ phi angle between Lip-D5 ECDs than

between D2-D5 ECDs (three-way rmANOVA; $F_{(2,40)} = 3.73$, $p = 0.033$; $p_{LSD} = 0.011$). These results further confirm the somatotopic organization of the tested body-sites ECDs, but with less pronounced differences along these directions than along the dorso-ventral direction. The $\Delta\theta$ analysis also revealed a significant interaction between relative EDs and sides ($F_{(2,40)} = 3.43$, $p = 0.042$), but which did not survive post-hoc tests (all p values > 0.05). Running separate two-way rmANOVAs (Session*Side) on each relative ED further revealed a significant difference between sides for the $\Delta\theta$ angle found between Lip and D2 ECDs ($F_{(1,20)} = 4.91$, $p = 0.038$), with a significantly smaller $\Delta\theta$ angle for the right side than for the left. No further differences were found for D2-D5 & Lip-D5 $\Delta\theta$ angles.

Overall, these differences in absolute and relative distances clearly demonstrate the somatotopic organization of the ECDs modelling the sources of the first prominent component evoked by tactile stimulation. In addition, some differences between body sides were observed, with smaller overall eccentricity of ECDs, larger D2-D5 ED, smaller Lip-D2 ED, and smaller $\Delta\theta$ angle between Lip-D2 for the right side, as compared with the left.

The next section focuses on the primary goal of this study, i.e., the quantification of the possible RSS-induced changes among individuals. Given the systematic differences observed between body-sites for several measures, and our strong hypotheses, the three-way rmANOVA (Session*Area*Side) was systematically followed by a separate two-way rmANOVA (Session*Side) for each body-site.

RSS-induced changes:

Comparing the dipole shift across sessions, no significant difference between body-sites was observed, all areas exhibiting a similar amount of shift that was significantly different from zero (Figure 14; 6 t-tests, all $t_{(20)}$ values > 6.80 , all p values $< 10^{-5} \ll p_{Bonf} = 0.008$). This unspecific shift was on average of 6.32mm (± 0.82).

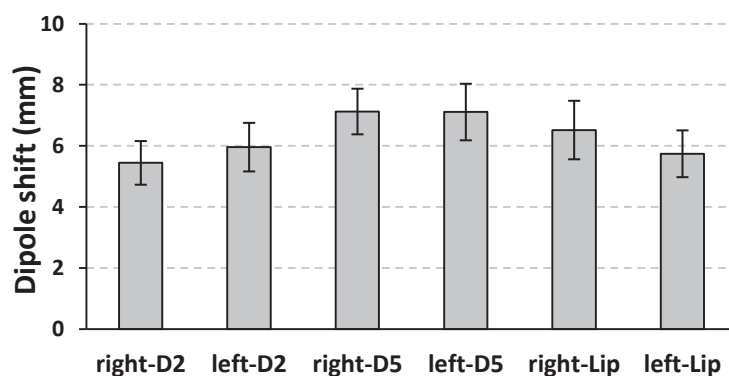


Figure 14. Mean dipole shift (mm) obtained after RSS for each of the tested body-sites.

To investigate the direction of these shifts, the Pre and Post localization of the dipoles was first compared for each of the **Polar coordinates** (Figure 16). A significant interaction was found between the eccentricity (i.e., radius) of body-site ECDs and sessions (three-way rmANOVA; $F_{(2,40)} = 3.31, p = 0.047$), revealing a tendency for an increased eccentricity for the lips after RSS ($p_{LSD} = 0.059$). Running a separate two-way rmANOVA (Session*Side) on each body-site confirmed this tendency for the lips only ($F_{(1,20)} = 3.53, p = 0.075$). In contrast, no RSS-induced changes in ECD location were observed for theta and phi angles.

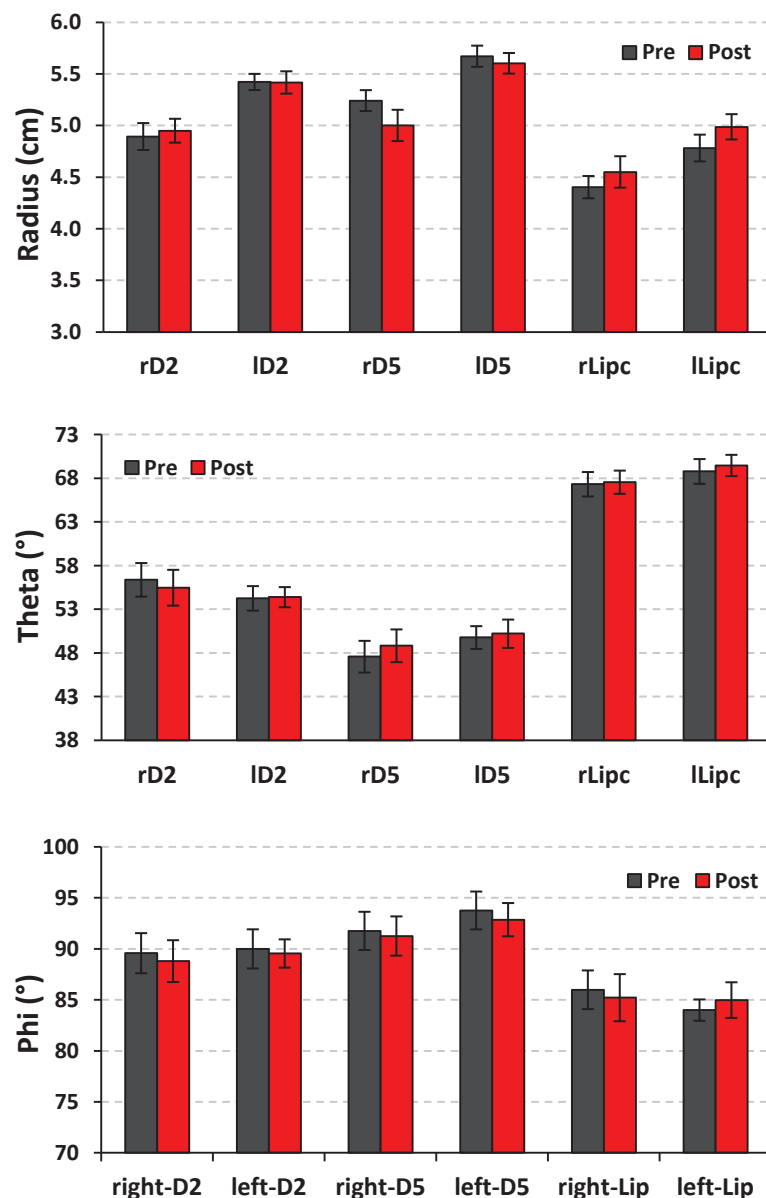


Figure 15. Mean Polar coordinates of the ECDs of each tested body-site (i.e., right- and left-D2, right- and left-D5, right- and left-Lip), Pre (black) and Post (red) RSS. **Top:** Mean eccentricity (or radius), in mm. **Centre:** Mean theta angle in degrees. **Bottom:** Mean phi angle in degrees. Note that the sign of the phi angles was inverted for the left body-sites (normally negative) to allow comparison with the right body-sites.

When computing the relative Euclidean Distance (ED) between body-sites (Figure 16), a significant interaction between sessions and relative EDs was found (three-way rmANOVA; $F_{(2,40)} = 4.48, p = 0.017$), with an increase of the Lip-D2 ED after RSS ($p_{LSD} = 0.014$; Figure 16). Running a separate two-way rmANOVA (Session*Side) on each body-site further confirmed this increase in the ED between the lip and D2 after RSS, regardless of the side ($F_{(1,20)} = 8.27, p = 0.009$). The two other relative EDs analyzed separately (i.e., D2-D5 and Lip-D5) did not show any RSS-induced effect. Similar analyses performed separately on each Cartesian coordinate (x, y and z) did not reveal any further effects (see Supplemental Results).

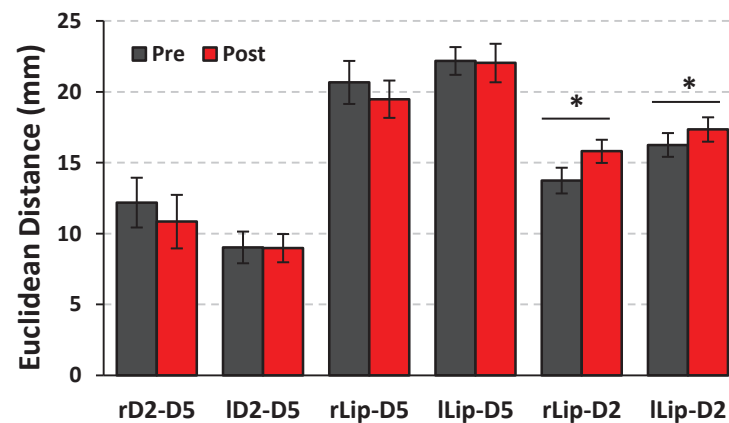


Figure 16. Mean relative Euclidean Distance (mm) between body-sites, Pre (black) and Post (red) RSS. r/lD2-D5: distance between D2 and D5 of the right or left side; r/lLip-D5: distance between Lip and D5 of the right or left side; r/lLip-D2: distance between Lip and D2 of the right or left side.

The relative displacement of ECDs was assessed by analyzing RSS-induced changes in their differential Polar **coordinates** (Figure 17). For all body-sites, Δ radius distances were smaller after RSS (three-way rmANOVA; $F_{(1,20)} = 5.56, p = 0.030$). Running separate two-way rmANOVAs (Session*Side) on each of the relative distances revealed a significant decrease in the relative eccentricity between the lip and D5 after RSS only ($F_{(1,20)} = 5.56, p = 0.029$). No RSS-induced effect was found for D2-D5 or Lip-D2 relative distances. A significant decrease of the $\Delta\theta$ angle was observed after RSS between D2 and D5 only (three-way rmANOVA; $F_{(2,40)} = 3.55, p = 0.038; p_{LSD} = 0.032$). Separate two-way rmANOVAs (Session*Side) on each relative distance revealed a significant increase of the $\Delta\theta$ angle between the Lips and D2 after RSS ($F_{(1,20)} = 6.40, p = 0.020$). No effect was observed for D2-D5 & Lip-D5 $\Delta\theta$ angles. Similarly, no RSS-induced changes were observed for $\Delta\phi$ angles.

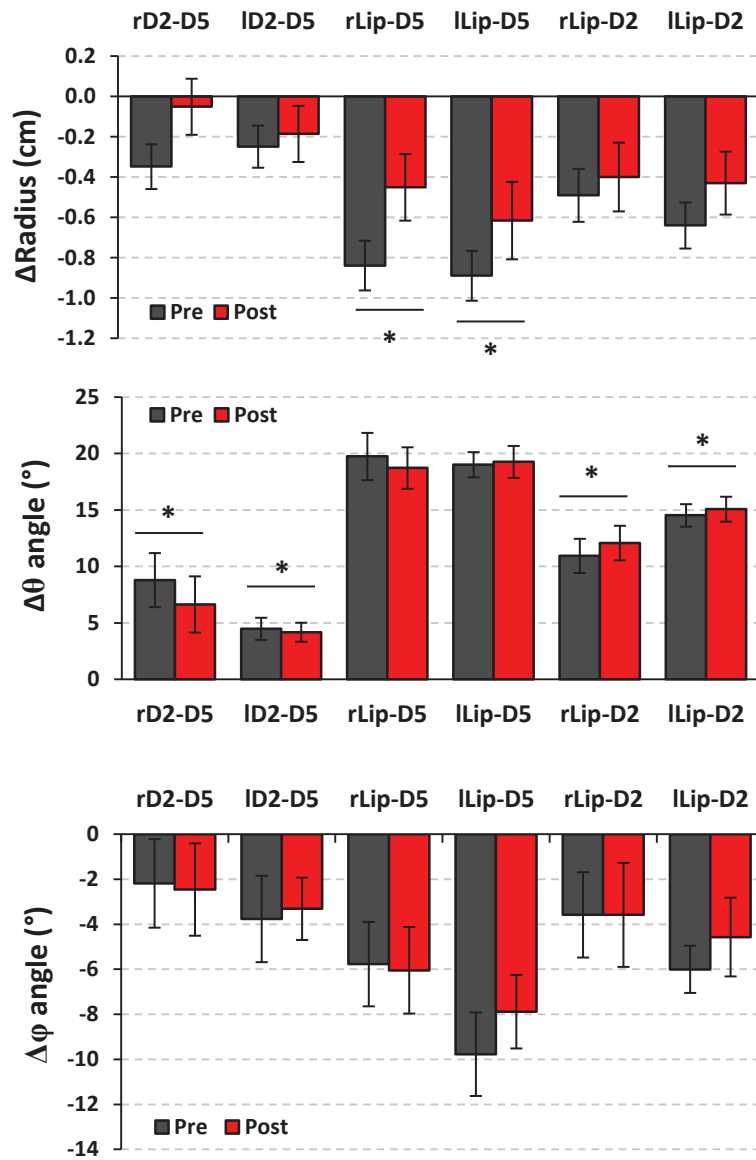


Figure 17. Mean differential Polar coordinates between the ECDs of the tested body-sites, Pre (black) and Post (red) RSS. **From top to bottom:** Mean Δeccentricity (or radius, in mm), mean Δtheta and mean Δphi angles, both in degrees. Note that the sign of the phi angles was inverted for the left body-sites (normally negative) to allow comparison with the right body-sites. r/lD2-D5: distance between D2 and D5 of the right or left side; r/lLip-D5: distance between Lip and D5 of the right or left side; r/lLip-D2: distance between Lip and D2 of the right or left side.

Altogether, we report after RSS an increased Lip-D2 ED, associated with a decrease in Lip-D5 eccentricity, a decreased Δtheta angle between D2 and D5, and an increased Lip-D2 Δtheta angle.

Dipole strength was significantly different across body-sites (Figure 18; $F_{(2,40)} = 9.36$, $p < 5 \cdot 10^{-4}$), the lips exhibiting significantly higher dipole strength than the fingertips (both p_{Bonf} values < 0.023). In addition, a significant interaction between sessions and sides was found

($F_{(1,20)} = 4.50$, $p = 0.047$), with the dipole strengths obtained at the Post-session being significantly higher for the right body-sites than for the left ones ($p_{LSD} = 0.027$). Given the difference between lips and fingertips, their datasets were separately submitted to two-way rmANOVAs (Session*Side). While no significant difference was observed for the lips, the strength of D5 dipoles was significantly smaller than that of D2 dipoles ($F_{(1,20)} = 5.11$, $p = 0.035$). In addition, an interaction with the finger side was revealed ($F_{(1,20)} = 5.29$, $p = 0.032$), the left-D5 dipole being weaker than both left- and right-D2 dipoles (both p_{LSD} values < 0.022), and right-D5 having a weaker dipole strength than left-D2 ($p_{LSD} = 0.027$). Finally, note the tendency for an inverse pattern between left- and right-D2 ($p = 0.086$), suggesting that right-D2 dipole strength increased after RSS while left-D2 strength decreased.

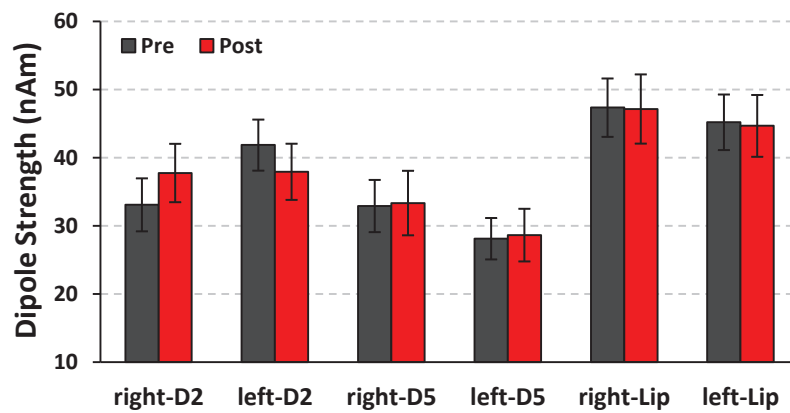


Figure 18. Mean dipole strength (nAm) of the first prominent component obtained Pre (black) and Post (red) RSS for each of the tested body-sites: right- and left-D2, right- and left-D5, right- and left-Lip.

Finally, no significant linear correlation was found between changes in dipole localization (ED, Δ radius or $\Delta\theta$ angles) and 2PDT changes (all p values > 0.05).

Discussion

The purpose of this study was to assess the neurophysiological substrates underlying the RSS-induced plastic changes recently observed across the hand-face border and to evaluate how they relate to the perceptual changes. In agreement with our previous reports (Muret et al., 2014, study 2 in this thesis), we found that three hours of RSS at the right-D2 fingertip improved spatial acuity not only at this finger, but also at both sides of the upper-lip, while the homologous left-D2 was unaffected. Additionally, in this present study we report for the first time the absence of behavioural effects on both little fingers. In parallel with these behavioural changes, dipole model source analyses revealed after RSS: (i) an increased distance between Lip and D2 dipoles (ED and $\Delta\theta$ angle), (ii) a decrease in Lip-D5 relative eccentricity, and (iii) a decreased distance between D2 and D5 dipoles ($\Delta\theta$ angle). In addition, the dipole strengths after RSS were found to be stronger for the right body-sites than for the left ones. Altogether, these results first confirm the existence of cross-border changes following RSS, with relative changes between the stimulated finger and the lip, but also suggest that changes are widespread - reaching the other hemisphere. Finally, these results underline the dynamic property of somatotopic maps, which likely fluctuate with time depending on the use, configuration, and stimulation of body-sites.

Behavioural results

In agreement with our previous findings (Muret et al., 2014), we report that three hours of RSS at right-D2 improved tactile acuity not only at this fingertip, but also at both sides of the upper-lip. However, smaller behavioural effects were observed in the present study than in the previous report (Muret et al., 2014). Indeed, a higher proportion of participants did not exhibit the right-D2 threshold decrease, which is the marker of the effectiveness of the RSS procedure. In addition, a lower proportion showed the mutual decrease at both right-D2 and the lips, and the average threshold decreases were lower. Altogether, these facts suggest a lower efficiency of the RSS procedure in this study, which resulted in a lower “transfer” of the effects towards the face. A possible explanation arises from the type of stimulation used during the MEG mapping procedure. Indeed, one has to consider that the repetitive stimulation performed during the MEG mapping could have itself induced some cortical reorganization. More importantly, note that the tapping-like pneumatic stimulation used during the mapping procedure with quite short and jittered ISIs (400-600ms) is highly similar to the RSS procedure. The main difference between these two procedures arises from the fact that instead of stimulating right-D2 only, during the mapping body-sites were randomly stimulated, which could be considered as an “asynchronous”

stimulation of these regions. Given that asynchronous RSS protocols across fingers have been shown to result in spatial acuity impairments (Hodzic et al., 2004; Kalisch et al., 2007), it is possible that the mapping procedure somewhat interfered with the RSS procedure. This could explain the lower RSS-induced behavioural changes reported here. Moreover, the longer time interval between tactile threshold assessments and the RSS procedure due to the interleaved MEG sessions (~1h instead of ~15min) could also have played a role in producing the smaller behavioural effects. Indeed, while the threshold decrease has been reported to be significant 2h after RSS (Godde et al., 2000), it was undoubtedly on the way back to baseline levels.

Despite the possible interfering factors described above, similar mean effects were observed at the group level, as well as at the individual level when considering participants for whom RSS was effective. In addition to replicating the effects at right-D2 and both sides of the upper-lip, we report that similar to left-D2, RSS at right-D2 does not affect the thresholds at both little fingers. This result is in line with previous reports of no change at the adjacent finger (right-D3; Godde et al., 2000; Muret et al., in preparation), and supports the idea that RSS-induced perceptual changes are limited to the stimulated finger and do not spread to other fingers within the hand, likely through intracortical **inhibitory** connections underlying lateral inhibition (Simões et al., 2001; Négyessy et al., 2013).

ECDs as a source model

The quality of the ECDs was confirmed by the high GoF observed across both body-sites and sessions. This ensured that our models explained more than 95% of the variance, which is the gold-standard in dipole model source analysis (see Hämäläinen et al., 1993; Kakigi et al., 2000). Note that the higher GoF observed for the lips compared to the fingertips is likely to arise from a systematic, even if small, ipsilateral activity induced by finger stimulation (Schnitzler et al., 1995; Sutherland and Tang, 2006; Hadoush et al., 2010), which we did not systematically model. In addition, the incertitude in our dipole localizations was on average below 1mm (i.e., 5mm³ on average, 52mm³ maximum), which is relatively small considering the spatial resolution that MEG offers and the values usually reported in the literature (i.e., Elbert et al., 1995; Flor et al., 1995: < 300mm³; Hlushchuk et al., 2004; Suzuki et al., 2004: < 1cm³; Knecht et al., 1998: < 300cm³). Altogether, these parameters demonstrate the reliability of our ECDs to model the relatively simple activity evoked within the primary somatosensory cortex following finger and face stimulation.

Because of the nature of the stimulation employed for the mapping procedure (i.e., mechanical), and given the orientation of SI subregions and the fact that MEG sensors record

predominantly the activity arising tangentially from the scalp (Hämäläinen et al., 1993), these responses are likely to arise from activity within BA3b (i.e., anterior wall of the post-central gyrus) and BA2 (i.e., posterior wall of the post-central gyrus), with BA1 activity possibly weighting the resulting fields. Intracranial recording studies have confirmed that BA3b and BA1 contribute the most to the peak in the type of evoked response examined here (Baumgartner et al., 1993).

Somatotopic organization

Consistent with the classical somatotopic organization of the primary somatosensory cortex (Penfield and Rasmussen, 1950; Nakamura et al., 1998), polar coordinates and Euclidean distances revealed that dipoles of D5, D2 and the Lip were sequentially more ventral and anterior. The largest differences between body-sites were observed along the dorso-ventral direction (i.e., y axis and theta angle), and some differences between body sides were also observed. First, dipole eccentricities were globally smaller for the right body side (i.e., left hemisphere), than for the left (i.e., right hemisphere). This result suggests an asymmetry between hemispheres, which has already been reported using MEG but following electrical median nerve stimulation (Jung et al., 2003, 2008). Surprisingly, in contrast to the hemispheric asymmetries reported in the primary motor cortex (e.g., Amunts et al., 1996), these studies also showed that this asymmetry of somatosensory representations was not correlated with handedness (Jung et al., 2003, 2008). Thus, the cause and functional relevance of such interhemispheric asymmetry remains to be clarified for the somatosensory domain. In addition to this overall asymmetry, the ED between D2 and D5 dipoles was significantly larger for the right body-sites than for the left. This difference is consistent with previous reports (Imai et al., 2003) and suggests a larger somatosensory representation of the dominant hand. Supporting this view, it has been reported that the rostral area of the post-central gyrus is more extended in the left than in the right hemisphere (Jung et al., 2003). Finally, there was also an asymmetry in dipole localization between the lip and D2 finger, as several measures (ED, Δ theta and z) revealed a smaller distance between their dipoles for the right side. Together with the larger D2-D5 distance mentioned above and the absence of Lip-D5 asymmetry, this novel result suggests a higher proximity between the lip and D2 representations in the left hemisphere, either due to a smaller D1 representation in between them, to a smaller lip representation (but in this case we would have expected differences in dipole strength), or more likely due to more overlapping representations than in the right hemisphere. But this remains to be investigated.

As expected from the shorter conduction pathways, shorter peak latencies were observed for the lips than for the fingers. But surprisingly, shorter latencies were observed for the left fingers than for the right ones. This unexpected result could come from differences in the membrane fixation since different experimenters fixed the membranes on the left and right body sites, or from "lateralization" but in this case we might have expected to see shorter latencies for the dominant hand). Note that even in the case of different fixations, this would have led to differences in stimulation intensity, which typically alter the dipole strength and latency (the higher the intensity, the higher the dipole strength and the lower the latency), but not localization (e.g., Hoshiyama and Kakigi, 2001; Otsuru et al., 2011). All possible precautions were taken to minimize the variability in stimulation location using the UV-visible marks. Moreover, the relative comparison of sessions also account for such differences. Finally, the dipole strength was larger for the lips compared to the fingertips, and - ignoring the differences between body sides - also larger for D2 compared to D5. Given that the current dipole strength is hypothesized to be an indicator of the net strength of cortical polarization, which reflects the total number of synchronously firing neurons contributing to the stimulus-driven cortical response (Williamson and Kaufman, 1990), these differences can reflect a larger/smaller neuronal population (i.e., representation) for the lip/D5. Such differences in cortical magnification are thought to be related to the differential sensitivity/acuity across body-sites, arising from the differential densities of receptors embedded in the skin.

RSS-induced changes

Despite the reliability of our ECDs (see above), a shift of approximately 6mm was observed across sessions for the ECDs of all body-sites. Such unspecific changes in dipole location could arise from an altered re-positioning of the participant's head inside the MEG helmet during the two recording sessions, co-registration errors, or systematic head motion. However, since all body-sites were stimulated within a given block, these possible causes can be excluded as one would have expected the ECD locations for the different regions to be similarly affected at the individual level, which was not the case. In line with this, a systematic shift at the individual level would have left the relative distances unaltered, which is again not the case. Furthermore, localization of head position was carefully checked at the beginning of each block ensuring the stability of the head position throughout the recording. These causes excluded, one remaining possibility is that the membranes/stimulators might have been attached slightly differently across body-sites and sessions, resulting in slightly different intensities of stimulation. However, changes in stimulation intensity have typically been shown to alter the dipole strength and

latency (the higher the intensity, the higher the dipole strength and the lower the latency), but not its localization (e.g., Hoshiyama and Kakigi, 2001; Otsuru et al., 2011). These methodological aspects being unlikely responsible for these 6mm shifts, our data suggest instead a real shift of all body-sites in different directions, as we found changes in their relative distances.

Similarly to the behavioural results, the repetitive stimulation performed during the MEG mapping could have itself induced some cortical reorganization which could explain these shifts. In line with this, task-free somatosensory stimulation paradigms have been shown to induce cortical changes depending on their stimulus properties (Braun et al., 2000b). Thus, despite the fact that each body-site received the exact same amount of stimuli and that stimuli were randomized, this repetitive stimulation may have led to some cortical changes. More importantly, note that the tapping-like pneumatic stimulation used during the mapping procedure with quite short and jittered ISIs (400-600ms) is highly similar to the RSS procedure. The main difference arises from the fact that body-sites were randomly stimulated instead of solely right-D2, which could be considered as an “asynchronous” stimulation of these regions. Given that such asynchronous stimulation were found to result in a segregation of cortical representations (e.g., Hodzic et al., 2004), this may have interfered with the RSS-induced cortical changes (as for the perceptual ones). Despite all these considerations, given that the exact same procedure was followed during each session, the Pre/Post design of this study allow for a direct estimation of the RSS-induced changes.

Following RSS at right-D2, a decrease in eccentricity was observed for all body-sites, suggesting a “deepening” or downward shift of all dipoles. However, further analysis revealed that this effect was mainly driven by a decreased eccentricity between the lip and D5 dipoles. Given the sequential distribution of the dipoles, one possibility is that each body-site may have slightly shifted down towards the lips, but that the “cumulative” effect made the shift significant for D5 only. Consistent with the shift of D5 towards the lip, a decreased $\Delta\theta$ angle was found between D2 and D5 dipoles. Finally, an increased distance between the lip and D2 dipoles was observed with two measures ($\Delta\theta$ and ED), suggesting that their dipoles moved apart from each other. Thus, another possibility is that D2 and Lip dipoles shifted towards that of D5, but that D2 shifted more than the lip. Given that an enlargement of the cortical representation of right-D2 has been reported by our team and others using fMRI (Pleger et al, 2003; Hodzic et al, 2004; Muret et al, in preparation), a possible explanation is that the enlargement of right-D2 displaced the lip representation away from it, while D5 moved towards D2/Lip. The tendency for an increased dipole strength for right-D2 is consistent with right-D2 enlargement. However,

given that the dipole strength for the lips and D5 did not change (not even a tendency), it is unlikely that right-D2 enlargement occurred to the detriment of the lip and D5 representations, as would be expected by the classically-defined “invasion” idea. Instead, these relative shifts are likely to have not altered the adjacent representations, but rather their relative overlap.

Importantly, the RSS-induced effects reported here were not influenced by body sides, suggesting changes in dipole location in both the left and right hemisphere. Given the strong transcallosal connectivity (at least between BA2s), changes in the hemisphere ipsilateral to the right-D2 which received the RSS may arise from a transfer, likely through right-D2 representations and/or the lips whose representations are known to be bilateral (more than fingers). Another alternative would be that RSS induces plastic changes primarily within the thalamus, then projecting to both hemispheres.

The only side-specific changes we observed were a higher dipole strength for the right body-sites than the left after RSS. Given that the current dipole strength is hypothesized to be an indicator of the net strength of cortical polarization, which reflects the total number of synchronously firing neurons contributing to the stimulus-driven cortical response (Williamson and Kaufman, 1990), these enhanced dipole strengths suggest a potentiation of the representations among the left hemisphere. This is consistent with the postulated mechanisms underlying RSS.

Conclusion

To conclude, in addition to the improved spatial discrimination at the RSS-stimulated finger (right-D2) and to both sides of the upper-lip, the present study reveals that the tactile acuity at both little fingers is not affected by the RSS procedure. Associated with these perceptual changes, dipole source analysis revealed relative shifts of all dipoles (Lip, D2 and D5), resulting in an increased distance between the sources of the Lips and D2, and a decreased distance between the little fingers and both the Lip and D2. After RSS, dipole strengths for the right body-sites (ipsilateral to RSS) were stronger than those of the left side. Altogether, these results first confirm the existence of cross-border changes following RSS, with relative changes between the stimulated finger and the lip, but also suggest that RSS induces widespread changes reaching the other hemisphere.

Supplementary Results

A three-way rmANOVA (Session*Body-sites*Side) revealed a significant difference between the relative distance between body-sites along the **x axis** ($F_{(2,40)} = 4.87, p = 0.013$), the distance between Lip and D5 being larger than that between D2 and D5 ($p_{LSD} = 0.004$). Running separate two-way rmANOVAs (Session*Side) on each relative distance did not reveal any further effect or interaction. Similar analysis performed on the relative distance between body-sites along the **y axis** did not reveal any significant differences.

Conversely, along the **z axis** a significant difference between the relative distance between body-sites was found (three-way rmANOVA; $F_{(2,40)} = 35.24, p < 10^{-6}$). Post-hoc analyses revealed that the distance along the **z axis** between body-sites gradually and significantly increased from D2-D5, to Lip-D2, the largest distance being between the Lip and D5 (all p_{LSD} values $< 5 \times 10^{-4}$). In addition, a significant interaction between relative distances and sides was found ($F_{(2,40)} = 4.76, p = 0.014$), coming from a larger distance between the Lip and D2 for the left areas than for the right ones ($p_{LSD} = 0.005$). Running separate two-way rmANOVAs (Session*Side) on each relative distance further confirmed this effect ($F_{(1,20)} = 10.53, p = 0.004$).

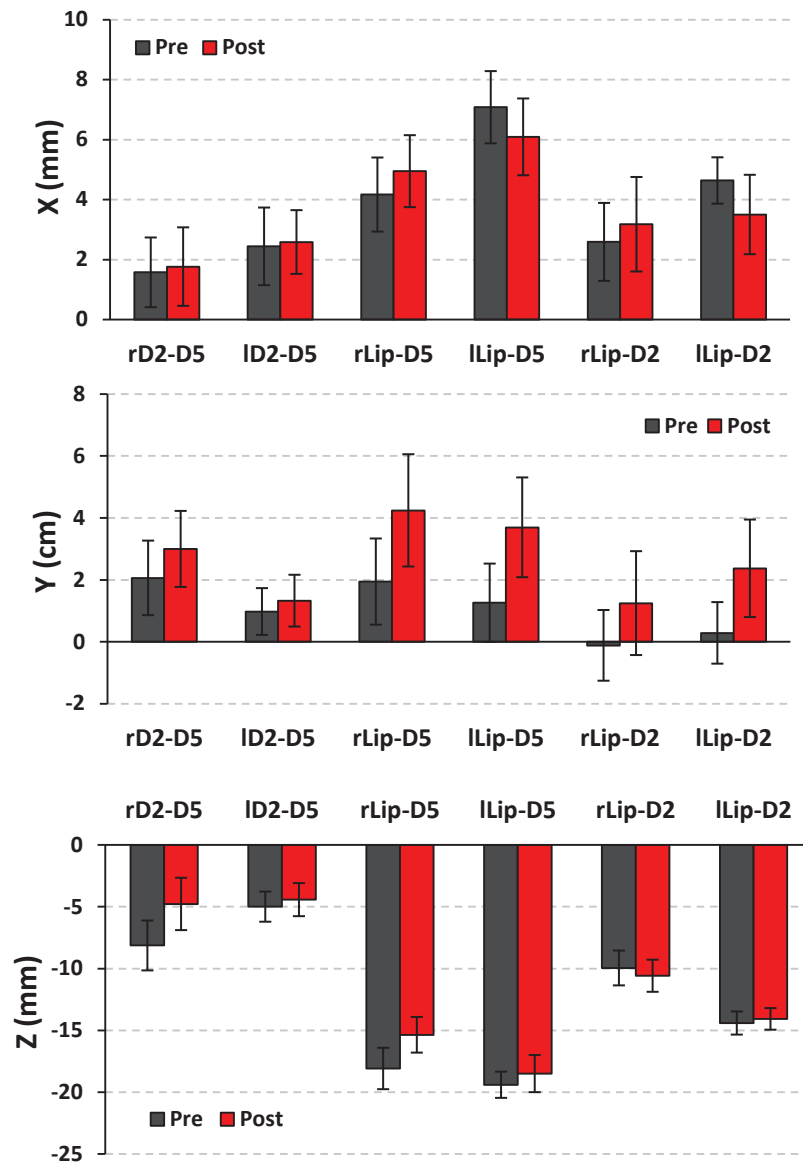


Figure S1. Mean relative distance (mm) between body-sites along the x (top), y (middle) and z (bottom) axis, Pre (black) and Post (red) RSS. Note that for the y axis, the sign was inverted for the left body-sites (normally negative) to allow comparison with the right body-sites. r/lD2-D5: distance between D2 and D5 of the right or left side; r/lLip-D5: distance between Lip and D5 of the right or left side; r/lLip-D2: distance between Lip and D2 of the right or left side.

References

- Amunts K, Schlaug G, Schleicher A, Steinmetz H, Dabringhaus A, Roland PE, Zilles K (1996) Asymmetry in the human motor cortex and handedness. *Neuroimage* 4:216–222.
- Baumgartner C, Doppelbauer A, Sutherling WW, Lindinger G, Levesque MF, Aull S, Zeitlhofer J, Deecke L (1993) Somatotopy of human hand somatosensory cortex as studied in scalp EEG. *Electroencephalogr Clin Neurophysiol* 88:271–279.
- Beste C, Dinse HR (2013) Learning without training. *Curr Biol* 23:R489–R499.
- Blatow M, Nennig E, Durst A, Sartor K, Stippich C (2007) fMRI reflects functional connectivity of human somatosensory cortex. *Neuroimage* 37:927–936.
- Braun C, Wilms A, Schweizer R, Godde B, Preissl H, Birbaumer N (2000) Activity patterns of human somatosensory cortex adapt dynamically to stimulus properties. *Neuroreport* 11:2977–2980.
- Clark SA, Allard T, Jenkins WM, Merzenich MM (1988) Receptive fields in the body-surface map in adult cortex defined by temporally correlated inputs. *Nature* 332:444–445.
- Craig JC, Johnson KO (2000) The Two-Point Threshold : Not a Measure of Tactile Spatial Resolution. *Am Psychol Soc* 9:29–32.
- Devonshire IM, Papadakis NG, Port M, Berwick J, Kennerley AJ, Mayhew JEW, Overton PG (2012) Neurovascular coupling is brain region-dependent. *Neuroimage* 59:1997–2006.
- Dinse HR, Kleibel N, Kalisch T, Ragert P, Wilimzig C, Tegenthoff M (2006) Tactile coactivation resets age-related decline of human tactile discrimination. *Ann Neurol* 60:88–94.
- Dinse HR, Ragert P, Pleger B, Schwenkreis P, Tegenthoff M (2003) Pharmacological modulation of perceptual learning and associated cortical reorganization. *Science* 301:91–94.
- Disbrow E a, Hinkley LBN, Roberts TPL (2003) Ipsilateral representation of oral structures in human anterior parietal somatosensory cortex and integration of inputs across the midline. *J Comp Neurol* 467:487–495.
- Dutta A, Kambi N, Raghunathan P, Khushu S, Jain N (2013) Large-scale reorganization of the somatosensory cortex of adult macaque monkeys revealed by fMRI. *Brain Struct Funct* 219:1305–1320.
- Eickhoff SB, Grefkes C, Fink GR, Zilles K (2008) Functional lateralization of face, hand, and trunk representation in anatomically defined human somatosensory areas. *Cereb cortex* 18:2820–2830.
- Elbert T, Pantev C, Wienbruch C, Rockstroh B, Taub E (1995) Increased cortical representation of the fingers of the left hand in string players. *Science* (80-) 270:305–307.
- Flor H, Elbert T, Knecht S, Wienbruch C, Pantev C, Birbaumer N, Larbig W, Taub E (1995) Phantom-limb pain as a perceptual correlate of cortical reorganization following arm amputation. *Nature* 375:482–484.
- Gibson GO, Makinson CD, Sathian K (2009) Tactile co-activation improves detection of afferent spatial modulation. *Exp Brain Res* 194:409–417.
- Godde B, Ehrhardt J, Braun C (2003) Behavioral significance of input-dependent plasticity of human somatosensory cortex. *Neuroreport* 14:543–546.
- Godde B, Stauffenberg B, Spengler F, Dinse HR (2000) Tactile coactivation-induced changes in spatial discrimination performance. *J Neurosci* 20:1597–1604.

- Hadoush H, Inoue K, Nakanishi K, Kurumadani H, Sunagawa T, Ochi M (2010) Ipsilateral primary sensorimotor cortical response to mechanical tactile stimuli. *Neuroreport* 21:108–113.
- Hämäläinen M, Hari R, Ilmoniemi RJ, Knuutila J, Lounasmaa O V (1993) Magnetoencephalography - theory, instrumentaton, and applications to noninvasive studies of the working human brain. *Rev Mod Phys* 65:413–497.
- Harrar V, Spence C, Makin TR (2014) Topographic generalization of tactile perceptual learning. *J Exp Psychol Hum Percept Perform* 40:15–23.
- Harris JA, Harris IM, Diamond ME (2001) The topography of tactile learning in humans. *J Neurosci* 21:1056–1061.
- Hlushchuk Y, Forss N, Hari R (2004) Distal-to-proximal representation of volar index finger in human area 3b. *Neuroimage* 21:696–700.
- Hodzic A, Veit R, Karim AA, Erb M, Godde B (2004) Improvement and decline in tactile discrimination behavior after cortical plasticity induced by passive tactile coactivation. *J Neurosci* 24:442–446.
- Hoffmeyer HW, Enager P, Thomsen KJ, Lauritzen MJ (2007) Nonlinear neurovascular coupling in rat sensory cortex by activation of transcallosal fibers. *J Cereb Blood Flow Metab* 27:575–587.
- Hoshiyama M, Kakigi R (2001) Two evoked responses with different recovery functions in the primary somatosensory cortex in humans. *Clin Neurophysiol* 112:1334–1342.
- Hoshiyama M, Ryusuke K, Koyama S, Kitamura Y, Shimojo M, Watanabe S, Kakigi R (1996) Somatosensory evoked magnetic fields following stimulation of the lip in humans. *Electroencephalogr Clin Neurophysiol* 100:96–104.
- Hu K-S, Kwak J, Koh K-S, Abe S, Fontaine C, Kim H-J (2007) Topographic distribution area of the infraorbital nerve. *Surg Radiol Anat* 29:383–388.
- Huttunen JK, Gröhn O, Penttonen M (2008) Coupling between simultaneously recorded BOLD response and neuronal activity in the rat somatosensory cortex. *Neuroimage* 39:775–785.
- Iannetti G., Porro C., Pantano P, Romanelli P., Galeotti F, Cruccu G (2003) Representation of different trigeminal divisions within the primary and secondary human somatosensory cortex. *Neuroimage* 19:906–912.
- Imai T, Kamping S, Breitenstein C, Pantev C, Lütkenhöner B, Knecht S (2003) Learning of tactile frequency discrimination in humans. *Hum Brain Mapp* 18:260–271.
- Inoue K, Nakanishi K, Hadoush H, Kurumadani H, Hashizume A, Sunagawa T, Ochi M (2013) Somatosensory mechanical response and digit somatotopy within cortical areas of the postcentral gyrus in humans: an MEG study. *Hum Brain Mapp* 34:1559–1567.
- Jain N, Catania KC, Kaas JH (1997) Deactivation and reactivation of somatosensory cortex after dorsal spinal cord injury. *Nature* 386:495–498.
- Johnson KO, Phillips JR (1981) Tactile spatial resolution. I. Two-point discrimination, gap detection, grating resolution, and letter recognition. *J Neurophysiol* 46:1177–1192.
- Jung P, Baumgärtner U, Bauermann T, Magerl W, Gawehn J, Stoeter P, Treede R-D (2003) Asymmetry in the human primary somatosensory cortex and handedness. *Neuroimage* 19:913–923.
- Jung P, Baumgärtner U, Magerl W, Treede R-D (2008) Hemispheric asymmetry of hand representation in human primary somatosensory cortex and handedness. *Clin Neurophysiol* 119:2579–2586.

- Kakigi R, Hoshiyama M, Shimojo M, Naka D, Itomi K, Nakamura A, Yamasaki H, Watanabe S, Xiang J, Maeda K, Lam K (2000) The somatosensory evoked magnetic fields. *Prog Neurobiol* 61:495–523.
- Kalisch T, Tegenthoff M, Dinse HR (2007) Differential effects of synchronous and asynchronous multifinger coactivation on human tactile performance. *BMC Neurosci* 8:58.
- Knecht S, Henningsen H, Höhling C, Elbert T, Flor H, Pantev C, Taub E (1998) Plasticity of plasticity? Changes in the pattern of perceptual correlates of reorganization after amputation. *Brain* 121:717–724.
- Lin C-CK, Sun Y, Huang C-I, Yu C-Y, Ju M-S (2010) Cortical activation by tactile stimulation to face and anterior neck areas: an fMRI study with three analytic methods. *Hum Brain Mapp* 31:1876–1885.
- Mertens M, Lütkenhöner B, Lu B (2000) Efficient neuromagnetic determination of landmarks in the somatosensory cortex. *Clin Neurophysiol* 111:1478–1487.
- Mogilner A, Nomura M, Ribary U, Jagow R, Lado F, Rusinek H, Llinás R (1994) Neuromagnetic studies of the lip area of primary somatosensory cortex in humans: evidence for an oscillotopic organization. *Exp brain Res* 99:137–147.
- Moore CI, Cao R (2008) The hemo-neural hypothesis: on the role of blood flow in information processing. *J Neurophysiol* 99:2035–2047.
- Muret D, Dinse HR, Macchione S, Urquizar C, Farnè A, Reilly KT (2014) Touch improvement at the hand transfers to the face. *Curr Biol* 24:R736–R737.
- Muret D, Martuzzi R, Dinse HR, Reilly KT, Blanke O, Farnè A (n.d.) Cortical correlates of perceptual changes transferring from the finger to the lips in human SI revealed by 7T fMRI.
- Nakamura A, Yamada T, Goto A, Kato T, Ito K, Abe Y, Kachi T, Kakigi R (1998) Somatosensory homunculus as drawn by MEG. *Neuroimage* 7:377–386.
- Négyessy L, Pálfi E, Ashaber M, Palmer C, Jákl B, Friedman RM, Chen LM, Roe AW (2013) Intrinsic horizontal connections process global tactile features in the primary somatosensory cortex: neuroanatomical evidence. *J Comp Neurol* 521:2798–2817.
- Nevalainen P, Ramstad R, Isotalo E, Haapanen M-L, Lauronen L (2006) Trigeminal somatosensory evoked magnetic fields to tactile stimulation. *Clin Neurophysiol* 117:2007–2015.
- Nguyen BT, Tran TD, Hoshiyama M, Inui K, Kakigi R (2004) Face representation in the human primary somatosensory cortex. *Neurosci Res* 50:227–232.
- Oldfield RC (1971) The assessment and analysis of handedness: the Edinburgh inventory. *Neuropsychologia* 9:97–113.
- Onishi H, Oyama M, Soma T, Kubo M, Kirimoto H, Murakami H, Kameyama S (2010) Neuromagnetic activation of primary and secondary somatosensory cortex following tactile-on and tactile-off stimulation. *Clin Neurophysiol* 121:588–593.
- Otsuru N, Inui K, Yamashiro K, Urakawa T, Keceli S, Kakigi R (2011) Effects of prior sustained tactile stimulation on the somatosensory response to the sudden change of intensity in humans: an magnetoencephalography study. *Neuroscience* 182:115–124.
- Parianen Lesemann FH, Reuter E-M, Godde B (2015) Tactile stimulation interventions: Influence of stimulation parameters on sensorimotor behavior and neurophysiological correlates in healthy and clinical samples. *Neurosci Biobehav Rev* 51:126–137.

- Penfield W, Boldrey E (1937) Somatic motor and sensory representation in the cerebral cortex of man as studied by electrical stimulation. *Brain* 60:389–443.
- Penfield W, Rasmussen T (1950) *The cerebral cortex of man: a clinical study of localization of function*. New York Macmillan Compagny.
- Pilz K, Veit R, Braun C, Godde B (2004) Effects of co-activation on cortical organization and discrimination performance. *Neuroreport* 15:2669–2672.
- Pleger B, Dinse HR, Ragert P, Schwenkreis P, Malin JP, Tegenthoff M (2001) Shifts in cortical representations predict human discrimination improvement. *Proc Natl Acad Sci USA* 98:12255–12260.
- Pleger B, Foerster A-F, Ragert P, Dinse HR, Schwenkreis P, Malin J-P, Nicolas V, Tegenthoff M (2003) Functional imaging of perceptual learning in human primary and secondary somatosensory cortex. *Neuron* 40:643–653.
- Pons TP, Garraghty PE, Ommaya AK, Kaas JH, Taub E, Mishkin M (1991) Massive cortical reorganization after sensory deafferentation in adult macaques. *Science* 252:1857–1860.
- Rosa MJ, Kilner J, Blankenburg F, Josephs O, Penny W (2010) Estimating the transfer function from neuronal activity to BOLD using simultaneous EEG-fMRI. *Neuroimage* 49:1496–1509.
- Schnitzler A, Salmelin R, Salenius S, Jousm V, Hari R (1995) Tactile information from the human hand reaches the ipsilateral primary somatosensory cortex. *Neurosci Lett* 200:25–28.
- Simões C, Mertens M, Forss N, Jousmäki V, Lange J, Lütkenhöner B, Hari R (2001) Functional overlap of finger representations in human SI and SII cortices. *J Neurophysiol* 86:1661–1665.
- Stavrinou ML, Penna S Della, Pizzella V, Torquati K, Cianflone F, Franciotti R, Bezerianos A, Romani GL, Rossini PM (2007) Temporal dynamics of plastic changes in human primary somatosensory cortex after finger webbing. *Cereb Cortex* 17:2134–2142.
- Stoeckel MC, Pollok B, Schnitzler A, Seitz RJ (2007) Studying the human somatosensory hand area: A new way to compare fMRI and MEG. *J Neurosci Methods* 164:280–291.
- Sutherland MT, Tang AC (2006) Reliable detection of bilateral activation in human primary somatosensory cortex by unilateral median nerve stimulation. *Neuroimage* 33:1042–1054.
- Suzuki T, Shibukawa Y, Kumai T, Shintani M (2004) Face area representation of primary somatosensory cortex in humans identified by whole-head magnetoencephalography. *Jpn J Physiol* 54:161–169.
- Tandon S, Kambi N, Lazar L, Mohammed H, Jain N (2009) Large-scale expansion of the face representation in somatosensory areas of the lateral sulcus after spinal cord injuries in monkeys. *J Neurosci* 29:12009–12019.
- Tecchio F, Rossini P., Pizzella V, Cassetta E, Pasqualetti P, Romani G. (1998) A neuromagnetic normative data set for hemispheric sensory hand cortical representations and their interhemispheric differences. *Brain Res Protoc* 2:306–314.
- Thees S, Blankenburg F, Taskin B, Curio G, Villringer A (2003) Dipole source localization and fMRI of simultaneously recorded data applied to somatosensory categorization. *Neuroimage* 18:707–719.
- Tuunanen PI, Kavec M, Jousmäki V, Usenius J-P, Hari R, Salmelin R, Kauppinen RA (2003) Comparison of BOLD fMRI and MEG characteristics to vibrotactile stimulation. *Neuroimage* 19:1778–1786.
- Wang X, Merzenich MM, Sameshima K, Jenkins WM (1995) Remodelling of hand representation in adult cortex determined by timing of tactile stimulation. *Nature* 378:71–75.

- Weiss T, Miltner WHR, Liepert J, Meissner W, Taub E (2004) Rapid functional plasticity in the primary somatomotor cortex and perceptual changes after nerve block. *Eur J Neurosci* 20:3413–3423.
- Williamson SJ, Kaufman L (1990) Evolution of neuromagnetic topographic mapping. *Brain Topogr* 3:113–127.
- Wühle A, Mertiens L, Rüter J, Ostwald D, Braun C (2010) Cortical processing of near-threshold tactile stimuli: an MEG study. *Psychophysiology* 47:523–534.
- Wühle A, Preissl H, Braun C (2011) Cortical processing of near-threshold tactile stimuli in a paired-stimulus paradigm--an MEG study. *Eur J Neurosci* 34:641–651.
- Yvert B, Bertrand O, Echallier JF, Pernier J (1996) Improved dipole localization using local mesh refinement of realistic head geometries: An EEG simulation study. *Electroencephalogr Clin Neurophysiol* 99:79–89.
- Zhu Z, Disbrow E a, Zumer JM, McGonigle DJ, Nagarajan SS (2007) Spatiotemporal integration of tactile information in human somatosensory cortex. *BMC Neurosci* 8:1–14.

GENERAL DISCUSSION

I. Main results

In addition to its strong social and emotional valence, touch plays a critical role in our daily life to grasp and manipulate objects, or simply walk. Touch was also one of the first senses to be investigated in the brain of both human and non-human primates using intracranial recordings and cortical stimulation procedures, due to the easy access to the post-central gyrus where the primary somatosensory cortex (SI) is located. These early and groundbreaking experiments revealed the peculiar somatotopic organization of the primary somatosensory areas, and gave rise to the so-called *Homunculus*. However, while most of the tactile information arising from our body surface is represented following an order similar to the physical continuity of our skin, the hand and the face representations generate a major discontinuity within the homunculus by their direct cortical proximity. The border separating these two representations has been widely used as a somatotopic landmark to study one of the most fascinating features of our brain, its capacity for reorganization. In the 90s, groundbreaking electrophysiological studies revealed that deprivation-induced somatosensory plasticity, until then thought to be limited to a few millimetres, could actually cross the hand-face border. While it has been known for a long time that increasing inputs also leads to cortical changes typically associated with perceptual benefits, whether such plasticity can cross the hand-face border remains unknown. My thesis work aimed to investigate this question using a protocol of repetitive somatosensory stimulation (RSS) known to induce transient somatosensory plasticity associated with tactile acuity improvements, which until my work were thought to be largely local (i.e., finger-specific).

In a first behavioural study, we showed that three hours of RSS at the tip of the right index finger improved tactile discrimination not only at the stimulated fingertip, but also at both sides of the unstimulated upper-lip and at the right cheek. In contrast, the left index finger was unaffected. These findings provide the first evidence that passively *increasing* input to the hand can positively affect tactile perception at a region of the body that is cortically close, but physically distant. Given that, although limited in number, horizontal intracortical connections exist between the hand and face representations (Manger et al., 1997; Florence et al., 1998; Fang et al., 2002), and can undergo hebbian-based plastic changes (Marik and Hickmott, 2009; Paullus and Hickmott, 2011), we hypothesized that the remote behavioural changes induced by RSS could arise from plastic changes spreading across the SI hand-face border via these connections. Together with the fact that an expansion and a shift of the cortical representation of

the RSS-stimulated finger (i.e., right-D2) has been repeatedly reported in SI (Pleger et al., 2001, 2003; Godde et al., 2003; Hodzic et al., 2004), the behavioural results of this first study bring to the following predictions: (i) the lip representations may also be affected and enlarged after RSS at right-D2, (ii) such an enlargement would possibly lead to a shift of their centre of gravity or dipole sources, and (iii) these shifts might be toward the RSS-stimulated finger.

To investigate these hypotheses two imaging studies were then conducted. In the first, ultra-high field fMRI (7T) was used: 1) to more precisely examine the RSS-induced cortical plasticity within SI, by allowing for a fine grained identification of the possibly differential contributions of the three Brodmann areas involved in tactile information processing (BA 3b, 1 and 2); and 2) to assess the spatial limits of this adaptive plasticity and whether it alters the representation of other fingers or of the face. In addition to replicating the behavioural results of the first study, we found a significant enlargement of right-D2 positive BOLD response (PBR) within the contralateral SI, more specifically, within the BA3b and BA1 sub-regions. Additionally, a decrease in right-D3 PBR and an increase in Lips negative BOLD response (NBR) were found within the contralateral BA3b, while a decrease in left-D2 PBR and an increase in D1 NBR were found within the contralateral BA1. These results clearly demonstrate a major contribution of BA3b and BA1 SI sub-regions to RSS-induced effects, and reveal that these effects are not as spatially limited as previously thought, given that changes were observed at body-parts that were not RSS-stimulated. This study also provides evidence for the existence of a complex pattern of intermingled positive and negative BOLD responses which could underlie RSS-induced changes across the hand-face border. Finally, for the first time an increased BOLD signal following RSS was reported within the contralateral BA4a area, and within the ipsilateral PPC, and these activations were correlated both with right-D2 and left-Lip discrimination improvements. This latter result suggests that a simple stimulation such as RSS may lead to consistent changes in higher-order multi-sensory associative cortical areas, and thus opens-up a new field of research to investigate the contribution of these areas to the RSS-induced increase in tactile spatial discrimination.

Complementarily, MEG was used in the second imaging study to assess the neurophysiological substrates of the RSS-induced plastic changes. The transfer of behavioural improvement from the finger to the upper-lips was confirmed for the third time, and neuromagnetic data analyzed using dipole source models revealed an increased distance between Lip and D2 sources after RSS, and conversely a decreased distance between Lip-D5 and D2-D5 sources. While further analyses are required to fully clarify the origin of these relative shifts, this last study supports the existence of cross-border changes following RSS of

right-D2, and confirms that the contralateral representation of each side of the upper-lip is affected. Finally, given that an unspecific shift not explained by methodological considerations was found, these results further suggest a dynamic modulation of somatotopic maps.

In addition to raising the question of assessing the cortical correlates of RSS-induced changes, the first study also raised the question of whether RSS may affect the perception at other fingers (i.e., what are the limits of the behavioural effects of RSS). While the first question was addressed with the two imaging studies mentioned above, this second question was addressed with a transversal approach through the two studies, the same critical body-sites as those tested in the first study being retested each time together with new ones, in order to respectively replicate and extend the behavioural results of study 1. These tests revealed a relatively high finger-selectivity of RSS effects, as no perceptual changes were observed neither at the adjacent finger (study 2), nor at both little fingers (study 5).

In the following sections, I will first underline some methodological aspects to take into consideration regarding this work, then I will discuss the implications of our behavioural results regarding the concept of learning, before discussing the possible mechanisms underlying RSS-induced changes. Finally, I will close the discussion with a more speculative section underlining some similarities between the status of the hand and the face regarding somatosensory perception, and how these two body-parts are conjointly involved in some of our most fundamental functions.

II. Methodological considerations

One of the limitations of the imaging studies arises from the stimulation used during the mapping procedures. Indeed, concerning the fMRI study, while brushing was delivered to the lips by rotating a shaft, the stimulation was manually delivered to the fingertips using a brush. Thus, despite the invariant frequency of stimulation, the use of casts, and all the care in delivering a nearly constant and reliable stimulation, some variability in the intensity of stimulation may have occurred. In addition, the fact that the experimenter had to use different hands to deliver the stimulation to each side of the participant's hand might also have contributed to some differences across body sides. To circumvent this source of variability, we expressed the amount of BOLD activation as a percentage of the total volume evoked by a given body side (i.e. the sum of all body-parts from this hemi-body) and sessions. Moreover, even if quite different from the RSS stimulation and equally administered to all body-parts, the stimulation performed during both mapping procedures might have altered or interfered with the RSS-induced effects. In addition, note that we intentionally chose to perform a simple mapping

procedure using passive (i.e., brush or pneumatic) stimulation rather than involving a spatial discrimination task. This choice was made in order to replicate the RSS-induced enlargement of the right-D2 representation, which had been previously reported in a similar context (Pleger et al., 2003).

Finally, the different types of tactile stimulation used across the different mapping procedures (i.e., two sharp static probes for 2PDT, brushing involving tactile motion during fMRI recordings, and tapping-like static stimulation during RSS and MEG recordings) could differentially recruit tactile afferents. Indeed, according to the traditional view, the 2PDT task is likely to preferentially involve slowly adapting afferents (SAI, Merkel cell-neurite complexes; see Phillips and Johnson, 1981; Johnson and Hsiao, 1992), while the brushing stimuli performed during the fMRI mapping procedure may preferentially recruit fast adapting afferents (FAI, Meissner's corpuscles) due to their sensitivity to low-frequency moving stimulus (Lofvenberg and Johansson, 1984). But the texture stimuli induced by the brush are likely to involve SAI afferents too (Blake et al., 1997). Finally, the tapping stimulation delivered during the RSS procedure may have preferentially recruited SAI and FAI afferents due to the fact that it was delivered at a low-frequency feature and did not contain tactile motion (Lofvenberg and Johansson, 1984). However, we can see that SAI afferents and slowly adapting afferents of type II (SAII, Ruffini's corpuscles) are likely involved in all procedures due to their sensitivity to skin stretch and sustained downward pressure (Knibestöl and Vallbo, 1970). And more importantly, while the traditional view is that the different classes of afferents serve different functions and lead to a segregation of these submodalities, recent evidence shows that most afferent classes are excited by most tactile stimuli and that information from all afferent classes are likely to converge and to be integrated together at least at the cortical level (for a review see Saal and Bensmaia, 2014). This suggests that all afferent classes should be taken into account to explain perceptual judgments. In addition, both mechanical stimulations are likely to provide complementary views on the RSS-induced effects, given that brushing stimuli were more complex and dynamic.

A last methodological consideration concerns the analysis of CoG. Indeed, given the large variability in sulcal geometry across individuals, localization of group activation in S1 could (and will) be optimized by implementing surface-based cortical mapping techniques, instead of simply calculating the Euclidean distances.

III. Training-dependent vs training-independent learning

One of the main contributions of the present work arises from the demonstration that the RSS-induced acuity improvement thought to be local, actually **transfers** from the hand to the face without losing its beneficial aspect. At the perceptual level, any process leading to the acquisition or reinforcement/improvement of a skill is commonly referred to as learning. While it is well known that practice and training are usually required to learn a skill, for instance in music and sport domains (e.g., Elbert et al., 1995; Draganski et al., 2004; Hashimoto et al., 2004), perception and behaviour can also change simply via passive exposure to sensory stimulation protocols (Recanzone et al., 1992a; Pleger et al., 2001, 2003; Dinse et al., 2003; Seitz and Dinse, 2007; Ragert et al., 2008; Beste et al., 2011). Such procedures, of which RSS is part, are referred to as training-independent learning processes (see Beste and Dinse, 2013 for a review). Consequently, improvements in tactile acuity similar to those reported in this work have also been reported following extensive somatosensory training, either over a life span such as in Braille reading (Pascual-Leone and Torres, 1993; Sterr et al., 1998a, 1998b; Van Boven et al., 2000; Goldreich and Kanics, 2003; Wan et al., 2010; Norman and Bartholomew, 2011; Wong et al., 2011), or over shorter time-scales (Recanzone et al., 1992d; Wang et al., 1995; Spengler et al., 1997; Harris et al., 2001). But several lines of evidence suggest that these protocols do not tap into the same neural mechanisms as the training-independent protocol used in the present study, which is completely passive and devoid of attentional or cognitive control processes.

Unlike the rapid changes reported here and in previous work using the RSS paradigm (Godde et al., 2000, 2003; Pleger et al., 2001, 2003; Dinse et al., 2006), training-induced improvements typically require days or weeks of attention-**demanding** training and practice (Spengler et al., 1997; Sathian and Zangaladze, 1998; Kaas et al., 2013a; Harrar et al., 2014). Also, in contrast with the present and previous results of RSS studies, training-induced tactile improvement has been found to **transfer** to the homologous finger on the opposite hand (Spengler et al., 1997; Sathian and Zangaladze, 1998; Kaas et al., 2013a; Harrar et al., 2014). Furthermore, while some perceptual learning studies report that improvement is transferred to adjacent fingers (Sathian and Zangaladze, 1997; Harris et al., 2001; Harrar et al., 2014), the possible transfer to other body-parts in the same hemi-body has rarely been investigated. The one study in which changes at remote body-parts were examined found that expert Braille readers (i.e. long-term trained) had enhanced tactile perception compared with controls at the fingertips, but not at the lips (Wong et al., 2011). Thus, together with our results showing - in

agreement with the RSS literature (Godde et al., 2000; Pleger et al., 2001, 2003; Dinse et al., 2006) - the absence of transfer of learning to the homologous and adjacent fingers, and with the disengagement from attentional processes and repetitive training, the RSS-induced training-independent learning seems to dissociate from training-dependent processes and might involve different mechanisms. Disentangling between training-independent (i.e., RSS-like) and training-dependent learning processes was further ensured by the control group in the first study that enabled us to isolate the RSS-induced effects from any effects possibly due to familiarization by repeated exposure to the 2PDT task, and additionally controlled for daily fluctuations in tactile discrimination.

Perceptual learning **specificity**, and conversely **generalization**, is widely regarded as an indication of the neurological site of the learning process. This translates into the following reasoning: the more perceptual learning transfers (i.e., to other body-parts), the less topographically organized and the more integrative are the brain areas involved in learning processes. Alternatively, learning involving topographically organized somatosensory areas, or higher order (non-primary) areas that are not necessarily topographically organized but receive direct inputs from somatotopic areas, should either not transfer at all, or transfer but following a “gradient-like” topographic pattern. Given that electrophysiological studies show a gradual increase in RF complexity from BA3b to BA2, with RFs spanning over a single finger within BA3b, adjacent fingers within BA3b and BA1, or adjacent and homologous fingers within BA2 (Hyvärinen and Poranen, 1978; Iwamura et al., 1980, 1993, 1994), the pattern of transfer of training-dependent learning (Sathian and Zangaladze, 1998; Harris et al., 2001; Kaas et al., 2013a; Harrar et al., 2014) suggests that plastic changes within BA1 and BA2 may underlie such learning. In contrast, different patterns of transfer are reported with training-independent learning, such as RSS. The present work contributes to investigating their limits, and extends these patterns to more distant body-parts. In the following section, the pattern of specificity/generalization of RSS-induced learning will be discussed in light of our neuroimaging results and of the possible mechanisms subserving them.

IV. Underlying mechanisms:

a. RSS-induced local plasticity

RSS has been repeatedly used as a means to alter input statistics in order to study the plastic mechanisms underlying somatosensory training-independent learning. RSS consists of an ecological stimulation directly adapted from classical Hebbian protocols and relies on mechanisms including spike-timing-dependent plasticity such as LTP & LTD of synaptic transmission (see Chapter 3 of the Introduction, page 125). Among the arguments supporting this notion is the short time-scale over which the RSS-induced changes occur, which excludes any structural changes. Rather, together with the fact that RSS-induced changes were found to be dependent on NMDA receptor activation (Dinse et al., 2003) - known to be involved in synaptic plasticity (Bliss and Collingridge, 1993; Nicoll and Malenka, 1995) - and were associated with an increased cortical excitability that is considered a typical signature of effective LTP induction (Höffken et al., 2007), RSS is more likely to induce changes in synaptic efficiency. This hypothesis is further supported by a recent modelling study showing that RSS-like consecutive repetitions of temporally structured stimuli induce Hebbian-like long-term modifications of synaptic weights (Phoka et al., 2012). Thus, the RSS-induced expansion of the cortical representation of the stimulated finger, previously reported in SI (Pleger et al., 2001, 2003; Godde et al., 2003; Hodzic et al., 2004) and that we presently report in BA3b and BA1 (study 2), is likely to arise from recruitment of latent connections and/or from fast modulations of local synaptic efficiency. The tendency for an increased dipole strength observed for the stimulated finger (study 3) is also in line with this possibility. Such a recruitment of processing resources is the likely substrate for the improved discrimination observed at the stimulated fingertip, even if we did not replicate the previously reported correlation (Pleger et al., 2001, 2003). In addition to refining our knowledge about these local plastic changes, the present work provides new evidence for a pattern of specificity and generalization of RSS-induced learning that differs from classical training-dependent learning procedures.

b. Specificity/generalization of the RSS-induced learning

First, and in agreement with the RSS literature (Godde et al., 2000; Pleger et al., 2001, 2003; Dinse et al., 2003), no change in tactile discrimination was observed at the **homologous finger** (i.e., left-D2; study 1, 2 and 3). Together with the absence of an effect on left-D5, which has never been tested in previous reports, these results demonstrate that RSS-induced learning does not transfer to the homologous hand. Given that we found most of the RSS-induced BOLD

signal changes within BA3b and BA1 (study 2), the lack of interhemispheric transfer of learning is consistent with the fact that no or few bilateral RFs have been reported in these sub-regions for the fingers (Iwamura et al., 1993, 2001; Iwamura, 2000). In addition, an increased ipsilateral response was found for the stimulated finger (likely NBR), as well as a decreased contralateral PBR for the homologous finger. These changes are likely to reflect **interhemispheric inhibition** processes mediated by transcallosal reciprocal connections between homotopic cortical areas (Schnitzler et al., 1995). This is further supported by the fact that BOLD changes for the homologous finger were observed within BA1 where more transcallosal connections have been reported than in BA3b (Killackey et al., 1983). These interhemispheric projections make excitatory contacts onto pyramidal cells and interneurons, and thus give rise to both excitation through the former cells, and inhibition through the inhibitory interneurons (Carr and Sesack, 1998). In humans, the behavioural effects of this interhemispheric inhibition have been revealed by the fact that anaesthesia of one hand improves tactile acuity in the homologous hand (Werhahn et al., 2002; Björkman et al., 2004b).

Within the “stimulated” hand, our behavioural findings suggest that RSS does not affect the other fingers, or at least the **adjacent finger** right-D3 (study 2) and the most distant right-D5 (study 3). While the former result corroborates the previous observation made on a small sample of participants (Godde et al., 2000), we further report a decrease in the contralateral PBR (i.e., representation) for the adjacent finger after RSS (study 2). This response decrease was located in BA3b, where an increased response was instead observed for the RSS-stimulated finger. Altogether, these results suggest the involvement of **lateral inhibition** processes mediated by intracortical horizontal connections (Jones and Powell, 1970) through GABAergic activity (Li et al., 2002). Functionally, such processes are considered to subserve the suppressive interaction over the brain response observed when, for instance, two fingers are simultaneously stimulated. This suppressive interaction has been repeatedly observed both in non-human (e.g. Friedman et al., 2008; Lipton et al., 2010), and human primates (Gandevia et al., 1983; Hoechstetter et al., 2001; Simões et al., 2001; Tanosaki et al., 2002; Ruben et al., 2006; Severens et al., 2010), and exhibits the feature of decreasing with distance (i.e., the more distant are the simultaneously stimulated fingers, the less “interference”). However, this kind of suppressive interaction has also been found between body-parts located farther from each other. For instance, simultaneous tactile stimulation of the forearm and finger significantly reduces the finger’s evoked response (Tanosaki et al., 2004). Similarly, anaesthesia of a limited portion of the right forearm by means of a local anaesthetic cream results in tactile improvement on the right hand (Björkman et al., 2004a). Interestingly, the existence of similar connections between hand and face

representations has also been demonstrated in BA3b, with stimulation of the face (forehead) resulting in a significant attenuation of the SEFs evoked by concurrent stimulation of the thumb (Tanosaki et al., 2003). Interestingly, this attenuation was observed only for the earliest component (N20m), reflecting BA3b activity (Kakigi et al., 1996; Tanosaki et al., 2002). In contrast, the next component (P30m) whose origin is less clear, was significantly enhanced by concurrent tactile stimulation to the face, whereas it was systematically attenuated by tactile stimulation to other digits (Tanosaki et al., 2002). This difference in the suppressive interaction observed within the hand, and between the hand and the face, suggests the involvement of different mechanisms subserving their interaction, and is consistent with the complex pattern of PBR/NBR observed in our fMRI results (study 2). But before discussing this, I would like to emphasize that the hypothesis that RSS-induced changes lateral inhibition processes is further supported by recent studies showing that RSS modulates intracortical inhibition (Wilimzig et al., 2012) and paired-pulse inhibition (Höffken et al., 2007).

Finally, one of the main results of the present work is that RSS at a fingertip results in an improved discrimination at the **face**. This remote effect was found for both sides of the upper-lip (study 1, 2, 3), and for the right-cheek (study 1). While this pattern may appear surprising at the first glance, its origin may arise from some features of the SI face representation. Indeed, an increasing number of studies (including our study 2) suggest that the tactile information arising from the face and in particular the lips, is represented in both hemispheres (Nagamatsu et al., 2000; Disbrow et al., 2003a; Nevalainen et al., 2006; Blatow et al., 2007; Nash et al., 2010). This has been linked with the fact that body midline regions are represented in SI of both hemispheres in cats (Manzoni et al., 1980), macaque monkeys (Taoka et al., 1998; Iwamura et al., 2001) and humans (Fabri et al., 2005). In agreement with this, the cheek, which is located farther from the body midline, was found to be more unilaterally represented than the lip (Nevalainen et al., 2006). Notably, our study 2 also provides the first evidence of (i) NBRs evoked by tactile stimulation of the upper-lips, which are (ii) co-localized with the classical (i.e. PBR-based) hand representation, and (iii) expand in the contralateral BA3b sub-region following RSS at the index finger. While the exact nature and distribution of these NBRs has to be further investigated, the “special” pattern of hand-face suppressive interaction reported by Tanosaki and colleagues (1993), together with the RSS-induced modulation of intracortical inhibition (Höffken et al., 2007; Wilimzig et al., 2012), bring us to suggest that these Lip NBRs may reflect processes resembling surround inhibition. Given the co-localization of these responses with the hand representation and the overlaps observed at the SI hand-face junction, the increased Lip NBRs may reflect an increased inhibition of the hand-face junction. This could

explain the increased distance observed between Lip and D2 dipole sources (study 3). The absence of a decrease in the Lip PBR (which would be expected in the case of true inhibition), further suggests a complex relationship between PBRs and NBRs, but also underlines the fact that we still lack some potentially critical bridges between BOLD responses and neurophysiological activity.

While this needs further investigation, it is worth emphasizing that similar complex patterns of intermingled up-regulation and down-regulation of excitatory and inhibitory factors (i.e., glutamatergic and GABAergic) have been reported following intracortical microstimulation (ICMS) of the SI hindpaw representation in rats (Benali et al., 2008), a protocol conceptually close to RSS. Interestingly, the authors found a large increase in excitation in a zone corresponding to the reorganized cortical area, which was limited in space by an increased “long-range” inhibition spanning over the forepaw representation and motor cortex. Similar lateral inhibition, notably expressed by NBRs, was also reported using ultra-high field fMRI in the barrel cortex of rodents (De Celis Alonso et al., 2008; Kennerley et al., 2012), the NBRs being associated with reduced multi-unit activity in deep layers (Kennerley et al., 2012; see Figure 48 upper panel). Interestingly, another electrophysiological study found that horizontal projections result in a layer-specific ratio between two opposing conductances competing for cortical space (Adesnik and Scanziani, 2010; see Figure 48 lower panel). Thus, the co-localization that we observed between lip NBRs and finger PBRs may also reflect processes occurring in two distinct cortical layers, likely interacting. But the nature of this interaction remains to be elucidated.

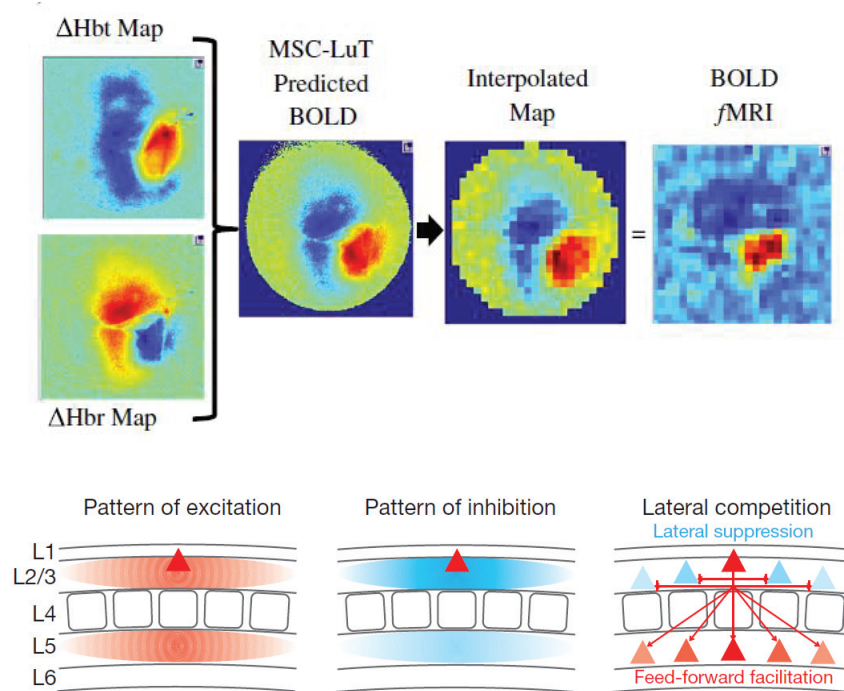


Figure 48. **Upper panel** [from Kennerley et al., 2012]: Spatial predictions of BOLD from underlying hemodynamics for a representative animal. Spatial maps of changes in HbT and Hbr are input into a Monte Carlo simulation of MR signal attenuation to predict the BOLD signal. The resulting BOLD prediction is subsampled so it can be directly compared to the concurrent fMRI data. **Lower panel** [from Adesnik and Scanziani, 2010]: schematic of the spatial overlap between excitation (left) and inhibition (centre) across and within layers. The resulting lateral suppression within layer 2/3 and feed-forward excitation of layer 5 leads to the lateral expansion of a cortical domain at the expense of its neighbours (right).

It is worth noting that these results obtained for the face are quite surprising when considering the finger specificity of RSS-induced effects previously described. However, it is worth emphasizing that the effects of D2-RSS have not been systematically investigated on the adjacent thumb. Only one study reported the absence of shift of the thumb's dipole source (Pleger et al., 2001). In contrast, we observed an enhanced NBR for the thumb in BA1 (study 2), similar to that observed for the lips in BA3b. While the presence of this effect within BA1 is consistent with the higher complexity (i.e., responding to multiple fingers) of RFs in BA1 compared to BA3b (Hyvarinen and Poranen, 1978; Iwamura et al., 1980, 1993; Sur, 1980), the increased NBR suggests the involvement of a process similar for D1 and the Lips. Thus RSS-induced perceptual changes at this finger are possible, and this possibility is currently being investigated.

Before finishing this section, I would like to underline the similarity between some of our results and those reported by Jenkins and colleagues in 1990. Indeed, monkeys trained to maintain contact with a rotating disk stimulating their fingertips exhibited an **expansion** of the cortical representations of these stimulated digits similar to the one we found for right-D2 in study 2. In addition, the borders between the representations of individual digits and digit segments **shifted in parallel**. This resembles the unspecific and non monodirectional shifts of fingers and lip dipole sources observed in study 3, and CoGs in study 2. Interestingly, Jenkins and colleagues also recorded a significant **lateral translocation of the borders** between the representations of the hand and the face, similar to the increased Lip-D2 distance observed in study 3. Finally, the rostral border of BA3b was also shifted towards BA3a, which is normally activated by deep (proprioceptive) receptors, suggesting a **potentiation of cutaneous over deep receptor activation**, which is consistent with the increase in activity observed for right-D2 in study 2.

c. Site of action of RSS

While RSS effects have been mainly investigated at the cortical level, the RSS-induced cortical reorganization could arise from plastic changes induced in the **thalamus**. But several lines of evidence suggest that this alternative is unlikely. First, a series of intracortical and intrathalamic microstimulation (ICMS/ITMS) experiments (see Dinse et al., 1997) showed that: (i) in contrast to the well-known extensive cortical reorganization following ICMS, using the analogous protocol in VPL (ITMS) induced only moderate changes in the reorganization of the somatosensory thalamic maps; and (ii) similar protocols, but designed to explore the capacities of transfer of plastic changes either retrogradely (from VPL to SI) or anterogradely (from SI to VPL), revealed an anterograde effect of ICMS over VPL RFs (enlarged), but no retrograde effect of ITMS over SI. Taken together, these results reveal a small but significant corticothalamic transfer of short-term plastic changes, but no substantial evidence for a thalamocortical transfer. Given that ICMS protocols rely on the same Hebbian rules as RSS, the thalamic contribution to the RSS-induced cortical reorganization is likely to be small. Second, the activity-dependent expansion of digit RFs induced by coincident stimulation of multiple adjacent fingers was reported in BA3b, but no apparent RF change was found in the thalamus of the same monkeys (Wang et al., 1995). Finally, even if in a different context, RF changes following sensory enrichment (after nerve cut and regeneration) were observed in monkeys at the cortical level, but not at the thalamic level (Florence et al., 2001). Thus, while our results do not preclude subcortical contributions, which remain to be investigated, these lines of evidence

suggest a rather small subcortical contribution to activity-dependent plastic changes observed at the cortical level.

In contrast, given the consistent cortical reorganization reported following RSS here and in the literature (Pleger et al., 2001, 2003; Godde et al., 2003; Hodzic et al., 2004), we propose that the RSS-induced plastic changes arise predominantly from modulation of the activity within both the finger and face (at least lips and cheek) cortical representations. In SI, the border between these two representations, also called the hand/face junction, is characterized by the presence of neurons that receive input from both the contralateral hand and face (Dreyer et al., 1975; see Figure 49). This overlap between the hand and face representations was confirmed and further associated with a strong interconnectivity between these representations through horizontal intracortical connections (Manger et al., 1997; Florence et al., 1998; Fang et al., 2002; Steen et al., 2007), which were found to overlap (Manger et al., 1997). Although more limited in number in New World monkeys (Fang et al., 2002) than in macaque monkeys (Manger et al., 1997; Florence et al., 1998) or rats (Steen et al., 2007), these connections are likely to subserve the excitatory and inhibitory responses that can be evoked across the hand-face border in rats (Hickmott and Merzenich, 1998; Burns and Hickmott, 2003). Interestingly, these cross-border connections can undergo Hebbian plasticity induced by tetanic (Paullus and Hickmott, 2011) or pairing protocols (Marik and Hickmott, 2009). Thus, we propose that the local changes induced in the finger representation by RSS transfer to the lip representation through these horizontal intracortical connections, whose strength might also be modulated. Moreover, this model is further supported by the fact that LTP of these connections was found to be dependent on NMDA receptors activation (Marik and Hickmott, 2009), as were the RSS-induced cortical and perceptual changes (Dinse et al., 2003). Our results, and in particular the intermingled positive and negative BOLD responses (study 2) may represent the first evidence of cortical activity that could be assigned to such horizontal intracortical connections in humans, but also of their involvement and/or modulation in/by training-independent learning (i.e., RSS), which appears to result in adaptive perceptual changes at both sides of the hand-face border.

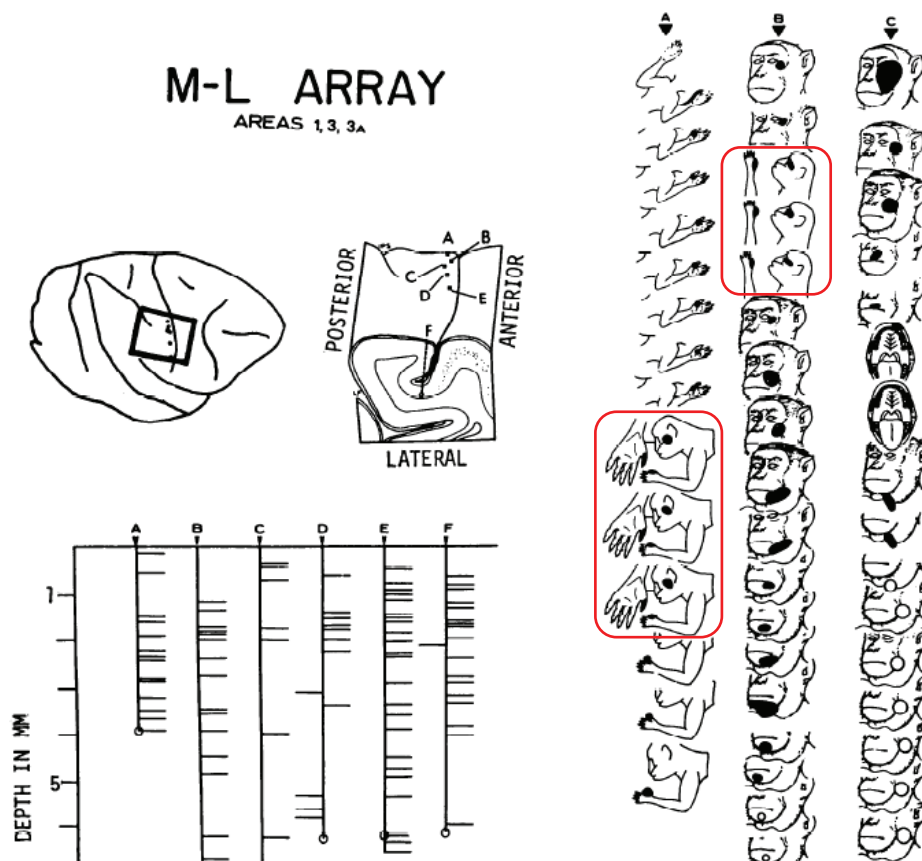


Figure 49 [modified from Dreyer et al., 1975]. Reconstruction of six microelectrode penetrations (A-F) arrayed from medial to lateral in SI. **Left:** Each penetration is represented as a vertical line and each neuron isolated as a horizontal line whose position along the vertical reflects its depth below the cortical surface. **Right:** Sequences of figurines which depict, in the order in which they were encountered, the size and location of the RF for each neuron isolated in the three first penetrations (A-C). Black symbols represent cutaneous RFs, while white symbols represent deep RFs (i.e., proprioceptive). Neurons presenting RFs on both the hand and the face are highlighted in red.

Finally, given the distributed network of cortical areas involved in the processing of tactile information (see section V. Chapter 1, page 63), we cannot exclude that RSS may also act on higher-order cortical areas. On the contrary, RSS has already been reported to induce an expanded activation within SII, similar to that observed in SI (Pleger et al., 2003; Hodzic et al., 2004). Given that SII is less somatotopically organized (Del Gratta et al., 2000), one could wonder whether the hand and lip may share more common substrates in SII than in SI, thus resulting in a transferred behavioural effect across body parts. While the field of view of our fMRI study did not allow for analysis of SII, this alternative is worth investigating. Further analysis of our MEG data, and notably of components at longer latencies, might provide some answers. However, the reduced somatotopy in SII, and in particular the lack of behavioural

effect on the left cheek following RSS on right-D2 (Muret et al., 2014), do not seem to favour a critical involvement of SII in our effects.

Interestingly, though unexpectedly, our second study also revealed RSS-induced changes in the anterior part of the primary motor cortex (BA4a) and in the posterior parietal cortex (PPC). While BA4a is primarily a motor area, its implication in tactile form discrimination has been reported (Bodegård et al., 2001), as well as in the processing of complex tactile stimuli (Terumitsu et al., 2009), and in haptic discrimination tasks (Geyer et al., 1996; Eickhoff et al., 2005). In addition, even passive tactile stimulation engages the precentral gyrus (Francis et al., 2000; Moore and Schady, 2000). However, the precise roles of motor areas in tactile perception remain to be clarified. Interestingly, the enhanced activity that we report in BA4a might also be the substrate for the improved sensorimotor performance reported after RSS (Kalisch et al., 2008, 2010), and to be related to the RSS-induced changes in resting state connectivity (mu-rhythm) observed within distributed sensorimotor cortical areas (Freyer et al., 2012). Lastly, the increased activity observed within PPC, a highly associative area, opens up a multitude of possible implications regarding the impact of RSS. Indeed, the wide range of functions subserved by PPC includes multisensory (Huang et al., 2012; Sereno and Huang, 2014) and sensorimotor integration, movement planning (Astafiev et al., 2003; Hanakawa et al., 2003; Diedrichsen et al., 2004), but also the integration of visuo-tactile inputs to promote and guide arm, hand but also face and lip movements and coordination (e.g., in reaching to grasp an object). More closely related to the context in which we report this increased activity, in addition to the apparent involvement of PPC in the perceptual changes induced by RSS (i.e., the correlation we report), PPC has been found to be activated in cases of complex and moving tactile stimulation (Fabri et al., 1999, 2001) similar to the brushing used in our fMRI mapping. Thus, the enhanced PPC activation following RSS could reflect changes in the perception of such complex tactile stimuli, an idea which has yet to be investigated. The emergence of an enhanced PPC activity after RSS might also reflect changes in tactile remapping in external space (Azañón et al., 2010), and more globally in higher-order body representation maps and in the conscious body image (see Longo et al., 2010 for a review). Altogether, these different lines of evidence suggest that RSS affects a rather widespread network of cortical areas, and thus underlines its potential impact over higher functions than simply two-point tactile discrimination, which might nevertheless improve performance on such a relatively simple discriminative task.

It is worth noting that the emergence of an enhanced PPC activity after RSS might also reflect tonically increased somatosensory attention (see Macaluso and Maravita, 2010). Attention interacting with sensory processing has been found to promote learning transfer (Ahissar and Hochstein, 1997; Weber et al., 2005). In addition, previous work demonstrated that attentional demands can induce transient representational changes within SI (Iguchi et al., 2001, 2002; Braun et al., 2002). For instance, changes in the relative distance between finger ECDs quite similar to those reported in our third study, were found during somatosensory tasks involving global to local attentional demands (Braun et al., 2000a). This suggests that the topographic organization of SI is dynamically modulated to achieve the best state (see Freyer et al., 2013; Ritter et al., 2015) and distribution to perform a given somatosensory task. However, neither the mapping procedures nor RSS involved attentional tasks, but the fact that right-D2 was the only body-site to be stimulated may have shifted the attention of participants towards this body-part. If true, such an attentional shift could account for some of the acuity improvement observed at this fingertip, but not for the improvement observed at the upper-lips. In addition, previous reports including a previous study from our group (Muret et al., 2014), reported no behavioural improvement in participants receiving either no stimulation (stimulator off), or single-point-like stimulation (Pleger et al., 2003; Ragert et al., 2008). Thus, the behavioural improvement as well as the cortical changes reported here cannot be explained by spatial tactile attention processes.

Finally, RSS-induced plasticity could also start as early in the pathway as at the **mechanoreceptor level**. Indeed, Merkel cells were recently found to actively tune the touch-dome afferents (SAI) and thus the mechanosensory responses, to facilitate high spatio-temporal acuity (Maksimovic et al., 2014). Given that Merkel cells make 'synapse-like' contacts with SAI afferents (see Halata et al., 2003; Nakatani et al., 2014 for review), a potentiation of these peripheral synapses may also happen and could be involved in Hebbian-like perceptual learning. However, while such peripheral changes may partially contribute to local effects (i.e., those induced on the RSS-stimulated site) their contribution can be readily ruled out in our studies for the RSS-induced remote perceptual changes on the lips and cheek.

V. The hand and the face: evidence for a singular “coupling”?

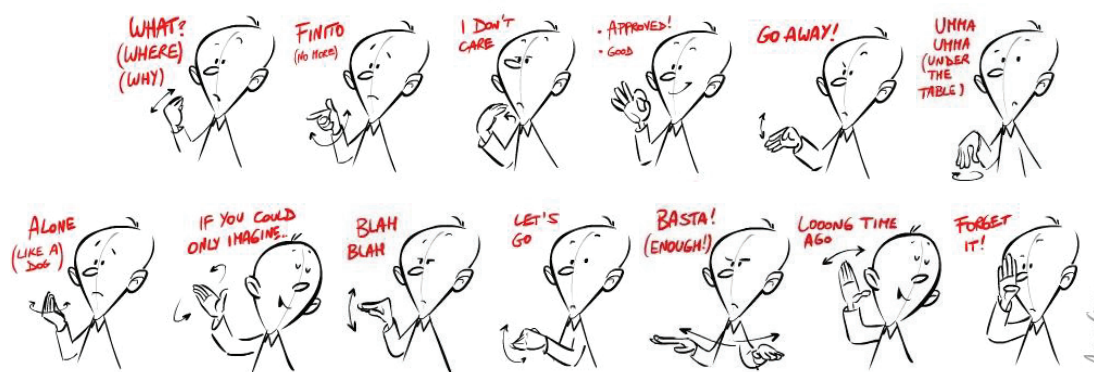
In this section, I will shortly describe some evidence underlining that our hands and face share a peculiar link along our life and in several of our daily-life activities. I allow myself here a more speculative section to highlight what I personally consider to be a “singular relationship” between these two body parts. If we consider the few points I will raise as the “visible part of the iceberg”, one could speculate that the results found in the present work arise from the bottom part of that iceberg, i.e., a hand-face interaction at one of their lowest somatosensory levels.

a. Foetal development, cortical magnification & sensitivity

Touch is the first sense to develop in utero, Montagu (1978, p. 195) reporting tactile responses to a hair stroking the cheek of a foetus at around 8 weeks gestational age. Cutaneous sensitivity of the embryonic body then extends to the genital area by week 10, to the palms by week 11, the soles by week 12, the abdomen and buttocks by week 17, and by week 32 every part of the body is responsive to the gentle stroke of a single hair. This developmental hierarchy of tactile sensitivity is reflected by the fact that the earliest sites developing cutaneous sensitivity also possess the greatest number and variety of sensory receptors in adults. Consequently, they are also represented cortically with larger areas of primary somatosensory cortex. Among the different body-parts, the face and the hand are the two regions that exhibit the highest cortical magnification, and consequently the highest sensitivity and discrimination abilities (see Chapter 1, page 48). In addition, while most of the tactile information arising from our body surface is represented following an order similar to the physical continuity of our skin, the hand and the face representations generate a major discontinuity by their direct cortical proximity. While the reason of such discontinuity remains unknown, one can assume that it should be functionally relevant. Among the different hypotheses, Farah (1998) proposed that the discontinuity occurs because “mechanisms of self-organization, in combination with the normal position of the foetus in the womb will incline the map towards just this organization.” In the womb, the foetus generally has its hands abutting its face, and its feet the genitalia, creating coactivations of the respective body parts. But is this discontinuity present only because of this developmental “coactivation”? Or is there other functions developing during adulthood that maintain a link between hands and face? In the following sections I will briefly provide an overview of two functions in which these two body parts are actively coupled: language and eating behaviour.

b. Language

As visual guidance of facial movements is impossible, accurate movements for speech (and mastication) require an established body schema that is formed via the information from mechanoreceptors in the skin, mucosa, periodontium, and proprioceptors in the facial (and masticatory) muscles and in the jaw joints. In addition, language production and perception has been found not to rely on speech only, but also to body communicational postures and gestures (McNeil, 1992). Among the most important features of this latter way of communicating, the face obviously plays a major role with its wide range of expressions, but hands postures and movements also bring a non negligible amount of information, far more than body posture. Our hands usually complete what we cannot express with our words or facial expressions. This body and especially hand communication achieves its apogee in sign language, and is commonly stereotyped in Italians' gestures (see Figure 50).



modified from <http://www.mymodernmet.com/profiles/blogs/>

Figure 50. Sketches illustrating few common Italian gestures (small dedication to Alessandro and the Italian people from the lab ;-)).

In addition, when communicating with each other, we have this trend (more or less developed according to someone's personality) to constantly physically interact and touch each other. For example, when asking for more attention from our interlocutor, one may grasp his arm in addition to coming closer to that person. And obviously when trying to comfort someone, one is likely to end up hugging that person. All this touch-mediated communication is mostly mediated by the hands. Moreover, considering well-known mirror neuron system (Rizzolatti and Craighero, 2004; Rizzolatti and Fabbri-Destro, 2008), one can assume that in order to produce a consistent body communication but also to perceive it, we need to simultaneously integrate the hand and face expression and gesture, but also the proprioceptive and cutaneous sensation accompanying these movements. Mirror-neurons have been reported in area F5, the superior temporal gyrus, but also in BA7b and PF in the rostral part of IPL (see Rizzolatti and Craighero,

2004). Obviously, the motor component is the most relevant when considering body communication, but one can wonder what can be the proprioceptive and cutaneous counterpart of such integration.

c. Eating behaviour or the “bring-to-the-mouth neurons”

Similar to the guidance of facial movements for speech, guidance of facial and hands movements for eating behaviour relies on both mechano and proprio-receptors embedded in the skin, muscles and joints of both the lower face surrounding the mouth, and the glabrous skin of the hand. For the hand, an additional proprioceptive input from the arm (shoulder/elbow/wrist) is necessary for the arm/hand to adjust their respective positions on their way to the mouth. But perception of mouth conformation (independent of jaw movement) is mostly based on information from cutaneous afferents because of the apparent lack of muscle spindles in facial muscles. During eating behaviour, mechanoreceptive inputs are particularly important for precision grip, for instance in order to grasp a fork and maintain it in the hand while moving the arm, to finally reach with precision the desired position, for instance the mouth. Then, once the food (or any other thing, like fork-glass-spoon or even a cigarette) has reached the mouth location, mechanoreceptive information from the lips is necessary to get the feedback that the fork and food reached the desired position. Overall, bringing something to the mouth requires a highly precise “synchronization” between hand and mouth-lips position and precision grip. This holds also for smoking behaviour during which the person has to maintain the cigarette in place and synchronize hand/arm and lips actions and grip.

The posterior parietal (Stepniewska et al., 2009a, 2009b) and ventral premotor (Gentilucci et al., 2012) cortices are involved in generating such as hand-to-mouth movements. Intracortical microstimulation (ICMS) of the dorsal PPC of galagos monkeys (Stepniewska et al., 2009b), corresponding to BA7, evoked at least three main categories of complex forelimb movements in different portions of PPC: hand-to-mouth (or hand-to-body), defensive (either protective or avoidance), and reaching. Hand-to-mouth movements were usually evoked from more rostralateral sites than defensive movements, while ventral PPC commonly represented defensive face movements. Injection of tracers in the hand-to-mouth zone of anterior PPC (defined by ICMS) revealed major connections with hand representations in somatosensory and motor fields but not with direct auditory and visual inputs (Stepniewska et al., 2009a). The most rostral portion of the hand-to-mouth zone maintained these connections, although projections from premotor cortex were not found. An injection at the caudal border, possibly also involving the defensive movement zone, labelled fewer neurons in area 3a, 3b and 1-2, and a few neurons

in visual area dorsal V3 (Stepniewska et al., 2009a). Thus, associative areas such as PPC are likely to affect lower relays of the somatosensory pathway, and may thus affect somatosensory perception.

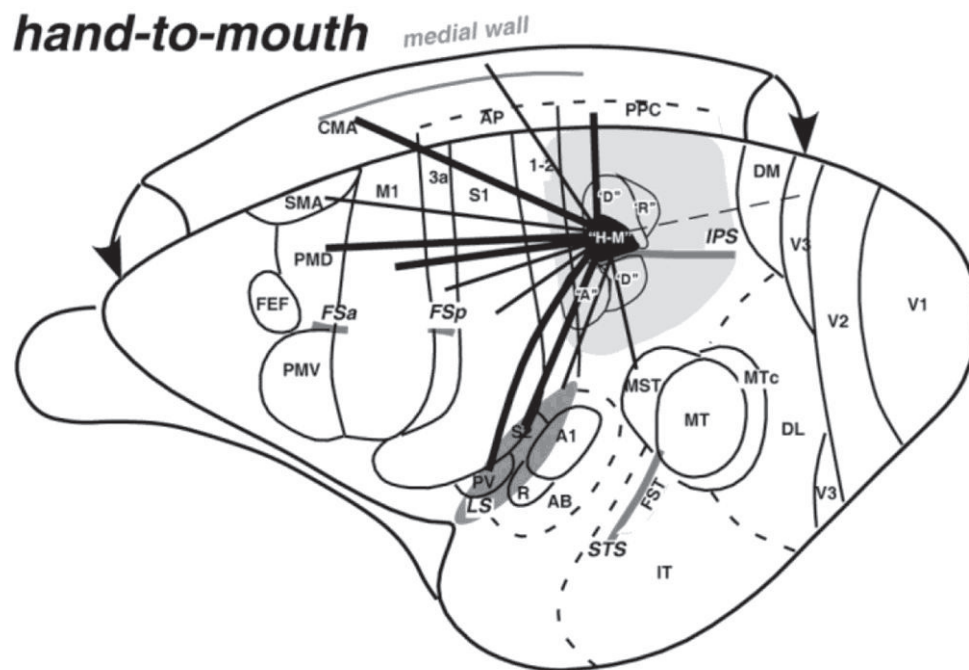


Figure 51 [modified from Stepniewska et al., 2009a]. Summary of corticocortical connections (indicated by black lines) of the hand-to-mouth zone (filled with black) of PPC in the galago monkey brain. Thick lines represent strong connections, and thin lines represent weak connections. The hand-to-mouth zone has major connections with somatosensory and motor fields, while being isolated from direct auditory and visual inputs. Sulci are marked with dark gray, and the entire region explored by ICMS is marked with light gray. A, aggressive; D, defensive forelimb or face; H-M, hand-to-mouth; R, reach.

Altogether, these few lines of evidence point toward the fact that the hand and the face interact together along the entire somatosensory pathway, correspondingly are both involved in both low and high level functions.

CONCLUSION & FOLLOW-UP

To conclude, in contrast to the theoretical framework within which deprivation-induced plastic changes across the hand-face border have been interpreted as a sign of ‘competition’, we report a non-competitive and adaptive transfer of perceptual changes across the hand-face border, with repetitive stimulation of the hand resulting in enhanced tactile performance at the face. This finding suggests that cross-border plasticity mechanisms also include ‘facilitation-based’ processes, revealed here through training-independent perceptual learning. We additionally found that these behavioural results were accompanied by substantial cortical changes involving a complex pattern of activation and deactivation potentially underlying changes in the balance between excitatory and inhibitory processes. Finally, we report that associative cortical areas may also be affected and involved in training-independent learning. While further investigations are required to understand the exact nature of the pattern of cortical activity in which we report changes, and the implication of associative areas, our results imply that training-independent learning, appears to affect more cortical areas than previously thought and promotes perceptual and cortical changes not only locally, but also remotely, and in particular across the hand-face border. Such a pattern of transfer underlines the potentially interesting impact of training-independent procedures in promoting adaptive plastic changes in the context of rehabilitation. Indeed, if a passive stimulation of a given body part could help to recover sensitivity from another body part, it would be useful to optimize this protocol to find new therapeutic tools to help patients with somatosensory disorders, like stroke patients.

Some promising results going in this direction have shown that RSS improves sensorimotor performance in stroke patients (Smith et al., 2009; Kattenstroth et al., 2012), but also compensates for age-related declines in sensitivity (Kalisch et al., 2008, 2010, 2012a, 2012b). In addition, given the passive feature of RSS, this protocol could be easily combined with other rehabilitation methods. In line with this, a recent study showed that repetitive motor training combined with RSS improves motor performance (Ladda et al., 2014). Thus, RSS appears to be a potentially interesting method to efficiently enhance haptic and sensorimotor abilities. Conversely, its potential impact on pain has not been investigated yet. The only hint regarding this aspect is not very encouraging, given that RSS was found to improve finger dexterity, but did not change pain thresholds (Kowalewski et al., 2012). However, the protocol of stimulation may need to be slightly adapted as a function of the to-be-achieved aim. For instance, some cases might require the implementation of asynchronous stimulation between body-parts instead

of synchronous. Some encouraging results going in this direction have been reported in amputees, whose phantom limb pain was reduced following an asynchronous stimulation of their residual limb and lip (Huse et al., 2001). Altogether, these lines of evidence point towards the need to further investigate the potential outcomes of RSS for functional rehabilitation, and to achieve a better understanding of the mechanisms subserving RSS training-independent learning.

In this direction, it would be interesting to implement further analyses of our imaging data. Regarding the **fMRI study**, a first step would be to confirm our results with a more robust delineation of BAs based on cytoarchitectonic probabilistic maps. Then, it would be interesting to directly compare positive and negative BOLD responses by analyzing their relative overlap at the individual level. This would also allow confirmation of the co-localization of the lip negative response within the hand positive response. For the **MEG study**, the analysis of dipole orientation would provide some additional information regarding the contribution of the different sub-regions (BAs). Indeed, if RSS differentially alters activity in BA3b, BA1, but also BA2, the net extracellular current oriented tangentially to the scalp (i.e., detected by MEG sensors) might be slightly modulated, which could result in dipole orientation changes. Another direct follow-up would be to analyze the other SEF components, to investigate whether RSS alters earlier or more associative brain areas, but also to compute the distributed sources of the somatosensory evoked activity. This approach requires no apriori regarding the number of sources generating the external field and thus would provide a reliable way of estimating the sources involved and modulated by our procedure. Finally, a more exploratory analysis in the time-frequency domain might also reveal an impact of RSS over some frequency bands, such as the mu and beta bands involved in sensorimotor processing. For both fMRI and MEG data, the analysis of CoG displacement could also be optimized by implementing surface-based cortical mapping techniques.

Other possible follow-up imaging studies include recording brain activity while participants are performing the two-point discrimination task, which would provide a complementary way of evaluating the cortical substrates involved in the RSS-induced changes in tactile acuity. It would be also interesting to investigate whether the functional but also resting state connectivity between hand and face representations is modulated by RSS. Finally, the use SEP recordings in the context of protocols of tactile interference would be interesting to further investigate the existence of lateral inhibition processes between the hand and the face suggested by the present work.

At the behavioural level, a direct follow-up would be to assess whether RSS at the index finger affects tactile perception at the thumb. This point is currently being investigated. Then, regarding the potential impact of RSS for somatosensory rehabilitation, it will be crucial to investigate whether the application of RSS on the face can affect finger tactile acuity. Given that the negative BOLD response obtained for the lip was co-localized with the positive response of all fingers, such a protocol is likely to result in a non-selective effect on all fingers.

REFERENCES

- Adesnik H, Scanziani M (2010) Lateral competition for cortical space by layer-specific horizontal circuits. *Nature* 464:1155–1160.
- Ahissar M, Hochstein S (1997) Task difficulty and the specificity of perceptual learning. *Nature* 387:401–406.
- Akatsuka K, Noguchi Y, Harada T, Sadato N, Kakigi R (2008) Neural codes for somatosensory two-point discrimination in inferior parietal lobule: An fMRI study. *Neuroimage* 40:852–858.
- Allard T, Clark SA, Jenkins WM, Merzenich MM (1991) Reorganization of somatosensory area 3b representations in adult owl monkeys after digital syndactyly. *J Neurophysiol* 66:1048–1058.
- Amunts K, Schlaug G, Schleicher A, Steinmetz H, Dabringhaus A, Roland PE, Zilles K (1996) Asymmetry in the human motor cortex and handedness. *Neuroimage* 4:216–222.
- Andersen RA, Buneo CA (2002) Intentional maps in posterior parietal cortex. *Annu Rev Neurosci* 25:189–220.
- Armstrong-James M, Fox K (1987) Spatiotemporal convergence and divergence in the rat S1 “barrel” cortex. *J Comp Neurol* 263:265–281.
- Arthurs O. J, Boniface S. J (2003) What aspect of the fMRI BOLD signal best reflects the underlying electrophysiology in human somatosensory cortex? *Clin Neurophysiol* 114:1203–1209.
- Arthurs OJ, Donovan T, Spiegelhalter DJ, Pickard JD, Boniface SJ (2007) Intracortically distributed neurovascular coupling relationships within and between human somatosensory cortices. *Cereb Cortex* 17:661–668.
- Astafiev S V, Shulman GL, Stanley CM, Snyder AZ, Van Essen DC, Corbetta M (2003) Functional organization of human intraparietal and frontal cortex for attending, looking, and pointing. *J Neurosci* 23:4689–4699.
- Avillac M, Ben Hamed S, Duhamel J-R (2007) Multisensory integration in the ventral intraparietal area of the macaque monkey. *J Neurosci* 27:1922–1932.
- Azañón E, Longo MR, Soto-Faraco S, Haggard P (2010) The posterior parietal cortex remaps touch into external space. *Curr Biol* 20:1304–1309.
- Backes W., Mess W., van Kranen-Mastenbroek V, Reulen JP. (2000) Somatosensory cortex responses to median nerve stimulation: fMRI effects of current amplitude and selective attention. *Clin Neurophysiol* 111:1738–1744.
- Bao R, Wei P, Li K, Lu J, Zhao C, Wang Y, Zhang T (2012) Within-limb somatotopic organization in human SI and parietal operculum for the leg: an fMRI study. *Brain Res* 1445:30–39.
- Baranyi A, Fehér O (1981) Synaptic facilitation requires paired activation of convergent pathways in the neocortex. *Nature* 290:413–415.
- Barbay S, Peden EK, Falchook G, Nudo RJ (1999) Sensitivity of neurons in somatosensory cortex (S1) to cutaneous stimulation of the hindlimb immediately following a sciatic nerve crush. *Somatosens Mot Res* 16:103–114.
- Batista AP, Buneo CA, Snyder LH, Andersen RA (1999) Reach plans in eye-centered coordinates. *Science* (80-) 285:257–260.

- Baumgartner C, Doppelbauer A, Deecke L, Barth DS, Zeitlhofer J, Lindinger G, Sutherling WW (1991) Neuromagnetic investigation of somatotopy of human hand somatosensory cortex. *Exp Brain Res* 87:641–648.
- Baumgartner C, Doppelbauer A, Sutherling WW, Lindinger G, Levesque MF, Aull S, Zeitlhofer J, Deecke L (1993) Somatotopy of human hand somatosensory cortex as studied in scalp EEG. *Electroencephalogr Clin Neurophysiol* 88:271–279.
- Baumgärtner U, Iannetti GD, Zambreanu L, Stoeter P, Treede R-D, Tracey I (2010) Multiple somatotopic representations of heat and mechanical pain in the operculo-insular cortex: a high-resolution fMRI study. *J Neurophysiol* 104:2863–2872.
- Benali A, Weiler E, Benali Y, Dinse HR, Eysel UT (2008) Excitation and inhibition jointly regulate cortical reorganization in adult rats. *J Neurosci* 28:12284–12293.
- Bentley WJ, Li JM, Snyder AZ, Raichle ME, Snyder LH (2014) Oxygen level and LFP in task-positive and task-negative areas : bridging BOLD fMRI and electrophysiology. *Cereb Cortex*:1–12.
- Besle J, Sánchez-Panchuelo R-M, Bowtell R, Francis S, Schluppeck D (2013a) Single-subject fMRI mapping at 7 T of the representation of fingertips in S1: a comparison of event-related and phase-encoding designs. *J Neurophysiol* 109:2293–2305.
- Besle J, Sánchez-Panchuelo R-M, Bowtell R, Francis S, Schluppeck D (2013b) Event-related fMRI at 7T reveals overlapping cortical representations for adjacent fingertips in S1 of individual subjects. *Hum Brain Mapp* 35:2027–2043.
- Beste C, Dinse HR (2013) Learning without training. *Curr Biol* 23:R489–R499.
- Beste C, Wascher E, Güntürkün O, Dinse HR (2011) Improvement and impairment of visually guided behavior through LTP- and LTD-like exposure-based visual learning. *Curr Biol* 21:876–882.
- Birbaumer N, Lutzenberger W, Montoya P, Larbig W, Unertl K, Töpfner S, Grodd W, Taub E, Flor H (1997) Effects of regional anesthesia on phantom limb pain are mirrored in changes in cortical reorganization. *J Neurosci* 17:5503–5508.
- Björkman A, Rosén B, Lundborg G (2004a) Acute improvement of hand sensibility after selective ipsilateral cutaneous forearm anaesthesia. *Eur J Neurosci* 20:2733–2736.
- Björkman A, Rosén B, van Westen D, Larsson E-M, Lundborg G (2004b) Acute improvement of contralateral hand function after deafferentation. *Neuroreport* 15:1861–1865.
- Björkman A, Weibull A, Olsrud J, Henrik Ehrsson H, Rosén B, Björkman-Burtscher IM (2012) Phantom digit somatotopy: a functional magnetic resonance imaging study in forearm amputees. *Eur J Neurosci*:1–9.
- Björkman A, Weibull A, Rosén B, Svensson J, Lundborg G (2009) Rapid cortical reorganisation and improved sensitivity of the hand following cutaneous anaesthesia of the forearm. *Eur J Neurosci* 29:837–844.
- Blake DT, Hsiao SS, Johnson KO (1997) Neural coding mechanisms in tactile pattern recognition: the relative contributions of slowly and rapidly adapting mechanoreceptors to perceived roughness. *J Neurosci* 17:7480–7489.
- Blake DT, Strata F, Kempter R, Merzenich MM (2005) Experience-dependent plasticity in S1 caused by noncoincident inputs. *J Neurophysiol* 94:2239–2250.

- Blankenburg F, Ruben J, Meyer R, Schwiemann J, Villringer A (2003a) Evidence for a rostral-to-caudal somatotopic organization in human primary somatosensory cortex with mirror-reversal in areas 3b and 1. *Cereb Cortex* 13:987–993.
- Blankenburg F, Taskin B, Ruben J, Moosmann M, Ritter P, Curio G, Villringer A (2003b) Imperceptible stimuli and sensory processing impediment. *Science* (80-) 299:1864.
- Blatow M, Nennig E, Durst A, Sartor K, Stippich C (2007) fMRI reflects functional connectivity of human somatosensory cortex. *Neuroimage* 37:927–936.
- Bliem B, Tegenthoff M, Dinse HR (2008) Cholinergic gating of improvement of tactile acuity induced by peripheral tactile stimulation. *Neurosci Lett* 434:129–132.
- Bliss TVP, Lomo T (1973) Long-lasting potentiation of synaptic transmission in the dentate area of the unanaesthetized rabbit following stimulation of the perforant path. *J Physiol* 232:357–374.
- Bliss T V, Collingridge GL (1993) A synaptic model of memory: long-term potentiation in the hippocampus. *Nature* 361:31–39.
- Bodegård A, Geyer S, Grefkes C, Zilles K, Roland PE (2001) Hierarchical processing of tactile shape in the human brain. *Neuron* 31:317–328.
- Bogdanov S, Smith J, Frey SH (2012) Former hand territory activity increases after amputation during intact hand movements, but is unaffected by illusory visual feedback. *Neurorehabil Neural Repair* 26:604–615.
- Boorman L, Kennerley AJ, Johnston D, Jones M, Zheng Y, Redgrave P, Berwick J (2010) Negative blood oxygen level dependence in the rat: a model for investigating the role of suppression in neurovascular coupling. *J Neurosci* 30:4285–4294.
- Borsook D, Becerra L, Fishman S, Edwards A, Jennings CL, Stojanovic M, Papinicolas L, Ramachandran VS, Gonzalez RG, Breiter H (1998) Acute plasticity in the human somatosensory cortex following amputation. *Neuroreport* 9:1013–1017.
- Borsook D, Burstein R, Becerra L (2004) Functional imaging of the human trigeminal system: Opportunities for new insights into pain processing in health and disease. *J Neurobiol* 61:107–125.
- Braun C, Haug M, Wiech K, Birbaumer N, Elbert T, Roberts LE (2002) Functional organization of primary somatosensory cortex depends on the focus of attention. *Neuroimage* 17:1451–1458.
- Braun C, Schweizer R, Elbert T, Birbaumer N, Taub E (2000a) Differential activation in somatosensory cortex for different discrimination tasks. *J Neurosci* 20:446–450.
- Braun C, Schweizer R, Heinz U, Wiech K, Birbaumer N, Topka H (2003) Task-specific plasticity of somatosensory cortex in patients with writer's cramp. *Neuroimage* 20:1329–1338.
- Braun C, Wilms A, Schweizer R, Godde B, Preissl H, Birbaumer N (2000b) Activity patterns of human somatosensory cortex adapt dynamically to stimulus properties. *Neuroreport* 11:2977–2980.
- Brecht M, Roth A, Sakmann B (2003) Dynamic receptive fields of reconstructed pyramidal cells in layers 3 and 2 of rat somatosensory barrel cortex. *J Physiol* 553:243–265.
- Bressler D, Spotswood N, Whitney D (2007) Negative BOLD fMRI response in the visual cortex carries precise stimulus-specific information. *PLoS One* 2.
- Brodmann K (1909) Vergleichende Lokalisationslehre der Grosshirnrinde in ihren Prinzipien dargestellt auf Grund des Zellenbaues. Johann Ambrosius Barth Verlag, Leipzig.

- Brookes M, Woolrich M, Luckhoo H, Price D, Hale, Stephenson M, Barnes G, Smith S, Morris P (2011) Investigating the electrophysiological basis of resting state networks using magnetoencephalography. *PNAS* 108:16783–16788.
- Brown PB, Pubols LM, Millecchial J, Gladfelter WE, Culberson JC, Covalt-Dunning D, Sonty R V., Millecchia RJ (1991) Somatotopic Organization of Single Primary Afferent Axon Projections to Cat Spinal Cord Dorsal Horn. *J Neurosci* 11:298–309.
- Bruehlmeier M, Dietz V, Leenders KL, Roelcke U, Missimer J, Curt A (1998) How does the human brain deal with a spinal cord injury? *Eur J Neurosci* 10:3918–3922.
- Bruns P, Camargo CJ, Campanella H, Esteve J, Dinse HR, Röder B (2014) Tactile Acuity Charts: A Reliable Measure of Spatial Acuity Sathian K, ed. *PLoS One* 9:e87384.
- Buchner H, Kauert C, Radermacher I (1995) Short-term changes of finger representation at the somatosensory cortex in humans. *Neurosci Lett* 198:57–59.
- Buonomano D V, Merzenich MM (1998) Cortical plasticity: from synapses to maps. *Annu Rev Neurosci* 21:149–186.
- Burbaud P, Doegle C, Gross C, Bioulac B (1991) A quantitative study of neuronal discharge in areas 5, 2, and 4 of the monkey during fast arm movements. *J Neurophysiol* 66:429–443.
- Burns S a., Hickmott PW (2003) Effect of representational borders on responses of supragranular neurons in rat somatosensory cortex. *Brain Res* 985:108–111.
- Burton H, Fabri M (1995) Ipsilateral intracortical connections of physiologically defined cutaneous representations in areas 3b and 1 of macaque monkeys: projections in the vicinity of the central sulcus. *J Comp Neurol* 355:508–538.
- Burton H, Fabri M, Alloway K (1995) Cortical areas within the lateral sulcus connected to cutaneous representations in areas 3b and 1: a revised interpretation of the second somatosensory area in macaque monkeys. *J Comp Neurol* 355:539–562.
- Byrne J a., Calford MB (1991) Short-term expansion of receptive fields in rat primary somatosensory cortex after hindpaw digit denervation. *Brain Res* 565:218–224.
- Calford MB, Tweedale R (1988) Immediate and chronic changes in responses of somatosensory cortex in adult flying-fox after digit amputation. *Nature* 332:446–448.
- Calford MB, Tweedale R (1990) Interhemispheric transfer of plasticity in the cerebral cortex. *Science* (80-) 249:805–807.
- Calford MB, Tweedale R (1991) Acute changes in cutaneous receptive fields in primary somatosensory cortex after digit denervation in adult flying fox. *J Neurophysiol* 65:178–187.
- Caminiti R, Ferraina S, Johnson PB (1996) The sources of visual information to the primate frontal lobe: A novel role for the superior parietal lobule. *Cereb Cortex*:319–328.
- Campbell WW (1999) Guidelines in electrodiagnostic medicine. *Muscle Nerve* 8:171–205.
- Cannestra AF, Black KL, Martin N a., Cloughesy T, Burton JS, Rubinstein E, Woods RP, Toga AW (1998) Topographical and temporal specificity of human intraoperative optical intrinsic signals. *Neuroreport* 9:2557–2563.
- Carlson M (1981) Characteristics of sensory deficits following lesions of Brodmann's areas 1 and 2 in the postcentral gyrus of *Macaca mulatta*. *Brain Res* 204:424–430.

- Carr DB, Sesack SR (1998) Callosal terminals in the rat prefrontal cortex: Synaptic targets and association with GABA-immunoreactive structures. *Synapse* 29:193–205.
- Castillo EM, Papanicolaou AC (2005) Cortical representation of dermatomes: MEG-derived maps after tactile stimulation. *Neuroimage* 25:727–733.
- Catani M, Dell’Acqua F, Vergani F, Malik F, Hodge H, Roy P, Valabregue R, Thiebaut de Schotten M (2012) Short frontal lobe connections of the human brain. *Cortex* 48:273–291.
- Cerkevich CM, Qi H-X, Kaas JH (2013) Thalamic input to representations of the teeth, tongue, and face in somatosensory area 3b of macaque monkeys. *J Comp Neurol* 521:3954–3971.
- Chang C, Shyu BC (2001) A fMRI study of brain activations during non-noxious and noxious electrical stimulation of the sciatic nerve of rats. *Brain Res* 897:71–81.
- Chapin JK (1986) Laminar differences in sizes, shapes, and response profiles of cutaneous receptive fields in the rat SI cortex. *Exp Brain Res* 62:549–559.
- Chen CJ, Liu HL, Wei FC, Chu NS (2006) Functional MR imaging of the human sensorimotor cortex after toe-to-finger transplantation. *Ajnr Am J Neuroradiol* 27:1617–1621.
- Chen LM, Friedman RM, Ramsden BM, LaMotte RH, Roe a W (2001) Fine-scale organization of SI (area 3b) in the squirrel monkey revealed with intrinsic optical imaging. *J Neurophysiol* 86:3011–3029.
- Chen TL, Babiloni C, Ferretti A, Perrucci MG, Romani GL, Rossini PM, Tartaro A, Del Gratta C (2008) Human secondary somatosensory cortex is involved in the processing of somatosensory rare stimuli: an fMRI study. *Neuroimage* 40:1765–1771.
- Chen TL, Babiloni C, Ferretti A, Perrucci MG, Romani GL, Rossini PM, Tartaro A, Del Gratta C (2010) Effects of somatosensory stimulation and attention on human somatosensory cortex: an fMRI study. *Neuroimage* 53:181–188.
- Chowdhury S a, Greek K a, Rasmusson DD (2004) Changes in corticothalamic modulation of receptive fields during peripheral injury-induced reorganization. *Proc Natl Acad Sci U S A* 101:7135–7140.
- Chung YG, Han SW, Kim H-S, Chung S-C, Park J-Y, Wallraven C, Kim S-P (2014) Intra- and inter-hemispheric effective connectivity in the human somatosensory cortex during pressure stimulation. *BMC Neurosci* 15:43.
- Churchill JD, Arnold LL, Garraghty PE (2001) Somatotopic reorganization in the brainstem and thalamus following peripheral nerve injury in adult primates. *Brain Res* 910:142–152.
- Clark SA, Allard T, Jenkins WM, Merzenich MM (1986) Cortical map reorganization following neurovascular island skin transfers on the hands of adult owl monkeys. *Soc Neurosci Abstr* 12:391.
- Clark SA, Allard T, Jenkins WM, Merzenich MM (1988) Receptive fields in the body-surface map in adult cortex defined by temporally correlated inputs. *Nature* 332:444–445.
- Coghill RC, Gilron I, Iadarola MJ (2001) Hemispheric lateralization of somatosensory processing. *J Neurophysiol* 85:2602–2612.
- Cohen D (1968) Magnetoencephalography: evidence of magnetic fields produced by alpha-rhythm currents. *Science (80-)* 161:784–786.
- Cohen D (1972) Magnetoencephalography: detection of the brain’s electrical activity with a superconducting magnetometer. *Science (80-)* 175:664–666.

- Cohen YE, Andersen RA (2002) A common reference frame for movement plans in the posterior parietal cortex. *Nat Rev Neurosci* 3:553–562.
- Cooke DF, Taylor CSR, Moore T, Graziano MSA (2003) Complex movements evoked by microstimulation of the ventral intraparietal area. *Proc Natl Acad Sci U S A* 100:6163–6168.
- Coq J-O, Qi H, Collins CE, Kaas JH (2004) Anatomical and functional organization of somatosensory areas of the lateral fissure of the New World titi monkey (*Callicebus moloch*). *J Comp Neurol* 476:363–387.
- Coq JO, Xerri C (1998) Environmental enrichment alters organizational features of the forepaw representation in the primary somatosensory cortex of adult rats. *Exp brain Res* 121:191–204.
- Coq JO, Xerri C (2000) Age-related alteration of the forepaw representation in the rat primary somatosensory cortex. *Neuroscience* 99:403–411.
- Coq JO, Xerri C (2001) Sensorimotor experience modulates age-dependent alterations of the forepaw representation in the rat primary somatosensory cortex. *Neuroscience* 104:705–715.
- Craig AD (Bud) (2009) How do you feel--now? The anterior insula and human awareness. *Nat Rev Neurosci* 10:59–70.
- Craig JC, Johnson KO (2000) The Two-Point Threshold : Not a Measure of Tactile Spatial Resolution. *Am Psychol Soc* 9:29–32.
- Cronholm B (1951) Phantom limbs in amputees; a study of changes in the integration of centripetal impulses with special reference to referred sensations. *Acta Psychiatr Neurol Scand Suppl* 72:1–310.
- Cusick CG, Gould HJ (1990) Connections between area 3b of the somatosensory cortex and subdivisions of the ventroposterior nuclear complex and the anterior pulvinar nucleus in squirrel monkeys. *J Comp Neurol* 292:83–102.
- Cusick CG, Wall JT, Felleman DJ, Kaas JH (1989) Somatotopic organization of the lateral sulcus of owl monkeys : Area 3b , SII , and a ventral somatosensory area. *J Comp Neurol* 282:169–190.
- Dan Y, Poo M (2006) Spike timing-dependent plasticity : from synapse to perception. *Physiol Rev*:1033–1048.
- Dan Y, Poo M-M (2004) Spike timing-dependent plasticity of neural circuits. *Neuron* 44:23–30.
- Darian-Smith I, Johnson KO (1977) Thermal sensibility and thermoreceptors. *J Invest Dermatol* 69:146–153.
- DaSilva AFM, Becerra L, Makris N, Strassman AM, Gonzalez RG, Geatrakis N, Borsook D (2002) Somatotopic activation in the human trigeminal pain pathway. *J Neurosci* 22:8183–8192.
- Davis KD, Kiss ZHT, Luo L, Tasker RR, Lozano AM, Dostrovsky JO (1998) Phantom sensations generated by thalamic microstimulation. *Nature* 391:385–387.
- De Celis Alonso B, Lowe AS, Dear JP, Lee KC, Williams SCR, Finnerty GT (2008) Sensory inputs from whisking movements modify cortical whisker maps visualized with functional magnetic resonance imaging. *Cereb Cortex* 18:1314–1325.
- Debowy DJ, Ghosh S, Ro JY, Gardner EP (2001) Comparison of neuronal firing rates in somatosensory and posterior parietal cortex during prehension. *Exp Brain Res* 137:269–291.

- Del Gratta C, Della Penna S, Ferretti A, Franciotti R, Pizzella V, Tartaro A, Torquati K, Bonomo L, Romani GL, Rossini PM (2002) Topographic Organization of the Human Primary and Secondary Somatosensory Cortices: Comparison of fMRI and MEG Findings. *Neuroimage* 17:1373–1383.
- Del Gratta C, Penna S Della, Tartaro A, Ferretti A, Torquati K, Bonomo L, Romani GL, Rossini PM (2000) Topographic organization of the human primary and secondary somatosensory areas. *Neuroreport* 11:2035–2043.
- Dellon AL, Kallman CH (1983) Evaluation of functional sensation in the hand. *J Hand Surg Am* 8:865–870.
- Derdikman D, Hildesheim R, Ahissar E, Arieli A, Grinvald A (2003) Imaging spatiotemporal dynamics of surround inhibition in the barrels somatosensory cortex. *J Neurosci* 23:3100–3105.
- Devonshire IM, Papadakis NG, Port M, Berwick J, Kennerley AJ, Mayhew JEW, Overton PG (2012) Neurovascular coupling is brain region-dependent. *Neuroimage* 59:1997–2006.
- Devor A, Ulbert I, Dunn AK, Narayanan SN, Jones SR, Andermann ML, Boas D a, Dale AM (2005) Coupling of the cortical hemodynamic response to cortical and thalamic neuronal activity. *PNAS* 102:3822–3827.
- Di Russo F, Committeri G, Pitzalis S, Spitoni G, Piccardi L, Galati G, Catagni M, Nico D, Guariglia C, Pizzamiglio L (2006) Cortical plasticity following surgical extension of lower limbs. *Neuroimage* 30:172–183.
- Diamond ME, Armstrong-James M, Ebner FF (1993) Experience-dependent plasticity in adult rat barrel cortex. *PNAS* 90:2082–26.
- Diedrichsen J, Nambisan R, Kennerley SW, Ivry RB (2004) Independent on-line control of the two hands during bimanual reaching. *Eur J Neurosci* 19:1643–1652.
- Dinse HR, Goode B, Hilger T, Haupt SS, Spengler F, Zepka R (1997) Short-term functional plasticity of cortical and thalamic sensory representations and its implication for information processing. *Brain Plast Adv Neurol* 73:159–178.
- Dinse HR, Kleibel N, Kalisch T, Ragert P, Wilimzig C, Tegenthoff M (2006) Tactile coactivation resets age-related decline of human tactile discrimination. *Ann Neurol* 60:88–94.
- Dinse HR, Ragert P, Pleger B, Schwenkreis P, Tegenthoff M (2003) Pharmacological modulation of perceptual learning and associated cortical reorganization. *Science* 301:91–94.
- Dinse HR, Recanzone GH, Merzenich MM (1993) Alterations in correlated activity parallel ICMS-induced representational plasticity. *Neuroreport* 5:173–176.
- Disbrow E a, Hinkley LBN, Roberts TPL (2003a) Ipsilateral representation of oral structures in human anterior parietal somatosensory cortex and integration of inputs across the midline. *J Comp Neurol* 467:487–495.
- Disbrow E, Litinas E, Recanzone GH, Padberg J, Krubitzer L (2003b) Cortical connections of the second somatosensory area and the parietal ventral area in macaque monkeys. *J Comp Neurol* 462:382–399.
- Disbrow E, Litinas E, Recanzone GH, Slutsky D, Krubitzer L (2002) Thalamocortical connections of the parietal ventral area (PV) and the second somatosensory area (S2) in macaque monkeys. *Thalamus Relat Syst* 1:289.
- Disbrow E, Roberts TIM, Krubitzer L (2000) Somatotopic organization of cortical fields in the lateral sulcus of Homo sapiens : evidence for SII and PV. *J Comp Neurol* 418:1–21.

- Dostrovsky JO, Millar J, Wall PD (1976) The immediate shift of afferent drive of dorsal column nucleus cells following deafferentation: a comparison of acute and chronic deafferentation in gracile nucleus and spinal cord. *Exp Neurol* 52:480–495.
- Draganski B, Gaser C, Busch V, Schuierer G, Bogdahn U, May A (2004) Changes in grey matter induced by training. *Nature* 427:311–312.
- Dreyer DA, Loe PR, Met CB, Whitsel BL (1975) Representation of head and face in postcentral gyrus of the macaque. *J Neurophysiol* 38:714–733.
- Druschky K, Kaltenhäuser M, Hummel C, Druschky A, Pauli E, Huk WJ, Stefan H, Neundörfer B (2002) Somatotopic organization of the ventral and dorsal finger surface representations in human primary sensory cortex evaluated by magnetoencephalography. *Neuroimage* 15:182–189.
- Dupont E, Canu MH, Langlet C, Falempin M (2001) Time course of recovery of the somatosensory map following hindpaw sensory deprivation in the rat. *Neurosci Lett* 309:121–124.
- Dutta A, Kambi N, Raghunathan P, Khushu S, Jain N (2013) Large-scale reorganization of the somatosensory cortex of adult macaque monkeys revealed by fMRI. *Brain Struct Funct* 219:1305–1320.
- Dykes RW, Sur M, Merzenich MM, Kaas JH, Nelson RJ (1981) Regional segregation of neurons responding to quickly adapting, slowly adapting, deep and pacinian receptors within thalamic ventroposterior lateral and ventroposterior inferior nuclei in the squirrel monkey. *Neuroscience* 6:1687–1692.
- Eickhoff SB, Amunts K, Mohlberg H, Zilles K (2006a) The human parietal operculum. II. Stereotaxic maps and correlation with functional imaging results. *Cereb Cortex* 16:268–279.
- Eickhoff SB, Grefkes C, Fink GR, Zilles K (2008) Functional lateralization of face, hand, and trunk representation in anatomically defined human somatosensory areas. *Cereb cortex* 18:2820–2830.
- Eickhoff SB, Grefkes C, Zilles K, Fink GR (2007a) The somatotopic organization of cytoarchitectonic areas on the human parietal operculum. *Cereb Cortex* 17:1800–1811.
- Eickhoff SB, Heim S, Zilles K, Amunts K (2006b) Testing anatomically specified hypotheses in functional imaging using cytoarchitectonic maps. *Neuroimage* 32:570–582.
- Eickhoff SB, Paus T, Caspers S, Grosbras M-H, Evans AC, Zilles K, Amunts K (2007b) Assignment of functional activations to probabilistic cytoarchitectonic areas revisited. *Neuroimage* 36:511–521.
- Eickhoff SB, Schleicher A, Zilles K, Amunts K (2006c) The human parietal operculum. I. Cytoarchitectonic mapping of subdivisions. *Cereb Cortex* 16:254–267.
- Eickhoff SB, Stephan KE, Mohlberg H, Grefkes C, Fink GR, Amunts K, Zilles K (2005) A new SPM toolbox for combining probabilistic cytoarchitectonic maps and functional imaging data. *Neuroimage* 25:1325–1335.
- Elbert T, Candia V, Altenmüller E, Rau H, Sterr A, Rockstroh B, Pantev C, Taub E (1998) Alteration of digital representations in somatosensory cortex in focal hand dystonia. *Neuroreport* 9:3571–3575.
- Elbert T, Flor H, Birbaumer N, Knecht S, Hampson S, Larbig W, Taub E (1994) Extensive reorganization of the somatosensory cortex in adult humans after nervous system injury. *Neuroreport* 5:2593–2597.
- Elbert T, Pantev C, Wienbruch C, Rockstroh B, Taub E (1995) Increased cortical representation of the fingers of the left hand in string players. *Science* (80-) 270:305–307.

- Elbert T, Sterr A, Flor H, Rockstroh B, Knecht S, Pantev C, Wienbruch C, Taub E (1997) Input-increase and input-decrease types of cortical reorganization after upper extremity amputation in humans. *Exp brain Res* 117:161–164.
- Endo T, Spenger C, Tominaga T, Brené S, Olson L (2007) Cortical sensory map rearrangement after spinal cord injury: fMRI responses linked to Nogo signalling. *Brain* 130:2951–2961.
- Ergenzinger ER, Glasier MM, Hahm JO, Pons TP (1998) Cortically induced thalamic plasticity in the primate somatosensory system. *Nat Neurosci* 1:226–229.
- Erzurumlu RS, Chen Z-F, Jacquin MF (2006) Molecular determinants of the face map development in the trigeminal brainstem. *Anat Rec A Discov Mol Cell Evol Biol* 288:121–134.
- Essick GK, Edin BB (1995) Receptor encoding of moving tactile stimuli in Humans. II. The mean response of individual low-threshold mechanoreceptors to motion across the receptive field. *J Neurosci* 15:848–864.
- Essick GK, James A, McGlone FP (1999) Psychophysical assessment of the affective components of non-painful touch. *Neuroreport* 10:2083–2087.
- Fabri M, Polonara G, Del Pesce M, Quattrini a, Salvolini U, Manzoni T (2001) Posterior corpus callosum and interhemispheric transfer of somatosensory information: an fMRI and neuropsychological study of a partially callosotomized patient. *J Cogn Neurosci* 13:1071–1079.
- Fabri M, Polonara G, Quattrini A, Salvolini U, Del Pesce M, Manzoni T (1999) Role of the corpus callosum in the somatosensory activation of the ipsilateral cerebral cortex: An fMRI study of callosotomized patients. *Eur J Neurosci* 11:3983–3994.
- Fabri M, Polonara G, Salvolini U, Manzoni T (2005) Bilateral cortical representation of the trunk midline in human first somatic sensory area. *Hum Brain Mapp* 25:287–296.
- Faggin BM, Nguyen KT, Nicolelis MAL (1997) Immediate and simultaneous sensory reorganization at cortical and subcortical levels of the somatosensory system. *PNAS* 94:9428–9433.
- Fan X, Jin WY, Wang YT (2014) The NMDA receptor complex: a multifunctional machine at the glutamatergic synapse. *Front Cell Neurosci* 8.
- Fang P, Jain N, Kaas JH (2002) Few intrinsic connections cross the hand-face border of area 3b of new world monkeys. *J Comp Neurol* 454:310–319.
- Farah MJ (1998) Why does the somatosensory homunculus have hands next to face and feet next to Genitals? A hypothesis. *Neural Comput* 10:1983–1985.
- Farnè A, Roy AC, Giraux P, Dubernard JM, Sirigu A (2002) Face or hand, not both: perceptual correlates of reafferentation in a former amputee. *Curr Biol* 12:1342–1346.
- Feldman DE (2000) Timing-based LTP and LTD at vertical inputs to layer II/III pyramidal cells in rat barrel cortex. *Neuron* 27:45–56.
- Feldman DE, Brecht M (2005) Map plasticity in somatosensory cortex. *Science* (80-) 310:810–815.
- Feldmeyer D, Brecht M, Helmchen F, Petersen CCH, Poulet JF a, Staiger JF, Luhmann HJ, Schwarz C (2013) Barrel cortex function. *Prog Neurobiol* 103:3–27.
- Ferretti A, Del Gratta C, Babiloni C, Caulo M, Arienzo D, Tartaro A, Rossini PM, Romani GL (2004) Functional topography of the secondary somatosensory cortex for nonpainful and painful stimulation of median and tibial nerve: an fMRI study. *Neuroimage* 23:1217–1225.

- Fitzgerald PJ, Lane JW, Thakur PH, Hsiao SS (2006) Receptive field (RF) properties of the macaque second somatosensory cortex: RF size, shape and somatotopic organisation. *J Neurosci* 26:6485–6495.
- Flor H, Diers M (2009) Sensorimotor training and cortical reorganization. *NeuroRehabilitation* 25:19–27.
- Flor H, Elbert T, Knecht S, Wienbruch C, Pantev C, Birbaumer N, Larbig W, Taub E (1995) Phantom-limb pain as a perceptual correlate of cortical reorganization following arm amputation. *Nature* 375:482–484.
- Flor H, Elbert T, Mühlhnickel W, Pantev C, Wienbruch C, Taub E (1998) Cortical reorganization and phantom phenomena in congenital and traumatic upper-extremity amputees. *Exp brain Res* 119:205–212.
- Florence SL, Boydston L a, Hackett T a, Lachoff HT, Strata F, Niblock MM (2001) Sensory enrichment after peripheral nerve injury restores cortical, not thalamic, receptive field organization. *Eur J Neurosci* 13:1755–1766.
- Florence SL, Garraghty PE, Wall JT, Kaas JH (1994) Sensory afferent projections and area 3b somatotopy following median nerve cut and repair in macaque monkeys. *Cereb Cortex* 4:391–407.
- Florence SL, Hackett T a, Strata F (2000) Thalamic and cortical contributions to neural plasticity after limb amputation. *J Neurophysiol* 83:3154–3159.
- Florence SL, Kaas JH (1995) Large-scale reorganization at multiple levels of the somatosensory pathway follows therapeutic amputation of the hand in monkeys. *J Neurosci* 15:8083–8095.
- Florence SL, Taub HB, Kaas JH (1998) Large-scale sprouting of cortical connections after peripheral injury in adult macaque monkeys. *Science* (80-) 282:1117–1121.
- Florence SL, Wall JT, Kaas JH (1989) Somatotopic organization of inputs from the hand to the spinal gray and cuneate nucleus of monkeys with observations on the cuneate nucleus of humans. *J Comp Neurol* 286:48–70.
- Florence SL, Wall JT, Kaas JH (1991) Central projections from the skin of the hand in squirrel monkeys. *J Comp Neurol* 311:563–578.
- Foell J, Bekrater-Bodmann R, Diers M, Flor H (2013) Mirror therapy for phantom limb pain: brain changes and the role of body representation. *Eur J pain* 18:729–739.
- Fogassi L, Gallese V, Buccino G, Craighero L, Fadiga L, Rizzolatti G (2001) Cortical mechanism for the visual guidance of hand grasping movements in the monkey: A reversible inactivation study. *Brain* 124:571–586.
- Forss N, Jousmäki V, Hari R (1995) Interaction between afferent input from fingers in human somatosensory cortex. *Brain Res* 685:68–76.
- Fox K (1992) A critical period for experience-dependent synaptic plasticity in rat barrel cortex. *J Neurosci* 15:1826–1838.
- Fox MD, Snyder AZ, Vincent JL, Corbetta M, Van Essen DC, Raichle ME (2005) The human brain is intrinsically organized into dynamic, anticorrelated functional networks. *PNAS* 102:9673–9678.
- Fox K, Wallace H, Glazewski S (2014BC) Is there a thalamic component to experience-dependent cortical plasticity? *Philos Trans R Soc London Ser B, Biol Sci* 357:17091709–17091715.

- Francis ST, Kelly EF, Bowtell R, Dunseath WJ, Folger SE, McGlone F (2000) fMRI of the responses to vibratory stimulation of digit tips. *Neuroimage* 11:188–202.
- Frey SH, Bogdanov S, Smith JC, Watrous S, Breidenbach WC (2008) Chronically deafferented sensory cortex recovers a grossly typical organization after allogenic hand transplantation. *Curr Biol* 18:1530–1534.
- Freyer F, Becker R, Dinse HR, Ritter P (2013) State-dependent perceptual learning. *J Neurosci* 33:2900–2907.
- Freyer F, Reinacher M, Nolte G, Dinse HR, Ritter P (2012) Repetitive tactile stimulation changes resting-state functional connectivity — implications for treatment of sensorimotor decline. *Medicine (Baltimore)* 6:1–11.
- Friedman DP, Murray E a (1986) Thalamic connectivity of the second somatosensory area and neighboring somatosensory fields of the lateral sulcus of the macaque. *J Comp Neurol* 252:348–373.
- Friedman RM, Chen LM, Roe AW (2004) Modality maps within primate somatosensory cortex. *Proc Natl Acad Sci U S A* 101:12724–12729.
- Friedman RM, Chen LM, Roe AW (2008) Responses of Areas 3b and 1 in Anesthetized Squirrel Monkeys to Single- and Dual-Site Stimulation of the Digits. :3185–3196.
- Frostig RD (2006) Functional organization and plasticity in the adult rat barrel cortex: moving out-of-the-box. *Curr Opin Neurobiol* 16:445–450.
- Gandevia SC, Burke D, McKeon BB (1983) Convergence in the somatosensory pathway between cutaneous afferents from the index and middle fingers in man. *Exp brain Res* 50:415–425.
- Gandevia SC, Phegan CM (1999) Perceptual distortions of the human body image produced by local anaesthesia, pain and cutaneous stimulation. *J Physiol* 514:609–616.
- Garraghty PE, Hanes DP, Florence SL, Kaas JH (1994) Pattern of peripheral deafferentation predicts reorganizational limits in adult primate somatosensory cortex. *Somatosens Mot Res* 11:109–117.
- Garraghty PE, Kaas JH (1991) Large-scale functional reorganization in adult monkey cortex after peripheral nerve injury. *Proc Natl Acad Sci U S A* 88:6976–6980.
- Gentilucci M, Benuzzi F, Gangitano M, Grimaldi S (2012) Grasp With Hand and Mouth : A Kinematic Study on Healthy Subjects Grasp With Hand and Mouth : A Kinematic Study on Healthy Subjects. *J Neurophysiol*:1685–1699.
- Gentilucci M, Fogassi L, Luppino G, Matelli M, Camarda R, Rizzolatti G, Camarda R, Fogassi L, Gentilucci M, Luppino G, Matelli M (1988) Functional organization of inferior area 6 in the macaque monkey. *Exp Brain Res* 71:475–490.
- Georgiadis JR, Kortekaas R, Kuipers R, Nieuwenburg A, Pruim J, Reinders a a TS, Holstege G (2006) Regional cerebral blood flow changes associated with clitorally induced orgasm in healthy women. *Eur J Neurosci* 24:3305–3316.
- Geyer S, Ledberg A, Schleicher A, Kinomura S, Schormann T, Bürgel U, Klingberg T, Larsson J, Zilles K, Roland PE (1996) Two different areas within the primary motor cortex of man. *Nature* 382:805–807.
- Geyer S, Schleicher A, Zilles K (1999) Areas 3a, 3b, and 1 of human primary somatosensory cortex. Microstructural organization and interindividual variability. *Neuroimage* 10:63–83.

- Geyer S, Schormann T, Mohlberg H, Zilles K (2000) Areas 3a, 3b, and 1 of human primary somatosensory cortex. Spatial normalization to standard anatomical space. *Neuroimage* 11:684–696.
- Ghazanfar AA, Nicolelis MAL (1999) Spatiotemporal properties of layer V neurons of the rat primary somatosensory cortex. *Cereb cortex* 9:348–361.
- Gibson GO, Craig JC (2005) Tactile spatial sensitivity and anisotropy. *Percept Psychophys* 67:1061–1079.
- Gibson GO, Makinson CD, Sathian K (2009) Tactile co-activation improves detection of afferent spatial modulation. *Exp Brain Res* 194:409–417.
- Gibson JR, Beierlein M, Connors BW (1999) Two networks of electrically coupled inhibitory neurons in neocortex. *Nature* 402:75–79.
- Gilbert CD, Sigman M, Crist RE (2001) The neural basis of perceptual learning. *Neuron* 31:681–697.
- Giraux P, Sirigu A, Schneider F, Dubernard JM (2001) Cortical reorganization in motor cortex after graft of both hands. *Nat Neurosci* 4:691–692.
- Godde B, Berkefeld T, David-Jürgens M, Dinse HR (2002) Age-related changes in primary somatosensory cortex of rats: evidence for parallel degenerative and plastic-adaptive processes. *Neurosci Biobehav Rev* 26:743–752.
- Godde B, Ehrhardt J, Braun C (2003) Behavioral significance of input-dependent plasticity of human somatosensory cortex. *Neuroreport* 14:543–546.
- Godde B, Spengler F, Dinse HR (1996) Associative pairing of tactile stimulation induces somatosensory cortical reorganization in rats and humans. *Neuroreport* 8:281–285.
- Godde B, Stauffenberg B, Spengler F, Dinse HR (2000) Tactile coactivation-induced changes in spatial discrimination performance. *J Neurosci* 20:1597–1604.
- Golaszewski SM, Bergmann J, Christova M, Kunz AB, Kronbichler M, Rafolt D, Gallasch E, Staffen W, Trinka E, Nardone R (2012) Modulation of motor cortex excitability by different levels of whole-hand afferent electrical stimulation. *Clin Neurophysiol* 123:193–199.
- Goldreich D, Kanics IM (2003) Tactile acuity is enhanced in blindness. *J Neurosci* 23:3439–3445.
- Goloshevsky AG, Silva AC, Dodd SJ, Koretsky AP (2008) BOLD fMRI and somatosensory evoked potentials are well correlated over a broad range of frequency content of somatosensory stimulation of the rat forepaw. *Brain Res* 1195:67–76.
- Goltz D, Pleger B, Thiel S, Villringer A, Müller MM (2013) Sustained spatial attention to vibrotactile stimulation in the flutter range: relevant brain regions and their interaction. *PLoS One* 8:e84196.
- Goodwin AW, Wheat HE (2004) Sensory signals in neural populations underlying tactile perception and manipulation. *Annu Rev Neurosci* 27:53–77.
- Graziano A, Jones EG (2009) Early withdrawal of axons from higher centers in response to peripheral somatosensory denervation. *J Neurosci* 29:3738–3748.
- Graziano MS a, Cooke DF (2006) Parieto-frontal interactions, personal space, and defensive behavior. *Neuropsychologia* 44:2621–2635.
- Greenspan JD (1997) Nociceptors and the peripheral nervous system's role in pain. *J Hand Ther* 10:78–85.

- Grefkes C, Fink GR (2005) The functional organization of the intraparietal sulcus in humans and monkeys. *J Anat* 207:3–17.
- Grefkes C, Geyer S, Schormann T, Roland P, Zilles K (2001) Human somatosensory area 2: observer-independent cytoarchitectonic mapping, interindividual variability, and population map. *Neuroimage* 14:617–631.
- Greicius MD, Krasnow B, Reiss AL, Menon V (2003) Functional connectivity in the resting brain: a network analysis of the default mode hypothesis. *PNAS* 100:253–258.
- Grüsser SM, Winter C, Mühlhnickel W, Denke C, Karl A, Villringer K, Flor H (2001a) The relationship of perceptual phenomena and cortical reorganization in upper extremity amputees. *Neuroscience* 102:263–272.
- Grüsser SM, Winter C, Schaefer M, Fritzsche K, Benhidjeb T, Tunn P, Schlag PM, Flor H (2001b) Perceptual phenomena after unilateral arm amputation: a pre-post-surgical comparison. *Neurosci Lett* 302:13–16.
- Gu X, Fortier P a (1996) Early enhancement but no late changes of motor responses induced by intracortical microstimulation in the ketamine-anesthetized rat. *Exp Brain Res* 108:119–128.
- Guillery RW (1995) Anatomical evidence concerning the role of the thalamus in corticocortical communication : a brief review. *J Anat* 187:583–592.
- Gustin SM, Peck CC, Cheney LB, Macey PM, Murray GM, Henderson L a (2012) Pain and plasticity: is chronic pain always associated with somatosensory cortex activity and reorganization? *J Neurosci* 32:14874–14884.
- Hadoush H, Inoue K, Nakanishi K, Kurumadani H, Sunagawa T, Ochi M (2010) Ipsilateral primary sensorimotor cortical response to mechanical tactile stimuli. *Neuroreport* 21:108–113.
- Hadoush H, Sunagawa T, Nakanishi K, Ochi M (2012) Somatosensory cortical plasticity after toe-to-index transfer. *Neuroreport* 23:1000–1005.
- Haenzi S, Stefanics G, Lanaras T, Calcagni M, Ghosh A (2014) Altered cortical activation from the hand after facial botulinum toxin treatment. *Ann Clin Transl Neurol* 1:64–68.
- Hagen MC, Zald DH, Thornton T a, Pardo J V (2002) Somatosensory processing in the human inferior prefrontal cortex. *J Neurophysiol* 88:1400–1406.
- Haines DE (2003) *Neuroanatomy: an atlas of structures, sections and systems* (Wilkins LW&, ed)., 6th editio.
- Haines DE (2013) *Fundamental Neuroscience for Basic and Clinical Applications*, 4th Editio. Elsevier.
- Halata Z, Grim M, Bauman KI (2003) Friedrich Sigmund Merkel and his “Merkel cell”, morphology, development, and physiology: review and new results. *Anat Rec Part A* 271A:225–239.
- Halligan PW, Marshall JC, Wade DT (1994) Sensory disorganization and perceptual plasticity after lmb amputation: a follwo-up study. *Neuroreport*.
- Halligan PW, Marshall JC, Wade DT, Davey J, Morrison D (1993) Thumb in cheek? Sensory reorganization and perceptual plasticity after limb amputation. *Neuroreport* 4:233–236.
- Hämäläinen M, Hari R, Ilmoniemi RJ, Knuutila J, Lounasmaa O V (1993) Magnetoencephalography - theory, instrumentaton, and applications to noninvasive studies of the working human brain. *Rev Mod Phys* 65:413–497.

- Hanakawa T, Immisch I, Toma K, Dimyan M a, Van Gelderen P, Hallett M (2003) Functional properties of brain areas associated with motor execution and imagery. *J Neurophysiol* 89:989–1002.
- Hansson T, Brismar T (1999) Tactile stimulation of the hand causes bilateral cortical activation: a functional magnetic resonance study in humans. *Neurosci Lett* 271:29–32.
- Harel N, Lee S-P, Nagaoka T, Kim D-S, Kim S-G (2002) Origin of negative blood oxygenation level-dependent fMRI signals. *J Cereb blood flow Metab* 22:908–917.
- Harrar V, Spence C, Makin TR (2014) Topographic generalization of tactile perceptual learning. *J Exp Psychol Hum Percept Perform* 40:15–23.
- Harris J a, Miniussi C, Harris IM, Diamond ME (2002) Transient storage of a tactile memory trace in primary somatosensory cortex. *J Neurosci* 22:8720–8725.
- Harris JA, Harris IM, Diamond ME (2001) The topography of tactile learning in humans. *J Neurosci* 21:1056–1061.
- Hartline HK (1938) The response of single optic nerve fibers of the vertebrate eye to illumination of the retina. *Am J Physiol* 121:400–415.
- Hashimoto I, Mashiko T, Kimura T, Imada T (1999a) Are there discrete distal-proximal representations of the index finger and palm in the human somatosensory cortex? A neuromagnetic study. *Clin Neurophysiol* 110:430–437.
- Hashimoto I, Saito Y, Iguchi Y, Kimura T, Fukushima T, Terasaki O, Sakuma K (1999b) Distal-proximal somatotopy in the human hand somatosensory cortex: a reappraisal. *Exp Brain Res* 129:467–472.
- Hashimoto I, Suzuki A, Kimura T, Iguchi Y, Tanosaki M, Takino R, Haruta Y, Taira M (2004) Is there training-dependent reorganization of digit representations in area 3b of string players? *Clin Neurophysiol* 115:435–447.
- Health M, Murray EA, Mishkin M (1984) Relative contributions of SII and area 5 to tactile discrimination in monkeys. *Behav Brain Res* 11:67–83.
- Hebb DO (1949) *The organization of behavior*, New York: .
- Henderson L a, Gustin SM, Macey PM, Wrigley PJ, Siddall PJ (2011) Functional reorganization of the brain in humans following spinal cord injury: evidence for underlying changes in cortical anatomy. *J Neurosci* 31:2630–2637.
- Hickmott PW, Merzenich MM (1998) Single-cell correlates of a representational boundary in rat somatosensory cortex. *J Neurosci* 18:4403–4416.
- Hickmott PW, Steen PA (2005) Large-scale changes in dendritic structure during reorganization of adult somatosensory cortex. *Nat Neurosci* 8:140–142.
- Hlushchuk Y, Forss N, Hari R (2004) Distal-to-proximal representation of volar index finger in human area 3b. *Neuroimage* 21:696–700.
- Hlushchuk Y, Hari R (2006) Transient suppression of ipsilateral primary somatosensory cortex during tactile finger stimulation. *J Neurosci* 26:5819–5824.
- Hlustík P, Solodkin A, Gullapalli RP, Noll DC, Small SL (2001) Somatotopy in human primary motor and somatosensory hand representations revisited. *Cereb cortex* 11:312–321.
- Hodzic A, Veit R, Karim AA, Erb M, Godde B (2004) Improvement and decline in tactile discrimination behavior after cortical plasticity induced by passive tactile coactivation. *J Neurosci* 24:442–446.

- Hoechstetter K, Rupp A, Stancák A, Meinck HM, Stippich C, Berg P, Scherg M (2001) Interaction of tactile input in the human primary and secondary somatosensory cortex--a magnetoencephalographic study. *Neuroimage* 14:759–767.
- Höffken O, Lenz M, Höckelmann N, Dinse HR, Tegenthoff M (2012) Noradrenergic modulation of human visual cortex excitability assessed by paired-pulse visual-evoked potentials. *Neuroreport* 23:707–711.
- Höffken O, Veit M, Knossalla F, Lissek S, Bliem B, Ragert P, Dinse HR, Tegenthoff M (2007) Sustained increase of somatosensory cortex excitability by tactile coactivation studied by paired median nerve stimulation in humans correlates with perceptual gain. *J Physiol* 584:463–471.
- Hoffmeyer HW, Enager P, Thomsen KJ, Lauritzen MJ (2007) Nonlinear neurovascular coupling in rat sensory cortex by activation of transcallosal fibers. *J Cereb Blood Flow Metab* 27:575–587.
- Hoshiyama M, Kakigi R (2001) Two evoked responses with different recovery functions in the primary somatosensory cortex in humans. *Clin Neurophysiol* 112:1334–1342.
- Hoshiyama M, Kakigi R, Koyama S, Kitamura Y, Shimoio M, Watanabe S (1995) Somatosensory evoked magnetic fields after mechanical stimulation of the scalp in humans. *Neurosci Lett* 195:29–32.
- Hoshiyama M, Kakigi R, Koyama S, Watanabe S, Shimojo M (1997) Activity in posterior parietal cortex following somatosensory stimulation in man: magnetoencephalographic study using spatio-temporal source analysis. *Brain Topogr* 10:23–30.
- Hoshiyama M, Ryusuke K, Koyama S, Kitamura Y, Shimojo M, Watanabe S, Kakigi R (1996) Somatosensory evoked magnetic fields following stimulation of the lip in humans. *Electroencephalogr Clin Neurophysiol* 100:96–104.
- Hozumi J, Sumitani M, Yozu A, Tomioka T, Sekiyama H, Miyauchi S, Yamada Y (2011) Oral local anesthesia successfully ameliorated neuropathic pain in an upper limb suggesting pain alleviation through neural plasticity within the central nervous system: a case report. *Anesthesiol Res Pract* 2011:984281.
- Hu K-S, Kwak J, Koh K-S, Abe S, Fontaine C, Kim H-J (2007) Topographic distribution area of the infraorbital nerve. *Surg Radiol Anat* 29:383–388.
- Huang R-S, Chen C, Tran AT, Holstein KL, Sereno MI (2012) Mapping multisensory parietal face and body areas in humans. *Proc Natl Acad Sci U S A* 109:18114–18119.
- Huffman KJ, Krubitzer L (2001) Area 3a: topographic organization and cortical connections in marmoset monkeys. *Cereb Cortex* 11:849–867.
- Huse E, Preissl H, Larbig W, Birbaumer N (2001) Phantom limb pain. *Lancet* 358:2001.
- Huttunen JK, Gröhn O, Penttonen M (2008) Coupling between simultaneously recorded BOLD response and neuronal activity in the rat somatosensory cortex. *Neuroimage* 39:775–785.
- Hyvärinen J (1981) Regional distribution of functions in parietal association area 7 of the monkey. *Brain Res* 206:287–303.
- Hyvärinen J, Poranen A (1978) Receptive field integration and submodality convergence in the hand area of the post-central gyrus of the alert monkey. *J Physiol* 283:539–556.
- Iannetti G., Porro C., Pantano P, Romanelli P., Galeotti F, Cruccu G (2003) Representation of different trigeminal divisions within the primary and secondary human somatosensory cortex. *Neuroimage* 19:906–912.

- Iguchi Y, Hoshi Y, Hashimoto I (2001) Selective spatial attention induces short-term plasticity in human somatosensory cortex. *Neuroreport* 12:3133–3136.
- Iguchi Y, Hoshi Y, Tanosaki M, Taira M, Hashimoto I (2002) Selective attention regulates spatial and intensity information processing in the human primary somatosensory cortex. *Neuroreport* 13:2335–2339.
- Imai T, Kamping S, Breitenstein C, Pantev C, Lütkenhöner B, Knecht S (2003) Learning of tactile frequency discrimination in humans. *Hum Brain Mapp* 18:260–271.
- Inoue K, Nakanishi K, Hadoush H, Kurumadani H, Hashizume A, Sunagawa T, Ochi M (2013) Somatosensory mechanical response and digit somatotopy within cortical areas of the postcentral gyrus in humans: an MEG study. *Hum Brain Mapp* 34:1559–1567.
- Itomi K, Kakigi R, Maeda K, Hoshiyama M (2000) Dermatome versus homunculus; detailed topography of the primary somatosensory cortex following trunk stimulation. *Clin Neurophysiol* 111:405–412.
- Iwamura Y (1998) Hierarchical somatosensory processing. *Curr Opin Neurobiol* 8:522–528.
- Iwamura Y (2000) Bilateral receptive field neurons and callosal connections in the somatosensory cortex. *Philos Trans R Soc Lond B Biol Sci* 355:267–273.
- Iwamura Y, Iriki A, Tanaka M (1994) Bilateral hand representation in the postcentral somatosensory cortex. *Nature* 369:554–556.
- Iwamura Y, Tanaka M (1978) Postcentral neurons in hand region of area 2: their possible role in the form discrimination of tactile objects. *Brain Res* 150:662–666.
- Iwamura Y, Tanaka M, Hikosaka O (1980) Overlapping representation of fingers in the somatosensory cortex (area 2) of the conscious monkey. *Brain Res* 197:516–520.
- Iwamura Y, Tanaka M, Sakamoto M, Hikosaka O (1993) Rostrocaudal gradients in the neuronal receptive field complexity in the finger region of the alert monkey's postcentral gyrus. *Exp Brain Res* 92:360–368.
- Iwamura Y, Taoka M, Iriki A (2001) Bilateral activity and callosal connections in the somatosensory cortex. *Neurosci* 7:419–429.
- Jacobs K, Donoghue J (1991) Reshaping the cortical motor map by unmasking latent intracortical connections. *Science* (80-) 251:944–947.
- Jain N (2002) Adult brain plasticity - what is revealed is exciting, what is hidden is critical. *J Biosci* 27:439–442.
- Jain N, Catania KC, Kaas JH (1997) Deactivation and reactivation of somatosensory cortex after dorsal spinal cord injury. *Nature* 386:495–498.
- Jain N, Florence SL, Kaas JH (1995) Limits on plasticity in somatosensory cortex of adult rats: hindlimb cortex is not reactivated after dorsal column section. *J Neurophysiol* 73:1537–1546.
- Jain N, Florence SL, Qi HX, Kaas JH (2000) Growth of new brainstem connections in adult monkeys with massive sensory loss. *Proc Natl Acad Sci U S A* 97:5546–5550.
- Jain N, Qi H, Catania KC, Kaas JH (2001) Anatomic correlates of the face and oral cavity representations in the somatosensory cortical area 3b of monkeys. *J Comp Neurol* 429:455–468.
- Jain N, Qi H-X, Collins CE, Kaas JH (2008) Large-scale reorganization in the somatosensory cortex and thalamus after sensory loss in macaque monkeys. *J Neurosci* 28:11042–11060.

- Jamali S, Ross B (2013) Somatotopic finger mapping using MEG: toward an optimal stimulation paradigm. *Clin Neurophysiol* 124:1659–1670.
- Jasmin L, Rabkin SD, Granato A, Boudah A, Ohara PT (2003) Analgesia and hyperalgesia from GABA-mediated modulation of the cerebral cortex. *Nature* 424:316–320.
- Jenkins WM, Merzenich MM (1987) Reorganization of neocortical representations after brain injury: a neurophysiological model of the bases of recovery from stroke. *Prog Brain Res* 71:249–266.
- Jenkins WM, Merzenich MM, Ochs MT, Allard T, Guic-Robles E (1990) Functional reorganization of primary somatosensory cortex in adult owl monkeys after behaviorally controlled tactile stimulation. *J Neurophysiol* 63:82–104.
- Johansson RS (1978) Tactile sensibility in the human hand: receptive fields characteristics of mechanoreceptive units in the glabrous skin area. *J Physiol* 281:101–123.
- Johansson RS, Trulsson M, Olsson KA, Westberg KG (1988) Mechanoreceptor activity from the human face and oral mucosa. *Exp brain Res* 72:204–208.
- Johansson RS, Vallbo AB (1979) Tactile sensibility in the human hand: relative and absolute densities of four types of mechanoreceptive units in glabrous skin. *J Physiol*:283–300.
- Johnson KO (2001) The roles and functions of cutaneous mechanoreceptors. *Curr Opin Neurobiol* 11:455–461.
- Johnson KO, Hsiao SS (1992) Neural mechanisms of tactual form and texture perception. *Annu Rev Neurosci* 15:227–250.
- Johnson KO, Phillips JR (1981) Tactile spatial resolution. I. Two-point discrimination, gap detection, grating resolution, and letter recognition. *J Neurophysiol* 46:1177–1192.
- Johnson PB, Ferraina S, Bianchi L, Caminiti R (1996) Cortical networks for visual reaching: Physiological and anatomical organization of frontal and parietal lobe arm regions. *Cereb Cortex* 6:102–119.
- Jones EG (1993) GABAergic neurons and their role in cortical plasticity in primates. *Cereb Cortex* 3:361–372.
- Jones EG (2000) Cortical and subcortical contributions to activity-dependent plasticity in primate somatosensory cortex. *Annu Rev Neurosci* 23:1–37.
- Jones EG, Coulter JD, Hendry SHC (1978) Intracortical connectivity of architectonic fields in the somatic sensory, motor and parietal cortex of monkeys. *J Comp Neurol* 181:291–348.
- Jones EG, Friedman DP (1982) Projection pattern of functional components of thalamic ventrobasal complex on monkey somatosensory cortex. *J Neurophysiol* 48:521–544.
- Jones EG, Friedman DP, Hendry SHC (1982) Thalamic basis of place- and modality-specific columns in monkey somatosensory cortex: a correlative anatomical and physiological study. *J Neurophysiol* 48:545–568.
- Jones EG, Pons TP (1998) Thalamic and brainstem contributions to large-scale plasticity of primate somatosensory cortex. *Science* (80-) 282:1121–1125.
- Jones EG, Powell TPS (1969) Connexions of the somatic sensory cortex of the rhesus monkey. II. Contralateral cortical connexions. *Brain* 92:717–730.
- Jones EG, Powell TPS (1970) Connexions of the somatic sensory cortex of the rhesus monkey. III. Thalamic connexions. *Brain* 93:37–56.

- Jung P, Baumgärtner U, Bauermann T, Magerl W, Gawehn J, Stoeter P, Treede R-D (2003) Asymmetry in the human primary somatosensory cortex and handedness. *Neuroimage* 19:913–923.
- Jung P, Baumgärtner U, Magerl W, Treede R-D (2008) Hemispheric asymmetry of hand representation in human primary somatosensory cortex and handedness. *Clin Neurophysiol* 119:2579–2586.
- Jung S-C, Shin H-C (2002) Reversible changes of presumable synaptic connections between primary somatosensory cortex and ventral posterior lateral thalamus of rats during temporary deafferentation. *Neurosci Lett* 331:111–114.
- Kaas AL, van de Ven V, Reithler J, Goebel R, Ven V van de (2013a) Tactile perceptual learning: learning curves and transfer to the contralateral finger. *Exp brain Res* 224:477–488.
- Kaas AL, van Mier H, Visser M, Goebel R (2013b) The neural substrate for working memory of tactile surface texture. *Hum Brain Mapp* 34:1148–1162.
- Kaas JH (1999) Commentary: Is most of neural plasticity in the thalamus cortical? *PNAS* 96:7622–7623.
- Kaas JH (2005) The future of mapping sensory cortex in primates: three of many remaining issues. *Philos Trans R Soc Lond B Biol Sci* 360:653–664.
- Kaas JH, Florence SL, Jain N (1999) Subcortical contributions to massive cortical reorganizations. *Neuron* 22:657–660.
- Kaas JH, Nelson RJ, Sur M, Dykes RW, Merzenich MM (1984) The somatotopic organization of the ventroposterior thalamus of the squirrel monkey, *Saimiri sciureus*. *J Comp Neurol* 226:111–140.
- Kaas JH, Nelson RJ, Sur M, Lin CS, Merzenich MM (1979) Multiple representations of the body within the primary somatosensory cortex of primates. *Science* (80-) 204:1977–1979.
- Kaas JH, Pons TP (1988) The somatosensory system of primates. In: Steklis HD, Erwin J, editors. *Neurosciences*. New York: Alan R. Liss, pp 421–468.
- Kaas JH, Qi H-X, Burish MJ, Gharbawie O a, Onifer SM, Massey JM, Massey M (2008) Cortical and subcortical plasticity in the brains of humans, primates, and rats after damage to sensory afferents in the dorsal columns of the spinal cord. *Exp Neurol* 209:407–416.
- Kakigi R, Hoshiyama M, Shimojo M, Naka D, Itomi K, Nakamura A, Yamasaki H, Watanabe S, Xiang J, Maeda K, Lam K (2000) The somatosensory evoked magnetic fields. *Prog Neurobiol* 61:495–523.
- Kakigi R, Koyama S, Hoshiyama M, Kitamura Y, Shimojo M, Watanabe S, Nakamura A (1996) Effects of tactile interference stimulation on somatosensory evoked magnetic fields. *Neuroreport* 7:405–408.
- Kalisch T, Kattenstroth J, Kowalewski R, Tegenthoff M, R H, Dinse HR (2012a) Cognitive and tactile factors affecting human haptic performance in later life. *PLoS One* 7:e30420.
- Kalisch T, Kattenstroth J-C, Kowalewski R, Tegenthoff M, Dinse HR (2012b) Age-related changes in the joint position sense of the human hand. *Clin Interv Aging* 7:499–507.
- Kalisch T, Ragert P, Schwenkreis P, Dinse HR, Tegenthoff M (2009) Impaired tactile acuity in old age is accompanied by enlarged hand representations in somatosensory cortex. *Cereb Cortex* 19:1530–1538.
- Kalisch T, Tegenthoff M, Dinse HR (2007) Differential effects of synchronous and asynchronous multifinger coactivation on human tactile performance. *BMC Neurosci* 8:58.

- Kalisch T, Tegenthoff M, Dinse HR (2008) Improvement of sensorimotor functions in old age by passive sensory stimulation. *Clin Interv Aging* 3:673–690.
- Kalisch T, Tegenthoff M, Dinse HR (2010) Repetitive electric stimulation elicits enduring improvement of sensorimotor performance in seniors. *Neural Plast* 2010:690531.
- Kang R, Herman D, MacGillis M, Zarzecki P (1985) Convergence of sensory inputs in somatosensory cortex: interactions from separate afferent sources. *Exp brain Res* 57:271–278.
- Kannurpatti SS, Biswal BB (2004) Negative functional response to sensory stimulation and its origins. *J Cereb blood flow Metab* 24:703–712.
- Karl A, Birbaumer N, Lutzenberger W, Cohen LG, Flor H (2001) Reorganization of motor and somatosensory cortex in upper extremity amputees with phantom limb pain. *J Neurosci* 21:3609–3618.
- Kastrup A, Baudewig J, Schnaudigel S, Huonker R, Becker L, Sohns JM, Dechent P, Klingner C, Witte OW (2008) Behavioral correlates of negative BOLD signal changes in the primary somatosensory cortex. *Neuroimage* 41:1364–1371.
- Kattenstroth J-C, Kalisch T, Peters S, Tegenthoff M, Dinse HR (2012) Long-term sensory stimulation therapy improves hand function and restores cortical responsiveness in patients with chronic cerebral lesions. Three single case studies. *Front Hum Neurosci* 6:244.
- Katz DB, Simon SA, Moody A, Nicolelis MAL (1999) Simultaneous reorganization in thalamocortical ensembles evolves over several hours after perioral capsaicin injections. *J Neurophysiol* 82:963–977.
- Katz J (1992) Psychophysical correlates of phantom limb experience. *J Neurol Neurosurg Psychiatry* 55:811–821.
- Kell CA, von Kriegstein K, Rösler A, Kleinschmidt A, Laufs H (2005) The sensory cortical representation of the human penis: revisiting somatotopy in the male homunculus. *J Neurosci* 25:5984–5987.
- Kelso SR, Ganong A H, Brown TH (1986) Hebbian synapses in hippocampus. *PNAS* 83:5326–5330.
- Kennerley AJ, Mayhew JE, Boorman L, Zheng Y, Berwick J (2012) Is optical imaging spectroscopy a viable measurement technique for the investigation of the negative BOLD phenomenon? A concurrent optical imaging spectroscopy and fMRI study at high field (7 T). *Neuroimage* 61:10–20.
- Kenshalo DR, Giesler GJ, Leonard RB, Willis WD (1980) Responses of neurons in primate ventral posterior lateral nucleus to noxious stimuli. *J Neurophysiol* 43:1594–1614.
- Kew JJ, Halligan PW, Marshall JC, Passingham RE, Rothwell JC, Ridding MC, Marsden CD, Brooks DJ (1997) Abnormal access of axial vibrotactile input to deafferented somatosensory cortex in human upper limb amputees. *J Neurophysiol* 77:2753–2764.
- Killackey HP, Gould HJ, Cusick CG, Pons TP, Kaas JH (1983) The relation of corpus callosum connections to architectonic fields and body surface maps in sensorimotor cortex of new and old world monkeys. *J Comp Neurol* 219:384–419.
- Kim S-G, Ogawa S (2012) Biophysical and physiological origins of blood oxygenation level-dependent fMRI signals. *J Cereb Blood Flow Metab* 32:1188–1206.
- Kimura J (2013) *Electrodiagnosis in diseases of nerve and muscle: principles and practice*, Oxford Uni.
- Kis Z, Farkas T, Rábl K, Kis E, Kóródi K, Simon L, Marusin I, Rojik I, Toldi J (1999) Comparative study of the neuronal plasticity along the neuraxis of the vibrissal sensory system of adult rat

- following unilateral infraorbital nerve damage and subsequent regeneration. *Exp brain Res* 126:259–269.
- Klingner CM, Hasler C, Brodoehl S, Witte OW (2010) Dependence of the negative BOLD response on somatosensory stimulus intensity. *Neuroimage* 53:189–195.
- Klingner CM, Hasler C, Brodoehl S, Witte OW (2014) Excitatory and inhibitory mechanisms underlying somatosensory habituation. *Hum Brain Mapp* 35:152–160.
- Klingner CM, Huonker R, Flemming S, Hasler C, Brodoehl S, Preul C, Burmeister H, Kastrup A, Witte OW (2011) Functional deactivations: multiple ipsilateral brain areas engaged in the processing of somatosensory information. *Hum Brain Mapp* 32:127–140.
- Knecht S, Henningsen H, Elbert T, Flor H, Höhling C, Pantev C, Taub E, Hohling C (1996a) Reorganizational and perceptual changes after amputation. *Brain* 119:1213–1219.
- Knecht S, Henningsen H, Höhling C, Elbert T, Flor H, Pantev C, Taub E (1998) Plasticity of plasticity? Changes in the pattern of perceptual correlates of reorganization after amputation. *Brain* 121:717–724.
- Knecht S, Kunesch E, Schnitzler A (1996b) Parallel and serial processing of haptic information in man: Effects of parietal lesions on sensorimotor hand function. *Neuropsychologia* 34:669–687.
- Knibestol M (1973) Stimulus-response functions of rapidly adapting mechanoreceptors in the human glabrous skin area. *J Physiol* 245:427–452.
- Knibestöl M, Vallbo ÅB (1970) Single unit analysis of mechanoreceptor activity from the human glabrous skin. *Acta Physiol Scand* 80:178–195.
- Kopietz R, Sakar V, Albrecht J, Kleemann AM, Schöpf V, Yousry I, Linn J, Fesl G, Wiesmann M (2009) Activation of primary and secondary somatosensory regions following tactile stimulation of the face. *Clin Neuroradiol* 19:135–144.
- Korvenoja A (2007) Comparison and integration of MEG and fMRI in the study of somatosensory and motor systems.
- Kowalewski R, Kattenstroth J, Kalisch T, Dinse HR (2012) Improved acuity and dexterity but unchanged touch and pain thresholds following repetitive sensory stimulation of the fingers. *Neural Plast* 2012.
- Krause T, Kurth R, Ruben J, Schwiemann J, Villringer K, Deuchert M, Moosmann M, Brandt S, Wolf K-J, Curio G, Villringer A (2001) Representational overlap of adjacent fingers in multiple areas of human primary somatosensory cortex depends on electrical stimulus intensity: an fMRI study. *Brain Res* 899:36–46.
- Krunitzer L a, Kaas JH (1987) Thalamic connections of three representations of the body surface in somatosensory cortex of gray squirrels. *J Comp Neurol* 265:549–580.
- Krunitzer L a, Kaas JH (1992) The somatosensory thalamus of monkeys: cortical connections and a redefinition of nuclei in marmosets. *J Comp Neurol* 319:123–140.
- Krunitzer L a, Sesma M a, Kaas JH (1986) Microelectrode maps, myeloarchitecture, and cortical connections of three somatotopically organized representations of the body surface in the parietal cortex of squirrels. *J Comp Neurol* 250:403–430.
- Krunitzer L, Clarey J, Tweedale R, Elston G, Calford M (1995) A redefinition of somatosensory areas in the lateral sulcus of macaque monkeys. *15:3821–3839*.

- Kurth R, Villringer K, Curio G, Wolf K-J, Krause T, Repenthin J, Schwiemann J, Deuchert M, Villringer A (2000) fMRI shows multiple somatotopic digit representations in human primary somatosensory cortex. *Neuroreport* 11:1487–1491.
- Lacour JP, Dubois D, Pisani A, Ortonne JP (1991) Anatomical mapping of Merkel cells in normal human adult epidermis. *Br J Dermatol* 125:535–542.
- Ladda AM, Pfannmoeller JP, Kalisch T, Roschka S, Platz T, Dinse HR, Lotze M (2014) Effects of combining 2 weeks of passive sensory stimulation with active hand motor training in healthy adults. *PLoS One* 9:e84402.
- Lane RD, Bennett-clarke CA, Chiaia NL, Killackey HP, Rhoades RW (1995) Lesion-induced reorganization in the brainstem is not completely expressed in somatosensory cortex. *PNAS* 92:4264–4268.
- Langlet C, Canu MH, Falempin M (1999) Short-term reorganization of the rat somatosensory cortex following hypodynamia-hypokinesia. *Neurosci Lett* 266:145–148.
- Leinonen L, Hyvärinen J, Nyman G, Linnankoski I (1979) I. Functional properties of neurons in lateral part of associative area 7 in awake monkeys. *Exp Brain Res* 34:321–333.
- Lenz FA, Garonzik IM, Zirh TA, Dougherty PM (1998) Neuronal activity in the region of the thalamic principal sensory nucleus (ventralis caudalis) in patients with pain following amputations. *Neuroscience* 86:1065–1081.
- Li CX, Callaway JC, Waters RS (2002) Removal of GABAergic inhibition alters subthreshold input in neurons in forepaw barrel subfield (FBS) in rat first somatosensory cortex (SI) after digit stimulation. *Exp Brain Res* 145:411–428.
- Liao C-C, Qi H-X, Reed JL, Miller DJ, Kaas JH (2014) Congenital foot deformation alters the topographic organization in the primate somatosensory system. *Brain Struct Funct* Oct:1–24.
- Liepert J, Oreja-Guevara C, Cohen LG, Tegenthoff M, Hallett M, Malin J-P (1999) Plasticity of cortical hand muscle representation in patients with hemifacial spasm. *Neurosci Lett* 272:33–36.
- Liepert J, Tegenthoff M, Malin JP (1995) Changes of cortical motor area size during immobilization. *Electroencephalogr Clin Neurophysiol* 97:382–386.
- Lin C-CK, Sun Y, Huang C-I, Yu C-Y, Ju M-S (2010) Cortical activation by tactile stimulation to face and anterior neck areas: an fMRI study with three analytic methods. *Hum Brain Mapp* 31:1876–1885.
- Lin CS, Merzenich MM, Sur M, Kaas JH (1979) Connections of areas 3b and 1 of the parietal somatosensory strip with the ventroposterior nucleus in the owl monkey (*Aotus trivirgatus*). *J Comp Neurol* 185:355–372.
- Lin L-D, Murray GM, Sessle BJ (1994) Functional properties of single neurons in the primate face primary somatosensory cortex. I. Relations with trained orofacial motor behaviors. *J Neurosci* 14:2377–2390.
- Lipton ML, Fu K-MG, Branch C a, Schroeder CE (2006) Ipsilateral hand input to area 3b revealed by converging hemodynamic and electrophysiological analyses in macaque monkeys. *J Neurosci* 26:180–185.
- Lipton ML, Liszewski MC, O’Connell MN, Mills A, Smiley JF, Branch C a, Isler JR, Schroeder CE (2010) Interactions within the hand representation in primary somatosensory cortex of primates. *J Neurosci* 30:15895–15903.

- Liu LC, Gaetz WC, Bosnyak DJ, Roberts LE (2000) Evidence for fusion and segregation induced by 21 Hz multiple-digit stimulation in humans. *Neuroreport* 11:2313–2318.
- Lockwood PL, Iannetti GD, Haggard P (2013) Transcranial magnetic stimulation over human secondary somatosensory cortex disrupts perception of pain intensity. *Cortex* 49:2201–2209.
- Lofvenberg J, Johansson RS (1984) Regional differences and interindividual variability in sensitivity to vibration in the glabrous skin of the human hand. *Brain Res* 301:65–72.
- Logothetis NK, Pauls J, Augath M, Trinath T, Oeltermann A (2001) Neurophysiological investigation of the basis of the fMRI signal. *Nature* 412:150–157.
- Löken LS, Wessberg J, Morrison I, McGlone F, Olausson H (2009) Coding of pleasant touch by unmyelinated afferents in humans. *Nat Neurosci* 12:547–548.
- Longo MR, Azañón E, Haggard P, Aza E (2010) More than skin deep: body representation beyond primary somatosensory cortex. *Neuropsychologia* 48:655–668.
- Lorente de No R (1938) Architectonics and structure of the cerebral cortex. *Physiol Nerv Syst*:291–330.
- Lotze M, Grodd W, Birbaumer N, Erb M, Huse E, Flor H (1999) Does use of a myoelectric prosthesis prevent cortical reorganization and phantom limb pain? *Nat Neurosci* 2:501–502.
- Lu L, Gainey MA, Goldbeck JE, Feldman DE (2014) Rapid homeostasis by disinhibition during whisker map plasticity. *Proc Natl Acad Sci U S A* 111:1616–1621.
- Lundborg G, Rosén B (2004) The two-point discrimination test - Time for a re-appraisal ? *J Hand Surg Am* 29B:418–422.
- Macaluso E, Maravita A (2010) The representation of space near the body through touch and vision. *Neuropsychologia* 48:782–795.
- Mackel R, Brink EE, Wittkowsky G (1985) Properties of cutaneous mechanosensitive afferents during the early stages of regeneration in man. *Brain Res* 329:49–69.
- Maeda K, Kakigi R, Hoshiyama M, Koyama S (1999) Topography of the secondary somatosensory cortex in humans : a magnetoencephalographic study. *Neuroreport* 10:301–306.
- Makin TR, Cramer AO, Scholz J, Hahamy A, Henderson Slater D, Tracey I, Johansen-Berg H (2013a) Deprivation-related and use-dependent plasticity go hand in hand. *Elife* 2:1–15.
- Makin TR, Scholz J, Filippini N, Henderson Slater D, Tracey I, Johansen-Berg H (2013b) Phantom pain is associated with preserved structure and function in the former hand area. *Nat Commun* 4:1–8.
- Maksimovic S, Nakatani M, Baba Y, Nelson AM, Marshall KL, Wellnitz SA, Firozi P, Woo S-H, Ranade S, Patapoutian A, Lumpkin EA (2014) Epidermal Merkel cells are mechanosensory cells that tune mammalian touch receptors. *Nature* 509:617–621.
- Maldjian JA, Gottschalk A, Patel RS, Detre JA, Alsop DC (1999) The sensory somatotopic map of the human hand demonstrated at 4 Tesla. *Neuroimage* 10:55–62.
- Malinen S, Renvall V, Hari R (2014) Functional parcellation of the human primary somatosensory cortex to natural touch. *Eur J Neurosci* 39:738–743.
- Malinen S, Schürmann M, Hlushchuk Y, Forss N, Hari R (2006) Improved differentiation of tactile activations in human secondary somatosensory cortex and thalamus using cardiac-triggered fMRI. *Exp brain Res* 174:297–303.

- Manger PR, Woods TM, Jones EG (1995) Representation of the face and intraoral structures in area 3b of the squirrel monkey (*Saimiri sciureus*) somatosensory cortex, with special reference to the ipsilateral representation. *J Comp Neurol* 362:597–607.
- Manger PR, Woods TM, Jones EG (1996) Representation of face and intra-oral structures in area 3b of macaque monkey somatosensory cortex. *J Comp Neurol* 371:513–521.
- Manger PR, Woods TM, Muñoz A, Jones EG (1997) Hand/face border as a limiting boundary in the body representation in monkey somatosensory cortex. *J Neurosci* 17:6338–6351.
- Manzoni T, Barbaresi P, Bellardinelli E, Caminiti R (1980) Callosal projections from the two body midlines. *Exp brain Res* 39:1–9.
- Manzoni T, Barbaresi P, Conti F (1984) Callosal mechanism for the interhemispheric transfer of hand somatosensory information in the monkey. *Behav Brain Res* 11:155–170.
- Marasco PD, Kuiken TA (2010) Amputation with median nerve redirection (targeted reinnervation) reactivates forepaw barrel subfield in rats. *J Neurosci* 30:16008–16014.
- Marfurt CF, Rajchert DM (1991) Trigeminal primary afferent projections to “non-trigeminal” areas of the rat central nervous system. *J Comp Neurol* 303:489–511.
- Margolis DJ, Lütcke H, Helmchen F (2014) Microcircuit dynamics of map plasticity in barrel cortex. *Curr Opin Neurobiol* 24:76–81.
- Marik SA, Hickmott PW (2009) Plasticity of horizontal connections at a functional border in adult rat somatosensory cortex. *Neural Plast* 2009:294192.
- Markram H, Lübke J, Frotscher M, Sakmann B (1997) Regulation of synaptic efficacy by coincidence of postsynaptic APs and EPSPs. *Science* (80-) 275:213–215.
- Martinez M, Delcour M, Russier M, Zennou-Azogui Y, Xerri C, Coq J-O, Brezun J-M (2010) Differential tactile and motor recovery and cortical map alteration after C4-C5 spinal hemisection. *Exp Neurol* 221:186–197.
- Martuzzi R, van der Zwaag W, Farthouat J, Gruetter R, Blanke O (2014) Human finger somatotopy in areas 3b, 1, and 2: A 7T fMRI study using a natural stimulus. *Hum Brain Mapp* 35:213–226.
- Matthews PB (1988) Proprioceptors and their contribution to somatosensory mapping: complex messages require complex processing. *Can J Physiol Pharmacol* 66:430–438.
- Mauguière F, Merlet I, Forss N, Vanni S, Jousmäki V, Adeleine P, Hari R (1997) Activation of a distributed somatosensory cortical network in the human brain. A dipole modelling study of magnetic fields evoked by median nerve stimulation. Part I: Location and activation timing of SEF sources. *Electroencephalogr Clin Neurophysiol* 104:281–289.
- Maunsell JHR, van Essen DC (1983) The connections of the middle temporal visual area (MT) and their relationship to a cortical hierarchy in the macaque monkey. *J Neurosci* 3:2563–2586.
- McGlone F, Kelly EF, Trulsson M, Francis ST, Westling G, Bowtell R (2002) Functional neuroimaging studies of human somatosensory cortex. *Behav Brain Res* 135:147–158.
- McGlone F, Reilly D (2010) The cutaneous sensory system. *Neurosci Biobehav Rev* 34:148–159.
- McNeil D (1992) *Hand and mind* (Press TU of C, ed). Chicago and London.
- Mertens M, Lütkenhöner B, Lu B (2000) Efficient neuromagnetic determination of landmarks in the somatosensory cortex. *Clin Neurophysiol* 111:1478–1487.

- Merzenich MM, Jenkins WM (1993) Reorganization of cortical representations of the hand following alterations of skin inputs induced by nerve injury, skin island transfers, and experience. *J Hand Ther* 6:89–104.
- Merzenich MM, Kaas JH, Sur M, Lin CS (1978) Double representation of the body surface within cytoarchitectonic areas 3b and 1 in “ SI ” in the Owl monkey (*Aotus trivirgatus*). *J Comp Neurol* 181:41–74.
- Merzenich MM, Kaas JH, Wall J, Nelson RJ, Sur M, Felleman D (1983a) Topographic reorganization of somatosensory cortical areas 3b and 1 in adult monkeys following restricted deafferentation. *Neuroscience* 8:33–55.
- Merzenich MM, Kaas JH, Wall JT, Sur M, Nelson RJ, Felleman DJ, Francisco S (1983b) Progression of change following median nerve section in the cortical representation of the hand in areas 3b and 1 in adult owl and squirrel monkeys. *Neuroscience* 10:639–665.
- Merzenich MM, Nelson RJ, Kaas JH, Stryker MP, Jenkins WM, Zook JM, Cynader MS, Schoppmann A (1987) Variability in hand surface representations in areas 3b and 1 in adult owl and squirrel monkeys. *J Comp Neurol* 258:281–296.
- Merzenich MM, Nelson RJ, Stryker MP, Cynader MS, Schoppmann A, Zook JM (1984) Somatosensory cortical map changes following digit amputation in adult monkeys. *J Comp Neurol* 224:591–605.
- Meunier S, Garnero L, Ducorps A, Mazières L, Lehericy S, Tézenas du Montcel S, Renault B, Vidailhet M (2001) Human brain mapping in dystonia reveals both endophenotypic traits and adaptive reorganization. *Ann Neurol* 50:521–527.
- Mima T, Nagamine T, Nakamura K, Shibasaki H (1998) Attention modulates both primary and second somatosensory cortical activities in humans: a magnetoencephalographic study. *J Neurophysiol* 80:2215–2221.
- Miyamoto JJ, Honda M, Saito DN, Okada T, Ono T, Ohyama K, Sadato N (2006) The representation of the human oral area in the somatosensory cortex: a functional MRI study. *Cereb cortex* 16:669–675.
- Mogilner A, Grossman JA, Ribary U, Joliot M, Volkmann J, Rapaport D, Beasley RW, Llinás RR (1993) Somatosensory cortical plasticity in adult humans revealed by magnetoencephalography. *PNAS* 90:3593–3597.
- Mogilner A, Nomura M, Ribary U, Jagow R, Lado F, Rusinek H, Llinás R (1994) Neuromagnetic studies of the lip area of primary somatosensory cortex in humans: evidence for an oscillotopic organization. *Exp brain Res* 99:137–147.
- Molander C, Grant G (1986) Laminar distribution and somatotopic organization of primary afferent fibers from hindlimb nerves in the dorsal horn. A study by transganglionic transport of horseradish peroxidase in the rat. *Neuroscience* 19:297–312.
- Montagu A (1978) *Touching - The Human Significance of the Skin*, Second edi. Harper & Row, publishers.
- Montoya P, Ritter K, Huse E, Larbig W, Braun C, To S, Lutzenberger W, Grodd W, Flor H, Birbaumer N, Töpfner S (1998) The cortical somatotopic map and phantom phenomena in subjects with congenital limb atrophy and traumatic amputees with phantom limb pain. *Eur J Neurosci* 10:1095–1102.
- Moore CE., Schady W (2000) Investigation of the functional correlates of reorganization within the human somatosensory cortex. *Brain* 123:1883–1895.

- Moore CI, Cao R (2008) The hemo-neural hypothesis: on the role of blood flow in information processing. *J Neurophysiol* 99:2035–2047.
- Moore CI, Crosier E, Greve DN, Savoy R, Merzenich MM, Dale AM (2013) Neocortical correlates of vibrotactile detection in humans. *J Cogn Neurosci* 25:49–61.
- Moore CI, Stern CE, Dunbar C, Kostyk SK, Gehi A, Corkin S (2000) Referred phantom sensations and cortical reorganization after spinal cord injury in humans. *Proc Natl Acad Sci USA* 97:14703–8.
- Moulton EA, Pendse G, Morris S, Aiello-Lammens M, Becerra L, Borsook D (2009) Segmentally arranged somatotopy within the face representation of human primary somatosensory cortex. *Hum Brain Mapp* 30:757–765.
- Mountcastle V (1997) The columnar organization of the neocortex. *Brain* 120:701–722.
- Mountcastle VB, Lynch JC, Georgopoulos A, Sakata H, Acuna C (1975) Posterior parietal association cortex of the monkey: command functions for operations within extrapersonal space. *J Neurophysiol* 38:871–908.
- Mullinger KJ, Mayhew SD, Bagshaw a P, Bowtell R, Francis ST (2014) Evidence that the negative BOLD response is neuronal in origin: a simultaneous EEG-BOLD-CBF study in humans. *Neuroimage* 94:263–274.
- Muret D, Dinse HR, Macchione S, Urquizar C, Farnè A, Reilly KT (2014) Touch improvement at the hand transfers to the face. *Curr Biol* 24:R736–R737.
- Muret D, Martuzzi R, Dinse HR, Reilly KT, Blanke O, Farnè A (n.d.) Cortical correlates of perceptual changes transferring from the finger to the lips in human SI revealed by 7T fMRI.
- Myers MI, Peltier AC, Li J (2013) Evaluating dermal myelinated nerve fibers in skin biopsy. *Muscle Nerve* 47:1–11.
- Nagamatsu K, Nakasato N, Hatanaka K, Kanno A, Iwasaki M, Yoshimoto T, Nakasato CAN (2000) Neuromagnetic localization of N15, the initial cortical response to lip stimulus. *Neuroreport* 12:1–5.
- Nakamura A, Yamada T, Goto A, Kato T, Ito K, Abe Y, Kachi T, Kakigi R (1998) Somatosensory homunculus as drawn by MEG. *Neuroimage* 7:377–386.
- Nakashita S, Saito DN, Kochiyama T, Honda M, Tanabe HC, Sadato N (2008) Tactile-visual integration in the posterior parietal cortex: a functional magnetic resonance imaging study. *Brain Res Bull* 75:513–525.
- Nakatani M, Maksimovic S, Baba Y, Lumpkin E a (2014) Mechanotransduction in epidermal Merkel cells. *Pflugers Arch*.
- Nardone R, Höller Y, Brigo F, Seidl M, Christova M, Bergmann J, Golaszewski S, Trinka E (2013) Functional brain reorganization after spinal cord injury: systematic review of animal and human studies. *Brain Res* 1504:58–73.
- Nash PG, MacEfield VG, Klineberg IJ, Gustin SM, Murray GM, Henderson L a. (2010) Bilateral activation of the trigeminothalamic tract by acute orofacial cutaneous and muscle pain in humans. *Pain* 151:384–393.
- Navarro X (2009) Neural plasticity after nerve injury and regeneration. *Int Rev Neurobiol* 87:483–505.
- Neal JW, Pearson RC a, Powell TPS (1987) The cortico-cortical connections of area-7b, PF, in the parietal lobe of the monkey. *Brain Res* 419:341–346.

- Neal JW, Pearson RCA, Powell TPS (1986) The organization of the corticocortical projection of area 5 upon area 7 in the parietal lobe of the monkey. *Brain Res* 381:164–167.
- Négyessy L, Pálfi E, Ashaber M, Palmer C, Jákli B, Friedman RM, Chen LM, Roe AW (2013) Intrinsic horizontal connections process global tactile features in the primary somatosensory cortex: neuroanatomical evidence. *J Comp Neurol* 521:2798–2817.
- Nelson AJ, Chen R (2008) Digit somatotopy within cortical areas of the postcentral gyrus in humans. *Cereb cortex* 18:2341–2351.
- Nelson RJ, Kaas JH (1981) Connections of the ventroposterior nucleus of the thalamus with the body surface representations in cortical areas 3b and 1 of the cynomolgus macaque, (*Macaca fascicularis*). *J Comp Neurol* 199:29–64.
- Nelson RJ, Sur M, Felleman DJ, Kaas JH (1980) Representations of the body surface in postcentral parietal cortex of *Macaca fascicularis*. *J Comp Neurol* 192:611–643.
- Nevalainen P, Ramstad R, Isotalo E, Haapanen M-L, Lauronen L (2006) Trigeminal somatosensory evoked magnetic fields to tactile stimulation. *Clin Neurophysiol* 117:2007–2015.
- Nguyen BT, Inui K, Hoshiyama M, Nakata H, Kakigi R (2005) Face representation in the human secondary somatosensory cortex. *Clin Neurophysiol* 116:1247–1253.
- Nguyen BT, Tran TD, Hoshiyama M, Inui K, Kakigi R (2004) Face representation in the human primary somatosensory cortex. *Neurosci Res* 50:227–232.
- Nicolelis M a. ., Ghazanfar A a, Faggin BM, Votaw S, Oliveira LM. (1997) Reconstructing the engram: simultaneous, multisite, many single neuron recordings. *Neuron* 18:529–537.
- Nicolelis MAL, Chapin JK (1994) Spatiotemporal structure ensembles of the thalamus of somatosensory in the rat ventral responses of posterior medial nucleus. *J Neurosci* 14:3511–3532.
- Nicolelis MAL, Lin RCS, Woodward DJ, Chapin JK (1993) Induction of immediate spatiotemporal changes in thalamic networks by peripheral block of ascending cutaneous information. *Nature* 361:533–536.
- Nicoll RA, Malenka RC (1995) Contrasting properties of two forms of long-term potentiation in the hippocampus. *Nature* 377:115–118.
- Nihashi T, Naganawa S, Sato C, Kawai H, Nakamura T, Fukatsu H, Ishigaki T, Aoki I (2005) Contralateral and ipsilateral responses in primary somatosensory cortex following electrical median nerve stimulation--an fMRI study. *Clin Neurophysiol* 116:842–848.
- Niu J, Ding L, Li JJ, Kim H, Liu J, Li H, Moberly A, Badea TC, Duncan ID, Son Y-J, Scherer SS, Luo W (2013) Modality-based organization of ascending somatosensory axons in the direct dorsal column pathway. *J Neurosci* 33:17691–17709.
- Nolano M, Provitera V, Caporaso G, Stancanelli A, Leandri M, Biasiotta A, Cruccu G, Santoro L, Truini A (2013) Cutaneous innervation of the human face as assessed by skin biopsy. *J Anat* 222:161–169.
- Nolano M, Provitera V, Crisci C, Stancanelli A, Wendelschafer-Crabb G, Kennedy WR, Santoro L (2003) Quantification of myelinated endings and mechanoreceptors in human digital skin. *Ann Neurol* 54:197–205.
- Noppeney U, Waberski TD, Gobelé R, Buchner H (1999) Spatial attention modulates the cortical somatosensory representation of the digits in humans. *Neuroreport* 10:3137–3141.
- Nordin M (1990) Low-threshold mechanoreceptive and nociceptive units with unmyelinated (C) fibres in the human supraorbital nerve. *J Physiol* 426:229–240.

- Norman JF, Bartholomew AN (2011) Blindness enhances tactile acuity and haptic 3-D shape discrimination. *Attention, Perception, Psychophys* 73:2323–2331.
- Nyberg G, Blomqvist A (1985) The somatotopic organization of forelimb cutaneous nerves in the brachial dorsal horn: an anatomical study in the cat. *J Comp Neurol* 242:28–39.
- Ogawa S, Lee TM, Kay AR, Tank DW (1990) Brain magnetic resonance imaging with contrast dependent on blood oxygenation. *PNAS* 87:9868–9872.
- Ohye C, Shibasaki T, Hirato M, Kawashima Y, Matsumura M (1990) Strategy of selective VIM thalamotomy guided by microrecording. *Stereotact Funct Neurosurg* 54:186–191.
- Ojemann JG, Silbergeld DL (1995) Cortical stimulation mapping of phantom limb rolandic cortex. *J Neurosurg* 82:641–644.
- Okada Y (1983) Neurogenesis of evoked magnetic fields. *Biomagn an interdisciplinary approach*.
- Olausson H, Lamarre Y, Backlund H, Morin C, Wallin BG, Starck G, Ekholm S, Strigo I, Worsley K, Vallbo ÅB, Bushnell MC (2002) Unmyelinated tactile afferents signal touch and project to insular cortex. *Nat Neurosci* 5:900–904.
- Oldfield RC (1971) The assessment and analysis of handedness: the Edinburgh inventory. *Neuropsychologia* 9:97–113.
- Onishi H, Oyama M, Soma T, Kubo M, Kirimoto H, Murakami H, Kameyama S (2010) Neuromagnetic activation of primary and secondary somatosensory cortex following tactile-on and tactile-off stimulation. *Clin Neurophysiol* 121:588–593.
- Otsuru N, Inui K, Yamashiro K, Urakawa T, Keceli S, Kakigi R (2011) Effects of prior sustained tactile stimulation on the somatosensory response to the sudden change of intensity in humans: an magnetoencephalography study. *Neuroscience* 182:115–124.
- Overduin S a, Servos P (2004) Distributed digit somatotopy in primary somatosensory cortex. *Neuroimage* 23:462–472.
- Padberg J, Cerkevich C, Engle J, Rajan AT, Recanzone G, Kaas J, Krubitzer L (2009) Thalamocortical connections of parietal somatosensory cortical fields in macaque monkeys are highly divergent and convergent. *Cereb cortex* 19:2038–2064.
- Padberg J, Franca JG, Cooke DF, Soares JGM, Rosa MGP, Fiorani M, Gattass R, Krubitzer L (2007) Parallel evolution of cortical areas involved in skilled hand use. *J Neurosci* 27:10106–10115.
- Padberg J, Krubitzer L (2006) Thalamocortical connections of anterior and posterior parietal cortical areas in New World Titi monkeys. *J Comp Neurol* 497:416–435.
- Pandya DN, Kuypers HGJM (1969) Cortico-cortical connections in the rhesus monkey. *Brain Res* 13:13–36.
- Pandya DN, Seltzer B (1982) Intrinsic connections and architectonics of posterior parietal cortex in the rhesus monkey. *J Comp Neurol* 204:196–210.
- Panetsos F, Nunez A, Avendano C (1995) Local anaesthesia induces immediate receptive fields changes in nucleus gracilis and cortex. *Neuroreport* 7:150–152.
- Paré M, Smith AM, Rice FL (2002) Distribution and Terminal Arborizations of Cutaneous Mechanoreceptors in the Glabrous Finger Pads of the Monkey. *J Comp Neurol* 445:347–359.

- Parianen Lesemann FH, Reuter E-M, Godde B (2015) Tactile stimulation interventions: Influence of stimulation parameters on sensorimotor behavior and neurophysiological correlates in healthy and clinical samples. *Neurosci Biobehav Rev* 51:126–137.
- Pascual-Leone A, Peris M, Tormos JM, Pascual Pascual-Leone A, Catala MD (1996) Reorganization of human cortical motor output maps following traumatic forearm amputation. *Neuroreport*.
- Pascual-Leone A, Torres F (1993) Plasticity of the sensorimotor cortex representation of the reading finger in Braille readers. *Brain* 116:39–52.
- Passow S, Specht K, Adamsen TC, Biermann M, Brekke N, Craven AR, Ersland L, Grüner R, Kleven-Madsen N, Kvernenes O-H, Schwarzmüller T, Olesen RA, Hugdahl K (2015) Default-mode network functional connectivity is closely related to metabolic activity. *Hum Brain Mapp*.
- Paul RL, Merzenich M, Goodman H (1972) Representation of slowly and rapidly adapting cutaneous mechanoreceptors of the hand in Brodmann's areas 3 and 1 of *Macaca Mulatta*. *Brain Res* 36:229–249.
- Pauling L, Coryell CD (1936) The magnetic properties and structure of hemoglobin, oxyhemoglobin and carbonmonoxyhemoglobin. *PNAS* 22:210–216.
- Paullus JR, Hickmott PW (2011) Diverse excitatory and inhibitory synaptic plasticity outcomes in complex horizontal circuits near a functional border of adult neocortex. *Brain Res* 1416:10–25.
- Pei Y, Denchev P V, Hsiao SS, Craig JC, Bensmaia SJ (2009) Convergence of submodality-specific input onto neurons in primary somatosensory cortex. *J Neurosci* 102:1843–1853.
- Penfield W, Boldrey E (1937) Somatic motor and sensory representation in the cerebral cortex of man as studied by electrical stimulation. *Brain* 60:389–443.
- Penfield W, Jasper H (1954) *Epilepsy and the functional anatomy of the human brain*. London J A Churchill 159:105–106.
- Penfield W, Rasmussen T (1950) *The cerebral cortex of man: a clinical study of localization of function*. New York Macmillan Compagny.
- Petersen CCH (2007) The functional organization of the barrel cortex. *Neuron* 56:339–355.
- Petoe MA, Jaque FAM, Byblow WD, Stinear CM (2013) Cutaneous anesthesia of the forearm enhances sensorimotor function of the hand. *J Neurophysiol* 109:1091–1096.
- Pettit MJ, Schwark HD (1976) Receptive field reorganization in dorsal column nuclei during temporary denervation. *Science* 262(5142):2054–6.
- Peyron R, Garcia-Larrea L, Grégoire M-C, Costes M, Convers P, Lavenne F, Mauguière F, Michel D, Laurent B (1999) Haemodynamic brain responses to acute pain in humans. Sensory and attentional networks. *Brain* 122:1765–1779.
- Phillips CG, Powell TPS, Wiesendanger M (1971) Projection from low-threshold muscle afferents of hand and forearm to area 3a of baboon's cortex. *J Physiol* 217:419–46.
- Phillips JR, Johnson KO (1981) Tactile spatial resolution . II . Neural representation of bars, edges, and gratings in monkey primary afferents. *J Neurophysiol* 46:1192–203.
- Phoka E, Wildie M, Schultz SR, Barahona M (2012) Sensory experience modifies spontaneous state dynamics in a large-scale barrel cortical model. *J Comput Neurosci* 33:323–39.
- Pihko E, Lauronen L (2004) Somatosensory processing in healthy newborns. *Exp Neurol* 190:S2–S7.

- Pilz K, Veit R, Braun C, Godde B (2004) Effects of co-activation on cortical organization and discrimination performance. *Neuroreport* 15:2669–2672.
- Pleger B, Dinse HR, Ragert P, Schwenkreis P, Malin JP, Tegenthoff M (2001) Shifts in cortical representations predict human discrimination improvement. *Proc Natl Acad Sci USA* 98:12255–60.
- Pleger B, Foerster A-F, Ragert P, Dinse HR, Schwenkreis P, Malin J-P, Nicolas V, Tegenthoff M (2003) Functional imaging of perceptual learning in human primary and secondary somatosensory cortex. *Neuron* 40:643–53.
- Polley DB, Kvasnák E, Frostig RD (2004) Naturalistic experience transforms sensory maps in the adult cortex of caged animals. *Nature* 429:67–71.
- Pons TP, Garraghty PE, Cusick CG, Kaas JH (1985) A sequential representation of the occiput, arm, forearm and hand across the rostrocaudal dimension of areas 1, 2 and 5 in macaque monkeys. *Brain Res* 335:350–353.
- Pons TP, Garraghty PE, Friedman DP, Mishkin M (1987) Physiological evidence for serial processing in somatosensory cortex. *Science* (80-) 237:417–20.
- Pons TP, Garraghty PE, Mishkin M (1992) Serial and parallel processing of tactual information in somatosensory cortex of rhesus monkeys. *J Neurophysiol* 68:518–27.
- Pons TP, Garraghty PE, Ommaya AK, Kaas JH, Taub E, Mishkin M (1991) Massive cortical reorganization after sensory deafferentation in adult macaques. *Science* 252:1857–60.
- Pons TP, Kaas JH (1985) Connections of area 2 of somatosensory cortex with the anterior pulvinar and subdivisions of the ventroposterior complex in macaque monkeys. *J Comp Neurol* 240:16–36.
- Pons TP, Kaas JH (1986) Corticocortical connections of area 2 of somatosensory cortex in macaque monkeys: a correlative anatomical and electrophysiological study. *J Comp Neurol* 248:313–335.
- Porter LL (1997) Morphological characterization of a cortico-cortical relay in the cat sensorimotor cortex. *Cereb cortex* 7:100–9.
- Pouchelon G, Frangeul L, Rijli FM, Jabaudon D (2012) Patterning of pre-thalamic somatosensory pathways. *Eur J Neurosci* 35:1533–9.
- Pourrier SD, Nieuwstraten W, Cranenburgh B Van, Schreuders TAR, Stam HJ, Selles RW (2010) Three cases of referred sensation in traumatic nerve injury of the hand: implications for understanding central nervous system reorganization. *J Rehabil Med* 42:357–61.
- Powell TPS, Mountcastle VB (1959a) Some aspects of the functional organization of the cortex of the postcentral gyrus of the monkey: a correlation of findings obtained in a single unit analysis with cytoarchitecture. *Bull Johns Hopkins Hosp* 105:133–62.
- Powell TPS, Mountcastle VB (1959b) The cytoarchitecture if the postcentral gyrus of the monkey *Macaca mulatta*. *Bull Johns Hopkins Hosp* 105:108–31.
- Provitera V, Nolano M, Pagano A, Caporaso G, Stancanelli A, Santoro L (2007) Myelinated nerve endings in human skin. *Muscle Nerve* 35:767–75.
- Purves D, Augustine GJ, Fitzpatrick D, Hall WC, LaMantia A-S, McNamara JO, Williams SM (2004) *Neuroscience*, third edition.
- Qi H, Kaas JONH (2006) Organization of primary afferent projections to the gracile nucleus of the dorsal column system of primates. *J Comp Neurol* 499:183–217.

- Qi H-X, Kaas JH, Reed JL (2014) The reactivation of somatosensory cortex and behavioral recovery after sensory loss in mature primates. *Front Syst Neurosci* 8:1–14.
- Qi H-X, Lyon DC, Kaas JH (2002) Cortical and thalamic connections of the parietal ventral somatosensory area in marmoset monkeys (*Callithrix jacchus*). *J Comp Neurol* 443:168–82.
- Ragert P, Kalisch T, Bliem B, Franzkowiak S, Dinse HR (2008) Differential effects of tactile high- and low-frequency stimulation on tactile discrimination in human subjects. *BMC Neurosci* 9:9.
- Raichle ME (1998) Behind the scenes of functional brain imaging: a historical and physiological perspective. *PNAS* 95:765–72.
- Raichle ME, MacLeod A M, Snyder A Z, Powers WJ, Gusnard D A, Shulman GL (2001) A default mode of brain function. *PNAS* 98:676–82.
- Ramachandran VS (1993) Behavioral and magnetoencephalographic correlates of plasticity in the adult human brain. *Proc Natl Acad Sci USA* 90:10413–20.
- Ramachandran VS, Hirstein W (1998) The perception of phantom limbs. The D. O. Hebb lecture. *Brain* 121:1603–30.
- Ramachandran VS, Rogers-Ramachandran D, Stewart M (1992a) Perceptual correlates of massive cortical reorganization. *Science* (80-) 258:1159–60.
- Ramachandran VS, Stewart M, Rogers-Ramachandran DC (1992b) Perceptual correlates of massive cortical reorganization. *Neuroreport* 3:583–6.
- Ramirez A, Pnevmatikakis E A, Merel J, Paninski L, Miller KD, Bruno RM (2014) Spatiotemporal receptive fields of barrel cortex revealed by reverse correlation of synaptic input. *Nat Neurosci* 17:866–875.
- Randolph M, Semmes J (1974) Behavioral consequences of selective subcortical ablations in the postcentral gyrus of *Macaca Mulatta*. *Brain Res* 70:55–70.
- Rasmusson D (1996) Changes in the organization of the ventroposterior lateral thalamic nucleus after digit removal in adult raccoon. *J Comp Neurol* 364:92–103.
- Rasmusson DD (1982) Reorganization of raccoon somatosensory cortex following removal of the fifth digit. *J Comp Neurol* 205:313–326.
- Rasmusson DD, Turnbull BG (1983) Immediate effects of digit amputation on SI cortex in the raccoon: unmasking of inhibitory fields. *Brain Res* 288:368–370.
- Rausell E, Bickford L, Manger PR, Woods TM, Jones EG (1998) Extensive divergence and convergence in the thalamocortical projection to monkey somatosensory cortex. *J Neurosci* 18:4216–4232.
- Recanzone GH, Jenkins WM, Hradek GT, Merzenich MM (1992a) Progressive improvement in discriminative abilities in adult owl monkeys performing a tactile frequency discrimination task. *J Neurophysiol* 67:1015–1030.
- Recanzone GH, Merzenich MM, Dinse HR (1992b) Expansion of the cortical representation of a specific skin field in primary somatosensory cortex by intracortical microstimulation. *Cereb cortex* 2:181–196.
- Recanzone GH, Merzenich MM, Jenkins WM (1992c) Frequency discrimination training engaging a restricted skin surface results in an emergence of a cutaneous response zone in cortical area 3a. *J Neurophysiol* 67:1057–1070.

- Recanzone GH, Merzenich MM, Jenkins WM, Grajski K a, Dinse HR (1992d) Topographic reorganization of the hand representation in cortical area 3b owl monkeys trained in a frequency-discrimination task. *J Neurophysiol* 67:1031–1056.
- Recanzone GH, Merzenich MM, Schreiner CE (1992e) Changes in the distributed temporal response properties of SI cortical neurons reflect improvements in performance on a temporally based tactile discrimination task. *J Neurophysiol* 67:1071–1091.
- Reinisch CM, Tschachler E (2005) The touch dome in human skin is supplied by different types of nerve fibers. *Ann Neurol* 58:88–95.
- Ritter P, Born J, Brecht M, Dinse HR, Heinemann U, Pleger B, Schmitz D, Schreiber S, Villringer A, Kempter R (2015) State-dependencies of learning across brain scales. *Front Comput Neurosci* 9:1–21.
- Rizzolatti G, Craighero L (2004) The mirror-neuron system. *Annu Rev Neurosci* 27:169–192.
- Rizzolatti G, Fabbri-Destro M (2008) The mirror system and its role in social cognition. *Curr Opin Neurobiol* 18:179–184.
- Robinson CJ, Burton H (1980a) Somatic submodality distribution within the second somatosensory (SII), 7b, retroinsular, postauditory, and granular insular cortical areas of M. fascicularis. *J Comp Neurol* 192:93–108.
- Robinson CJ, Burton H (1980b) Organization of somatosensory receptive fields in cortical areas 7b, retroinsular, postauditory and granular insula of M. fascicularis. *J Comp Neurol* 192:69–92.
- Rocco MM, Brumberg JC (2007) The sensorimotor slice. *J Neurosci Methods* 162:139–147.
- Roland PE, O’Sullivan B, Kawashima R (1998) Shape and roughness activate different somatosensory areas in the human brain. *PNAS* 95:3295–3300.
- Rosa MJ, Kilner J, Blankenburg F, Josephs O, Penny W (2010) Estimating the transfer function from neuronal activity to BOLD using simultaneous EEG-fMRI. *Neuroimage* 49:1496–1509.
- Rosselet C, Zennou-Azogui Y, Escoffier G, Kirmaci F, Xerri C (2008) Experience-dependent changes in spatiotemporal properties of cutaneous inputs remodel somatosensory cortical maps following skin flap rotation. *Eur J Neurosci* 27:1245–1260.
- Rosselet C, Zennou-Azogui Y, Xerri C (2006) Nursing-induced somatosensory cortex plasticity: temporally decoupled changes in neuronal receptive field properties are accompanied by modifications in activity-dependent protein expression. *J Neurosci* 26:10667–10676.
- Rossini PM, Martino G, Narici L, Pasquarelli A, Peresson M, Pizzella V, Tecchio F, Torrioli G, Romani GL (1994) Short-term brain “plasticity” in humans: transient finger representation changes in sensory cortex somatotopy following ischemic anesthesia. *Brain Res* 642:169–177.
- Rothmund Y, Schaefer M, Grüsser SM, Flor H (2005) Localization of the human female breast in primary somatosensory cortex. *Exp brain Res* 164:357–364.
- Rowe MJ, Turman AB, Murray GM, Zhang HQ (1996) Parallel organisation of somatosensory cortical areas I and II for tactile processing. *Clin Exp Pharmacol Physiol* 23:931–938.
- Roy CS, Sherrington CS (1980) On the regulation of the blood-supply of the brain. *J Physiol* 11:85–158.
- Ruben J, Krause T, Taskin B, Blankenburg F, Moosmann M, Villringer A (2006) Subarea-specific suppressive interaction in the BOLD responses to simultaneous finger stimulation in human primary somatosensory cortex: evidence for increasing rostral-to-caudal convergence. *Cereb cortex* 16:819–826.

- Ruben J, Schwiemann J, Deuchert M, Meyer R, Krause T, Curio G, Villringer K, Kurth R, Villringer A (2001) Somatotopic organization of human secondary somatosensory cortex. *Cereb Cortex* 11:463–473.
- Rushworth MFS, Nixon PD, Passingham RE (1997a) Parietal cortex and movement. I. Movement selection and reaching. *Exp Brain Res* 117:292–310.
- Rushworth MFS, Nixon PD, Passingham RE (1997b) Parietal cortex and movement. II. Spatial representation. *Exp Brain Res* 117:311–323.
- Saal HP, Bensmaia SJ (2014) Touch is a team effort : interplay of submodalities in cutaneous sensibility. *Trends Neurosci* 37:689–697.
- Sadato N, Ibañez V, Deiber MP, Hallett M (2000) Gender difference in premotor activity during active tactile discrimination. *Neuroimage* 11:532–540.
- Sakai M, Suga N (2001) Plasticity of the cochleotopic (frequency) map in specialized and nonspecialized auditory cortices. *PNAS* 98:3507–3512.
- Sakamoto K, Nakata H, Kakigi R (2008) Somatosensory-evoked magnetic fields following stimulation of the tongue in humans. *Clin Neurophysiol* 119:1664–1673.
- Sakata H, Taira M, Murata A, Mine S (1995) Neural mechanisms of visual guidance of hand action in the parietal cortex of the monkey. *Cereb cortex* 5:429–438.
- Sakata H, Takaoka Y, Kawarasaki A, Shibutani H (1973) Somatosensory properties of neurons in the superior parietal cortex (area 5) of the rhesus monkey. *Brain Res* 64:85–102.
- Sánchez-Panchuelo R-M, Besle J, Beckett A, Bowtell R, Schluppeck D, Francis S, Sanchez-panchuelo RM (2012) Within-digit functional parcellation of Brodmann areas of the human primary somatosensory cortex using functional magnetic resonance imaging at 7 tesla. *J Neurosci* 32:15815–15822.
- Sánchez-Panchuelo R-M, Besle J, Mougin O, Gowland P, Bowtell R, Schluppeck D, Francis S (2014) Regional structural differences across functionally parcellated Brodmann areas of human primary somatosensory cortex. *Neuroimage* 93:221–230.
- Sanchez-Panchuelo RM, Francis S, Bowtell R, Schluppeck D (2010) Mapping human somatosensory cortex in individual subjects with 7T functional MRI. *J Neurophysiol* 103:2544–2556.
- Sathian K, Deshpande G, Stilla R (2013) Neural changes with tactile learning reflect decision-level reweighting of perceptual readout. *J Neurosci* 33:5387–5398.
- Sathian K, Zangaladze A (1997) Tactile learning is task specific but transfers between fingers. *Percept Psychophys* 59:119–128.
- Sathian K, Zangaladze A (1998) Perceptual learning in tactile hyperacuity : complete intermanual transfer but limited retention. *Exp Brain Res* 118:131–134.
- Sathian K, Zangaladze A (2002) Feeling with the mind ' s eye : contribution of v isual cortex to tactile perception. *Behav Brain Res* 135:127–132.
- Sathian K, Zangaladze C a a, Hoffman JM, Grafton ST (1997) Feeling with the mind ' s eye. *Neuroreport* 8:3877–3881.
- Sato K, Nariai T, Sasaki S, Yazawa I, Mochida H, Miyakawa N, Momose-Sato Y, Kamino K, Ohta Y, Hirakawa K, Ohno K (2002) Intraoperative intrinsic optical imaging of neuronal activity from subdivisions of the human primary somatosensory cortex. *Cereb cortex* 12:269–280.

- Sato K, Nariai T, Tanaka Y, Maehara T, Miyakawa N, Sasaki S, Momose-Sato Y, Ohno K (2005) Functional representation of the finger and face in the human somatosensory cortex: intraoperative intrinsic optical imaging. *Neuroimage* 25:1292–1301.
- Schaefer M, Noennig N, Heinze H-J, Rotte M (2006) Fooling your feelings: artificially induced referred sensations are linked to a modulation of the primary somatosensory cortex. *Neuroimage* 29:67–73.
- Schäfer K, Blankenburg F, Kupers R, Grüner JM, Law I, Lauritzen M, Larsson HBW (2012) Negative BOLD signal changes in ipsilateral primary somatosensory cortex are associated with perfusion decreases and behavioral evidence for functional inhibition. *Neuroimage* 59:3119–3127.
- Schlieper S, Dinse HR (2012) Perceptual improvement following repetitive sensory stimulation depends monotonically on stimulation intensity. *Brain Stimul* 5:647–651.
- Schneider RJ, Friedman DP, Mishkin M (1993) A modality-specific somatosensory area within the insula of the rhesus monkey. *Brain Res* 621:116–120.
- Schnitzler A, Salmelin R, Salenius S, Jousm V, Hari R (1995) Tactile information from the human hand reaches the ipsilateral primary somatosensory cortex. *Neurosci Lett* 200:25–28.
- Schouenborg J, Kalliomaki J, Gustavsson P, Rosén I (1986) Field potentials evoked in rat primary somatosensory cortex (SI) by impulses in cutaneous AB- and C-fibres. *Brain Res* 397:86–92.
- Schwartz TH, Chen LM, Friedman RM, Spencer DD, Roe AW (2004) Intraoperative optical imaging of human face cortical topography: a case study. *Neuroreport* 15:1527–1531.
- Schweisfurth M a, Frahm J, Schweizer R (2014) Individual fMRI maps of all phalanges and digit bases of all fingers in human primary somatosensory cortex. *Front Hum Neurosci* 8:658.
- Schweisfurth M a, Schweizer R, Frahm J (2011) Functional MRI indicates consistent intra-digit topographic maps in the little but not the index finger within the human primary somatosensory cortex. *Neuroimage* 56:2138–2143.
- Schweizer R, Braun C, Fromm C, Wilms A, Birbaumer N (2001) The distribution of mislocalizations across fingers demonstrates training-induced neuroplastic changes in somatosensory cortex. *Exp Brain Res* 139:435–442.
- Schweizer R, Voit D, Frahm J (2008) Finger representations in human primary somatosensory cortex as revealed by high-resolution functional MRI of tactile stimulation. *Neuroimage* 42:28–35.
- Seitz AR, Dinse HR (2007) A common framework for perceptual learning. *Curr Opin Neurobiol* 17:148–153.
- Sellien H, Ebner FF (2007) Rapid plasticity follows whisker pairing in barrel cortex of the awake rat. *Exp Brain Res* 177:1–14.
- Sengelaub D., Muja N, Mills A., Myers W., Churchill J., Garraghty P. (1997) Denervation-induced sprouting of intact peripheral afferents into the cuneate nucleus of adult rats. *Brain Res* 769:256–262.
- Sereno MI, Huang R-S (2014) Multisensory maps in parietal cortex. *Curr Opin Neurobiol* 24:39–46.
- Servos P, Engel S a, Gati J, Menon R (1999) fMRI evidence for an inverted face representation in human somatosensory cortex. *Neuroreport* 10:1393–1395.
- Servos P, Zacks J, Rumelhart DE, Glover GH (1998) Somatotopy of the human arm using fMRI. *Neuroreport* 9:605–609.

- Severens M, Farquhar J, Desain P, Duysens J, Gielen C (2010) Transient and steady-state responses to mechanical stimulation of different fingers reveal interactions based on lateral inhibition. *Clin Neurophysiol* 121:2090–2096.
- Shanks MF, Powell TPS (1981) An electron microscopic study of the termination of thalamocortical fibres in area 3b, 1 and 2 of the somatic sensory cortex in the monkey. *Brain Res* 218:35–47.
- Sherrington CS (1906) *The integrative action of the nervous system*. New York: C Scribner and Sons.
- Shibasaki H (2008) Human brain mapping: Hemodynamic response and electrophysiology. *Clin Neurophysiol* 119:731–743.
- Shimojo M, Kakigi R, Hoshiyama M, Koyama S, Kitamura Y, Watanabe S (1996) Differentiation of receptive fields in the sensory cortex following stimulation of various nerves of the lower limb in humans: a magnetoencephalographic study. *J Neurosurg* 85:255–262.
- Shin H-C, Park S, Son J, Sohn J-H (1995) Responses from new receptive fields of VPL neurones following deafferentation. *Neuroreport* 7:33–36.
- Shmuel A, Augath M, Oeltermann A, Logothetis NK (2006) Negative functional MRI response correlates with decreases in neuronal activity in monkey visual area V1. *Nat Neurosci* 9:569–577.
- Shmuel A, Yacoub E, Pfeuffer J, Van de Moortele PF, Adriany G, Hu X, Ugurbil K (2002) Sustained negative BOLD, blood flow and oxygen consumption response and its coupling to the positive response in the human brain. *Neuron* 36:1195–1210.
- Shoham D, Grinvald A (2001) The cortical representation of the hand in macaque and human area S-I: high resolution optical imaging. *J Neurosci* 21:6820–6835.
- Simões C, Mertens M, Forss N, Jousmäki V, Lange J, Lütkenhöner B, Hari R (2001) Functional overlap of finger representations in human SI and SII cortices. *J Neurophysiol* 86:1661–1665.
- Simoies EL, Bramati I, Rodrigues E, Franzoi A, Moll J, Lent R, Tovar-Moll F (2012) Functional expansion of sensorimotor representation and structural reorganization of callosal connections in lower limb amputees. *J Neurosci* 32:3211–3220.
- Simons DJ (1978) Response properties of vibrissa units in rat SI somatosensory neocortex. *J Neurophysiol* 41:798–820.
- Sloan HL, Austin VC, Blamire a. M, Schnupp JWH, Lowe a. S, Allers K a., Matthews PM, Sibson NR (2010) Regional differences in neurovascular coupling in rat brain as determined by fMRI and electrophysiology. *Neuroimage* 53:399–411.
- Smith PS, Dinse HR, Kalisch T, Johnson M, Walker-Batson D (2009) Effects of repetitive electrical stimulation to treat sensory loss in persons poststroke. *Arch Phys Med Rehabil* 90:2108–2111.
- Smits E, Gordon DC, Witte S, Rasmusson DD, Zarzecki P (1991) Synaptic potentials evoked by convergent somatosensory and corticocortical inputs in raccoon somatosensory cortex : substrates for plasticity. *J Neurophysiol* 66:688–695.
- Snyder LH, Batista AP, Andersen RA (1997) Coding of intention in the posterior parietal cortex. *Nature* 386:167–170.
- Spengler F, Dinse HR (1994) Reversible relocation of representational boundaries of adult rats by intracortical microstimulation. *Neuroreport* 5:949–953.
- Spengler F, Godde B, Dinse HR (1995) Effects of ageing on topographic organization of somatosensory cortex. *Neuroreport* 6:469–473.

- Spengler F, Roberts TPL, Poeppel D, Byl N, Wang X, Rowley HA, Merzenich MM (1997) Learning transfer and neuronal plasticity in humans trained in tactile discrimination. *Neurosci Lett* 232:151–154.
- Squire LR, Bloom FE, Spitzer NC, du Lac S, Ghosh A, Berg D (2008) *Fundamental Neuroscience*, third edition.
- Srinivasan MA, Whitehouse JM, LaMotte RH (1990) Tactile detection of slip: surface microgeometry and peripheral neural codes. *J Neurophysiol* 63:1323–1332.
- Stanton GB, Cruce WL, Goldberg ME, Robinson DL (1977) Some ipsilateral projections to areas PF and PG of the inferior parietal lobule in monkeys. *Neurosci Lett* 6:243–250.
- Stavrinou ML, Penna S Della, Pizzella V, Torquati K, Cianflone F, Franciotti R, Bezerianos A, Romani GL, Rossini PM (2007) Temporal dynamics of plastic changes in human primary somatosensory cortex after finger webbing. *Cereb Cortex* 17:2134–2142.
- Steen PA, Mason M, Pham L, Lefebvre Y, Hickmott PW (2007) Axonal bias at a representational border in adult rat somatosensory cortex (S1). *J Comp Neurol* 500:634–645.
- Stepniewska I, Cerkevich CM, Fang P-CY, Kaas JH (2009a) Organization of the posterior parietal cortex in galagos: II. Ipsilateral cortical connections of physiologically identified zones within anterior sensorimotor region. *J Comp Neurol* 517:783–807.
- Stepniewska I, Fang P-CY, Kaas JH (2009b) Organization of the posterior parietal cortex in galagos: I. Functional zones identified by microstimulation. *J Comp Neurol* 517:765–782.
- Sterr A, Green L, Elbert T (2003) Blind Braille readers mislocate tactile stimuli. *Biol Psychol* 63:117–27.
- Sterr A, Müller MM, Elbert T, Rockstroh B (1998a) Changed perceptions in Braille readers. *Nature* 391:134–5.
- Sterr A, Müller MM, Elbert T, Rockstroh B, Pantev C, Taub E (1998b) Perceptual correlates of changes in cortical representation of fingers in blind multifinger Braille readers. *J Neurosci* 18:4417–4423.
- Stilla R, Deshpande G, LaConte S, Hu X, Sathian K (2007) Posteromedial parietal cortical activity and inputs predict tactile spatial acuity. *J Neurosci* 27:11091–11102.
- Stippich C, Hofmann R, Kapfer D, Hempel E, Heiland S, Jansen O, Sartor K (1999) Somatotopic mapping of the human primary somatosensory cortex by fully automated tactile stimulation using functional magnetic resonance imaging. *Neurosci Lett* 277:25–28.
- Stoeckel MC, Pollok B, Schnitzler A, Seitz RJ (2007) Studying the human somatosensory hand area: A new way to compare fMRI and MEG. *J Neurosci Methods* 164:280–291.
- Stoeckel MC, Pollok B, Schnitzler A, Witte OW, Seitz RJ (2004) Use-dependent cortical plasticity in thalidomide-induced upper extremity dysplasia: Evidence from somaesthesia and neuroimaging. *Exp Brain Res* 156:333–341.
- Stoesz MR, Zhang M, Weisser VD, Prather SC, Mao H, Sathian K (2003) Neural networks active during tactile form perception: common and differential activity during macrospatial and microspatial tasks. *Int J Psychophysiol* 50:41–49.
- Stringer EA, Chen LM, Friedman RM, Gatenby C, Gore JC (2011) Differentiation of somatosensory cortices by high-resolution fMRI at 7 T. *Neuroimage* 54:1012–1020.
- Sur M (1980) Receptive fields of neurons in areas 3b and 1 of somatosensory cortex in monkeys. *Brain Res* 198:465–471.

- Sur M, Garraghty PE, Bruce CJ (1985) Somatosensory cortex in macaque monkeys: laminar differences in receptive field size in areas 3b and 1. *Brain Res* 342:391–395.
- Sur M, Nelson RJ, Kaas JH (1982) Representations of the body surface in cortical areas 3b and 1 of squirrel monkeys: comparisons with other primates. *J Comp Neurol* 211:177–192.
- Sur M, Wall JT, Kaas JH (1981) Modular segregation of functional cell classes within the postcentral somatosensory cortex of monkeys. *Science* (80-) 212:1059–1061.
- Sutherland MT, Tang AC (2006) Reliable detection of bilateral activation in human primary somatosensory cortex by unilateral median nerve stimulation. *Neuroimage* 33:1042–1054.
- Sutherling WW, Levesque MF, Baumgartner C (1992) Cortical sensory representation of the human hand: size of finger regions and nonoverlapping digit somatotopy. *Neurology* 42:1020–1028.
- Suzuki T, Shibukawa Y, Kumai T, Shintani M (2004) Face area representation of primary somatosensory cortex in humans identified by whole-head magnetoencephalography. *Jpn J Physiol* 54:161–169.
- Swadlow H a (2003) Fast-spike interneurons and feedforward inhibition in awake sensory neocortex. *Cereb Cortex* 13:25–32.
- Tamburin S, Manganotti P, Marzi CA, Fiaschi A, Zanette G (2002) Abnormal somatotopic arrangement of sensorimotor interactions in dystonic patients. *Brain* 125:2719–2730.
- Tamura Y, Shibukawa Y, Shintani M, Kaneko Y, Ichinohe T (2008) Oral structure representation in human somatosensory cortex. *Neuroimage* 43:128–135.
- Tandon S, Kambi N, Lazar L, Mohammed H, Jain N (2009) Large-scale expansion of the face representation in somatosensory areas of the lateral sulcus after spinal cord injuries in monkeys. *J Neurosci* 29:12009–12019.
- Tanji J, Wise SP (1981) Submodality distribution in sensorimotor cortex of the unanesthetized monkey. *J Neurophysiol* 45:467–481.
- Tanosaki M, Hashimoto I (2004) Serial N20m dipoles in somatosensory evoked magnetic fields move along the distal-proximal representation of the digit area 3b of the human cortex. *Neurosci Lett* 359:175–179.
- Tanosaki M, Iguchi Y, Hoshi Y, Hashimoto I (2003) Tactile interference to the face affects magnetic responses elicited by electric thumb stimulation. *Clin Neurophysiol* 114:2118–2123.
- Tanosaki M, Iguchi Y, Kimura T, Takino R, Hashimoto I (2004) Functional connectivity between forearm and digits representations in human somatosensory area 3b. *Clin Neurophysiol* 115:2638–2644.
- Tanosaki M, Suzuki A, Takino R, Kimura T, Iguchi Y, Kurobe Y, Haruta Y, Hoshi Y, Hashimoto I (2002) Neural mechanisms for generation of tactile interference effects on somatosensory evoked magnetic fields in humans. *Clin Neurophysiol* 113:672–680.
- Taoka M, Toda T, Iriki a., Tanaka M, Iwamura Y (2000) Bilateral receptive field neurons in the hindlimb region of the postcentral somatosensory cortex in awake macaque monkeys. *Exp Brain Res* 134:139–146.
- Taoka M, Toda T, Iwamura Y (1998) Representation of the midline trunk, bilateral arms, and shoulders in the monkey postcentral somatosensory cortex. *Exp Brain Res* 123:315–322.
- Taylor KS, Anastakis DJ, Davis KD (2009) Cutting your nerve changes your brain. *Brain* 132:3122–3133.

- Taylor KS, Davis KD (2009) Stability of tactile- and pain-related fMRI brain activations: An examination of threshold-dependent and threshold-independent methods. *Hum Brain Mapp* 30:1947–1962.
- Taylor MJ, Saliba E, Laugier J (1996) Use of evoked potentials in preterm neonates. *Arch Dis Child* 74:F70–F76.
- Tecchio F, Rossini P., Pizzella V, Cassetta E, Pasqualetti P, Romani G. (1998) A neuromagnetic normative data set for hemispheric sensory hand cortical representations and their interhemispheric differences. *Brain Res Protoc* 2:306–314.
- Terumitsu M, Ikeda K, Kwee IL, Nakada T (2009) Participation of primary motor cortex area 4a in complex sensory processing: 3.0-T fMRI study. *Neuroreport* 20:679–683.
- Thees S, Blankenburg F, Taskin B, Curio G, Villringer A (2003) Dipole source localization and fMRI of simultaneously recorded data applied to somatosensory categorization. *Neuroimage* 18:707–719.
- Thibodeau GA, Patton KT (1999) *Anatomy & physiology*.
- Thulborn KR, Waterton JC, Matthews PM, Radda GK (1982) Oxygenation dependence of the transverse relaxation-time of water protons in whole-blood at high-field. *Biochim Biophys Acta* 714:265–270.
- Tinazzi M, Zanette G, Polo A, Volpato D, Manganotti P, Bonato C, Testoni R, Fiaschi A (1997) Transient deafferentation in humans induces rapid modulation of primary sensory cortex not associated with subcortical changes: a somatosensory evoked potential study. *Neurosci Lett* 223:21–24.
- Tinazzi M, Zanette G, Volpato D, Testoni R, Bonato C, Manganotti P, Miniussi C, Fiaschi A (1998) Neurophysiological evidence of neuroplasticity at multiple levels of the somatosensory system in patients with carpal tunnel syndrome. *Brain* 121:1785–1794.
- Toda T, Taoka M (2002) Integration of the upper and lower lips in the postcentral area 2 of conscious macaque monkeys (*Macaca fuscata*). *Arch Oral Biol* 47:449–456.
- Toda T, Taoka M (2004) Converging patterns of inputs from oral structures in the postcentral somatosensory cortex of conscious macaque monkeys. *Exp brain Res* 158:43–49.
- Tong J, Mao O, Goldreich D (2013) Two-point orientation discrimination versus the traditional two-point test for tactile spatial acuity assessment. *Front Hum Neurosci* 7.
- Tremere L, Hicks TP, Rasmusson DD (2001a) Expansion of receptive fields in raccoon somatosensory cortex in vivo by GABA A receptor antagonism: implications for cortical reorganization. *Exp Brain Res* 136:447–455.
- Tremere L, Hicks TP, Rasmusson DD (2001b) Role of inhibition in cortical reorganization of the adult raccoon revealed by microiontophoretic blockade of GABA A receptors. *J Neurophysiol* 86:94–103.
- Tuunanen PI, Kavec M, Jousmäki V, Usenius J-P, Hari R, Salmelin R, Kauppinen RA (2003) Comparison of BOLD fMRI and MEG characteristics to vibrotactile stimulation. *Neuroimage* 19:1778–1786.
- Vallbo AB, Johansson RS (1978) The tactile sensory innervation of the glabrous skin of the human hand. In: *Active Touch, the Mechanism of Recognition of Objects by Manipulation*, pp 29–54.
- Vallbo AB, Johansson RS (1984) Properties of cutaneous mechanoreceptors in the human hand related to touch sensation. *Hum Neurobiol* 3:3–14.

- Vallbo ÅB, Olausson H, Wessberg J (1999) Unmyelinated afferents constitute a second system coding tactile stimuli of the human hairy skin. *J Neurophysiol* 81:2753–2763.
- Van Boven RW, Hamilton RH, Kauffman T, Keenan JP, Pascual-Leone A (2000) Tactile spatial resolution in blind Braille readers. *Neurology* 54:2230–2236.
- Van Boven RW, Johnson KO (1994) The limit of tactile spatial resolution in humans: Grating orientation discrimination at the lip, tongue, and finger. *Neurology* 44:2361–2366.
- Van der Zwaag W, Kusters R, Magill A, Gruetter R, Martuzzi R, Blanke O, Marques JP (2013) Digit somatotopy in the human cerebellum: a 7T fMRI study. *Neuroimage* 67:354–362.
- Van Westen D, Fransson P, Olsrud J, Rosén B, Lundborg G, Larsson E-M, Westen D Van (2004) Fingersomatotopy in area 3b: an fMRI-study. *BMC Neurosci* 5:28.
- Vanzetta I, Grinvald A (2008) Coupling between neuronal activity and microcirculation: implications for functional brain imaging. *HFSP J* 2:79–98.
- Vega-Bermudez F, Johnson KO (1999) Surround suppression in the responses of primate SA1 and RA mechanoreceptive afferents mapped with a probe array. *J Neurophysiol* 81:2711–2719.
- Vega-Bermudez F, Johnson KO (2004) Fingertip skin conformance accounts, in part, for differences in tactile spatial acuity in young subjects, but not for the decline in spatial acuity with aging. *Percept Psychophys* 66:60–67.
- Vingerhoets G (2014) Contribution of the posterior parietal cortex in reaching, grasping, and using objects and tools. *Front Psychol* 5:1–17.
- Vitureira N, Letellier M, Goda Y (2012) Homeostatic synaptic plasticity: from single synapses to neural circuits. *Curr Opin Neurobiol* 22:516–521.
- Vogt B a, Pandya DN (1978) Cortico-cortical connections of somatic sensory cortex (areas 3, 1 and 2) in the rhesus monkey. *J Comp Neurol* 177:179–191.
- Vogt C, Vogt O (1919) Allgeimeinere Ergebnisse unserer Hirnforschung. *J Psychol Neurol Leipzig* 25:279–462.
- Wade AR, Rowland J (2010) Early suppressive mechanisms and the negative blood oxygenation level-dependent response in human visual cortex. *J Neurosci* 30:5008–5019.
- Wall JT (1988) Variable organization in cortical maps of the skin as an indication of the lifelong adaptive capacities of circuits in the mammalian brain. *TINS* 11:549–557.
- Wall JT, Felleman DJ, Kaas JH (1983) Recovery of normal topography in the somatosensory cortex of monkeys after nerve crush and regeneration. *Science* (80-) 221:771–773.
- Wan CY, Wood AG, Reutens DC, Wilson SJ (2010) Congenital blindness leads to enhanced vibrotactile perception. *Neuropsychologia* 48:631–635.
- Wang X, Merzenich MM, Sameshima K, Jenkins WM (1995) Remodelling of hand representation in adult cortex determined by timing of tactile stimulation. *Nature* 378:71–75.
- Weber B, Treyer V, Oberholzer N, Jaermann T, Boesiger P, Brugger P, Regard M, Buck A, Savazzi S, Marzi C a (2005) Attention and interhemispheric transfer: a behavioral and fMRI study. *J Cogn Neurosci* 17:113–123.
- Weber EH (1996) E. H. Weber on the Tactile Senses, Hove: Erlb.
- Weiss T, Miltner WHR, Liepert J, Meissner W, Taub E (2004) Rapid functional plasticity in the primary somatomotor cortex and perceptual changes after nerve block. *Eur J Neurosci* 20:3413–3423.

- Werhahn KJ, Mortensen J, Boven RW Van, Zeuner KE, Cohen LG (2002) Enhanced tactile spatial acuity and cortical processing during acute hand deafferentation. *Nat Neurosci* 5:936–938.
- Whitsel BL, Rustioni A, Dreyer D a, Loe PR, Allen EE, Metz CB (1978) Thalamic projections to SI in macaque monkey. *J Comp Neurol* 178:385–410.
- Wigström H, Gustafsson B (1986) Postsynaptic control of hippocampal long-term potentiation. *J Physiol* 81:228–236.
- Wilent WB, Contreras D (2005) Dynamics of excitation and inhibition underlying stimulus selectivity in rat somatosensory cortex. *Nat Neurosci* 8:1364–1370.
- Wilimzig C, Ragert P, Dinse HR (2012) Cortical topography of intracortical inhibition influences the speed of decision making. *PNAS* 109:3107–3112.
- Will B, Dalrymple-Alford J, Wolff M, Cassel JC (2008) The concept of brain plasticity-Paillard's systemic analysis and emphasis on structure and function (followed by the translation of a seminal paper by Paillard on plasticity). *Behav Brain Res* 192:2–7.
- Williamson SJ, Kaufman L (1990) Evolution of neuromagnetic topographic mapping. *Brain Topogr* 3:113–127.
- Wong M, Gnanakumaran V, Goldreich D (2011) Tactile spatial acuity enhancement in blindness: evidence for experience-dependent mechanisms. *J Neurosci* 31:7028–7037.
- Woolsey CN, Fairman D (1946) Contralateral, ipsilateral, and bilateral representation of cutaneous receptors in somatic areas I and II of the cerebral cortex of pig, sheep, and other mammals. *Surgery* 19:684–702.
- Wrigley PJ, Press SR, Gustin SM, Macefield VG, Gandevia SC, Cousins MJ, Middleton JW, Henderson L a, Siddall PJ (2009) Neuropathic pain and primary somatosensory cortex reorganization following spinal cord injury. *Pain* 141:52–59.
- Wu C-S, Ballester Rosado CJ, Lu H-C (2011) What can we get from “barrels”: the rodent barrel cortex as a model for studying the establishment of neural circuits. *Eur J Neurosci* 34:1663–1676.
- Wu CWH, Kaas JH (2002) The effects of long-standing limb loss on anatomical reorganization of the somatosensory afferents in the brainstem and spinal cord. *Somatosens Mot Res* 19:153–163.
- Wühle A, Mertiens L, Rüter J, Ostwald D, Braun C (2010) Cortical processing of near-threshold tactile stimuli: an MEG study. *Psychophysiology* 47:523–534.
- Wühle A, Preissl H, Braun C (2011) Cortical processing of near-threshold tactile stimuli in a paired-stimulus paradigm--an MEG study. *Eur J Neurosci* 34:641–651.
- Xerri C (2012) Plasticity of cortical maps: multiple triggers for adaptive reorganization following brain damage and spinal cord injury. *Neurosci* 18:133–148.
- Xerri C, Coq JO, Merzenich MM, Jenkins WM (1996) Experience-induced plasticity of cutaneous maps in the primary somatosensory cortex of adult monkeys and rats. *J Physiol Paris* 90:277–287.
- Xerri C, Merzenich MM, Peterson BE, Jenkins W (1998) Plasticity of primary somatosensory cortex paralleling sensorimotor skill recovery from stroke in adult monkeys. *J Neurophysiol* 79:2119–2148.
- Xerri C, Stern JM, Merzenich MM (1994) Alterations of the cortical representation of the rat ventrum induced by nursing behavior. *J Neurosci* 14:1710–1721.

- Xu J, Wall JT (1999) Functional organization of tactile inputs from the hand in the cuneate nucleus and its relationship to organization in the somatosensory cortex. *J Comp Neurol* 411:369–389.
- Yang TT, Gallen CC, Ramachandran VS, Cobb S, Schwartz BJ, Bloom FE (1994) Noninvasive detection of cerebral plasticity in adult human somatosensory cortex. *Neuroreport* 5:701–704.
- Yang TT, Gallen CC, Schwartz BJ, Bloom FE (1993) Noninvasive somatosensory homunculus mapping in humans by using a large-array biomagnetometer. *PNAS* 90:3098–3102.
- Yau JM, Connor CE, Hsiao SS (2013) Representation of tactile curvature in macaque somatosensory area 2. *J Neurophysiol* 109:2999–3012.
- Yvert B, Bertrand O, Echallier JF, Pernier J (1996) Improved dipole localization using local mesh refinement of realistic head geometries: An EEG simulation study. *Electroencephalogr Clin Neurophysiol* 99:79–89.
- Zamorano AM, Riquelme I, Kleber B, Altenmüller E, Hatem SM, Montoya P (2015) Pain sensitivity and tactile spatial acuity are altered in healthy musicians as in chronic pain patients. *Front Hum Neurosci* 8:1–9.
- Zarei M, Stephenson JD (1996) Ipsilateral and bilateral receptive fields in rat primary somatosensory cortex. *Neuroreport* 7:647–651.
- Zarzecki P et al. (1993) Synaptic mechanisms of cortical representational plasticity : somatosensory and corticocortical EPSPs in reorganized raccoon SI cortex. *J Neurophysiol*.
- Zarzecki P, Blum PS, Bakker DA, Herman D (1983) Convergence of sensoru inputs upon projection neurons of somatosensory cortex: vestibular, neck, head, and forelimb inputs. *Exp brain Res* 50:408–414.
- Zarzecki P, Wiggin DM (1982) Convergence of sensory inputs upon projection neurons of somatosensory cortex. *Exp brain Res* 48:28–42.
- Zeharia N, Hertz U, Flash T, Amedi A (2012) Negative blood oxygenation level dependent homunculus and somatotopic information in primary motor cortex and supplementary motor area. *PNAS* 109:18565–18570.
- Zhang M, Mariola E, Stilla R, Stoesz M, Mao H, Hu X, Sathian K (2005) Tactile discrimination of grating orientation: fMRI activation patterns. *Hum Brain Mapp* 25:370–377.
- Zhu Z, Disbrow E a, Zumer JM, McGonigle DJ, Nagarajan SS (2007) Spatiotemporal integration of tactile information in human somatosensory cortex. *BMC Neurosci* 8:1–14.